Desarrollo de metodologías analíticas sostenibles para el estudio de heterociclos de interés farmacéutico

Víctor González Ruiz

Tesis doctoral

Facultad de Farmacia - Universidad Complutense de Madrid
Febrero de 2014

Desarrollo de metodologías analíticas sostenibles para el estudio de heterociclos de interés farmacéutico

Memoria presentada para optar al grado de
Doctor por la Universidad Complutense de Madrid

Víctor González Ruiz

Bajo la dirección de:

Profª. Drª. Mª Antonia Martín Carmona
Profª. Drª. Ana Isabel Olives Barba

Febrero de 2014

S. D. de Química Analítica
Facultad de Farmacia
Universidad Complutense de Madrid

Development of sustainable analytical methodologies to study pharmaceutically relevant heterocycles

Víctor González-Ruiz

Ph.D. Thesis

February 2014

Tipografías:

Los pies de figuras, encabezados de tablas y páginas, títulos de partes y capítulos, y otros textos de apoyo, se han compuesto usando la familia Adobe Clean, creada originalmente por Robert Slimbach para Adobe en 2009.

El cuerpo del texto está compuesto usando la familia Gulliver, diseñada en 1993 por Gerard Unger para ser usada en aplicaciones en las que el ahorro de espacio y la facilidad de la lectura fueran prioritarios.

Imagen de portada:

Algunos de los compuestos empleados en el trabajo que se recoge en esta memoria (luotonina A, norharmano y β-ciclodextrina). Cromatograma obtenido al separar todos los antitumorales estudiados bajo condiciones optimizadas (Capítulo 13). Tres de las columnas cromatográficas empleadas: Waters Spherisorb, Phenomenex Luna C-18 y Phenomenex Kinetex C-18. *Fotografía: VGR*. **Contraportada**: imagen representativa de la estructura de una partícula core-shell. Complejo ternario Top1-DNA-topotecán.

ISBN y Depósito Legal: en trámite.

A mis padres.

A Elena.

Con todo mi cariño y mi gratitud.

Thanks to mother nature who, through separation,
has created beauty and bounty from formless matter.

J. Calvin Giddins, Unified Separation Science (1991).

Una experiencia de aprendizaje es cuando alguien tiene que decirte:
"¿Sabes eso que acabas de hacer? Pues no lo hagas más"

Douglas Adams, El salmón de la duda: haciendo autostop por la galaxia una última vez (2005).

Financiación

El trabajo recogido en la presente memoria ha sido posible gracias a los siguientes proyectos y becas:

- Beca de Formación de Profesorado Universitario 2008 (Ministerio de Educación)
- Beca de Iniciación a la Actividad Investigadora 2008 (Universidad Complutense de Madrid)
- Beca de Investigación asociada al Grupo de Investigación UCM-CAM 920234
- Fondos del Grupo de Investigación Heterociclos de Interés Biológico (UCM-CAM 920234, Universidad Complutense de Madrid, Comunidad Autónoma de Madrid)
- Fondos del Proyecto CTQ2009-11312 (Ministerio de Ciencia e Innovación)
- Fondos del Proyecto CTQ2006-13351 (Ministerio de Ciencia e Innovación)

Acto de lectura y defensa pública

El acto de lectura y defensa pública de esta tesis doctoral tuvo lugar en la Facultad de Farmacia de la Universidad Complutense de Madrid el día 10 de abril de 2014, ante el siguiente tribunal:

- **Presidenta:** Profª. Drª. Paloma Yáñez-Sedeño Orive
  Catedrática. Departamento de Química Analítica, Facultad de Ciencias Químicas, Universidad Complutense de Madrid.
- **Vocal:** Profª. Drª. María Celia García Álvarez-Coque
  Catedrática. Departamento de Química Analítica, Facultad de Química, Universidad de Valencia.
- **Vocal:** Profª. Drª. Ana María García Campaña
  Catedrática. Departamento de Química Analítica, Facultad de Ciencias, Universidad de Granada.
- **Vocal:** Dr. Ángel de la Puerta García-Barroso
  Investigador. Departamento de Análisis Instrumental y Química Ambiental, Instituto de Química Orgánica General, Consejo Superior de Investigaciones Científicas, Madrid.
- **Secretario:** Prof. Dr. Pedro Andrés Carvajales
  Profesor Titular. Sección Departamental de Química Analítica, Facultad de Farmacia, Universidad Complutense de Madrid.

El tribunal le otorgó la calificación máxima de “sobresaliente *cum laude*”.

Agradecimientos

Ésta es la última parte de la tesis que escribo. Dicen que es la más complicada; eso lo averiguaré en los próximos minutos. Lo que es seguro es que será la más leída, así que tiene que estar a la altura de las expectativas. Confío en que mis dedos sean fieles a lo que quiere decir mi corazón.

Tengo que agradecer a la Sección Departamental de Química Analítica de la Facultad de Farmacia que haya puesto a mi disposición todos sus recursos para poder trabajar. A las profesoras M. Carmen Martín y Sofía Ródenas, Directoras de la Sección Departamental durante mi paso por ella, por todo su interés y paciencia cuando ha habido que hacer papeles y lo han puesto todo de su parte. A Benito del Castillo, Decano de la Facultad de Farmacia en mis años de estudiante y cuando me incorporé al laboratorio. Y al resto de compañeros del departamento que me han enseñado y han compartido sus experiencias e historias conmigo, gracias.

Al Departamento de Química Analítica de la Facultad de Ciencias Químicas, que ha facilitado con su mejor voluntad cuanta burocracia ha tenido que pasar por sus manos. Al Decano de la Facultad de Farmacia, Rafael Lozano, y a la Vicedecana de Programación Docente y Posgrado, Begoña Elorza, por su buena disposición y su ayuda con todos los trámites del Programa Oficial de Posgrado "Farmacia".

A mis Directoras, Ana Olives y Toñi Martín, les agradezco el tiempo y el esfuerzo que me han dedicado todos estos años; sólo ellas saben cuánto ha sido. Gracias por haber compartido cafés, revisiones al detalle, horas delante del ordenador, tardes garabateando planes de trabajo, plazos que se acababan, interminables charlas sobre ciencia (y todo lo demás). Y, sobre todo, gracias por confiar en mí y alentar mis iniciativas, por respaldarme y brindarme vuestro apoyo, por escucharme y ayudarme en los malos momentos, por hacerlo todo posible y por tratarme con tanto cariño. Toñi, Ana: gracias por todo.

Muchas gracias al profesor José Carlos Menéndez por haber estado siempre dispuesto a ayudarnos, por las correcciones del inglés, por facilitar el acceso a reactivos, equipos, software, material, instalaciones... Por tus útiles discusiones, por tu ayuda con las resonancias, por tu pragmatismo aplastante, por las charlas sobre programas y Macs y, especialmente, por ese humor cuya concentración de protones hace que el perclórico parezca sosa.

Por supuesto, a los departamentos de Química Orgánica y Farmacéutica y de Bioquímica y Biología Molecular II, de la Facultad de Farmacia, por haberme acogido como uno más en nuestras colaboraciones.

Y si hablo de esos departamentos, tengo que hablar de lo más importante: la gente que he encontrado allí. Ellos han sido los compañeros que he tenido durante estos años de laboratorio. Gracias, *piccola Italia*. Gracias por vuestra amistad y por haber estado a mi lado dentro y fuera de la facultad. Giammarco, gracias por tu generosidad y tu sentido del humor. Matteo, gracias por estar siempre ahí y hacer de amortiguador entre ML y yo. Giulia, gracias por tu ayuda con el modelado y el *docking*, y por tener siempre una sonrisa. Pascual, gracias por ser el *padre* de las luotoninas. Tamara, Irene, Jackie: *las chicas del 36*. Gracias por haberme enseñado los secretos del laboratorio de biología molecular y del cuarto de cultivos (sin desesperar en el intento). Y gracias, sobre todo, por vuestra comprensión y por estar siempre dispuestas a escuchar.

Elisa, Pierluigi, mis únicos compañeros de poyata. Cómplices y amigos. Los culpables de mi mejor época en el laboratorio. Gracias por vuestra amistad, por haberme ayudado a sobrellevar a R, por esos momentos de locura tan divertidos, por el radio-reloj, por ser tan como sois, cada uno de una manera, y por haberme dejado aprender tanto de vosotros.

Alberto, cómo te he echado de menos este último año. Cómo he extrañado los cafés de cada día, las comidas en Odontología, las discusiones que había que zanjar a golpe de Wikipedia, mis preguntas de biología molecular, tus preguntas de química. Gracias por ayudarme tanto, animarme en los peores momentos, estar siempre ahí, dentro y fuera de la facultad. Por llevarme la contraria, por saber las cosas más frikis, por esas dos semanas en Nueva York, por ser tan rockero y tan de Carabanchel. Pero, especialmente, gracias por inspirarme, porque eres un ejemplo de todas las virtudes que un investigador debe tener. Gracias, Lara, por

tantas risas y por tu entusiasmo al hablar conmigo de tipografías, diseño, o lo que se terciara, mientras todos los demás ponían cara de póquer.

Gracias al profesor Gregorio Carcedo. Por tus consejos para cuidarme en el día a día; por encontrar siempre una ecuación que me tranquilizara; por tu ayuda, sin la que los *kinetic plots* nunca hubieran salido adelante; por estar siempre dispuesto a echar una mano; por compartir conmigo el secreto de qué libros son los mejores; por animarme y tener siempre una sonrisa; y por tomarte tan bien las comparaciones. Muchas gracias, Gregorio, de veras.

También quiero agradecer a Juan Pajares aquella conversación que tuvimos un día de año nuevo en Valladolid. Gracias, Juan, porque aquello era lo que necesitaba para empezar a buscar la luz al final del túnel.

Rosa, ya sabes que el día que tú te marches el laboratorio se vendrá abajo. Gracias por ser tan *facilitadora*, por estar siempre disponible para remangarte y arrimar el hombro, por tener una solución inmediata para todo, por tantas charlas y por tranquilizarme cada día antes de que los alumnos entraran al laboratorio de prácticas.

Gracias, Carlos; gracias, Ana. Por vuestra amistad, por tantas comidas, cafés, charlas, y buenos momentos. Gracias, Miriam, por tus chistes breves que nos han hecho reír estos últimos meses. Gracias, Lily, por tu amistad y por tu ánimo *a dar el paso*.

Gracias a María Ortiz, Paloma Salas, Álex Buendía, María del Mar Hilillo, Alejandra Ruiz, Clara Torralbo y, especialmente, a Víctor Cervera y Miguel Largo; a todos, gracias por haberme enseñado tantas cosas. Yami, gracias por tu optimismo, tu capacidad de trabajo, y tu generosidad. Louise, tak *for caring about every little detail and for your perfectionism.* Gracias a Andrés León por haber sido un ejemplo de cómo trabajar en un laboratorio de química analítica.

A todos los amigos que me han acompañado durante todos estos años y, algunos, durante muchos más. Paco, Vero, con vosotros he pasado muchos de los mejores momentos de los últimos años, ya lo sabéis; gracias por vuestra amistad incondicional. Javi, gracias por seguir estando al pie del cañón más de veinticinco años después; por esos paseos y esas conversaciones. Gari, gracias por tu programa "Acabe la tesis en un año"; casi funciona. Adrie, gracias por tantos buenos ratos, por tu serenidad y tus sabias palabras. Marigel, gracias por tu positividad, por tantos buenos consejos, por tu vitalidad. Nacho, gracias por esa generosidad tan tuya. Miguel, si no fuera por ti... gracias por tu cuerda locura. Agus, Flor, gracias por estar siempre dispuestas a convertir en buenos los malos momentos. Héctor, gracias por tu humor gallego. Yasmina, gracias por no haber dejado de estar ahí nunca. Anne, *danke schön* por compartir con nosotros tu Berlín preferido cada verano. Áurea, gracias por ser maestra y amiga.

Rosa, Asun, gracias por mimarme, por darme tanto a cambio de nada, por quererme y cuidarme y hacerme vuestro niño. Gracias, de veras, de todo corazón. Gracias, Quino, por mostrar cómo la felicidad se encuentra en las cosas sencillas de la vida. Gracias, tito Pepe, por ser un ejemplo de dedicación al trabajo duro y bien hecho. Gracias, abuelos, porque siento que me seguís acompañando e inspirando cada día.

Papá, mamá: GRACIAS. Sin vosotros absolutamente nada habría sido posible. Gracias por tantas noches sin dormir, por darnos lo que teníais y lo que no teníais, por educarnos para ser buenas personas y ser ejemplo de ello, por recordarme cada día que podría ser lo que yo me propusiera, por tantos kilómetros caminados juntos, y por inculcarme las dos virtudes más importantes de una persona de ciencia: curiosidad y espíritu crítico.

Elena, gracias por haber hecho magia con mi vida. Gracias por haber conseguido que algo tan difícil como describir la felicidad sea tan fácil como decir: "Despertar junto a ti, cada mañana, cada día del resto de mi vida".

Gracias a mis enemigos, que creo que son pocos, y a mis *dificultadores*, que son algunos más, porque también a ellos debo parte de lo que he aprendido estos años.

Y gracias también a ti. Siento haberte olvidado en estos párrafos, pero tú sabes que sin tu granito de arena, esto no hubiera salido adelante. Gracias.

Viajando entre Palencia y Madrid, 26 de febrero de 2014.

Tabla de Contenidos

Resumen

1. Introducción

El cáncer, junto con las enfermedades cardiovasculares y las neurodegenerativas, son las patologías no transmisibles de mayor impacto social en los países con mayor índice de riqueza, aunque no sólo en ellos [1]. Este impacto se debe no únicamente a las consecuencias derivadas del hecho de padecer la enfermedad, sino también al coste económico que suponen. Por esta razón, la búsqueda de nuevos agentes terapéuticos y de técnicas analíticas que permitan el diagnóstico precoz de estas patologías en sus estadios primarios constituyen un campo de actividad continuada y renovada [2].

Las estrategias terapéuticas basadas en los fármacos antitumorales requieren un conocimiento minucioso de su mecanismo de acción y de su interacción con las macromoléculas biológicas, así como de su metabolización en los orgánulos celulares. La búsqueda de nuevas dianas terapéuticas abre un amplio abanico de posibilidades [3,4], y, en este sentido, los compuestos con actividad inhibidora de topoisomerasas constituyen una esperanzadora realidad. Algunos alcaloides utilizados desde antaño en medicina tradicional china poseen esta actividad, destacando entre ellos la camptotecina y la luotonina A, si bien esta actividad también se ha encontrado en los alcaloides derivados de β-carbolina.

En los últimos 10 años, se ha ido arraigando cada vez con más fuerza en la comunidad científica la necesidad de desarrollar metodologías analíticas sostenibles, no sólo con el fin de preservar el entorno que han de poder disfrutar futuras generaciones, sino también desde el punto de vista del ahorro energético y la economía molecular. De este modo se han ido introduciendo distintas metodologías y técnicas analíticas con la finalidad de reducir el impacto medioambiental de las ya existentes [5]. A día de hoy, la cromatografía de líquidos (HPLC) es la técnica analítica de mayor proyección y aplicación en el desarrollo farmacéutico, así como en otros ámbitos (plantas de producción, control de calidad de materias primas y de productos terminados, laboratorios clínicos, etc...) La producción de residuos de disolventes orgánicos como consecuencia de los análisis realizados es algo inherente a la mayoría de modalidades de HPLC y, por ello, la reducción en la generación de los mismos constituye un reto atractivo en el contexto de la Química Analítica Sostenible. Welch [6] afirma que cada cromatógrafo de líquidos (trabajando a pleno rendimiento en un entorno industrial) genera aproximadamente 1 L de residuos orgánicos cada 24 h. Por ello, ha sugerido distintas alternativas como el empleo de disolventes orgánicos biodegradables en clara sintonía con lo propuesto por Kerton [7] y De La Guardia [8].

2. Objetivos

En la presente memoria se plantea un objetivo general consistente en el desarrollo y la aplicación de metodologías analíticas sostenibles, apoyándose en tres objetivos específicos:

1.- Desarrollo de metodologías sostenibles en cromatografía de líquidos, encaminadas a la reducción de residuos orgánicos en HPLC. Este objetivo se desglosa en los siguientes:

1.1.- Reducción de la generación de residuos mediante la reducción del diámetro de las columnas empleando fases estacionarias convencionales.

1.2.- Reducción del volumen de disolventes orgánicos mediante el empleo de fases estacionarias de núcleo de sílice tipo “core shell” gracias a la reducción del tiempo de análisis.

1.3.- Utilización de fases móviles sostenibles (alcoholes) mediante la incorporación de ciclodextrinas como aditivos en las mismas.

2.- Empleo de técnicas espectroscópicas miniaturizadas. Demostrar el valor de las técnicas de lectura en placas multipocillos para la reducción del volumen de reactivos y residuos en una aplicación de relevancia en la industria farmacéutica: estudios de solubilidad de fármacos.

3.- Aplicación de las metodologías desarrolladas a la resolución de un problema de interés analítico y social: análisis de alcaloides antitumorales inhibidores de topoisomerasa 1. Desarrollo de

técnicas que permitan la determinación de su actividad biológica.

3. Metodología experimental

Se han utilizado cromatógrafos de líquidos (HPLC) con detección fluorimétrica. Además de las determinaciones espectrofotométricas y espectrofluorimétricas, llevadas a cabo en nuestros laboratorios, también se han utilizado espectrómetros de masas y de RMN de distintos centros de apoyo a la investigación.

4. Resultados

En este trabajo se ha llevado a cabo por primera vez, la caracterización espectrofluorimétrica de la luotonina A y de una serie de derivados de nueva síntesis. Las técnicas de ^{1}H- y ^{13}C-RMN han permitido verificar que los dos nitrógenos básicos son susceptibles de protonarse, a pesar de ser bases extremadamente débiles. Los equilibrios de protonación de en estado excitado de los dos nitrógenos no transcurren de modo independiente en medio acuoso, mientras que las titulaciones en medio no acuoso permiten evidenciar puntos isoemisivos en el caso de algunos de ellos. Existe una buena correlación estructura química-basicidad para el conjunto de los derivados estudiados.

De acuerdo con los objetivos planteados, nos propusimos desarrollar una metodología de separación utilizando una fase estacionaria frecuentemente empleada (columna C-18, Spherisorb, 5 µm, 150 × 4.6 mm) combinada con una fase móvil de acetonitrilo. Los distintos experimentos nos permitieron descartar la elución isocrática (incluyendo distintos modificadores orgánicos) y finalmente se seleccionó una elución en gradiente que permitía la separación de 6 de los 7 derivados de luotonina A en tiempos de análisis de 22 minutos. La metodología fue validada con LODs de 2,0 × 10^{-10} M, precisiones intra- e inter-día con RSD inferiores al 6% y adecuada exactitud, con valores de error relativo inferiores al 10%. La metodología desarrollada se aplicó a la determinación de los antitumorales en muestras de suero humano fortificadas con los analitos.

En una segunda etapa, y en la idea de reducir el consumo de disolvente orgánico sin sacrificar la eficacia, nos planteamos el empleo de una fase estacionaria análoga pero utilizando columnas de menor diámetro interno (columnas de partículas totalmente porosas C-18, 5 µm, 150 × 3.0 mm), utilizando también acetonitrilo como componente orgánico de la fase móvil, y elución en gradiente. En estas condiciones se consigue no sólo mantener la eficacia, sino incrementarla a la vez que se logra la separación y resolución de los 7 derivados de la luotonina A y de la camptotecina utilizada como patrón interno en un tiempo de análisis significativamente menor.

Con el objetivo de mejorar la selectividad de la separación, se ha estudiado la influencia de la naturaleza química de la fase estacionaria, comparando columnas con fases estacionarias C-18, fenil-hexil (PH) y pentafluoro-fenil-propil (PFP). En esta última fase estacionaria se lograron separaciones rápidas empleando como componente orgánico metanol, si bien se vio comprometida la resolución de los compuestos 4 y 5. Por ello, para lograr separaciones de elevada eficacia en tiempos de análisis cortos se optó por el empleo de fases estacionarias de partículas de sílice superficialmente porosa, tipo “core-shell” (C-18, PH y PFP 2,6 µm, 50 × 3.0 mm) que aportan varias ventajas a la cromatografía de líquidos. La superficie porosa hace que se puedan utilizar tamaños de partícula inferiores (2,6-2,7 µm) manteniendo presiones muy inferiores a las que se obtendrían con partículas del mismo tamaño totalmente porosas. Este hecho permite la utilización de equipos de HPLC convencionales sin necesidad de recurrir a inversiones en bombas de UHPLC capaces de trabajar a presiones mayores.

Se ha realizado el estudio termodinámico y cinético del comportamiento de las columnas de partículas total y superficialmente porosas. Los resultados obtenidos ponen de manifiesto el mejor comportamiento cromatográfico de las columnas empaquetadas con partículas “core-shell”. Las graficas de van’t Hoff nos han permitido determinar las entalpías de la separación, y los gráficos de van Deemter y cinéticos hacen posible comparar la eficacia de estas columnas y determinar los parámetros óptimos de eficacia y tiempo de análisis. En función de su selectividad, se eligió la fase estacionaria C-18 superficialmente porosa y se estudiaron distintas modalidades de gradiente. De esta manera conseguimos una separación eficaz de los ocho compuestos en tiempos de análisis un 50% más cortos (9 minutos) que con las columnas de sílice totalmente porosa y con un ahorro de acetonitrilo superior al 70%. Todo ello conlleva un ahorro del tiempo y de la energía empleados en el análisis de cada muestra. Para las condiciones experimentales óptimas se validó el método analítico, obteniendo excelentes parámetros de calidad. La metodología desarrollada se ha aplicado a la determinación de los antitumorales en cultivos celulares.

Otro de los aspectos susceptibles de modificarse en HPLC para mejorar la sostenibilidad de la técnica es la fase móvil. En este sentido, nos decantamos por la incorporación de ciclodextrinas, CDs (oligosacáridos macrocíclicos naturales, obtenidos mediante fermentación, no tóxicos y

completamente biodegradables) en las fases móviles. Las CDs introducen un equilibrio secundario al proceso de separación cromatográfica, y debido a su hidrosolubilidad son capaces de solubilizar analitos hidrofóbicos que alojan en el interior de sus cavidades. Por esta razón, permiten el empleo de fase móviles mayoritariamente acuosas. Así, para la separación de β-carbolinas, se logra reducir la proporción de disolvente orgánico a un 50% en el caso del metanol y a un 30% en el caso del etanol cuando la fase estacionaria es C-18. Si se utiliza como fase estacionaria C-1, en ese caso, la proporción de metanol se reduce a un 40% y la de etanol a un 25%. Los resultados obtenidos demuestran que el consumo de disolvente orgánico en la metodología propuesta en esta memoria es de unos 4 mL por carrera en comparación a los 6-14 mL utilizados por otros autores. Además, nuestro trabajo emplea alcoholes en vez de acetonitrilo. Este análisis se combinó con SPE para desarrollar y validar un método que permitiera la cuantificación de β-carbolinas en sueros humanos.

Las técnicas espectroscópicas miniaturizadas en formato de placas multi-pocillo permiten alcanzar una reducción de entre 10-20 veces en el volumen requerido para llevar a cabo determinaciones analíticas. En esta memoria se describe la aplicación de estas metodologías a los ensayos de solubilidad de fármacos. Mientras que en la determinación espectrofluorimétrica miniaturizada que hemos desarrollado sólo se requieren 300 µL de acetonitrilo por ensayo, en la determinación convencional por HPLC se necesitan entre 6 y 7 mL. Además del considerable ahorro de disolvente orgánico y de los desechos generados, este formato permite analizar un elevado número de muestras en un periodo de tiempo corto y de forma automatizada, analizándose simultáneamente patrones y problemas.

Considerando que la luotonina A ha sido utilizada en medicina tradicional china, entre otras razones por su actividad antitumoral, resulta de indudable interés el estudio de la actividad biológica *in vitro* de sus derivados. La luotonina A está estructuralmente relacionada con la camptotecina, que es el compuesto modelo los inhibidores de la enzima topoisomerasa I. Las analogías y diferencias estructurales, geométricas y químicas, hacen de la luotonina un candidato ideal para el estudio de la inhibición de la actividad de esta enzima, contribuyendo a profundizar en las interacciones que se establecen en el complejo ternario topoisomerasa-fármaco-ADN, un ejemplo del aún no muy bien conocido "paradigma de la inhibición interfacial".

La actividad antitumoral de los compuestos estudiados se ha ensayado utilizando como modelo líneas celulares tumorales de carcinoma cervical (HeLa), adenocarcinoma de pulmón (A549) y adenocarcinoma de colon (SW480). Los compuestos más lipófilos (**5**-**7**), muestran una mayor actividad, destacando la del compuesto **7**, que se convierte en uno de los pocos derivados de luotonina A descritos hasta la fecha que superan la potencia citotóxica del alcaloide natural. Esta actividad en cultivos celulares tumorales se correlaciona con la capacidad de inhibir la enzima impidiendo el desenrollamiento del ADN. Este comportamiento se ha cuantificado y se manifiesta de manera más acusada en el caso de los compuestos **4**, **6** y **7**. Se ha evaluado el papel de los sustituyentes sobre la estructura de luotonina A en la estabilización del complejo ternario mediante experimentos de modelado molecular y "docking", habiéndose descrito un nuevo modo de unión al complejo enzima-ADN que parece ser el responsable de la elevada actividad antitumoral de algunos de los derivados estudiados.

5. Conclusiones

Se han planteado distintas estrategias para lograr determinaciones cromatográficas más sostenibles empleando como modelos alcaloides del grupo de la pirroloquinazolina (luotonina A) y de las β-carbolinas. Se ha logrado reducir en más de un 50% el tiempo de análisis mediante el empleo de fases estacionarias de tipo "core-shell". Esta metodología de separación acoplada al sistema de pretratamiento de las muestras por precipitación en placa multi-pocillo conlleva una reducción total en el consumo de disolventes orgánicos superior al 70%.

Como estrategia alternativa se ha demostrado que la combinación de fases estacionarias convencionales con fases móviles que incorporan ciclodextrinas como aditivos en las fases móviles reducen el consumo de disolventes orgánicos hasta un 50%, con una generación de residuos mínima y de bajo impacto ambiental, al tratarse de macrociclos naturales completamente biodegradables, y permitiendo la sustitución del acetonitrilo por alcoholes. Se han caracterizado mediante espectrofluorimetría una biblioteca de compuestos (la luotonina A y 6 análogos de nueva síntesis), evidenciando las peculiaridades de sus equilibrios ácido-base. Se ha demostrado que la miniaturización de las técnicas espectroscópicas facilita los ensayos de solubilidad de fármacos, ahorrado reactivos, disolventes y tiempo, a la vez que posibilita la determinación semi-automática de un elevado número de muestras. La actividad biológica de estos compuestos se ha demostrado por su capacidad de inhibir la topoisomerasa 1. Los

sustituyentes en el anillo B de la luotonina A han demostrado ser claves para su actividad antitumoral, existiendo buena correlación entre los datos experimentales, en líneas celulares tumorales y los que predicen los modelos teóricos mediante técnicas de modelado molecular ("docking").

6. Referencias

1. World Health Organization. WHO Cancer Fact Sheet number 297. WHO Fact Sheets (2011).
2. A. I. Olives, B. del Castillo, M. A. Martín, Técnicas analíticas luminiscentes y de separación aplicadas a la identificación y cuantificación de biomarcadores, en F. Ortega Ortiz de Apodaca, Biomarcadores: analítica, diagnóstico y terapéutica, Monografía XXX, Real Academia Nacional de Farmacia, Madrid, 2010.
3. C. Avendaño, J. C. Menéndez, Medicinal chemistry of anticancer drugs. Elsevier, Amsterdam, 2008.
4. V. R. Adams, T. J. Burke (Eds.), Camptothecins in Cancer Therapy, Humana Press Inc., Totowa, NJ, 2005.
5. L.H Keith., L.U. Gron, J.L. Young, Chem. Rev., 2007, 107, 2695-2708.
6. C. J. Welch, N. Wu, M. Biba, R. Hartman, T. Brkovic, X. Gong, R. Helmy, W. Schafer, J. Cuff, Z. Pirzada, L Zhou, Trend. Anal. Chem., 2010, 29, 667-680.
7. F. M. Kerton, Alternative Solvents for Green Chemistry, RSC, Cambridge, 2009.
8. M. de la Guardia, S. Armenta, Green Analytical Chemistry. Theory and Practice, vol 57, en D. Barceló (Ed.), Comprehensive Analytical Chemistry, Elsevier, Amsterdam, 2010.

Summary

1. Introduction

Cancer, along with cardiovascular and neurodegenerative diseases, are the noncommunicable diseases having a biggest impact in developed countries [1]. Such an impact is caused not only by the illness itself, but also by its economic consequences. These facts have prompted the search for new therapeutic agents and analytical techniques allowing for the early diagnosis of these illnesses, renewing the interest in these research fields [2].

Therapeutic strategies based upon the use of anticancer drugs demand a close knowledge of their mechanisms of action, their modes of interaction with biological macromolecules, and their metabolites arising after intracellular processes.

Targeted therapy has opened a whole new horizon in cancer treatment [3,4], and topoisomerase I is one of the most promising anticancer drug targets. Some alkaloids isolated from plants that have been employed for centuries in traditional Chinese medicine, specially camptothecin and luotonin A, have been shown to act as topoisomerase I inhibitors. Other natural products, such as the β-carboline alkaloids, have also been recently found to exert this action.

For the past ten years, the need for developing sustainable methodologies has strengthened among many researches, not only due to the need for caring and protecting our legacy to future generations, but also in order to save reagents and energy. With this aim, a plethora of analytical methodologies able to fulfil these goals have been developed, and many existing ones have been adapted appropriately [5]. Nowadays, liquid chromatography (HPLC) is the analytical technique with the biggest relevance in pharmaceutical development, as well as in other fields (manufacturing plants, quality control of raw materials and finished products, clinical chemistry laboratories…). The production of wastes containing organic solvents is a drawback inherent to most chromatographic separation modes and, consequently, reducing the amount of organic solvents has become a major challenge for analytical chemists. Welch [6] calculates that a full-time working HPLC system in an industrial environment produces up to 1L of organic solvent residues daily. To reduce this volume, several alternatives such as the use of biodegradable solvents have been proposed following the principles suggested by Kerton [7] and de la Guardia [8].

2. Aims of the work

In the present thesis, our driving motivation is developing and applying sustainable analytical methodologies, a goal that can be divided into three parts:

1.- Development of sustainable methodologies for liquid chromatography, aimed at reducing the volume of organic solvents employed in HPLC. This goal can be divided as follows:

1.1.- Use of conventional columns with a smaller internal diameter in order to reduce the working flow rates.

1.2.- Use of core-shell columns allowing for higher efficiencies and shorter run times.

1.3.- Replacement of acetonitrile with alcohols as organic solvent, by using cyclodextrins as mobile phase additives.

2.- Development of miniaturized spectroscopic techniques proving the value of these techniques to carry out routine analyses with full analytical validity while reducing the amount of organic solvents required. Application to a relevant problem: determining the solubility values of drugs under development.

3.- Application of the developed methodologies to a problem of analytical and social relevance: analysis of alkaloids behaving as topoisomerase 1 inhibitors. Development of analytical

techniques allowing the study of their biological activities.

3. Experimental methods

Liquid chromatography systems with fluorescence detectors have been employed. Spectrophotometric and fluorimetric assays have also been developed in our laboratories. Further instrumentation (NMR and mass spectrometers) were used at Research Support facilities ascribed to our and other universities.

4. Results

In this work we have carried out, for the first time, the spectrofluorimetric characterization of luotonin A and a series of new analogues. ^{1}H- and ^{13}C-NMR techniques have evidenced that both basic nitrogens can be protonated, although they behave as extremely weak bases. In aqueous media, proton transfer equilibria can coexist for both nitrogens simultaneously, while in non-aqueous titration experiments, isoemissive points appear for some of the compounds. A good correlation was found between the chemical structures and the basicities of the library of compounds.

We have developed an analytical method to quantify the alkaloids under study employing a conventional, widely used stationary phase (C-18, Spherisorb, 5 µm, 150 × 4.6 mm) and a mobile phase containing acetonitrile. Although different organic modifiers were assayed, isocratic elution had to be discarded. Finally, a gradient elution was able to separate six out of the seven luotonin A derivatives in a 22-minute run time. The methodology was fully validated with LOD around 2.0×10^{-10} M, intra- and inter-day precisions below the 6% RSD, and adequate accuracy with relative errors under 10%. This methodology was used to analyse the alkaloids in fortified human serum samples.

In a second step, and with the aim to reduce the organic solvent consumption without reducing the efficiency, we assayed a related stationary phase packed into columns with smaller inner diameters (fully porous particles, C-18, 5 µm, 150 × 3 mm), also using a gradient elution with water and acetonitrile. Under these conditions, we were able not only to keep the efficiency of the analysis, but also to improve it while achieving the full separation of all of the compounds in a notably shorter analysis time.

In an effort to improve the selectivity of the separation, we studied the influence of the chemical nature of the stationary phase on the separation of the compounds by comparing C-18-, pentaflurophenylpropyl- (PFP) and phenylhexyl- (PH) functionalized columns. In the PH stationary phase we were able to achieve very fast separations using methanol, but at the expense of not resolving compounds 4 and 5. Next, we explored the possibilities of stationary phases packed with core-shell particles (C-18, PFP and PH, 2.6 µm, 50 × 3 mm) that afford several advantages in liquid chromatography. The porous shell keeps the backpressures under 400 bar even when small particles are employed, thus avoiding the need for UHPLC pumps.

We conducted a thermodynamic and kinetic study comparing fully-porous and core-shell packed columns. Our results evidenced the improved chromatographic properties of the columns packed with core-shell particles. Van't Hoff plots allowed us to determine the enthalpies driving the separation process, and van Deemter and kinetic plots made it possible to determine the optimum parameters of efficiency and analysis time. Based on its selectivity, we finally chose a C-18 core-shell stationary phase to develop and optimize different gradient profiles. With this method we achieved an efficient separation of the eight compounds within an analysis time 50% shorter (9 minutes) than the one required with the fully porous particles and saving over 75% of the organic solvent. Excellent figures of merit were obtained when the method was fully validated for the determination of the compounds in spiked samples of cell lysates.

Another component of the HPLC analyses that can be modified to improve the sustainability of the technique is the composition of the mobile phase. Among the many options available, we decided to try the effect of cyclodextrins (CDs): natural, atoxic macrocyclic oligosaccharides. CDs introduce an additional equilibrium into the separation process, and they are able to solubilize highly lipophilic molecules through inclusion into their apolar cavities. For this reason, they allow the use of mobile phases with high water contents. When applied to the separation of β-carbolines on C-18 stationary phases, these properties allow the use of methanol contents as low as 50% (30% in the case of ethanol). When C-1 stationary phases were employed, the organic solvent proportion was reduced to 40% for methanol and 25% for ethanol. A total volume of only 4 mL of solvent per run was needed, compared to the 6-14 mL reported in previous papers.

Furthermore, our work uses alcohols instead of the more toxic acetonitrile. This analysis was coupled to SPE to develop and validate a method to quantify β-carbolines in human serum samples.

Miniaturized spectroscopic techniques in multi-well plate format allow a 20-fold reduction in the volume needed for the analytical determination. In another part of this thesis we describe how the advantages of this design can be applied to drug solubility assays. While in the conventional HPLC determination 6-7 mL are needed, using the multi-well plate format we reduced the volume of organic solvent required for a determination down to 300 µL. This approach not only allows the automated analysis of a large number of samples in a short time span, but it also dramatically reduces the solvent and time consumption.

Taking into account that the antitumour and anti-inflammatory properties of luotonin A had been used for centuries in traditional Chinese medicine, it becomes evident that the in vitro study of its biological activity is an important issue in the characterization of new derivatives. Luotonin A is structurally related to the potent anticancer compound camptothecin, a model topoisomerase 1 inhibitor. Chemical analogies and differences between camptothecin and luotonin A turn the latter into an ideal candidate to study the complex mechanisms underlying the inhibition of this enzyme, allowing for a better comprehension of the interactions established in thr enzyme-DNA-drug complex that are the drivers of the not fully understood "interfacial inhibition paradigm".

The antitumor activities of the compounds were assayed on several different cancer cell lines: cervix carcinome (HeLa), lung adenocarcinome (A549) and colon adenocarcinome (SW480). The most lipophilic compounds (**5**-**7**) exhibited a higher degree of cytotoxic activity. The results from compound **7** are specially remarkable, as it is one of the few luotonin A derivatives that has shown a higher cytotoxicity than the natural alkaloid to date. This activity, found in cell cultures, correlates well with the topoisomerase 1 inhibition showed in enzymatic assays. We also evaluated the role of the substituents on the luotonin A backbone by means of molecular docking calculations, and from the results obtained we have described a new mode of binding to the enzyme-DNA complex which explains the remarkable potency of some of the studied derivatives.

5. Conclusions

We have developed several strategies to achieve more sustainable chromatographic analyses, using as a model alkaloids derived from luotonin A and β-carboline. By using core-shell stationary phases, we have shortened the analysis time of a previously described methodology by more than 50%. Coupled to a multi-well plate clean-up procedure, we have dropped the volume of organic solvents needed by more than 70%. As an alternative, the use of cyclodextrins as mobile phase additives and conventional columns has allowed a 50% drop in the organic solvent consumption and also the replacement of acetonitrile by alcohols, which are more environmentally friendly solvents.

Spectrofluorimetry was employed to characterize for the first time the luminescent properties of luotonin A and its six derivatives, evidencing their peculiar acid-base properties. By means of a miniaturized spectroscopy assay based on a multi-well plate format, we have proved the applicability of such kind of assays to routine determinations commonly carried out during the development of new drugs. The newly designed protocol allowed for a fast, automatized determination of the solubility of drugs in a HPLC-independent manner, saving time, reagents, and processing a large number of samples simultaneously.

The biological activity of these compounds has been studied, and their ability to inhibit the topoisomerase 1 enzyme has been quantified. Substituents on the B ring of luotonin A have been proved to play a key role on the activity of their derivatives, some of which show a remarkable antitumor activity due to their singular mode of binding to the enzyme-DNA complex.

6. Bibliography

1. World Health Organization. WHO Cancer Fact Sheet number 297. WHO Fact Sheets (2011).
2. A. I. Olives, B. del Castillo, M. A. Martín, Técnicas analíticas luminiscentes y de separación aplicadas a la identificación y cuantificación de biomarcadores, en F. Ortega Ortiz de Apodaca, Biomarcadores: analítica, diagnóstico y terapéutica, Monografía XXX, Real Academia Nacional de Farmacia, Madrid, 2010.

3. C. Avendaño, J. C. Menéndez, Medicinal chemistry of anticancer drugs. Elsevier, Amsterdam, 2008.
4. V. R. Adams, T. J. Burke (Eds.), Camptothecins in Cancer Therapy, Humana Press Inc., Totowa, NJ, 2005.
5. L.H Keith., L.U. Gron, J.L. Young, Chem. Rev., 2007, 107, 2695-2708.
6. C. J. Welch, N. Wu, M. Biba, R. Hartman, T. Brkovic, X. Gong, R. Helmy, W. Schafer, J. Cuff, Z. Pirzada, L Zhou, Trend. Anal. Chem., 2010, 29, 667-680.
7. F. M. Kerton, Alternative Solvents for Green Chemistry, RSC, Cambridge, 2009.
8. M. de la Guardia, S. Armenta, Green Analytical Chemistry. Theory and Practice, vol 57, en D. Barceló (Ed.), Comprehensive Analytical Chemistry, Elsevier 2010.

PARTE 1

Introducción

- El tratamiento del cáncer a través de la inhibición de la enzima topoisomerasa 1: derivados de la camptotecina y de la luotonina A
- Técnicas analíticas empleadas para el análisis de los derivados de la camptotecina y de la luotonina A
- Relevancia biológica y técnicas aplicables al análisis de alcaloides con estructura de β-carbolina
- Panorámica de la química analítica sostenible
- Técnicas espectroscópicas en formato de alto rendimiento en el contexto de la química analítica sostenible
- La cromatografía de líquidos en el contexto de la química analítica sostenible
- Fases móviles respetuosas con el medio ambiente
- Core-shell particles: leading the way to a renewed HPLC
- Recursos para mejorar la sostenibilidad de la etapa de pretratamiento de las muestras

Esta página se ha dejado en blanco intencionadamente.

1

El tratamiento del cáncer a través de la inhibición de la enzima topoisomerasa 1: derivados de la camptotecina y de la luotonina A

ABSTRACT ▶ El cáncer es una pandemia mundial con tendencia ascendente tanto en los países más desarrollados como en los de menor riqueza. Junto con la cirugía y la radioterapia, la quimioterapia antitumoral es uno de los pilares básicos en el tratamiendo de esta enfermedad. En la búsqueda de fármacos más selectivos y con menos efectos adversos, en los años 60 se descubrió que un alcaloide natural, la camptotecina, ejercía una potente actividad citotóxica sobre varios tipos de tumores. Tras caer en el olvido por sus efectos adversos, el interés por la camptotecina se reavivó dos décadas más tarde al descubrir que su mecanismo de acción es la inhibición de la topoisomerasa 1 humana. Esta enzima es capaz de deshacer el superenrollamiento que aparece en la doble hélice del ADN, permitiendo así el desarrollo de procesos celulares vitales como la replicación, la transcripción o la reparación del material genético. El hallazgo de su diana farmacológica alentó la búsqueda de análogos de camptotecina modificados químicamente para mejorar su farmacocinética y disminuir sus efectos adversos. En la actualidad, tres análogos de camptotecina están aprobados para su uso clínico, y otros muchos se encuentran en etapas avanzadas de desarrollo. Sin embargo, el talón de aquiles de los derivados de la camptotecina sigue siendo el anillo tipo lactona que presentan en su estructura y que los hace químicamente inestables. En 2003 se descubrió otro alcaloide natural, la luotonina A, que era estructuralmente análogo de la camptotecina pero tenía un anillo bencénico en lugar del anillo de lactona. Sorprendentemente, y a pesar de que su actividad era menor que la de la camptotecina, resultó también ser citotóxico contra distintas líneas celulares tumorales. Este descubrimiento ha abierto la puerta a la búsqueda de una nueva familia de inhibidores de topoisomerasa 1 que carezcan del inestable anillo lactona y presenten una actividad mejorada con respecto a la de la luotonina A natural.

> *Nadie, ni siquiera bajo tortura, puede decir con exactitud qué es un tumor*
>
> J. Ewing, 1916

1. Cáncer y quimioterapia

1.1. Patología del cáncer

El cáncer es un conjunto de más de cien enfermedades que tienen como denominador común la presencia de procesos anormales de división y crecimiento celulares. Cuando el desarrollo y la proliferación de la célula escapan al estrecho control al que están sometidos en condiciones fisiológicas, la división celular sigue generando nuevas células aunque el organismo no las necesite, y las células envejecidas no mueren cuando deberían hacerlo. Las células que así crecen y se dividen de manera anómala forman una masa de tejido que se denomina tumor.

Un tumor se considera benigno cuando las células que lo han originado no se diseminan a otras partes del cuerpo. Eso hace que generalmente se pueden extraer por cirugía y, en la mayoría de los casos, no tienden a reaparecer. Por el contrario, en el caso de los tumores malignos o cancerosos, las células pueden invadir tejidos adyacentes, desprenderse y diseminarse a regiones distantes del organismo dando lugar a la aparición de nuevos tumores.

El proceso por el que una célula normal se convierte en cancerosa es generalmente prolongado en el tiempo, y suele estar favorecido por la acción simultánea de varios factores externos [1]. Debido a que la malignización implica una compleja serie de cambios en la genética de la célula, se puede considerar que cada cáncer, en cada paciente, presenta caracteres exclusivos. Esa naturaleza única constituye una de las mayores barreras a salvar en el tratamiento de la enfermedad.

1.1.1. Las señas de identidad del cáncer

Hanahan y Weinberg delimitaron en 2000 [2] y actualizaron en 2011 [3] las

> *El tumor no es una masa aislada de células cancerosas en proliferación. En realidad, es un tejido de naturaleza compleja que incluye múltiples tipos celulares no sólo cancerosos, sino también células sanas reclutadas por el tumor, que forman el estroma asociado al mismo y son fundamentales para hacer posible su progresión.*

Hanahan y Weinberg, *The hallmarks of cancer*

características que definen a las células cancerosas, lo que llamaron "the hallmarks of cancer". Estas señas de identidad son distintivas de las células cancerosas y complementarias entre sí, permitiendo el crecimiento tumoral y la diseminación a otras zonas del organismo, y se enumeran a continuación (Figura 1):

Señalización proliferativa sostenida

En los tejidos normales, la secreción de factores de crecimiento que guían a las células a lo largo del ciclo celular se encuentra estrechamente controlada con el fin de que el crecimiento y la división estén supeditados al mantenimiento de la estructura y la funcionalidad tisulares. Las células cancerosas desarrollan uno o varios mecanismos que les permiten escapar de este control, entrando en un estado de proliferación continua. Algunos de ellos son la secreción autocrina de factores proliferativos, la sobreexpresión de receptores para estos factores, o la inducción a que las células del estroma del tumor aumenten la producción de los mismos.

Evasión de supresores del crecimiento

Las células cancerosas también son capaces de evitar los programas que regulan negativamente la proliferación celular. Se han descrito decenas de genes supresores que operan en una intrincada red para limitar el crecimiento y proliferación celulares por medio de vías de senescencia y apoptosis activadas por diversos mecanismos externos e internos. Mutaciones en estas proteínas pueden hacer que la célula escape de estas rutas de control.

Resistencia a la muerte celular

La apoptosis (o muerte celular programada) debería activarse en respuesta al envejecimiento y a diferentes tipos de estrés que sufren las células cancerosas durante la tumorogénesis o como resultado de la terapia antitumoral. De nuevo, alteraciones en las proteínas implicadas en las cascadas de activación de la apoptosis, ya sea por vía extríniseca o intrínseca, permiten a la célula sobrevivir de manera incontrolada.

Inmortalidad replicativa

Los telómeros son complejos nucleoproteicos con repeticiones en tándem de la secuencia TTAGGG, que se encuentran en los extremos de los cromosomas, y en células normales se van acortando con cada división celular. En ausencia de telómeros de suficiente longitud, la estabilidad del material genético celular se ve comprometida. Para hacer posible un número de divisiones celulares ilimitado, las células tumorales reactivan la enzima telomerasa, la transcriptasa inversa encargada de mantener la longitud de los telómeros.

Inducción de angiogénesis

El tejido tumoral en desarrollo necesita riego sanguíneo que le suministre oxígeno y nutrientes, y le permita desprenderse de los residuos del metabolismo celular. En un adulto sano, la angiogénesis (ramificación de vasos sanguíneos) se encuentra detenida salvo en circuns-

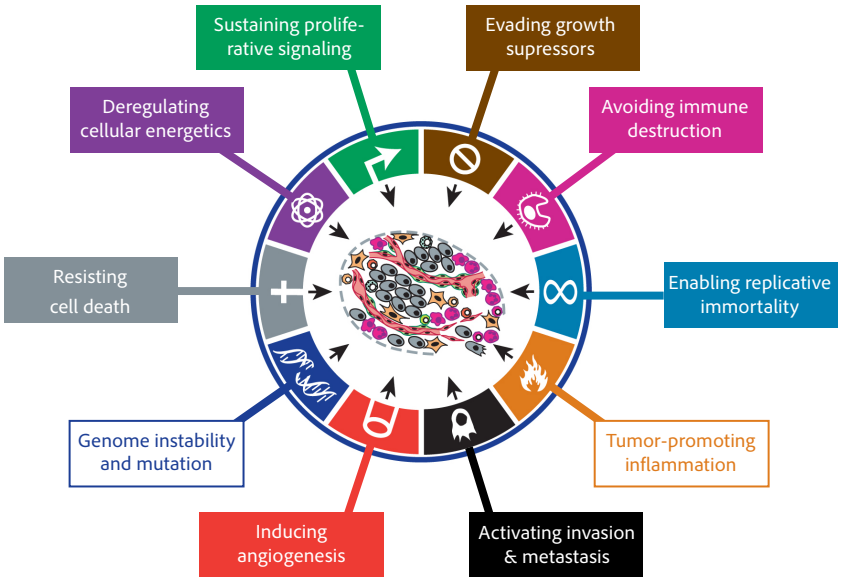

Figura 1.
Las 8 señas de identidad del cáncer y las dos características posibilitadoras que se asocian al mismo [3].

tancias concretas como la regeneración de heridas o la menstruación. Sin embargo, los tumores segregan señales capaces de favorecer la angiogénesis en los vasos circundantes, recibiendo así suficiente riego sanguíneo.

Activación de la invasión y la metástasis

Las células tumorales suelen presentar una disminución en la expresión de proteínas de adhesión celulares que contribuyen a la integridad de los tejidos en los que se encuentran. En cambio, la sobreexpresión de proteínas implicadas en la migración contribuye a su movilidad y capacidad invasiva en otros tejidos.

Reprogramación del metabolismo energético de la célula

Las células cancerosas exhiben características propias relacionadas con la organización energética, como un aumento de los transportadores para la captación de glucosa, o el uso preferente de la glucolisis citoplasmática en lugar de la fosforilación oxidativa mitocondrial para obtener ATP. La hiperactivación de esta vía, menos eficiente energéticamente, podría estar justificada por la producción de intermedios metabólicos que se incorporan a diversas rutas biosintéticas.

Evasión del sistema inmune

La secreción de algunas citoquinas, así como el reclutamiento de células inflamatorias, parecen ayudar al tumor a evitar activamente la respuesta inmune que de otro modo lo eliminaría.

Inestabilidad genómica e inflamación promotora del tumor

Existen dos mecanismos que, aunque no son consideradas *hallmarks* del cáncer, sí se pueden entender como características posibilitadoras del mismo. El aumento de las tasas de mutación en células en proceso de tumorogénesis parece ser clave en el desarrollo de las características que finalmente las convierten en cancerosas. Por otro lado, la presencia de células inflamatorias es común en muchos tumores y facilita el desarrollo del mismo al secretar factores de crecimiento y facilitar la angiogénesis.

1.1.2. Iniciación, promoción y progresión del cáncer

De manera histórica, se ha establecido un modelo bifásico del desarrollo de las células cancerosas en función de la naturaleza del agente externo al que son expuestas [4].

Iniciación

En el primer período, las células entran en contacto con un agente capaz de reaccionar con el ADN provocando cambios permanentes en el mismo (mutaciones). Muchas sustancias químicas no poseen esta característica per sé, sino que requieren una metabolización previa para convertirse en verdaderos iniciadores. Ésta es la razón por la que algunas sustancias sólo son carcinogénicas en determinados tejidos con determinada capacidad metabólica.

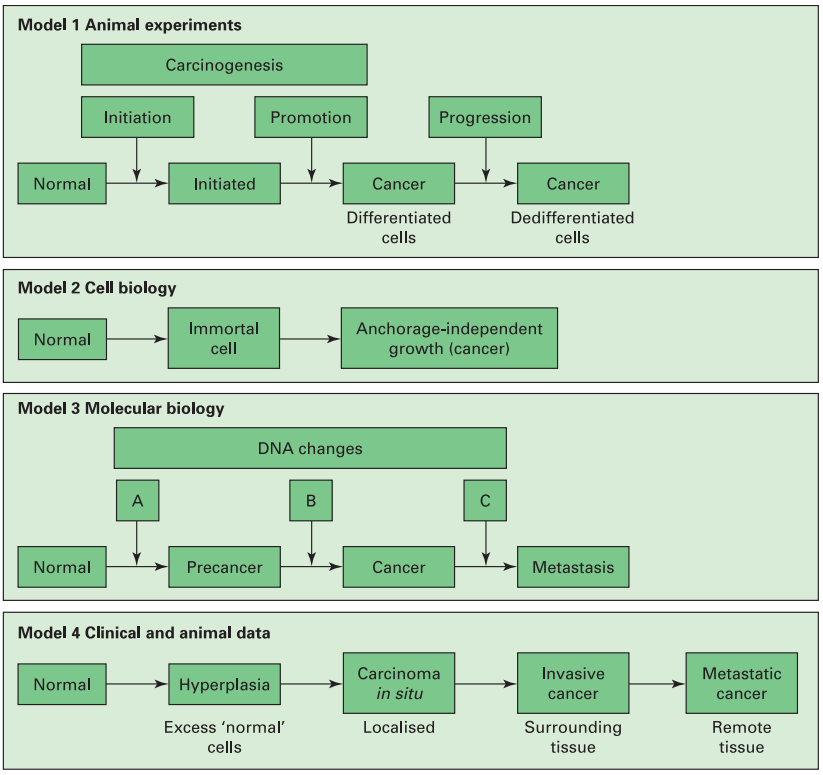

Figura 2.
Clasificación de las etapas de la carcinogénesis atendiendo a distintos criterios [4].

Promoción

Una vez que una célula ha sido mutada por un iniciador, es susceptible en una segunda fase a los efectos de los promotores. Estas sustancias activan rutas de señalización celulares que aumentan la proliferación celular.

Progresión

Se refiere a la evolución del tumor formado por la acción consecutiva de las dos etapas anteriores para adquirir características de malignidad que lo hacen irreversible; implicando, comúnmente, alteraciones en el cariotipo celular.

1.1.3. Etapas del desarrollo tumoral

Desde un punto de vista clínico, la evolución del cáncer se puede dividir en las siguientes etapas (Figura 2)

Hiperplasia

Las células se dividen de manera descontrolada, aunque su aspecto es aún normal.

Displasia

Mutaciones adicionales llevan a un crecimiento cada vez más descontrolado, y el tejido comienza a desorganizarse.

Carcinoma in situ

Más alteraciones acentúan la anormalidad del aspecto de las células. Muchas se desdiferencian y pierden características propias del tejido en que se originaron. Aún no han cruzado la lámina basal del tejido

Cáncer

Las células anormales invaden tejidos adyacentes y/o se diseminan a regiones distales.

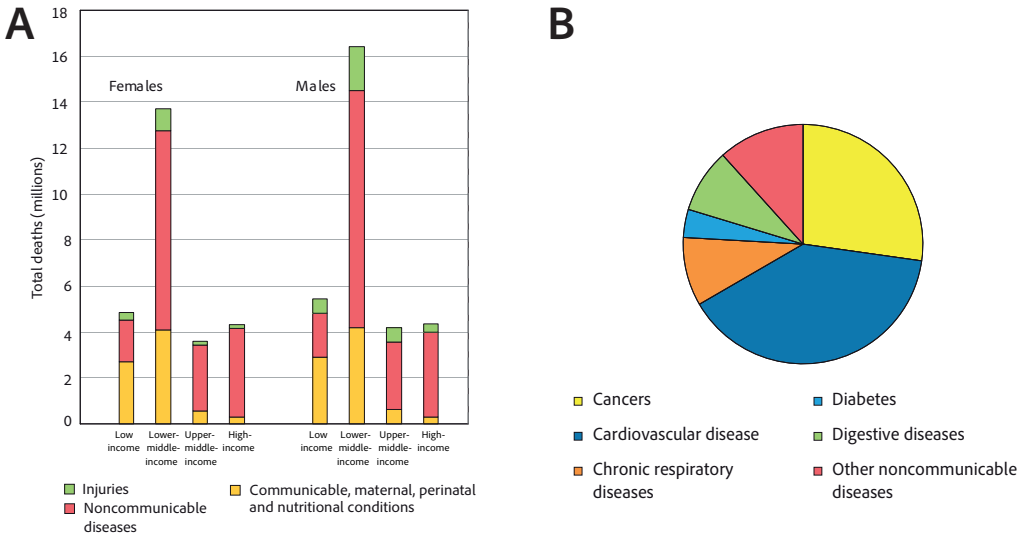

Figura 3. (A) Muertes totales agrupadas por sexo y según los niveles de riqueza definidos por el Banco Mundial, 2008. (B) Proporción de muertes globales por ENT en menores de 70 años, según causa de la muerte, 2008 [6].

1.2. Epidemiología del cáncer

A lo largo de sus vidas, aproximadamente una de cada tres personas recibirá en algún momento un diagnóstico de cáncer. Esta enfermedad, geográfica y étnicamente omnipresente, se percibe con mayor gravedad en las sociedades occidentales como la nuestra. En ellas, desde la perspectiva de la riqueza, la longevidad y la erradicación de la mayoría de enfermedades infecciosas, contemplamos perplejos cómo la solución para este grave problema no acaba de llegar. Este estado de preocupación se alimenta, además, de la ignorancia, de las afirmaciones infundadas y de las anécdotas llamativas. La espera de descubrimientos que parecen estar siempre "a la vuelta de la esquina" puede llevar en ocasiones a la búsqueda de alternativas en opciones alejadas de la medicina ortodoxa [5].

La Organización Mundial de la Salud clasifica el cáncer dentro del conjunto de las enfermedades no transmisibles (ENT; Noncommunicable diseases, NCD en inglés). De los 57 millones de muertes contabilizadas en todo el mundo en 2008, 36 millones (un 63%) fueron debidas a ENT. Las ENT comprenden, principalmente, enfermedades cardiovasculares (48% de las muertes por ENT), cáncer (21%), enfermedad pulmonar obstructiva crónica, y diabetes. Salvo en la región de África, la mortalidad por ENT supera a la suma de todas las muertes causadas por enfermedades transmisibles, maternales, perinatales y por desnutrición. En contra de la creencia popular, el 80% de las muertes por ENT ocurrieron en países con índices de riqueza bajos o medios, y de hecho fueron la causa más frecuente de muerte en estos países con la excepción de los del Continente africano (Figura 3A) [6].

En 2008, se estima que aparecieron un total de 12,7 millones de casos de cáncer en el mundo, y se produjeron 7,6 millones de muertes por cáncer. Un 56% de los nuevos casos y un 63% de las muertes tuvieron lugar en países con un bajo índice de desarrollo [7,8]. La previsión es que hasta 2030, el incremento en los casos de cáncer en estos países (82%) será notablemente mayor que en los de riqueza media-alta y alta (58 y 40% respectivamente) [6]. Son también los países más pobres aquellos que presentan mayor incidencia de cánceres asociados con infecciones (virus del papiloma humano, virus de las hepatitis B y C y *Helicobacter pilori*), los cuales suponen un 18% de los casos de cáncer a nivel mundial (Figura 3B) [6].

Los datos preliminares de GLOBOCAN 2012 [9] confirman que la tendencia es al alza, con 14,1 millones de nuevos casos, 8,2 millones de muertes y 32,6 millones de diagnósticos de cáncer en los cinco años precedentes. De ellos, un 57% de los nuevos casos y un 65% de los nuevos diagnósticos, ocurrieron en las regiones menos desarrolladas del planeta.

En las regiones con mayor índice de desarrollo humano (IDH) en 2008, los cánceres de pulmón, mama, colon-recto y próstata sumaron la mitad de los casos totales de cáncer, mientras que en las de IDH medio, los de esófago, estómago e hígado fueron también comunes. En total, estos siete tipos de cáncer fueron responsables del 62% de los casos en zonas con IDH medio y alto. En las áreas de menor IDH, el cáncer de cérvix fue más frecuente que el de mama y el de hígado. Las regiones con IDH medio o alto muestran una tendencia al descenso de la incidencia de cáncer de cérvix y estómago, mientras que para los de mama, próstata y colon se observa un comportamiento contrario (Figura 4) [10].

En el año 2010 las ENT fueron responsables de un 91% de todas las muertes registradas en España. El cáncer causó el 27% de la mortalidad total, lo que lo sitúa como la segunda causa de mortalidad en nuestro país, por detrás sólo de las enfermedades cardiovasculares (Figura 5) [11]. A nivel mundial, se espera que la incidencia de nuevos casos de cáncer aumente de 12,7 millones en 2008 a 22,2 millones en 2030 [10].

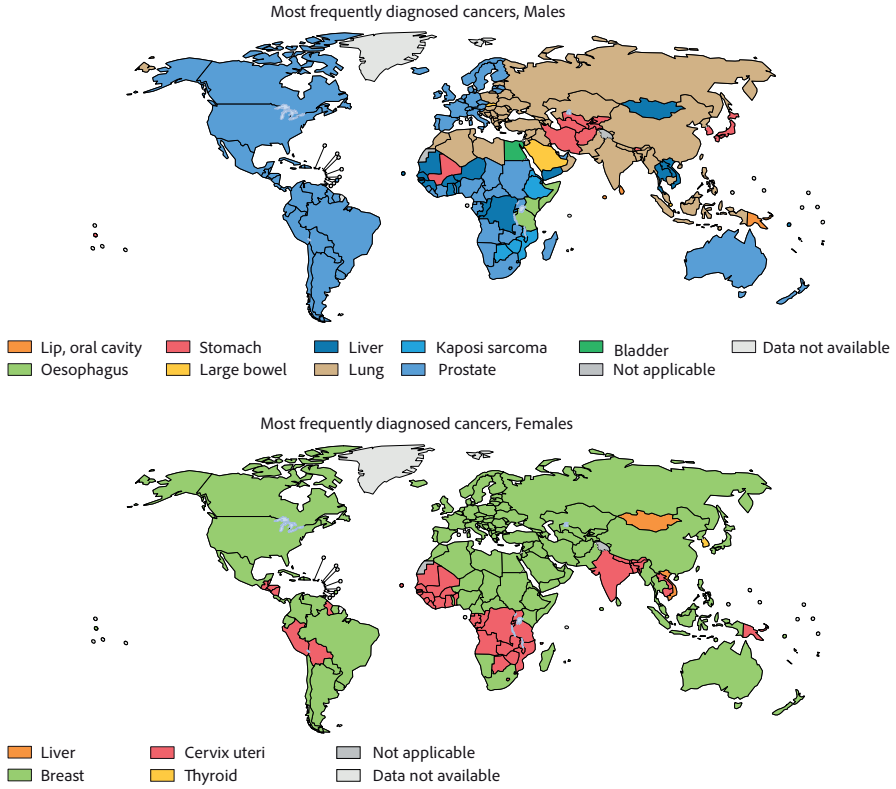

Figura 4.
Tipos de cáncer más diagnosticados, clasificados por sexo y país, en 2008 [6].

Al drama humano que supone el cáncer, hay que añadir los costes sanitarios directos y los costes económicos indirectos derivados del mismo. En 2010, los National Institutes of Health de Estados Unidos estimaban que, solo en ese país, el coste total atribuible al cáncer fue de 263.800 millones de dólares: 102.800 millones por costes médicos directos (total por todo el gasto sanitario); 20.900 millones de dólares por costes indirectos de morbilidad (pérdida de productividad debida a enfermedad); y 140.100 millones por costes indirectos de mortalidad (productividad perdida por muerte prematura) [12].

1.3. Quimioterapia del cáncer

1.3.1. Introducción

El proceso patológico del cáncer es tan complejo y cambiante a lo largo de la evolución de la enfermedad en un paciente, que hace necesario que su tratamiento sea objeto de un abordaje interdisciplinar por parte de equipos de profesionales especializados en diferentes áreas de la medicina. Las principales modalidades del tratamiento son la cirugía, la radioterapia y la quimioterapia, aunque el diagnóstico por imagen, la enfermería y la psicología resultan igualmente indispensables en la correcta atención a los pacientes [13].

En el caso de los tumores sólidos, habitualmente se recurre a la extirpación quirúrgica seguida de radioterapia y quimioterapia como técnicas adyuvantes. En tumores ubicados en zonas que desempeñan funciones vitales, como el cerebro y la médula espinal, suele preferirse la radioterapia. Por último, en cánceres diseminados como la leucemia, la quimioterapia directa suele ser el recurso de elección.

En la quimioterapia, se usan fármacos citotóxicos o citostáticos para provocar la muerte o detener la proliferación, respectivamente, de las células malignizadas. Generalmente, la especificidad de este tipo de fármacos sólo consiste en su mayor efecto sobre células en rápida proliferación. Eso provoca muchos de sus efectos adversos y, por lo tanto, son comunes los efectos indeseables sobre médula ósea (neutropenia, anemia, trombocitopenia), folículo piloso (alopecia), y células de las mucosas gastrointestina-

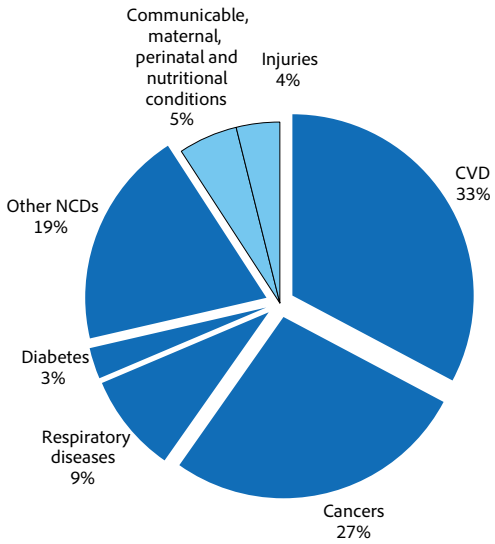

Figura 5.
Mortalidad proporcional en España, en porcentaje sobre el total de muertes, para ambos sexos y todas las edades, 2010 [11].

les (diarrea y aftas). A ellos se suman frecuentemente otros sobre sistema nervioso e hígado [13]. En la actualidad se dispone de unos 30 fármacos citotóxicos que se emplean rutinariamente en la práctica clínica de la quimioterapia anticancerosa. Gracias a la quimioterapia, han mejorado considerablemente las expectativas de supervivencia en cánceres de mama, colon, testículo, ovario, sarcoma, y varios tumores hematológicos [13]. Algunos de los quimioterápicos más frecuentemente utilizados pueden verse en la Figura 6.

1.3.2. Compuestos formadores de aductos con el ADN

Estos fármacos son capaces de formar enlaces covalentes con las bases del ADN. Suelen administrarse como profármacos y requieren una activación metabólica previa para transformarse en citotóxicos. Los compuestos monofuncionales distorsionan la doble hélice de ADN e interfieren con la acción de las polimerasas. Los bifuncionales, pueden producir crosslinking o entrecruzamiento entre bases de la misma o distintas cadenas de ADN, impidiendo también el funcionamiento de las enzimas que actúan sobre el material genético.

Dentro de este grupo de encuentran los agentes alquilantes, como la ciclofosfamida o las nitrosoureas; los derivados del platino (cisplatino, carboplatino y oxaliplatino) y la mitomicina C.

1.3.3. Antimetabolitos

Son sustancias que, por su analogía estructural con metabolitos celulares imprescindibles para la síntesis de biomoléculas, interfieren con su metabolismo y causan depleción intracelular de los mismos. Algunos de los más comunes son el metotrexato (un inhibidor de la dihidrofolato reductasa que impide la síntesis de la timidina), el 5-fluorouracilo (que inhibe la timidilato sintasa tras ser metabolizado a 5-flurodesoxiuridina monofosfato y, además, se incorpora fraudulentamente al ARN), el arabinósido de citosina (citarabina o ara-C, que acaba con la reserva intracelular de desoxicitidina y se comporta como falso nucleótido), o los antimetabolitos de purina (tioguanina, mercaptopurina), que inhiben enzimas implicadas en la síntesis de la guanina.

1.3.4. Derivados de la antraciclina

La doxorubicina y la epirubicina ejercen varios efectos citotóxicos sobre el ADN. Por un lado, se intercalan provocando un desenrollamiento parcial de la doble hélice. También generan radicales libres, y se unen a la topoisomerasa II, provocando roturas en las cadenas de ADN.

1.3.5. Inhibidores de la funcionalidad del huso mitótico

La vinca (*Catharanthus roseus*) es el origen de varios alcaloides naturales (vincristina, vinblastina y vinorelbina) que impiden la polimerización de la tubulina que forma el huso durante la mitosis. Los taxanos (paclitaxel y docetaxel), por el contrario, son inhibidores de la despolimerización, dando lugar a husos aberrantes.

1.3.6. Inhibidores de las topoisomerasas

Las topoisomerasas son enzimas encargadas de disminuir el grado de superenrollamiento del ADN para permitir los procesos de replicación y transcripción. Son de uso clínico tanto los inhibidores de la topoisomerasa I (topotecán, irinotecán) como los de la topoisomerasa II (epipodofilotoxinas, como el etopósido). En los siguientes apartados de este capítulo se puede encontrar una descripción mucho más detallada del funcionamiento de la topoisomerasa I y su inhibición por derivados de la camptotecina y la luotonina A, que constituyen el objeto de la mayor parte del trabajo recogido en esta memoria.

1.3.7. Terapia hormonal

Como se ha explicado anteriormente, en los países con mayores índices de riqueza los cánceres de mama y próstata son los más comunes en mujeres y hombres, respectivamente. En ambos casos, la proliferación celular en estado no patológico está ligada a la presencia de esteroides sexuales, estrógenos en las mujeres y andrógenos en los hombres. Como relativamente pocas células del organismo poseen estos receptores, la quimioterapia basada en esta estrategia posee un buen grado de especificidad. Este objetivo se puede alcanzar bien evitando la síntesis de las hormonas esteroideas, o bien, bloqueando sus receptores en las células tumorales. La administración de LHRH (*luteinising hormone releasing hormone* u hormona liberadora de hormona luteinizante), de inhibidores de la aromatasa (suicidas como el formestano o reversibles como el anastrozol), o de antagonistas de los receptores como tamoxifeno o flutamida ejercen así sus efectos citostáticos y citotóxicos.

1.3.8. Terapia inmunológica

La inmunoterapia activa consiste en la aministración de vacunas elaboradas con fragmentos microbiológicos o tumorales (de células de melanoma o de *Mycobacterium tuberculosis*, por ejemplo), mientras que la pasiva implica el uso de anticuerpos (rituximab, tocilizumab, ofatumumab) o reticulocitos. También se usan mediadores del sistema inmune como los interferones (IFN-α), las interleucinas (IL-2) o los factores estimulantes de colonias de granulocitos y monocitos (GM-CSF).

1.3.9. Terapia fotodinámica

Las porfirinas portadoras de moléculas de oxígeno pueden absorber luz en la región de 630 nm y convertir el O_2 unido a ellas en oxígeno singlete/radical superóxido $O_2^{\bullet}$. El superóxido tiene una semivida muy corta (<0,04 μs), lo que hace

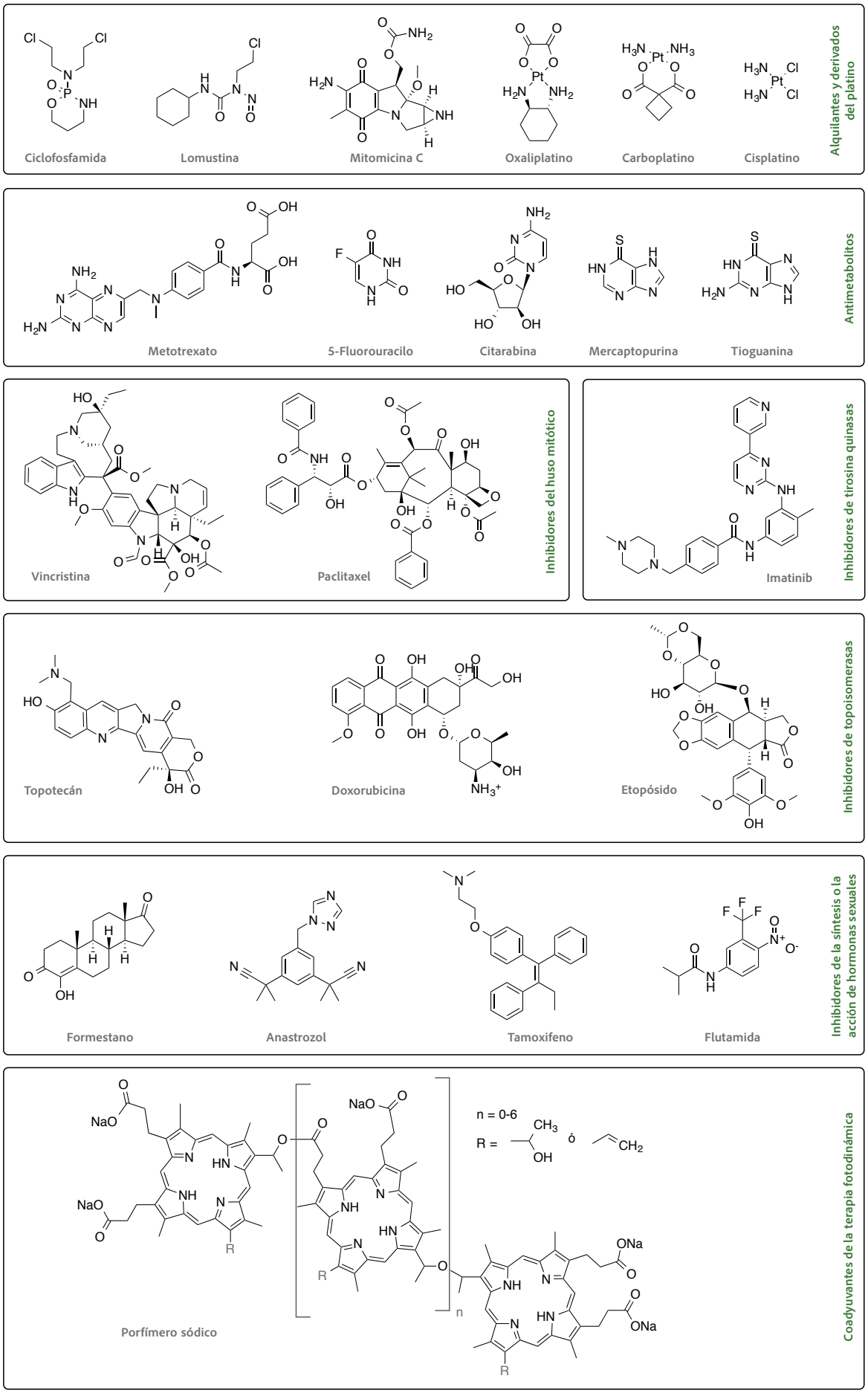

Figura 6. Estructuras químicas de algunos de los agentes quimioterápicos mencionados en el texto

que el alcance de su acción (aproximadamente 0,02 µm desde el lugar de generación), sea muy pequeño en comparación con el tamaño de una célula (unos 10 µm). Por ello, aunque las porfirinas se administren por vía sistémica, su efecto es muy localizado y se limita a la región en la que se aplique la luz. El daño provocado por el radical superóxido activa vías de apoptosis capaces de circunvalar algunos mecanismos de resistencia típicos de células cancerosas. Se suele utilizar una forma polimérica denominada porfímero sódico.

1.3.10. Nuevas formas de tratamiento

El mejor conocimiento de algunos de los mecanismos moleculares implicados en el cáncer está haciendo posible el desarrollo de fármacos más selectivos dirigidos a estas nuevas dianas terapéuticas. Dada su diversidad de acción, pueden a su vez dividirse en varios grupos:

- Inhibidores de tirosina-quinasas: Imatinib, trastuzumab, cetuximab
- Inhibidores de la angiogénesis y la metástasis: bevacizumab, neovastat, vitaxin.
- Silenciadores de genes: pueden silenciarse oncogenes usando siRNAs específicos, como el oblimersen.

2. Inhibición de la topoisomerasa 1 (Top1)

2.1. Biología molecular de Top1

Se dice que una supervuelta es negativa cuando tiende a desenrollar la doble hélice, que por sí misma está enrollada a derechas. Por el contrario, son positivas las supervueltas que tienden a superenrollar más a la doble hélice en el mismo sentido que está enrollada por sí misma [17].

Para que todo el genoma de una célula quepa en su núcleo (o, de manera análoga, en el nucleoide bacteriano), el material genético debe compactarse superenrollándose sobre sí mismo y sobre las histonas [14]. Sin embargo, debido a la naturaleza de doble hélice del ADN, para la mayoría de los procesos que requieren acceder a la información que ésta contiene, ambas cadenas deben separarse ya sea temporalmente (transcripción, recombinación) o permanentemente (replicación) [15]. Al no poder girar libremente, ya sea por su tamaño o por la unión a histonas, la apertura de la doble hélice genera tensión torsional a ambos lados del punto de separación: por delante de la horquilla de replicación o transcripción aparece superenrollamiento positivo (lo que apelmaza el ADN e impide que la separación de las cadenas continúe); y negativo (que tiende a extender el ADN y facilitar la formación de estructuras topológicas anómalas) por detrás de la misma (Figura 7) [16,17].

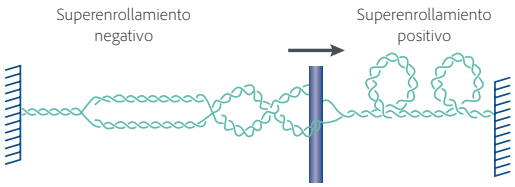

Figura 7.
El problema del superenrollamiento que se acumula por delante y por detrás del punto de avance de la maquinaria de replicación, transcripción o reparación del ADN. Los bloques rallados a ambos lados representan la unión del ADN a las histonas nucleares, que impiden la libre rotación del mismo [16].

Las topoisomerasas son la maquinaria que la naturaleza emplea para resolver el singular problema que supone el superenrollamiento de la doble hélice del ADN. Este inconveniente topológico surge cuando los superenrollamientos deben deshacerse y volverse a generar durante los procesos de replicación, transcripción, recombinación, reparación y remodelación de la cromatina [18].

Las topoisomerasas son proteínas ubicuas presentes en los tres reinos de la vida: eucariotas, arqueobacterias y eubacterias [16]. Recientemente se ha propuesto que el origen de las actuales topoisomerasas podría remontarse a varias subfamilias de enzimas virales que posteriormente se diseminaron de manera independiente a diferentes linajes celulares [19]. Todas las topoisomerasas comparten una tirosina como elemento común en su centro activo. Este aminoácido lleva a cabo un ataque nucleofílico sobre el esqueleto fosfodiéster del ADN, formándose en esta reacción de transesterificación una rotura reversible del ADN, que queda unido covalentemente a la enzima por uno de sus extremos. Esta reacción es altamente reversible, y una vez que las modificaciones topológicas han tenido lugar, una segunda transesterificación inversa de la primera, libera la enzima y restaura la integridad del ADN [20].

Las topoisomerasas se clasifican en dos grandes familias según su mecanismo de acción. Las topoisomerasas tipo II son homodiméricas, cortan las dos hebras del ADN uniéndose covalentemente al extremo 5', requieren ATP y Mg^{2+} para funcionar, y pueden relajar tanto superenrollamiento positivo como negativo [15]. Las topoisomerasas de tipo I sólo cortan una de las dos hebras del ADN, y pueden dividirse en

> *"El genoma de una célula humana contiene unos 3×10^9 pares de bases, lo que corresponde a una longitud de aproximadamente 1,8 m. Todo ese ADN debe compactarse hasta caber en un núcleo con un tamaño medio de 6 µm, o visto de otro modo: la circunferencia de ese núcleo es aproximadamente un millón de veces más pequeña que la longitud del genoma que alberga."*
>
> Y. Pommier, 2010 [14]

Topoisomerasas humanas			kDa	P-Tyr	ΔLk	Mg^{2+},ATP
	Tipo IA	Top3α	112	5'	+1	Mg^{2+}
		Top3β	97	5'	+1	Mg^{2+}
	Tipo IB	Top1	100	3'	±1	No
		Top1mt	70	3'	±1	No
	Tipo IIA	Top2α	170 (x2)	5'	±2	Ambos
		Top2β	180 (x2)	5'	±2	Ambos

Figura 8.
Esquema mostrando la clasificación de las topoisomerasas humanas, así como las características distintitvas de cada grupo.

dos subfamilias: las Top1A y las Top1B. Las del tipo A sólo pueden relajar superenrollamiento negativo, se unen covalentemente a la hebra escindible por el extremo 5' de la misma y requieren Mg^{2+} aunque no ATP. Las de tipo B, por el contrario, no dependen de cofactores, pueden relajar ambos tipos de superenrollamiento y se unen a la hebra cortada por el extremo 3' de la misma [14,21].

El genoma humano contiene seis genes de topoisomerasa que codifican otras tantas enzimas (Figura 8): dos de tipo IB, (TOP1 y TOP1MT o mitocondrial), dos IA (TOP3α y TOP3β), y dos IIA (TOP2α y TOP2β) [22]. Los inhibidores de topoisomerasas tienen una gran relevancia farmacológica, ya que se emplean extensamente como antibióticos y antitumorales. Las quinolonas antibacterianas (ácido nalidíxico, ciprofloxacino o levofloxacino entre otras) inhiben las topoisomerasas bacterianas de tipo IIA sin afectar a las humanas. Los inhibidores de topoisomerasas con actividad antitumoral actúan selectivamente sobre las enzimas tipo II humanas (doxorubicinas, etopósido) o las de tipo I (irinotecán, topotecán). Debido a que la topoisomerasa humana de tipo IB (la topoisomerasa 1 o Top1) es la diana farmacológica de las moléculas objeto de esta memoria, en adelante nos centraremos en sus características.

La Top1 no guarda homología estructural con el resto de topoisomerasas, y puede relajar por completo tanto superenrollamiento positivo como negativo. Tiene un peso molecular de 100 kDa, está constituida por 765 aminoácidos y tiene cuatro dominios diferenciados (Figura 9): el N-terminal (1-214), el principal o *core* (215-635), el de unión o *linker* (636-712) y el C-terminal (713-765) [23].

El dominio N-terminal contiene cuatro secuencias de localización nuclear que interaccionan con proteínas del núcleo, así como otras responsables de interacción con el ADN, tanto en su unión, como en el control del proceso de rotación. El *core* contiene todos los residuos del centro activo a excepción de la tirosina catalítica, y se encuentra dividido en tres subdominios I, II y III. La secuencia del *linker* está poco conservada, y este dominio es prescindible para la actividad de la enzima. Aunque sus posibles funciones son todavía poco conocidas, parece estar implicado en el control de la velocidad de rotación durante el desenrollamiento [24] y mejora la sensibilidad a camptotecina. Por último, en la región C-terminal se encuentra la Tyr723 que hace posibles las reacciones de transesterificación [15,25].

Se denominan topoisómeros a cada uno de los distintos niveles de superenrollamiento que puede presentar una misma molécula de ADN.

La enzima se cierra como una pinza sobre la doble hélice de ADN, atrapándola entre los subdominios I y II del *core* (que forman lo que en la bibliografía se denomina "la tapa") y el subdominio III en la parte inferior. Ambas partes se encuentran conectadas por una corta región flexible que actúa como bisagra [25]. Tanto la región del dominio que está más próxima al DNA como el hueco central de la enzima, poseen un potencial electrostático positivo que les permite establecer numerosas interacciones con los grupos fosfato de la doble hélice cargados negativamente. Sólo las bases (-1) y (+2) establecen contactos directos con la enzima a

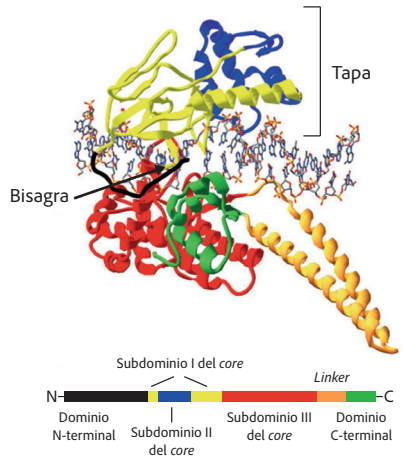

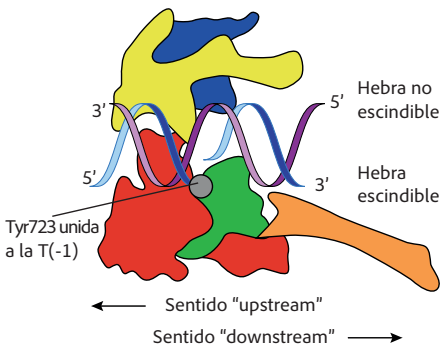

Figura 9.
Topoisomerasa 1 humana. Izquierda: principales elementos estructurales y localización de los dominios en el gen que la codifica. Derecha: orientación durante la acción catalítica de la enzima.

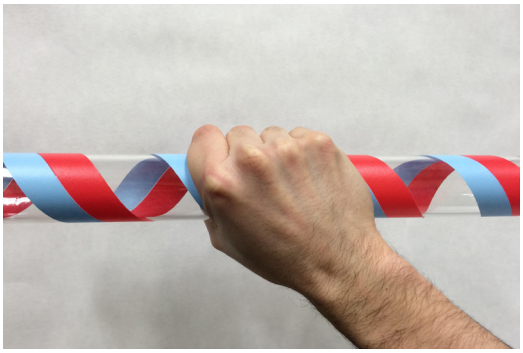

Figura 10.
La topoisomerasa 1 se cierra sobre la doble cadena de ADN de manera muy similar a como lo hace una mano al asir un objeto cilíndrico.

través de la Lys532 y la Arg364 por el lado del surco menor [26].

La Top1 tiene preferencia por las regiones de ADN con superenrollamientos o curvaturas, al parecer, debido a una secuencia de aminoácidos de la región *linker* que es capaz de interaccionar con distintos puntos del ADN cuando la hélice se encuentra en este estado [27] y a su capacidad de reconocer curvaturas tridimensionales [28]. A diferencia de otras enzimas, la Top1 no reconoce secuencias concretas en el ADN. Sin embargo, en presencia de camptotecina, muestra una mayor afinidad por los motivos 5'-[A/T][G/C][A/T]T(-1)↓G(+1)-3' en las bases (-4) a (+1) de la hebra escindible (nótese la importancia de la T en posición (-1), que sólo ocasionalmente puede ser sustituida por una C) [29-33]. También se ha sugerido que la base en posición (-2) de la hebra no escindible podría ser relevante [32]. En el centro activo de la enzima existe una péntada de aminoácidos cuya distribución espacial está muy conservada entre todas las topoisomerasas IB, formada por Arg488, Lys532, Arg590, [His632/Asn] (en el dominio *core*) y Tyr723 (en el dominio C-terminal) [34]. Los cuatro aminoácidos situados en el *core* sirven para anclar el ADN por el nucleótido en el que se va a producir el corte: la Lys532 se une al átomo O-2 de la timidina en posición (-1) y las argininas y la His632 forman interacciones electrostáticas con el grupo fosfato de la timidina. Por su lado, la Tyr723 es responsable de la transesterificación en sí al formar el enlace DNA-3'-fosfotirosina [26].

Como se ha mencionado anteriormente, la enzima se cierra como una mano sobre el ADN dejando un canal de entre 15 y 20 Å (Figura 10) [23]. Una vez que las dos macromoléculas se han acoplado, el O-4 de la Tyr723 lleva a cabo un ataque nucleofílico sobre el fosfato de la T(-1) pasando por un estado de transición pentacoordinado que estabilizan los aminoácidos del centro activo [35]. El extremo 3' de la hebra escindible queda de este modo unido covalentemente a la enzima, mientras que el extremo 5' se libera y puede rotar sin necesidad de más energía que la del propio superenrollamiento presente en el ADN y, por lo tanto, de manera ATP-independiente (Figura 11) [18].

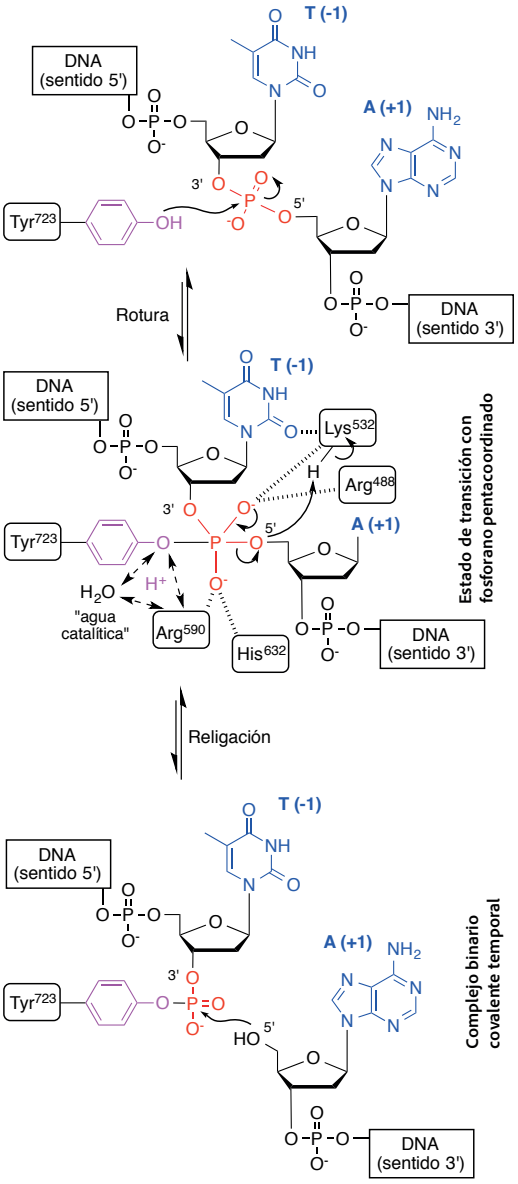

Figura 11.
Ciclo catalítico de la Top1 [20,26].

Debido a su naturaleza, el proceso de giro se denomina "rotación controlada" (Figura 12) [15,36]. Tras los primeros estudios sobre el mecanismo de la topoisomerasa 1, se pensó que el mecanismo de desenrollamiento era posible por medio del giro libre de la parte "downstream" de la hebra escindida. Sin embargo, estudios posteriores han revelado que este giro en realidad no es totalmente libre, sino que se encuentra parcialmente frenado (de ahí el término de "rotación controlada") por la fricción entre el DNA y los aminoácidos del canal de la enzima. El número de vueltas en que la enzima puede reducir el superenrollamiento en cada ciclo catalítico es proporcional al torque (y, por lo tanto, al nivel de superenrollamiento inicial) de la hebra de ADN [37,38].

Durante cada giro, es necesario que tengan lugar alteraciones conformacionales en la enzima (principalmente la apertura parcial del

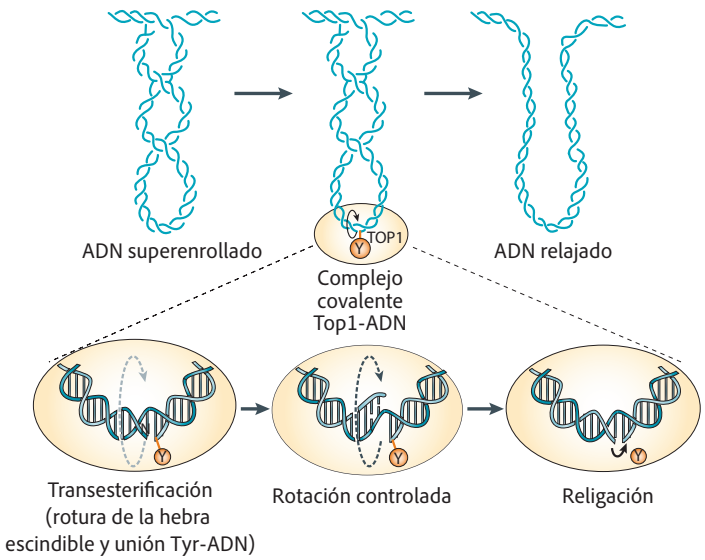

Figura 12.
Esquema resumen de la acción de la Top1 sobre el ADN superenrollado [36].

canal) para acomodar la doble hélice durante la rotación. Este hecho da lugar a un perfil energético en forma de sierra [38]. Existe un punto de cada vuelta de la doble hélice en el que el extremo 5' de la hebra escindible vuelve a alinearse con extremo 3' cortado, y en ese momento existe una probabilidad de que se produzca la segunda transesterificación que restaura la integridad de la hebra, y libera la enzima [37,38]. Una enzima puede llevar a cabo este ciclo de apertura, rotación y religación a una velocidad de hasta 6000 veces por minuto [16].

2.2. Quimioterapia basada en la inhibición de Top1: derivados de la camptotecina.

En los años 50, el Dr. Jonathan Hartwell del NCI (National Cancer Institute) comenzó un programa de cribado de compuestos en busca de actividad antitumoral [39]. Hartwell se interesó por incluir en el proyecto los extractos vegetales de un investigador del U. S. Department of Agriculture, el Dr. Monroe E. Wall, que hasta entonces trabajaba en fitosteroides útiles como precursores de cortisona.

Inicialmente se ensayaron más de mil extractos, y entre ellos destacó el de la corteza del árbol asiático *Camptotheca acuminata* por mostrar una potente actividad *in vivo* frente a modelos de adenocarcinoma murino. En 1958, el grupo de Wall (que en 1960 se había trasladado al Research Triangle Institute para centrar su ámbito investigación en los antitumorales) identificó la camptotecina (Figura 13) como un nuevo alcaloide responsable de su actividad, y en 1966 describió su estructura mediante difracción de rayos X con la ayuda de Mansukh C. Wani [40]. Este grupo fue también responsable en ese mismo período del descubrimiento de otro de los antitumorales de origen natural más importantes en la actualidad: el taxol.

En vista de la prometedora acción antitumoral de la camptotecina, se iniciaron ensayos clínicos para estudiar su efectividad. Con el propósito de mejorar su limitada solubilidad, se administró la sal sódica obtenida por hidrólisis básica del anillo de lactona (Figura 13).

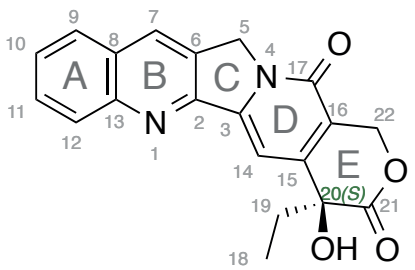

$C_{20}H_{16}N_2O_4$	348,36 g/mol
CAS	7689-03-4
PubChem	CID 2538
DrugBank	DB04690
ChemSpider	22775
UNII	XT3Z54Z28A
KEGG	C01897
ChEBI	CHEBI:27656
ChEMBL	CHEMBL65
Sigma-Aldrich	C9911

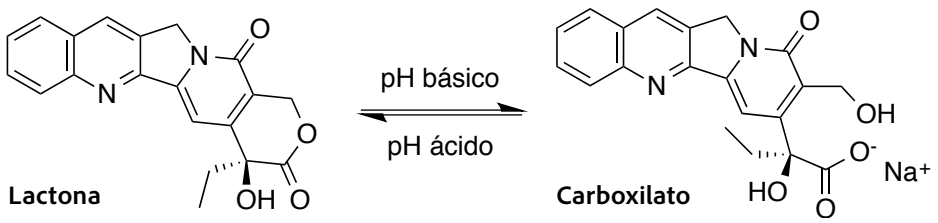

Figura 13.
Estructura química de la camptotecina, y equilibrio establecido entre las formas abierta y cerrada de la δ-lactona presente en el anillo E.

> *Los alcaloides son un grupo diverso de moléculas de bajo peso molecular que contienen nitrógeno en su estructura y están presentes en aproximadamente un 20% de las especies de plantas. Su papel suele ser el de protegerlas de herbívoros, virus, bacterias o plantas competidoras. Los alcaloides de origen natural se han empleado a lo largo de la historia de la humanidad con fines tan diversos como la caza, las ejecuciones, el armamento bélico o el tratamiento de enfermedades.*

Sorprendentemente, los resultados de estos ensayos mostraron una pobre actividad antitumoral clínica y unos marcados efectos adversos, entre los que destacaban la mielosupresión y la cistitis hemorrágica [41-43]. Debido a que para obtener algún beneficio terapéutico era necesario administrar dosis elevadas con efectos adversos erráticos e imprevisibles, el desarrollo clínico de la camptotecina fue abandonado a principios de los 70. Sólo investigaciones llevadas a cabo años después desvelaron el porqué de estos hechos. Por un lado, la forma carboxilato presenta una actividad inhibitoria de la Top1 muy limitada en comparación con la forma cerrada de la camptotecina [44] y, además, tiene una elevada afinidad por el dominio II de la albúmina sérica humana [45-47]. Por otro lado, la forma carboxilato se excreta por vía renal, y el pH ácido de la orina causa el cierre del anillo a la forma lactona mucho más activa, desencadenando la grave toxicidad observada sobre el epitelio vesical [48].

No fue hasta la década de los años 80 cuando el interés por la camptotecina volvió a despertarse tras descubrir que su diana farmacológica era la Top1 [49,50], iniciándose el desarrollo de análogos con farmacocinética y estabilidad mejoradas que llevó al uso clínico del topotecán y el irinotecán [51].

La Figura 14 recoge las estructuras de los análogos de camptotecina actualmente en uso y en diferentes etapas del desarrollo clínico.

La camptotecina es un alcaloide indol-monoterpenoide modificado, aislado originalmente de la corteza de *Camptotheca acuminata* (familia *Nyssaceae*), un árbol de hoja caduca de hasta 20 m de altura que crece silvestre en el sur de China y el Tíbet [52]. Este árbol ha sido ampliamente utilizado en la medicina tradicional china (MTC) para combatir los tumores y la inflamación [53]. En MTC, el árbol es conocido como "árbol feliz" o "árbol del cáncer", y se denomina *xi shu* (chino simplificado, 喜树). Sin embargo, la camptotecina se ha llegado a encontrar en hasta nueve especies de diferentes órdenes filogenéticos [54]. En *C. acuminata*, la mayor concentración se encuentra en las hojas jóvenes (lo que confirma su papel defensivo en la planta), seguido de las semillas y la corteza [54].

Las rutas sintéticas de los alcaloides indol-monoterpenoides provienen del triptófano y el geraniol, que confluyen biosintéticamente en la estrictosidina. Esta familia de alcaloides comprende, entre otros, la ibogaína, la reserpina, la yohimbina, la vincristina, la elipticina y la quinina. Actualmente, el suministro de camptotecina para la industria farmacéutica depende de extractos de *C. acuminata* y *Nothapodytes foetida*. Varios grupos trabajan en el desarrollo de otros métodos de obtención del alcaloide, como cultivos *in vitro* de raíces de *C. acuminata* y *Ophiorrhiza pumila* transformadas con *Agrobacterium rhizogenes* (Figura 15), o el empleo de enzimas de la ruta biosintética del alcaloide para su producción a gran escala [55].

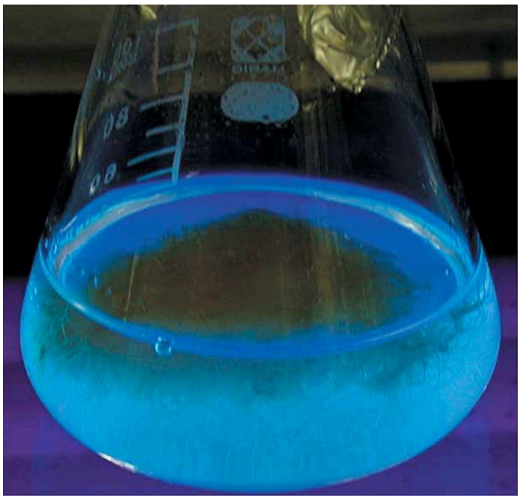

Figura 15.
Excreción de camptotecina al medio de cultivo por raíces transformadas de *Ophiorrhiza pumila*. Se observa la fluorescencia de la camptotecina al iluminarla con luz ultravioleta [55].

Un hecho particularmente interesante es que las plantas que producen camptotecina presentan mutaciones puntuales en sus Top1 que las hacen resistentes al efecto del alcaloide [56]. En concreto, se han identificado tres mutaciones habituales en *C. acuminata*, *O. pumila* y *Ophiorrhiza liukiuensis*: Asn421Lys, Leu530Ile y Asn722Ser (según la numeración de los aminoácidos en la enzima humana). Curiosamente, la mutación en la posición 722 es idéntica a la encontrada en tumores humanos resistentes a camptotecina.

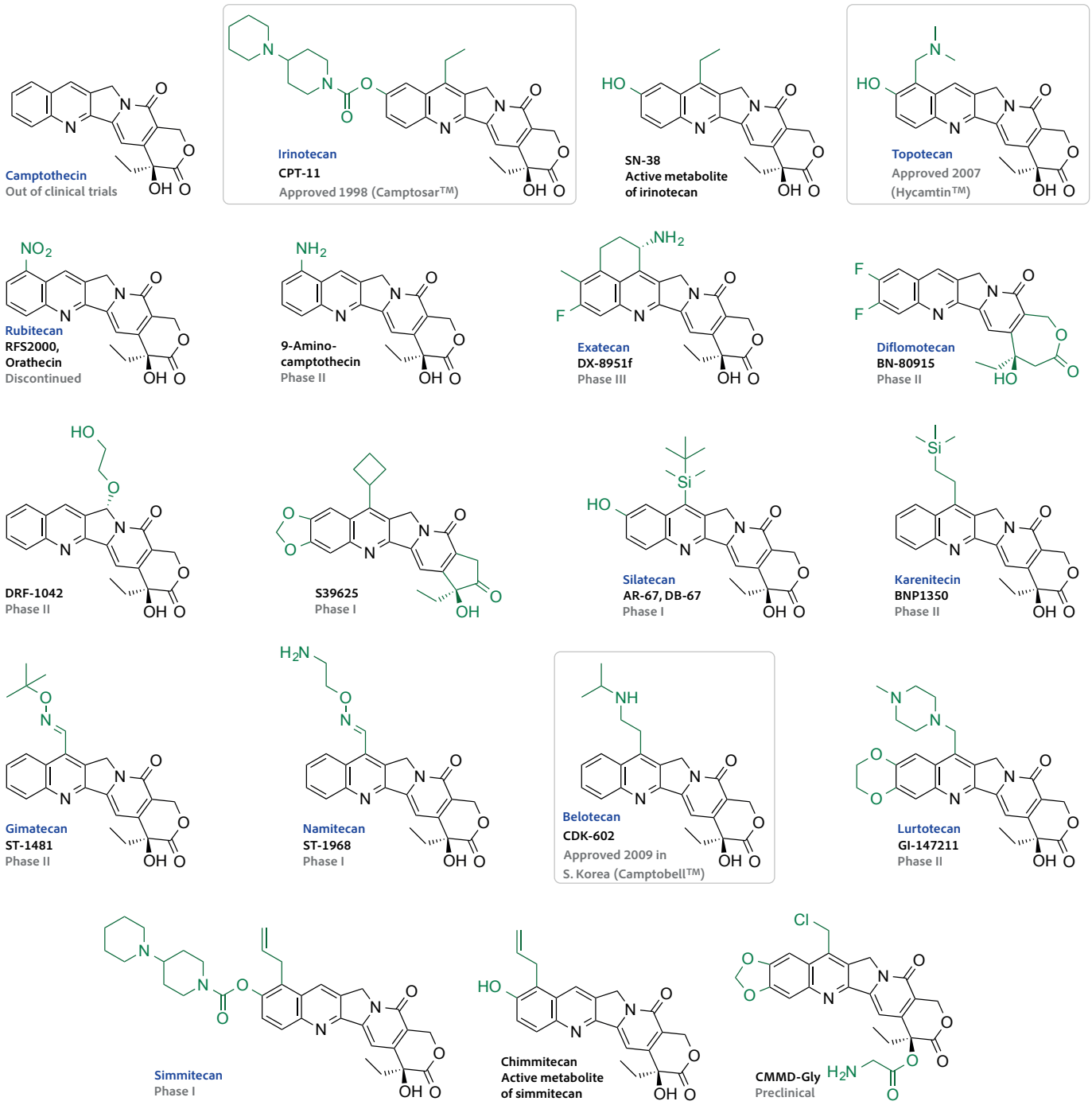

Figura 14A.
Estructuras químicas de derivados de la camptotecina en diferentes etapas de desarrollo clínico. Se muestran enmarcadas las de los tres análogos actualmente aprobados: irinotecán (un profármaco de la molécula activa, SN-38), topotecán y belotecán (aprobado sólo en Corea del Sur). La información recogida en esta figura es un compendio de:
-Vincent J. Venditto and Eric E. Simanek, Cancer Therapies Utilizing the Camptothecins: A Review of the in Vivo Literature, Mol. Pharmaceutics, 2010, 7 (2), 307–349, DOI: 10.1021/mp900243b
-Zhe-yi Hu, Xiu-xue Li, Fei-fei Du, Jun-ling Yang, Wei Niu, Fang Xu, Feng-qing Wang, Chuan Li and Yan Sun, Pharmacokinetic evaluation of the anticancer prodrug simmitecan in different experimental animals, Acta Pharmacologica Sinica, 2013, 34, 1437-1448 , DOI:10.1038/aps.2013.74
-Qingqing Huang, Lei Wang and Wei Lu, Evolution in medicinal chemistry of E-ring-modified Camptothecin analogs as anticancer agents, European Journal of Medicinal Chemistry, 2013, 63, 746–757, DOI: 10.1016/j.ejmech.2013.01.058

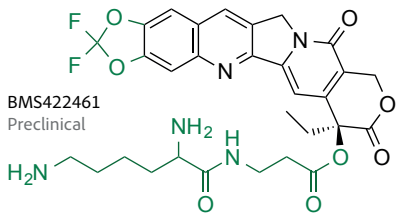

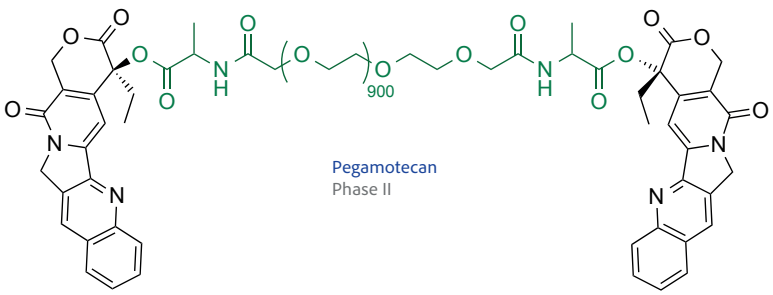

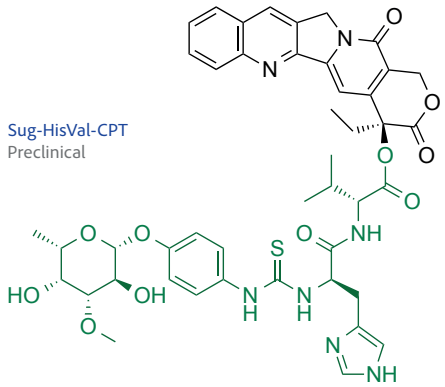

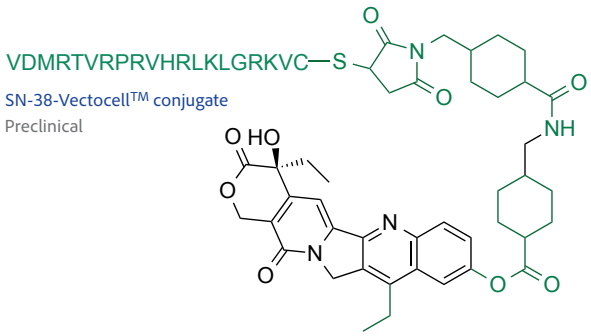

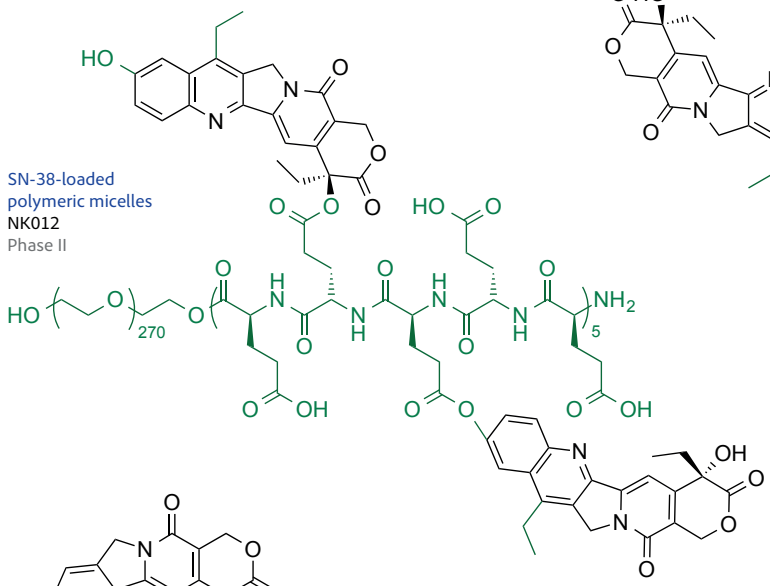

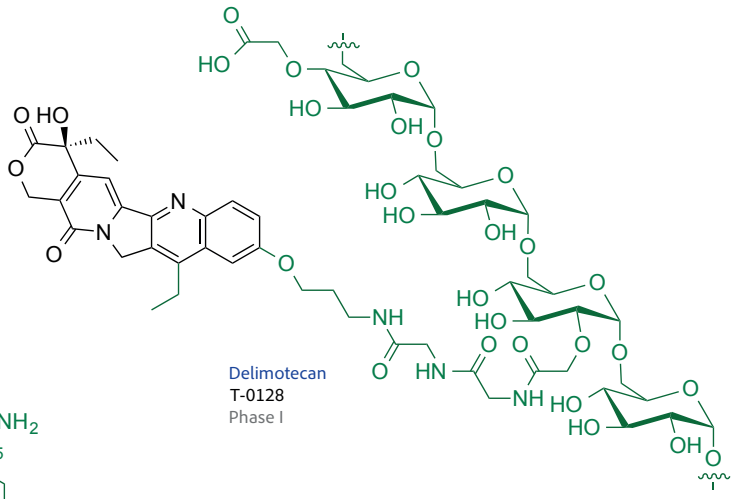

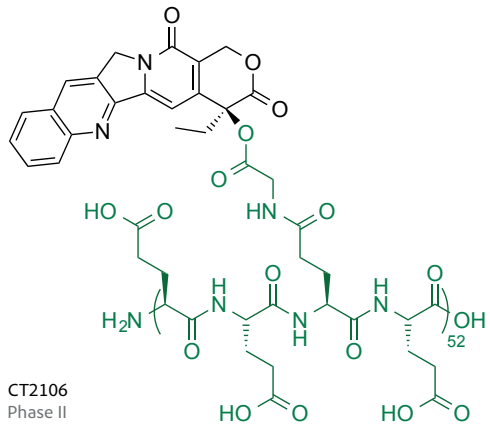

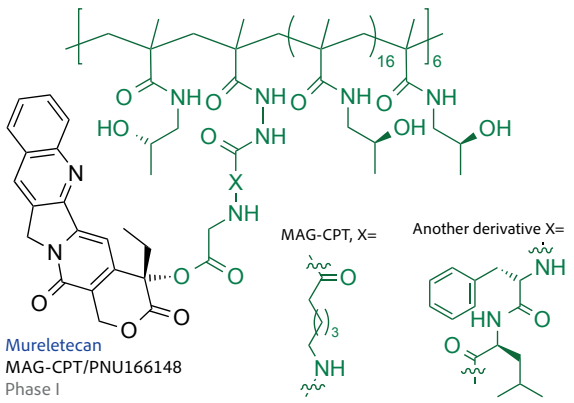

Figura 14B. (Esta página y la opuesta)
Estructuras químicas de derivados de la camptotecina en diferentes etapas de desarrollo clínico. La conjugación con polipéptidos y oligosacáridos es un recurso que está resultando de gran ayuda para mejorar la biodisponibilidad y penetración celular de estos fármacos.

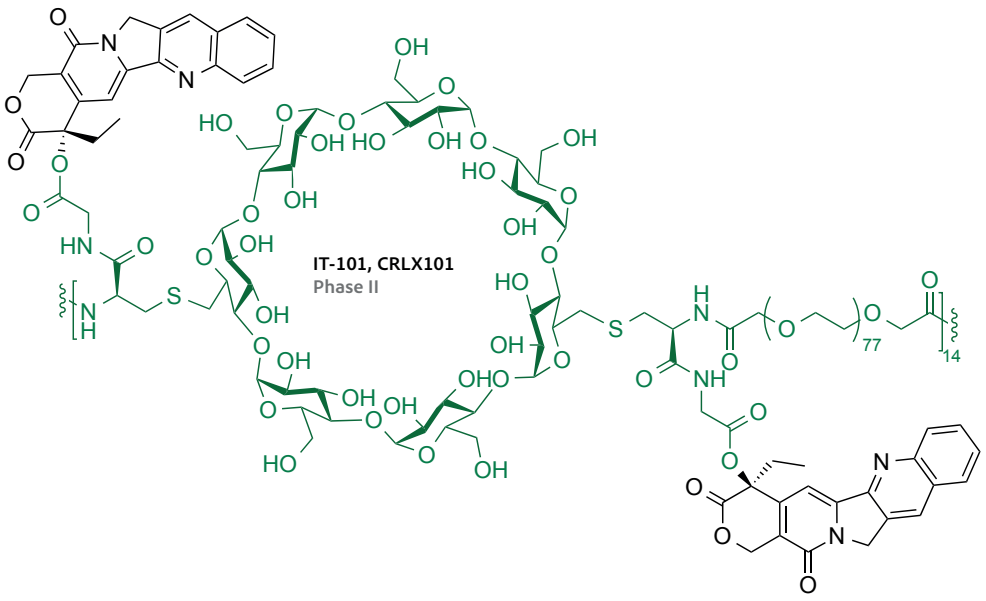
IT-101, CRLX101
Phase II

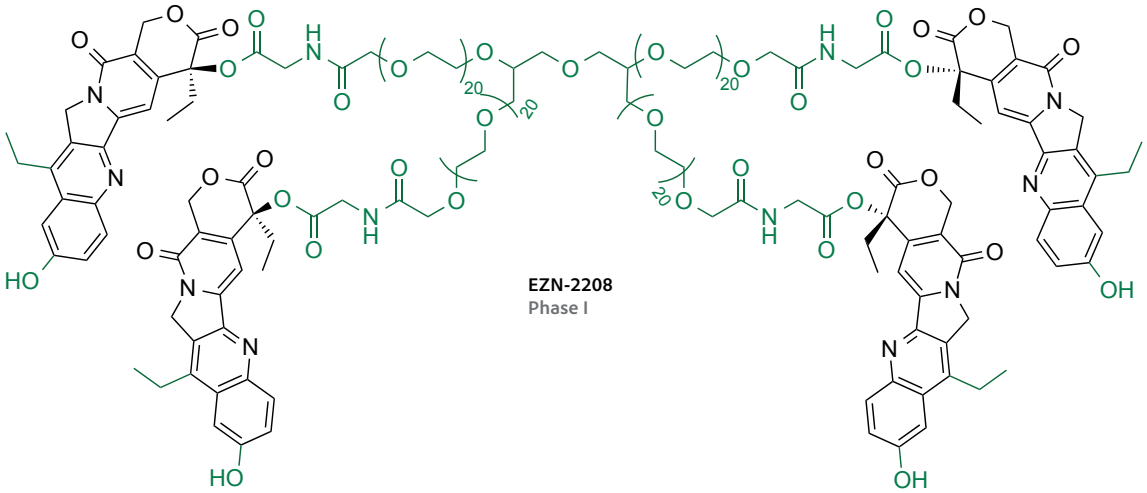
EZN-2208
Phase I

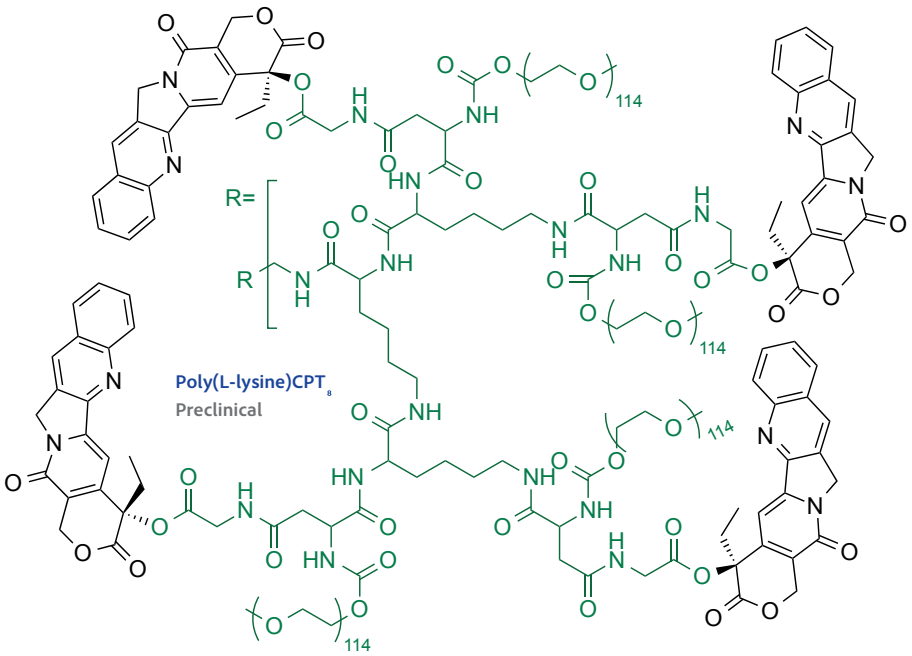
R=
Poly(L-lysine)CPT8
Preclinical

Figura 16.
Estructura química de la luotonina A.

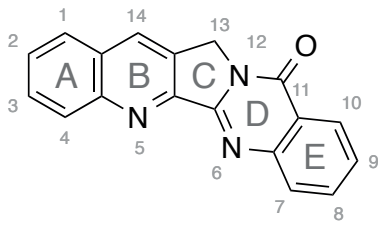

$C_{18}H_{11}N_3O$	285,31 g/mol
CAS number	205989-12-4
PubChem	CID 10334120
ChemSpider	8509579
ChEBI	CHEBI:121720
ChEMBL	CHEMBL19163
Sigma-Aldrich	L4045

2.3. Luotonina A y derivados.

En 1997 se describieron el aislamiento y la caracterización de la luotonina A (Figura 16), a partir de los extractos (fracciones *n*-hexano, benceno y cloroformo) de *Peganum nigellastrum* Bunge (*Zygophyllaceae*) [57]. Esta hierba perenne, de 10 a 25 cm de alto, se encuentra extendida por el centro y el norte de China, Mongolia y áreas meridionales de Rusia [58]. *P. nigellastrum* (骆驼蒿, *luo tuo hao* en chino simplificado) ha sido utilizada en MTC para tratar afecciones reumáticas, abscesos e inflamaciones.

La luotonina A fue el primer alcaloide pirroloquinazolinoquinolínico descrito en la literatura científica. Los alcaloides de quinazolina, incluyendo las vasicina, tienen al ácido antranílico como un paso clave en su biosíntesis. La luotonina A coexiste en la planta con otros alcaloides quinazolínicos y tiene una vasicinona en su estructura, por lo que se ha propuesto que su biosíntesis implique la condensación de vasicinona y ácido antranílico [57].

La CI_{50} (concentración inhibitoria 50) es la concentración de un fármaco que causa la inhibición del crecimiento del 50% de las células en estudio.

En el mismo artículo en el que por primera vez se describía su aislamiento y estructura, se demostró también su actividad citotóxica sobre cultivos de leucemia murina P-388 [57]. A pesar de su evidente similitud estructural con la camptotecina, hubo que esperar seis años hasta que el grupo de Hecht obtuvo pruebas concluyentes de que ambas moléculas compartían la inhibición de Top1 como mecanismo de acción de su citotoxicidad [59]. Las CI_{50} obtenidas en el caso de la luotonina A eran unas diez veces superiores a las de la camptotecina. Sin embargo, estos resultados contradecían un hecho que, hasta entonces, se había aceptado como irrefutable: la lactona del anillo E de la camptotecina aumentaba la potencia del alcaloide, pero no era indispensable para su actividad. El hallazgo de este nuevo farmacóforo abrió la puerta para superar el cuello de botella que suponía obtener análogos de camptotecina sustituidos en el anillo E, ya que los derivados de la luotonina A modificados en este anillo presentaban mejor accesibilidad sintética.

Desde entonces, se han desarrollado varias rutas sintéticas para acceder a derivados de luotonina A modificados en distintas posiciones. El efecto de estas sustituciones sobre la actividad antitumoral se detalla a continuación, y han sido revisados por Ma [60] y más recientemente por Liang [61].

2.4. Mecanismo de acción de la camptotecina y la luotonina A: el paradigma de la inhibición interfacial

2.4.1. Modelos de interacción en el complejo ternario camptotecina-ADN-Top1

A mediados de la década de los 80 se descubrió que la toxicidad de la camptotecina estaba mediada por la inhibición de la Top1, y que en presencia del alcaloide era posible aislar productos de ADN que presentaban una rotura en una de sus hebras y se encontraban unidos covalentemente a la enzima [49,50].

Como se ha comentado anteriormente, la afinidad que determina la unión de las topoisomerasas al ADN pasa más por el reconocimiento del estado topológico de superenrollamiento del mismo que por el reconocimiento de secuencias de nucleótidos concretas. Lo que sí se observó es que los puntos por los que el ADN aparecía fragmentado y unido covalentemente a la Top1 en presencia de camptotecina sí presentaban una secuencia consenso de nucleótidos [29]. Poco después, se puso de manifiesto que la maquinaria replicativa celular también jugaba un papel en la toxicidad de la camptotecina [62,63]. Todo ello sugería que la topoisomerasa no era afectada por la camptotecina de una manera habitual (como la inhibición competitiva o la alostérica) sino que el ADN y sus procesos tenían una relevancia clave en la actividad.

En 1989, Champoux propuso de manera formal el mecanismo de acción in vivo de la camptotecina, cuyos detalles se han ido conociendo con posterioridad [64]. Según este modelo, la camptotecina es capaz de unirse exclusivamente, de manera no covalente y altamente específica, al complejo covalente formado entre el ADN y la Top1 cuando ésta está ejerciendo su actividad catalítica. Es decir, una vez que la Top1 se ha acoplado al ADN y la Tyr723 se encuentra unida covalentemente a la T(-1), es cuando se forma el sitio de unión de la camptotecina. Al situarse en él, el alcaloide debía estabilizar de algún modo el complejo covalente, dificultando la última parte de la reacción en la que el ADN se religaba y la enzima era liberada. Esto explicaría por qué en presencia de camptotecina podían aislarse los complejos covalentes ADN-Top1, pero si el alcaloide se retiraba, la enzima seguía siendo activa. Estos resultados fueron comple-

mentados poco tiempo después por el grupo de Pommier [30].

En los complejos binarios ADN-Top1 se observó que el nucleótido (-1) con respecto al punto de corte era siempre una T. Esta observación se repetía tanto en ausencia como en presencia de camptotecina. Sin embargo, el caso de la posición (+1) era diferente: el nucleótido que aparecía con más frecuencia era la G, pero sólo en presencia de camptotecina. En ausencia del alcaloide, cualquiera de los cuatro nucleótidos se encontraba con igual probabilidad [65]. Ello indicaba que la unión de la camptotecina estaba de algún modo favorecida por la G(+1), lo que apuntaba a una interacción entre ambas. También resultaba evidente que la camptotecina interaccionaba con el centro activo de la enzima además del ADN, ya que mutaciones puntuales en la asparagina contigua a la Tyr723 del centro activo conferían a las células tumorales resistencia al alcaloide [66].

En 1998, el grupo de Pommier publicó los resultados de un trabajo de modelado molecular [67] en el que se sugería una estructura para el complejo ternario ADN-Top1-camptotecina. En él, la camptotecina se situaba entre los pares de bases (-1) y (+1) y paralela a ellos, con la parte cóncava de la molécula orientada hacia el surco mayor del ADN, y el anillo E hacia la hebra escindible. En este modelo, la camptotecina interaccionaba por apilamiento π-π con los pares de bases, y por puentes de hidrógeno con los aminoácidos del centro activo y el ADN: el carbonilo del anillo D con un hidroxilo de la ribosa de T(-1), el OH 20 de la lactona con el oxígeno de la cadena lateral de la Asn722 y el carbonilo del anillo E con el enlace amida de la Asn722.

> *A lo largo del tiempo, se han ido sumando evidencias de que la diana farmacológica de la camptotecina es la Top1, entre las que merece la pena destacar las siguientes[62]:*
> - *La camptotecina natural inhibe* in vitro *la acción de la Top1 aislada.*
> - *La camptotecina no es tóxica frente a levaduras mutadas para silenciar la expresión de Top1.*
> - *Las líneas celulares seleccionadas por su resistencia a camptotecina presentan mutaciones puntuales en los genes que codifican la Top1.*
> - *Las plantas que producen camptotecina de forma natural presentan una mutación puntual en sus Top1.*

La primera evidencia experimental de la estructura de los complejos ADN-Top1 y ADN-Top1-camptotecina fue publicada en 1998 por el grupo de Champoux y Hol con dos artículos publicados en Science que mostraban su estructura elucidada por medio de difracción de rayos X [23,26] (Figura 17). En ellos se hace un extensivo análisis sobre la estructura de la proteína (no se trataba de la proteína nativa, sino de los dominios *core* y C-terminal reconstituidos),

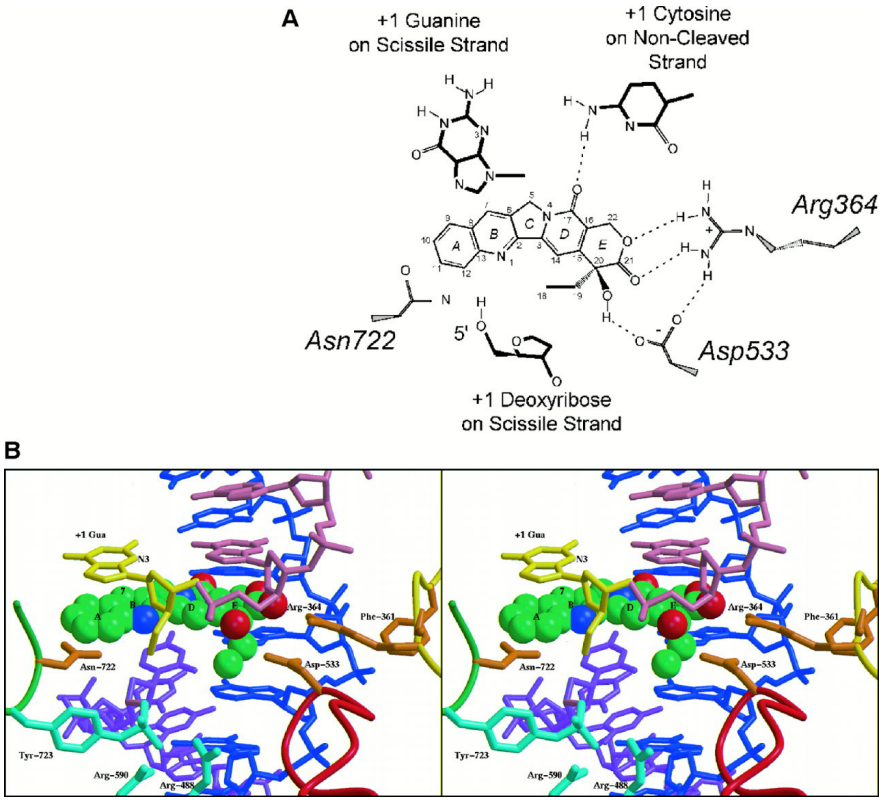

Figura 17.
(A) Esquema de los enlaces de hidrógeno y apilamientos entre el complejo Top1-DNA y la camptotecina.
(B) Vista estereográfica del modo de unión propuesto. La camptotecina (verde) se apila entre la G(+1) (amarillo) y la cadena lateral de la Asn722 (naranja). La hebra escindible se muestra en magenta claro y oscuro, en sentidos "upstream" y "downstream" respectivamente [23].

y se establecen las interacciones clave observadas entre la proteína, el ADN y el fármaco. La proteína contacta a través del canal central con los pares de bases (-4) a (+6) del ADN , estableciendo con ellos enlaces de hidrógeno e interacciones electrostáticas a través de los grupos fosfato. También hay interacciones electrostáticas entre el dominio *linker* y los fosfatos del ADN. Hay un único enlace de hidrógeno específico entre la Lys532 y el oxígeno carbonílico (O-2) de la T(-1) en la hebra escindible, lo que explica la preferencia por esta base en dicha posición. El fosfato de la T(-1) forma enlaces de hidrógeno con la Arg488 y la Arg590. En estos trabajos se propone una hipótesis para la unión de la camptotecina al complejo binario ADN-Top1 que difiere del de apilamiento de Pommier. En primer lugar, la molécula de camptotecina se orienta con el lado cóncavo hacia la hebra escindible, y el anillo E hacia el surco menor del ADN. Por otro lado, la G(+1) se desplaza fuera de la doble hélice por rotación del esqueleto fosfodiéster y queda apilada con los anillos A y B de la camptotecina, que también se apilarían con la cadena plana conjugada de la Asn722. El carbonilo del anillo D establecería un enlace de hidrógeno con la C(+1) de la hebra no escindible. La Arg364 interaccionaría con los dos oxígenos de la función lactona del anillo E, y con la Asp533, que a su vez podría formar un enlace de hidrógeno con el hidroxilo en 20. La Arg364 puede también interaccionar con la G(+2) y con los oxígenos de las ribosas en posiciones (+2) y (+3) de la hebra escindible. Arg488, Arg590 y His632 serían capaces de estabilizar el estado de transición pentacoordinado propuesto para el mecanismo catalítico de doble transesterificación.

El mismo grupo describió poco después la estructura de un complejo con C en lugar de T en posición (-1) [68]. La C es otra base pirimidínica y por eso puede establecerse un enlace de hidrógeno entre la Lys532 y el oxígeno carbonílico de la C análogo al que se forma con la T de la secuencia consenso. Otro interesante hallazgo de este estudio fue una molécula de agua cristalizada a distancia de enlace de hidrógeno de la Arg590. La Tyr723 del sitio activo estaría también a distancia de enlace de hidrógeno de esta molécula de agua y del átomo de fósforo del grupo fosfato escindible. Todo ello parece indicar que esta molécula de agua podría comportarse como base para tomar el protón de la Tyr723, para activarla como nucleófilo antes del ataque al grupo fosfato del ADN. Esta hipótesis está respaldada por la cercanía de la Tyr723 también a la Arg590, que reduciría su pKa favoreciendo la formación del enolato. Además, una rotación en el grupo fosfato escindible que lo sitúa a una corta distancia de la Lys532 indica que ésta debe considerarse parte del centro activo al estabilizar el estado de transición. Por su parte, la His632 puede jugar un doble papel en el proceso catalítico: por un lado, estabilizar el estado de transición pentacoordinado del fósforo, y por otro, protonar el grupo hidroxilo 5' de la ribosa saliente tras el ataque de la Tyr723 al fosfato. Así, según esta publicación, el centro activo de la Top1 estaría formado por Tyr723, Arg590, Arg488, His632, Lys532 y una molécula de agua catalítica (Figura 18).

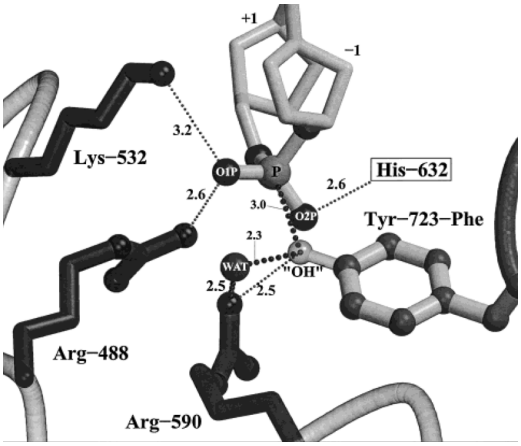

Figura 18.
Papel de la molécula catalítica de agua propuesta en [68], que actuaría como base para el mecanismo enzimático de la Top1.

Un artículo posterior de Kerrigan y Pilch [69] describía los resultados de un trabajo de modelado molecular en el que se comparaban varios modos de interacción (Figura 19), entre ellos, el propuesto por Pommier [67] y uno basado en el de Hol [23] pero en el que la G(+1) no se encontraba rotada (Figura 19A).

En este trabajo, los intentos de simular un modo de intercalación totalmente paralela a las bases (el propuesto por Pommier) acabaron con la molécula de camptotecina expelida al surco mayor y sin establecer contactos significativos con el complejo ADN-Top1. Por el contrario, el modelo basado en el de Hol, en el que la interacción es intercalativa pero la molécula se sitúa perpendicular al eje de las bases, con el anillo E orientado hacia el surco menor y la parte cóncava hacia la hebra escindible, obtuvo el mejor resultado en cuanto a estabilidad energética. En este modelo, los dos oxígenos de la función lactona del anillo E interaccionan por puentes de hidrógeno con la Arg364. El hidroxilo en 20 puede establecer enlaces de hidrógeno tanto con el N-3 de la G(+1) como con un oxígeno de la ribosa. El N del anillo B de la camptotecina podría interaccionar tanto con el protón del N-3 de la T(-1) como con el amino de la A complementaria a la T(-1). Esta misma A también interacciona con el anillo C de la camptotecina por apilamiento. Esta conformación deja las posiciones 7, 9 y 10 de la camptotecina expuestas hacia el surco mayor del ADN, lo que concuerda con que los sustituyentes voluminosos en esas posiciones sean bien tolerados.

En 2002, se publicó la estructura de un complejo ternario con topotecán, elucidada por di-

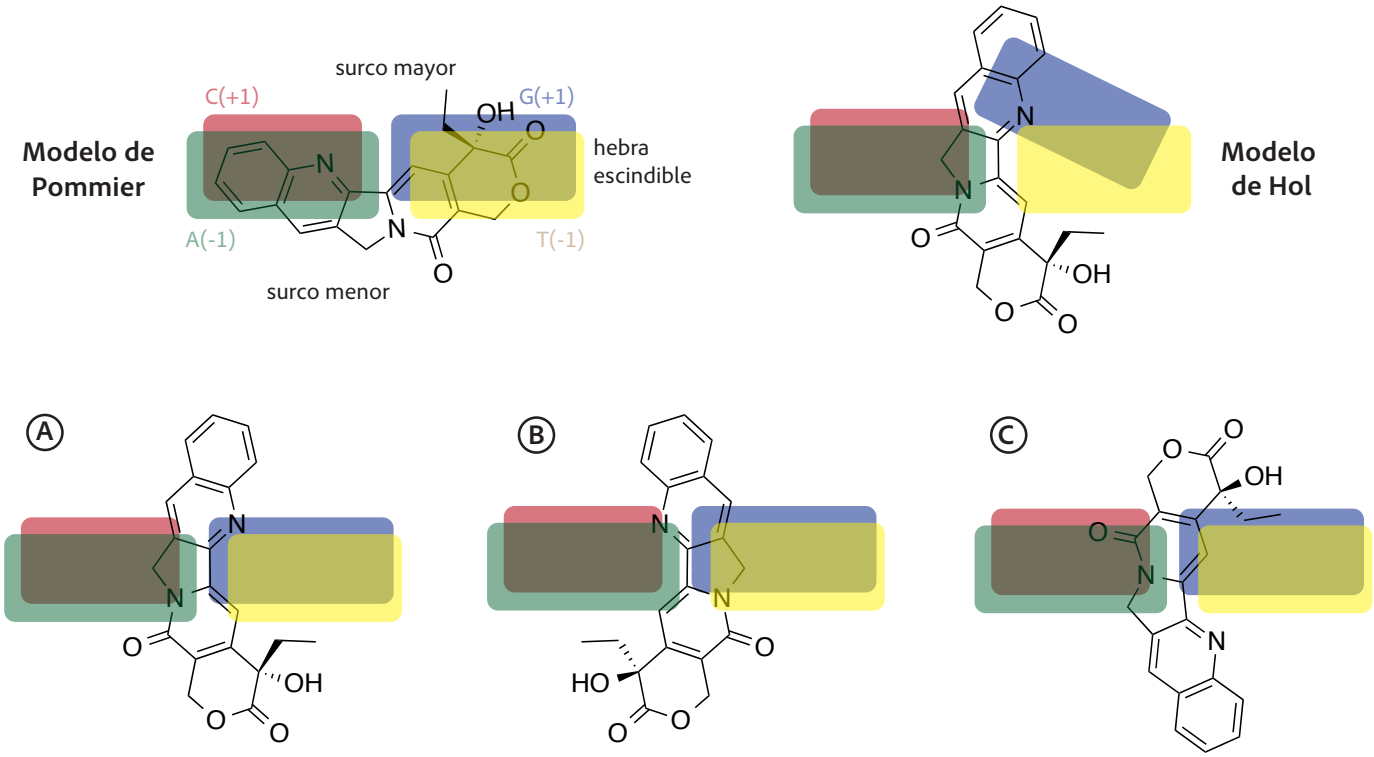

Figura 19.
Vista esquemática de los distintos modos de interacción comparados por Kerrigan y Pilch [69].

fracción de rayos X [70]. En él se puede apreciar cómo el topotecán se intercala entre los pares de bases (+1) y (-1). El sistema pentacíclico se apila con los pares de bases en la misma posición que ocupa el par (+1) en la estructura del complejo ADN-Top1, con la parte cóncava hacia el surco menor y el anillo E entre los nucleótidos de la hebra escindible. En este caso, la molécula se alinea paralelamente a los ejes de los pares de bases, a diferencia de los modelos computacionales que proponían una intercalación parcial. La intercalación del topotecán es posible en el hueco que se forma por simple rotación del enlace fosfodiéster de la hebra no escindible, y no requiere ni la rotación de una base fuera de la hélice (modelo de Hol) ni la ruptura de enlaces de hidrógeno entre los pares de bases del ADN. El desapilamiento energéticamente desfavorable de los pares de bases (+1) y (-1) estaría compensado por la rotación del fosfato entre ellas hasta situarse a distancia de enlace de hidrógeno con los nitrógenos de la cadena principal de Arg362 y Gly363. Este fosfato también interacciona con la cadena lateral de la Lys374. La intercalación del topotecán desplaza 3,6 Å el par de bases (+1) y 8 Å el hidroxilo 5' escindido, hasta situarlo fuera del alcance de la Tyr723, imposibilitando la religación. En la estructura se aprecia la posibilidad de formar un enlace de hidrógeno entre la Asp533 y el hidroxilo en posición 20 de la camptotecina. Este modelo presenta varias ventajas destacables: en primer lugar, las posiciones 7, 9 y 10 quedan orientadas hacia el surco mayor; en segundo, demuestra que hay suficiente espacio para albergar los anillos E expandidos de siete miembros de la familia de las homocamptotecinas; y por último, este modelo también es compatible con que la camptotecina interaccione con el complejo ADN-Top1 en la forma carboxilato abierta, que hasta entonces se consideraba incapaz de unirse al mismo.

Pommier había propuesto en 2000 [71] una hipótesis según la cual la rotación del ADN durante el desenrollamiento desplazaba a la G(+1) fuera de la doble hélice. Aunque Champoux también hablaba en su modelo de la rotación de la G(+1) [23], la diferencia entre ambas teorías estriba en que mientras que en el modelo de Champoux la G(+1) rotada quedaba apilada con la camptotecina, en el modelo de Pommier la G(+1) se desplazaba y generaba un hueco para la unión de la camptotecina, pero quedando tan lejos que el apilamiento no era posible. Basado en este modelo, el grupo de Pommier propuso en 2002 otro modo de interacción generado computacionalmente [72], esta vez para SN-38, el metabolito activo del topotecán. La G(+1) quedaría estabilizada fuera de la doble hélice por una red de enlaces de hidrógeno con Asp533, Arg488 y Arg590. El SN-38 se colocaría apilado entre los pares de bases, perpendicular a ellos, con el lado cóncavo hacia la hebra no escindible y con el anillo D sobre la T(-1) y el anillo A proyectado hacia el surco mayor, donde el hidroxilo del SN-38 formaría un enlace de hidrógeno con la Asn352 (Figura 20).

Además de este enlace sólo posible en el caso de SN-38, el resto de la estructura (común con la camptotecina) establecería varios enlaces de hidrógeno adicionales: el carbonilo de la lactona con los aminoácidos Lys532 y Asp533, el

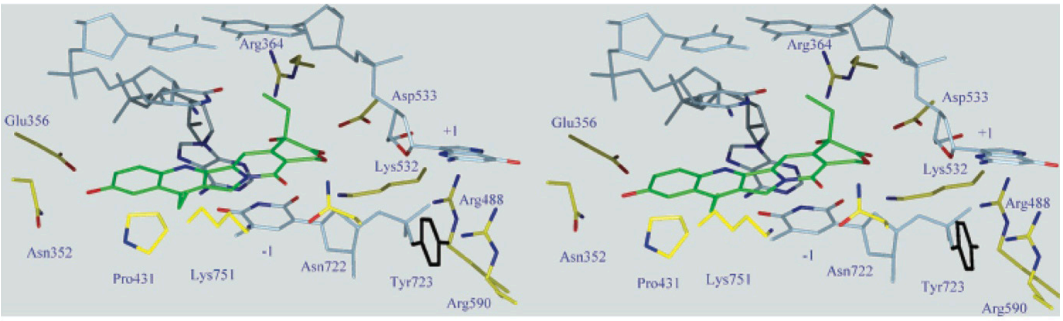

Figura 20. Diagrama esteroegráfico del modo de interacción propuesto por Laco para SN-38 en [72]. Nótese cómo la G(+1) ha sido rotada fuera de su emplazamiento.

hidroxilo en 20 con la Lys532 y el carbonilo de la T(-1), y el carbonilo del anillo D con la Asn722.

En 2004, los resultados de un trabajo de modelado molecular llevado a cabo con homocamptotecina arrojaron una colocación análoga de la molécula en el complejo ternario [73].

El mismo grupo que había descrito en 2002 la estructura del complejo ternario con topotecán por difracción de rayos X, logró en 2005 cristalizar y describir la estructura del complejo ternario con camptotecina [74]. La posición y orientación de la camptotecina era prácticamente idénticas a la hallada para el topotecán. De entre seis posibles modos de apilamiento, esta colocación fue también confirmada como la más estable termodinámicamente por modelado molecular con cálculos *ab initio* considerando las interacciones π-π establecidas entre la campotecina y los pares de bases (+1) y (-1) [75]. Simulaciones con otros derivados de camptotecina llevan también a esa disposición de manera preferencial [76].

Una reciente simulación ha estudiado la dinámica del complejo durante 25 ns [77]. Para ello han utilizado el complejo ternario con topotecán cristalizado por Staker [70]. La mayoría de interacciones propuestas en el análisis difractográfico del trabajo original se mantienen más del 95% del tiempo de la simulación. Este trabajo revela dos interacciones de hidrógeno adicionales: la de la Lys532 con los oxígenos carbonílico e hidroxilo del anillo E del topotecán, y la de la Arg364 con los anillos B y E del antitumoral. En la publicación también se describe cómo la presencia del topotecán aumenta la rigidez de la región "downstream" del ADN y cómo la Lys532 se mantiene siempre a más de 8 Å del hidroxilo 5' de la G(+1) haciendo imposible la catálisis básica de la segunda transesterificación, hechos ambos que dificultan la religación de la hebra escindible. Por medio de la misma técnica, el grupo ha explicado también cómo la red de enlaces de hidrógeno entre la Top1 y las bases del ADN en el sitio activo es responsable de la preferencia por la presencia de una timina en posición (-1) con respecto al punto de corte en el que la camptotecina actúa como inhibidor [78].

El análisis informático de las estructuras cristalográficas de los complejos ternarios con camptotecina y topotecán llevó al grupo de Pommier [79] a proponer un farmacóforo para los compuestos inhibidores de topoisomerasa I. Las características que lo definen son: interacciones aromáticas sobre los anillos A, B y D, aceptores de enlaces hidrógeno en el nitrógeno quinolónico y el oxígeno cíclico de la lactona, y donadores de enlaces de hidrógeno en el hidroxilo en 20 (Figura 21). Por otro lado, un estudio empleando resonancia paramagnética de electrón en combinación con marcaje de spin dirigido (SDSL-EPR) ha permitido determinar que el tiempo que permanece unida la camptotecina en el complejo ternario está en el orden de cientos de microsegundos [80].

Laco ha comparado recientemente [81], por medio de métodos computacionales, el modelo de intercalación deducido de la estructura cristalográfica del complejo ternario con topotecán [70], y el modelo del nucleótido rotado propuesto por él mismo por medio de modelado

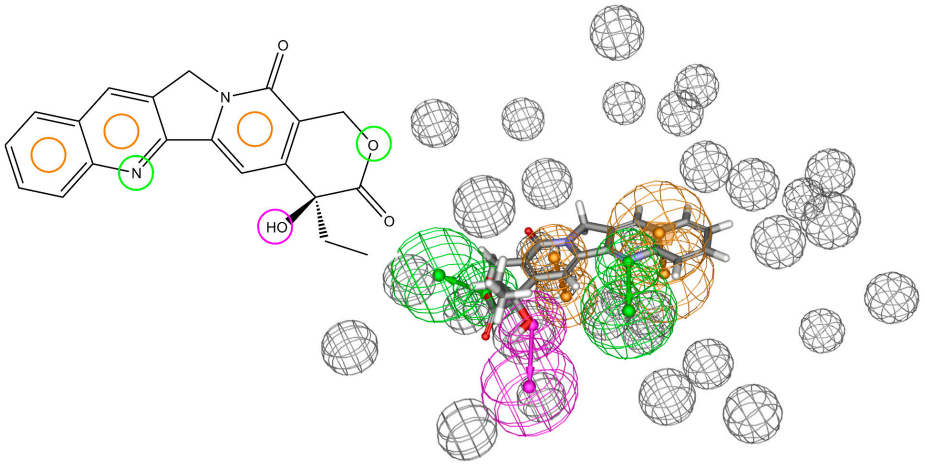

Figura 21. Farmacóforo hallado por modelado molecular para los inhibidores de Top1, en representaciones 2D (izquierda) y 3D (derecha). Los aceptores de enlaces de hidrógeno están marcados en verde, los donadores en magenta y los grupos capaces de establecer interacciones de apilamiento, en naranja. Las esferas grises son puntos de impedimento estérico [79].

molecular [73]. En el estudio se hace docking de varios compuestos (entre ellos la 20-cloro-camptotecina y la 10,11-difluoro-camptotecina) en los sitios activos propuestos por ambos modelos. Laco llega a la conclusión de que las estabilidades de los complejos ternarios calculadas usando el modelo del nucleótido rotado se correlacionan mejor con la actividad citotóxica real de los compuestos.

En resumen, se puede decir que existen varios modelos propuestos para el modo en el que la camptotecina y sus derivados se unen al complejo ADN-Top1. Todas comparten el hecho de que la camptotecina se intercala entre los pares de bases (-1) y (+1) del ADN después de que la enzima corte la hebra, modificando la geometría del sitio activo de modo que se dificulta la religación del ADN y probablemente se ralentiza su giro. Sin embargo, y aunque hay algunos puntos consensuados, la orientación de la molécula, el número de interacciones que establece con aminoácidos de la proteína y la necesidad o no de que la G(+1) rote fuera de la hélice de ADN, son aún objeto de discusión por parte de varios grupos.

2.4.2. El paradigma de la inhibición interfacial

El modo de acción de los inhibidores de Top1 es especial, porque no establecen enlaces covalentes con la enzima, ni interaccionan con sitios de inhibición alostérica de las mismas. Por el contrario, el sitio de unión no covalente de estos inhibidores aparece en, y solamente en, la interfaz que se forma entre el ADN y la Top1. Este modo de interacción es poco habitual, y lo comparte un relativamente pequeño grupo de moléculas (como la colchicina, la ciclosporina, la ecteinascidina 743, la rapamicina, el paclitaxel o la vinblastina, Figura 22) que sólo pueden unirse en puntos de las interfaces que se forma entre macromoléculas biológicas (Figura 23).

La singularidad de este hecho llevó a Pommier a proponer el concepto que denominó "el paradigma de la inhibición interfacial", y que ha venido revisando ampliamente a lo largo de diversas publicaciones [14,16,21,22,25,36,82-84].

Las características esenciales de los inhibidores interfaciales son [22]:

- Tienen como diana a un sistema o máquina molecular con dos o más componentes, que pueden ser proteínas y/o ácidos nucleicos.
- Se acoplan a la interfaz generada cuando los componentes se unen entre sí.
- El sitio exacto de unión del inhibidor se genera como consecuencia de los movimientos de la máquina macromolecular.
- Presentan una alta estereoselectividad.
- Su unión es generalmente reversible, por enlaces de hidrógeno, interacciones π-π o quelación de metales.

Otro hecho destacable es que, mientras que la Top1 no es imprescindible para la supervivencia celular (otras topoisomerasas pueden suplirla, al menos temporalmente), sin embargo, su inhibición lleva a la muerte celular. Por ello, Pommier describe cómo no es la inhibición de la actividad catalítica, sino el "atrapamiento" del complejo, el responsable de la apoptosis [16]. Es decir, que a la inhibición le siguen una serie de acontecimientos moleculares, aún no totalmente conocidos, que median en el desencadenamiento de la muerte celular.

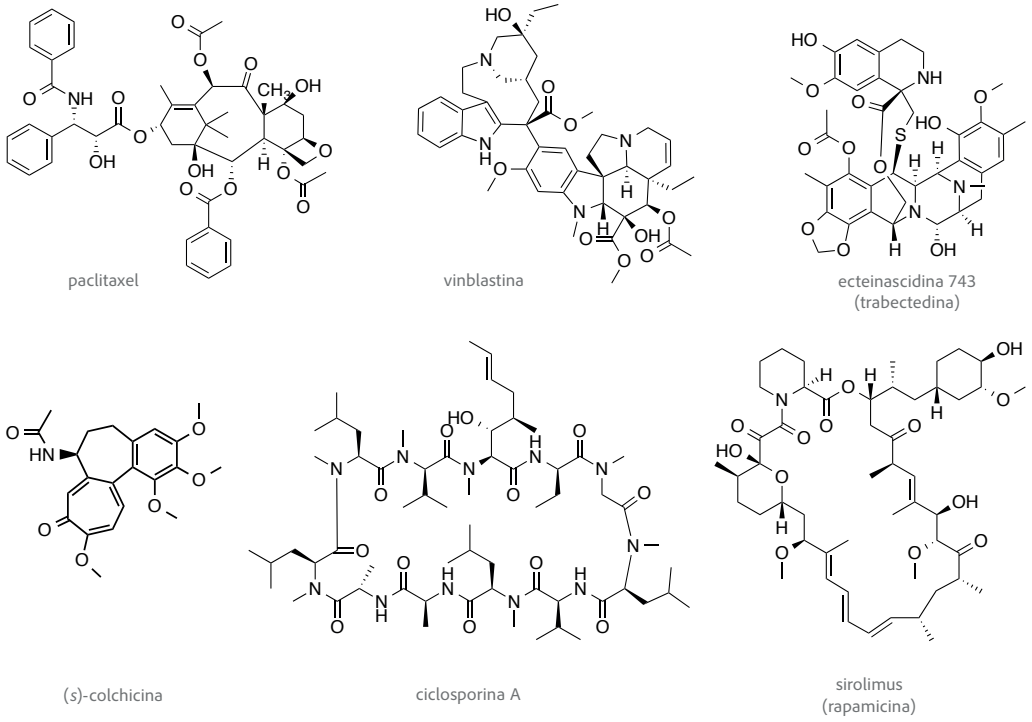

Figura 22.
Algunos de los inhibidores interfaciales mejor conocidos [22], grupo de moléculas al que pertenecen la camptotecina y la luotonina A. Todos tienen potentes actividades farmacológicas como antitumorales o inmunosupresores.

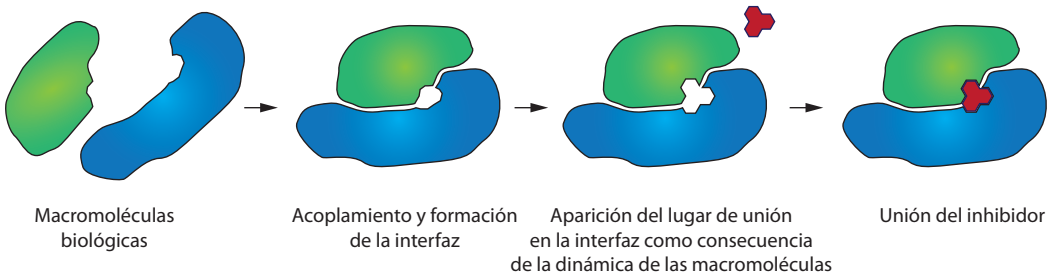

Figura 23. Formación del lugar de unión de un inhibidor interfacial.

2.4.3. Consecuencias moleculares de la inhibición de Top1

Desde las primeras investigaciones sobre la biología molecular detrás de la acción farmacológica de la camptotecina, se sabe que la unión de los análogos de camptotecina al ADN, al impedir la religación de la hebra escindible, prolonga la semivida de la unión covalente ADN-Top1, lo que provoca una acumulación del complejo ternario en las células [85].

Una de las primeras explicaciones a la muerte celular fue el modelo colisional. Como se ha explicado antes, la Top1 avanza por el ADN desenrollándolo para permitir el acceso a la maquinaria de transcripción/replicación/reparación. La acción de la camptotecina puede hacer que la Top1 quede atrapada covalentemente en un punto del ADN. Al seguir avanzando, la maquinaria enzimática que va tras ella colisionaría contra el complejo atrapado, lo que sería suficiente para provocar la rotura de la hebra no escindible del ADN. De ese modo se produciría la rotura de ambas hebras de la doble hélice: la escindible por la acción catalítica de la Top1, y la no escindible por el choque con la maquinaria enzimática [86].

Por otro lado, la formación de los complejos ternarios activa cascadas de señalización celular que implican a proteínas como Rad9, Bcl-2, Bcl-xL y c-abl, responsables de iniciar el proceso de la apoptosis y, por lo tanto, acabando con la viabilidad de la célula (Capítulo 4 de la ref. [25]). Además, parece que vías de reparación del ADN que podrían revertir los complejos (BRCA1, 53BP1 o MDC1) pueden tener un nivel de activación menor o nulo en células tumorales [21,36].

2.5. Relación estructura actividad

2.5.1. Derivados de la camptotecina

Existe un gran número de publicaciones en las que se describen diversas modificaciones sobre la estructura original de la camptotecina, así como la repercusión de éstas en la estabilidad, farmacocinética y potencia inhibitoria de los fármacos. Como consecuencia, ha sido posible establecer un mapa de las modificaciones que más condicionan estos parámetros en los análogos de camptotecina descritos hasta el momento [87,88] (Figura 24).

2.5.2 Derivados de la luotonina A

Las síntesis de derivados de la luotonina A modificados en distintas posiciones son mucho menos numerosas que las de la camptotecina. No obstante, es posible determinar cuáles son las sustituciones más favorables, permitidas o desfavorables sobre la estructura de la luotoni-

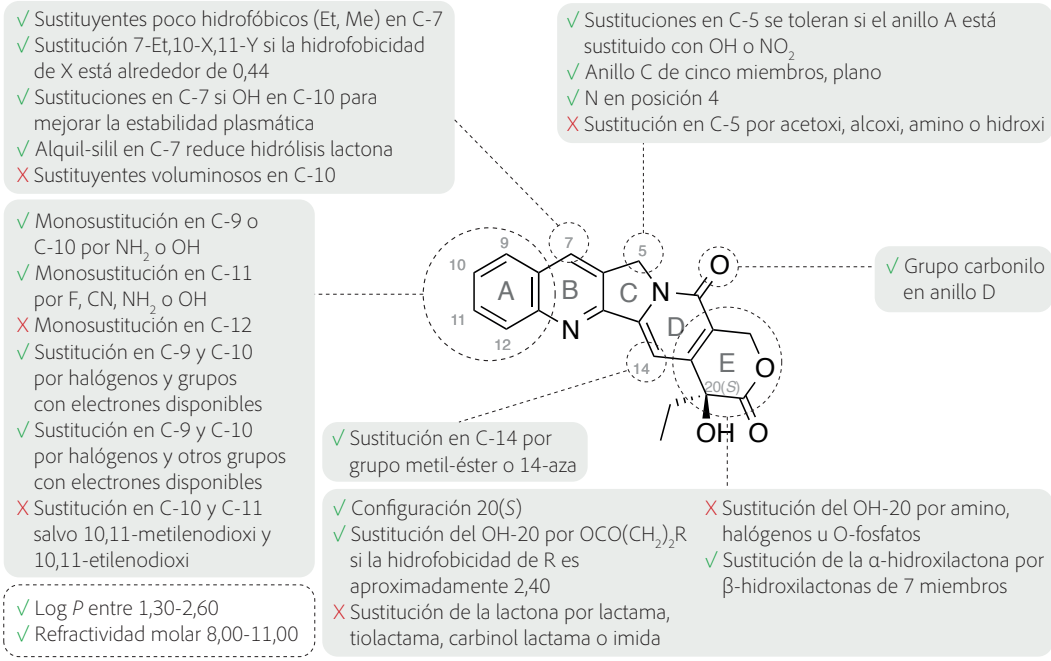

Figura 24. Modificaciones descritas sobre el núcleo básico de la camptotecina, y repercusión sobre su actividad biológica

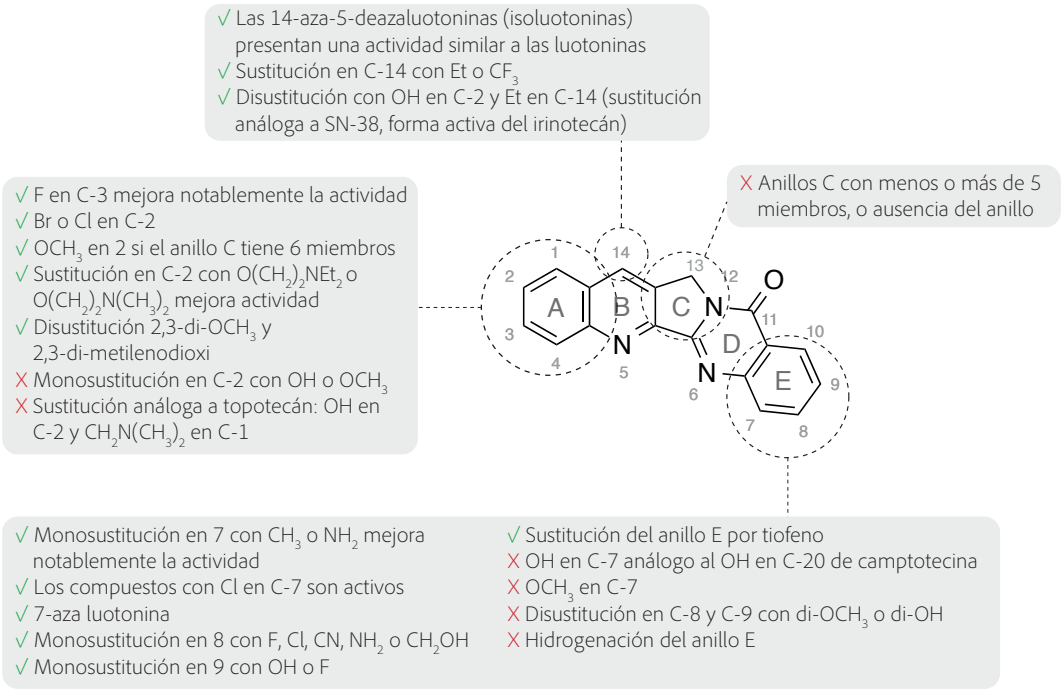

Figura 25.
Influencia de distintos sustituyentes en las propiedades farmacológicas de los derivados de luotonina A.

na A en base a las publicaciones sobre su síntesis [57,59,60,89-94] y a una reciente revisión que recoge algunas de ellas [61]. Se han recopilado en el esquema de la Figura 25.

2.6. Derivados de la camptotecina utilizados en la práctica clínica

2.6.1. Irinotecán

El irinotecán (Figura 14A) es un derivado hidrosoluble de la camptotecina aprobado en 1998 para su uso clínico y comercializado con los nombres de Camptosar y Campto [88]. En realidad, se trata de un profármaco de la molécula activa, SN-38, que requiere la hidrólisis del carbamato presente en C-10 por la carboxilesterasa-2 humana y la enzima P450 3A. SN-38 presenta una buena estabilidad del anillo de lactona comparado con el profármaco. Su uso terapéutico principal es en casos de cáncer colorrectal y gastroesofágico con presencia de metástasis refractario a otros tratamientos [95,96], aunque también es frecuente en la terapio de los glioblastomas, sarcomas y cáncer de cérvix [16]. El aclaramiento mayoritario es por vía hepática, a través de glucuronización por la uridina-difosfato glucuronosil-transferasa 1A1 (UGT1A1), una enzima cuyo polimorfismo es el principal responsable de la necesidad de ajustes interindividuales en la dosis [97].

2.6.2. Topotecán

El topotecán (Figura 14A) se introdujo en la práctica clínica en 2007 bajo el nombre comercial de Hycamtin. Su indicación terapéutica aprobada es como fármaco de segunda línea en cáncer ovárico con metástasis y el cáncer de pulmón de células pequeñas [95]. También es de aplicación en glioblastomas y sarcomas [16]. Este fármaco ha demostrado su eficacia en la administración por vía oral [88].

2.6.3. Belotecán

Este fármaco (Figura 14A) tiene indicaciones terapéuticas aprobadas desde 2009 sólo en Corea del Sur, en casos de cáncer de ovario recurrente o en cáncer de pulmón de células pequeñas [88]. Su nombre comercial es Camptobell.

La información contenida en este capítulo puede complementarse con dos completos libros sobre el tema [25,98] y varias recientes revisiones [61,88,97].

3. Referencias

1. H.-O. Adami, D.J.D.J. Hunter, D. Trichopoulos, Textbook of cancer epidemiology, 2nd ed., Oxford University Press, Oxford, 2008.
2. D. Hanahan, R.A. Weinberg, The Hallmarks of Cancer, Cell. 100 (2000), 57-70.
3. D. Hanahan, R.A. Weinberg, Hallmarks of cancer: the next generation, Cell. 144 (2011) 646–674.
4. R.J.B. King, M.W. Robins, Cancer biology, 3rd ed., Pearson/Prentice Hall, Harlow, 2006.
5. M. Greaves, Cancer: The evolutionary disease, Oxford University Press, Oxford, 2001.
6. A. Alwan, ed., Global status report on noncommunicable diseases 2010. World Health Organization, Geneva, 2011.
7. J. Ferlay, H.-R. Shin, F. Bray, D. Forman, C. Mathers, D.M. Parkin, Estimates of worldwide burden of cancer in 2008: GLOBOCAN 2008, Int. J. Cancer. 127 (2010) 2893–2917.
8. A. Jemal, F. Bray, M.M. Center, J. Ferlay, E. Ward, D. Forman, Global cancer statistics, CA-Cancer J. Clin. 61 (2011) 69–90.

9. J. Ferlay, I. Soerjomataram, M. Ervik, R. Dikshit, S. Eser, C. Mathers, et al., GLOBOCAN 2012 v1.0, Cancer Incidence and Mortality Worldwide: IARC CancerBase No. 11, Wiley Subscription Services, Inc., A Wiley Company, Lyon, 2013.
10. F. Bray, A. Jemal, N. Grey, J. Ferlay, D. Forman, Global cancer transitions according to the Human Development Index (2008–2030): a population-based study, Lancet Oncol. 13 (2012) 790–801.
11. A. Alwan, T. Armstrong, M. Cowan, L. Riley, Noncommunicable Diseases - Country Profiles 2011, World Health Organization, Geneva, 2011.
12. American Cancer Society, Cancer Facts & Figures 2010, 2010 ed., American Cancer Society, Atlanta, 2010.
13. B. Levin, P. Boyle, eds., World cancer report 2008, International Agency for Research on Cancer - WHO Press, Lyon, 2008.
14. Y. Pommier, E. Leo, H. Zhang, C. Marchand, DNA topoisomerases and their poisoning by anticancer and antibacterial drugs, Chem. Biol. 17 (2010) 421–433.
15. J.J. Champoux, DNA topoisomerases: Structure, function, and mechanism, Annu Rev Biochem. 70 (2001) 369–413.
16. Y. Pommier, Drugging topoisomerases: lessons and challenges, ACS Chem. Biol. 8 (2013) 82–95.
17. J.C. Wang, Cellular roles of DNA topoisomerases: a molecular perspective, Nat. Rev. Mol. Cell Biol. 3 (2002) 430–440.
18. S.H. Chen, N.-L. Chan, T.-S. Hsieh, New mechanistic and functional insights into DNA topoisomerases, Annu Rev Biochem. 82 (2013) 139–170.
19. P. Forterre, D. Gadelle, Phylogenomics of DNA topoisomerases: their origin and putative roles in the emergence of modern organisms, Nucleic Acids Res. 37 (2009) 679–692.
20. C. Bailly, Homocamptothecins: potent topoisomerase I inhibitors and promising anticancer drugs, Crit Rev Oncol Hematol. 45 (2003) 91–108.
21. Y. Pommier, DNA topoisomerase I inhibitors: chemistry, biology, and interfacial inhibition, Chem Rev. 109 (2009) 2894–2902.
22. Y. Pommier, C. Marchand, Interfacial inhibitors: targeting macromolecular complexes, Nat Rev Drug Discov. 11 (2012) 25–36.
23. M.R. Redinbo, J.J. Champoux, L. Stewart, P. Kuhn, W.G. Hol, Crystal structures of human topoisomerase I in covalent and noncovalent complexes with DNA, Science. 279 (1998) 1504–1513.
24. J.R. Olesen, C. Skouboe, B.O. Krogh, T. Straub, F. Boege, S. Velmurugan, et al., Residues within the N-terminal domain of human topoisomerase I play a direct role in relaxation, J. Biol. Chem. 276 (2001) 20220–20227.
25. Y. Pommier, DNA Topoisomerases and Cancer, Springer, New York, 2011.
26. J.J. Champoux, L. Stewart, M.R. Redinbo, X. Qiu, W.G. Hol, A model for the mechanism of human topoisomerase I, Science. 279 (1998) 1534–1541.
27. Z. Yang, J.J. Champoux, J.F. Carey, Mutational analysis of the preferential binding of human topoisomerase I to supercoiled DNA, Febs J. 276 (2009) 5906–5919.
28. Z. Yang, D. Li, S. Hiew, M.T. Ng, W. Yuan, H. Su, et al., Recognition of forcible curvature in circular DNA by human Topoisomerase I, Chem. Commun. 47 (2011) 11309–11311.
29. B. Thomsen, S. Mollerup, B. Bonven, R. Frank, H. Blöcker, O.F. Nielsen, et al., Sequence specificity of DNA topoisomerase I in the presence and absence of camptothecin, The EMBO Journal. 6 (1987) 1817–1823.
30. C. Jaxel, G. Capranico, D. Kerrigan, K.W. Kohn, Y. Pommier, Effect of local DNA sequence on topoisomerase I cleavage in the presence or absence of camptothecin, J. Biol. Chem. 266 (1991) 20418–20423.
31. F.M. Siu, Y. Pommier, Sequence selectivity of the cleavage sites induced by topoisomerase I inhibitors: a molecular dynamics study, Nucleic Acids Res. (2013).
32. C. Punchihewa, M. Carver, D. Yang, DNA sequence selectivity of human topoisomerase I-mediated DNA cleavage induced by camptothecin, Protein Sci. 18 (2009) 1326–1331.
33. P. Fiorani, G. Chillemi, C. Losasso, S. Castelli, A. Desideri, The different cleavage DNA sequence specificity explains the camptothecin resistance of the human topoisomerase I Glu418Lys mutant, Nucleic Acids Res. 34 (2006) 5093–5100.
34. N.M. Baker, R. Rajan, A. Mondragón, Structural studies of type I topoisomerases, Nucleic Acids Res. 37 (2009) 693–701.
35. J.B. Leppard, J.J. Champoux, Human DNA topoisomerase I: relaxation, roles, and damage control, Chromosoma. 114 (2005) 75–85.
36. Y. Pommier, Topoisomerase I inhibitors: camptothecins and beyond, Nat Rev Cancer. 6 (2006) 789–802.
37. D.A. Koster, V. Croquette, C. Dekker, S. Shuman, Friction and torque govern the relaxation of DNA supercoils by eukaryotic topoisomerase IB, Nature. 434 (2005) 671–674.
38. J. Wereszczynski, I. Andricioaei, Free Energy Calculations Reveal Rotating-Ratchet Mechanism for DNA Supercoil Relaxation by Topoisomerase IB and its Inhibition, Biophys J. 99 (2010) 869–878.
39. N.H. Oberlies, D.J. Kroll, Camptothecin and taxol: historic achievements in natural products research, J Nat Prod. 67 (2004) 129–135.
40. M.E. Wall, M.C. Wani, C.E. Cook, K.H. Palmer, A.T. McPhail, G.A. Sim, Plant Antitumor Agents. I. The Isolation and Structure of Camptothecin, a Novel Alkaloidal Leukemia and Tumor Inhibitor from *Camptotheca acuminata,* J Am Chem Soc. 88 (1966) 3888–3890.
41. J.A. Gottlieb, A.M. Guarino, J.B. Call, V.T. Oliverio, J.B. Block, Preliminary pharmacologic and clinical evaluation of camptothecin sodium (NSC-100880), Cancer Chemother Rep. 54 (1970) 461–470.
42. F.M. Muggia, P.J. Creaven, H.H. Hansen, M.H. Cohen, O.S. Selawry, Phase I clinical trial of weekly and daily treatment with camptothecin (NSC-100880): correlation with preclinical studies, Cancer Chemother Rep. 56 (1972) 515–521.

43. C.G. Moertel, A.J. Schutt, R.J. Reitemeier, R.G. Hahn, Phase II study of camptothecin (NSC-100880) in the treatment of advanced gastrointestinal cancer, Cancer Chemother Rep. 56 (1972) 95–101.
44. B.C. Giovanella, H.R. Hinz, A.J. Kozielski, J.S. Stehlin, R. Silber, M. Potmesil, Complete growth inhibition of human cancer xenografts in nude mice by treatment with 20-(S)-camptothecin, Cancer Res. 51 (1991) 3052–3055.
45. G.L. Beretta, F. Zunino, Relevance of extracellular and intracellular interactions of camptothecins as determinants of antitumor activity, Biochem Pharmacol. 74 (2007) 1437–1444.
46. Z. MI, H. Malak, T. Burke, Reduced Albumin-Binding Promotes the Stability and Activity of Topotecan in Human Blood, Biochemistry. 34 (1995) 13722–13728.
47. M.P. Marszałł, A. Buciński, S. Kruszewski, B. Ziomkowska, A new approach to determine camptothecin and its analogues affinity to human serum albumin, J Pharm Sci. 100 (2011) 1142–1146.
48. J.F. Pizzolato, L.B. Saltz, The camptothecins, Lancet. 361 (2003) 2235–2242.
49. Y.H. Hsiang, R. Hertzberg, S. Hecht, L.F. Liu, Camptothecin induces protein-linked DNA breaks via mammalian DNA topoisomerase I, J. Biol. Chem. 260 (1985) 14873–14878.
50. Y.H. Hsiang, L.F. Liu, Identification of mammalian DNA topoisomerase I as an intracellular target of the anticancer drug camptothecin, Cancer Res. 48 (1988) 1722–1726.
51. M. Potmesil, Camptothecins - From Bench Research to Hospital Wards, Cancer Res. 54 (1994) 1431–1439.
52. Harvard University Herbaria, Missouri Botanical Garden, *Camptotheca acuminata* in Flora of China at eFloras.org, eFloras.org. 13 (n.d.) 300.
53. T. Efferth, P.C.H. Li, V.S.B. Konkimalla, B. Kaina, From traditional Chinese medicine to rational cancer therapy, Trends Mol Med. 13 (2007) 353–361.
54. A. Lorence, C. Nessler, Camptothecin, over four decades of surprising findings, Phytochem. 65 (2004) 2735–2749.
55. S. Sirikantaramas, T. Asano, H. Sudo, M. Yamazaki, K. Saito, Camptothecin: therapeutic potential and biotechnology, Curr Pharm Biotechnol. 8 (2007) 196–202.
56. S. Sirikantaramas, M. Yamazaki, K. Saito, Mutations in topoisomerase I as a self-resistance mechanism coevolved with the production of the anticancer alkaloid camptothecin in plants, Proc Natl Acad Sci USA. 105 (2008) 6782–6786.
57. Z. Ma, Y. Hano, T. Nomura, Y. Chen, Two new pyrroloquinazolinoquinoline alkaloids from *Peganum nigellastrum*, Heterocycles. 46 (1997) 541–546.
58. Harvard University Herbaria, Missouri Botanical Garden, Peganum nigellastrum in Flora of China at eFloras.org, eFloras.org. (n.d.) 43.
59. Ali Cagir, Shannon H Jones, Rong Gao, A. Brian M Eisenhauer, S.M. Hecht, Luotonin A. A Naturally Occurring Human DNA Topoisomerase I Poison, J Am Chem Soc. 125 (2003) 13628–13629.
60. Z. Ma, Y. Hano, T. Nomura, Luotonin A: A lead toward anti-cancer agent development, Heterocycles. 65 (2005) 2203–2219.
61. J.L. Liang, H.C. Cha, Y. Jahng, Recent advances in the studies on luotonins, Molecules. 16 (2011) 4861–4883.
62. S. Castelli, A. Coletta, I. D'Annessa, P. Fiorani, C. Tesauro, A. Desideri, Interaction between natural compounds and human topoisomerase I, Biol. Chem. 393 (2012) 1327–1340.
63. Y.H. Hsiang, M.G. Lihou, L.F. Liu, Arrest of replication forks by drug-stabilized topoisomerase I-DNA cleavable complexes as a mechanism of cell killing by camptothecin, Cancer Res. 49 (1989) 5077–5082.
64. J.J. Champoux, S.E. Porter, The basis for camptothecin enhancement of DNA breakage by eukaryotic topoisomerase I, Nucleic Acids Res. 17 (1989) 8521–8532.
65. Y. Pommier, P. Pourquier, Y. Fan, D. Strumberg, Mechanism of action of eukaryotic DNA topoisomerase I and drugs targeted to the enzyme, BBA-Gene Struct Expr. 1400 (1998) 83–106.
66. A. Fujimori, W.G. Harker, G. Kohlhagen, Y. Hoki, Y. Pommier, Mutation at the catalytic site of topoisomerase I in CEM/C2, a human leukemia cell line resistant to camptothecin, Cancer Res. 55 (1995) 1339–1346.
67. Y. Fan, J.N. Weinstein, K.W. Kohn, L.M. Shi, Y. Pommier, Molecular Modeling Studies of the DNA–Topoisomerase I Ternary Cleavable Complex with Camptothecin, J Med Chem. 41 (1998) 2216–2226.
68. J.J. Champoux, M.R. Redinbo, W.G.J. Hol, Novel Insights into Catalytic Mechanism from a Crystal Structure of Human Topoisomerase I in Complex with DNA, Biochemistry. 39 (2000) 6832–6840.
69. A. John E Kerrigan, Daniel S Pilch, A Structural Model for the Ternary Cleavable Complex Formed between Human Topoisomerase I, DNA, and Camptothecin, Biochemistry, 40 (2001) 9792-9798.
70. B. Staker, K. Hjerrild, M. Feese, C. Behnke, The mechanism of topoisomerase I poisoning by a camptothecin analog, Proc Natl Acad Sci USA. 99 (2002) 15387-15392.
71. Y. Pommier, G. Laco, G. Kohlhagen, J. Sayer, H. Kroth, D. Jerina, Position-specific trapping of topoisomerase I–DNA cleavage complexes by intercalated benzo [a]-pyrene diol epoxide adducts at the 6-amino group of adenine, Proc Natl Acad Sci USA. 97 (2000) 10739-10744.
72. G.S. Laco, J.R. Collins, B.T. Luke, H. Kroth, J.M. Sayer, D.M. Jerina, et al., Human Topoisomerase I Inhibition: Docking Camptothecin and Derivatives into a Structure-Based Active Site Model, Biochemistry. 41 (2002) 1428–1435.
73. G. Laco, W. Du, G. Kohlhagen, J. Sayer, D. Jerina, T. Burke, et al., Analysis of human topoisomerase I inhibition and interaction with the cleavage site +1 deoxyguanosine, via in vitro experiments and molecular modeling studies, Bioorgan Med Chem. 12 (2004) 5225–5235.
74. B.L. Staker, M.D. Feese, M. Cushman, Y. Pommier, D. Zembower, L. Stewart, et al., Structures of three classes of anticancer agents bound

to the human topoisomerase I-DNA covalent complex, J Med Chem. 48 (2005) 2336–2345.

75. X. Xiao, M. Cushman, An ab initio quantum mechanics calculation that correlates with ligand orientation and DNA cleavage site selectivity in camptothecin-DNA-topoisomerase I ternary cleavage complexes, J Am Chem Soc. 127 (2005) 9960–9961.
76. C. Samorì, A. Guerrini, G. Varchi, G. Fontana, E. Bombardelli, S. Tinelli, et al., Semisynthesis, Biological Activity, and Molecular Modeling Studies of C-Ring-Modified Camptothecins, J Med Chem. 52 (2009) 1029–1039.
77. G. Mancini, I. D'Annessa, A. Coletta, N. Sanna, G. Chillemi, A. Desideri, Structural and Dynamical Effects Induced by the Anticancer Drug Topotecan on the Human Topoisomerase I – DNA Complex, PLoS ONE. 5 (2010) e10934 EP-
78. A. Coletta, A. Desideri, Role of the protein in the DNA sequence specificity of the cleavage site stabilized by the camptothecin topoisomerase IB inhibitor: a metadynamics study, Nucleic Acids Res. 41 (2013) 9977–9986.
79. M.N. Drwal, K. Agama, L.P.G. Wakelin, Y. Pommier, R. Griffith, Exploring DNA topoisomerase I ligand space in search of novel anticancer agents, PLoS ONE. 6 (2011) e25150 EP.
80. A. Ricci, J. Marinello, M. Bortolus, A. Sánchez, A. Grandas, E. Pedroso, et al., Electron paramagnetic resonance (EPR) study of spin-labeled camptothecin derivatives: a different look of the ternary complex, J Med Chem. 54 (2011) 1003–1009.
81. G.S. Laco, Evaluation of two models for human topoisomerase I interaction with dsDNA and camptothecin derivatives, PLoS ONE. 6 (2011) e24314 EP.
82. Y. Pommier, J. Cherfils, Interfacial inhibition of macromolecular interactions: nature's paradigm for drug discovery, Trends Pharmacol. Sci. 26 (2005) 138–145.
83. Y. Pommier, C. Marchand, Interfacial inhibitors of protein-nucleic acid interactions, Curr Med Chem:Anti-Cancer Agents. 5 (2005) 421–429.
84. Y. Pommier, Camptothecins and Topoisomerase I: A Foot in the Door. Targeting the Genome Beyond Topoisomerase I with Camptothecins and Novel Anticancer Drugs: Importance of DNA Replication, Repair and Cell Cycle Checkpoints, Curr Med Chem: Anti-Cancer Agents. 4 (2004) 429–434.
85. J.L. Nitiss, J.C. Wang, Mechanisms of cell killing by drugs that trap covalent complexes between DNA topoisomerases and DNA, Mol Pharmacol. 50 (1996) 1095–1102.
86. Y.-H. Hsiang, M.G. Lihou, L.F. Liu, Arrest of Replication Forks by Drug-stabilized Topoisomerase I-DNA Cleavable Complexes as a Mechanism of Cell Killing by Camptothecin, Cancer Res. 49 (1989) 5077–5082.
87. R.P. Verma, C. Hansch, Camptothecins: a SAR/QSAR study, Chem Rev. 109 (2009) 213–235.
88. K.M. Kacprzak, Chemistry and Biology of Camptothecin and its Derivatives, in: K.G. Ramawat, J.-M. Mérillon (Eds.), Natural Products, Springer, Berlin, 2013: pp. 643–682.
89. S. Dallavalle, L. Merlini, G. Beretta, S. Tinelli, F. Zunino, Synthesis and cytotoxic activity of substituted Luotonin A derivatives, Bioorganic & Medicinal Chemistry Letters. 14 (2004) 5757–5761.
90. A. Cagir, S. Jones, B. Eisenhauer, R. Gao, S. Hecht, Synthesis and biochemical properties of E-ring modified luotonin A derivatives, Bioorganic & Medicinal Chemistry Letters. 14 (2004) 2051–2054.
91. A. Cagir, B.M. Eisenhauer, R. Gao, S.J. Thomas, S.M. Hecht, Synthesis and topoisomerase I inhibitory properties of luotonin A analogues, Bioorganic & Medicinal Chemistry. 12 (2004) 6287–6299.
92. K. Nacro, C.(C.) Zha, P.R. Guzzo, R.J. Herr, D. Peace, T.D. Friedrich, Synthesis and topoisomerase poisoning activity of A-ring and E-ring substituted luotonin A derivatives, Bioorganic & Medicinal Chemistry. 15 (2007) 4237–4246.
93. A. Rahman, D. Kim, J. Liang, E. Lee, Y. Na, K. Jun, et al., Synthesis and Biological Properties of Luotonin A Derivatives, Bull. Korean Chem. Soc. 29 (2008) 1988–1992.
94. M.-C. Tseng, Y.-W. Chu, H.-P. Tsai, C.-M. Lin, J. Hwang, Y.-H. Chu, One-pot synthesis of luotonin A and its analogues, Org Lett. 13 (2011) 920–923.
95. V.J. Venditto, E.E. Simanek, Cancer therapies utilizing the camptothecins: a review of the in vivo literature, Mol Pharm. 7 (2010) 307–349.
96. D.C. Gilbert, A.J. Chalmers, S.F. El-Khamisy, Topoisomerase I inhibition in colorectal cancer: biomarkers and therapeutic targets, Br. J. Cancer. 106 (2012) 18–24.
97. J. Moukharskaya, C. Verschraegen, Topoisomerase 1 inhibitors and cancer therapy, Hematol. Oncol. Clin. North Am. 26 (2012) 507–525.
98. V.R. Adams, T.G. Burke, T.G. Burke, Camptothecins in Cancer Therapy, Springer, Totowa, 2007.

2

Técnicas analíticas empleadas para el análisis de los derivados de la camptotecina y de la luotonina A

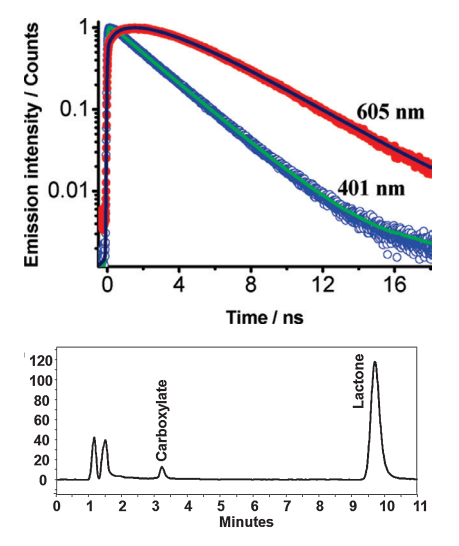

ABSTRACT ▶ El análisis de las moléculas derivadas de la camptotecina y de la luotonina A constituye un apasionante objeto de trabajo. Por un lado, su intensa fluorescencia convierte a la detección fluorimétrica en el método de elección para su detección analítica y muchos de los estudios relacionados con su fisicoquímica. Por otro, el equilibio de apertura y cierre del anillo tipo lactona (en el caso de los derivados de la camptotecina) y un complejo equilibrio de protonación (en el de los derivados de la luotonina A) plantea el desafío de desarrollar estrategias capaces de distinguir todas las formas que pueden coexistir simultáneamente. La gráfica de la parte superior muestra cómo la fluorescencia con resolución temporal permite distinguir las desactivaciones de las formas neutra y protonada de la camptotecina en una misma disolución. El cromatograma de la parte inferior es un ejemplo de cómo la separación por HPLC permite diferenciar las fracciones correspondientes a la forma intacta y abierta de un derivado de la camptotecina, siempre que las condiciones de recogida, pretratamiento y separación sean cuidadosamente elegidas para evitar la interconversión de una forma en otra. *Imágenes tomadas de las referencias 6 y 55.*

1. Luminiscencia de la camptotecina y fármacos derivados

1.1. Introducción

Muchos compuestos con actividad antitumoral como los derivados de antraciclinas, de la doxorubicina, de la elipticina, o de los indolocarbazoles, presentan una estructura heterocíclica con varios anillos aromáticos que, por lo general, hace que muestren una notable fluorescencia nativa [1]. Esta característica está presente también en los antitumorales con actividad inhibidora de topoisomerasa 1, tanto en la camptotecina como en la luotonina A, y puede ser utilizada con fines analíticos [2].

Desde el punto de vista espectrofluorimétrico, la camptotecina es un compuesto con un singular atractivo, ya que, al igual que ocurre con otros derivados de quinolina, la transición $n \rightarrow \pi^*$ puede intercambiar su energía con la transición $\pi \rightarrow \pi^*$ dependiendo de la naturaleza del disolvente, y así observarse el fenómeno denominado inversión de niveles [3].

1.2. Equilibrios de protonación

Aunque a comienzos de la década de los 90 se realizaron los primeros estudios espectroscópicos sobre la camptotecina [4], los trabajos pioneros en este campo se deben a Dey y Warner, quienes estudiaron el comportamiento de la camptotecina en disolución acuosa en el intervalo pH/H_o de -2 a 13. La titulación de la camptotecina lleva a estos autores a proponer los valores de pK_a = 0,7 y de pK_a^*= 1,18 correspondientes a la desprotonación de la camptotecina en estados fundamental y excitado respectivamente [5]. Por otro lado, la hidrólisis del anillo de lactona se produce lentamente a valores de pH de 5,0 o inferiores; sin embargo, es casi inmediata a valores por encima de pH 7,0 (Figura 1A), y la forma carboxilato abierta resultante tiene propiedades espectroscópicas diferentes.

Debido a las distintas formas de la camptotecina que pueden coexistir en disolución acuosa (protonada/desprotonada, lactona/carboxilato, fundamental/excitada) y considerando que los espectros de emisión de las distintas especies químicas pueden superponerse e interferir entre sí, las técnicas de fluorescencia con resolución temporal son de extremada utilidad para distinguir la proce-

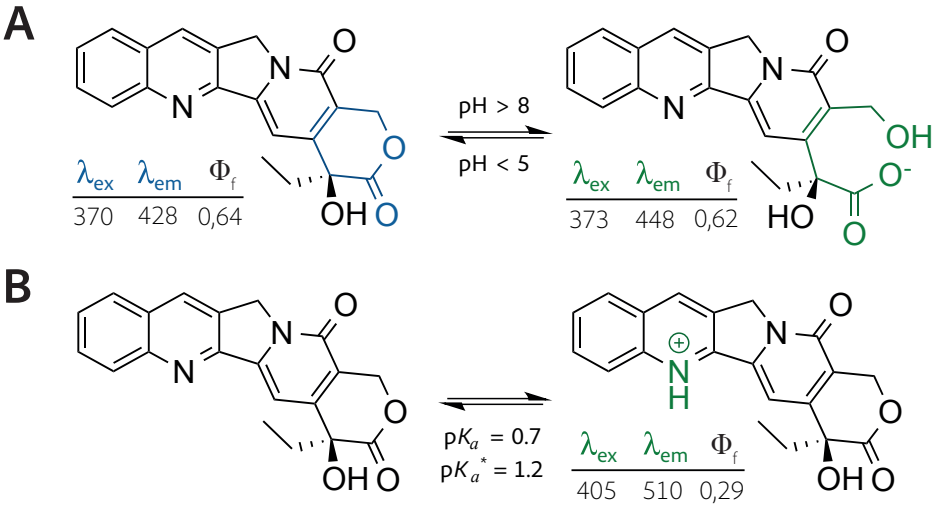

Figura 1. (A) Reacción de apertura del anillo de lactona y (B) equilibrio de protonación de la camptotecina, con las longitudes de onda de excitación y emisión características de cada forma (en nm), y sus rendimientos cuánticos [5].

dencia de las distintas emisiones observables en función de los tiempos de vida de fluorescencia de la camptotecina y sus derivados [6,7] (Figura 1B). Mediante la aplicación de estas técnicas se ha determinado que el nitrógeno tipo quinolina de la camptotecina presenta un pK_a* de 1,85. Las especies catiónica y neutra de la camptotecina coexisten en el intervalo de pH comprendido entre 1,5 y 3,0, pudiéndose distinguir por el valor de sus tiempos de vida de fluorescencia, correspondiendo el de la forma neutra a τ = 3,76 ns y el de la forma catiónica a τ = 2,83 ns. Las medidas de resolución temporal confirman y a la vez complementan los datos obtenidos mediante las medidas de fluorescencia convencional descritos por Dey y Warner, y además permiten establecer que el proceso de transferencia de protón en estado excitado es dependiente de la difusión.

En otros estudios se ha descrito cómo afecta el disolvente a la emisión de fluorescencia de la camptotecina, la importancia de la capacidad formadora de puentes de hidrógeno del disolvente sobre el rendimiento cuántico de la camptotecina y la contribución del entorno a que la naturaleza de la transición electrónica sea de tipo $n \rightarrow \pi^*$ o $\pi \rightarrow \pi^*$ [8].

1.3. Efecto del disolvente

En la Tabla 1 se recogen los parámetros de fluorescencia de la camptotecina en diferentes disolventes. La naturaleza del disolvente evaluada como parámetros de polaridad —constante dieléctrica o $E_T(30)$—, la capacidad de esta-

Tabla 1. Propiedades luminiscentes de la camptotecina en diferentes disolventes.

Disolvente	λ_{ex}	λ_{em}	Φ_f	τ_f
Ciclohexano	385, 368, 278, 257	420 (Espectro resuelto)	0,47	2,78
Benceno*	387, 369	424	0,56	
Dietil éter	384, 368, 292, 255	422	0,50	2,94
1,4-Dioxano	385, 368, 292, 254	425	0,52	2,97
Tetrahidrofurano	385, 369, 280, 256	424 / 422*	0,52 / 0,62*	2,96
1,2-Dimetoxietano	383, 367, 290, 254	424	0,53	3,05
Diclorometano*	381, 364, 287, 254	420	0,57	
Cloroformo	378, 364, 290, 256	422 / 420*	0,45 / 0,61*	2,51
Acetato de etilo*	380, 363, 289,254	422	0,59	
Isopropanol*	373, 358, 288, 253	420	0,62	
Acetonitrilo	377, 364, 289, 253	422 / 420*	0,54 / 0,69*	3,15
Etanol	369, 290, 253	428	0,60	3,52
Metanol	369, 289, 253	428 / 421*	0,61 / 0,62*	3,69
Etilenglicol	372, 290, 255	431	0,62	3,54
Tampón (pH = 5,1)	370, 252	428	0,64	3,99
Tampón (pH =7,02)*		420	0,76	

Valores tomados de [8] excepto los marcados con (*), que provienen de [11].

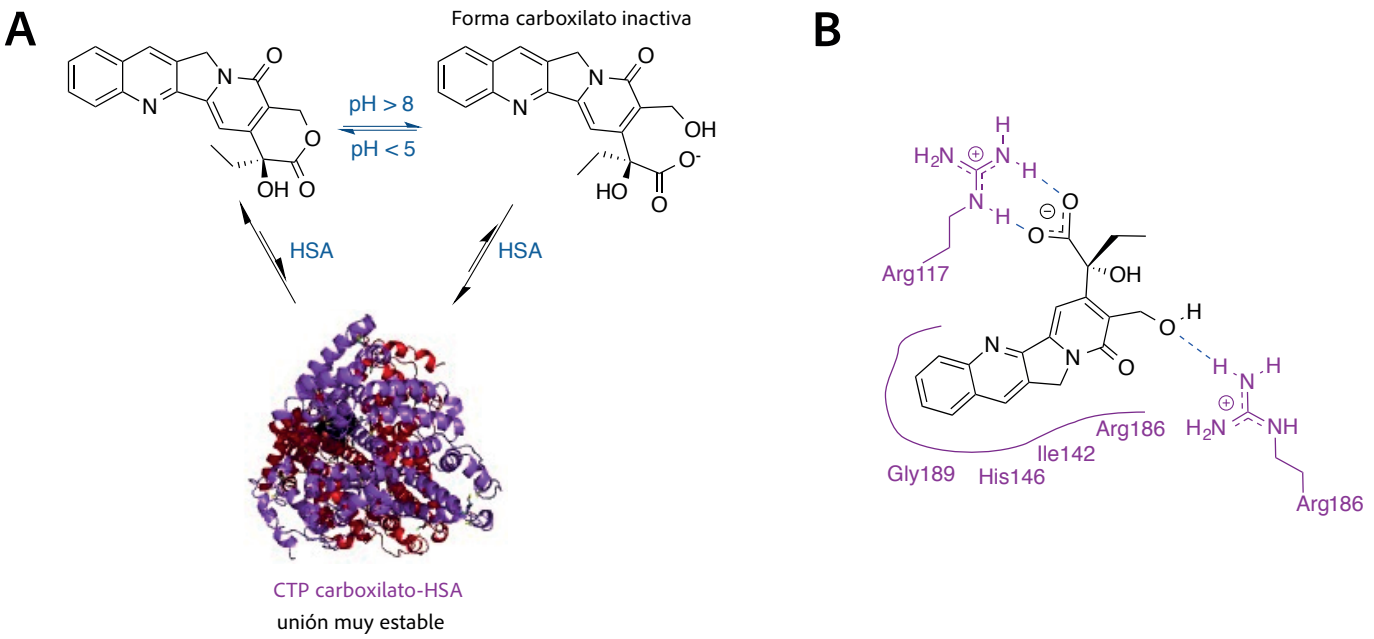

Figura 2.
(A) Unión de la camptotecina a la albúmina sérica humana preferentemente en su forma carboxilato. (B) Interacciones establecidas por la camptotecina carboxilato con la albúmina sérica humana. Tomado de PDB ref. 4L9K [Wang *et al.*, Biochim. Biophys. Acta (2013) 1830, 5356-5374]

blecer enlaces de hidrógeno, de aceptar o donar protones o su viscosidad, influyen no sólo en la la posición de los máximos o en el rendimiento cuántico de fluorescencia (Φ_f), sino también en los tiempos de vida de fluorescencia (τ_f) y en las constantes de desactivación radiante y no radiante de los estados excitados. Se ha estudiado cómo la capacidad de formar enlaces de hidrógeno de distintos disolventes influye en el equilibrio de transferencia de protón en estado excitado del topotecán [9].

Un estudio similar para el derivado 9-aminocamptotecina pone de manifiesto la relevancia de la introducción de pequeños sustituyentes (grupo amino) sobre la estructura pentacíclica de la camptotecina. Así, los rendimientos cuánticos de fluorescencia obtenidos para la 9-aminocamptotecina en disolventes polares son significativamente más bajos (entre 150 y 200 veces inferiores) que los correspondientes a la camptotecina [10], y sólo en cloroformo se obtienen valores de Φ_f semejantes para ambos compuestos.

Las modificaciones en la posición de los máximos y en el rendimiento cuántico de fluorescencia (Φ_f) como consecuencia del disolvente han sido utilizadas por Posokhov *et al.* [11] para determinar el momento dipolar de la camptotecina en estado excitado. Los resultados experimentales se correlacionan con los datos estimados a partir de cálculos teóricos. Además, en este estudio se pone de manifiesto que la molécula de camptotecina es extremadamente sensible al quenching por cobalto.

1.4. Medidas de anisotropía de fluorescencia

Debido a la notable fluorescencia nativa de la camptotecina, y de sus análogos de utilidad en clínica irinotecán y topotecán, se ha aplicado la anisotropía de fluorescencia en los estudios de interacción de estos compuestos antitumorales con membranas [12], nucleótidos como la guanina [13], polidesoxirribonucleótidos [14], macromoléculas como el ADN [15] o interaccionando con el surco menor del ADN [16]. Estos mismo autores han confirmado mediante electroforesis en gel que el topotecán es capaz de fracturar el ADN circular superenrrollado en ausencia de la topoisomerasa [17]. Los estudios de interacción del topotecán con el ADN ponen de manifiesto la mayor afinidad que presentan estos antitumorales por las zonas de la doble hélice ricas en pares de bases de tipo guanina y citosina [18].

Es relevante la unión de camptotecina o de sus derivados a proteínas como la albúmina sérica humana [19,20] (Figura 2). Esta proteína presente en la sangre es determinante para el transporte sérico del fármaco hacia su lugar de acción y, a su vez, es clave en la inactivación del antitumoral en torrente circulatorio debido a su unión estable con la forma carboxilato. Este fenómeno se produce tanto con la camptotecina como con los derivados que presentan un anillo E de lactona sin modificar. La medida de la fluorescencia y de la anisotropía de fluorescencia han permitido estudiar la inactivación en plasma del análogo de camptotecina 7-*terc*-butildimetilsil-10-hidroxicamptotecina (DB-67) y de su éster en menos de 2 horas. Esto es debido a que a pH fisiológico tiene lugar la apertura del anillo de lactona, y la forma abierta se une a la albúmina sérica humana haciendo imposible restablecer el equilibrio de formación de la lactona en presencia de ésta [21]. Estudios similares se han llevado a cabo para otros análogos [22].

1.5. HPLC

Desde el punto de vista analítico, la detección por fluorescencia en HPLC es la técnica de elección para la determinación de camptotecina, como se describe a continuación. Como ejemplo de la relevancia clínica de este recurso, cabe señalar que la determinación por HPLC o por HPTLC con detección fluorimétrica es la técnica utilizada en las unidades de citostáticos de los servicios de farmacia hospitalaria [23]. Se ha podido mejorar la sensibilidad y la selectividad de la determinación espectrofluorimétrica de la 7-etil-10-hidroxicamptotecina (SN-38) mediante el empleo de medios organizados (micelas y ciclodextrinas), un recurso que se ha aplicado a la cuantificación de este compuesto en orina humana [24].

1.6. Formación de complejos con CDs

La camptotecina y sus derivados son moléculas atractivas también para el estudio espectrofluorimétrico de la formación de complejos de inclusión con ciclodextrinas. Entre otras razones que justifiquen su estudio cabe señalar el incremento en estabilidad química del alcaloide y en su hidrosolubilidad, lo que mejora su biodisponibilidad. Se ha descrito el incremento en la solubilidad de la camptotecina entre 10 y 50 veces en presencia de α-CD, β-CD, γ-CD, (2-hidroxipropil)-β-CD, dimetil-β-CD (aleatoriamente sustituida) y dimetil-γ-CD (aleatoriamente sustituida). Los incrementos en las solubilidades son mayores para las CD sustituidas con respecto a las correspondientes CDs nativas [25]. En ese mismo trabajo se demuestra que la inclusión en las cavidades de las CDs dificulta el equilibrio de hidrólisis de la camptotecina. Este efecto es más marcado en el caso de la dimetil-β-CD. En los ensayos de disolución y liberación se ha observado una importante mejora en la liberación de este antitumoral gracias a la inclusión de la camptotecina en nanopartículas anfifílicas poliméricas de ciclodextrina [26].

La solubilización de la camptotecina es dependiente del pH, por lo que se ha estudiado mediante HPLC con detección de fluorescencia el proceso de inclusión a distintos valores de pH para hallar los valores de las constantes de afinidad que presentan en cada caso las formas lactona y carboxilato. Las constantes de asociación para los complejos CPT/(2-hidroxipropil)-β-CD son mayores para la forma lactona que para la forma carboxilato [27].

Con el fin de determinar los valores de sus constantes de asociación, la inclusión de la camptoptecina y algunas homocamptotecinas con β-CD y (2-hidroxipropil)-β-CD se ha estudiado mediante espectrofluorimetría, espectrometría de masas, HPLC con columnas quirales de ciclodextrinas y electroforesis capilar incorporando CDs al tampón de separación [28].

2. Luminiscencia de la luotonina A y sus análogos

A pesar de la relevancia biológica y su interés terapéutico como inhibidor de topoisomerasa 1, hasta el momento no se habían descrito sus propiedades luminiscentes. Los primeros trabajos que describen las propiedades fluorescentes de la luotonina A, su rendimiento cuántico de fluorescencia, la influencia del disolvente en sus propiedades químicas y espectroscópicas, así como los procesos de transferencia de protón en estado excitado (ESPT) constituye uno de los objetivos de esta memoria.

Sólo recientemente las propiedades espectrofluorimétricas de la luotonina A han sido objeto del interés de otro grupo de investigación [29], observándose una notable fluorescencia con un rendimiento cuántico en agua (véase Tabla 2), cercana a la del sulfato de quinina (Φ_f = 0,546) utilizado como referencia. La fluorescencia de este compuesto es dependiente del entorno, mostrando una mayor intensidad en agua que en disolventes de menor polaridad. Asimismo, se ha puesto de manifiesto cómo la formación de enlaces de hidrógeno con el disolvente prolonga el tiempo de vida del estado excitado y constituye un primer paso a la protonación fotoinducida de la molécula (Figura 3). También se ha descrito la capacidad de formar complejos de estequiometría 1:1 con metales como la Ag^+, el Zn^{2+} o el Cd^{2+}; por ello, se ha propuesto como sensor para la detección selectiva de estos cationes.

En otros trabajos de nuestro grupo, se ha estudiado la interacción de la luotonina A con el ADN usando la amortiguación de su fluorescencia por determinados quenchers (I^- y Co^{2+},) [30] (Figura 4). La titulación espectrofluorimétrica con ADN, los valores de anisotropía de fluorescencia, así como los ensayos de desplazamiento del bromuro de etidio permiten afirmar que el modo de unión al ADN que presentan la luotonina A y dos análogos de nueva síntesis es a través del surco menor de la doble hélice. El hecho de que estos compuestos se unan únicamente al ADN de doble cadena, unido a los cambios que esta unión provocan en su fluorescencia, hacen de este tipo de moléculas unos excelentes sen-

Tabla 2. Valores de rendimiento cuántico y tiempo de vida de fluorescencia de la luotonina A en diferentes disolventes [29].

Disolvente	Φ_f	τ_f
Tolueno	0,046	0,15
Diclorometano	0,098	0,37
Acetonitrilo	0,082	0,43
Etanol	0,100	0,54
Agua	0,460	2,70

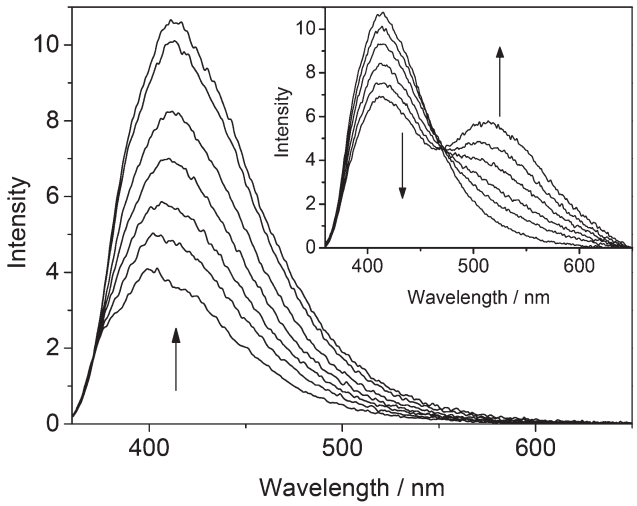

Figura 3.
Espectros de emisión de fluorescencia de la luotonina A en CH_2Cl_2 en presencia de cantidades crecientes (0-65 mM) de hexafluoro-2-propanol como donador de enlaces de hidrógeno. El recuadro superior corresponde a un exceso del reactivo (0-0,58 M). Nótese cómo a concentraciones mayores del alcohol, aparece el máximo de emisión correspondiente a la forma protonada [29].

sores fluorescentes para la detección de la hibridación del ADN.

Al igual que en el caso de la camptotecina, existe un interés creciente en el estudio de los complejos de inclusión de luotonina A con α–CD, β-CD, γ-CD nativas. Se han estudiado estos complejos mediante espectrofotometría de absorción UV-Vis, espectrometría de RMN y espectrometría de masas, si bien por el momento no se han estudiado mediante espectrofluorimetría. Los datos experimentales obtenidos en la caracterización de estos complejos se han comparado con las predicciones de los cálculos teóricos de química cuántica [31]. En consecuencia, la caracterización espectrofluorimétrica de los complejos de inclusión luotonina A con CDs es aún un campo por explorar.

3. Análisis cromatográfico de camptotecina y análogos

Un desafío en el análisis cromatográfico de la camptotecina lo constituye la presencia del anillo de lactona. Puesto que, como se ha explicado, es susceptible de hidrolizarse a pH fisiológico, en los estudios farmacocinéticos de la camptotecina y sus derivados se hace necesario poder cuantificar la fracción de fármaco que permanece intacto y, por tanto, mantiene su actividad biológica. Distintas revisiones recopilan las metodologías cromatográficas que permiten la separación y cuantificación de estos antitumorales [32-36]. Algunos de estos artículos de revisión ponen especial énfasis en los procedimientos de tratamiento analítico previo a la cuantificación por HPLC [37].

En la Tabla 3 se recogen diferentes metodologías analíticas (cromatográficas, espectroscópicas y electroanalíticas) para la determinación de camptotecina y sus análogos inhibidores de topoisomerasa I.

Figura 4.
Demostración de la interacción preferente del compuesto 2 (ver Parte Experimental, Resultados y Discusión) con el ADN de doble cadena (dsDNA). El incremento de la anisotropía de fluorescencia y el quenching producido como consecuencia de la interacción con la macromolécula son mucho menores en el caso del ADN de cadena sencilla [30].

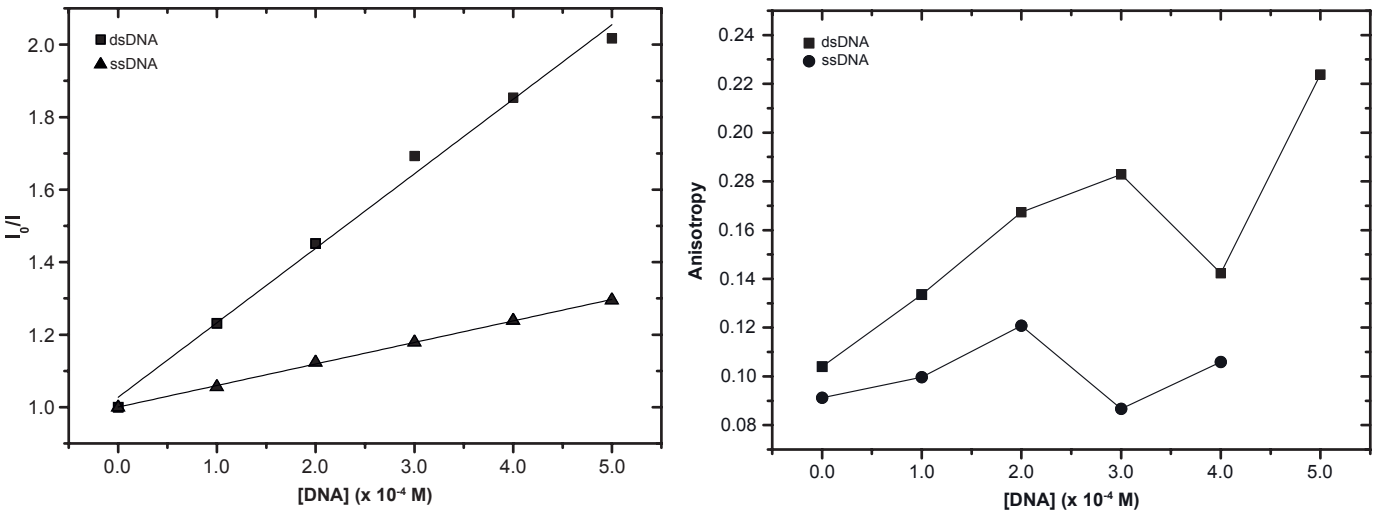

Tabla 3. Ejemplos de de análisis de camptotecina y algunos de sus derivados en distintas matrices (continúa en página siguiente).

Analito/muestra	Técnica analítica	Comentarios	Ref.
Camptotecina en *Nothapodytes foetida*	HPLC-UV. FE: C-18. FM: MeCN:tampón fosfato de amonio, 45:55, v:v. Elución isocrática. Detección a λ_{max} = 254 nm	Comparación de métodos de extracción: agitación magnética, ultrasonidos, microondas y Soxhlet	[38]
Camptotecina y gimatecán / Pureza enantiomérica	HPLC-MS/MS. FE: Quiral. FM: *n*-hexano:CH_2Cl_2, 50:50, v:v	Sin pretratamiento	[39]
Separación quiral de los enantiomeros de namitecán	HPLC-UV y -MS. FE: Columnas de quiralidad inversa. FM: *n*-hexano: CH_2Cl_2, 40:60, v:v	Sin pretratamiento	[40]
Resolución de enantiómeros de derivados de homocamptotecina	HPLC-DAD. FE: Chiracel OD-H. FM: hexano:2-propanol. Elución isocrática	Sin pretratamiento	[41]
Determinación de pureza enantiomérica en derivados de homocamptotecina	CZE-FD. Tampón de separación: fosfato 75 mM y trietanolamina (pH 2,5) : MeCN, 95:5, v:v. Se incorpora β-ciclodextrina sulfatada o carboximetil-β-ciclodextrina como selectores quirales	Sin pretratamiento	[42]
Liberación de camptotecina vehiculizada en nanopartículas de sílice de superficie modificada	HPLC	Precipitación de las proteínas séricas con ácido tricloroacético, centrifugación. Disolución del sobrenadante en la fase móvil	[43]
Camptotecina / órganos de animales a los que se les ha administrado vehiculizada como nano-partículas de lípidos sólidos	UFLC-FD. FE: C-18 . FM: Gradiente, trietilamina y ácido acético pH = 5,5: MeCN. 1,2 mL/min, 30 °C	Desproteinización con ácido fosfórico 0,15 M y MeCN. Agitación y centrifugación	[44]
Camptotecina y 10-hidroxicamptotecina / plasma humano	HPLC-UV-Vis, -FD y -MS. FE: C-18 . FM: MeOH:tampón fosfato (pH=3,9), 50:50, v:v; 0,8 mL/min. Detección a λ_{max} = 254 nm y a λ_{ex} = 370, λ_{em} = 440 nm	Congelación a -20 °C, centrifugación y SPME on-line. SPME: capilar de poli(ácido metaacrílico - dimetacrilato de etilénglicol) monolítico	[45]
10-hidroxicamptotecina / tejido hepático de ratón	HPLC-FD. FE: C-18. FM: H_2O:MeCN elución en gradiente. Caudal 1,5 mL/min. Tiempo de separación 25 min. Detección: λ_{ex} = 383, λ_{em} = 553 nm	Tejido hepático homogeneizado con fosfato de sodio al 1%. Agitación con CH_2Cl_2 y centrifugación. El sobrenadante se lava, liofiliza y redisuelve en FM	[46]
10-hidroxicamptotecina / cultivos celulares	HPLC-FD. FE: Diamosil C-18 . FM: disolución tampón de ácido fosfórico y trietilamina (pH 3,0):MeCN, 75:25, v:v. Elución isocrática, 1,0 mL/min, 35 °C. Detección: λ_{ex} = 382, λ_{em} = 528 nm	Lisis por sonicación en frío. Desproteinización con ácido fosfórico. Extracción con acetato de etilo. El sobrenadante se evapora y se reconstituye con la FM	[47]
10-metoxicamptotecina y su metabolito 10-hidroxicamptotecina / plasma de rata	HPLC-MS. FE: fenil silano. FM: Gradiente acetato de amonio (pH 3,0):MeCN.	Desproteinización con ácido acético. Extracción con éter dietílico. Sobrenadante se evapora y redisuelve en FM	[48]
Camptotecina y sus ésteres acetilado (CZ44) y propanoilado (CZ48) en el anillo de lactona / plasma de ratón	HPLC-FD. FE: Synergi C-18. FM: gradiente, CH_3COOH 0,1% (pH 3,0):MeCN. 1,2 mL/min. . Detección: λ_{ex} = 380, λ_{em} = 418 nm	Desproteinización con ácido acético. Extracción con éter dietílico. Sobrenadante se evapora y redisuelve en FM con MeCN:H_2O	[49]
Camptotecina (lactona y forma abierta) y SN-38) / células y tejidos tumorales	HPLC-DAD -FD. FE: C-18 . FM: Gradiente, MeOH:acetato de amonio	Lisis por sonicación en frío. SPE	[50]
9-nitrocamptotecina y 9-aminocamptotecina / suero humano	HPLC-DAD y -FD. FE: C-8. FM: MeOH:tampón fosfato pH 2,5 (10 mM), 48:52, v:v	SPE (C-18)	[51]
9-nitrocamptotecina formas lactona y carboxilato / suero humano	HPLC-UV. FE: C-8 (25 cm, 4,0 mm, 5 µm). FM: MeCN:H_2O (pH 3,5) 43:57, v:v. Detección a λ_{max} = 370 nm	Desproteinización con MeCN en frío. El sobrenadante se evapora y redisuelve en FM	[52]
Glucuorónido de 9-aminocamptotecina / líneas celulares tumorales	HPLC-FD. FE: C-18 . FM: MeOH:tampón fosfato pH 6,5 (5 mM), 50:50, v:v. Detección: λ_{ex} = 300-395, λ_{em} = 430-470 nm. Para el análisis de topotecán y 10-hidroxicamptotecina, FM: MeCN:trietilamna (3%)/CH_3COOH pH 5,5; 80:20; v:v	Desproteinización con MeOH en frío. Dilución de los sobrenadantes con MeCN: trietilamna (3%), pH 5,5 (ajustado con CH_3COOH)	[53]
Camptotecina y tiocamptotecina / estudio del equilibrio de hidrólisis	HPLC-UV-Vis y -FD. FE: fenil silano. FM: tampón acético/acetato de dietil amina:MeCN. Detección: λ_{ex} = 370, λ_{em} = 421 nm	Desarrollo del método cromatográfico, N/A pretratamiento.	[54]
AR-67 en forma lactona y carboxilato / sangre completa	HPLC-FD. FE: C-18. FM: tampón acetato de amonio (pH=6,5)/dihidrógeno fosfato de tetrabutil amonio:MeCN, 65:35, v:v, 1 mL/min.	Lisis de eritrocitos, desproteinización con MeOH en frío. Dilución previa a análisis	[55]

Tabla 3. (continuación).

Analito/muestra	Técnica analítica	Comentarios	Ref.
Irinotecán y SN-38 / plasma de rata	HPLC-FD. FE: C-18. FM: MeCN:tampón fosfato (pH 6,4); 25:75, v:v. Detección: λ_{ex} = 380, λ_{em} = 540 nm	Desproteinización con MeCN:MeOH	[56]
Irinotecán y SN-38/plasma y bilis de rata	HPLC-UV. FE: C-18. FM: Gradiente, MeCN:ácido fosfórico (pH 3,0). 1 mL/min	Precipitación de las proteínas con MeCN frío con un 1% de CH_3COOH	[57]
Irinotecán y SN-38 / plasma de rata	HPLC-FD. FE: C-18. FM: fosfato 50 mM (pH 4,0)/0,2% de heptanosulfonato de sodio:MeCN, 30:70, v:v. λ_{ex} = 380, λ_{em} = 540 nm	Precipitación de proteínas con SDS y ácido fosfórico	[58]
Irinotecán y sus dos principales metabolitos activos, SN-38 y su glucurónido, SN-38G / plasma humano	HPLC-MS/MS. FE: C-18 . FM: gradiente, HCOOH 0,05%: MeCN. 0,3 mL/min,30 °C	Desproteinización con MeCN. Evaporación del disolvente y reconstitución con la FM	[59]
Irinotecán y su metabolitos activos/plasma de oveja. Determinación tanto de las formas lactonas como de las formas abiertas	HPLC-FD. FE: C-18. FM: tampón fosfato pH 3.0: MeCN, 72:28, v:v. 1,45 mL/min. Detección: λ_{ex} = 355, λ_{em} = 515 nm	Liofilización del plasma sin calor	[60]
Irinotecán y su metabolito activo/orina y saliva	CZE- y MEKCC-DAD. CZE: Potencial aplicado 25 kV. Tampón de separación: tampón borato (pH 8,8), conteniendo SDS y MeCN. MEKCC: FE: C-18. FM: Gradiente, MeCN:acetato de amonio	Desproteinización con MeCN:MeOH, adición de tampón de electroforesis y centrifugación. Orina desproteinizada con MeOH, adición de tampón de electroforesis y centrifugación	[61]
Irinotecán y sus principales metabolitos / plasma y saliva humana. Estudio farmacocinético. Correlación entre los niveles en plasma y saliva	HPLC-FD. FE: C-18. FM: gradiente, MeCN:tampón fosfato (pH 4,0). Detección: λ_{ex} = 370, λ_{em} = 470 nm	Desproteinización con MeCN:MeOH y acidificación con HCl	[62]
Irinotecán en glóbulos rojos y en sangre	HPLC-FD. FE: C-18. FM: MeOH:acetato de amonio 0,1 M + sulfato de tetrabutilamonio 0,01 M (pH=5,2), 35:60, v:v.	Liofilización. Reconstitución para análisis, desproteinización con $MeOH/HClO_4$	[63]
Irinotecán y su metabolito activo/saliva de enfermos de cáncer. Monitorización clínica	HPLC-FD. FE: C-18. FM: MeCN:fosfato 50 mM, (pH 3,0), 28:72, v:v/heptanosulfonato sódico 5 mM	Demostración de la buena correlación entre los niveles plasmáticos y los detectados en saliva	[64]
Irinotecán y su metabolito 4-piperidinopiperidina/Plasma humano. Farmacocinética en enfermos de cáncer	HPLC-MS (detector de triple cuadrupolo). FE: Fenilsilano . FM: MeCN:tampón acetato de amonio (pH=4,0), 80:20, v:v	Dilución con agua, centrifugación, SPE (C-18, MeOH:H_2O)	[65]
Metabolización del irinotecán / plasma humano	HPLC-FD. FE: C-18. FM: MeCN:fosfato de potasio 0,05 M (pH=3,5), 30:70, v:v. Detección: λ_{ex} = 373, λ_{em} = 428 nm	SPE C-18	[66]
Irinotecán y su metabolito activo SN-38 / plasma y tejidos de ratón	FE: fenil-silano. FM: MeCN:acetato de amonio 20 mM (pH=3,5), 35:65, v:v	Desproteinización por MeCN en placas de 96 pocillos. Evaporación y redisolución en FM	[67]
Irinotecán y su metabolito activo / líneas celulares tumorales. Estudios de acumulación	HPLC-FD. FE: C-18 . FM: MeCN:fosfato 50 mM/1-heptano sulfonato de sodio (pH 3,0) 27:73, v:v. Detección: λ_{ex} = 380, λ_{em} = 540 nm	Desproteinización con MeOH/HCl 0,1 M y sonicación	[68]
Irinotecán y topotecán / metodología para una unidad de quimioterapia	HPLC- y HPTLC-FD. FE: C-18 . FM: Gradiente, MeCN:di-hidrógeno fosfato de sodio 50 mM (pH 3,5), 50 °C. Detección: λ_{ex} = 355, λ_{em} = 515 nm	Dilución con MeOH:H_2O	[23]
Clorhidrato de irinotecán/Inyectables para administración intravenosa	HPLC-FD. FE: C-18. FM: 28:72 MeCN: dihidrógeno fosfato de sodio 50 mM / ácido heptanosulfónico 5 mM y trietilamina 0,03%	Dilución en FM	[69]
Metabolito activo del irinotecán (formas lactona y carboxilato) / nanopartículas	HPLC-UV. FE: C-18. FM: MeCN:di-hidrógeno fosfato potásico (pH=3,0):1-octano sulfonato de sodio, 40:30:30, v:v:v	Agitación rotatoria en disolución tampón fosfato (pH=7,4) a 37 °C. Centrifugación y filtración	[70]
Irinotecán, su metabolito activo SN-38 y su glucurónido, SN-38G en plasma humano y porcino.	UHPLC-MS. FE: C-18. FM: Gradiente, MeOH:HCOOH 0,1%.	Liofilización sin calor. Reconstitución y acidificación con HCOOH 1%. Centrifugación y SPE	[71]
Irinotecán / formas farmacéuticas comerciales	Voltamperometría diferencial de impulsos y comparación con HPLC. Electrodo de pasta de carbono modificado con nanotubos de carbono multicapa y azul de metileno polimerizado como mediador/indicador redox.	Dilución con monohidrogeno fosfato de sodio (pH=7,0, fuerza iónica ajustada a 0,1 M) como electrolito soporte	[72]

Tabla 3. (continuación).

Analito/muestra	Técnica analítica	Comentarios	Ref.
Trazas de camptotecina, en presentaciones comerciales de topotecán e irinotecán / Formas farmacéuticas	Determinación por fluorescencia inducida por láser mediante derivatización por vía fotoquímica	Derivatización en medio fuertemente básico. Comparación con HPLC-FD	[73]
Topotecán / Plasma y sangre completa	Fluorescencia con excitación de bifotónica con láser de 820 nm	Heparinización de las muestras	[74]
Topotecán formas lactona y carboxilato/suero humano	HPLC-FD. FE: RAM-MFP (*restricted access media-mixed functional phase*). FM: MeOH:fosfato potásico 0,05 M/1% trietilamina (pH=6,6), 13:87, v:v. Detección: λ_{ex} = 390, λ_{em} = 520 nm	Centrifugación.	[75]
Topotecán/modelo de permeabilidad y absorción intestinal	HPLC-DAD. FE: C-18 . FM: Gradiente, MeCN:fosfato (pH 3,0)	No es necesario pretratamiento	[76]
Exatecán, un derivado de camptotecina conjugado con un polialcohol de carboximetildextranos / sangre completa, eritrocitos y saliva	HPLC-FD. FE: C-18 . FM: CH_3COOH 0,1 M (pH=5,0):tetrahidrofurano, 15:1, v:v. ó CH_3COOH 0,1 M (pH=5,0): MeOH, 10:12, v:v. 60 °C. Detección: λ_{ex} = 375, λ_{em} = 445 nm	Desproteinización con MeCN, evaporación, reconstitución con FM	[77]
Gimatecán / plasma humano	HPLC-FD. FE: fenilhexil-silano. FM: HCOOH 0,1 M:MeCN:2-propanol, 5:4:0,1, v:v:v. Detección: λ_{ex} = 370, λ_{em} = 510 nm	Desproteinización con HCOOH:MeCN, dilución en FM	[78]
Gimatecán y su metabolito ST1698 / plasma humano	HPLC-FD. FE: fenilhexil-silano. FM: HCOOH 0,1 M:MeCN:2-propanol, 5:4:0,1, v:v:v. Detección: λ_{ex} = 370, λ_{em} = 510 nm	Desproteinización con HCl	[79]
Silatecanes / plasma y microsoma hepático de ratones	HPLC-MS (selected ion monitoring) y HPLC-FD. FE: C-18. FM: CH_3COOH (pH 7,2):MeOH, 55:45, v:v. (en algunos casos, 70:30. 0,25 mL/min. Detección λ_{ex} = 367-379, λ_{em} = 438-546 nm según compuesto	Desproteinización con MeOH:MeCN, dilución con FM	[80]
Luotonina A / microsomas hepáticos	HPLC-ESI-MS/MS. FE: C-18. FM: Gradiente, HCOOH 0,1 M:MeCN	Adición de acetato de etilo sobre las células hepáticas y centrifugación. Evaporación y reconstitución en HCOOH 0,1%:MeOH	[81]

FM: fase móvil; FE: fase estacionaria

Referencias

1. J. Aaron, S. Trajkovska, Fluorescence Studies of Anti-Cancer Drugs-Analytical and Biomedical Applications, Current Drug Targets. 7 (2006) 1067–1081.
2. S. Kruszewski, D.M. Kruszewska, Fluorescence spectroscopy in camptothecins studies, Acta Phys Pol, A. 118 (2010) 99–102.
3. G.G. Guilbault, Practical fluorescence, M. Dekker, New York, 1990.
4. J. Fassberg, V.J. Stella, A kinetic and mechanistic study of the hydrolysis of camptothecin and some analogues, J Pharm Sci. 81 (1992) 676–684.
5. J. Dey, I. Warner, Excited state tautomerization of camptothecin in aqueous solution, J Photochem Photobiol. 101 (1996) 21–27.
6. M.R. di Nunzio, B. Cohen, A. Douhal, Structural photodynamics of camptothecin, an anticancer drug in aqueous solutions, J. Phys. Chem. A. 115 (2011) 5094–5104.
7. M.R. di Nunzio, Y. Wang, A. Douhal, Structural Photodynamic Behavior of Topotecan, a Potent Anticancer Drug, in Aqueous Solutions at Different pHs, J Phys Chem B. 116 (2012) 8182–8190.
8. J. Dey, I. Warner, Spectroscopic and photophysical studies of the anticancer drug: Camptothecin, J Lumines. 71 (1997) 105–114.
9. M.R. di Nunzio, Y. Wang, A. Douhal, Structural spectroscopy and dynamics of inter- and intramolecular H-bonding interactions of topotecan, a potent anticancer drug, in organic solvents and in aqueous solution, J Phys Chem B. 116 (2012) 7522–7530.
10. J. Dey, I.M. Warner, Charge-transfer effects on the fluorescence spectra of 9-aminocamptothecin steady-state and time-resolved fluorescence studies, J Photochem Photobiol A: Chem. 116 (1998) 27–37.
11. Y. Posokhov, H. Biner, S. Içli, Spectral-luminescent and solvatochromic properties of anticancer drug camptothecin, J Photochem Photobiol A: Chem. 158 (2003) 13–20.
12. B. Selvi, S. Patel, M. Savva, Physicochemical characterization and membrane binding properties of camptothecin, J Pharm Sci. 97 (2008) 4379–4390.
13. K. Steenkeste, E. Guiot, F. Tfibel, P. Pernot, Camptothecins–guanine interactions: mechanism of charge transfer reaction upon photoactivation, Chem Phys. 275 (2002) 93–108.
14. S. Strel'tsov, S. Grokhovskii, I. Kudelina, V.A. Oleinikov, A.L. Zhuze, Interaction of Topotecan, DNA Topoisomerase I Inhibitor, with Double-Stranded Polydeoxyribonucleotides. 1. Topotecan Dimerization in Solution, Mol. Biol. (Mosk). 35 (2001) 365–373.
15. S.A. Strel'tsov, A.L. Mikheikin, I.D. Nechipurenko, Interaction of topotecan, DNA topoisomerase I inhibitor, with dual-stranded polydeoxyribonucleotides. II. Formation of a complex containing several DNA molecules in the presence of topotecan, Mol Biol (Mosk). 35 (2001) 374–381.
16. S.A. Strel'tsov, A.L. Mikheikin, S.L. Grokhovskii, V.A. Oleinikov, A.L. Zhuze, Interaction of topotecan, DNA topoisomerase I inhibitor, with double-stranded polydeoxyribonucleotides. III. Binding at the minor groove, Mol Biol (Mosk). 36 (2002) 400–411.
17. S.L. Grokhovskii, S.A. Strel'tsov, A.L. Zhuze, Interaction of topotecan, DNA topoisomerase I inhibitor, with dual-stranded polydeoxyribonucleotides. V. Topotecan is able to cause single- and double-strand breaks in ring superhelical DNA in the absence of enzyme, Mol Biol (Mosk). 37 (2003) 888–896.
18. S.A. Strel'tsov, A.L. Mikheikin, S.L. Grokhovskii, V.A. Oleinikov, I.A. Kudelina, A.L. Zhuze, Interaction of topotecan, DNA topoisomerase I inhibitor, with double-stranded polydeoxyribonucleotides. 4. Topotecan binds preferably to the GC base pairs of DNA, Mol Biol (Mosk). 36 (2002) 736–753.
19. H.-H. Sun, J. Zhang, Y.-Z. Zhang, L.-Y. Yang, L.-L. Yuan, Y. Liu, Interaction of human serum albumin with 10-hydroxycamptothecin: spectroscopic and molecular modeling studies, Mol. Biol. Rep. 39 (2012) 5115–5123.
20. T. Wybranowski, M. Cyrankiewicz, B. Ziomkowska, S. Kruszewski, The HSA affinity of warfarin and flurbiprofen determined by fluorescence anisotropy measurements of camptothecin, BioSystems. 94 (2008) 258–262.
21. S. Kruszewski, B. Ziomkowska, M. Cyrankiewicz, T. Wybranowski, The comparison of biophysical properties of DB-67 and its ester DB-67-4ABTFA determined by fluorescence spectroscopy methods, BioSystems. 94 (2008) 270–275.
22. S. Kruszewski, D. Bom, B. Ziomkowska, M. Cyrankiewicz, Affinity of new anticancer agent, DB-174, to membranes and HSA determined by fluorescence spectroscopy methods, Opt Appl. 36 (2006) 199–207.
23. E. Gravel, P. Bourget, L. Mercier, A. Paci, Fluorescence detection combined with either HPLC or HPTLC for pharmaceutical quality control in a hospital chemotherapy production unit: application to camptothecin derivatives, J Pharm Biomed Anal. 39 (2005) 581–586.
24. M.I. Rodríguez-Cáceres, D. Bohoyo Gil, I. Durán-Merá, M.C. Hurtado Sánchez, Spectrofluorimetric determination of SN-38, a promising new anti-tumor agent, in the presence and absence of organized media, Appl Spectrosc. 65 (2011) 298–306.
25. J. Kang, V. Kumar, D. Yang, P.R. Chowdhury, R.J. Hohl, Cyclodextrin complexation: influence on the solubility, stability, and cytotoxicity of camptothecin, an antineoplastic agent, Eur J Pharm Sci. 15 (2002) 163–170.

26. Y. Çirpanli, E. Bilensoy, A.L. Dogan, S. Çalis, Comparative evaluation of polymeric and amphiphilic cyclodextrin nanoparticles for effective camptothecin delivery, Eur J Pharm Biopharm. 73 (2009) 82–89.
27. A.M. Saetern, N.B. Nguyen, A. Bauer-Brandl, M. Brandl, Effect of hydroxypropyl-beta-cyclodextrin-complexation and pH on solubility of camptothecin, Int J Pharm. 284 (2004) 61–68.
28. C. Foulon, J. Tedou, T. Queruau Lamerie, C. Vaccher, J. Bonte, J.-F. Goossens, Assessment of the complexation degree of camptothecin derivatives and cyclodextrins using spectroscopic and separative methodologies, Tetrahedron: Asymmetry. 20 (2009) 2482–2489.
29. Z. Miskolczy, L. Biczók, Effect of hydrogen bonding and complexation with metal ions on the fluorescence of luotonin A, Photochem. Photobiol. Sci. 12 (2013) 936–943.
30. P. Mussardo, E. Corda, V. González-Ruiz, J. Rajesh, S. Girotti, M.A. Martín, et al., Study of non-covalent interactions of luotonin A derivatives and the DNA minor groove as a first step in the study of their analytical potential as DNA probes, Anal Bioanal Chem. 400 (2011) 321–327.
31. B. Ivanova, M. Spiteller, Novel pyrrolo-quinazolino-quinoline analogues of the natural alkaloids and their inclusion molecular complexes in the native cyclodextrins: experimental versus theoretical study, J Incl Phenom Macrocycl Chem. 76 (2013) 87–98.
32. S. Nussbaumer, P. Bonnabry, J.-L. Veuthey, S. Fleury-Souverain, Analysis of anticancer drugs: A review, Talanta. 85 (2011) 2265–2289.
33. M. Ramesh, P. Ahlawat, N.R. Srinivas, Irinotecan and its active metabolite, SN-38: review of bioanalytical methods and recent update from clinical pharmacology perspectives, Biomed Chromatogr. 24 (2010) 104–123.
34. T. Oguma, Antitumor drugs possessing topoisomerase I inhibition: applicable separation methods, J Chromatogr B. 764 (2001) 49–58.
35. M. Palumbo, C. Sissi, B. Gatto, S. Moro, G. Zagotto, Quantitation of camptothecin and related compounds, J Chromatogr B. 764 (2001) 121–140.
36. L. Zufía, A. Aldaz, J. Giráldez, Separation methods for camptothecin and related compounds, J Chromatogr B. 764 (2001) 141–159.
37. T.H. Tsai, Analytical approaches for traditional chinese medicines exhibiting antineoplastic activity, J Chromatogr B. 764 (2001) 27–48.
38. D.P. Fulzele, R.K. Satdive, Comparison of techniques for the extraction of the anti-cancer drug camptothecin from Nothapodytes foetida, J Chromatogr A. 1063 (2005) 9–13.
39. E. Badaloni, W. Cabri, A. Ciogli, R. Deias, F. Gasparrini, F. Giorgi, et al., Combination of HPLC "inverted chirality columns approach" and MS/MS detection for extreme enantiomeric excess determination even in absence of reference samples. Application to camptothecin derivatives, Anal Chem. 79 (2007) 6013–6019.
40. E. Badaloni, W. Cabri, A. Ciogli, I. D'Acquarica, R. Deias, F. Gasparrini, et al., Extending the use of "Inverted Chirality Columns Approach" for enantiomeric excess determination in absence of reference samples: Application to a water-soluble camptothecin derivative, J Chromatogr A. 1217 (2010) 1024–1032.
41. J.-F. Goossens, C. Foulon, C. Bailly, D. Bigg, J. Bonte, C. Vaccher, Chiral resolution of enantiomers of homocamptothecin derivatives, antitumor topoisomerase I inhibitors, using high performance liquid chromatography on polysaccharide-based chiral stationary phases, Chromatographia. 59 (2004) 305–313.
42. J.-F. Goossens, C. Mahieu, N. Dias, C. Bailly, P. Principe, J.-P. Bonte, et al., Chiral capillary electrophoretic determination of the enantiomeric purity of homocamptothecin derivatives, promising antitumor topoisomerase I inhibitors, using highly sulfated CDs and fluorescence detection, Environ Res. 27 (2006) 4717–4729.
43. P. Botella, I. Abasolo, Y. Fernández, C. Muniesa, S. Miranda, M. Quesada, et al., Surface-modified silica nanoparticles for tumor-targeted delivery of camptothecin and its biological evaluation, J Control Release. 156 (2011) 246–257.
44. S.M. Martins, T. Wendling, V.M.F. Gonçalves, B. Sarmento, D.C. Ferreira, Development and validation of a simple reversed-phase HPLC method for the determination of camptothecin in animal organs following administration in solid lipid nanoparticles, J Chromatogr B. 880 (2012) 100–107.
45. Y. Wen, Y. Fan, M. Zhang, Y.-Q. Feng, Determination of camptothecin and 10-hydroxycamptothecin in human plasma using polymer monolithic in-tube solid phase microextraction combined with high-performance liquid chromatography, Anal Bioanal Chem. 382 (2005) 204–210.
46. J. Zheng, H. Guo, N. Guo, W. Ma, L. Jing, R. Zhang, et al., A two-step pH-dependent liquid-liquid extraction combined with HPLC-fluorescence method for the determination of 10-hydroxycamptothecin in mouse liver tissue, Pharm Biol. 50 (2012) 954–961.
47. Y.-X. Zhao, J.-Q. Gao, H.-L. Qiao, H.-L. Chen, W.-Q. Liang, Development and validation of a sensitive reversed-phase HPLC method to determine intracellular accumulation of hydroxycamptothecin, J Pharm Biomed Anal. 41 (2006) 1007–1010.
48. J. Zheng, R. Zhang, C. Shao, Z. Hu, D. Wang, T. Yu, et al., Development and validation of a RP-HPLC method with fluorescence detection for simultaneous determination of 10-methoxycamptothecin and its metabolite 10-hydroxycamptothecin in rat plasma, J Chromatogr B. 903 (2012) 81–87.

49. X. Liu, Y. Wang, D. Vardeman, Z. Cao, B. Giovanella, Development and validation of a reverse-phase HPLC with fluorescence detector method for simultaneous determination of CZ48 and its active metabolite camptothecin in mouse plasma, J Chromatogr B. 867 (2008) 84–89.
50. G. Boyd, J. Smyth, D. Jodrell, J. Cummings, High-performance liquid chromatographic technique for the simultaneous determination of lactone and hydroxy acid forms of camptothecin and SN-38 in tissue culture media and cancer cells, Anal Biochem. 297 (2001) 15–24.
51. N. Shoemaker, H. Rosing, S. Jansen, P. Schöffski, J. Rizzo, J. Schellens, et al., Determination of 9-nitrocamptothecin and its metabolite 9-aminocamptothecin in human plasma using high-performance liquid chromatography with ultraviolet and fluorescence detection, J Chromatogr B. 775 (2002) 231–237.
52. K. Derakhshandeh, S. Dadashzadeh, Liquid chromatographic quantitation of the lactone and the total of lactone and carboxylate forms of 9-nitrocamptothecin in human plasma, J Chromatogr B. 818 (2005) 199–204.
53. Z.M. Prijovich, Y.-L. Leu, S.R. Roffler, Effect of pH and human serum albumin on the cytotoxicity of a glucuronide prodrug of 9-aminocamptothecin, Cancer Chemother Pharmacol. 60 (2007) 7–17.
54. M. Pistolozzi, G. Varchi, A. Degli Esposti, A. Guerrini, G. Sotgiu, M. Ballestri, et al., Camptothecin and thiocamptothecin: the role of sulfur in shifting the hydrolysis equilibrium towards the closed lactone form, ChemMedChem. 6 (2011) 1706–1714.
55. E. Tsakalozou, J. Horn, M. Leggas, An HPLC assay for the lipophilic camptothecin analog AR-67 carboxylate and lactone in human whole blood, Biomed Chromatogr. 24 (2010) 1045–1051.
56. X. Yang, Z. Hu, S.Y. Chan, B.C. Goh, W. Duan, E. Chan, et al., Simultaneous determination of the lactone and carboxylate forms of irinotecan (CPT-11) and its active metabolite SN-38 by high-performance liquid chromatography: application to plasma pharmacokinetic studies in the rat, J Chromatogr B. 821 (2005) 221–228.
57. T. Bansal, A. Awasthi, M. Jaggi, R. Khar, S. Talegaonkar, Development and validation of reversed phase liquid chromatographic method utilizing ultraviolet detection for quantification of irinotecan (CPT-11) and its active metabolite, SN-38, in rat plasma and bile samples: Application to pharmacokinetic studies, Talanta. 76 (2008) 1015–1021.
58. Z. Zhang, J. Yao, X. Wu, J. Zou, An Accurate Assay for Simultaneous Determination of Irinotecan and Its Active Metabolite SN-38 in Rat Plasma by LC with Fluorescence Detection, Chromatographia. 70 (2009) 399–405.
59. W. Zhang, G.E. Dutschman, X. Li, M. Ye, Y.-C. Cheng, Quantitation of Irinotecan and its two major metabolites using a liquid chromatography-electrospray ionization tandem mass spectrometric, J Chromatogr B. 877 (2009) 3038–3044.
60. M.-T. Baylatry, A.-C. Joly, J.-P. Pelage, L. Bengrine-Lefevre, J.-L. Prugnaud, A. Laurent, et al., Simple liquid chromatography method for the quantification of irinotecan and SN38 in sheep plasma: application to in vivo pharmacokinetics after pulmonary artery chemoembolization using drug eluting beads, J Chromatogr B. 878 (2010) 738–742.
61. F.F.C. Marques, A.L.M.C. Cunha, A. Sá, R.Q. Aucélio, Determination of the Camptothecin Derivatives CPT-11 and SN-38 in Urine and Saliva by Micellar Electrokinectic Chromatography, Analytical Letters. 45 (2012) 1849–1861.
62. S. Poujol, F. Pinguet, F. Malosse, C. Astre, M. Ychou, S. Culine, et al., Sensitive HPLC-fluorescence method for irinotecan and four major metabolites in human plasma and saliva: Application to pharmacokinetic studies, Clin Chem. 49 (2003) 1900–1908.
63. F.A. de Jong, R.H.J. Mathijssen, P. de Bruijn, W.J. Loos, J. Verweij, A. Sparreboom, Determination of irinotecan (CPT-11) and SN-38 in human whole blood and red blood cells by liquid chromatography with fluorescence detection, J Chromatogr B. 795 (2003) 383–388.
64. T. Takahashi, Y. Fujiwara, H. Sumiyoshi, T. Isobe, Salivary drug monitoring of irinotecan and its active metabolite in cancer patients, Cancer Chemother Pharmacol. 40 (1997) 449–452.
65. H.M. Dodds, S.J. Clarke, M. Findlay, J.F. Bishop, J. Robert, L.P. Rivory, Clinical pharmacokinetics of the irinotecan metabolite 4-piperidinopiperidine and its possible clinical importance, Cancer Chemother Pharmacol. 45 (2000) 9–14.
66. M. Shingyoji, Y. Takiguchi, R. Watanabe-Uruma, Y. Asaka-Amano, H. Matsubara, K. Kurosu, et al., In vitro conversion of irinotecan to SN-38 in human plasma, Cancer Sci. 95 (2004) 537–540.
67. S. Bardin, W. Guo, J. Johnson, S. Khan, A. Ahmad, J. Duggan, et al., Liquid chromatographic–tandem mass spectrometric assay for the simultaneous quantification of Camptosar® and its metabolite SN-38 in mouse plasma and tissues, J Chromatogr A. 1073 (2005) 249–255.
68. Z.-P. Hu, X.-X. Yang, X. Chen, E. Chan, W. Duan, S.-F. Zhou, Simultaneous determination of irinotecan (CPT-11) and SN-38 in tissue culture media and cancer cells by high performance liquid chromatography: application to cellular metabolism and accumulation studies, J Chromatogr B. 850 (2007) 575–580.
69. W.Y. Li, R.T. Koda, Stability of irinotecan hydrochloride in aqueous solutions, Am J Health Syst Pharm. 59 (2002) 539–544.
70. P. Ebrahimnejad, R. Dinarvand, A. Sajadi, M. Jafari, F. Movaghari, F. Atyabi, Development and Validation of an Ion-pair HPLC Chromatography for Simultaneous Determination of Lactone and Carboxylate Forms of SN-38 in Nano-

particles, Journal of Food and Drug Analysis. 17 (2009) 246–256.

71. X. Chen, C.J. Peer, R. Alfaro, T. Tian, S.D. Spencer, W.D. Figg, Quantification of irinotecan, SN38, and SN38G in human and porcine plasma by ultra high-performance liquid chromatography-tandem mass spectrometry and its application to hepatic chemoembolization, J Pharm Biomed Anal. 62 (2012) 140–148.
72. N. Karadas, S. Sanli, B. Akmese, B. Dogan-Topal, A. Can, S.A. Ozkan, Analytical application of polymethylene blue-multiwalled carbon nanotubes modified glassy carbon electrode on anticancer drug irinotecan and determination of its ionization constant value, Talanta. 115 (2013) 911–919.
73. F.F. de C. Marques, A.L.M.C. Da Cunha, R.Q. Aucélio, Laser induced fluorescence and photochemical derivatization for trace determination of camptothecin, Talanta. 83 (2010) 256–261.
74. T.G. Burke, H. Malak, I. Gryczynski, Z. Mi, J.R. Lakowicz, Fluorescence detection of the anticancer drug topotecan in plasma and whole blood by two-photon excitation, Anal Biochem. 242 (1996) 266–270.
75. J. Ma, Z. Jia, Z. Guo, P. Fan, R. Wang, Restricted-access material HPLC method for simultaneous determination of carboxylate and lactone forms of topotecan in human serum, J Anal Chem. 64 (2009) 823–827.
76. T. Bansal, M. Singh, G. Mishra, S. Talegaonkar, R.K. Khar, M. Jaggi, et al., Concurrent determination of topotecan and model permeability markers (atenolol, antipyrine, propranolol and furosemide) by reversed phase liquid chromatography: utility in Caco-2 intestinal absorption studies, J Chromatogr B. 859 (2007) 261–266.
77. O. Soepenberg, P. de Bruijn, J. Verweij, R. Atsumi, A. Sparreboom, Liquid chromatographic assays for DE-310, a novel camptothecin analog, and two major enzymatic products in human matrices, J Chromatogr B. 799 (2004) 15–22.
78. R. Frapolli, M. Zucchetti, C. Sessa, S. Marsoni, L. Viganò, A. Locatelli, et al., Clinical pharmacokinetics of the new oral camptothecin gimatecan: The inter-patient variability is related to α1-acid glycoprotein plasma levels, European Journal of Cancer. 46 (2010) 505–516.
79. S. Pace, F. Capocasa, C. Tallarico, R. Frapolli, M. Zucchetti, A. Longo, Determination of total and lactone form of a new camptothecin derivative gimatecan (ST1481) and its metabolite ST1698 in human plasma by high-performance liquid chromatography with fluorimetric detection, J Pharm Biomed Anal. 50 (2009) 507–514.
80. T.-K. Yeh, C.-M. Li, C.-P. Chen, J.-J. Chuu, C.-L. Huang, H.-S. Wang, et al., Antitumor activities and pharmacokinetics of silatecans DB-67 and DB-91, Pharmacol Res. 61 (2010) 108–115.
81. S. Lee, J. Lee, Y. Jahng, T.C. Jeong, D.H. Kim, Characterization of in vitro metabolites of luotonin A in human liver microsomes using electrospray/tandem mass spectrometry, Xenobiotica. 43 (2013) 527–533.

3

Relevancia biológica y técnicas aplicables al análisis de alcaloides con estructura de β-carbolina

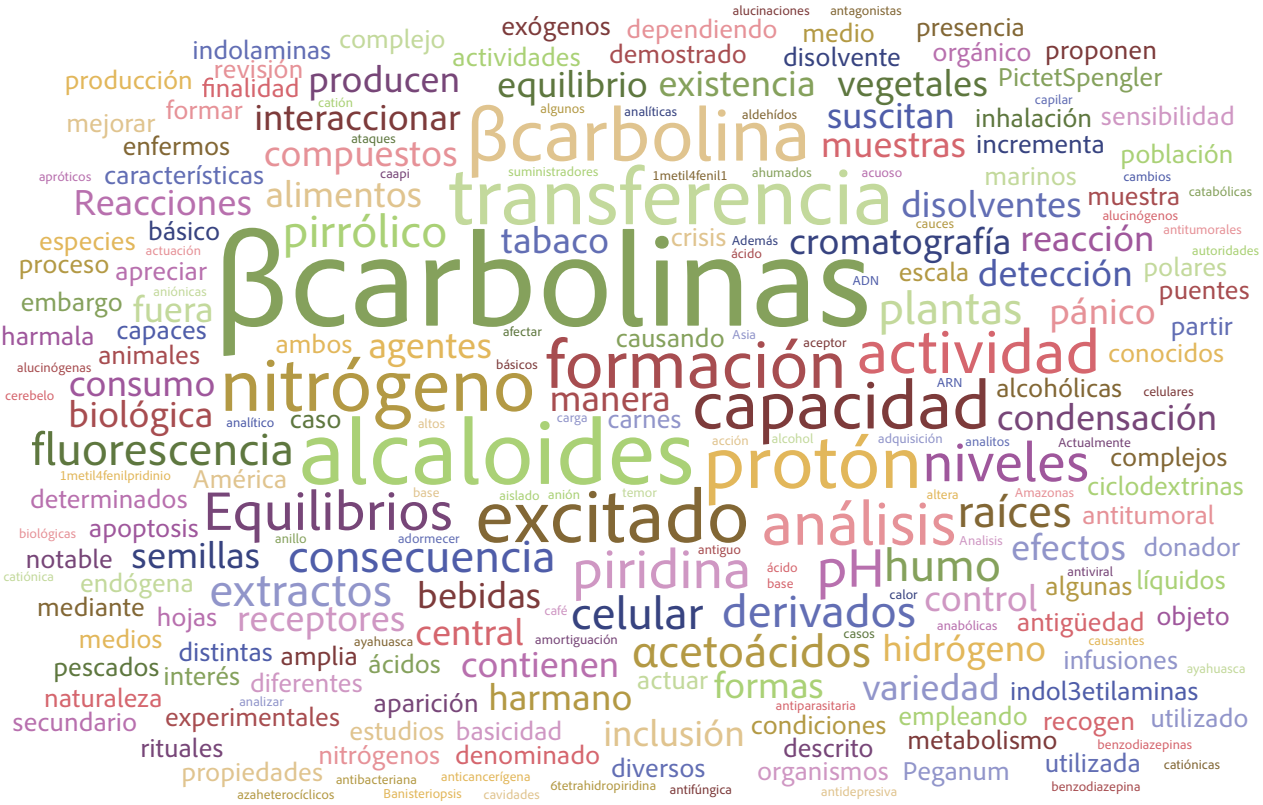

Nube de palabras que representa el número de veces que un término aparece en este capítulo

1. Origen de las β-carbolinas

Las β-carbolinas son un grupo de compuestos azaheterocíclicos naturales ampliamente distribuidos en la naturaleza [1,2]. La harmina y el harmano (Figura 1) son las primeras β-carbolinas conocidas y reciben su nombre por haberse aislado de los extractos de las semillas y de las raíces del *Peganum harmala* (*luo tuo peng*, chino simplificado: 骆驼蓬) [3-5].

Aunque estos alcaloides se caracterizaron por primera vez en plantas, también aparecen en animales, ya que se generan en el metabolismo secundario por condensación de indol-3-etilaminas con α-cetoácidos mediante la reacción de Pictet-Spengler (Figura 2). Por esta razón, se han calificado con el término paradójico, y a la vez expresivo, de "alcaloides indólicos de mamíferos" [6].

Además, se han encontrado en otros extractos vegetales como *Banisteriopsis caapi* [7], en diversas esponjas marinas [8,9], tunicados [10] y otros microorganismos marinos [11,12]. La presencia de estos alcaloides en una gran variedad de organismos marinos ha sido objeto de una reciente revisión [13]. También insectos, como las termitas, son capaces de producirlos [14].

La reacción de condensación entre indolaminas y aldehídos o α-cetoácidos también puede producirse de manera espontánea en numerosos alimentos, principalmente carnes y pescados. La aparición de β-carbolinas está favorecida en alimentos, tanto en los no cocinados (en los ahumados [15] o el queso [16]) como en el caso de aquellos alimentos que han sido sometidos a tratamiento de calor para su conservación. Análogamente están presentes en las carnes y los pescados muy

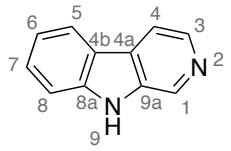

Norharmano (β-carbolina)
(**1**)

$C_{11}H_8N_2$	168,20 g/mol
CAS	244-63-3
PubChem	64961
ChemSpider	58486
UNII	94HMA1I78O
KEGG	C20157
ChEBI	109895
ChEMBL	275224
Sigma-Aldrich	N6252

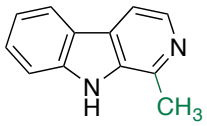

Harmano
(**2**)

$C_{12}H_{10}N_2$	182,23 g/mol
CAS	486-84-0
PubChem	5281404
ChemSpider	4444755
UNII	82D6J0535P
KEGG	C09209
ChEBI	12014
Sigma-Aldrich	103276

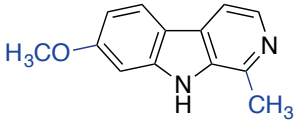

Harmina
(**3**)

$C_{13}H_{12}N_2O$	212,25 g/mol
CAS	442-51-3
PubChem	5280953
ChemSpider	4444445
UNII	4FHH5G48T7
KEGG	C06538
ChEBI	28121
ChEMBL	269538
Sigma-Aldrich	286044

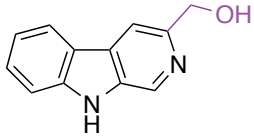

3-hidroximetil-β-carbolina
(**IS**)

$C_{12}H_{10}N_2O$	198,23 g/mol
CAS	65474-79-5
PubChem	5353338
ChemSpider	4510052
UNII	00QJ5EQT3E
Sigma-Aldrich	E004

Figura 1. Estructuras químicas de los alcaloides derivados de β-carbolina utilizados en el trabajo experimental que se recoge en esta memoria.

hechos [17]. Estos alcaloides se han detectado y cuantificado en bebidas alcohólicas [18], en el café [19] y en el humo del tabaco [20], y su presencia es de especial relevancia en las infusiones procedentes de las hojas, raíces y corteza de las plantas que producen β-carbolinas, como se comentará más adelante.

Varias revisiones exhaustivas recogen la formación y aparición de β-carbolinas a partir de las indolaminas y α-cetoácidos en una gran variedad de muestras (plantas, tejidos animales, bebidas alcohólicas, humo de tabaco, aire…) [5,21,22].

2. Actividad biológica y farmacológica de las β-carbolinas

Es notable la diversidad de actividades biológicas y farmacológicas descritas para los derivados de β-carbolina [23], lo cual puede explicarse considerando que son productos del metabolismo secundario que desempeñan distintos papeles en rutas anabólicas o catabólicas, como se ha revisado en varios artículos sobre su actividad biológica [24-26]. Los extractos vegetales que contienen estos alcaloides se han utilizado desde antiguo tanto en Asia Central como en América Central y del Sur por su actividad antiviral [27], antibacteriana y antifúngica [28], antiparasitaria [29] y anticancerígena, así como por sus propiedades alucinógenas ("ayahuasca").

Su actividad antitumoral se relaciona con la capacidad de interrumpir la maquinaria de replicación celular, bien sea interaccionando con los ácidos nucleicos, o bien, con algunas de las proteínas implicadas en dicho proceso. Se ha descrito su capacidad para interaccionar tanto con el ADN como con el ARN [30], llegando a comportarse como agentes co-mutagénicos dado que pueden actuar como intercalantes. Gracias a su interacción con los ácidos nucleicos son capaces de inducir apoptosis en líneas celulares de melanoma y de leucemia, actuando como citotóxicos y antitumorales [31-33]. Además se ha demostrado que su actividad antitumoral puede también ejercerse por inhibición de la topoisomerasa 1 humana [34], y por su capacidad de interaccionar con las α-tubulinas [35], en ambos casos conduciendo a las células a la apoptosis.

Se ha descrito que interaccionan con diversos receptores como los de benzodiazepinas, serotonina e imidazolina [36], actuando como antagonistas de los mismos y, por tanto, causando el efecto opuesto al que producen las benzodiazepinas. Estudios más recientes sugieren que estos alcaloides tienen actividad antidepresiva debido a que inhiben a las enzimas monoaminooxidasas (MAO) A y B [4]. También mejoran la capacidad cognitiva [37] al impedir la degradación de la dopamina por las MAO.

El papel de estos alcaloides en varios trastornos neurológicos es bien conocido. Se sabe

Figura 2. Reacción de Pictet-Spengler. Condensación de indol-3-etilaminas con α-cetoácidos para formar β-carbolinas.

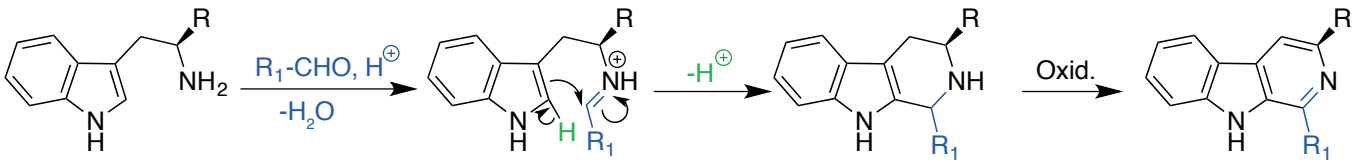

que son los agentes causantes del denominado "temor intrínseco" o crisis de pánico primarias. Estudios epidemiológicos *post mortem* han puesto de manifiesto que los niveles de harmano en cerebro y cerebelo, cuantificados mediante HPLC, están significativamente elevados con respecto a la población control [38] en enfermos que manifiestan crisis de pánico a lo largo de su vida. Parece que la generación de estos ataques podría estar relacionada con su elevada potencia para inducir alucinaciones [39].

Por otra parte, se ha demostrado que la producción endógena de β-carbolinas se incrementa como consecuencia de determinados trastornos neurológicos [40]. Se han estudiado los cambios en los niveles plasmáticos de β-carbolinas debido a factores exógenos como son la inhalación de humo de tabaco, la ingesta de alcohol o el consumo de heroína. Recientemente se ha descubierto que la producción endógena de β-carbolinio, al igual que de 1-metil-4-fenilpridinio a partir de determinados precursores exógenos como las tetrahidro β-carbolinas y la 1-metil-4-fenil-1,2,3,6-tetrahidropiridina respectivamente, producen neurotoxicidad y muerte celular debido a su actuación sobre el receptor dopaminérgico [41].

Los efectos alucinógenos de estos alcaloides eran ya bien conocidos por diferentes culturas desde hace siglos. Extractos vegetales que contienen estos compuestos se utilizaban con la finalidad de narcotizar a las víctimas en rituales que, en ocasiones, implicaban sacrificios humanos. Se sabe del uso tradicional por parte de algunas de las tribus del Amazonas [7,42,43], en las que era popular el consumo de estas hierbas en infusión, o bien la inhalación del humo de las hojas secas de las plantas que contienen estos alcaloides. Similares rituales están también documentados en la región de Irán desde tiempos remotos [44]. Actualmente, debido a los efectos psicotrópicos, las β-carbolinas suscitan una gran curiosidad en la población joven de Europa y América del Norte, entre los que ha crecido el consumo de bebidas e infusiones preparadas a base de semillas y raíces de *Peganum harmala*, en lo que se ha venido a denominar "la experiencia ayahusca" y la globalización de este preparado [45]. Dado el interés que suscitan y su carácter ilegal, es común la adquisición de estas mezclas de semillas y raíces a través de diversos suministradores en Internet [46], lo que constituye una serie amenaza de salud pública que ha puesto en guardia a numerosas autoridades.

3. Luminiscencia de las β-carbolinas

El anillo de β-carbolina presenta una notable fluorescencia intrínseca, la cual está condicionada por la diferente basicidad de los dos nitrógenos: el nitrógeno tipo pirrólico y el nitrógeno tipo piridina. El nitrógeno de tipo piridina es significativamente más básico que el nitrógeno pirrólico y la basicidad de ambos se incrementa en el estado excitado [47]. El nitrógeno tipo pirrólico puede desprotonarse en medio fuertemente básico fuera de la escala de pH (pH > 14). De esta manera, dependiendo del pH, pueden existir en el equilibrio una o más de las formas implicadas en el equilibrio de transferencia de protón que se muestra en la Figura 3. Debido a que las reacciones de transferencia de protón en estado excitado son más rápidas que la desactivación del mismo, es posible determinar las propiedades luminiscentes de cada una de las especies tanto en medio acuoso como orgánico [48]. Las reacciones de transferencia de protón en estado excitado en el caso de las β-carbolinas están fuertemente influenciadas por las características de polaridad de los disolventes y especialmente por la capacidad de estos de formar puentes de hidrógeno [49-51].

En disolventes orgánicos polares próticos, se ha podido apreciar la formación de complejos en estado excitado (exciplex), como consecuencia de la asociación entre el catión de la molécula de β-carbolina y el disolvente donador de protones [52]. Empleando la piridina como disolvente polar prótico, se puede apreciar la formación de puentes de hidrógeno entre los nitrógenos de la β-carbolina y el nitrógeno de la piridina. Estos enlaces de hidrógeno tienen como consecuencia la amortiguación (*quenching*) de la fluorescencia de la β-carbolina [53]. Al estudiar los equilibrios de transferencia de protón en estado excitado en disolventes polares apróticos, Sánchez-Coronilla *et al.* proponen la existencia de fototautómeros en estado excitado para explicar la formación del ion dipolar (zwitterion). Así, proponen la existencia de un proceso de transferencia de carga intramolecular entre el nitrógeno pirrólico (donador) y el nitrógeno tipo piridina (aceptor) [54].

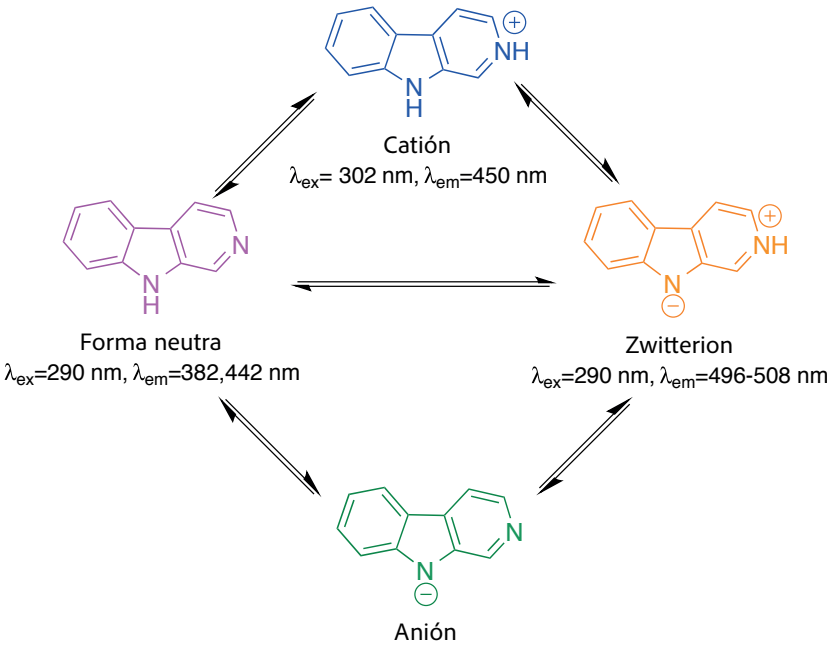

Figura 3.
Reacciones de transferencia de protón en estado excitado posibles en los derivados de β-carbolina. La formación del anión sólo se observa en medios fuertemente básicos, fuera de la escala de pH.

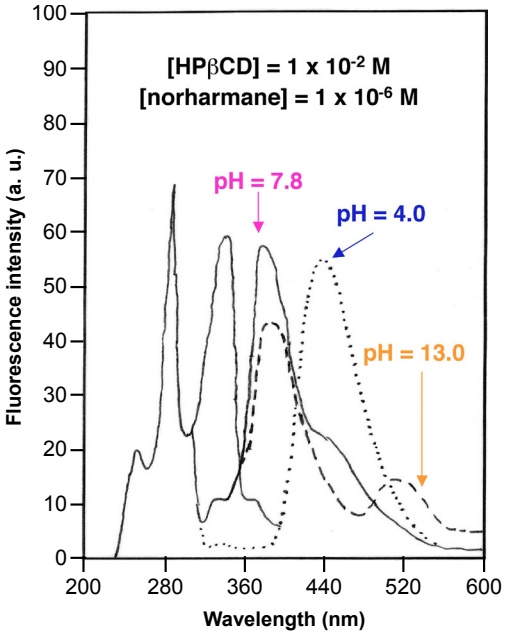

Figura 4. Espectros de fluorescencia de las especies catiónica, neutra y zwitteriónica del complejo de inclusión del norharmano y la HPβ-CD.

La existencia de los equilibrios de transferencia de protón en estado excitado es una propiedad que puede ser utilizada de forma valiosa desde el punto de vista analítico, si bien requiere un control estricto de las condiciones del entorno para evitar errores que sean consecuencia de dichos equilibrios. Dado que las formas catiónicas muestran rendimientos cuánticos de fluorescencia notablemente superiores a las formas neutras o aniónicas, se puede mejorar la sensibilidad en la detección de estos analitos en condiciones experimentales de pH ácido (Figura 4). Sin embargo, cuando se lleva a cabo el análisis en cromatografía de líquidos con detección fluorescente, el componente orgánico de la fase móvil puede afectar a los equilibrios de transferencia de protón. Por ello, para mejorar la sensibilidad del análisis fluorimétrico de estos alcaloides se ha utilizado como recurso la solubilización en medios micelares [55,56], así como la inclusión en las cavidades de las ciclodextrinas [57,58].

4. Análisis de las β-carbolinas

Debido al interés que suscitan las β-carbolinas como drogas ilícitas, a su amplia distribución en la naturaleza, a la variedad de matrices en las que se pueden encontrar, así como los diferentes niveles de concentración en los que se hallan dependiendo de la muestra a analizar, se hace necesario disponer de metodologías analíticas que posibiliten su determinación. La técnica más utilizada para el análisis de β-carbolinas es la cromatografía de líquidos empleando distintas modalidades de detección (UV-Vis, fluorescencia, electroquímica o por espectrometría de masas), si bien se ha descrito su separación y cuantificación por cromatografía de gases y por electroforesis capilar en multitud de trabajos que se escapan del alcance de la presente memoria.

En la Tabla 1 se recogen algunos ejemplos ilustrativos del análisis de β-carbolinas en distintas muestras y con características experimentales propias de la metodología desarrollada con tal finalidad.

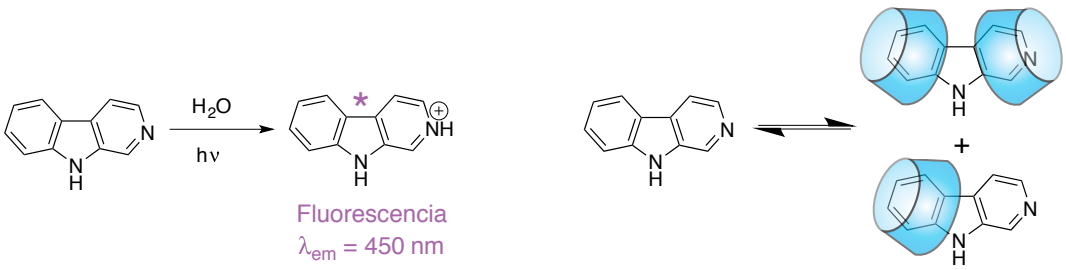

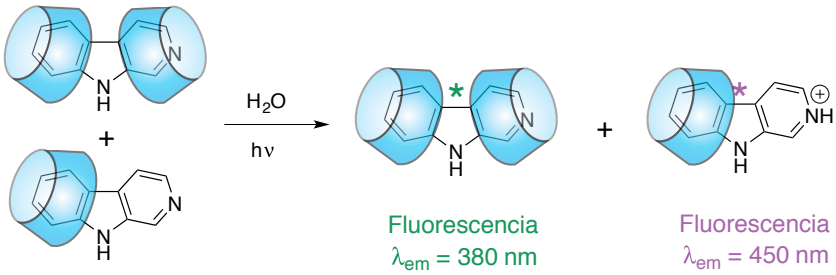

Figura 5. Equilibrios concomitantes de transferencia de protón en estado exitado y de formación de complejos de inclusión entre ciclodextrinas y β-carbolinas. La inclusión altera el equilibrio ácido-base.

Tabla 1. Ejemplos de determinación cuantitativa de β-carbolinas en distintas muestras.

Analito	Muestra	Detección	Comentarios	Ref.
Harmina, harmalina y sus metabolitos harmol y harmalol	Plasma de perro	UPLC-ESI-MS/MS	FE: C-18. FM: Gradiente, HCOOH 0,1% / MeCN. Desproteinización con MeCN	[59]
Derivados quirales de β-carbolina y melatonina.		NP-HPLC y CE	Revisión de los métodos analíticos y preparativos de HPLC y CE. La precisión y la sensibilidad de HPLC y CE son comparables. HPLC: FE: celulosa quiral. FM: EtOH/hexano. CE: la resolución quiral se obtiene mediante CDs en el tampón de separación	[60]
Harmina y harmalina	Microsomas hepáticos humanos	HPLC-ESI-MS	FE: C-18. Centrifugación en frío	[61]
β-carbolinas y aminas aromáticas	Humo de cigarrillos	HPLC-ESI-MS (dilución isotópica)	Método exacto, preciso y capaz de procesar un elevado número de muestras	[62]
β-carbolinas y sus metabolitos	Orina humana después de la ingesta de capsulas de extracto de "ayahuasca"	UHPLC-MS/MS	FE: C-18. FM: Gradiente, HCOOH 0,1% / MeCN. Hidrólisis enzimática de las muestras de orina. Dilución con FM	[63]
β-carbolinas y triptamina	Infusiones de ayahuasca	HPLC-ESI-MS/MS	FE: C-18. FM: Gradiente, HCOOH 0,1% / MeCN Hidrólisis enzimática de las muestras de orina. Dilución con FM	[64]
β-carbolinas	Semillas de *Peganum harmala*	HPTLC-Densitometría	FE: silicagel 60 (0,2 mm de espesor) FM: AcOEt:MeOH:NH_4 7:1:0,3, v:v:v. Extracción en MeOH a reflujo durante 1 h	[65]
Norharmano, harmano, harmina, harmalina y harmalol	Cerveza, café y queso	HPLC detección electroquímica	FE: C-18. FM: isocrática, MetOH:MeCN:fosfato pH 9,0 (20:20:60). Electrodos de pasta de carbono modificados con nanotubos	[18]
Harmano, harmina, harmalina y harmalol	Extractos de semillas de *Peganum harmala*	Espectrofotometría UV-Vis mediante calibración espectral multivariante por mínimos cuadrados parciales	Los mejores resultados se obtienen a pH < 9,0. Este método permite determinar simultáneamente los alcaloides a concentraciones de 0,15-10 µg/mL	[1]
Inhibición de la monoamino oxidasa (MAO) a través de la determinación β-carbolinas	Alimentos	HPLC-DAD, HPLC-FL y HPLC-MS	FE: C-18. FM: gradiente, fosfato amónico/MeCN. Extracción por SPE	[66]
β-carbolinas	Humo de tabaco	HPLC-DAD y HPLC-FD; GC-MS	Extracción por SPE	[67]
α- y β-carbolinas	Humo de tabaco	GC-MS sin necesidad de derivatización previa a la separación	Las α- y β-carbolinas se extraen de los filtros a través de los que se ha hecho pasar el humo con 50mL HCl 0,1 M que contiene ácido ascórbico 20mM	[20]
Imidazoquinolinas, imidazopiridinas, piridoimidazoles, α- y β-carbolinas	Carnes a la brasa y ahumadas	GC-MS con fuente de ionización por impacto de electrones.	Reacción de derivatización con *N*-metil-*N*-*terc*-butildimetilsilil-trifluoroacetamida. Buena sensibilidad y reproducibilidad	[17]
β-carbolinas	Cabello de individuos fumadores y no fumadores	HPLC-FD	Digestión enzimática del cabello seguida de derivatización con fluorescamina para evitar la cuantificación de las β-carbolinas que podría generarse durante la extracción	[68]
β-carbolinas y otros alcaloides.		HPLC-MS y CE-MS	Se revisan críticamente los distintos métodos de HPLC y CE con detección por MS. La ionización por ESI es la más frecuentemente utilizada	[2]
Tetrahidro β-carbolinas y sus ácidos carboxílicos	Vino, vinagre, salsa de soja, zumos, pan tostado, pescados ahumados	HPLC-FD	FE: C-18. FM: gradiente MeCN/fosfato amónico pH 3,0. Muy buena sensibilidad. SPE de intercambio iónico	[69]

Referencias

1. B. Hemmateenejad, A. Abbaspour, H. Maghami, R. Miri, M.R. Panjehshahin, Partial least squares-based multivariate spectral calibration method for simultaneous determination of beta-carboline derivatives in *Peganum harmala* seed extracts, Anal Chim Acta. 575 (2006) 290–299.
2. J. Stöckigt, Y. Sheludko, M. Unger, I. Gerasimenko, H. Warzecha, D. Stöckigt, High-performance liquid chromatographic, capillary electrophoretic and capillary electrophoretic–electrospray ionisation mass spectrometric analysis of selected alkaloid groups, J Chromatogr A. 967 (2002) 85–113.
3. Harvard University Herbaria, Missouri Botanical Garden, *Peganum harmala* in Flora of China at eFloras.org, eFloras.org. 11 (n.d.) 43.
4. T. Herraiz, D. González, C. Ancín-Azpilicueta, V.J. Arán, H. Guillén, β-Carboline alkaloids in *Peganum harmala* and inhibition of human monoamine oxidase (MAO), Food Chem Toxicol. 48 (2010) 839–845.
5. W. Pfau, K. Skog, Exposure to β-carbolines norharman and harman, J Chromatogr B. 802 (2004) 115–126.
6. T.D. Nikam, K.M. Nitnaware, M.L. Ahire, Alkaloids Derived from Tryptophan: Harmine and Related Alkaloids, in: K.G. Ramawat, J.-M. Mérillon (Eds.), Natural Products, Springer Berlin, 2013: pp. 553–574.
7. J.C. Callaway, Various alkaloid profiles in decoctions of Banisteriopsis caapi, J Psychoact Drugs. 37 (2005) 151–155.
8. W.D. Inman, W.M. Bray, N.C. Gassner, R.S. Lokey, K. Tenney, Y.Y. Shen, et al., A beta-Carboline Alkaloid from the Papua New Guinea Marine Sponge *Hyrtios reticulatus*, J Nat Prod. 73 (2010) 255–257.
9. R.D. Charan, T.C. McKee, K.R. Gustafson, L.K. Pannell, Thorectandramine, a novel β-carboline alkaloid from the marine sponge *Thorectandra sp*, Tetrahedron Lett. 43 (2002) 5201–5204.
10. T. Suzuki, T. Kubota, J. Kobayashi, Eudistomidins H-K, new β-carboline alkaloids from the Okinawan marine tunicate *Eudistoma glaucus*, Bioorg Med Chem Lett. 21 (2011) 4220–4223.
11. H. Huang, Y. Yao, Z. He, T. Yang, J. Ma, X. Tian, et al., Antimalarial β-carboline and indolactam alkaloids from *Marinactinospora thermotolerans*, a deep sea isolate, J Nat Prod. 74 (2011) 2122–2127.
12. A. Bratchkova, V. Ivanova, A. Gousterova, H. Laatsch, β-Carboline alkaloid constituents from a *Thermoactinomyces* sp. strain isolated from Livingston Island, Antarctica, Biotechnol. & Biotechnol. Equip. 26 (2012) 3005–3009.
13. J.W. Blunt, B.R. Copp, R.A. Keyzers, M.H.G. Munro, M.R. Prinsep, Marine natural products, Nat Prod Rep. 31 (2014) 160–258.
14. T. Chouvenc, N. Su, M. Elliott, Antifungal activity of the termite alkaloid norharmane against the mycelial growth of *Metarhizium anisopliae* and *Aspergillus nomius*, J Invertebr Pathol. 99 (2008) 345–347.
15. E. Papavergou, T. Herraiz, Identification and occurrence of 1, 2, 3, 4-tetrahydro-β-carboline-3-carboxylic acid: the main β-carboline alkaloid in smoked foods, Food Research International. 36 (2003) 843–848.
16. C. Naccari, M.T. Galceran, E. Moyano, M. Cristani, L. Siracusa, D. Trombetta, Presence of heterocyclic aromatic amines (HAS) in smoked "Provola" cheese from Calabria (Italy), Food Chem Toxicol. 47 (2009) 321–327.
17. S. Casal, E. Mendes, J.O. Fernandes, M.B.P.P. Oliveira, M.A. Ferreira, Analysis of heterocyclic aromatic amines in foods by gas chromatography–mass spectrometry as their tert.-butyldimethylsilyl derivatives, J Chromatogr A. 1040 (2004) 105–114.
18. L. Agüí, C. Peña-Farfal, P. Yáñez-Sedeño, J.M. Pingarrón, Determination of beta-carboline alkaloids in foods and beverages by high-performance liquid chromatography with electrochemical detection at a glassy carbon electrode modified with carbon nanotubes, Anal Chim Acta. 585 (2007) 323–330.
19. T. Herraiz, Identification and occurrence of the bioactive beta-carbolines norharman and harman in coffee brews, Food Addit Contam. 19 (2002) 748–754.
20. C. Smith, X. Qian, Q. Zha, S. Moldoveanu, Analysis of α-and β-carbolines in mainstream smoke of reference cigarettes by gas chromatography–mass spectrometry, J Chromatogr A. 1046 (2004) 211–216.
21. M. Sanz Alaejos, J.H. Ayala, V. González, A.M. Afonso, Analytical methods applied to the determination of heterocyclic aromatic amines in foods, J Chromatogr B. 862 (2008) 15–42.
22. T. Herraiz, Analysis of the bioactive alkaloids tetrahydro-β-carboline and β-carboline in food, J Chromatogr A. (2000) 483–499.
23. A. Peduto, R. Filosa, P. de Caprariis, V. De Feo, S. Li, P. Wang, et al., 1-Methoxy-Canthin-6-One and Related β-Carbolines: From Natural Compound to Synthesis and Biological Activities, in: Studies in Natural Products Chemistry, Elsevier, 2012: pp. 81–104.
24. R. Cao, W. Peng, Z. Wang, A. Xu, beta-Carboline alkaloids: biochemical and pharmacological functions, Curr Med Chem. 14 (2007) 479–500.
25. F.A. Khan, A. Maalik, Z. Iqbal, I. Malik, Recent pharmacological developments in β-carboline alkaloid "harmaline", Eur J Pharmacol. 721 (2013) 391–394.
26. K. Patel, M. Gadewar, R. Tripathi, S.K. Prasad, D.K. Patel, A review on medicinal importance, pharmacological activity and bioanalytical

aspects of beta-carboline alkaloid, Asian Pac J Trop Biomed. 2 (2012) 660–664.

27. J. Ishida, H.-K. Wang, M. Oyama, M.L. Cosentino, C.-Q. Hu, K.-H. Lee, Anti-AIDS Agents. 46. 1Anti-HIV Activity of Harman, an Anti-HIV Principle from *Symplocos setchuensis*, and Its Derivatives, J Nat Prod. 64 (2001) 958–960.
28. G. Nenaah, Antibacterial and antifungal activities of beta-carboline alkaloids of *Peganum harmala* (L) seeds and their combination effects, Fitoterapia. 81 (2010) 779–782.
29. C. Di Giorgio, F. Delmas, E. Ollivier, R. Elias, G. Balansard, P. Timon-David, In vitro activity of the beta-carboline alkaloids harmane, harmine, and harmaline toward parasites of the species *Leishmania infantum*, Exp. Parasitol. 106 (2004) 67–74.
30. S. Nafisi, Z.M. Malekabady, M.A. Khalilzadeh, Interaction of β-carboline alkaloids with RNA, DNA Cell Biol. 29 (2010) 753–761.
31. F. Zaker, A. Oody, A. Arjmand, A study on the antitumoral and differentiation effects of *Peganum harmala* derivatives in combination with ATRA on leukaemic cells, Arch Pharm Res. 30 (2007) 844–849.
32. R. Cao, W. Peng, H. Chen, X. Hou, H. Guan, Q. Chen, et al., Synthesis and in vitro cytotoxic evaluation of 1,3-bisubstituted and 1,3,9-trisubstituted beta-carboline derivatives, Eur J Med Chem. 40 (2005) 249–257.
33. H. Guan, H. Chen, W. Peng, Y. Ma, R. Cao, X. Liu, et al., Design of β-carboline derivatives as DNA-targeting antitumor agents, Eur J Med Chem. 41 (2006) 1167–1179.
34. A.M. Sobhani, S.-A. Ebrahimi, M. Mahmoudian, An in vitro evaluation of human DNA topoisomerase I inhibition by *Peganum harmala* L. seeds extract and its beta-carboline alkaloids, J Pharm Pharm Sci. 5 (2002) 19–23.
35. R. Ikeda, M. Kurosawa, T. Okabayashi, A. Takei, M. Yoshiwara, T. Kumakura, et al., 3-(3-Phenoxybenzyl)amino-β-carboline: a novel antitumor drug targeting α-tubulin, Bioorg Med Chem Lett. 21 (2011) 4784–4787.
36. R. Glennon, B. Grella, R. Tyacke, A. Lau, J. Westaway, A. Hudson, Binding of β-carbolines at imidazoline I2 receptors: a structure–affinity investigation, Bioorg Med Chem Lett. 14 (2004) 999–1002.
37. M. Gruss, D. Appenroth, A. Flubacher, C. Enzensperger, J. Bock, C. Fleck, et al., 9-Methyl-β-carboline-induced cognitive enhancement is associated with elevated hippocampal dopamine levels and dendritic and synaptic proliferation, J Neurochem. 121 (2012) 924–931.
38. E.D. Louis, P. Factor-Litvak, X. Liu, J.-P.G. Vonsattel, M. Galecki, W. Jiang, et al., Elevated brain harmane (1-methyl-9H-pyrido[3,4-b]indole) in essential tremor cases vs. controls, Neurotoxicology. 38 (2013) 131–135.
39. R.G. Santos, J. Landeira-Fernandez, R.J. Strassman, V. Motta, A.P.M. Cruz, Effects of ayahuasca on psychometric measures of anxiety, panic-like and hopelessness in Santo Daime members, J Ethnopharmacol. 112 (2007) 507–513.
40. E. Louis, W. Jiang, K. Pellegrino, E. Rios, P. Factor-Litvak, C. Henchcliffe, et al., Elevated blood harmane (1-methyl-9H-pyrido [3, 4-B] indole) concentrations in essential tremor, Neurotoxicology. 29 (2008) 294–300.
41. T. Herraiz, H. Guillén, J. Galisteo, Metabolite profile resulting from the activation/inactivation of 1-methyl-4-phenyl-1,2,3,6-tetrahydropyridine and 2-methyltetrahydro-β-carboline by oxidative enzymes, Biomed Res Int. 2013 (2013) 248608.
42. J.C. Callaway, Fast and Slow Metabolizers of Hoasca, J Psychoact Drugs. 37 (2005) 157–161.
43. D.J. McKenna, Clinical investigations of the therapeutic potential of ayahuasca: rationale and regulatory challenges, Pharmacol Therapeut. 102 (2004) 111–129.
44. A. Pieroni, H. Muenz, M. Akbulut, K.H.C. Baser, C. Durmuskahya, Traditional phytotherapy and trans-cultural pharmacy among Turkish migrants living in Cologne, Germany, J Ethnopharmacol. 102 (2005) 69–88.
45. K.W. Tupper, The globalization of ayahuasca: harm reduction or benefit maximization? Int. J. Drug Policy. 19 (2008) 297–303.
46. G. Frison, D. Favretto, F. Zancanaro, G. Fazzin, S. Ferrara, A case of β-carboline alkaloid intoxication following ingestion of *Peganum harmala* seed extract, Forensic Sci Int. 179 (2008) e37–e43.
47. G.G. Guilbault, Practical fluorescence, New York : M. Dekker, 1990.
48. M. Tapia, D. Reyman, M. Vinas, C. Carcedo, J. Poyato, Acid-base equilibria of methyl beta-carboline-3-carboxylate in aqueous solution, J Lumines. 101 (2003) 227–234.
49. A. Sánchez-Coronilla, M. Balón, M.A. Muñoz, C. Carmona, Influence of hydrogen bonding in the ground and the excited states of the isomers of the β-carboline anhydrobase (N_2-methyl-9H-pyrido[3,4-b]indole) in aprotic solvents, Chem Phys. 344 (2008) 72–78.
50. A.S. Coronilla, C. Carmona, M.A. Muñoz, M. Balón, Ground state isomerism and dual emission of the β-carboline anhydrobase (N_2-methyl-9H-pyrido[3,4-b]indole) in aprotic solvents, Chem Phys. 327 (2006) 70–76.
51. D. Reyman, M.J. Tapia, C. Carcedo, M.H. Viñas, Photophysical properties of methyl beta-carboline-3-carboxylate mediated by hydrogen-bonded complexes--a comparative study in different solvents, Biophys Chem. 104 (2003) 683–696.
52. C. Carmona, M. Balón, A.S. Coronilla, M.A. Muñoz, New Insights on the Excited-State Proton-Transfer Reactions of Betacarbolines: Ca-

tionic Exciplex Formation, J. Phys. Chem. A. 108 (2004) 1910–1918.

53. J. Hidalgo, A. Sánchez-Coronilla, M.A. Muñoz, C. Carmona, M. Balón, Fluorescence quenching of betacarboline (9H-pyrido[3,4-b]indole) induced by intermolecular hydrogen bonding with pyridines, J Lumines. 127 (2007) 671–677.
54. A. Sánchez-Coronilla, M. Balón, M.A. Muñoz, J. Hidalgo, C. Carmona, Ground state isomerism in betacarboline hydrogen bond complexes: The charge transfer nature of its large Stokes shifted emission, Chem Phys. 351 (2008) 27–32.
55. L. Martín, A.I. Olives, B. del Castillo, M.A. Martín, Fluorescence quenching of beta-carboline alkaloids in micellar media. A study to select the adequate surfactant to use in analytical techniques, Luminescence. 20 (2005) 152–161.
56. A. Mallick, N. Chattopadhyay, Photophysics of norharmane in micellar environments: a fluorometric study, Biophys Chem. 109 (2004) 261–270.
57. J. Prados, A. León, A.I. Olives, M.A. Martín, B. Castillo, Cyclodextrins modify the proton transfer photoreactions of norharmane, J Photochem Photobiol A: Chem. 173 (2005) 287–295.
58. L. Martín, A. León, A.I. Olives, B. Del Castillo, M.A. Martín, Spectrofluorimetric determination of stoichiometry and association constants of the complexes of harmane and harmine with beta-cyclodextrin and chemically modified beta-cyclodextrins, Talanta. 60 (2003) 493–503.
59. L. Zhang, L. Teng, C. Gong, W. Liu, X. Cheng, S. Gu, et al., Simultaneous determination of harmine, harmaline and their metabolites harmol and harmalol in beagle dog plasma by UPLC-ESI-MS/MS and its application to a pharmacokinetic study, J Pharm Biomed Anal. 85 (2013) 162–168.
60. E. Lipka, S. Yous, C. Furman, P. Carato, C. Deghaye, J.-P. Bonte, et al., Analytical and Preparative Chiral Separation of β-Carboline Derivatives, LDL Oxidation Inhibitors, Using HPLC and CE Methodologies: Determination of Enantiomeric Purity, Chromatographia. 75 (2012) 337–345.
61. T. Zhao, S.-S. Zheng, B.-F. Zhang, Y.-Y. Li, S.W.A. Bligh, C.-H. Wang, et al., Metabolic pathways of the psychotropic-carboline alkaloids, harmaline and harmine, by liquid chromatography/mass spectrometry and NMR spectroscopy, Food Chem. 134 (2012) 1096–1105.
62. L. Zhang, D.L. Ashley, C.H. Watson, Quantitative analysis of six heterocyclic aromatic amines in mainstream cigarette smoke condensate using isotope dilution liquid chromatography-electrospray ionization tandem mass spectrometry, Nicotine Tob Res. 13 (2011) 120–126.
63. E.H. McIlhenny, J. Riba, M.J. Barbanoj, R. Strassman, S.A. Barker, Methodology for and the determination of the major constituents and metabolites of the Amazonian botanical medicine ayahuasca in human urine, Biomed Chromatogr. 25 (2011) 970–984.
64. E.H. McIlhenny, K.E. Pipkin, L.J. Standish, H.A. Wechkin, R. Strassman, S.A. Barker, Direct analysis of psychoactive tryptamine and harmala alkaloids in the Amazonian botanical medicine ayahuasca by liquid chromatography-electrospray ionization-tandem mass spectrometry, J Chromatogr A. 1216 (2009) 8960–8968.
65. H. Pulpati, Y.S. Biradar, M. Rajani, High-performance thin-layer chromatography densitometric method for the quantification of harmine, harmaline, vasicine, and vasicinone in *Peganum harmala*, J AOAC Int. 91 (2008) 1179–1185.
66. T. Herraiz, C. Chaparro, Analysis of monoamine oxidase enzymatic activity by reversed-phase high performance liquid chromatography and inhibition by beta-carboline alkaloids occurring in foods and plants, J Chromatogr A. 1120 (2006) 237–243.
67. T. Herraiz, C. Chaparro, Human monoamine oxidase is inhibited by tobacco smoke: β-carboline alkaloids act as potent and reversible inhibitors, Biochem Biophys Res Commun. 326 (2005) 378–386.
68. H. Tsuchiya, High-performance liquid chromatographic analysis of beta-carbolines in human scalp hair, J Chromatogr A. 1031 (2004) 325–330.
69. T. Herraiz, Analysis of tetrahydro-beta-carboline-3-carboxylic acids in foods by solid-phase extraction and reversed-phase high-performance liquid chromatography combined with fluorescence detection, J Chromatogr A. 871 (2000) 23–30

Panorámica de la química analítica sostenible

Los últimos treinta años se han caracterizado por una mejora de los estándares de calidad de vida en los países industrializados. En determinados aspectos, ello ha tenido consecuencias negativas sobre el medio ambiente. La consciencia de que debemos preservar nuestro entorno para las generaciones futuras ha llevado a proponer alternativas que satisfagan los requisitos de conservación del medioambiente ("environmentally-friendly") en los distintos ámbitos de las ciencias experimentales.

En el campo de la Química Analítica, se han ido introduciendo metodologías, procedimientos y técnicas cuya finalidad es reducir el impacto medioambiental de los distintos métodos analíticos [1,2]. Desde el control de calidad de materias primas y productos terminados en la industria farmacéutica, las determinaciones analíticas en laboratorios oficiales (agencias de control de medicamentos, alimentos, contaminantes ambientales...) hasta en la rutina de los laboratorios de análisis clínicos, se ha intentado buscar métodos calificados como "verdes" o "sostenibles", que tiendan a disminuir los residuos generados en el proceso analítico (Figura 1), como sucede con las nuevas fases estacionarias disponibles en HPLC.

Por ello, se apuesta por la tendencia de transformación de las metodologías que, desarrolladas para un formato que podríamos denominar convencional, se han convertido en atractivas y útiles metodologías sostenibles [3]. Una gran parte de los procedimientos de pre-tratamiento analítico se ha transformado en sus equivalentes "micro" o miniaturizados.

La utilización de métodos sostenibles supone reducir el volumen de disolventes empleados, sustituir los disolventes tóxicos por otros que no lo sean y, en un siguiente paso, utilizar metodologías exentas de disolventes [4]. Complementariamente, debe reducirse el consumo energético y la generación de residuos así como mejorar el reciclado [5] de los mismos.

La etapa de preparación de la muestra es una de los pasos que podrían considerarse más contaminantes, ya que consume no sólo un elevado volumen de disolventes, sino también cantidades considerables de tiempo y energía [6]. De ahí el esfuerzo realizado en desarrollar nuevas metodologías más sostenibles.

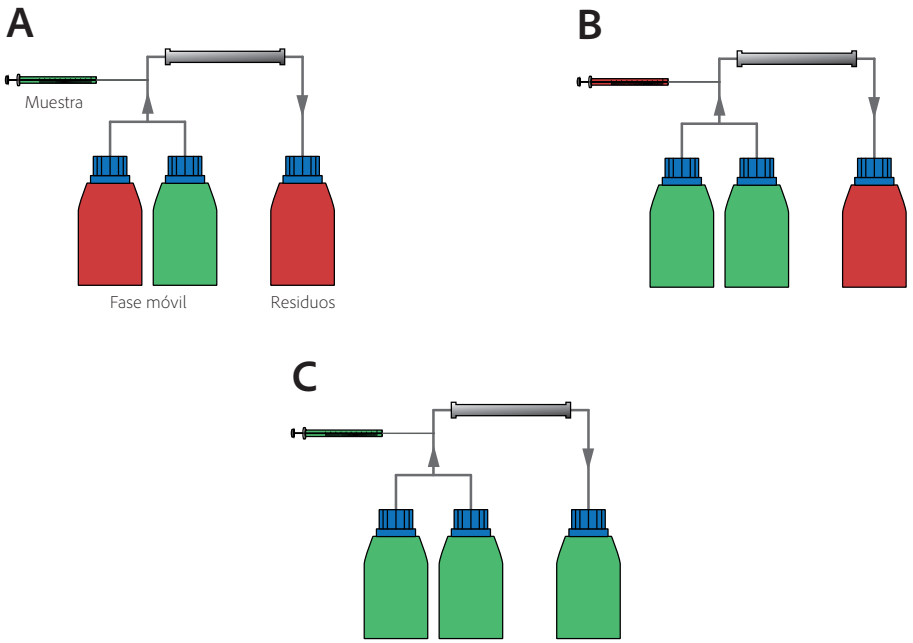

Figura 1.
Diferentes situaciones que se suelen presentar en cromatografía de líquidos, que ponen de manifiesto cómo todos los elementos del proceso cromatográfico han de tenerse en cuenta a la hora de mejorar su sostenibilidad. (A) y (B) Un componente de la fase móvil, o la muestra en sí, respectivamente, deben ser sujetos a modificaciones para intentar alcanzar la combinación óptima, (C).

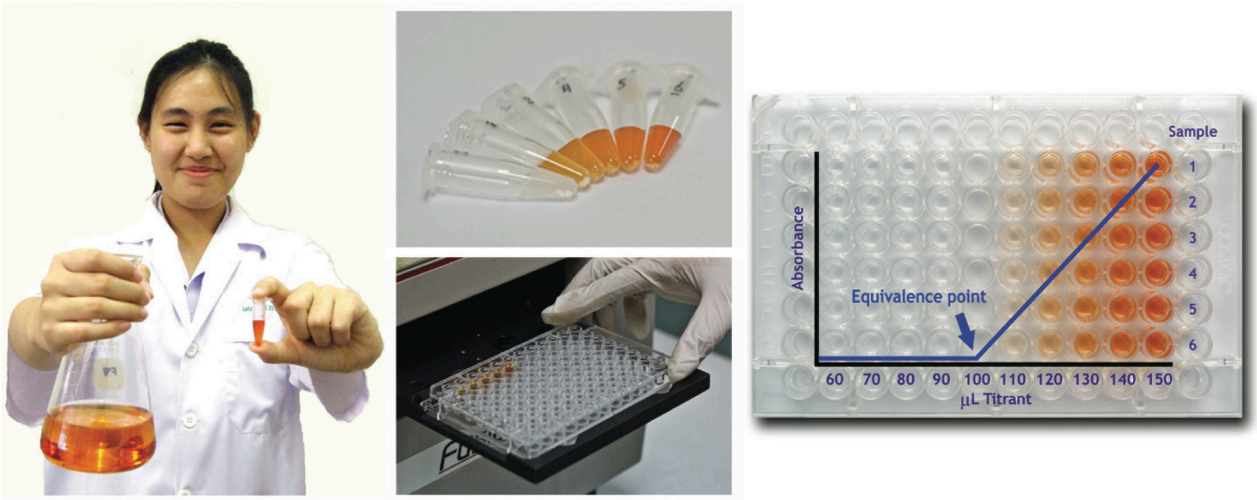

Figura 2.
La miniaturización y el uso de técnicas en formato de alto rendimiento requieren volúmenes de reacción mucho más pequeños que los métodos espectroscópicos en formato convencional [25].

Entre ellas, cabe señalar el auge de la utilización de líquidos iónicos [7-9], el desarrollo de nuevas técnicas de micro-extracción en fase líquida [10-13], el diseño de estrategias para la preparación de las muestras en el análisis de contaminantes orgánicos en cantidades traza [14], o la posibilidad de realizar la extracción en un solo paso empleando ciclodextrinas [15].

En la etapa de análisis de la muestra, la miniaturización, la automatización y el análisis, no sólo "on-line", sino "in-line", suponen un importante avance hacia el objetivo de la consecución de métodos sostenibles [16]. Resulta de especial interés el acoplamiento de métodos de pre-tratamiento verdes con técnicas capilares de análisis, tal es el caso de la micro-extracción en fase líquida con la electroforesis capilar [17]. Las diferentes estrategias para el análisis sostenible mediante técnicas cromatográficas, ya sean de gases o de líquidos, se han revisado recientemente considerando las aplicaciones de éstas en la determinación de alimentos y contaminantes ambientales [18]. Los métodos instrumentales empleados en rutina pueden hacerse sostenibles con matices o adaptaciones como, por ejemplo, el empleo de sistemas de medida en flujo (FIA) [19,20], o la utilización de las clásicas técnicas espectroscópicas en la modalidad de alto rendimiento ("High Throughput Screening") [21] permitiendo el análisis de las muestras a la vez que la realización de la curva de calibrado mediante los dispositivos de lectura "multi-pocillo" en placa (Figura 2) y utilizando volúmenes entre 10 y 50 veces inferiores a los requeridos en las medidas convencionales.

Otros ejemplos son la realización de medidas "in situ" mediante el empleo de sensores [22,23] y biosensores o la utilización de reacciones analíticas sencillas sobre papel (Paper µZone Plates) [24].

A priori, la forma más sencilla de transformar un técnica analítica convencional en una sostenible implica la miniaturización, ya que ello conlleva la reducción del volumen de disolventes y reactivos a utilizar, así como la consiguiente disminución en los residuos generados. Otra estrategia útil pasa por la disminución del tiempo de análisis, lo que a su vez conlleva un importante ahorro energético, este último es una de las características que deben poseer las metodologías analíticas sostenibles. En los apartados siguientes se describen las tendencias en el desarrollo de metodologías analíticas respetuosas con el medio ambiente enfocadas en el pretratamiento analítico de las muestras y las determinaciones cuantitativas mediante las técnicas espectroscópicas moleculares y en las separaciones por cromatografía de líquidos.

Referencias

1. L.H. Keith, L.U. Gron, J.L. Young, Green Analytical Methodologies, Chem Rev. 107 (2007) 2695–2708.
2. M. Tobiszewski, A. Mechlinska, J. Namiesnik, Green analytical chemistry--theory and practice, Chem Soc Rev. 39 (2010) 2869–2878.
3. M. de L. Guardia, Green analytical chemistry, Trends Anal Chem. 29 (2010) 577–577.
4. S. Armenta, S. Garrigues, M. de la Guardia, Green Analytical Chemistry, Trends Anal Chem. 27 (2008) 497–511.
5. S. Garrigues, S. Armenta, M. de la Guardia, Green strategies for decontamination of analytical wastes, Trends Anal Chem. 29 (2010) 592–601.
6. Y. Picó, L. Ramos, Editorial, Trends Anal Chem. 43 (2013) 1.
7. E. Aguilera-Herrador, R. Lucena, S. Cárdenas, M. Valcárcel, The roles of ionic liquids in sorptive microextraction techniques, Trends Anal Chem. 29 (2010) 602–616.
8. Z. Li, Y. Pei, H. Wang, J. Fan, J. Wang, Ionic liquid-based aqueous two-phase systems and their applications in green separation processes, Trends Anal Chem. 29 (2010) 1336–1346.
9. A.B. Pereiro, J.M.M. Araújo, J.M.S.S. Esperança, I.M. Marrucho, L.P.N. Rebelo, Ionic liquids in separations of azeotropic systems – A review, J Chem Thermodyn. 46 (2012) 2–28.
10. F. Pena-Pereira, I. Lavilla, C. Bendicho, Liquid-phase microextraction techniques within the framework of green chemistry, Trends Anal Chem. 29 (2010) 617–628.
11. A. Sarafraz-Yazdi, A. Amiri, Liquid-phase microextraction, Trends Anal Chem. 29 (2010) 1–14.
12. C. Mahugo-Santana, Z. Sosa-Ferrera, M.E. Torres-Padrón, J.J. Santana-Rodríguez, Application of new approaches

to liquid-phase microextraction for the determination of emerging pollutants, Trends Anal Chem. 30 (2011) 731–748.

13. J.M. Kokosa, Advances in solvent-microextraction techniques, Trends Anal Chem. 43 (2013) 2–13.
14. M. Tobiszewski, A. Mechlinska, B. Zygmunt, J. Namiesnik, Green analytical chemistry in sample preparation for determination of trace organic pollutants, Trends Anal Chem. 28 (2009) 943–951.
15. S. Mantegna, A. Binello, L. Boffa, M. Giorgis, C. Cena, G. Cravotto, A one-pot ultrasound-assisted water extraction/cyclodextrin encapsulation of resveratrol from Polygonum cuspidatum, Food Chem. 130 (2012) 746–750.
16. M. Farré, S. Pérez, C. Gonçalves, M.F. Alpendurada, D. Barceló, Green analytical chemistry in the determination of organic pollutants in the aquatic environment, Trends Anal Chem. 29 (2010) 1347–1362.
17. H.-Y. Xie, Y.-Z. He, Green analytical methodologies combining liquid-phase microextraction with capillary electrophoresis, Trends Anal Chem. 29 (2010) 629–635.
18. M. Tobiszewski, J. Namiesnik, Direct chromatographic methodsin the context of green analytical chemistry, Trends Anal Chem. 35 (2012) 67–73.
19. S. Kruanetr, S. Liawruangrath, N. Youngvises, A simple and green analytical method for determination of iron based on micro flow analysis, Talanta. 73 (2007) 46–53.
20. N.O. Soto, B. Horstkotte, J.G. March, P.L.L. de Alba, L.L. Martínez, V.C. Martín, An environmental friendly method for the automatic determination of hypochlorite in commercial products using multisyringe flow injection analysis, Anal Chim Acta. 611 (2008) 182–186.
21. T. Rojanarata, K. Sumran, P. Nateetaweewat, W. Winotapun, S. Sukpisit, P. Opanasopit, et al., Microscale chemistry-based design of eco-friendly, reagent-saving and efficient pharmaceutical analysis: a miniaturized Volhard's titration for the assay of sodium chloride, Talanta. 85 (2011) 1324–1329.
22. X.-D. Wang, O.S. Wolfbeis, Fiber-Optic Chemical Sensors and Biosensors (2008–2012), Anal Chem. 85 (2013) 487–508.
23. P. Yáñez-Sedeño, J.M. Pingarrón, J. Riu, F.X. Rius, Electrochemical sensing based on carbon nanotubes, Trends Anal Chem. 29 (2010) 939–953.
24. M. Vaher, M. Kaljurand, The development of paper microzone-based green analytical chemistry methods for determining the quality of wines, Anal Bioanal Chem. 404 (2012) 627–633.
25. Rojanarata, T. Green Pharmaceutical Chemistry for the Sustainability. Silpakorn University Science and Technology Journal, 6 (2012), 7–13.

Esta página se ha dejado en blanco intencionadamente

4

Técnicas espectroscópicas en formato de alto rendimiento en el contexto de la química analítica sostenible

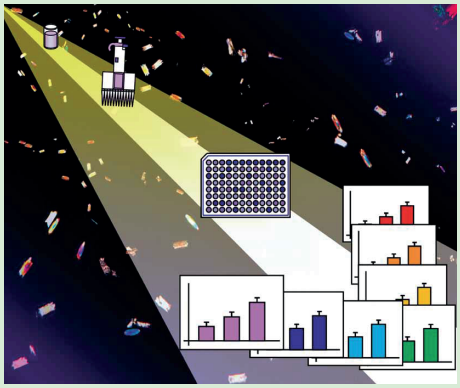

Portada del número de junio de 2010 de The Analyst

ABSTRACT ▶ Las técnicas analíticas en formato de alto rendimiento han evolucionado a gran velocidad en las últimas décadas, ya que permiten procesar un elevado número de muestras con un consumo mínimo de tiempo y de reactivos. El presente capítulo revisa las tendencias más recientes en los análisis espectroscópicos en formatos miniaturizados, dando especial relevancia a la reducción del impacto medioambiental de los mismos. Mientras que este tipo de ensayos está ampliamente extendido en análisis rutinarios en las áreas bioquímica y clínica, han encontrado una aplicación mucho menor en el campo de la espectroscopía analítica más clásica. Por ello, a continuación se recogen los ejemplos más relevantes publicados recientemente de cómo los análisis convencionales pueden adaptarse a formatos miniaturizados para reducir los volúmenes de reactivos empleados y, por tanto, los residuos generados por los mismos.

1. Introducción

Uno de los objetivos a alcanzar en el desarrollo de metodologías analíticas sostenibles es la reducción de los residuos generados en el procedimiento, así como la sustitución, en la medida de lo posible, de los reactivos tóxicos por otros que no lo sean. La miniaturización de las técnicas analíticas, a día de hoy, continúa siendo uno de las tendencias líderes en química analítica [1]. El empleo de técnicas miniaturizadas implica la reducción en el consumo de disolventes y reactivos así como de la cantidad de muestra a analizar.

Los ensayos de alto rendimiento (High Throughput Screening, HTS) combinan la detección de los analitos con técnicas sencillas y miniaturizadas de análisis (espectrofotometría de absorción UV-VIS o espectrofluorimetría) logrando el objetivo de la miniaturización de las técnicas analíticas a la vez que satisfacen los actuales requisitos de sostenibilidad. De esta forma, mediante los HTS, el consumo de reactivos, disolventes y analitos, así como la generación de residuos se ve reducida entre 10 y 100 veces con respecto a los mismos métodos en su versión no miniaturizada. Además, los ensayos de alto rendimiento aportan notables ventajas a las determinaciones analíticas e incrementan significativamente su robustez.

Los HTS cuentan desde hace tiempo con una extensa aplicación en los ensayos de actividad biológica de candidatos a fármacos [2,3] y, por tanto, tienen una gran popularidad en las industrias farmacéutica [4] y biotecnológica [5,6]. En los campos de la bioquímica y la biología molecular se vienen empleando rutinariamente desde hace años en un sinfín de aplicaciones, como las determinaciones de actividad enzimática (Figura 1) [7].

A día de hoy son una realidad en los ensayos de toxicidad [8], en los que en la modalidad tradicional implica un elevado gasto económico y el empleo de animales de experimentación. Sin embargo, la modalidad HTS cuantitativa emplea líneas celulares humanas, generando información valiosa a precio razonable. Diversos artículos de revisión [9-11] profundizan en las ventajas e inconvenientes de estas metodologías y en su expansión a otros campos científicos.

Los primeros dispositivos de lectura en pocillo de unos pocos microlitros se describen en 1954, sin embargo, es necesario esperar a la década de los 70 para que el formato de placas de 96 pocillos se popularizara, en parte gracias a su utilización en los inmunoensayos tipo ELISA. En 1991 aparece una publicación en cuyo título se incluye la denominación HTS [12]. Desde esas fechas, los avances tecnológicos han contribuido al desarrollo e implantación de los HTS como procedimientos reproducibles que utilizan volúmenes muy pequeños de reactivos junto

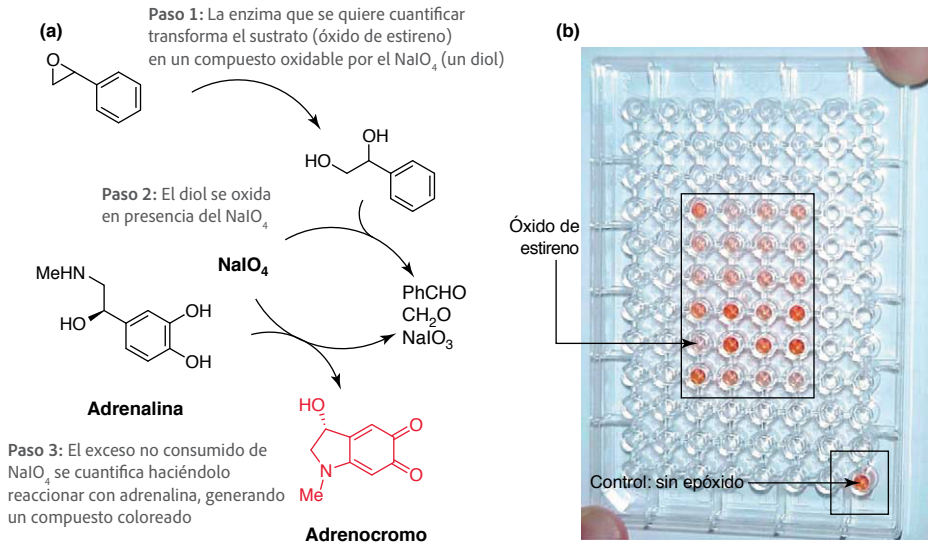

Figura 1. Aplicación de las técnicas de alto rendimiento a la cuantificación de la enzima epóxido hidrolasa. En una valoración por retroceso, se cuantifica el periodato de sodio en exceso que no se ha consumido [7].

con técnicas analíticas sensibles y robustas para la detección (basados en la medida de la absorbancia o de la fluorescencia) [13].

El éxito de estos ensayos en la industria farmacéutica fue extraordinario y, por ello, pasaron a utilizarse rutinariamente en los estudios de actividad de fármacos. La capacidad de ensayo se multiplicó al menos por 10, con un tiempo de análisis extraordinariamente reducido, requiriendo además menos espacio. En conjunto, la miniaturización incrementa las posibilidad de ensayar candidatos que mediante ensayos tradicionales no llegarían a estudiarse.

A pesar de que se han utilizado otras formas de detectar la respuesta analítica (radioensayos y radioinmunoensayos), las espectroscopías moleculares de absorción y de emisión son las que han logrado mayor aplicación y utilidad. Las medidas espectrofotométricas o espectrofluorimétricas en formatos miniaturizados de alto rendimiento presentan notables ventajas con respecto al empleo de las técnicas tradicionales, entre las que cabe citar:

- Estas técnicas espectroscópicas son sencillas y a la vez sensibles
- Se requieren volúmenes de muestra muy pequeños (10 µL o inferiores)
- Consumo de reactivos muy reducido
- Bajo coste
- Reducción del tiempo de análisis
- Elevado número de determinaciones simultáneas (96-1536)
- Análisis paralelo de patrones y muestras
- Buenas precisión y robustez

En la Figura 2 se muestra un ejemplo de la forma en que se llevan acabo los ensayos de alto rendimiento, y en la Tabla 1 se comparan las principales características de estas metodologías con las de formato tradicional.

A estas ventajas hay que unir el hecho de que se pueden utilizar para el análisis multimuestra en reacciones colorimétricas y fluorimétricas bien conocidas. Sin embargo, a pesar de su amplia aceptación en el campo de la biomedicina, existe un cierto reparo a su aplicación rutinaria en análisis químico cuantitativo. Este hecho obedece a diversas razones. La primera es que la sensibilidad de la determinación en el sistema multi-pocillo es menor, debido a lo reducido de los volúmenes y al recipiente donde se hace la medida. A pesar de ello, esta dificultad es de menor importancia cuando se utiliza detección por fluorescencia o quimioluminiscencia

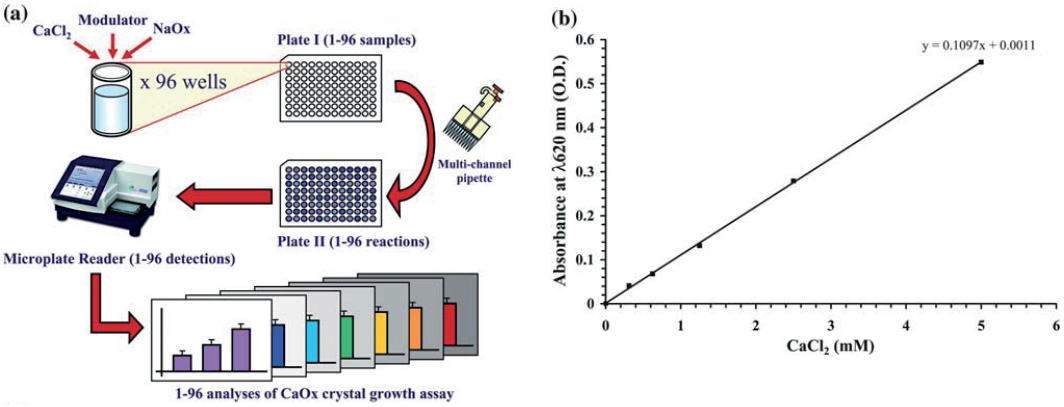

Figura 2. (a) Esquema que ilustra el concepto analítico de un ensayo de alto rendimiento y muestra las etapas del mismo. (b) Curva de calibrado obtenida mediante lectura espectrofotométrica en lector multipocillo en el intervalo de 0-5 mM de $CaCl_2$. [S. Chutipongtanatea, V. Thongboonkerd, Analyst, (2010) 135, 1309–1314].

Tabla 1. Comparación de las principales características de los formatos miniaturizado y tradicional. Adaptado de [10] y [11].

Parámetro	Formato tradicional	Formato HTS
Protocolo	Complejo, con numeroso pasos	Operaciones simples, generalmente adiciones
Reacción/ensayo	Ensayo en "un" tubo	Ensayo simultáneo en 96 "pocillos"
Volúmenes	~ 1 mL	~50-100 µL
Adición de los reactivos	Cada analito/reactivo se adiciona individualmente	Los analitos/reactivos se adicionan simultáneamente
Lectura	1:1	1:96
Formato de lectura	Individual: inspección visual, radiactividad, fluorescencia	Paralela y automática: radiactividad, luminiscencia, absorción UV-Vis
Tiempo de análisis	La determinación es lenta y laboriosa (minutos-horas)	La determinación es rápida y eficaz (segundos-minutos)
Analitos/ compuestos	Se ensayan ~20-50 compuestos/ semana	Se ensayan ~1.000-10.000 compuestos/semana
Características del cribado	Limitado el número y la diversidad	Ilimitado el numero y la diversidad
Evaluación de los resultados	Análisis estadístico de los datos obtenidos manualmente	Análisis estadístico automatizado de todos los datos obtenidos

debido a la elevada sensibilidad, por lo que se emplean ampliamente en determinaciones de interés biológico.

Las ventajas de esta modalidad de detección así como las interferencias que surgen como consecuencia de la auto-fluorescencia de numerosos entornos biológicos se han revisado críticamente [14]. En el caso de la detección por absorción UV-Vis, la menor sensibilidad puede comprometer algunas aplicaciones cuantitativas, como consecuencia de que la determinación se realiza midiendo la fracción de luz transmitida por la muestra en los pocillos con un camino óptico muy reducido, por tanto, los límites de detección que se alcancen no serán tan bajos como los obtenidos con procedimientos "en cubeta". Esta pérdida de sensibilidad, en numerosas ocasiones, se verá compensada por las otras cualidades que acompañan a los HTS.

2. Tratamiento estadístico de los datos

Está muy extendida la idea errónea de que los HTS, al ser metodologías de cribado, no tienen la fiabilidad requerida [15]. En este sentido, se ha sistematizado el tratamiento de los datos para darles validez estadística, introduciendo el denominado factor *Z* [16], que es una medida del efecto estadístico en los HTS, y que permite juzgar si la respuesta en un determinado ensayo tiene la significación suficiente como para garantizar la fiabilidad del resultado. El factor *Z* se calcula considerando la media y las desviaciones estándar tanto de los controles positivos (*p*) como de los negativos (*n*) (Ec. 1).

En esta ecuación, μ_p y μ_n son los valores de las medias obtenidas para los controles positivo y negativo respectivamente, y σ_p y σ_n son los valores de desviación estándar obtenidos para esos mismos controles. En la Tabla 2 se recogen los valores de *Z* y la calificación que recibe el en-

$$Z = 1 - \frac{3\left(\sigma_p + \sigma_n\right)}{\left|\mu_p - \mu_n\right|} \qquad \textbf{Ec. 1}$$

$$\frac{S}{N} = \frac{\mu_{max} - \mu_{min}}{\sigma_{min}} \qquad \textbf{Ec. 2}$$

$$\frac{S}{N} = \frac{\mu_{max} - \mu_{min}}{\sqrt{\sigma_{max}^2 + \sigma_{min}^2}} \qquad \textbf{Ec. 3}$$

$$\frac{S}{B} = \frac{\mu_{max}}{\mu_{min}} \qquad \textbf{Ec. 4}$$

Tabla 2. Características de los ensayos HTS en función de su valor de *Z*. Adaptado de [4].

Valor de *Z*	Interpretación
1,0	Ideal, el factor Z no puede exceder a 1,0
De 0,5 a 1,0	Ensayo excelente (12 desviaciones estándar entre μ_p y μ_n)
De 0 a 0,5	Ensayo en el límite de aceptabilidad
Menor que 0	Ensayo pobre. El solapamiento entre los controles positivos y negativos es muy grande para que pueda aceptarse el resultado como bueno

sayo en función de los mismos y el criterio de bondad del resultado.

En la validación de los ensayos de alto rendimiento es frecuente, igualmente, diferenciar entre la relación señal/ruido (S/N, *signal to noise*) y la relación señal/fondo (S/B, *signal to background*) (Ecs. 2-3).

La relación señal/ruido (S/N) es un valor que permite establecer la fuerza de la señal que proporciona una muestra real con respecto a la desviación estándar asociada al ruido de fondo. La relación señal/fondo (S/B), como se puede ver en la Ec. 4, no da información sobre el grado de dispersión de los datos y, por tanto, puede resultar inadecuada para la evaluación de los datos. Es aconsejable utilizarla junto con el valor *Z*, ya que dan una idea más completa del entorno en el que se desarrollan los HTS. Para la determinación de estos valores se utilizan las señales de los controles positivo y negativo. En el caso de la relación S/B se considera aceptable si ésta es igual o superior a 2.

Si se comparan las determinaciones "en cubeta" con las determinaciones en lector multi-pocillo, se puede apreciar un pérdida de sensibilidad con respecto a las medidas convencionales.

3. Ejemplos de aplicación

Como consecuencia de las ventajosas cualidades que presentan los HTS, poco a poco se ha ido extendiendo su campo de aplicación fuera del ámbito biológico propiamente dicho. Una metodología clásica para la determinación espectrofotométrica de la **vitamina C** en alimentos consiste en la formación de un complejo coloreado Fe^{2+}/dipiridilo. Al añadir una sal de Fe^{3+} a las muestras que contienen ascorbato, éste reduce el Fe^{3+} a Fe^{2+}, formándose ácido dehidroascórbico y el Fe^{2+} originado reacciona con el dipiridilo dando lugar a la aparición del color característico, que se puede cuantificar por la absorbancia a 550 nm. Así, se ha determinado el contenido en vitamina C en muestras de tomate de una forma rápida y sencilla al utilizar un sistema de lector multi-pocillo [17] acoplado a un espectrofotómetro. Los resultados obtenidos mediante los HTS, se comparan con el procedimiento de determinación de la vitamina C mediante espectrofluorimetría. Existe una gran concordancia en los valores cuantitativos obtenidos por HTS y el método de referencia. Además, los autores realizan un riguroso análisis comparativo de ambas metodologías, destacando que la cantidad de muestra analizada es entre 5-10 veces más pequeña que en el procedimiento convencional y que el costo en mano de obra especializada es unas 50 veces inferior por el ahorro de tiempo que los HTS conllevan.

Un claro ejemplo de cómo los HTS pueden ser utilizados para cuantificar y procesar un número de muestras elevado con un consumo reducido de disolventes es la determinación de cloruros mediante el procedimiento de Volhard [18]. La precipitación del **cloruro** se lleva a cabo en tubo de centrífuga de 2 mL, el precipitado obtenido se separa por centrifugación y seguidamente se procede a la valoración en placa de 96 pocillos con detección espectrofotométrica. En esta valoración, en modalidad HTS, el volumen de reactivo titulador es de unos 200 µL, siendo la concentración de la disolución tituladora 10 veces más diluida que en el procedimiento tradicional. La reducción en gasto de los reactivos y residuos varía entre 25 veces (residuos sólidos de AgCl y AgSCN), 50 veces (residuos líquidos y $AgNO_3$) y más de 200 veces el titulador (NH_4SCN) con respecto al procedimiento de referencia seguido (Farmacopea Británica). El HTS ha mostrando una muy buena exactitud (99,85-101,16%) y reproducibilidad (% RSD intra-ensayo 0,178% e inter-ensayo 0,051%).

La determinación del contenido de catión **amonio** en aguas costeras requiere métodos lo suficientemente sensibles como para detectar concentraciones de este ion inferiores a µM. El amoniaco generado a partir de catión amonio es capaz de reaccionar con el *o*-ftaldialdehído (OPA) [19] para dar lugar a isoindoles que presentan una notable fluorescencia a λ_{ex} = 360 nm, λ_{em} = 430 nm. Con el fin de incrementar la especificidad de la reacción y de evitar las interferencias debidas a los aminoácidos y la aminas primarias presentes en las muestras se ha propuesto la adición de sulfito al medio de reacción. El LOD obtenido en el HTS es 5 nM, ligeramente superior al obtenido mediante derivatización con OPA y detección en cubeta convencional (2 nM). La reproducibilidad evaluada

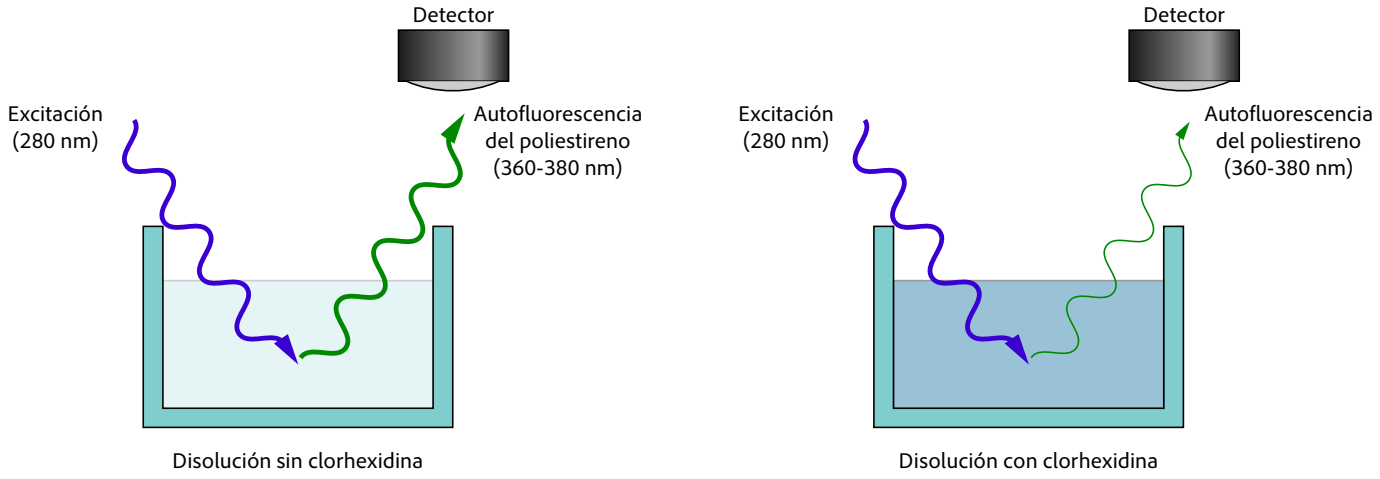

Figura 3.
Esquema que explica la determinación de clorhexidina mediante la reducción de la fluorescencia emitida por los pocillos transparentes de poliestireno. El poliestireno emite fluorescencia entre 360-380 nm cuando se excita con radiaciones de 280 nm. El grosor de las flechas ilustra cómo el pocillo que contiene clorhexidina presenta una menor lectura de fluorescencia que el pocillo que contiene el blanco correspondiente [21].

como coeficiente de variación porcentual osciló entre 0,4% y 4,5%, dependiendo de la salinidad de la muestra de agua. El método propuesto es exacto y rápido y no está sujeto a las interferencias debidas a la presencia de partículas en suspensión en el agua o muestras con un elevado contenido salino.

Otro ejemplo de eficacia en la reducción del volumen de disolventes y el tiempo de análisis lo proporciona la comparación de dos métodos clásicos de determinación de **lípidos** en tejidos animales. El método de Bligh–Dyer es un método gravimétrico de determinación del contenido total de lípidos previa extracción con un disolvente orgánico de la matriz en la que se encuentran. En el caso del método de Van Handel, la fracción lipídica extraída con un disolvente orgánico se hace reaccionar con vainillina en medio ácido dando lugar a un color rosa característico cuya intensidad es proporcional a la concentración de lípidos presentes en la muestra. El empleo de HTS con detección espectrofotométrica como una modificación/miniaturización [20] del procedimiento tradicional de Van Handel, permite reducir la cantidad de muestra a analizar en 100 veces, así como el volumen de disolvente orgánico 5 veces y el tiempo de análisis en más de 10 veces. Esta metodología es exacta y reproducible, sin embargo, hay que tener en cuenta que si el número de muestras a analizar supera el número de pocillos por placa, se deberá realizar una curva de calibrado adicional en cada placa. Esto es debido a que la intensidad del color desarrollado es dependiente del tiempo y todos los pocillos (muestras y patrones) deben leerse en menos de 5 minutos, lo cual es posible para una placa de 96 pocillos (tiempo de lectura 2 minutos).

La **clorhexidina** es un antiséptico muy utilizado en colutorios orales por sus buenas propiedades y especialmente porque reduce el riesgo de desarrollar caries. También se incluye en los barnices dentales para proteger las zonas afectadas durante una intervención. Se han descrito distintos métodos espectrofotométricos y cromatográficos para la determinación de clorhexidina, pero para poder llevarlo a cabo en pequeños volúmenes de muestra, los HTS se presentan como una alternativa atractiva. La determinación espectrofluorimétrica indirecta de clorhexidina en lector multipocillo se vale de la fluorescencia intrínseca que presentan las placas transparentes de poliestireno. Cuando las placas se iluminan con radiaciones UV de 280 nm emiten fluorescencia en la región de 360-380 nm. Estas placas son las que se utilizan en las medidas espectrofotométricas midiendo la radiación transmitida. La clorhexidina tiene un máximo de absorción a 280 nm, por ello, cuando los pocillos se rellenan con 150-200 µL de soluciones de clorhexidina de concentraciones crecientes, se observa una disminución en la intensidad de fluorescencia tal y como se muestra en la Figura 3. Se determinó la precisión y exactitud de la determinación, obteniéndose valores de coeficientes de variación intra-ensayo < 10% mientras que los correspondientes a los inter-ensayo fueron < 20%. Esta metodología ha permitido determinar el contenido de clorhexidina en barnices dentales [21] así como en muestras tomadas directamente de los dientes que se han tratado con estos barnices. Esta metodología facilita el procesado de un número elevado de muestras.

Basándose también en la auto-fluorescencia que presentan las placas, se ha propuesto la determinación de anión **fosfato** [22]. Se ha comparado la detección absorciométrica con la detección fluorimétrica, utilizando en ambos casos sistemas HTS. Las metodologías propuestas tiene la sensibilidad requerida para la detección de fosfato inorgánico en muestras de interés biológico, permitiendo la determinación de la actividad enzimática de la fosfatasa alcalina. El anión fosfato forma complejos con el ácido molíbdico y colorantes como el verde malaquita o el rojo quinaldina. Por otra parte, las placas blancas utilizadas en los lectores multipocillo para medidas de absorbancia, son capaces de emitir fluorescencia en la región de 460-640 nm cuando se excitan con radiaciones comprendidas entre 400-490 nm. Por tanto, esta emisión

de fluorescencia puede ser amortiguada si en los pocillos se depositan disoluciones de colorantes que absorban en la región de 400-490 nm. Éste es el caso de los complejos que forma el fosfato con el verde malaquita y el ácido molíbdico. La respuesta lineal, precisión y exactitud del método son adecuadas para la detección de fosfato. El análisis estadístico de las muestras medidas en placas de 384 pocillos proporciona relaciones S/B > 4,0 y un factor *Z* de 0,8, lo que demuestra la idoneidad del método propuesto. Los resultados obtenidos se comparan con los ensayos HTS con detección espectrofotométrica utilizando los mismos colorantes, si bien la sensibilidad del método espectrofotométrico es más pobre.

La sensibilidad de la detección espectrofotométrica es suficiente para la detección de **arsénico** en diversas muestras de suelos que, además, contienen fosfato como interferente. Así, Makris et al. [23] han desarrollado un HTS basado en la detección colorimétrica de As que ha demostrado ser rápido, exacto y económico para la determinación de As(III) y As(V) en cantidades traza, incluso en presencia de fosfatos en concentraciones 15 veces mayores que las del As. Se trata de una modificación del método del verde malaquita descrito para la determinación de P en forma de fosfato. As(III) y As(V) no desarrollan color con el método del verde malaquita (610 nm) empleado para el P. Los complejos de As-ácido molíbdico no son capaces de unirse al verde malaquita, sin embargo, la adición de ácido ascórbico hace que éste reaccione con los complejos molíbdicos tanto del As como del P desarrollado un color intenso en presencia del verde malaquita. Por tanto, si la muestra se divide en dos partes alícuotas, en una, gracias a la presencia del ácido ascórbico, se determinará el contenido de As y de P, y en la otra utilizando el procedimiento clásico del verde malaquita se determinará el contenido de P, y por diferencia se determinará el del As. Los resultados de las determinaciones de As en muestras de suelo presentaron recuperaciones del 84-118% con una buena reproducibilidad y estos resultados son concordantes con los obtenidos por ICP-MS. Entre las ventajas de este HTS, cabe señalar que los volúmenes de reactivo y muestra empleados fueron respectivamente de 120 µL y 200 µL. No solo se ahorra tiempo y reactivos, sino que la generación de residuos tóxicos se ve disminuida drásticamente. El ensayo HTS evita, además, riesgos inherentes a la manipulación de las muestras para su análisis por ICP-MS, incluyendo la formación especies volátiles de arsénico.

Las **aminas biogénicas** (histamina, putrescina, cadaverina, tiramina...) se denominan así porque aparecen de forma natural por acción de las bacterias que producen la descarboxilación de los aminoácidos. Su presencia en alimentos (carnes, pescados, quesos, huevos, salsas, setas...) tiene importancia no sólo porque son unos indicadores ideales del estado de conservación de los alimentos y de su frescura, sino porque su ingestión concomitante con ciertos fármacos conlleva la aparición de efectos indeseables en el organismo, como vasoconstricción periférica y crisis hipertensivas. Así mismo, está bien establecida su potencial acción carcinogénica. Por ello, la detección de estos compuestos en alimentos suscita un gran interés. Se ha puesto a punto un ensayo HTS que cumple la doble función: la de cribado, porque permite la detección visual en la placa de la presencia de aminas biogénicas; y también su determinación cuantitativa en pescados [24] con la sensibilidad requerida. Para ello, las aminas se hacen reaccionar con un derivado de una sal de pirilio comercial (Py-1) que muestra una intensa fluorescencia a 620 nm cuando se excita a 485 nm tras la reacción con las aminas. En el caso de la detección visual se observa el cambio de color como se puede apreciar en la Figura 4. Para la cuantificación por fluorimetría, se utilizó el método de adición estándar. La detección fluorimétrica, en placa opaca, permite alcanzar LOD de 0,16 a 0,59 µg/mL y % RSD de 0,92% a 2,79% dependiendo de la amina detectada. Si se compara el ensayo HTS con la determinación por HPLC o por GC-MS se produce una reducción significativa en el tiempo de análisis y en la manipulación de las muestras, ya que en el ensayo HTS la placa de 96 pocillos se incuba durante 10 minutos para que las aminas reaccionen con el Py-1 y tan solo 2 minutos para la lectura de la fluorescencia desarrollada en los pocillos, mientras que en los métodos cromatográficos se requieren entre 15

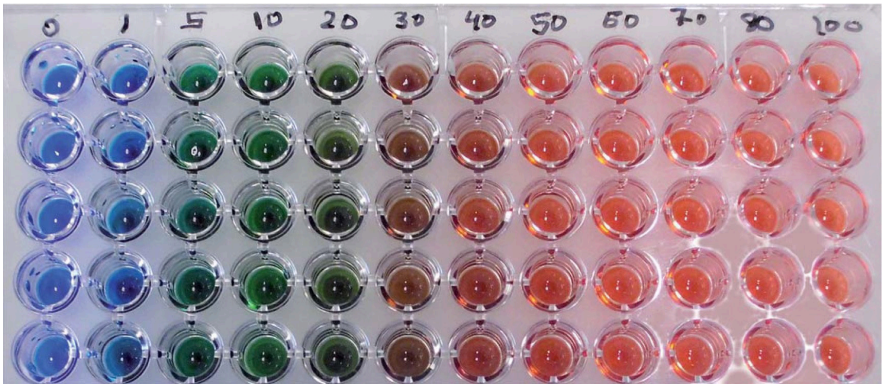

Figura 4.
Fotografía de una microplaca de 96 pocillos mostrando la gama y la intensidades de color para el producto de reacción de la histamina con el sensor Py-1. Las concentraciones de histamina varían entre 0 y 100 µg/mL [24].

y 30 minutos para la derivatización de las aminas y entre 20 y 30 minutos para la separación cromatográfica.

Las **quinonas** desempeñan distintos papeles a nivel biológico, por su carácter esencial (vitamina K), y también siendo claves en las cadenas de transporte de electrones y en los procesos de respiración celular. Por otra parte, están presentes en las estructuras de numerosos fármacos como antitumorales (doxorubicina y mitomicina), empleándose también en el tratamiento de enfermedades infecciosas, bacterianas o parasitarias. Su reactividad química, su capacidad de generar especies reactivas de oxígeno (ROS) cuando son sometidas a radiación UV y su persistencia en el entorno, hacen que tengan interés desde el punto de vista medioambiental. Todo ello suscita la necesidad de disponer de métodos analíticos para su identificación y cuantificación. Se ha desarrollado un ensayo HTS para la determinación de quinonas (vitamina K) [25] en muestras de suero humano basándose en la medida de la radiación quimioluminiscente del luminol inducida por las especies de oxígeno generadas por las quinonas. El ensayo de alto rendimiento presenta muy buena sensibilidad, con rangos lineales de 0,05 a 150 µM (LOD 0,01 µM), recuperaciones que varían entre 88% y 97% y coeficientes de variación intra-día e inter-día que varían entre un 4% y un 10%. La metodología propuesta presenta una validez y aplicabilidad similar a otros procedimientos de cuantificación de quinonas con un importante ahorro en tiempo (la respuesta quimioluminiscente de 96 muestras se mide en 125 s) y en reactivos, por lo que se propone como análisis de rutina para la determinación cuantitativa de quinonas tanto en materias primas como en formas farmacéuticas.

Las **heparinas** no fraccionadas (UFH) y las de bajo peso molecular (LMWHs) son poliaminosacáridos de composición compleja. Generalmente, las que se utilizan con fines terapéuticos son de origen porcino. Tienen una gran utilidad terapéutica por su actividad antitrombótica, ya que inhiben el factor X_a de la compleja cadena de coagulación. Además, presentan acción antiinflamatoria, antimetastásica y antiangiogénica. Su eficacia terapéutica hace que su empleo esté muy extendido. En 2008-2009 se desató una importante polémica, debido a la adulteración de las heparinas de uso humano con elevadas concentraciones de sulfato de condroitina poniendo de manifiesto que los controles analíticos [26] legales eran insuficientes y con trágicas consecuencias para numerosos enfermos bien en forma de reacciones adversas y llegando incluso a la muerte [27].

Para la determinación de los grupos aniónicos, las técnicas espectrofotométricas, las conductimétricas o las potenciométricas no poseen la sensibilidad necesaria y las técnicas electroforéticas son laboriosas y requieren un consumo elevado de tiempo. Aunque se ha propuesto el empleo de sensores electroquímicos o colorimétricos, también se ha propuesto su análisis mediante HTS [28] basado en el reconocimiento molecular de las heparinas por el "polímero H" (Figura 5) que tiene una alta afinidad por la heparina y que está compuesto por tres tipos de monómeros con grupos funcionales enlazados sobre un esqueleto de metacrilamida y que son capaces de interaccionar con las heparinas. El monomero "1" es un marcador fluorescente, normalmente cloruro de dansilo; el monómero "2" es *o*-aminometilfenilboronato, capaz de formar esteres cíclicos con los grupos glicol de la heparina; y el monómero "3", etilamonio, es capaz de establecer interacciones electrostáticas con los restos aniónicos de las heparinas. La interacción del polímero H con las heparinas provoca cambios en la intensidad de fluorescencia del marcador fluorescente. Sobre 180 µL de disolución problema de heparina, se adicionan 20 µL del polímero H. Después de incubar durante 10 min la placa de 96 pocillos, a temperatura ambiente, se procede a la lectura de forma automática a λ_{ex}= 320 nm, λ_{em}= 510 nm. La intensidades de fluorescencia de las distintas muestras fueron corregidas por sustracción de la intensidad de fluorescencia del polímero H medida en idénticas condiciones experimentales y empleado como control. De esta manera se han determinado distintas heparinas comer-

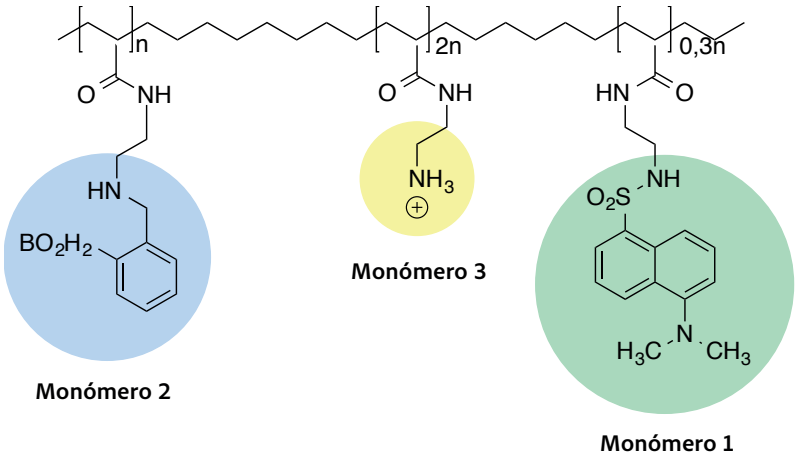

Figura 5.
Esquema de la estructura del polímero fluorescente "H" concebido para que sea capaz de reconocer al analito a través de unión covalente (resto de ácido borónico) y de interacciones electrostáticas ($-NH_3^+$). El sensor fluorescente (dansilo, resto aminonaftaleno sulfónico) modula y modifica su respuesta fluorescente en función de su grado de anclaje a la heparina [28].

ciales, de manera sensible, exacta y económica. En la Tabla 3 se recogen otros ensayos HTS para la detección de las impurezas en heparinas de uso humano.

Los **antibióticos** son un grupo de fármacos que se clasifican no sólo por su eficacia frente a determinados procesos patológicos (infecciosos) sino por su potencia frente a determinados microorganismos susceptibles de desencadenar tales infecciones. Para ello, lo mas frecuente es su valoración mediante ensayos biológicos determinando la concentración inhibitoria en los cultivos de los **microorganismos patógenos**. Se ha determinado la actividad de ofloxacino, ciprofloxacino, ampicilina y vancomicina frente a dos patógenos (*Streptococcus vestibularis* y *Pseudomonas fluorescens*) mediante el procedimiento clásico de cultivo en placa de agar, y se han comparado las valoraciones de concentración mínima inhibitoria con los resultados obtenidos con HTS y detección fluorimétrica así como electroforesis capilar con detección por fluorescencia inducida por láser [29]. Para la determinación de la actividad mediante el lector multipocillo, a un volumen de 200 µL de los microorganismos tratados con el correspondiente antibiótico, se añade 1 µL de una disolución 2 mM de ioduro de propidio. El propidio es un marcador fluorescente capaz de interaccionar con el ADN celular, pudiendo distinguir las células vivas de las células muertas debido a que se observa su fluorescencia roja (λ_{ex}= 488 nm, λ_{em} = 520 nm) en el caso de las células vivas, y fluorescencia verde (λ_{ex}= 488 nm, λ_{em} = 655 nm) en el caso de las células muertas, debido a que al penetrar en el núcleo se observa fluorescencia de resonancia por transferencia de energía (FRET). El cociente de las intensidades de emisión a 520 y 655 nm obtenidas con el lector multipocillo, proporciona un resultado cuantitativo y fiable del número de células vivas (no de colonias) según el tipo de antibiótico y su concentración en el que han sido incubadas. Los resultados son totalmente concordantes con los obtenidos con una técnica eminentemente cuantitativa como es la electroforesis capilar, utilizando el mismo marcador fluorescente.

Se ha demostrado la validez de los HTS para la determinación de **insecticidas neurotóxicos** como el paroxon en muestras de leche [30], mediante un inmunoanálisis tipo ELISA. La enzima, la acetilcolinesterasa, se inmoviliza sobre la superficie de poliestireno de los pocillos de la placa a través de los grupos amino y mediante la formación de enlaces cruzados con glutaraldehído. Se determina la actividad de la enzima inmovilizada sobre la placa en presencia y en ausencia de neurotóxico (insecticida), pudiéndose determinar la concentración de insecticida en función del grado de inhibición. El límite de detección se estableció en 0,5 µg L^{-1} con recuperaciones que oscilan entre 89% y 108%, por ello teniendo en cuenta que esta metodología permite procesar un número elevado de muestras en corto tiempo y a precio razonable, se considera un método de elección para la determinación de insecticidas en alimentos y garantizar así la seguridad a los consumidores.

A continuación, la Tabla 3 recoge de manera resumida las características de otros ensayos miniaturizados de relevancia desde el punto de vista de la sostenibilidad del análisis.

Tabla 3. Ensayos que reducen el volumen de reactivos consumidos y desechos producidos al llevarse a cabo en formato HTS o miniaturizado (continúa en página siguiente).

Analito	Muestra	Detección	Comentarios	Ref.
NH_4^+	Aguas dulces y aguas saladas de elevado contenido en sales y microorganismos	Fluorimétrica del producto de reacción con OPA	LOD 5 nM, excelente repetitividad, eficacia y robustez. Exacto y rápido. No interferencias de partículas en suspensión, elevado contenido salino, o ácidos orgánicos en las aguas rojas de marismas	[19]
Catión manganeso	Líneas celulares neuronales	El Mn amortigua la fluorescencia del marcador fura-2.	Almacenamiento y transporte del Mn en las células. Análisis estadístico con valores de factor *Z* diferentes dependiendo del lote	[31]
Ácidos orgánicos	Aguas residuales y lodos	Reacción con 1-naftiletilenodiamina y quenching de fluorescencia de OPA	Rango lineal de 3,9-2000 mg L^{-1}. Los resultados obtenidos se comparan con la determinación por GC, utilizada como técnica de referencia	[32]
Clorofila de algas	Aguas dulces y aguas marinas	Detección fluorimétrica de la fluorescencia de la clorofila	El crecimiento de algas como parámetro de medida de la calidad de las mismas. Utilidad en granjas y piscifactorías. Se emplean placas de 24 pocillos	[33]
Clorofila en medios de cultivo de algas	Inhibición por metales pesados del crecimiento de distintas variedades de algas	Detección de la fluorescencia de la clorofila	270 µL del cultivo de algas + 30 µL de disolución conteniendo el metal pesado en estudio. La inhibición del crecimiento de las algas depende de la toxicidad del metal y del tipo de alga	[34]
Sulfato de condroitina	Heparinas de uso humano	Detección espectrofotométrica	Se utiliza el polímero hidrosoluble 3-(2-(*N*-(*N*'-metilimidazol))etoxi)-4-metiltiofeno, LPTP) y digestión con heparinasa. Se detecta 0,003% p/p de sulfato de condroitina en muestras de heparina adicionadas. Visualmente se detecta un 0,1%	[35]
Glucógeno	Hepatocitos de rata	Detección fluorimétrica del derivado formado entre 2-{N-[7-nitrobenz-2-oxa-1, 3-diazol-4-il] amino}-2-desoxiglucosa y el glucógeno	El método permite conocer los niveles de gluógeno en hepatocitos en tiempo real	[36]
Hialorunano	Líneas celulares epiteliales (ECACC 93120839) expuestas a cloruro de benzalconio	Fluorescencia del diacetato de diclorofluoresceína hidrolizado como consecuencia de la sobreproducción de peróxido de hidrógeno (ROS) por las células sometidas a estrés	Hialorunano protege a las células frente a las especies reactivas de oxígeno que las células producen como respuesta al cloruro de benzalconio	[37]
Determinación de la actividad de caspasa-4	Lisados de líneas celulares de coriocarcinoma JGE-3	Medida de la fluorescencia de la 7-amino-4-trifluoro metilcumarina. Este reactivo es liberado de los péptidos marcados por acción de la caspasa-4	Las caspasas se activan en la apoptosis celular. Los resultados del lector multipocillo se comparan con los obtenidos por RP-HPLC-FD	[38]
Agentes antituberculosos	Inhibición de la actividad enzimática de la aminotransferasa del ácido 7,8-diaminopelargónico en el *Mycobacterium tuberculosis*	Se determina el grado de inhibición enzimática mediante derivatización fluorescente con OPA en presencia de mercaptoetanol	Método rápido, económico y sensible. Rango lineal de 20 nM a 50 µM. Los métodos previos son largos y tediosos	[39]
Agentes antifúngicos inhibidores de la homocitrato sintasa.	Inhibición de la actividad enzimática de la homocitrato sintasa	Se detecta la formación de CoA mediante la reacción del grupo tiol con el marcador fluorescente ácido 10-(2,5-dihidro-2, 5-di-oxo-1*H*-pirrol-1-il)-9-metoxi-3-oxo-, metil ester 3H-naftol(2,1-b) piran-S-carboxílico	20 min de incubación a temperatura ambiente, más 10 min adicionales después de adicionar el reactivo fluorogénico para que transcurra la reacción de derivatización. Factor *Z* de 0,73-0,82. CV de 7,9% a 14,9%	[40]
Inhibidores del receptor α-estrogénico	Receptor α-estrogénico	Medida de las fluorescencia del inhibidor α-estrogénico unido a fluoresceína y enlazado al receptor	En las células tumorales de cáncer de mama resistentes al tamoxifeno, el receptor α-estrogénico está sobrexpresado. Se emplean placas de 384 pocillos y volúmenes de 10 µL	[41]

Tabla 3. (continuación)

Analito	Muestra	Detección	Comentarios	Ref.
Inhibidores de quinasas	Extractos vegetales	Medida de la fluorescencia de un reactivo fluorogénico patentado	Los resultados se comparan con los obtenidos mediante la aplicación de un ELISA	[42]
Determinación de la actividad de 5-lipoxigenasa humana	Lipoxigenasa humana clonada	Medida de la fluorescencia del diacetato de diclorofluoresceína oxidado en presencia de 5-lipoxigenasa.	Se emplean placas de 384 pocillos. Además de la actividad enzimática, se determina la inhibición de 5-lipoxigenasa por diversos compuestos. El factor *Z* obtenido es 0,61	[43]
Determinación de la actividad de lisozima	Lisozima de *Micrococcus lysodeikticus*	Medida de la fluorescencia de la lisozima marcada con fluoresceína	Se compara el método de detección fluorimétrica en placas de 96 pocillos con el método de referencia turbidimétrico. El ensayo HTS es notablemente más sensible, exacto y rápido	[44]
Determinación de la actividad de lisozima en células humanas expuestas a saponinas	Líneas celulares epiteliales humanas HT-29 y líneas celulares monocito humanos THP-1	Medida de la fluorescencia de la lisozima marcada con fluoresceína	Se emplea el sobrenadante de los cultivos y se incuban 50 µL por pocillo durante 60 min, después se mide la fluorescencia cada 5 min	[45]
Determinación de la actividad hidrolítica de proteasas	Seroalbúmina bovina	Detección fluorimétrica del derivado de fluoresceína liberado del complejo con Cu^{2+}	Un compuesto análogo de fluoresceína es capaz de formar complejos con Cu^{2+} (no fluorescente). La presencia de los aminoácidos liberados por la proteasa, desplazan al Cu^{2+} y se desarrolla una notable fluorescencia de forma instantánea	[46]
Determinación de la actividad de kynurenina aminotransferasa (KYNA)	Líneas celulares y enzima nativa	Detección fluorimétrica debido a la capacidad de KYNA de formar un complejo fluorescente con Zn^{2+}	Comparación entre el ensayo HTS y la determinación por HPLC. Mediante el HTS la L- kynurenina se detecta directamente en el medio celular de forma rápida y con costo sensiblemente menor. Máxima concordancia entre los resultados HPLC vs. HTS	[47]
Compuestos con actividad protectora frente a especies reactivas de oxígeno	Mitocondria hepática	Medida de la fluorescencia del diacetato de diclorofluoresceína	Se emplean placas de 384 pocillos en las que se incuban durante 90 min el marcador fluorescente y los antioxidantes en presencia de las mitocondrias. Se han ensayado más de 75000 compuestos, de los que 5061 resultaron activos. El factor *Z* obtenido es 0,81	[48]
Genotóxicos (nitrosaminas, aminas aromáticas...)	Células de ovario de hámster	Cambios de la fluorescencia del sensor Hoescht	La emisión de fluorescencia del sensor cambia según se encuentre unido a la doble hélice o a un fragmento dañado del mismo	[49]
Detección simultánea de microorganismos patógenos (*E. coli, S. typhimurium*)	Potencial aplicación a alimentos	Medida de la fluorescencia del marcador (fluoresceína o Cy-3) que se intensifica al producirse la reacción inmunoanalítica antígeno-anticuerpo marcado	Inmunoensayo tipo sándwich. Los pocillos de la placa se recubren con estreptavidina y los anticuerpos se enlazan a través de la biotina. Se añade el analito (antígeno) y a continuación el fluoróforo se une al anticuerpo. El analito queda atrapado entre las dos capas de anticuerpos	[50]
Enterotoxina estafilocócica B	Muestras de alimentos adicionados (leche, mayonesa)	Detección colorimétrica miniaturizada en placa de 96 pocillos	El volumen de muestra utilizado es 5 µL, unas 10 veces menor que en el diseño de 96 pocillos tradicional. LOD 3,9 - 18,5 ng mL^{-1} dependiendo de la matriz	[51]
Enterotoxina estafilocócica B	Aguas fluviales, residuales y lodos. Agua potable. Carne de vacuno, jamón curado, zumos, leche. Mantequilla de cacahuete. Orina y suero humano.	Detección quimioluminescente acoplada a un enzimoinmunoensayo	Dos anticuerpos monoclonales reconocen específicamente diferentes epitopos de la enterotoxina B. El antígeno (enterotoxina) se une al anticuerpo que se ha unido previamente a la peroxidasa de rábano. La peroxidasa genera el H_2O_2 requerido para oxidar el luminol. LOD 0,01 ng mL^{-1};% CV intra- e inter-ensayo <13%. Sencillez y rapidez para un ensayo de utilidad en salud pública	[52]

Referencias

1. T. Křížek, A. Kubícková, Microscale separation methods for enzyme kinetics assays, Anal Bioanal Chem. 403 (2012) 2185–2195.
2. R. Macarron, Critical review of the role of HTS in drug discovery, Drug Discov Today. 11 (2006) 277–279.
3. B.T. Cunningham, L.G. Laing, Advantages and application of label-free detection assays in drug screening, Expert Opin. Drug Discov. 3 (2008) 891–901.
4. E.A. Martis, R. Radhakrishnan, R.R. Badve, High-throughput screening: the hits and leads of drug discovery-an overview, J App Pharm Sci. 1 (2011) 2–10.
5. J.L. Reymond, Spectrophotometric enzyme assays for high-throughput screening, Food Technol Biotechnol. 42 (2004) 265–269.
6. J. Wölcke, D. Ullmann, Miniaturized HTS technologies - uHTS, Drug Discov Today. 6 (2001) 637–646.
7. J.-P. Goddard, J.-L. Reymond, Enzyme assays for high-throughput screening, Curr Opin Biotechnol. 15 (2004) 314–322.
8. S.J. Shukla, R. Huang, C.P. Austin, M. Xia, The future of toxicity testing: a focus on in vitro methods using a quantitative high-throughput screening platform, Drug Discov Today. 15 (2010) 997–1007.
9. M.L. Kovarik, P.C. Gach, D.M. Ornoff, Y. Wang, J. Balowski, L. Farrag, et al., Micro total analysis systems for cell biology and biochemical assays, Anal Chem. 84 (2012) 516–540.
10. D.A. Pereira, J.A. Williams, Origin and evolution of high throughput screening, Br J Pharmacol. 152 (2007) 53–61.
11. J. Inglese, R.L. Johnson, A. Simeonov, M. Xia, W. Zheng, C.P. Austin, et al., High-throughput screening assays for the identification of chemical probes, Nat. Chem. Biol. 3 (2007) 466–479.
12. R. Macarron, M.N. Banks, D. Bojanic, D.J. Burns, D.A. Cirovic, T. Garyantes, et al., Impact of high-throughput screening in biomedical research, Nat Rev Drug Discov. 10 (2011) 188–195.
13. K. Aslan, P. Holley, C.D. Geddes, Microwave-Accelerated Metal-Enhanced Fluorescence (MAMEF) with silver colloids in 96-well plates: Application to ultra fast and sensitive immunoassays, High Throughput Screening and drug discovery, J. Immunol. Methods. 312 (2006) 137–147.
14. P. Gribbon, A. Sewing, Fluorescence readouts in HTS: no gain without pain? Drug Discov Today. 8 (2003) 1035–1043.
15. J. Inglese, D.S. Auld, A. Jadhav, R.L. Johnson, A. Simeonov, A. Yasgar, et al., Quantitative high-throughput screening: a titration-based approach that efficiently identifies biological activities in large chemical libraries, Proc Natl Acad Sci USA. 103 (2006) 11473–11478.
16. J.H. Zhang, A Simple Statistical Parameter for Use in Evaluation and Validation of High Throughput Screening Assays, J Biomol Screen. 4 (1999) 67–73.
17. R. Stevens, M. Buret, C. Garchery, Y. Carretero, M. Causse, Technique for rapid, small-scale analysis of vitamin C levels in fruit and application to a tomato mutant collection, J Agric Food Chem. 54 (2006) 6159–6165.
18. T. Rojanarata, K. Sumran, P. Nateetaweewat, W. Winotapun, S. Sukpisit, P. Opanasopit, et al., Microscale chemistry-based design of eco-friendly, reagent-saving and efficient pharmaceutical analysis: a miniaturized Volhard's titration for the assay of sodium chloride, Talanta. 85 (2011) 1324–1329.
19. P. Poulin, É. Pelletier, Determination of ammonium using a microplate-based fluorometric technique, Talanta. 71 (2007) 1500–1506.
20. L.S. Inouye, G.R. Lotufo, Comparison of macro-gravimetric and micro-colorimetric lipid determination methods, Talanta. 70 (2006) 584–587.
21. T. Attin, T. Abouassi, K. Becker, A. Wiegand, M. Roos, R. Attin, A new method for chlorhexidine (CHX) determination: CHX release after application of differently concentrated CHX-containing preparations on artificial fissures, Clin Oral Invest. 12 (2008) 189–196.
22. P. Zuck, G.T. O'Donnell, J. Cassaday, P. Chase, P. Hodder, B. Strulovici, et al., Miniaturization of absorbance assays using the fluorescent properties of white microplates, Anal Biochem. 342 (2005) 254–259.
23. K.C. Makris, P. Punamiya, D. Sarkar, R. Datta, Novel colorimetric method overcoming phosphorus interference during trace arsenic analysis in soil solution, Analyst. 133 (2008) 191–196.
24. H.A. Azab, S.A. El-Korashy, Z.M. Anwar, G.M. Khairy, M.-S. Steiner, A. Duerkop, High-throughput sensing microtiter plate for determination of biogenic amines in seafood using fluorescence or eye-vision, Analyst. 136 (2011) 4492–4499.
25. M.S. Elgawish, C. Shimomai, N. Kishikawa, K. Ohyama, K. Nakashima, N. Kuroda, Microplate analytical method for quinones by pulse photo-irradiation and chemiluminescence detection, Analyst. 137 (2012) 4802–4808.
26. Summary of 2nd Workshop on the Characterisation of Heparin Products, in: Nd Workshop on the Characterisation of Heparin Products, Strasbourg, 2008: pp. 1–15.
27. A.W. McMahon, R.G. Pratt, T.A. Hammad, S. Kozlowski, E. Zhou, S. Lu, et al., Description of hypersensitivity adverse events following administration of heparin that was potentially contaminated with oversulfated chondroitin sulfate in early 2008, Pharmacoepidemiol Drug Saf. 19 (2010) 921–933.
28. S. Lühn, T. Schrader, W. Sun, S. Alban, Development and evaluation of a fluorescence microplate assay for quantification of heparins and other sulfated carbohydrates, J Pharm Biomed Anal. 52 (2010) 1–8.

29. V. Hoerr, W. Ziebuhr, S. Kozitskaya, E. Katzowitsch, U. Holzgrabe, Laser-induced fluorescence-capillary electrophoresis and fluorescence microplate reader measurement: two methods to quantify the effect of antibiotics, Anal Chem. 79 (2007) 7510–7518.
30. Y. Zhang, Y. Cai, L. Li, Y. Qian, L. Lu, High-throughput biosensing of neurotoxic insecticides using polystyrene microplate-immobilized acetylcholinesterase, Anal. Methods. 4 (2012) 3830.
31. K.K. Kumar, A.A. Aboud, D.K. Patel, M. Aschner, A.B. Bowman, Optimization of fluorescence assay of cellular manganese status for high throughput screening, J. Biochem. Mol. Toxicol. 27 (2013) 42–49.
32. F. Robert-Peillard, E. Palacio-Barco, B. Coulomb, J.L. Boudenne, Development of a fluorescence-based microplate method for the determination of volatile fatty acids in anaerobically digested and sewage sludges, Talanta. 88 (2012) 230–236.
33. T.J. Waybright, D.E. Terlizzi, M.D. Ferrier, Chemical characterization of the aqueous algistatic fraction of barley straw (*Hordeum vulgare*) inhibiting Microcystis aeruginosa, J Appl Phycol. 21 (2009) 333–340.
34. A. Satoh, L.Q. Vudikaria, N. Kurano, S. Miyachi, Evaluation of the sensitivity of marine microalgal strains to the heavy metals, Cu, As, Sb, Pb and Cd, Environ Int. 31 (2005) 713–722.
35. C.D. Sommers, D.J. Mans, L.C. Mecker, D.A. Keire, Sensitive detection of oversulfated chondroitin sulfate in heparin sodium or crude heparin with a colorimetric microplate based assay, Anal Chem. 83 (2011) 3422–3430.
36. M.C. Louzao, B. Espiña, M.R. Vieytes, F.V. Vega, J.A. Rubiolo, O. Baba, et al., "Fluorescent glycogen" formation with sensibility for in vivo and in vitro detection, Glycoconj. J. 25 (2008) 503–510.
37. T. Pauloin, M. Dutot, J.-M. Warnet, P. Rat, In vitro modulation of preservative toxicity: high molecular weight hyaluronan decreases apoptosis and oxidative stress induced by benzalkonium chloride, Eur J Pharm Sci. 34 (2008) 263–273.
38. S. Koehn, M. Trueck, T.G. Poehlmann, E. Schleussner, U.R. Markert, L. Seyfarth, Assessment of caspase-4 released free AFC by RP-HPLC and fluorescence detection, J Chromatogr B. 874 (2008) 111–114.
39. S. Mann, L. Eveleigh, O. Lequin, O. Ploux, A microplate fluorescence assay for DAPA aminotransferase by detection of the vicinal diamine 7,8-diaminopelargonic acid, Anal Biochem. 432 (2013) 90–96.
40. S.L. Bulfer, T.J. McQuade, M.J. Larsen, R.C. Trievel, Application of a high-throughput fluorescent acetyltransferase assay to identify inhibitors of homocitrate synthase, Anal Biochem. 410 (2011) 133–140.
41. C. Mao, N.M. Patterson, M.T. Cherian, I.O. Aninye, C. Zhang, J.B. Montoya, et al., A new small molecule inhibitor of estrogen receptor alpha binding to estrogen response elements blocks estrogen-dependent growth of cancer cells, J. Biol. Chem. 283 (2008) 12819–12830.
42. I. Dufau, A. Lazzari, A. Samson, I. Pouny, F. Ausseil, Optimization of a homogeneous assay for kinase inhibitors in plant extracts, Assay Drug Dev Technol. 6 (2008) 673–682.
43. R.A. Pufahl, T.P. Kasten, R. Hills, J.K. Gierse, B.A. Reitz, R.A. Weinberg, et al., Development of a fluorescence-based enzyme assay of human 5-lipoxygenase, Anal Biochem. 364 (2007) 204–212.
44. R. Helal, M.F. Melzig, Determination of lysozyme activity by a fluorescence technique in comparison with the classical turbidity assay, Pharmazie. 63 (2008) 415–419.
45. R. Helal, M.F. Melzig, In vitro Effects of Selected Saponins on the Production and Release of Lysozyme Activity of Human Monocytic and Epithelial Cell Lines, Sci Pharm. 79 (2011) 337–349.
46. K.E.S. Dean, G. Klein, O. Renaudet, J.-L. Reymond, A green fluorescent chemosensor for amino acids provides a versatile high-throughput screening (HTS) assay for proteases, Bioorg Med Chem Lett. 13 (2003) 1653–1656.
47. J. Wong, W.J. Ray, A.Y. Kornilova, Development of a microplate fluorescence assay for kynurenine aminotransferase, Anal Biochem. 409 (2011) 183–188.
48. X.-P. Chen, G.-H. Du, High-throughput screening for reactive oxygen species scavengers targeting mitochondria, Methods Find Exp Clin Pharmacol. 30 (2008) 255–260.
49. C. Baumstark-Khan, G. Horneck, Results from the "Technical workshop on genotoxicity biosensing" on the micro-scale fluorometric assay of deoxyribonucleic acid unwinding, Anal Chim Acta. 593 (2007) 75–81.
50. A.G. Gehring, D.M. Albin, S.A. Reed, S.-I. Tu, J.D. Brewster, An antibody microarray, in multiwell plate format, for multiplex screening of foodborne pathogenic bacteria and biomolecules, Anal Bioanal Chem. 391 (2008) 497–506.
51. K.E. Sapsford, J. Francis, S. Sun, Y. Kostov, A. Rasooly, Miniaturized 96-well ELISA chips for staphylococcal enterotoxin B detection using portable colorimetric detector, Anal Bioanal Chem. 394 (2009) 499–505.
52. F. Liu, Y. Li, C. Song, B. Dong, Z. Liu, K. Zhang, et al., Highly sensitive microplate chemiluminescence enzyme immunoassay for the determination of staphylococcal enterotoxin B based on a pair of specific monoclonal antibodies and its application to various matrices, Anal Chem. 82 (2010) 7758–7765.

La cromatografía de líquidos en el contexto de la química analítica sostenible

La cromatografía de líquidos es una técnica analítica que se caracteriza por su versatilidad, sensibilidad, rapidez, capacidad de análisis de un elevado número de muestras y además acoplada a distintas modalidades de detección es una técnica no destructiva; por todo ello el número de aplicaciones analíticas de la misma se incrementa constantemente [1]. En la idea de hacer de ella una técnica respetuosa con el medio ambiente, en los últimos años se han introducido nuevas fases estacionarias, o bien, modificadores en las fases móviles que permiten reducir el consumo de disolventes orgánicos [2].

La reducción de la longitud de la columna, del diámetro interno de la misma, o del tamaño de las partículas que forman la fase estacionaria, conllevan una drástica reducción en el consumo de disolventes y la generación de residuos manteniendo o mejorando las características de eficacia y resolución tradicionalmente esperadas de la cromatografía de líquidos (Figura 1). El empleo de partículas de diámetro inferior a 2 µm ha dado lugar a la denominada UHPLC (Ultra High Presssure/Performance Liquid Chromatography) que posee las características anteriormente mencionadas pero que tiene el inconveniente de las elevadas presiones que se generan en el interior de la columna y, por ello, se hace necesario equipos dotados de bombas específicas con tal finalidad. Debido no sólo a la presión sino al calor generado, es frecuente que estas partículas de tan reducido tamaño se empaqueten en columnas capilares para facilitar la disipación de calor. Varios artículos de revisión resumen los aspectos más significativos del empleo de este tipo de fases estacionarias [3-6].

El empleo de nanopartículas (de Au o de Ag) funcionalizadas en las separaciones por cromatografía está suscitando muy recientemente un gran interés, lo que se debe en gran parte a que la tecnología de producción de este tipo de nanopartículas es altamente reproducible y permite la obtención de fases estacionarias muy específicas debido a la unión de antígenos y otros receptores biológicos. Alternativamente se pueden enlazar/inmovilizar sobre la superficie de las nanopartículas "receptores" de distintas clases (biológicos y abióticos) que le confieran una gran versatilidad a las fases estacionarias formadas con ellas [7,8].

Teniendo en cuenta que en todo proceso cromatográfico se puede optar por modificar la naturaleza de la fase estacionaria o bien de la fase móvil, a continuación consideraremos ambos como factores moduladores en el desarrollo de metodologías analíticas sostenibles.

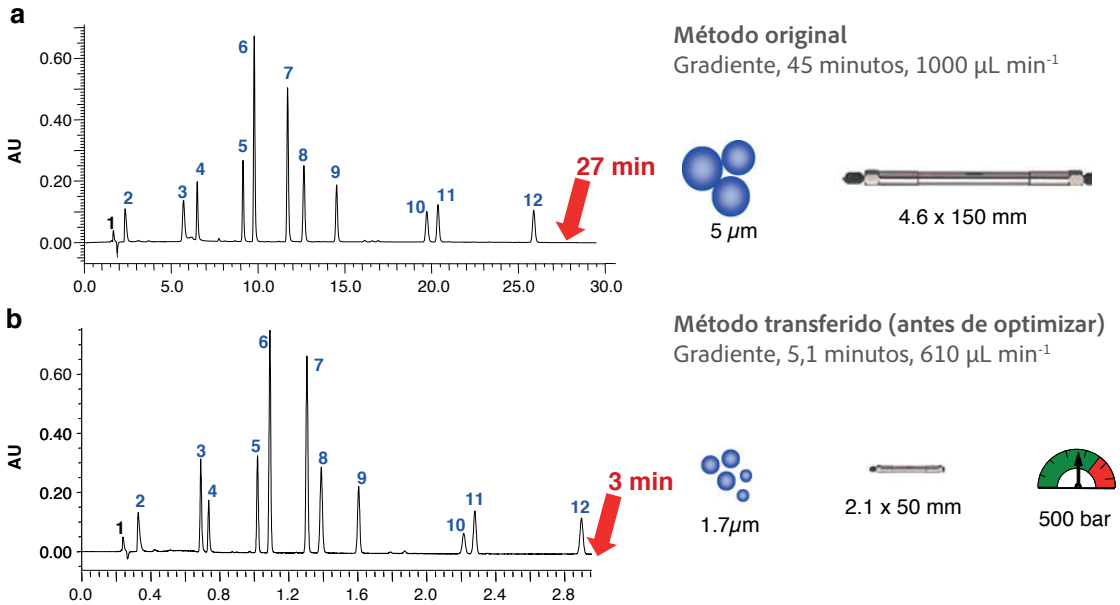

Figura 1.
Cromatogramas que muestran cómo el empleo de las nuevas fases estacionarias disponibles en cromatografía de líquidos permiten alcanzar no sólo mejores eficacias y rendimientos, sino también ahorros considerables en el consumo de disolventes y generación de residuos [9].

Referencias

1. P.W. Carr, D.R. Stoll, X. Wang, Perspectives on recent advances in the speed of high-performance liquid chromatography, Anal Chem. 83 (2011) 1890–1900.
2. T.L. Chester, Recent Developments in High-Performance Liquid Chromatography Stationary Phases, Anal Chem. 85 (2013) 579–589.
3. J.J. Salisbury, Fused-core particles: a practical alternative to sub-2 micron particles, J Chromatogr Sci. 46 (2008) 883–886.
4. F. Gritti, G. Guiochon, Mass transfer kinetics, band broadening and column efficiency, J Chromatogr A. 1221 (2012) 2–40.
5. Y. Wang, F. Ai, S.-C. Ng, T.T.Y. Tan, Sub-2 µm porous silica materials for enhanced separation performance in liquid chromatography, J Chromatogr A. 1228 (2012) 99–109.
6. G. Guiochon, F. Gritti, Shell particles, trials, tribulations and triumphs, J Chromatogr A. 1218 (2011) 1915–1938.
7. E. Guihen, Nanoparticles in modern separation science, Trends Anal Chem. 46 (2013) 1–14.
8. F.P. Zamborini, L. Bao, R. Dasari, Nanoparticles in measurement science, Anal Chem. 84 (2012) 541–576.
9. D. Guillarme, J. Ruta, S. Rudaz, J.-L. Veuthey, J.-L. New trends in fast and high-resolution liquid chromatography: a critical comparison of existing approaches. Anal Bioanal Chem, 397 (2010) 1069–1082

5

Fases móviles respetuosas con el medio ambiente

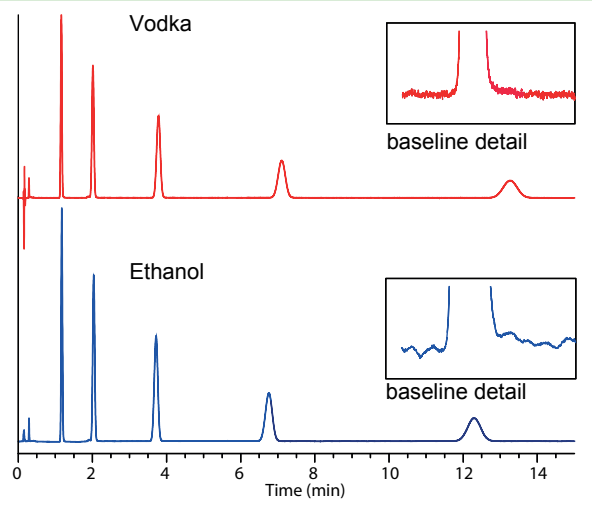

Welch, C. J. et al. (2010). Trends in Analytical Chemistry, 29(7), 667

ABSTRACT ▶ Las fases móviles en cromatografía suelen contener una proporción variable de disolvente orgánico. Hay intervenciones que pueden llevarse a cabo sobre la fase estacionaria (estructura, composición química, tamaño del empaquetamiento) para reducir el consumo de fase móvil, y éstas se revisarán en el siguiente capítulo. Sin embargo, uno de los recursos más inmediatos para disminuir el impacto medioambiental de las fases móviles es cambiar su composición para hacerlas más respetuosas con el medio ambiente. Existen dos aproximaciones a esta alternativa: la primera es la sustitución del componente orgánico (generalmente acetonitirlo) por otros con menos impacto ambiental, como los alcoholes o el carbonato de propileno. La segunda pasa por el uso de modificadores que, añadidos a la fase móvil, cambien sus características cromatográficas y permitan reducir la proporción de disolvente orgánico. Dentro de este grupo son destacables por su importancia los tensioactivos formadores de micelas y las ciclodextrinas.

1. Introducción

La mayoría de los disolventes orgánicos empleados en HPLC son compuestos volátiles capaces de dispersarse fácilmente en la atmósfera con los consiguientes riesgos en lo que a toxicidad y seguridad se refiere; de ahí que la reducción de la utilización de disolventes de impacto medioambiental sea objeto de diversos artículos de revisión [1-3]. Los dos disolventes más ampliamente utilizados en las separaciones por HPLC son metanol y acetonitrilo. Ambos poseen cualidades deseables tanto desde el punto de vista de la separación (fuerza eluyente, viscosidad, miscibilidad con el agua y otros disolventes orgánicos...) como por sus buenas características de cara a la detección. Sin embargo, el acetonitrilo es tóxico tanto en estado líquido como gaseoso y, además, sus residuos requieren un tratamiento químico especial que supone un elevado coste económico. Por otra parte, el metanol también es tóxico para los humanos y es causa de diversos efectos indeseados sobre los ecosistemas acuáticos. En consecuencia, desde el punto de vista de la sostenibilidad, en los últimos años se han desarrollado diferentes estrategias alternativas al empleo de metanol o acetonitrilo en las fases móviles.

El abanico de posibilidades comprende desde la utilización de disolventes y fases móviles sobrecalentadas constituidas por disolventes renovables, pasando por el empleo de líquidos iónicos, hasta otras modificaciones en la composición de la fase móvil como micelas o ciclodextrinas. Una modificación de la fase móvil es aceptable siempre que en el cambio no se sacrifiquen la eficacia y resolución de la técnica cromatográfica. Además, para cualquier técnica analítica modificada hacia la sostenibilidad es requisito imprescindible mantener la exactitud y reproducibilidad de la misma [4].

Estas estrategias encaminadas hacia la sostenibilidad no se emplean solamente en HPLC sino también en TLC y en HTLC [5,6]. En los apartados siguientes consideraremos las diferentes alternativas que conducen a fases móviles más sostenibles.

2. Separaciones mediante el empleo de fases móviles mayoritariamente acuosas

Las características químicas de algunos analitos hacen viable su separación en fases estacionarias convencionales, en gran parte debido a la gran diversidad de modificaciones químicas hoy en día comercialmente disponibles para las mismas, y empleando fases móviles cuya proporción acuosa supera el 90%. Así, compuestos muy polares e ioniza-

bles en función del pH de la fase móvil, como el ácido úrico y la creatinina, se pueden resolver y separar en menos de 5 minutos en fases estacionarias convencionales C-18 controlando el pH de la fase móvil (disolución acuosa de fosfato amónico 0,05 M, pH = 7,4). Esta metodología se ha aplicado a la determinación de estos compuestos en orina [7].

Compuestos de polaridad elevada como la niacina, la niacinamida (pertenecientes al grupo de la vitamina B) o el 4-acetamidofenol son susceptibles de separarse en columnas Hamilton PRP-1, constituidas por fases estacionarias poliméricas de poli(estireno-divinilbenceno) que forman un entramado polimérico capaz de resistir elevadas presiones, altas temperaturas, valores de pH entre 1 y 13 y fases móviles 100% acuosas sin que se produzcan los fenómenos de colapso que se observan en las tradicionales C-18 cuando se emplean fases móviles totalmente acuosas. Estas fases estacionarias muestran unas características de retención similares a las C-18 pero poseen distinta selectividad, dado que las características químicas de su soporte son diferentes. Se compara esta metodología de separación con las obtenidas empleando columnas clásicas Waters XTerra MS-C18. Las fases móviles son 100% acuosas y las temperaturas oscilan entre los 60 y 80 ºC. El método desarrollado se ha validado y se ha demostrado su utilidad para la determinación de niacina y niacinamida en cremas utilizadas en la regeneración y cuidado de la piel [8].

Una fase estacionaria constituida por un derivado polisacárido de metacriloilo establece interacciones hidrofílicas (HILIC) con los analitos a separar (cafeína, vitaminas hidrosolubles y melamina) posibilitando su separación utilizando como fase móvil MeCN:H_2O, 3:97, v:v [9].

Algunos fármacos, como la cafeína, el paracetamol y la propifenazona, que presentan un carácter hidrófilo, se separan pobremente en condiciones de fase inversa utilizando fases estacionarias C-18 debido a la mala retención de estos compuestos por una fase estacionaria hidrofóbica. La utilización de columnas de tipo amino tampoco contribuye a la resolución del problema. Sin embargo, el empleo de fases estacionarias de polietilenglicol (PEG) hace posible la resolución eficaz de los analitos empleando fases móviles casi completamente acuosas. Ello se debe a que los grupos éter del PEG retienen eficazmente a los analitos polares discriminándolos entre si y en tiempos de análisis de 7 min. La separación se lleva a cabo en elución isocrática, empleando como fase móvil una disolución acuosa de trietilamina al 0,04% cuyo pH se ha ajustado a un valor de 4,5 mediante el empleo de ácido acético. Los analitos se detectan a 210 nm mediante un detector UV de diodos en serie [10].

Las separaciones HILIC están siendo objeto de numerosos avances y un creciente uso con muy buena acogida por parte de muchos practicantes de la cromatografía [11].

3. Empleo de disolventes orgánicos sostenibles

Se ha llevado a cabo un estudio comparativo de las separaciones de diversos compuestos modelo (derivados de alquilbenceno, hidrocarburos aromáticos policíclicos y bases xánticas como la cafeína) empleando como fases móviles MeCN:H_2O, MeOH:H_2O o EtOH:H_2O. Los resultados obtenidos demuestran que la utilización de un gradiente adecuado de proporción creciente en etanol permite obtener eficacias y resoluciones análogas a las que se obtienen para las fases móviles de MeCN:H_2O o MeOH:H_2O, en tiempos de análisis muy similares e incluso inferiores. Por ello los autores proponen el empleo de etanol como alternativa a las fases móviles de acetonitrilo [12,13].

Durante los últimos años, y en parte debido a la crisis económica, se ha producido un notable descenso a nivel mundial en la demanda de acrilonitrilo. Dado que el acetonitrilo es uno de los productos secundarios de esta síntesis, la producción de este disolvente ha caído bruscamente, lo que ha incrementado su precio. Este hecho, unido a las razones anteriormente expuestas han motivado la búsqueda de disolventes alternativos al acetonitrilo para su utilización en HPLC.

3.1. Sustitución de acetonitrilo por alcoholes en las fases móviles

Un reciente estudio ha comparado la separación de nucleótidos y polinucletótidos, péptidos y proteínas como bradiquinina y angiotensina, mioglobina y seroalbúmina humana en fases estacionarias monolíticas C-18 y C-5 y empleando como agentes formadores de pares iónicos acetato de trietilamina, sulfato de tetrabutilamonio y ácido trifluoroacético. La elución se realizó en gradiente, siendo el disolvente A agua que incorpora el agente formador del par iónico, y el disolvente B distinto en cada caso:

- H_2O:MeCN(20:80, v:v)
- H_2O:EtOH (50:50, v:v)
- H_2O:*n*-propanol (50:50, v:v)
- MeOH (100%)

Las características de las fases metanólica y de *n*-propanol (*n*PrOH) no son suficientes en lo que a eficacia y resolución se refiere, comparadas con el acetonitrilo. Sin embargo, las fases móviles etanólica y de acetonitrilo son semejantes desde un punto de vista cromatográfico (Figura 1) y su sustitución supone un considerable ahorro no sólo económico (etanol 25€/L y acetonitrilo 80€/L, precios de 2009-2010)

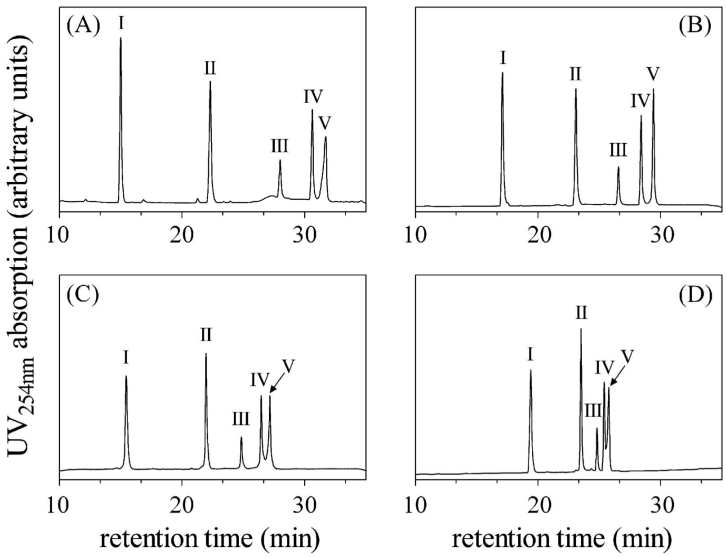

Figura 1.
Efecto de la composición de la fase móvil sobre la separación de polifosfatos de diadenosina. Fase estacionaria columna monolítica C-18. (A) Fase móvil H_2O:MeCN, 20:80, v:v (B) Fase móvil EtOH:H_2O (C) Fase móvil *n*PrOH:H_2O (D) MeOH:H_2O. En todos los casos la elución se llevó a cabo en gradiente con programación dependiente del disolvente orgánico empleado. Compuestos I-V: di-, tri-, tetra-, penta- y hexafosfato de diadenosina [14].

sino desde el punto de vista del bajo impacto medioambiental que posee el etanol [14].

También se ha utilizado el etanol para determinación simultánea del ácido ascórbico, del fosfato de ascorbilo, del palmitato de ascorbilo y del glucósido de ascorbilo en productos cosméticos. La composición de la fase móvil es un gradiente de etanol y tampón fosfato 50 mM conteniendo cloruro de sodio 0,1 M. El pH de la fase móvil demostró ser una variable crítica para la separación. La detección de los derivados de ácido ascórbico se realiza mediante su absorción en UV-Vis y se ha aplicado a la determinación de estos componentes en productos cosméticos de 6 firmas comerciales [15].

Se han propuesto fases móviles EtOH:H_2O, 30:70, v:v y MeOH:H_2O, 58:42, v:v, como alternativa al empleo de acetonitrilo para la separación de prednisolona en comprimidos y otras formas farmacéuticas demostrando no sólo que la eficacia de la separación se garantizaba, sino unos parámetros de calidad adecuados, junto con una buena robustez. El método propuesto satisface los requerimientos para el análisis de rutina y el control de calidad de este principio activo en la industria farmacéutica. Además, se realiza un análisis del ahorro en cuanto al coste del acetonitrilo con respecto al etanol en un momento de especial carestía del primero [16]. A pesar de que las fases móviles hidroetanólicas generan presiones más elevadas en la columna que las metanólicas o las de acetonitrilo, sin embargo, en ningún caso se sobrepasaron los 80 bares. Con la finalidad de evitar esta mayor presión inherente a las fases móviles hidroetanólicas, el empleo de columnas monolíticas constituye una atractiva alternativa [17].

La sustitución de acetonitrilo por metanol para la elución en gradiente de las antocianinas presentes en distintas variedades de fresas, frambuesas y arándanos ha dado muy buenos resultados en cuanto a recuperaciones y sensibilidad para la detección de los analitos. Se han empleado columnas convencionales de octadecilsilano (C-18) y un cromatógrafo con detector de diodos en serie. Para esta fase estacionaria, las fases móviles metanólicas proporcionan una buena resolución y eficacia con mejor selectividad y simetría en los picos que las fases móviles que utilizan acetonitrilo como componente orgánico de las mismas [18].

La separación y cuantificación de melamina en productos lácteos infantiles se ha realizado empleando una fase estacionaria C-18 y como fase móvil una disolución acuosa de ácido trifluoroacético 0,10% (pH = 2,4) y metanol en proporciones 10:90 (v:v). La presencia de ácido en la fase móvil tiene como consecuencia la protonación de los grupos silanol que no estén sustituidos en el proceso de *end-capping*, lo que contribuye a evitar las colas en los picos cromatográficos. La elevada proporción de metanol en la fase móvil hace que el tiempo de análisis sea de tan sólo 6 min por muestra, dado que el tiempo de retención de la melamina es de unos 4,6 min [19].

El isopropanol es otro de los disolventes alternativos para la sustitución del acetonitrilo en las fases móviles en HPLC. Sus características químicas son muy semejantes a las del metanol, si bien tiene una polaridad más baja (su constante dieléctrica es aproximadamente la mitad del valor correspondiente a la del metanol), por tanto presenta una adecuada fuerza eluyente. Si se compararan las fases móviles agua:isopropanol, éstas presentan una mayor viscosidad que las de H_2O:MeCN (similar también a las obtenidas para las mezclas H_2O:MeOH), por ello este hecho ha de tenerse en consideración cuando se emplean estas fases móviles en UHPLC. Estas fases móviles isopropanólicas se han utilizado para la separación y análisis de dendrímeros empleados en la formación de nanopartículas como estructuras base para la vehiculización de fármacos [20].

3.2. Empleo de carbonato de propileno

El carbonato de propileno (PC, Figura 2) es un disolvente incoloro e inodoro que presenta unas características que lo hacen adecuado para su uso en HPLC:

- Elevados valores de constante dieléctrica y momento dipolar, siendo capaz de inducir en los solutos interacciones de naturaleza dipolo-dipolo que facilitan su solubilización.
- Baja volatilidad, además de no ser inflamable.
- Es biodegradable, tiene muy bajo impacto ambiental y los riesgos derivados de la exposición al mismo se limitan a la irritación de mucosas.
- Su fuerza eluyente es comparable a la del acetonitrilo quedando incluido en el mismo grupo (Grupo VI) en la clasificación de Snyder [21,22].

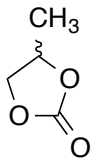

Figura 2. Estructura química del carbonato de propileno: (*R*,*S*)-4-metil-1,3-dioxolan-2-ona.

Entre las desventajas del carbonato de propileno cabe señalar [23]:

- No es completamente miscible con el agua, lo cual requiere siempre el empleo de un disolvente tipo metanol, EtOH o propanol para lograr la homogeneidad requerida para una fase móvil.
- Su densidad y viscosidad son más elevadas que la de los disolventes tradicionalmente utilizados en HPLC, lo cual implica que la presión generada en la columna y los fenómenos de resistencia a la transferencia de masa se van a ver seriamente afectados, ocasionando una pérdida de eficacia en las separaciones.
- Su elevado punto de ebullición y reducida tensión de vapor suponen un serio inconveniente para el empleo en las fases móviles en el caso de que la detección se realice mediante espectrometría de masas.

Este disolvente se ha empleado con éxito en el análisis de diversos compuestos de interés farmacéutico como hipolipemiantes del grupo de las estatinas con una fase móvil PC:EtOH:H_2O. Las separaciones se comparan con los métodos de referencia que utilizan acetonitrilo logrando eficacias similares y tiempos de análisis más reducidos en las fases móviles de PC:EtOH [23]. Al igual que en el caso de las estatinas, fases móviles que contienen carbonato de propileno han sido también utilizadas en la separación de antihipertensivos (Figura 3), obteniendo resultados comparables a los de las fases móviles con acetonitrilo [24].

Ansiolíticos como el alprazolam o antidepresivos como la sertralina, se han separado y cuantificado en comprimidos mediante HPLC con detección UV-Vis. Para ello se han empleado columnas C-18, fase móvil PC:MeOH 60:40 v:v que se añade sobre tampón de fosfato amónico (pH= 4,45) en una relación 50:50, v:v. Los resultados obtenidos se comparan con las separaciones que se llevan a cabo utilizando como fase móvil MeCN:tampón fosfato de amonio (pH= 4,45) en una relación 50:50, v:v [21,22].

4. Empleo de micelas como aditivos en las fases móviles

La cromatografía de líquidos por su naturaleza y esencia hace uso de disolventes que participando en los sucesivos equilibrios de transferencia de los solutos entre la fase móvil y la fase estacionaria tenga lugar el proceso de separación. El empleo de tensioactivos como aditivos en las fases móviles es un recurso ampliamente utilizado desde finales de la década de los ochenta

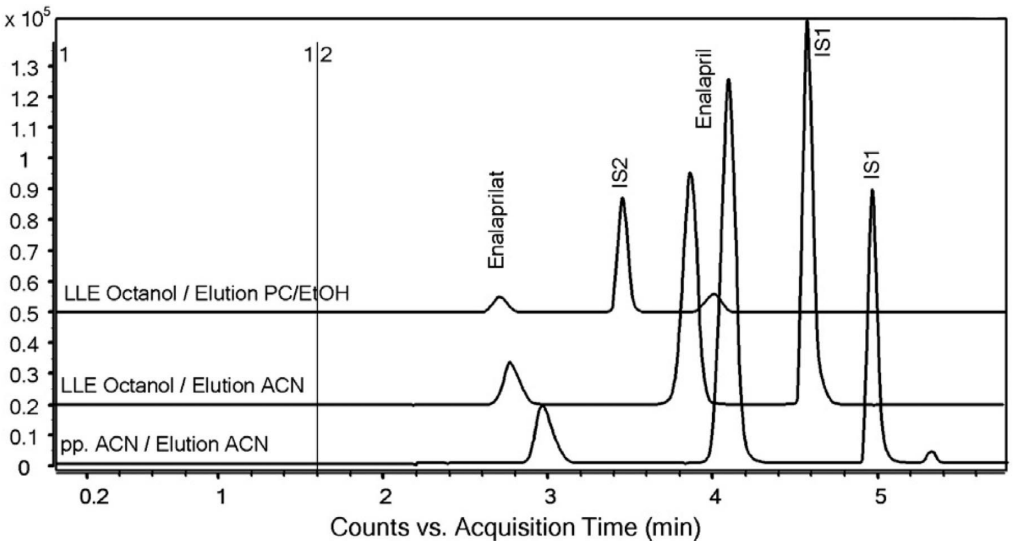

Figura 3. Cromatogramas mostrando la separación del enalaprilo y del maleato de enalaprilo en plasma humano mediante el empleo de fases estacionarias C-18 y elución en gradiente con fase móvil MeCN:H_2O conteniendo un 0,1% de HCOOH o bien fase móvil PC:EtOH (7:3, v:v) y agua conteniendo un 0,1% de HCOOH. En el cromatograma correspondiente a las disoluciones patrón los analitos no se han sometido al pretratamiento (extracción líquido-líquido) con 1-octanol [24].

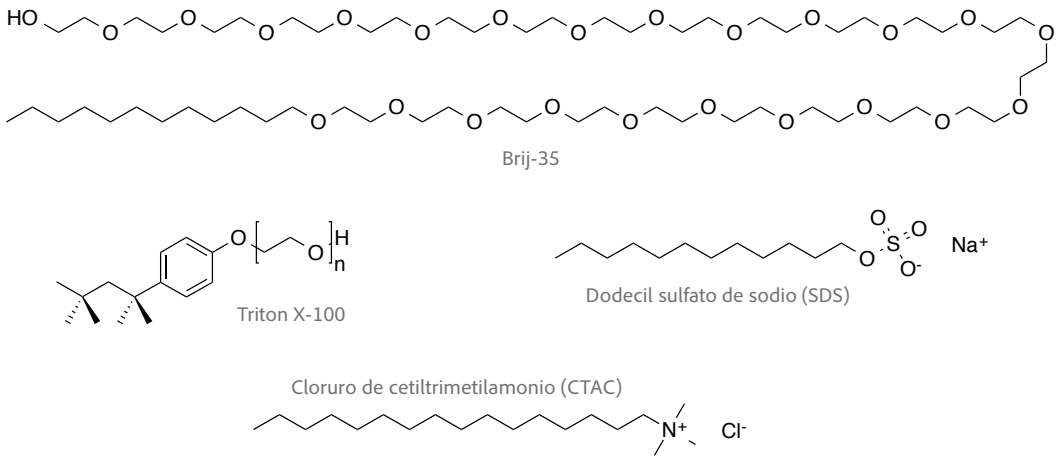

Figura 4.
Estructuras químicas de los tensioactivos más utilizados en cromatografía micelar.

[25]. En la búsqueda de alternativas sostenibles a las fases móviles convencionales la utilización de tensioactivos constituye un recurso de indudable interés [26].

Muchos tensioactivos son metabolizables a productos inocuos y biodegradables produciendo compuestos no tóxicos para el medio ambiente. La cromatografía de líquidos micelar permite la separación simultánea de compuestos hidrofílicos e hidrofóbicos, al igual que de especies cargadas o neutras en fases móviles hidro-orgánicas mayoritariamente acuosas (> 80%). En consecuencia, los tensioactivos (Figura 4) se emplean en cromatografía de líquidos en la modalidad de elución en fase inversa, si bien dependiendo de que su concentración sea inferior o superior a la concentración micelar crítica (CMC), el mecanismo de separación implicará la formación de pares iónicos con los analitos (concentración inferior a la CMC), o bien la compartimentalización de los analitos en las micelas formadas en la fase móvil (concentración superior a la CMC).

Los aspectos más novedosos de esta modalidad de cromatografía sostenible han sido revisados, poniendo especial atención a los nuevos tensioactivos como alternativa a los convencionalmente empleados [27]. Los distintos equilibrios implicados en las separaciones mediante cromatografía de líquidos empleando micelas has sido revisados y descritos rigurosamente [28] (Figura 5). Se describen las interacciones analito-micela frente a las analito-fase estacionaria, y se presentan los distintos modelos de retención en fases móviles exclusivamente micelares. La existencia de equilibrios concurrentes con los de distribución de los analitos entre las micelas y las fases estacionaria y móvil implican un control estricto de las variables que afectan a dichos equilibrios concurrentes, como son el pH o la adición de disolventes inmiscibles con el agua, como el 1-octanol.

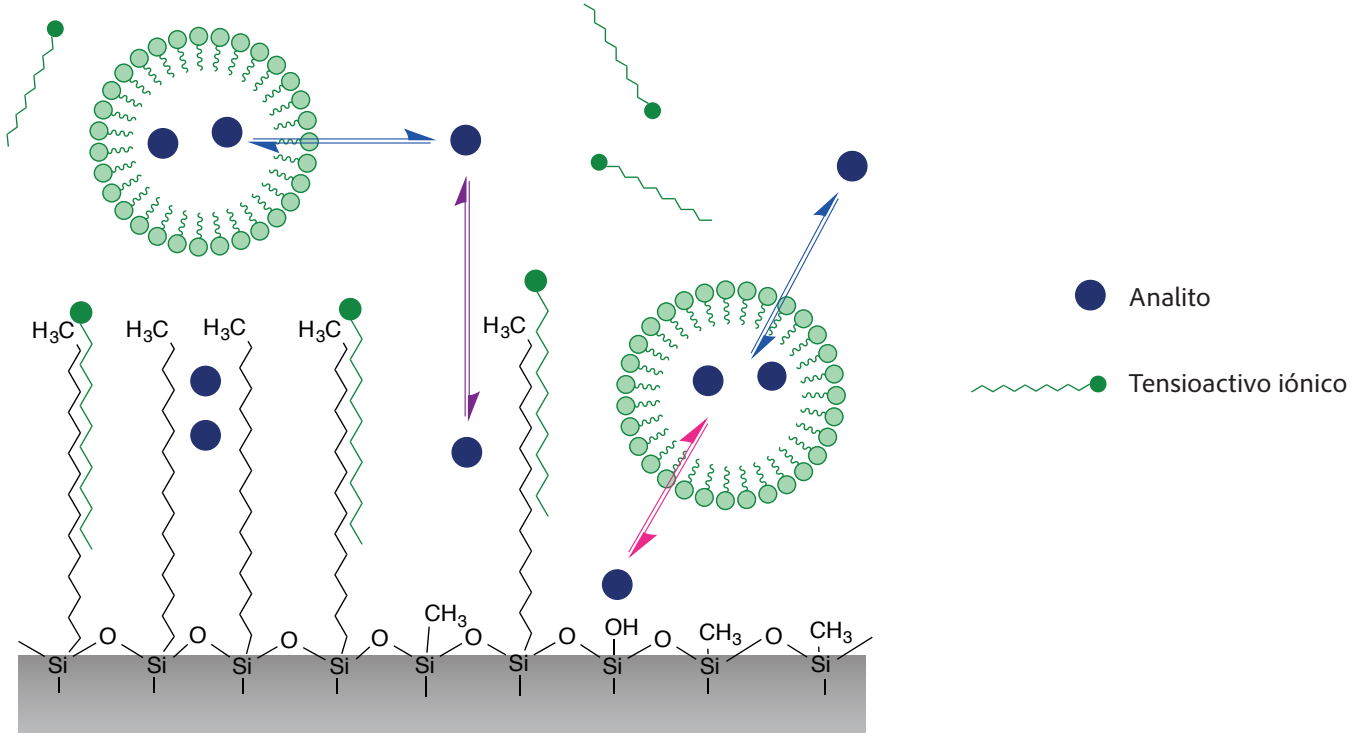

Figura 5.
Equilibrios de distribución cromatográficos que coexisten con el equilibrio secundario de solubilización de los analitos en las micelas.

4.1. High Submicelar Liquid Chromatography (HSLC)

En la modalidad denominada High Submicelar Liquid Chromatography (HSLC), los tensioactivos se encuentran en concentraciones superiores a la CMC en agua, sin embargo, la proporción relativamente alta de disolvente orgánico impide la formación de micelas [29]. La naturaleza del tensioactivo, el papel del disolvente orgánico y su proporción con respecto al componente acuoso de la fase móvil son determinantes para el mecanismo de separación en HSLC. La HSLC se ha aplicado con éxito a la determinación de antidepresivos tricíclicos empleando como fase móvil micelar Brij-35, un tensioactivo completamente biodegradable [30]. Sus bases teóricas, así como sus aplicaciones se han revisado recientemente [31].

4.2. Separaciones en fase inversa empleando fases móviles micelares

Una exhaustiva recopilación de la utilidad de la cromatografía micelar en las separaciones de fármacos analiza los factores que contribuyen al ensanchamiento de pico [32]. Como consecuencia de la lenta transferencia de masa de los solutos de la fase estacionaria a las micelas y viceversa, la eficacia de las separaciones se ve disminuida. La menor velocidad de los equilibrios de transferencia de los solutos en cromatografía micelar que contribuye al ensanchamiento de pico se ve compensada por la disminución de los valores de índice de retención, lo que hace que las eficacias sean análogas a las obtenidas en separaciones en fase inversa convencional (Figura 6).

Recientemente se ha descrito cómo pueden mejorarse las eficacias mediante la selección del componente orgánico de la fase móvil o mediante el incremento de la temperatura de la columna [33]. El efecto del SDS en la fase móvil sobre la eficacia, el perfil de pico y las anchuras de pico se ha estudiado en las separaciones de fármacos bloqueantes beta-adrenérgicos. Se realizó un estudio comparando fases móviles con diferente componente orgánico (metanol, etanol, propanol y acetonitrilo). Cuando las fases móviles incorporan acetonitrilo, el comportamiento cromatográfico del sistema en lo referente a anchuras de pico y eficacia es sensiblemente mejor que en el caso de los alcoholes lo cual puede explicarse considerando que el acetonitrilo evita la adsorción del SDS sobre el lecho de la fase estacionaria C-18 [34].

Los tensioactivos iónicos más frecuentemente utilizados son el dodecil sulfato de sodio y cloruro de *N*-cetil-trimetilamonio, y entre los no iónicos, el Brij-35 o el Triton X-100. Así, se ha comparado la separación de distintos fármacos (esteroides, sulfamidas, bloqueantes beta-adrenérgicos y diuréticos) empleando fases móviles que contienen distintos tensioactivos (dodecil sulfato de sodio, cloruro de *N*-cetil-trimetilamonio y Brij-35) y distintos componentes orgánicos (acetonitrilo, propanol y butanol). Los autores concluyen que las interacciones hidrofóbicas se ven escasamente afectadas por los cambios en la composición micelar de la fase móvil [35].

Utilizando como fases estacionaria C-18 y como componente micelar de la fase móvil dodecil sulfato de sodio (SDS) se ha propuesto un modelo de retención en cromatografía micelar basado en la aplicación de la ley de acción de masas al equilibrio de formación de las micelas en el seno de las fases móviles. La concentración de tensioactivo o la naturaleza del componente orgánico determinan el comportamiento de este equilibrio [36]. La combinación de fases estacionarias de tipo C-18 con fases móviles de ^{i}PrOH:H_2O, 10:90, v:v, que incorpora dodecil sulfato de sodio (SDS) en concentración superior a la CMC, hacen posible la separación de un grupo de anestésicos locales y de otro grupo de antihistamínicos con una buena sensibilidad y recuperaciones que oscilan entre el 92,4% y el 109,2% [37].

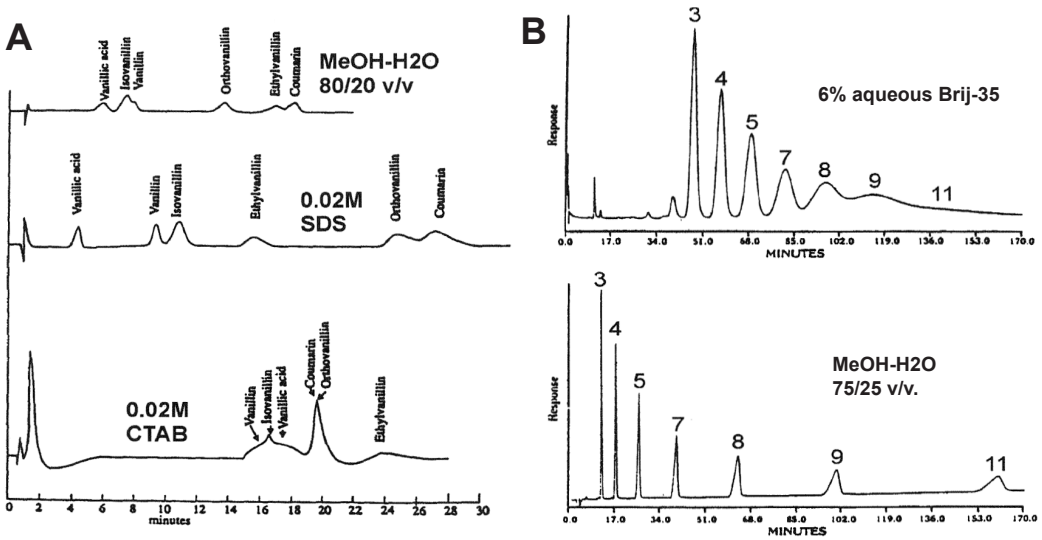

Figura 6.
(A) Influencia de la naturaleza del tensioactivo en cromatografía micelar sobre la fuerza eluyente y la selectividad. Separación de una mezcla de derivados de vainillina [25].
(B) Separación de alquilbencenos en disolución acuosa de Brij-35 al 6% y MeOH:H_2O, 75:25, v:v. [25]

Otra de las ventajas del empleo de fases móviles micelares es que, debido a la mejora en las características de la separación, se evita la utilización de gradientes, y además, en el caso de que los analitos se encuentren en muestras de alimentos o biológicas no se hace necesaria la precipitación previa a la separación de las proteínas. Teniendo en cuenta estas ventajas, Rambla-Alegre *et al.* [38] han llevado a cabo la determinación de antibióticos derivados de fluoroquinolonas en muestras de leche y huevos utilizando una fase móvil de dodecil sulfato de sodio 0,05 M disuelto en una disolución de dihidrógeno fosfato de sodio 0,01 M cuyo pH se ajustó a 3 empleando trietilamina al 0,5%. El componente orgánico de la fase móvil es *n*-butanol en una proporción en volumen del 10% con respecto al tampón fosfato que contiene la fase micelar de SDS. La metodología propuesta ha sido validada de acuerdo con la norma EC 2377/90 y ha demostrado poseer excelentes parámetros de calidad. Incidiendo en la ventaja de reducir el pretratamiento de las muestras gracias al empleo de tensioativos en las fases móviles, las aminas putrescina y cadaverina fueron derivatizadas con cloruro de 3,5-dinitrobenzoilo e inyectadas en el cromatógrafo, empleando para su separación una fase estacionaria C-18 y como fase móvil una disolución acuosa de tampón dihidrógeno fosfato de sodio 0,01 M que contiene SDS en concentración 0,15 M, a pH 7,0. Como componente orgánico se utilizó *n*-butanol en proporción en volumen de un 6% con respecto al componente acuoso (94%) [39]. Una fase móvil completamente acuosa compuesta por agua:SDS 69,3 mM, 50:1, v:v se ha utilizado con éxito para la separación de los antifúngicos blasticidina S y kasugamicina utilizando columnas Aqua 5 µm C-18 (Phenomenex) [40].

Se ha descrito de forma detallada y se ha desarrollado un modelo teórico para predecir el perfil de los picos y el comportamiento cromatográfico de los solutos relacionando la anchura de pico y el tiempo de retención, comparando fases móviles de MeCN:tampón citrato (en el intervalo de pH de 3,0 a 7,0) y las correspondientes fases MeCN:tampón con SDS como tensioactivo. La eficacia obtenida no sólo está relacionada con la concentración de SDS en la fase móvil, sino con la proporción de disolvente orgánico en la fase móvil para un valor dado de concentración de tensioactivo [41]. Igualmente, el SDS se ha utilizado como componente de la fase móvil, en fases mayoritariamente acuosas, para la determinación de diversas aminas aromáticas [42], hidroxitirosol en muestras de extractos de aceite de oliva [43], melamina en plasma y orina [44], y este mismo tóxico derivado de triazina en muestras de leche [45], paracetamol en supositorios mediante la formación de microemulsiones (incorporando entre otros componentes SDS, *n*-butanol y *n*-octano) [46], tamixifeno y endoxifeno [47] y sustancias dopantes en suero y orina de deportistas hasta 48 h después de haber sido consumidas [48].

Se ha desarrollado un método sostenible para la determinación de un grupo de colorantes sintéticos utilizados como aditivos en alimentos. Como fase estacionaria se utilizó una columna C-8, que al presentar menor hidrofobicidad que la clásica C-18 posibilita el empleo de una fase móvil con una proporción de agua próxima al 100% (tampón fosfato 50 mM, pH 7,0 con Triton X-100 al 0,25% en volumen con respecto a la disolución tampón). Esta metodología se ha aplicado a la determinación de colorantes (tartrazina, carmoisina, azul brillante, Ponceau 4R) en muestras de alimentos y de medicamentos [49].

4.3. Fases móviles que contienen microemulsiones

La formación de microemulsiones en las fases móviles en cromatografía de líquidos es una metodología con un potencial muy elevado para la separación de analitos que difieren notablemente en su polaridad. Un fase móvil de elevada polaridad con acido fosfórico (pH 3,0, 95,5%), *n*-butanol (2,5%) acetato de etilo (0,5%) y Brij-35 (1,5%) posibilita la separación y cuantificación de terbutalina en diversas formas farmacéuticas [50]. Esta modalidad de formación de sistemas micelares híbridos o microemulsiones se ha empleado en la determinación de las interacciones soluto-disolvente para compuestos antihistamínicos y fenetilaminas. Se ha utilizado como fase móvil disolución tampón de monohidrógeno fosfato de sodio 0,01 (pH 7,0), 1-pentanol y SDS. Las concentraciones del tensioactivo variaron entre 0,05 y 0,15 M y las del disolvente orgánico entre un 2 y un 6%, por lo que la proporción de agua en la fase móvil se sitúa en torno a un 95% [51].

5. Empleo de líquidos iónicos como aditivos en las fases móviles

Los líquidos iónicos poseen unas propiedades fisicoquímicas que los hacen adecuados para numerosos propósitos en el campo de la química analítica [52]. Algunas de sus aplicaciones en los procedimientos de extracción y purificación se comentan en el capítulo dedicado al pretratamiento de la introducción de esta memoria. La utilización de líquidos iónicos tanto en cromatografía de líquidos como en electroforesis capilar, formando parte de las fases móviles o bien incorporados a los materiales que componen las fases estacionarias (Figura 7), ya sea en cromatografía de líquidos o de gases, ha sido objeto de exhaustivos artículos de revisión [53-55].

Los líquidos iónicos pueden emplearse como aditivos en las fases móviles, como “High Performance Ionic Liquid Chromatography”, HPILC, [57] mostrando las siguientes características las separaciones en las que éstos se utilizan:

> *Hace unos años predije que los líquidos iónicos cambiarían la química orgánica. Actualmente es evidente que han cambiado y revolucionado todos aquellos aspectos de las química donde su utilización es posible*
>
> K. R. Seddon, [52]

- Reducción en los tiempos de retención de los solutos
- No producen modificación en el orden de retención de los solutos
- Su elevada viscosidad hace que la caída de presión originada en el interior de la columna sea extraordinariamente elevada, aún utilizando caudales muy reducidos.
- Poseen menor transparencia en la región UV que los disolventes orgánicos convencionales.

Hasta el momento, todos los trabajos publicados en los que se emplean líquidos iónicos (sales de alquilamonio) presentan menores eficacias cromatográficas y su capacidad contaminante no es inferior a la del metanol o del acetonitrilo. Por ello, teniendo en cuenta que son más costosos que los citados disolventes, es poco probable que en un futuro próximo los reemplacen [53].

Se ha estudiado el comportamiento cromatográfico del formiato de isopropilamonio como posible sustitutivo del metanol o el acetonitrilo en las fases móviles, ya que al determinar su valor de polaridad y de fuerza eluyente se ha hallado que son muy similares a los valores del metanol y el acetonitrilo. El comportamiento de este líquido iónico como modificador de las fases móviles se ha estudiado y se ha aplicado a la separación de acetofenona y niacinamida y de algunas proteínas como el citocromo C [58]. Uno de los inconvenientes de esta sal de amonio cuaternario es su elevada viscosidad, lo que tiene como consecuencia que el mezclado con el agua no sea homogéneo.

No obstante, los líquidos iónicos poseen la ventaja de reducir las colas de los picos en las separaciones de compuestos de carácter básico susceptibles de interaccionar con los grupos silanol ionizados libres que no hayan sido totalmente sustituidos en el proceso de "end-capping". Se ha propuesto la formación de pares iónicos entre los líquidos iónicos y los grupos silanol de la fase estacionaria así como la adsorción de los mismos sobre las fases C-18 [59]. Así, la adición de pequeñas cantidades de derivados de alquilamonio a las fases móviles mejora sustancialmente la simetría de los picos [60,61], habiéndose demostrado su utilidad en el caso de la separación de derivados de efedrina [62] y diversas catecolaminas. La mejora en la asimetría de los picos en las separaciones de fármacos de carácter básico del tipo bloqueantes beta-adrenérgicos ha sido estudiada de forma crítica. Se ha comparado la eficacia en la reducción de la asimetría de los picos mediante el empleo de cuatro líquidos iónicos (derivados de catión imidazolio) en la fase móvil con el comportamiento observado en presencia de trietilamina (como aditivo catiónico) y SDS (como aditivo aniónico) [56].

Se ha comparado el comportamiento cromatográfico de varios fenoles y algunos compuestos de carácter básico como piridina, anilina y cafeína al incluir en la fase móvil líquidos iónicos como tetrafluoroborato de 1-hexil-3-metilimidazolio con respecto a las fases móviles convencionales. Los valores de la relaciones de energía de solvatación lineal permiten explicar los equilibrios de distribución de los solutos en presencia de tetrafluroborato de 1-hexil-3-metil imidazolio [63]. Se ha estudiado cómo se modifican las separaciones cromatográficas de compuestos ácidos, básicos y también de carácter anfótero por la presencia de sales (Cl^- y PF_6^-) de 1-butil-3-metil imidazolio. Se obtienen separaciones adecuadas tanto en fases estacionarias C-18 como en fases de fenil-silano, si bien las interacciones creadas en la interfase de ambas fases estacionarias se ven afectadas de distinta manera por la presencia del líquido iónico en la fase móvil [64]. El empleo de fases móviles mayoritariamente acuosas es posible en el caso de la separación de compuestos altamente hidrofílicos, aminas biogénicas, y gracias al uso de

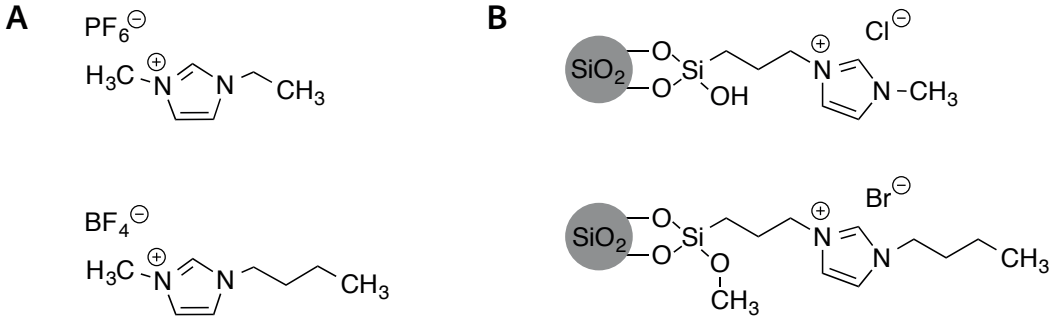

Figura 7. Líquidos iónicos más frecuentemente usados en cromatografía de líquidos. (A) líquidos iónicos empleados como aditivos en las fases móviles (B) Fases estacionarias de sílice modificada químicamente con líquidos iónicos derivados de imidazolio. [54,56].

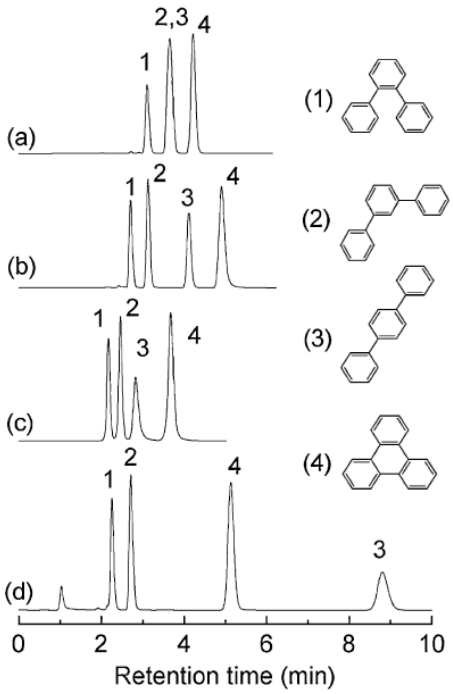

Figura 8.
Fases estacionarias modificadas con líquidos iónicos, comparación con otras fases estacionarias de referencia. (a) C-18 monolítica, (b) C-30 (tamaño de partícula 5 µm), (c) Sílice modificada químicamente con bromuro de *N*-octadecilimidazolio y (d) Sílice modificada químicamente con de *N*-octadecilimidazolio en la que el anión de este líquido iónico es el resto sulfonato del naranja de metilo [54].

hexafluorofosfato de 1-etil-3-metil imidazolio como líquido iónico en la fase móvil [65].

No puede pasarse por alto que los derivados de imidazolio con actividad óptica pueden aplicarse a la resolución quiral y a la determinación de pureza enantiomérica. Así, el empleo de líquidos iónicos quirales, es decir, sales de metilimidazolio unidas a un resto aminoacídico, permite la resolución de enantiómeros en fases estacionarias convencionales (C-18). Estos procedimientos utilizan sales de cobre al igual que en otras separaciones quirales y han posibilitado la separación del (*R*)- y del (*S*)-ofloxacino [66].

En la idea de demostrar la utilidad de los líquidos iónicos en HPLC, algunos derivados se han unido químicamente a la sílice [67], (Figura 8). Fases estacionarias de bromuro de 1-butil-3-heptilimidazolio se han aplicado a la separación de compuestos aromáticos [54,68,69]. Los resultados obtenidos con estas fases estacionarias no contribuyen a una mejora significativa de las separaciones con respecto a aquéllas que incorporan estos mismos líquidos iónicos en las fases móviles.

Puede afirmarse que, si bien los líquidos iónicos no mejoran ostensiblemente las separaciones cromatográficas, ya sea formando parte de la fase estacionaria o bien de la fase móvil, sin embargo, sí que contribuyen a incrementar la simetría de los picos cromatográficos.

6. Empleo de ciclodextrinas como aditivos en las fases móviles

Las ciclodextrinas (CDs) desempeñan un papel muy significativo en la mayoría de las áreas del análisis instrumental moderno [70-72], lo cual se debe a su capacidad para formar complejos de inclusión con una gran variedad de moléculas e iones en disoluciones acuosas. Estos macrociclos (Figuras 9 y 10) están constituidos por un número variable de unidades de (+)-β−D-glucopiranosa unidas mediante enlaces α−(1-4). Las ciclodextrinas naturales (α-, β- y γ-CD) contienen respectivamente 6, 7, y 8 residuos de (+)-β−D-glucopiranosa, poseen aspecto de cono truncado debido a la disposición espacial de las unidades de los azúcares, confiriendo al interior de la cavidad un carácter claramente apolar mientras que los bordes del tronco del cono son polares debido a la presencia de los grupos OH, que hacen de estas moléculas compuestos hidrosolubles. La característica común de estos derivados es su capacidad para formar complejos de inclusión tanto en estado sólido como en disolución. Los compuestos incluidos, de carácter hidrófobo o parcialmente hidrófilo, se alojan en el interior de la cavidad por interacciones de Van der Waals. El estudio de los complejos de inclusión con ciclodextrinas constituye una parcela apasionante dentro del campo de estudio de la química supramolecular.

Figura 9.
Detalles de las dos ciclodextrinas empleadas en el trabajo experimental de la presente memoria.

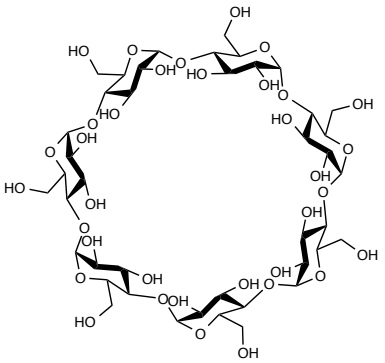

β-CD

$C_{42}H_{70}O_{35}$
1134,99 g/mol

CAS number	7585-39-9
PubChem	444041
ChemSpider	10469496
UNII	JV039JZZ3A
KEGG	D0240
ChEBI	CHEBI:495055
ChEMBL	389143
Sigma-Aldrich	C4767

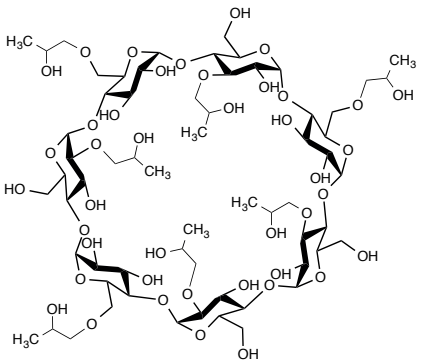

HPβ-CD

$C_{63}H_{112}O_{42}$
1541,55 g/mol (sustit. 1.0 M)
1460 g/mol (sustit. 0.8 M)

CAS number	128446-35-5
PubChem	14049689
UNII	1I96OHX6EK
ChEMBL	577294
Sigma-Aldrich	389145 (1.0 M)
Sigma-Aldrich	332607 (0.8 M)

El sustituyente 2-hidroxipropilo puede estar en distinta posición en cada subunidad de glucosa

El grado de sustitución pueden variar

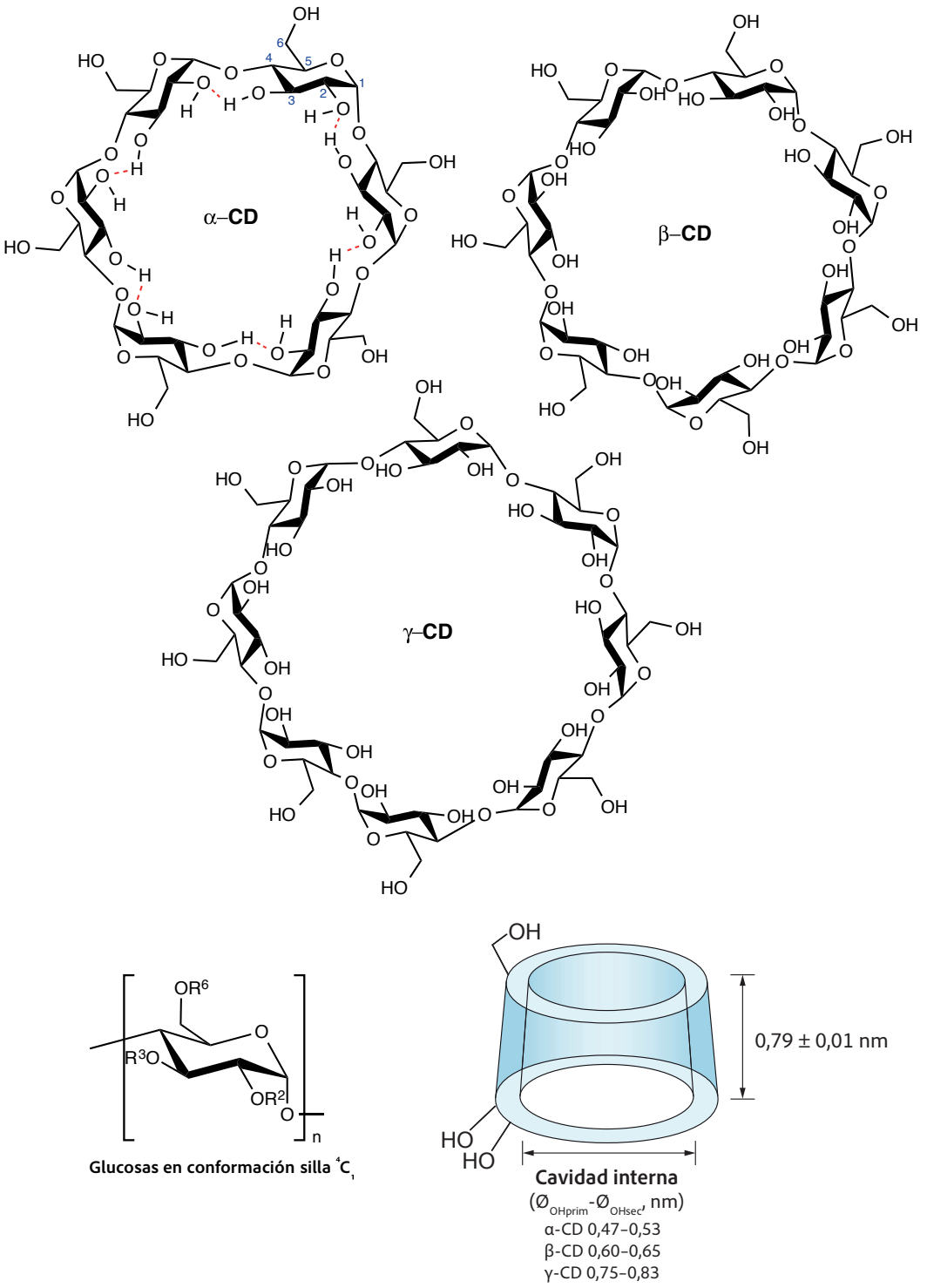

Figura 10. Estructuras químicas de las ciclodextrinas naturales mayoritarias. En la α-CD, se han indicado los enlaces de hidrógeno intramoleculares presentes en el borde de los hidroxilos secundarios. En la parte inferior se muestran la conformación tipo silla de la subunidad de glucopiranosa, y una visión esquemática de la cavidad de las ciclodextrinas con sus dimensiones más significativas. Adaptado de Davis & Brewster (2004) Nature Reviews Drug Discovery, 3(12), 1023–1035.

Los complejos de los analitos con diversas ciclodextrinas incrementan la sensibilidad de las determinaciones fluorimétricas debido al incremento en el rendimiento cuántico de fluorescencia y a la capacidad de las ciclodextrinas de solubilizar compuestos hidrofóbicos [73,74]. Muchas reacciones analíticas ven mejorada su sensibilidad gracias a la incorporación de diversas ciclodextrinas a los medios de reacción, así como en el caso de ciertas reacciones quimioluminiscentes en las que la mejora en la intensidad de quimioluminiscencia se atribuye al incremento en la velocidad de reacción y a la protección y estabilización de sus productos. Una de las características de los complejos de inclusión con las ciclodextrinas es que permiten observar fosforescencia a temperatura ambiente. Estas mejoras contribuyen a incrementar la sensibilidad y la selectividad tanto de los métodos luminiscentes como de las separaciones cromatográficas.

El empleo de ciclodextrinas como aditivos y modificadores de polaridad de las fases móviles en HPLC, o bien, formando parte de la fase esta-

Tabla 1. Ejemplos de ciclodextrinas modificadas disponibles comercialmente. Tomado de www.cyclolab.hu

Neutras	Catiónicas	Aniónicas
(2-hidroxipropil)-X-CD	6-monodesoxi-6-monoamino-β-CD hidrocloruro	carboximetil-X-CD sal sódica
acetil-X-CD aleatoriamente sustituida	heptakis(6-amino-6-desoxi)-β-CD heptahidrocloruro	(2-carboxietil)-X-CD
metil-X-CD aleatoriamente sustituida	(2-hidroxi-3-*N*,*N*,*N*-trimetilamino)propil-β-CD cloruro	succinil-X-CD
heptakis(2,6-di-*O*-metil)-β-CD		succinil-(2-hidroxipropil)-X-CD
heptakis(2,3,6-tri-*O*-metil)-β-CD		sulfobutil-β-CD
heptakis(2,3,6-tri-*O*-benzoil)-β-CD		X-CD fosfato sal sódica
6-monodesoxi-6-monoazido-β-CD		X-CD sulfato sal sódica
6-monodesoxi-6-monoiodo-β-CD		

Fluorescentes		Fases estacionarias HPLC modificadas con CDs
Fluoróforo	**CD**	
6-desoxi-6-[(5/6)-fluoresceiniltioureido]	β-CD, metil-β-CD, (2-hidroxipropil)-β-CD, carboximetil-β-CD	β-CD
6-desoxi-6-[(5/6)-rodaminiltioureido]	β-CD, metil-β-CD, (2-hidroxipropil)-β-CD, sulfobutil-β-CD	heptakis(2,3,6-tri-*O*-metil)-β-CD
		(2-hidroxipropil)-β-CD
		carboximetil-β-CD
		sulfobutil-β-CD

Las X indican que existe más de una CD nativa (α, β o γ) disponible con esa sustitución

cionaria constituye una elección muy atractiva frente a otras alternativas como tensioactivos, éteres corona, antibióticos macrólidos o calixarenos y ha sido objeto de diversas revisiones [75-79]. Este hecho se debe entre otras a las razones que, según Szejtli [80], se exponen a continuación:

- Son productos semisintéticos obtenidos a partir del almidón por una simple conversión enzimática.
- Se producen y se utilizan en la industria en grandes cantidades, sin embargo, no tienen impacto medioambiental negativo debido a que son compuestos naturales completamente biodegradables.
- A pesar de que sus precios fueron elevados, hoy en día los costos de producción han descendido considerablemente llegando a ser aceptables desde el punto de vista de su uso industrial.
- Gracias a su capacidad para formar complejos de inclusión, se modifican notablemente las características de las especies incluidas y esta encapsulación molecular hace que sean útiles en la fabricación de numerosos productos, así como su utilización en muy diversos métodos analíticos.
- Sus efectos secundarios y tóxicos son insignificantes. Por ello pueden emplearse en la elaboración de distintos productos para su uso humano en la industria química, farmacéutica, agroalimentaria y cosmética [81].

Además, en la actualidad es posible adquirir de manera comercial una gran variedad de ciclodextrinas semisintéticas, químicamente modificadas con distintos sustituyentes, como refleja la Tabla 1. Este hecho permite elegir, de entre las múltiples disponibles, aquella que presente las características que mejor se presten a resolver un determinado problema analítico.

Cuando las CDs se emplean como aditivos incorporados a las fases móviles en HPLC, permiten obtener buenas resoluciones de manera versátil, ya que se puede modificar la composición de la fase móvil según la separación lo requiera. Además, presentan la ventaja de permitir la presencia de un elevado contenido en agua en la fase móvil gracias a la mayor estabilidad de los complejos de inclusión en agua con respecto a los disolventes orgánicos. Por ello, se utilizan fases móviles mayoritariamente acuosas para la elución en fase inversa. La resolución en las separaciones es consecuencia de la formación de complejos de inclusión y es la parte hidrofóbica de los analitos la que interacciona con la cavidad apolar de las CDs. Por el contrario, el proceso de inclusión no es la fuerza conductora en el proceso de separación cuando se emplea la elución en fase orgánica polar. En este caso, las interacciones entre los analitos y los hidroxilos secundarios del borde de las cavidades de las CDs son las que determinan la selectividad en el proceso de separación.

La adición de CDs a las fases móviles modifica el equilibrio de distribución de los solutos entre la fase estacionaria y la fase móvil debido a la formación de complejos de inclusión con las CDs que permanecen en la fase móvil. Este he-

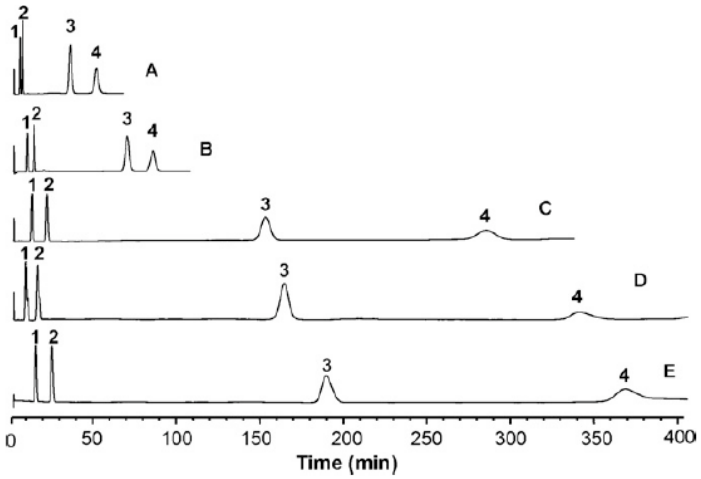

Figura 11. Separación cromatográfica de isoflavonoides, empleando distintas ciclodextrinas como aditivos en la fase móvil MeOH:H_2O, 25:75, v:v. La fase móvil contiene las siguientes ciclodextrinas en concentración 5 mM: (A) HP-β-CD (B) β-CD (C) α-CD (D) γ-CD (E) sin CD en la fase móvil [89].

cho tiene las siguientes consecuencias sobre el análisis cromatográfico:

- Reducción de los índices de retención.
- Disminución del tiempo de análisis.
- Mejora de la selectividad.
- Incremento de la eficacia.

Estos cambios quedan ejemplificados en la Figura 11.

La resolución de los analitos y la eficacia del proceso cromatográfico dependen de la concentración y del tipo de CD empleada, así como de las características de la fase móvil y de la fase estacionaria, siendo un parámetro importante a considerar la temperatura, ya que influye en todos los equilibrios mencionados. En la Figura 12 se muestra el equilibrio de distribución entre los analitos y la fase estacionaria/fase móvil, junto con el equilibrio secundario de distribución analitos y CD, propuesto por Sybilska [82]. Además, hay que considerar que los complejos de inclusión formados entre los analitos y las CDs también pueden distribuirse entre la fase estacionaria y la fase móvil de acuerdo con los equilibrios de distribución cromatográficos. La tendencia a incluirse en las cavidades de las CDs altera el equilibrio cromatográfico posibilitando la diferenciación y separación de los analitos en función de su afinidad por las cavidades de las CDs.

Las ventajas del empleo de las CDs como aditivos en las fases móviles en HPLC (MPA) frente a su empleo como integrantes de la fase estacionaria (CSP) pueden resumirse como sigue:

- El equilibrio de inclusión es reversible y selectivo.
- Buena estabilidad química de las CDs incluso a valores elevados de pH.
- Gran versatilidad al poder cambiar fácilmente de tipo de CD y también de fase estacionaria convencional.
- Elevada solubilidad tanto en agua como en disolventes orgánicos, especialmente en el

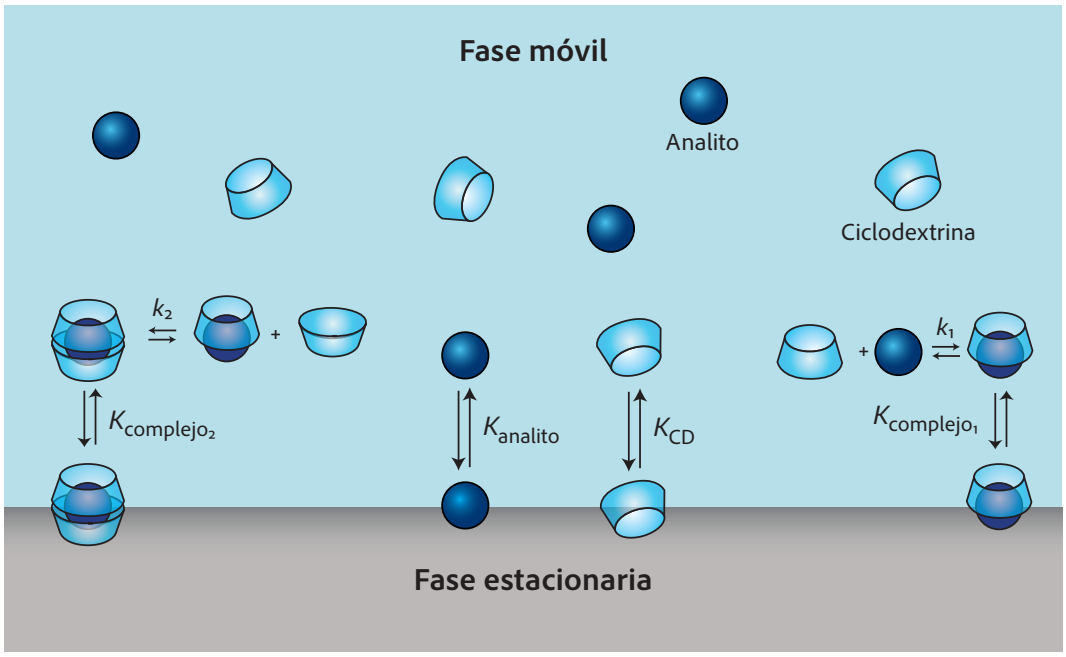

Figura 12. Equilibrios de inclusión y distribución que coexisten en las separaciones cromatográficas en presencia de ciclodextrinas como aditivos en las fases móviles.

caso de las CDs metiladas y carboximetiladas.

- Control de la eficacia del proceso cromatográfico según la concentración de CD presente en la fase móvil.
- Posibilidad de adsorción de las CDs sobre las fases estacionarias de baja polaridad creando una pseudofase estacionaria.

La principal desventaja de la incorporación de las CDs a las fases móviles es que para lograr una buena eficacia y resolución es necesario emplear concentraciones de CDs en las fases móviles próximas al límite de solubilidad de las mismas. Este hecho afecta y modifica la fase estacionaria siempre que no se tomen las precauciones debidas y se proceda a su regeneración de manera adecuada [83,84].

Las ciclodextrinas (CDs), al igual que otros cavitandos de síntesis, son capaces de reconocer molecularmente a una gran variedad de analitos en función del tamaño, estructura y disposición espacial de los distintos grupos de las moléculas a incluir. Por ello, se han utilizado con éxito como selectores quirales en cromatografía de líquidos [76,85], como ilustra la Figura 13. Estos derivados también han sido aplicados con este fin en electroforesis capilar (CZE) [86,87], ya que se pueden añadir en concentraciones elevadas a los tampones de separación.

Su uso en HPLC como selectores en la fase móvil está limitado por la concentración que se puede alcanzar en la fase móvil y también por su adsorción sobre las fases estacionarias [79]. El empleo de CDs como aditivos de las fases móviles aporta importantes beneficios y se han utilizado con éxito en la resolución de compuestos quirales como en la mejora de las separaciones de compuestos no quirales. La incorporación de CDs modificadas químicamente incrementa la capacidad de resolución de compuestos quirales [71].

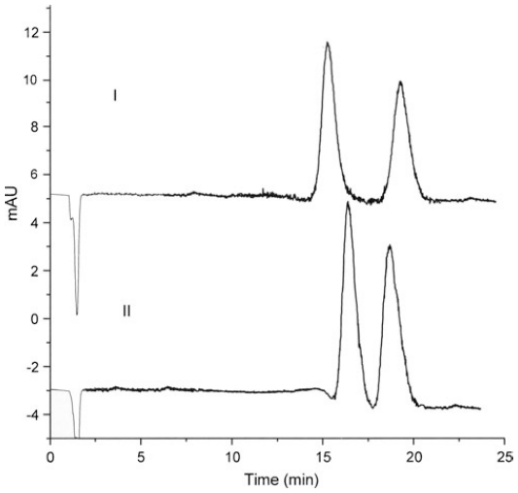

Figura 13. Cromatogramas ilustrando la resolución quiral de los enantiómeros de naproxeno (I) y de ketoprofeno (II) en fase móvil MeOH:tampón (pH 3,0) empleando HPβ-CD 15 mM como aditivo en la fase móvil [92].

Otra de las ventajas de la incorporación de CDs a las fases móviles en HPLC es que permiten reducir la proporción de disolventes orgánicos en las mismas sin disminuir la selectividad ni la resolución. Así, la selección adecuada de la fase estacionaria permite la utilización de fases móviles mayoritariamente acuosas, llegando incluso al 100% de agua. Por ello, estas modalidades de separación incorporando CDs como aditivos en las fases móviles han sido aplicadas en la mejora de la determinación de una gran variedad de compuestos.

En la Tabla 2 se incluyen ejemplos de separaciones que incluyen CDs como aditivos en las fases móviles.

Tabla 2. Ejemplos de aplicaciones en las que la separación de analitos por HPLC incluye CDs como modificadores de la fase móvil (continúa en página siguiente).

Analito	Condiciones de separación	CDs empleadas	Comentarios	Ref.
Enantiómeros del ácido fenil-láctico	Separación y resolución quiral. HPLC-UV. FE: C-18. FM: MeOH:H_2O / ácido TFA 0,05% y trietilamina (pH 2,5); 10:90, v:v	β-CD 10 mM, HPβ-CD 10 mM	La β-CD separa pero no resuelve los dos enantiómeros, mientras que la HPβ-CD resuelve ambos compuestos quirales	[88]
Insoflavonoides en extractos vegetales	HPLC-UV. FE: C-8. FM: MeOH:H_2O, 25:75, v:v	α-CD 5 mM, β-CD 5 mM, HPβ-CD, 5 mM, γ-CD 5 mM		[89]
Isoflavonas: formononetina y calcosina y sus correspondientes glicósidos	HPLC-FD. FE: C-18. FM:MeOH:H_2O. La proporción del disolvente orgánico depende de la concentración de CD en la fase móvil	HPβ-CD		[90]
Aminoácidos derivatizados con cloruro de dansilo	Cromatografía de líquidos capilar-FD. Separación y resolución quirales. Capilar abierto no tratado de poli(tetrafluoroetileno) de 100 µm de diámetro interno y 90 cm de longitud. FM: MeCN:AcOEt:H_2O	β-CD	Se produce un fenómeno de distribución radial de los analitos entre el agua, situada en el interior del capilar, y el componente orgánico situado en las paredes del capilar. Las CDs en la fase móvil actúan como pseudo-fase estacionaria	[91]
Fármacos antiinflamatorios no esteroideos	Cromatografía de líquidos capilar. Separación y resolución quiral. Capilar de 100 µm de diámetro interno y 10 cm de longitud. FE: Sílica totalmente porosa C-18, monolíticas C-18. FM: MeCN:tampón acetato de sodio 50 mM (pH 3,0), 30:70, v:v	2,3,6-trimetil-β-CD 30 mM, HPβ-CD (15-30 mM)		[92]
Catequinas	HPLC-UV FE: C-18 FM: MeOH:H_2O, 50:50, v:v	β-CD 15 mM		[93]
Pteroestilbeno en arándanos	HPLC-UV y HPLC-FD FE: C-8. FM: MeCN:H_2O, 12:88, v:v	β-CD 12 mM		[94]
Aflatoxinas B1, B2, G1 y G2	TLC FE: C-18 FM: MeOH:tampón	HP-β-CD		[95]
Clopidogrel	Separación por TLC y resolución quiral del *S*-clopidogrel de su impureza, el *R*-clopidogrel. FE: celulosa/acetato de celulosa. FM: ^{i}PrOH:H_2O, 60:40, v:v	β-CD 5 mM		[96]
Aminoácidos derivatizados con cloruro de dansilo	UHPLC-FD. Separación y resolución quiral. FE: C-18. FM: MeCN:-tampón acetato de trietilamonio (pH 4,7)	β-CD catiónica modificada químicamente con sustituyente de cloruro de pirrolinio		[97]
Antiinflamatorios no esteroideos	Separación y resolución quiral. FE: C-18. FM: MeOH:tampón fosfato (pH 4,0-5,5)	HPβ-CD 25 mM		[98]
Oxirresveratrol	HPLC-UV. FE: C-18. FM: MeOH:H_2O, 30:70, v:v	α-CD 4 mM, β-CD 4 mM, γ-CD 4 mM		[99]
Fármacos derivados de feniramina	Separación y resolución quiral. HPLC-UV. FE: C-18. FM: EtOH:H_2O, 35:65, v:v	β-CD, 2,6-dimetil-β-CD, 2,3,6-trimetil-β-CD, HPβ-CD, β-CD sulfatada		[100]
Esteroides e hidrocarburos aromáticos policíclicos	HPLC-UV. FE: C-18 FM: MeCN:H_2O, 20:80, v:v y EtOH:H_2O, 10:90, v:v	α-CD 10 mM, HPα-CD 10 mM, β-CD 10 mM, HPβ-CD 10 mM, γ-CD 10 mM, HPγ-CD 10 mM		[101]
trans-Resveratrol	HPLC-DAD. FE: Sílica modificada con zirconio y monocapa hidrofílica de tipo diol. FM: 100% acuosa de: tampón acetato (pH 4,0) tampón fosfato (pH 7,0-8,5) tampón borato (pH 9,0-10,0)	α-CD 0,5-2,0 mM, β-CD 0,5-2,0 mM, γ-CD, 0,5-2,0 mM		[102]

Tabla 2. (Continuación).

Analito	Condiciones de separación	CDs empleadas	Comentarios	Ref.
Mezclas racémicas de benzoína, 2-fenilciclohexanona, flavona, dianilida del ácidociclopropanodicarboxílico	Separación y resolución quiral. HPLC-UV. FE: C-18. FM: hexano:^{i}PrOH, 90:10, v:v	2,3,6-trimetil-β-CD		[103]
Nitrofurazona e hidroximetilnitrofurazona	HPLC-UV. FE: C-18. FM: MeCN:H_2O, 20:80, v:v	β-CD 5-30 mM, 2,6-dimetil-β-CD 5-30 mM	Separación y caracterización de los complejos de inclusión.	[104]
Hidroximetilnitrofurazona	HPLC-UV. FE: C-18. FM: MeCN:H_2O, 20:80, v:v	HPβ-CD (5-30 mM)	Separación y caracterización de los complejos de inclusión	[105]
Pantoprazol	Resolución quiral, HPLC-UV. FE: C-18. FM: MeCN:tampón fosfato (10 mM pH 2,5), 15:85, v:v	sulfobutiléter-β-CD 10 mM		[106]
Madecasósido y asiaticósido-B	HPLC-UV. FE: C-18. FM: MeOH:H_2O, 50:50, v:v	β-CD 4 mM		[107]
Duloxetina	Resolución quiral. HPLC-UV. FE: C-8 y C-18 y FE quiral incorporando vancomicina (Chirobiotic). FM: MeOH:H_2O, 35:65, v:v	HPβ-CD 60 mM		[108]
trans-Resveratrol	HPLC-DAD. FE: Cianopropilsilano. FM: MeOH:tampón fosfato (pH 2,0), 50:50, v:v, o bien MeOH:H_2O, 40:60, v:v	β-CD 1-7 mM		[109]
Norgestrel	Resolución quiral. HPLC-UV. FE: C-8 FM: MeCN:tampón fosfato (20 mM, pH 5,0), 30:70, v:v	HPβ-CD 25 mM		[110]
Citalopran	Separación y resolución quiral. FE: C-18. FM: MeCN:tampón acetato de trietilamina (0,1%, pH 4,0), 10:90, v:v	β-CD 12 mM	Resolución quiral con elevados factores de separación	[111]
Pindolol, indol y metoxiindol	HPLC-DAD. FE: C-18. FM: MeCN:tampón fosfato (pH 3,0), 32:68, v:v	β-CD		[112]
Sertralina	Separación y resolución quiral. HPLC-UV. FE: C-18 .FM: MeOH:tampón fosfato (pH 6,0), 15:85, v:v	HPβ-CD 18 mM		[113]
Ácidos triterpénicos pentacíclicos (betulínico, ursólico, olcanólico)	HPLC-UV. FE: C-18 FM: MeCN:tampón fosfato 0,02 M (pH 3,5), 70:30, v:v y MeCN:tampón fosfato 0,02 M (pH 3,5), 50:50, v:v	2,6-dimetil-β-CD, γ-CD 2,5 mM, HPγ-CD, 7,5 mM		[114]
Naproxeno	HPLC-DAD. FE: C-8. FM: MeOH:tampón fosfato (pH 7,0), 70:30, v:v	β-CD, metil-β-CD, HPβ-CD		[115]

DAD: detección con diodos en red. FD: detección fluorimétrica. UV: ultravioleta. FE: fase estacionaria. FM: fase móvil.

Referencias

1. L.H. Keith, L.U. Gron, J.L. Young, Green Analytical Methodologies, Chem Rev. 107 (2007) 2695–2708.
2. M. Tobiszewski, A. Mechlinska, J. Namiesnik, Green analytical chemistry-theory and practice, Chem Soc Rev. 39 (2010) 2869–2878.
3. M. Tobiszewski, J. Namiesnik, Direct chromatographic methods in the context of green analytical chemistry, Trends Anal Chem. 35 (2012) 67–73.
4. T. Rojanarata, Green Pharmaceutical Chemistry for the Sustainability, Silpakorn University Science and Technology Journal. 6 (2013) 7–13.
5. B. Kapalavavi, R. Marple, C. Gamsky, Y. Yang, Separation of sunscreens in skincare creams using greener high-temperature liquid chromatography and subcritical water chromatography, Int J Cosmet Sci. 34 (2012) 169–175.
6. A. Mohammad, N. Haq, A. Siddiq, Resolution of multicomponent mixture of amino acids using environmentally benign eluents: A green chromatographic approach, J. Sep. Sci. 33 (2010) 3619–3626.
7. J.-F. Jen, S.-L. Hsiao, K.-H. Liu, Simultaneous determination of uric acid and creatinine in urine by an eco-friendly solvent-free high performance liquid chromatographic method, Talanta. 58 (2002) 711–717.
8. Y. Yang, Z. Strickland, B. Kapalavavi, R. Marple, C. Gamsky, Industrial application of green chromatography-I. Separation and analysis of niacinamide in skincare creams using pure water as the mobile phase, Talanta. 84 (2011) 169–174.
9. Y. Li, J. Li, T. Chen, X. Liu, H. Zhang, Covalently bonded polysaccharide-modified stationary phase for per aqueous liquid chromatography and hydrophilic interaction chromatography, J Chromatogr A. 1218 (2011) 1503–1508.
10. D. Šatínský, I. Brabcová, A. Maroušková, P. Chocholouš, P. Solich, Green chromatography separation of analytes of greatly differing properties using a polyethylene glycol stationary phase and a low-toxic water-based mobile phase, Anal Bioanal Chem. 405 (2013) 6105–6115.
11. B. Buszewski, S. Noga, Hydrophilic interaction liquid chromatography (HILIC)-a powerful separation technique, Anal Bioanal Chem. 402 (2012) 231–247.
12. C.J. Welch, T. Brkovic, W. Schafer, X. Gong, Performance to burn? Re-evaluating the choice of acetonitrile as the platform solvent for analytical HPLC, Green Chem. 11 (2009) 1232–1238.
13. C.J. Welch, N. Wu, M. Biba, R. Hartman, T. Brkovic, X. Gong, et al., Greening analytical chromatography, Trends Anal Chem. 29 (2010) 667–680.
14. F. Brettschneider, V. Jankowski, T. Günthner, S. Salem, M. Nierhaus, A. Schulz, et al., Replacement of acetonitrile by ethanol as solvent in reversed phase chromatography of biomolecules, J Chromatogr B. 878 (2010) 763–768.
15. A. Balaguer, A. Chisvert, A. Salvador, Environmentally friendly LC for the simultaneous determination of ascorbic acid and its derivatives in skin-whitening cosmetics, J. Sep. Sci. 31 (2008) 229–236.
16. T. Rojanarata, Eco-friendly, operator-safe and cost-effective RP-HPLC method for stability-indicating assay of prednisolone tablets using ethanol-water as mobile phase, International Journal of Pharmacy and Pharmaceutical Sciences. Suppl 1 (2011) 444–448.
17. E. Destandau, E. Lesellier, Chromatographic Properties of Ethanol/Water Mobile Phases on Silica Based Monolithic C18, Chromatographia. 68 (2008) 985–990.
18. J.G. Bordonaba, P. Crespo, L.A. Terry, A new acetonitrile-free mobile phase for HPLC-DAD determination of individual anthocyanins in blackcurrant and strawberry fruits: A comparison and validation study, Food Chem. 129 (2011) 1265–1273.
19. G. Venkatasami, J.R. Sowa, A rapid, acetonitrile-free, HPLC method for determination of melamine in infant formula, Anal Chim Acta. 665 (2010) 227–230.
20. A.M. Desai, M. Andreae, D.G. Mullen, M.M.B. Holl, J.R. Baker, Acetonitrile shortage: use of isopropanol as an alternative elution system for ultra/high performance liquid chromatography, Anal. Methods. 3 (2011) 56–58.
21. B. Suvarna, N. Varsha, V. Pratibha, M. Soni, B. Ashok, Prospective Use of Propylene Carbonate as a Mobile Phase Component in RP-HPLC, International Journal of Research in Pharmacy and Science. 1 (2011) 15–28.
22. N. Varsha, B. Suvarna, V. Pratibha, M. Soni, B. Ashok, Replacement of acetonitrile by mixtures of propylene carbonate and methanol as organic modifier in mobile phases for rplc separation mechanism: application to the assay of alprazolam and sertraline in combined pharmaceutical formulations, J Liq Chromatogr Relat Technol. 35 (2012) 2643–2654.
23. F. Tache, S. Udrescu, F. Albu, F. Micele, A. Medvedovici, Greening pharmaceutical applications of liquid chromatography through using propylene carbonate-ethanol mixtures instead of acetonitrile as organic modifier in the mobile phases, J Pharm Biomed Anal. 75 (2013) 230–238.
24. M. Cheregi, F. Albu, S. Udrescu, N. Raducanu, A. Medvedovici, Greener bioanalytical approach for LC/MS-MS assay of enalapril and enalaprilat in human plasma with total replacement of acetonitrile throughout all analytical stages, J Chromatogr B. 927 (2013) 124–132.
25. A. Berthod, C. Garcia-Alvarez-Coque, Micellar liquid chromatography, Marcel Dekker, New York, 2000.

26. A. Mohammad, N. Haq, Green Eluents in Chromatography, in: Green Chemistry for Environmental Sustainability, CRC Press, Boca Raton, 2011: pp. 285–302.
27. M.J. Ruiz-Ángel, M.C. García-Álvarez-Coque, A. Berthod, New Insights and Recent Developments in Micellar Liquid Chromatography, Sep Purif Rev. 38 (2009) 45–96.
28. M.J. Ruiz-Ángel, S. Carda-Broch, J.R. Torres-Lapasió, M.C. García-Álvarez-Coque, Retention mechanisms in micellar liquid chromatography, J Chromatogr A. 1216 (2009) 1798–1814.
29. M.J. Ruiz-Ángel, J.R. Torres-Lapasió, M.C. García-Álvarez-Coque, S. Carda-Broch, Submicellar and micellar reversed-phase liquid chromatographic modes applied to the separation of beta-blockers, J Chromatogr A. 1216 (2009) 3199–3209.
30. J.J. Fernández-Navarro, M.J. Ruiz-Ángel, M.C. García-Álvarez-Coque, Reversed-phase liquid chromatography without organic solvent for determination of tricyclic antidepressants, J. Sep. Sci. 35 (2012) 1303–1309.
31. M.J. Ruiz-Ángel, S. Carda-Broch, M.C. García-Álvarez-Coque, High Submicellar Liquid Chromatography, Sep Purif Rev. 43 (2014) 124–154.
32. J. Esteve-Romero, S. Carda-Broch, M. Gil-Agustí, M.-E. Capella-Peiró, D. Bose, Micellar liquid chromatography for the determination of drug materials in pharmaceutical preparations and biological samples, Trends Anal Chem. 24 (2005) 75–91.
33. M.J. Ruiz-Ángel, S. Carda-Broch, M.C. García-Álvarez-Coque, Chromatographic Efficiency in Micellar Liquid Chromatography: Should it Be Still a Topic of Concern? Sep Purif Rev. 42 (2013) 1–27.
34. M.J. Ruiz-Ángel, S. Carda-Broch, M.C. García-Álvarez-Coque, Peak half-width plots to study the effect of organic solvents on the peak performance of basic drugs in micellar liquid chromatography, J Chromatogr A. 1217 (2010) 1786–1798.
35. J.R. Torres-Lapasió, M.J. Ruiz-Ángel, M.C. García-Álvarez-Coque, M.H. Abraham, Micellar versus hydro-organic reversed-phase liquid chromatography: a solvation parameter-based perspective, J Chromatogr A. 1182 (2008) 176–196.
36. L.P. Loginova, L.V. Samokhina, A.P. Boichenko, A.U. Kulikov, Micellar liquid chromatography retention model based on mass-action concept of micelle formation, J Chromatogr A. 1104 (2006) 190–197.
37. N. Youngvises, T. Chaida, S. Khonyoung, N. Kuppithayanant, W. Tiyapongpattana, A. Itharat, et al., Greener liquid chromatography using a guard column with micellar mobile phase for separation of some pharmaceuticals and determination of parabens, Talanta. 106 (2013) 350–359.
38. M. Rambla-Alegre, M.A. Collado-Sánchez, J. Esteve-Romero, S. Carda-Broch, Quinolones control in milk and eggs samples by liquid chromatography using a surfactant-mediated mobile phase, Anal Bioanal Chem. 400 (2011) 1303–1313.
39. M.-L. Chin-Chen, D. Bose, J. Esteve-Romero, J. Peris-Vicente, M. Rambla-Alegre, S. Carda-Broch, Determination of Putrescine and Tyramine in Fish by Micellar Liquid Chromatography with UV Detection Using Direct Injection, The Open Analytical Chemistry Journal. 5 (2011) 22–26.
40. S. Cheng, C.C. Kwan, C. Lo, Simultaneous Analysis of Blasticidin S and Kasugamycin with Micellar Liquid Chromatography, J Food Drug Anal. 19 (2011) 452–456.
41. J.J. Baeza-Baeza, M.J. Ruiz-Ángel, M.C. García-Álvarez-Coque, Prediction of peak shape in hydro-organic and micellar-organic liquid chromatography as a function of mobile phase composition, J Chromatogr A. 1163 (2007) 119–127.
42. S.-K. Mourya, D. Bose, A. Durgbanshi, J. Esteve-Romero, S. Carda-Broch, Determination of some banned aromatic amines in waste water using micellar liquid chromatography, Anal. Methods. 3 (2011) 2032.
43. M. Rambla-Alegre, S. Marco-Peiró, J. Peris-Vicente, B. Beltrán-Martinavarro, M.A. Collado-Sánchez, S. Carda-Broch, et al., Analytical determination of hydroxytyrosol in olive extract samples by micellar liquid chromatography, Food Chem. 129 (2011) 614–618.
44. S. Marco-Peiró, B. Beltrán-Martinavarro, M. Rambla-Alegre, J. Peris-Vicente, J. Esteve-Romero, Validation of an analytical methodology to quantify melamine in body fluids using micellar liquid chromatography, Talanta. 88 (2012) 617–622.
45. M. Rambla-Alegre, J. Peris-Vicente, S. Marco-Peiró, B. Beltrán-Martinavarro, J. Esteve-Romero, Development of an analytical methodology to quantify melamine in milk using micellar liquid chromatography and validation according to EU Regulation 2002/654/EC, Talanta. 81 (2010) 894–900.
46. E. McEvoy, S. Donegan, J. Power, K. Altria, Optimisation and validation of a rapid and efficient microemulsion liquid chromatographic (MELC) method for the determination of paracetamol (acetaminophen) content in a suppository formulation, J Pharm Biomed Anal. 44 (2007) 137–143.
47. E.O. Aranda, J. Esteve-Romero, M. Rambla-Alegre, J. Peris-Vicente, D. Bose, Development of a methodology to quantify tamoxifen and endoxifen in breast cancer patients by micellar liquid chromatography and validation according to the ICH guidelines, Talanta. 84 (2011) 314–318.

48. M.J. Ruiz-Ángel, S. Carda-Broch, M.C. García-Álvarez-Coque, Micellar liquid chromatography in doping control, Bioanalysis. 1 (2009) 1225–1241.
49. M. Khanavi, M. Hajimahmoodi, A.M. Ranjbar, M.R. Oveisi, M.R.S. Ardekani, G. Mogaddam, Development of a Green Chromatographic Method for Simultaneous Determination of Food Colorants, Food Anal Methods. 5 (2011) 408–415.
50. M.S. Althanyan, K.H. Assi, B.J. Clark, J. Hanaee, Microemulsion high performance liquid chromatography (MELC) method for the determination of terbutaline in pharmaceutical preparation, J Pharm Biomed Anal. 55 (2011) 397–402.
51. M. Gil-Agustí, J. Esteve-Romero, M.H. Abraham, Solute-solvent interactions in micellar liquid chromatography. Characterization of hybrid micellar systems of sodium dodecyl sulfate-pentanol, J Chromatogr A. 1117 (2006) 47–55.
52. M. Freemantle, New frontiers for ionic liquids, Chem Eng News Archive. 85 (2007) 23–26.
53. A. Berthod, M.J. Ruiz-Ángel, S. Carda-Broch, Ionic liquids in separation techniques, J Chromatogr A. 1184 (2008) 6–18.
54. L. Vidal, M.-L. Riekkola, A. Canals, Ionic liquid-modified materials for solid-phase extraction and separation: a review, Anal Chim Acta. 715 (2012) 19–41.
55. V. Pino, M. Germán-Hernández, A. Martín-Pérez, J.L. Anderson, Ionic Liquid-Based Surfactants in Separation Science, Sep Sci Technol 47 (2012) 264–276.
56. J.J. Fernández-Navarro, M.C. García-Álvarez-Coque, M.J. Ruiz-Ángel, The role of the dual nature of ionic liquids in the reversed-phase liquid chromatographic separation of basic drugs, J Chromatogr A. 1218 (2011) 398–407.
57. Y. Fukaya, A. Tsukamoto, K. Kuroda, H. Ohno, High performance "ionic liquid" chromatography, Chem Commun. 47 (2011) 1994–1996.
58. M.P. Collins, L. Zhou, S.E. Camp, N.D. Danielson, Isopropylammonium formate as a mobile phase modifier for liquid chromatography, J Chromatogr Sci. 50 (2012) 869–876.
59. X. Xiaohua, Z. Liang, L. Xia, J. Shengxiang, Ionic liquids as additives in high performance liquid chromatography, Anal Chim Acta. 519 (2004) 207–211.
60. R. Kaliszan, M.P. Marszałł, M. Jan Markuszewski, T. Bczek, J. Pernak, Suppression of deleterious effects of free silanols in liquid chromatography by imidazolium tetrafluoroborate ionic liquids, J Chromatogr A. 1030 (2004) 263–271.
61. M.P. Marszałł, R. Kaliszan, Application of Ionic Liquids in Liquid Chromatography, Crit Rev Anal Chem. 37 (2007) 127–140.
62. L. He, W. Zhang, L. Zhao, X. Liu, S. Jiang, Effect of 1-alkyl-3-methylimidazolium-based ionic liquids as the eluent on the separation of ephedrines by liquid chromatography, J Chromatogr A. 1007 (2003) 39–45.
63. M. Tian, S. Li, K.H. Row, Retention mechanism of some solutes using ionic liquids as mobile phase modifier in RP-high-performance liquid chromatography (HPLC), Korean J. Chem. Eng. 28 (2010) 357–363.
64. J. Flieger, A. Czajkowska-Zelazko, Ionic Liquids As Mobile Phase Additives In Reversed-Phase High Performance Liquid Chromatography, J Liq Chromatogr Relat Technol. 34 (2011) 2224–2242.
65. J. Flieger, A. Czajkowska-Zelazko, Comparison of chaotropic salt and ionic liquid as mobile phase additives in reversed-phase high-performance liquid chromatography of biogenic amines, J. Sep. Sci. 34 (2011) 733–739.
66. W. Bi, M. Tian, K.H. Row, Chiral separation and determination of ofloxacin enantiomers by ionic liquid-assisted ligand-exchange chromatography, Analyst. 136 (2011) 379–387.
67. W. Bi, J. Zhou, K.H. Row, Preparation and Application of Ionic Liquid-Modified Stationary Phases in High Performance Liquid Chromatography, Sep Sci Technol. 47 (2012) 360–369.
68. Y. Sun, B. Cabovska, C.E. Evans, T.H. Ridgway, A.M. Stalcup, Retention characteristics of a new butylimidazolium-based stationary phase, Anal Bioanal Chem. 382 (2005) 728–734.
69. Y. Sun, A.M. Stalcup, Mobile phase effects on retention on a new butylimidazolium-based high-performance liquid chromatographic stationary phase, J Chromatogr A. 1126 (2006) 276–282.
70. S. Fakayode, M. Lowry, K. Fletcher, X. Huang, A. Powe, I. Warner, Cyclodextrins host-guest chemistry in analytical and environmental chemistry, Curr Anal Chem. 3 (2007) 171–181.
71. H. Dodziuk, ed., Cyclodextrins and Their Complexes, Wiley-VCH, Weinheim, 2006.
72. C.A. Schalley, ed., Analytical Methods in Supramolecular Chemistry, Wiley-VCH, Weinheim, 2012.
73. R.N. Dsouza, U. Pischel, W.M. Nau, Fluorescent dyes and their supramolecular host/guest complexes with macrocycles in aqueous solution, Chem Rev. 111 (2011) 7941–7980.
74. A. Douhal, ed., Cyclodextrin Materials Photochemistry, Photophysics and Photobiology, Elsevier, Amsterdam, 2006.
75. L. Yu, S. Wang, S. Zeng, Chiral mobile phase additives in HPLC enantioseparations, Methods Mol. Biol. 970 (2013) 221–231.
76. K. Kalíková, M. Riesová, E. Tesarová, Recent chiral selectors for separation in HPLC and CE, Cent Eur J Chem. 10 (2012) 450–471.
77. A. Cavazzini, L. Pasti, A. Massi, N. Marchetti, F. Dondi, Recent applications in chiral high performance liquid chromatography: a review, Anal Chim Acta. 706 (2011) 205–222.

78. E. Schneiderman, A.M. Stalcup, Cyclodextrins: a versatile tool in separation science, J. Chromatogr. B Biomed. Sci. Appl. 745 (2000) 83–102.
79. T. Cserháti, E. Forgacs, Cyclodextrins in Chromatography, The Royal Society of Chemistry, Cambridge, 2003.
80. J. Szejtli, Introduction and General Overview of Cyclodextrin Chemistry, Chem Rev. 98 (1998) 1743–1754.
81. E. Bilensoy, ed., Cyclodextrins in Pharmaceutics, Cosmetics, and Biomedicine, John Wiley & Sons, Inc, Hoboken, 2011.
82. M. Asztemborska, A. Bielejewska, K. Duszczyk, D. Sybilska, Comparative study on camphor enantiomers behavior under the conditions of gas-liquid chromatography and reversed-phase high-performance liquid chromatography systems modified with alpha- and beta-cyclodextrins, J Chromatogr A. 874 (2000) 73–80.
83. A.G. León, A.I. Olives, M.A. Martín, B. del Castillo, The role of β-cyclodextrin and hydroxypropyl β-cyclodextrin in the secondary chemical equilibria associated to the separation of β-carbolines by HPLC, J Incl Phenom Macrocycl Chem. 57 (2007) 577–583.
84. A. León, A.I. Olives, B. del Castillo, M.A. Martín, Influence of the presence of methyl cyclodextrins in high-performance liquid chromatography mobile phases on the separation of [beta]-carboline alkaloids, J Chromatogr A. 1192 (2008) 254–258.
85. Z. Juvancz, J. Szejtli, The role of cyclodextrins in chiral selective chromatography, Trends Anal Chem. 21 (2002) 379–388.
86. F. Kitagawa, K. Otsuka, Recent progress in capillary electrophoretic analysis of amino acid enantiomers, J Chromatogr B. 879 (2011) 3078–3095.
87. Z. Juvancz, R.B. Kendrovics, R. Iványi, L. Szente, The role of cyclodextrins in chiral capillary electrophoresis, Electrophoresis. 29 (2008) 1701–1712.
88. J. Xu, W. Zhao, Y. Ning, M. Bashari, Y. Chen, Z. Jin, et al., Enantiomer separation of phenyllactic acid by HPLC with HP-β-cyclodextrin as chiral mobile phase additive, J Incl Phenom Macrocycl Chem. 76 (2013) 461–465.
89. A. Zeng, J. Xing, C. Wang, J. Song, C. Li, X. Yang, et al., Simultaneous analysis and retention behavior of major isoflavonoids in Radix Puerariae lobatae and Radix Puerariae thomsonii by high performance liquid chromatography with cyclodextrins as a mobile phase modifier, Anal Chim Acta. 712 (2012) 145–151.
90. B. Feng, J. Jin, C. Wang, J. Song, G. Yang, A. Zeng, Analysis and retention behavior of isoflavone glycosides and aglycones in Radix Astragali by HPLC with hydroxypropyl-β-cyclodextrin as a mobile phase additive, J. Sep. Sci. 35 (2012) 3469–3476.
91. Y. Kudo, H. Kan, N. Jinno, M. Hashimoto, K. Tsukagoshi, Separation of dansyl-DL-amino acids by open tubular capillary chromatography based on tube radial distribution phenomenon of the ternary mixed carrier solvents, Anal. Methods. 4 (2012) 906–912.
92. A. Rocco, A. Maruška, S. Fanali, Cyclodextrins as a chiral mobile phase additive in nano-liquid chromatography: comparison of reversed-phase silica monolithic and particulate capillary columns, Anal Bioanal Chem. 402 (2012) 2935–2943.
93. W. Bi, S. Li, K.H. Row, Eco-friendly separation of catechins using cyclodextrins as mobile phase additives in RP-HPLC, Phytochem. Anal. 23 (2011) 308–314.
94. P. Rodríguez-Bonilla, J.M. López-Nicolás, L. Méndez-Cazorla, F. García-Carmona, Development of a reversed phase high performance liquid chromatography method based on the use of cyclodextrins as mobile phase additives to determine pterostilbene in blueberries, J Chromatogr B. 879 (2011) 1091–1097.
95. D.A. Larionova, I.Y. Goryacheva, C. Van Peteghem, S. De Saeger, Thin-layer chromatography of aflatoxins and zearalenones with β-cyclodextrins as mobile phase additives, World Mycotoxin J. 4 (2011) 113–117.
96. D. Antic, S. Filipic, B. Ivkovic, K. Nikolic, D. Agbaba, Direct separation of clopidogrel enantiomers by reverse-phase planar chromatography method using β-cyclodextrin as a chiral mobile phase additive, Acta Chromatogr. 23 (2011) 235–245.
97. Y. Xiao, T.T.Y. Tan, S.-C. Ng, Enantioseparation of dansyl amino acids by ultra-high pressure liquid chromatography using cationic β-cyclodextrins as chiral additives, Analyst. 136 (2011) 1433–1439.
98. J. Ye, W. Yu, G. Chen, Z. Shen, S. Zeng, Enantiomeric separation of 2-arylpropionic acid nonsteroidal anti-inflammatory drugs by HPLC with hydroxypropyl-beta-cyclodextrin as chiral mobile phase additive, Biomed Chromatogr. 24 (2010) 799–807.
99. P. Rodríguez-Bonilla, J.M. López-Nicolás, F. García-Carmona, Use of reversed phase high pressure liquid chromatography for the physicochemical and thermodynamic characterization of oxyresveratrol/beta-cyclodextrin complexes, J Chromatogr B. 878 (2010) 1569–1575.
100. A. Kwaterczak, K. Duszczyk, A. Bielejewska, Comparison of chiral separation of basic drugs in capillary electrophoresis and liquid chromatography using neutral and negatively charged cyclodextrins, Anal Chim Acta. 645 (2009) 98–104.
101. P.K. Zarzycki, H. Ohta, Y. Saito, K. Jinno, Interaction of native alpha-cyclodextrin, beta-cyclodextrin and gamma-cyclodextrin and their hydroxypropyl derivatives with selected organic low molecular mass compounds at elevated

and subambient temperature under RP-HPLC conditions, Anal Bioanal Chem. 391 (2008) 2793–2801.

102. J. López-Nicolás, F. García-Carmona, Rapid, simple and sensitive determination of the apparent formation constants of trans-resveratrol complexes with natural cyclodextrins in aqueous medium using HPLC, Food Chem. 109 (2008) 868–875.

103. L. Yuan, Effect of mobile phase additive on chiral separation, Sep Purif Technol. 63 (2008) 701–705.

104. N.F.S. de Melo, R. Grillo, A.H. Rosa, L.F. Fraceto, Interaction between nitroheterocyclic compounds with beta-cyclodextrins: phase solubility and HPLC studies, J Pharm Biomed Anal. 47 (2008) 865–869.

105. R. Grillo, N.F.S. de Melo, C.M. Moraes, R. de Lima, C.M.S. Menezes, E.I. Ferreira, et al., Study of the interaction between hydroxymethylnitrofurazone and 2-hydroxypropyl-beta-cyclodextrin, J Pharm Biomed Anal. 47 (2008) 295–302.

106. J. Guan, J. Yang, Y. Bi, S. Shi, F. Yan, F. Li, Determination of the enantiomeric impurity in S-(−)pantoprazole using high performance liquid chromatography with sulfobutylether-beta-cyclodextrin as chiral additive, J Sep Sci. 31 (2008) 288–293.

107. J. Pan, G. Kai, C. Yuan, R. Jin, Separation and Determination of the Structural Isomers of Madecassoside by HPLC Using β-Cyclodextrin as Mobile Phase Additive, Chromatographia. 66 (2007) 121–123.

108. J. Yang, X. Lu, Y. Bi, F. Qin, F. Li, Chiral Separation of Duloxetine and Its R-Enantiomer by LC, Chromatographia. 66 (2007) 389–393.

109. J. López-Nicolás, E. Núñez-Delicado, A. Pérez-López, Á. Barrachina, P. Cuadra-Crespo, Determination of stoichiometric coefficients and apparent formation constants for β-cyclodextrin complexes of trans-resveratrol using reversed-phase liquid chromatography, J Chromatogr A. 1135 (2006) 158–165.

110. J. Ye, G. Chen, S. Zeng, Enantiomeric separation of norgestrel by reversed phase high-performance liquid chromatography using eluents containing hydroxypropyl-beta-cyclodextrin in stereoselective skin permeation study, J Chromatogr B. 843 (2006) 289–294.

111. A. El-Gindy, S. Emara, M.K. Mesbah, G.M. Hadad, Liquid chromatography determination of citalopram enantiomers using beta-cyclodextrin as a chiral mobile phase additive, J AOAC Int. 89 (2006) 65–70.

112. C. Gazpio, M. Sánchez, I.X. García-Zubiri, I. Vélaz, C. Martínez-Ohárriz, C. Martín, et al., HPLC and solubility study of the interaction between pindolol and cyclodextrins, J Pharm Biomed Anal. 37 (2005) 487–492.

113. D. Chen, S. Jiang, Y. Chen, Y. Hu, HPLC determination of sertraline in bulk drug, tablets and capsules using hydroxypropyl-beta-cyclodextrin as mobile phase additive, J Pharm Biomed Anal. 34 (2004) 239–245.

114. B. Claude, P. Morin, M. Lafosse, P. Andre, Evaluation of apparent formation constants of pentacyclic triterpene acids complexes with derivatized β- and γ-cyclodextrins by reversed phase liquid chromatography, J Chromatogr A. 1049 (2004) 37–42.

115. S. Rozou, E. Antoniadou-Vyza, Chromatographic behaviour of naproxen–cyclodextrin complexes, J Chromatogr A. 1041 (2004) 187–194.

6

Core-shell particles: leading the way to a renewed HPLC

Submitted to Trends in Analytical Chemistry. González-Ruiz, V., Olives, A. I., Martín, M. A..

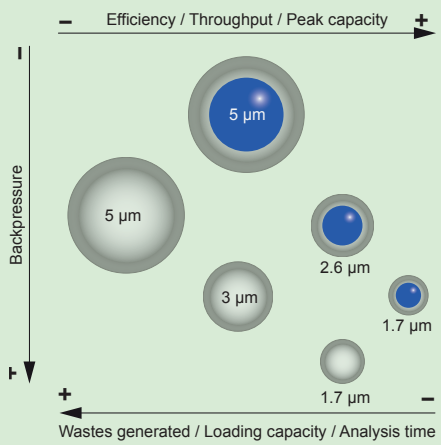

ABSTRACT ▶ In this review we present the latest highlights and trends on the use of core-shell particles as stationary phases in liquid chromatography. These superficially porous particles have a diameter between 1.3 and 5 µm, with a solid silica core and a highly homogeneous porous surface that confers them excellent performance compared to the fully porous ones. The use of these columns is exponentially growing since their first large-scale manufacturing in 2006, and they are becoming an outbreaking trend in the analysis of biological, toxicological and pharmaceutically interesting compounds. Herein we review the landmarks of their timeline since the conceptual beginnings in the 60's to their commercial availability nowadays. The main theoretical aspects responsible for their surprisingly good chromatographic behaviour and analytical features are explained by the use of the van Deemter equation and their kinetic characteristics. We also review the state-of-the-art analytical applications taking advantage of this column technology that is leading the current revolution in liquid chromatography.

Ms. ID ▼
TRAC-D-13-00167

ABBREVIATIONS ▼

- **AOAC:** Association of the Official Analytical Chemists
- **CPC:** Centrifugal Partition Chromatography
- **DAD:** Diode Array Detector
- **DNA:** Deoxyribonucleic acid
- **ELSD:** Evaporative Light Scattering Detector
- **FL:** Fluorescence Detection
- **HETP:** Height Equivalent to a Theoretical Plate
- **HILIC:** Hydrophilic Interaction Liquid Chromatography
- **HPLC:** High Performance Liquid Chromatography
- **I.D.:** Inner Diameter or Internal Diameter
- **LC:** Liquid Chromatography
- **LLE:** Liquid-Liquid Extraction
- **MS:** Mass Spectrometry
- **NSAIDs:** Non-Steroidal Anti-inflammatory Drugs
- **O.D.:** Outer Diameter
- **PFP:** Pentafluorophenyl
- **POISe:** Performance Optimized Injection Sequence
- **SIA:** Sequential Injection Analysis
- **SLE:** Solid Liquid Extraction
- **SPE:** Solid Phase Extraction
- **UHPLC:** Ultra High Performance / Pressure Liquid Chromatography
- **UV-Vis:** Ultraviolet-visible spectral region / detection

1. Introduction

Liquid chromatography is a powerful quantitative technique strongly grounded in many analytical fields because of its versatility, sensitivity, rapidity, non-destructive nature and economical advantages. It is widely employed in a plethora of different analytical applications comprising countless analytes, matrices and purposes [1-3].

In the last decades a renewed interest in the development of sustainable analytical methodologies has aimed at the reduction of wastes and reagents [4]. According to Welch [5], one single conventional HPLC instrument equipped with a traditional column generates approximately 1 L of solvent waste per day. The proportion of organic solvents is often high in these wastes. Meanwhile, the current challenges in chemical analysis are demanding improved liquid chromatography methods able to afford better efficiency, higher resolution and sensitivity, and shorter analysis times. An example of that is the large number of recent innovations that have focused on stationary phases to provide more efficient solutions to liquid chromatography analysts [6].

Trying to achieve a greener and more powerful liquid chromatography, the length and diameter of the columns, as well as the size of the particles packed into them, have been downscaled. The development of these narrow-bore HPLC columns together with the breakout of ultra high performance liquid chromatography (UHPLC) using smaller particles, made possible to maintain or boost the classical good analytical features of HPLC while improving its environmentally friendliness. UHPLC columns packed with sub-2 µm fully-porous particles dramatically increased the column performance. This made possible very fast separations requiring smaller amounts of solvents, at the expense of generating very high backpressures because of the small particle diameter. These high-pressure conditions require special hardware able to handle them, and so an investment on renewed instruments. As an alternative to avoid the need for dedicated UHPLC systems, superficially porous particles arose as a new technology able to yield efficiencies comparable to those of UHPLC (running fast, efficient and solvent-saving separations) without the inconvenience of dealing with high pressures [7]. The possibility to use conventional HPLC systems already present in the labs afforded

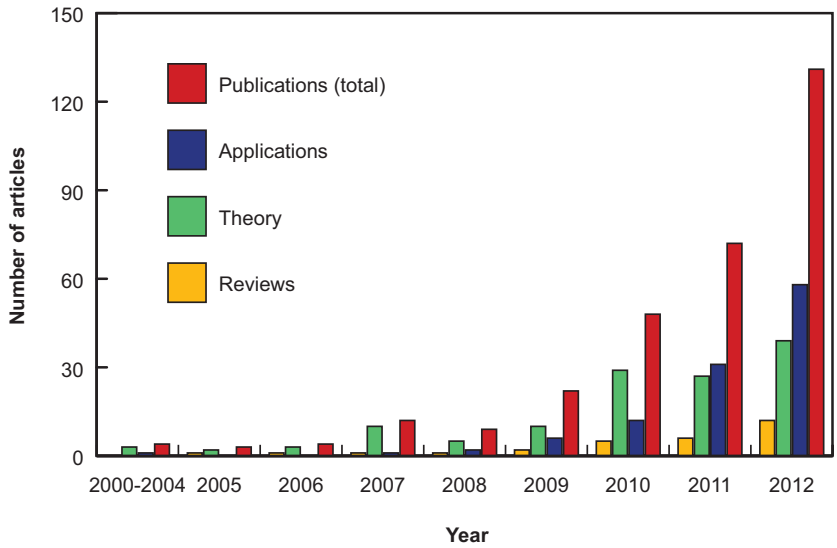

Figure 1. Evolution of the total number of papers dealing with core-shell particles according to several databases.

immediate economical advantages over UHPLC. The reduction in the run time and solvents consumption achieved by superficially porous particles, together with their higher efficiency and resolution, makes them an alternative to totally porous particles clearly lighting the way to the future that liquid chromatography seems to face [8].

In the last three years, a considerable number of reviews have been devoted to describe the behaviour of the core-shell particles and to compare them to the totally porous (UHPLC) [9-13]. Other articles focus on capillary chromatography with sub-2 µm fully porous and superficially porous particles [14] as well as on the aspects regarding the nature of the interactions in fully-porous silica or core-shell silica particles [15]. The theoretical aspects of core-shell particles and the mechanisms responsible for their high efficiency have been deeply reviewed [16]. The strategies to minimize several causes of band broadening have been proposed [11]. Wang *et al.* revised the advantages and applications of the liquid chromatography employing superficially porous particles with sub-2 µm and sub-3 µm diameters [17].

Most of the reviews and research articles dedicated to core-shell particles (Figure 1) focus either in the fundamentals or in analytical applications of this columns, so our aim is merging both sides in the present review to provide the interested readers with the most attractive analytical capabilities as well as enough theoretical background to fine-tune their methods and squeeze most of this new column technology.

2. An outlook on the development of core-shell silica particles

The concept of solid core silica particles coated with a porous shell was first proposed by Horváth and Kirkland at the end of the 60's, but the production of such particles under high-quality standards had to overcome many difficulties over the following decades. The work was pioneered by Horváth [18] using 50-100 µm beads coated with a porous thin layer in gas chromatography aimed at reducing the tailing of peaks. Later, he applied this technology to ionic exchange liquid chromatography [19,20]. Knox studied how decreasing the particle size affected the chromatographic efficiency also in gas chromatography [21]. This idea was worked and assayed by Kirkland showing that the particles coated with controlled surface porosity support exhibited better behaviour in the resistance to the mass transfer equilibrium [22].

These particles were commercialized under several brands and employed as stationary phases for liquid-liquid chromatography in the early 70's. During the 1980's decade Unger and independently Horváth and Kalghatji developed truly superficially porous particles and used them to separate mixtures of proteins and peptides, although they were abandoned due to their low load capacity [23,24]. In 1992, Kirkland developed a new methodology to prepare 5 µm core-shell particles, which were later successfully marketed for the separation of proteins [25]. Kirkland also emphasized in the characteristics of the superficially silica particles [26] and in their applications to the chromatographic analysis of macromolecules due to their excellent kinetic properties for the retention of molecules with such a high molecular weight [27]. The large-scale production and commercialization of 2.7 µm shell particles had to wait until 2006, when Halo started manufacturing columns able to yield excellent efficiencies for small molecules and unveiling the potential of this new technology in liquid chromatographic analysis.

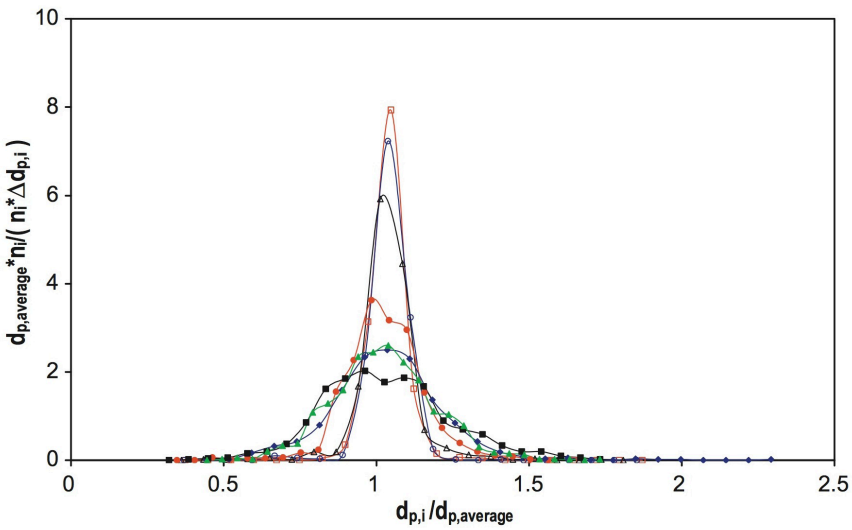

Figure 2.
Normalized size distribution of core-shell (empty symbols) and fully-porous (filled symbols) particles from various manufacturers. Taken from Figure 2 on Cabooter *et al* (2010). Journal of Chromatography A, 1217(45), 7074–7081.

3. Structure, preparation and properties of core-shell particles

The presence of the distinctive non porous silica nuclei coated by successive porous layers affords outstanding features to the chromatographic behaviour of these particles. As explained on the following sections, several reasons account for that. First, column permeability is increased, so higher flow rates can be achieved at lower working pressures. Second, the high homogeneity and roughness of the particles obtained with this process improves the packing process of the column, avoiding the band broadening caused by multiple inter-particle paths. Third, the existence of a reduced porous region in the particles drops the band broadening caused by intra-particle paths and diffusion processes. And fourth, the higher thermal conductivity afforded by the solid silica nucleus improves heat dissipation thus reducing the existence of radial temperature gradients that contribute to band broadening. They also exhibit a reduction in the retention factors and so in the time of analyses, increasing even further the already high efficiencies due to the abovementioned reasons.

3.1. Preparation

The characteristic structure of core-shell particles employed in chromatography comprises two different parts. The first one is an inner core with a diameter between 0.9 and 3.7 µm made from solid silica. Less often, other inorganic (aluminium, gold or carbon) or organic materials (a polymer or a mixture of polymers) can be employed to build the core. The second part is a shell formed by successive layers of controlled-porosity, chemically modified silica. Together, the nucleus and the shell conform spherical particles with a narrow particle size distribution (Figure 2) of a total diameter that can be tuned between 1.3 and 5 µm.

Chaudhuri and Paria [28] described the different approaches to obtain core-shell particles. Taking into account that a narrow distribution of the size of the particles is a critical issue for chromatography applications, the "bottom-up" approach (synthesis from inner to outer layers, Figure 3A) has shown to yield the best results in terms of efficiency of the process and homogeneity of the obtained particles. Such methodologies are based upon the protocol by Stober [29], which allows synthesizing virtually monodisperse non-porous silica particles that will become the future nuclei. Although other methodologies were applied earlier [30], nowadays the following concentrical layer-by-layer growing of porous silica shells over the nuclei is achieved by taking advantage of the self-organizing properties of cationic surfactants and organic polymers [31]. Such organic elements constitute a temporary backbone helping the silica grow in an organized fashion, allowing for fine control of pore size and layer thickness, and achieving a high level of homogeneity over time (Figure 3B). As discussed later, this high degree of homogeneity explains many of the fascinating chromatographic features of core-shell particles.

Alternative synthetic methodologies have been proposed with the aim to save the time required for the multiple step that are necessary for the layer to layer technique. This is the case of the one-pot synthesis of silica spheres-on-spheres that improve the morphology and the size distribution of the core-shell particles [32]. The influence of the initiators for producing shells with different structures has been also described [33]. The use of particles with a solid core possessing other chemical nature than silica was also explored, thus spherical carbon and nanodiamond particles have been employed as core and layer-by-layer coated with chemically functionalized polymers. These stationary phases posses very high hydrolytic stability at extreme pH-values, with higher efficiencies and very low back pressures [34]. A

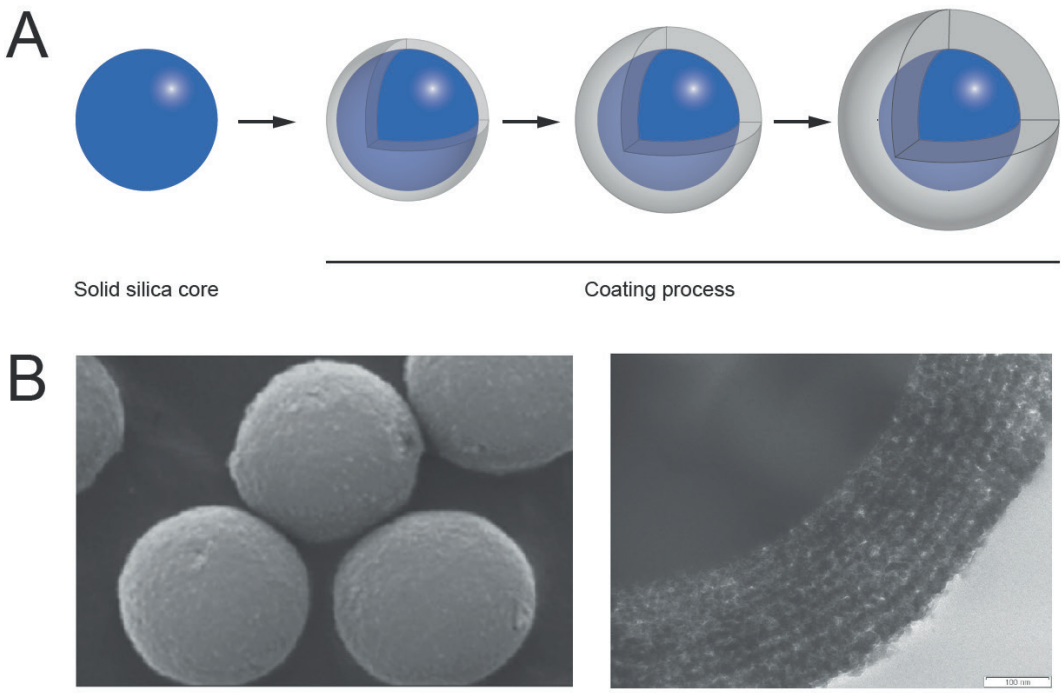

Figure 3. (A) Scheme showing the bottom-up, building process of a typical core-shell particle. (B) Scanning electron microscopy images of 2.6 (left) and 1.7 µm (right) Kinetex core-shell particles. The result of layer-by-layer synthesis process is clearly visible on the image on the right. (B) is taken from [41].

similar deposition approach has been employed for the preparation of core-shell diamond particles and they have been successfully applied as stationary phases in HPLC as well as support for solid phase extraction [35]. A sol-gel approach producing highly regular silica elements with an adequate external porosity, was employed to produce porous-shell pillar-array columns, thus conjugating separation efficiency and peak capacity and retention [36]. The surface of silica cores has also been activated employing metallic species like Al(III) for subsequent chemical vapour deposition of carbon. This resulted in a carbon clad core-shell silica particle which retains the properties of a carbon phase, and has been found to be very useful for chromatographic separations [37].

A recent publication [38], used trans-(1*R*,2*R*)-diaminocyclohexane to functionalize core-shell particles allowing for fast, enantioselective separations. Core-shell particles incorporating cyclodextrins and cyclodextrins polymers into the shells have been successfully produced and structurally characterized [39]. Although the authors propose the use of such nanoparticles as drugs carriers and delivery systems, this technology could be also applied to chiral chromatographic separations.

3.2. Morphology

Details concerning morphology of packed beds i.e. size distribution, shape, and surface roughness, have been deduced from confocal laser scanning microscopy images [40]. The physical characteristics, including porosities, of commercially columns have been evaluated (Kinetex C-18 and Halo C-18) showing exceptional features with regard to the classical C-18 columns [41]. An exhaustive study of more than 10 columns of superficially porous particles was conducted employing carotenoids as model analytes, and their chromatographic behaviour was compared to fully-porous C-18 stationary phases [42].

Less frequently, the role of the geometry of the porous shell particles on the chromatographic behaviour of these stationary phases has been considered. As explained later, the enhancement of the mass transfer kinetics is a consequence of the particles geometry that modifies the diffusion time of the analyte molecules on the stationary phase. Fellinger [43] has shown that the diffusion times for a Halo 2.7 µm are equivalent to a totally porous stationary phase of 1.8 µm, and even better results were obtained for Kinetex 2.6 µm, since its chromatographic behaviour is equivalent to a 1.34 µm fully porous stationary phase.

3.3. Thickness and porosity of the shell

The total thickness of the porous layer is a critical factor in the contribution to the global porosity of the particles [44]. Porosity exerts a notable influence on the chromatographic behaviour [9]. The resolution of analytes can be improved with core-shell particles possessing thinner porous surface if the eluting strength of the mobile phase is reduced to compensate for the smaller retention factor yielded by the drop in surface area of the particle [45]. The chromatographic behaviour of superficially porous particles of the same overall size, when possessing different solid core diameters and different porous shell thicknesses, is clearly influenced by the internal, external and total porosities of the particles that modify the eddy and longitudinal

diffusion as well as the mass transfer resistance, as explained later [46,47].

Porosity, surface area, particle distribution of the fully porous and superficially porous silica particles have been evaluated and determined by scanning electron microscopy, pycnometry and inverse size exclusion chromatography. The values obtained were discussed in connection with those reported by the manufacturers (Table 1) [48]. The porosities of fully and superficially porous particles have been compared [49] and, as expected, the total porosity is lower in the case of the core-shell particles (0.540) than in the case of totally porous traditional silica (0.645), what can be explained considering that the solid core affords a reduction in the number of total pores per silica particle. However the external porosity of the columns possessing core-shell particles present higher value (0.432) than those obtained for the columns packed with traditional silica particles of 3 µm of diameter (0.383). Similar porosity values have been reported and discussed comparing fully and superficially porous particles as well as monolithic columns [50]. Different models for the determination of external porosities and diffusion in superficially porous particles have been developed and applied [51,52].

Additional considerations about the pore diameter must be taken into account. As explained below, the molecular weight of the analytes conditions the selection of the pore diameter of the core-shell particles adequate for their separation [12,53,54]. In most cases, small molecules with low molecular weights require the diameter of the surface pores of the particles to be around 80 Å. On the other hand, in the case of proteins and other biomolecules, a pore di-

Table 1. Commercially available core-shell columns for liquid chromatography and some of their most relevant characteristics. The number of application notes published by each manufacturer is also indicated

Manufacturer	Brand	Appl. Notes#	Pore size: Chemistries	O. D. | shell thickness (µm)	Surf. area (m^2/g)*	Max. press. (bar)
Advanced Materials Technology	HALO	-	90 Å: C-18, C-8, phenyl-hexyl, pentafluorophenyl, RP-amide, cyano, HILIC, OH5	4.6 | 0.6 2.7 | 0.5	150	600
			160 Å: C-18			
Agilent	Poroshell	61	120 Å: C-18, C-8, phenyl-hexyl, SB-Aq, RP-amide, cyano, HILIC	2.7 | 0.5 5 | 0.25	130	600
			300 Å: C-3, C-8, C-18			
ChromaNik	SunShell	-	90 Å: C-18, C8, pentafluorophenyl, phenyl, 2-EP, -HILIC amide, 2-ethylpyridine	2.6 | 0.5	150	590
			160 Å: C-18, RP-AQUA, hexafunctional C-18			
			300 Å: hexa-functional C-18			
Macherey-Nagel	NucleoShell	-	90 Å: C-18, phenyl-hexyl, pentafluorophenyl, HILIC-ammonium-sulfonic acid	2.7 | 0.5	130	600
Nanologica (Glantreo	Eiroshell	-	100 Å: naked silica, derivatisation upon request	1.7 | 0.15 2.6 | 0.4	130	
Perkin Elmer	Brownlee SPP	11	90 Å: C-18, C-8, phenyl-hexyl, pentafluorophenyl, RP-amide, HILIC	2.7 | 0.5		
			160 Å: C-18			
Phenomenex	Kinetex / Aeris	471	Kinetex 100 Å: C18, XB-C18, C8, phenyl-hexyl, pentafluorophenyl, HILIC	1.3 | 0.2 1.7 | 0.23 2.6 | 0.35 5 | 0.67	200	1000
			Aeris Peptide: C-18	1.7 | 0.22 3.6 | 0.5		
			Aeris Widepore: C-18, C-8, C-4	3.6 | 0.2		
Sigma-Aldrich (Supelco)	Ascentis Express	16	90 Å: C-18, ES-C-18-peptide, C-8, phenyl-hexyl, pentafluorophenyl, RP-amide, ES-cyano, HILIC, OH5	5 | 0.6 2.7 | 0.5	135	1000
			160 Å: C-18			
Thermo Scientific	Accucore	67	80 Å: C-30, C18, amide-embeded C-18, C-8, C-4, phenyl-hexyl, phenyl-X, pentafluorophenyl, urea-HILIC, amide-HILIC, aQ	2.6 4	130	1000
			150 Å: C-18, C-4, amide-HILIC			
Waters	Cortecs	6	90 Å: C-18, HILIC	1.6 | 0.24		

#Data in this table was updated on September 2013
**The surface area values are referred to the 2.6 or 2.7 µm particles of each brand*

ameter near between 150-300 Å is required as it ensures enough penetration of the molecules into the porous shell. This is why most manufacturers offer two separate lines of products, one with 80-90 Å pores and other with 150-300 Å pores, each one intended to separate analytes within different molecular weight ranges.

3.4. Thermal conductivity

An important factor to be considered is the effective thermal conductivity of the columns packed with solid-core particles. A low thermal conductivity is responsible for the formation of radial temperature gradients into the column, what spoils their efficiency causing peak broadening and even peak split. The thermal conductivity of core-shell particles is larger than the one of fully porous particles due to the presence of the highly conductive solid core (closer to the optimum value of 30-40 W/m/K). Thus, the heat generated at higher flow rates can be better dissipated avoiding the appearance of such thermal gradients, what improves the homogeneity of the migration velocities of the molecules along the column, yielding narrower peaks [55].

Table 1 also shows the core-shell columns commercially available by the third quarter of 2013, their trade-marks, particle sizes, porosities, chemical variations, some physicochemical parameters and applications notes developed by their manufacturers. Although still scarce, the developing interest on 5.0 µm particles is reflected on the growing number of columns being packed with this size of core-shell particles. This is due to the fact that they allow an immediate improvement of already-validated methods just by replacing classical 5 µm fully-porous columns, improving the efficiency, affording a similar load capacity and working at lower backpressures. This kind of packing materials have been proved to afford a minimum reduced HETP similar to that of a theoretical 3.2 µm fully-porous particles but generating half the backpressure, or to be as efficient as second-generation monolithic columns while allowing working pressures up to 600 bar [56]. At the opposite end of the size range, the newest 1.3 µm core-shell particles have recently unveiled their striking performance by reaching peak capacities 20-40% higher than those of 1.7 µm fully porous particles [57].

$$H = A + \frac{B}{u} + Cu \qquad \text{Eq. 1}$$

$$h = a + \frac{b}{v} + cv \qquad \text{Eq. 2}$$

$$P = \phi \frac{u\eta L}{d_p^2} \qquad \text{Eq. 3}$$

4. Theoretical aspects of the chromatographic behaviour in core-shell silica particles

Exhaustive and critical evaluation of the models and the equations employed to describe the mass transfer kinetics of the solutes in core-shell particles have been reported [11,53,58,59]. The differences among the velocities of the molecules of the same analyte migrating along the column cause the broadening of the chromatographic peak, what leads to an increase in the height equivalent to a theoretical plate. The different causes accounting for peak broadening are modelled by the classical van Deemter equation (Equation 1, Figure 4). In this model, three different terms (A, B and C) sum their contributions up to raise the HETP value (H) –it is to say, to decrease the column efficiency:

Equation 2 uses H and u in their reduced forms, h and ν, and is often employed with physicochemical comparison purposes. From Equation 1 and Equations 10 and 12 on Table 2, it is clear that A-term and C-terms directly depend on the particle diameter and, therefore, the re-

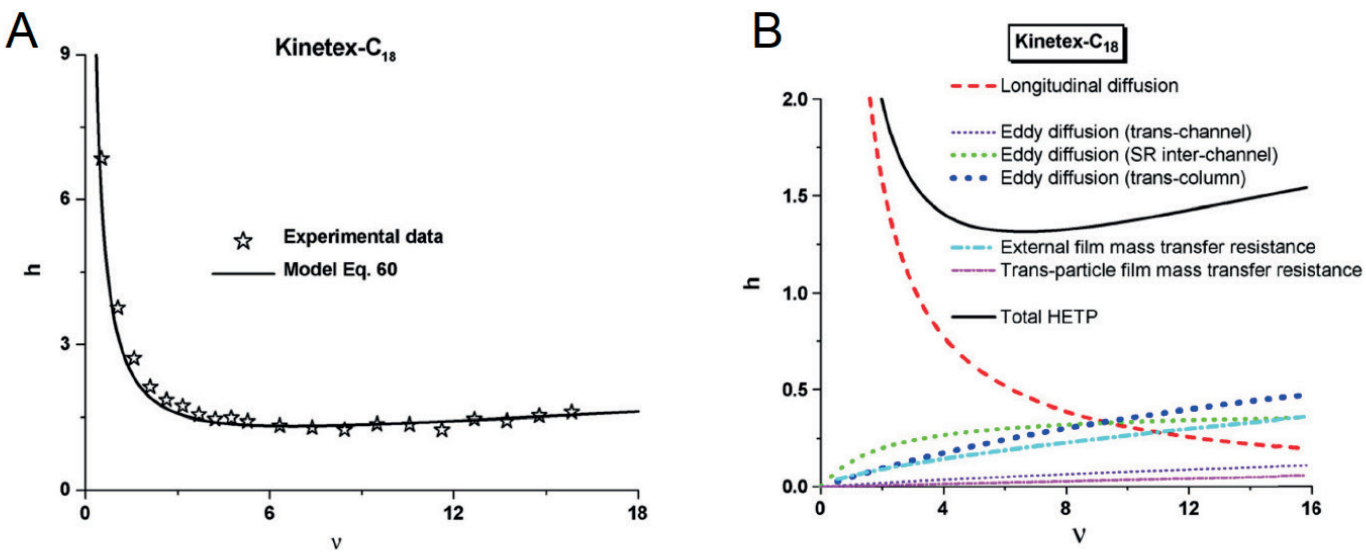

Figure 4. (A) Agreement between the efficiency values experimentally found, and the theoretically calculated ones after measuring the different parameters involved in the van Deemter equation for the separation of naphtho[2,3-*a*]pyrene on a 2.6 µm Kinetex-C18 column. (B) Contribution of each parameter to the total HETP. [68]

Table 2. Equations and parameters defined according to the classical chromatographic kinetic model

#	Parameter, (symbol)	Equation	Variables
1	Dead time (t_0) Retention time (t_R),	$t_0 = \frac{L}{u_0} \quad t_R = \frac{L}{u_x}$	L: column length, u_0: linear velocity of the mobile phase for the dead time, u_x: linear velocity of the analyte x into the column
2	Plate Number (N)	$N = \frac{L}{H} = \left(\frac{t_R}{\sigma}\right)^2$	L: column length, H: Plate height
3	Plate Height or height equivalent to a theoretical plate (H)	$H = \frac{L}{N} = \frac{\sigma^2}{L}$	L: column length, N: plate number, σ^2: variance
4	Variance (σ^2)	$\sigma^2 = \frac{L\,w_b}{4\,t_r} = \frac{L\,w_{1/2}}{2.354\,t_R}$	L: column length, σ^2: variance, w_b: width at the base, $w_{1/2}$: width at half height, t_R: retention time
5	Plate Height or height equivalent to a theoretical plate (H)	$H = \frac{L}{N} = \frac{\sigma^2}{t_R^2} L$	L: column length, N: Plate number, σ^2: variance, t_R: retention time
6	Plate Number (N)	$N = 16\left(\frac{t_R}{w_b}\right)^2 = 5.54\left(\frac{t_R}{w_{1/2}}\right)^2$	t_R: retention time, w_b: width at the base, $w_{1/2}$: width at half height,
7	Reduced Plate Height (h)	$h = \frac{H}{d_p}$	H: height equivalent to a theoretical plate, d_p: particle size
8	Reduced Linear Velocity of the Mobile Phase (v)	$v = \frac{u\,d_p}{D_M}$	u: linear velocity of the mobile phase, d_p: particle size, D_M: diffusion coefficient of analytes in the mobile phase.
9	Van Deemter's equation	$H = A + \frac{B}{u} + Cu \quad h = a + \frac{b}{v} + cv$	H: height equivalent to a theoretical plate , u: linear velocity of the mobile phase
10	A-term of the van Deemter's equation	$A = 2\lambda d_p$	A: diffusion eddy term, d_p: particle diameter of the column packing material, λ: structure factor of the packing material
11	B- term of the van Deemter's equation	$B = 2\gamma D_M$	B: longitudinal diffusion term, D_M: diffusion coefficient of analytes in the mobile phase, γ: constant related to quality of packing material (tortuosity/obstruction)
12	C- term of the van Deemter's equation	$C = C_S + C_M$	C: mass transfer resistance
13	Mass transfer resistance in the stationary phase (C_S)	$C_S = \frac{f_s(k')d_f^2}{D_S}$	f_S: function of the stationary phase, k': retention factor, d_f: thickness of the film liquid coating on the stationary phase, D_S: diffusion coefficient of analytes in the stationary phase
14	Mass transfer resistance in the mobile phase (C_M)	$C_M = \frac{f_M(k')d_p^2}{D_M}$	f_M: function of the mobile phase, k': retention factor, d_p: particle diameter of the column packing material, D_M: diffusion coefficient of analytes in the mobile phase
15	Pressure drop (ΔP)	$\Delta P = \phi\frac{u\eta L}{d_p^2} = \frac{u_0\eta L}{K_V}$	ΔP: pressure drop, ϕ: flow resistance factor, L: column length, u: linear velocity of the mobile phase, η: mobile phase viscosity, d_p: particle diameter of the column packing, K_V: column permeability based on u_0
16	Plate number (N)	$N = \frac{\Delta P}{\eta}\left(\frac{K_V}{u_0 H}\right)$	N: plate number, ΔP: pressure drop, η: mobile phase viscosity, u_0: linear velocity of non-retained solute, K_V: column permeability, H: height equivalent to a theoretical plate
17	Dead (void) time (t_0)	$t_0 = \frac{\Delta P}{\eta}\left(\frac{K_V}{u_0^2}\right)$	t_0: dead (void) time, ΔP: pressure drop, η: mobile phase viscosity, u_0: linear velocity of non-retained solute, K_V: column permeability
18	Colum permeability (K_V)	$K_V = \frac{u\eta L}{\Delta P}$	u: linear velocity , η: mobile phase viscosity, L: column length, ΔP: pressure drop
19	Equation employed in kinetic plots (Desmet modification)	$\frac{t_0}{N^2} = \frac{\eta}{\Delta P}\left(\frac{H^2}{K_V}\right)$	t_0: dead (void) time, N: plate number, ΔP: pressure drop, η: mobile phase viscosity, of non-retained solute, K_V: column permeability, H: height equivalent to a theoretical plate

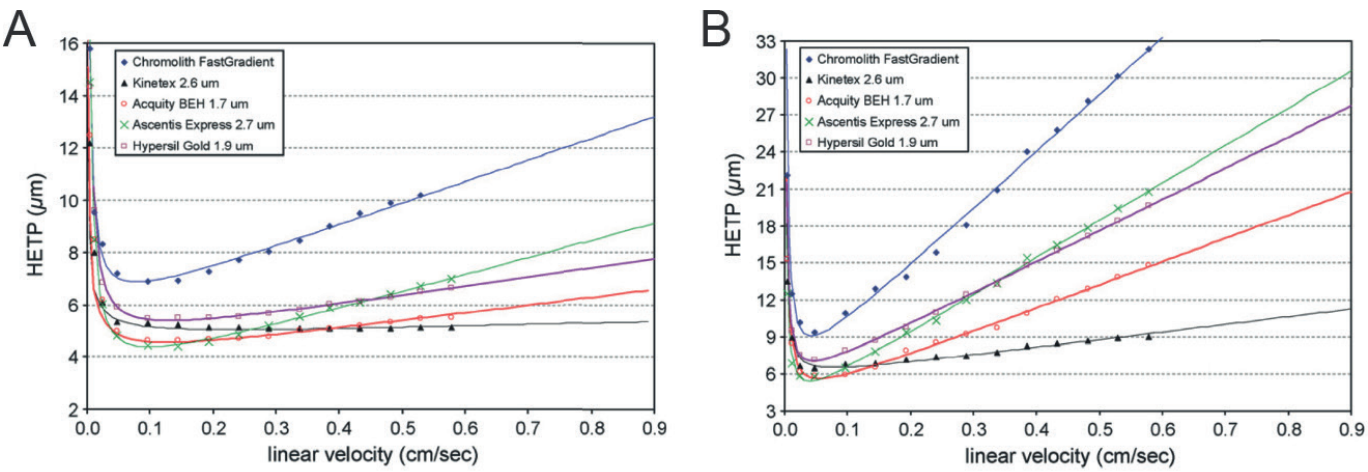

Figure 5. Comparison of the van Deemter plots obtained by using different monolith, core-shell and fully porous columns. Note the larger slope of the plot at high flow rates (C-term-driven region) when a high molecular weight compound is analysed (B), and how the minimum HETP values obtained for 2.6 µm core-shell particles are similar to those of 1.7 µm fully porous ones. Taken from [79].

duction of the size of the particles enhances the performance of the separation. Nevertheless, this leads to an immediate drawback: columns packed with smaller particles present a lower permeability and this causes higher backpressures according to the Darcy's law (Equation 3). It means that optimal flow rates for fully porous particles will generate backpressures several times higher in columns packed with sub-3 µm or sub-2 µm than in the case of 5 µm. However, this can be bypassed by using superficially porous particles: the solid core increases the permeability of the chromatographic bed and as a consequence core-shell particles generate lower backpressures that fully porous particles of the same diameter [60]. As higher flow rates can be employed, this contributes to a reduction in the axial (longitudinal) diffusion component of the peak broadening, the B-term, in the van Deemter equation. Kirkland developed the core-shell silica particles with the aim to reduce the diffusion path of the molecules into the pores. Actually, the intra-particle diffusion path in the core-shell particles is reduced in comparison to traditional totally porous particles, decreasing the C-term, although this reduction has been experimentally found to be much lesser than theoretically expected [16].

The combination of large efficiencies and resolutions with reduced backpressures is the consequence of several additive physical and chemical factors that are determined by the unique characteristics of superficially silica particles and their packing.

The significant differences among the total porosities of the fully and superficially porous stationary phases induced to Gritti *et al.* [49] to consider the superficial velocity (u_S) instead of the lineal velocity (u_0) to calculate the HETP values in both types of stationary phases. The superficial velocity can be obtained from the product of the total porosity (ϵ_t) by the lineal velocity. For molecules with low molecular weights, the minimum H value found in the van Deemter equation is lower in the case of superficially porous than in totally porous stationary phases. At velocities faster than the optimum, the efficiency reached with core-shell particles is at least two times higher than those obtained using fully porous particles. This can be explained considering the effects of the core-shell structure on the A, B and C terms on the van Deemter equation (Figure 5).

The efficiency and kinetic behaviour of different columns packed with core-shell particles have been compared taking into account the particle size (1.7 µm, 2.6 µm and 2.7 µm). The influence of the inner diameter of the columns (4.6 mm and 2.1 mm) was also considered. Surprisingly, the reduced plate heights were better in the case of 4.6 mm I. D. columns than for 2.1 mm I. D. columns with the same kind of packing. The relative velocity biases were comparable for both types of I. D. columns, and the diffusion terms (A and B) were found to be greater for narrow-bore columns than in classical columns of 4.6 mm inner diameter [61]. Other factors such as extra-column contributions, peak variances [62], band profiles, or frictional heating have also been evaluated and discussed.

More recently, the reproducibility of the kinetic performance have been studied on 2.1 mm and 4.6 mm × 100 mm columns packed with core shell particles manufactured by different commercial suppliers. The A-term presents poor reproducibility, possibly due to the difficulties in reaching the same packing procedure [63]. The relative standard deviations of this coefficient depend on the nature of the analytes (proteins and low molecular weight molecules) as well as the inner diameter of the columns. The columns with lower I. D (2.1 mm) present better reproducibility for both types of analytes at highest reduced velocity. B-term is highly reproducible with very low relative standard deviations. The changes in the C-term are negligible in comparison to the eddy diffusion coefficient [64].

4.1. The A-term in the van Deemter equation

The A-term or eddy dispersion term reveals the differences of the analytes speed with regard to the average velocity of the mobile phase

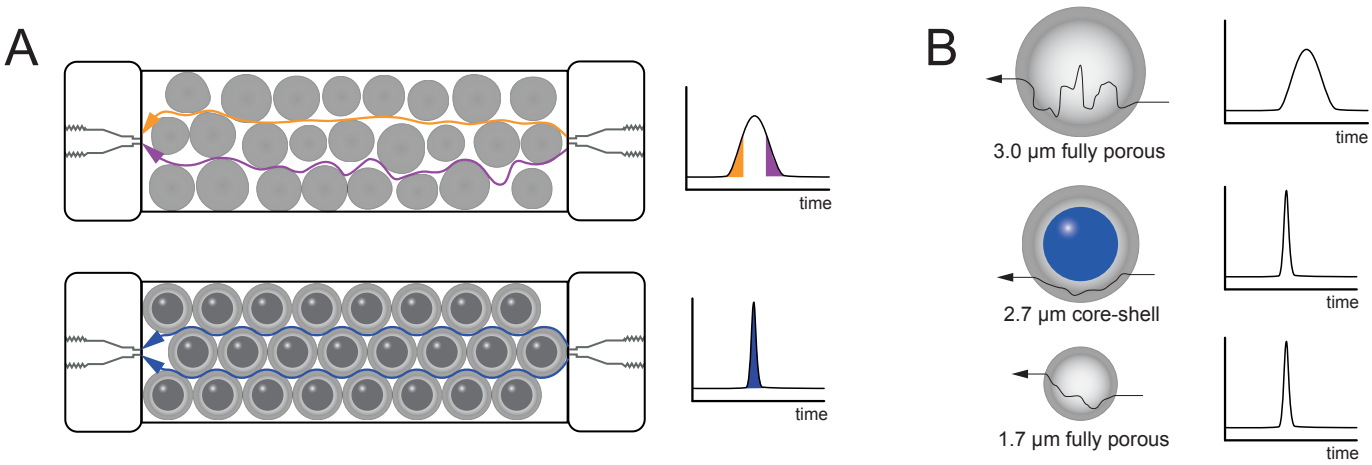

Figure 6.
(A) Effect of the larger packing homogeneity afforded by the core-shell particles on the A-term of the van Deemter equation. (B) Difference in the intra-particle diffusion between fully-porous and core-shell particles.

due to the existence of different inter- and intra-particle routes [65] (Figure 6).

Cabooter *et al.* have demonstrated that there is a strong relation between the particle size distribution and the quality of the packing. In most cases, the almost monodisperse particle size of the core-shell particles increases the overall column packing homogeneity, thus reducing the A-term of the van Deemter equation (Figure 6A, Eq. 10 on Table 2) [66]. As a consequence of this, a reduction of up to 20% in the A-term has been found in the case of core-shell particles [49].

The differences in the migration velocities of a solute between the centre and the wall of the column can be voltamperometically determined by means of appropriate microelectrodes. Such measurements showed that the velocity bias decreases for increasing analyte retention factors [67]. Similar studies of the bed of columns packed with core-shell particles (Halo-C-18 and Kinetex C-18) revealed a greater radial homogeneity for the Halo particles [68].

The decrease in the A-term of the van Deemter equation as consequence of the reduction either of the inter-channel or of the trans-column velocity biases were determined and remained unclear [69]. The experimental procedures for evaluating the trans-channel eddy diffusion, short inter-range eddy diffusion and trans-column eddy diffusion in totally and superficially porous particles have been deeply revised by these authors [70]. Several experimental protocols have been applied to the determination of the eddy diffusion for commercially available core-shell silica columns [71]. The satisfactory performance of these columns has been shown to be due to their exceptionally low eddy and axial diffusions.

The influence of the shell porosity, the core-to-shell ratio and the surface roughness have been found to be critical parameters affecting the homogeneity of the packing and thus to the A-term. Several authors have studied and discussed how the eddy diffusion is modified by these variables. Although results vary among different columns and manufacturers, an overall reduction in the eddy dispersion has been described for the core-shell particles compared to the fully-porous ones. Some of the most remarkable findings on this issue include the difficulties to homogeneously pack sub 2 µm core-shell particles in narrow-bore columns, the existence of an optimum core-to-shell ratio [72], the relevance of the roughness of the external surface of the core-shell [73], and the influence of the particle size on the quality of the packed bed (bigger core-shell particles are potentially more homogeneously packed) [74].

4.2. The B-term in the van Deemter equation

The longitudinal diffusion process is caused by the axial diffusion of the analytes driven by their own gradients of concentration as the bands progress along the chromatographic bed. Higher flow rates minimize this effect (Figure 7). As the higher permeability of core-shell packed columns allows working at faster flow rates, these columns achieve an important performance enhancement with regard to totally porous particles showing B-term values around a 25% lower. This observation is suggested to come from the much shorter retention times, what hampers the axial diffusion [49].

Gritti and Guiochon found that in the case of superficially porous particles, the B-term is not a linear function of the distribution constant, K [70]. The reduced values (usually negligible) of the B-term can be explained considering that the axial diffusion does not proceed in the solid core. The volume of the solid cores in the column represents around 25% of the total column volume with important consequences in the decrease of the values of B-term.

4.3. The C-term in the van Deemter equation

C-term quantifies the mass-transfer resistances between the mobile and the stationary phase. In the case of totally porous particles, the increase in the flow rates produces an important increase in the C-term. The decrease of C-term

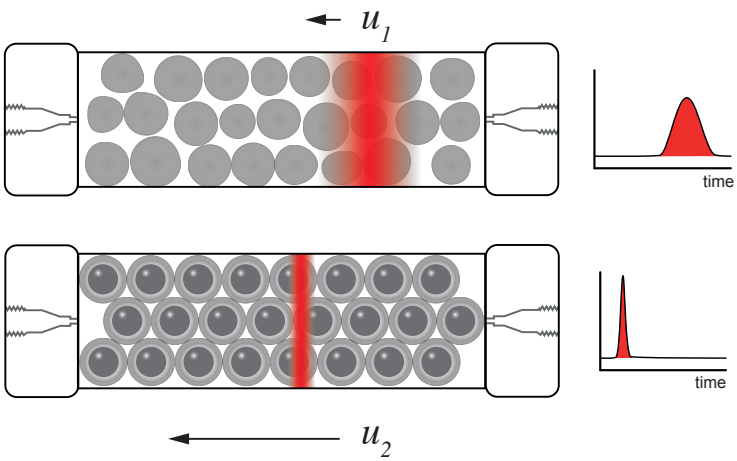

Figure 7.
Illustration showing the effect of the velocity of the mobile phase on the axial diffusion.

and therefore the improvement in the performance of the separation is consequence of the increase in the external surface area of the shell that eases the distribution of the molecules inside the particles allowing a rapid equilibrium of the analytes onto stationary and into mobile phases to be reached [75].

As with other of their characteristic, a part of the success of the core-shell particles to reduce the C-term takes the root in the way they are built. The layer-by-layer synthesis of the porous shell onto the solid core allows to produce large and homogeneous mesopores (300 Å) improving the mass transfer kinetics. The trans-particle mass transfer resistance coefficient results very low in the case of molecules with low molecular weight. In the case of proteins and peptides, the mass-transfer resistance depends principally on the accessibility of the mesopores and the openings of the pores placed on the external surface of the shells [69], which is also largely improved in wide pore core-shell particles.

In contrast with the general conviction, the mass-transfer resistance is quite small or negligible for small molecules, either for fully porous or core-shell particles. This is why the reduction in the value of the C-term in core-shell particles with regard to totally porous is only significant in the case of high molecular weigh compounds and fast flow rates [69]. Biomolecules of higher molecular weights require specially synthesized particles with larger mesopores to be able to penetrate into them [53], and more efficient separations are obtained for 160 Å pore size in comparison with 90 Å pore size for the same core-shell particles of 2.7 µm [76]. The structure of the external shells possessing large mesopores of (200 - 300 Å) facilitates the penetration of proteins into the stationary phase [54].

The experimental determination of the values of the C-term in columns packed with totally and superficially porous particles has been carried out employing both small molecules and biomolecules. In the case of superficially porous silica, small peptides present lower mass transfer resistance on superficially (2.7 µm) than in totally porous (3.0 µm) particles. The compounds with higher molecular weights (proteins) present low diffusivities, and thus they can reach the mass transfer equilibrium faster than in totally porous particles, yielding smaller C-terms than in traditional columns (Figure 8) [49].

The experimental values obtained for the C-term in Halo (2.7 µm, core-shell), Luna (3.0 µm, totally porous) and Atlantis (3.0 µm, totally porous) were compared with the expected theoretical C-term values. Surprisingly, the C-term was found to be larger in the tested core-shell particles than in the conventional fully porous stationary phases. Nevertheless, the contribution of the A- and B-terms to the total value of H made the columns to show a better performance [77].

The C-term is particularly reduced in the case of core-shell particles of 1.7 µm applied to the separation both low molecular weight compounds and proteins. An improvement of 50% in the plate heights compared to the core-shell

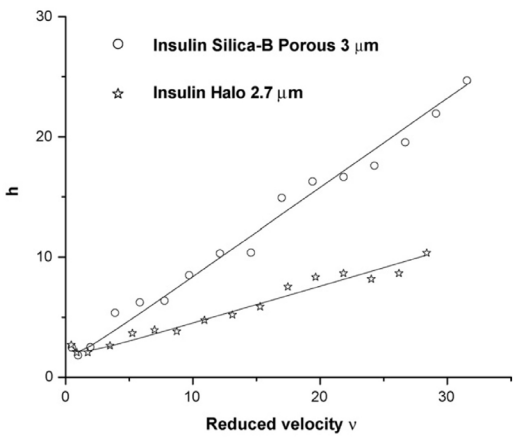

Figure 8.
Insulin is a good example of how the mass transfer equilibrium of large molecules is remarkably improved by using core-shell particles (stars), as shown by the lower slope of C-term branch of the van Deemter plot. Taken from [49].

particles of 2.7 µm was obtained by Fekete *et al.* [78]. Kinetex columns were compared with Ascentis Express core-shell columns and monolithic columns showing the shortest analysis time and more efficient separations in a wide range of velocities. Moreover, Kinetex columns presented a low value and flat C-term for the separation of small molecules in comparison to the other core-shell or monolithic columns studied [79].

Proteins are interesting subject to study the mass transfer kinetics in core-shell particles also employing low-polarity stationary phases such as C-4 and C-18. The excellent mass transfer characteristics of C-18 columns packed with superficially porous particles of 3.6 µm were compared to those obtained using C-18 fully porous particles of 1.7 µm. The retention behaviour was a combination of the hydrophobic and ion exchange and hydrogen bonding mechanisms. The two last modes of interaction contributed to the band broadening, but it was found to be compensated by the good C-term [80].

5. Other physicochemical and operational advantages of fused-core silica particles

5.1. The frictional heating

The percolation of the pressurized mobile phase through and into the pores of the stationary phase generates frictional heating. The adsorption-desorption of the solute from the bed of the column is also responsible for generating heat into the column. Such heat is unevenly distributed inside the packed bed because of two reasons: the mobile phase progressively increases its temperature while advancing along the column (generating an axial temperature gradient), and the heat exchange mainly happens through the column's wall (causing a radial temperature gradient). These gradients account for local differences in the viscosity of the mobile phase and, thus, different flow velocities. The retention factor of an analyte also becomes inhomogeneous because it depends on the temperature.

When temperature gradients are radial, different molecules of the same analyte will migrate at different velocities and with different retention factors, depending on their distance from the column axis, what will ultimately contribute to broaden the analyte band. Gritti and Guiochon have recently proved that the radial temperature gradient can be mitigated by operating the column in an insulating (with low heat absorption capacity) environment, such as still air. On the contrary, a media with a larger conductivity (i. e. water bath) drains the heat and hampers reaching a thermal equilibrium, increasing the magnitude of the radial temperature gradient, and consequently boosting the negative effects of the frictional heating on the separation, particularly at higher flow rates [81].

$$h = a + \frac{b}{v} + cv + h_{\text{heat}} \qquad \textbf{Eq. 4}$$

The van Deemter equation can be modified to take into account the effects of the frictional heating on the efficiency, by adding its contribution to the plate height (Eq. 4), being h_{heat} the contribution of the thermal heterogeneity of the packed bed. Gritti and Guiochon determined the frictional heating for columns packed with totally and superficially porous silica of 1.7 µm [82]. The experimental results obtained are in agreement with those derived from theoretical considerations and they have shown that frictional heating is significantly lower in the case of superficially silica particles in comparison with the totally porous particles. In connection with this behaviour, the efficiencies obtained at different flow rates (0.2-1.10 mL min^{-1}) are 1.5 to 5 times higher for the core-shell silica particles than for the totally porous particles.

Other comparative study of different columns (2.7 µm core shell, 1.7 µm core shell and 1.7 µm fully porous) showed that columns packed with core-shell particles are much more efficient in heat dissipation that the totally porous ones. These effects can be explained on the basis that the solid core, which has a much better thermal conductivity that the porous silica, represents around 40% of the particle volume and about 25% of the total volume of the column, thus affording its characteristic high thermal conductivity to the porous shell stationary phases [83].

A recent paper came to the conclusion that the role of frictional heating is almost negligible when short, narrow-bore columns are employed, even when high pressures are generated by a packed bed of core-shell particles as small as 1.3 µm, because the heat dissipation power of the column is directly related to its dimensions [57].

5.2. The backpressure

One of the most outstanding advantages of the core shell particles is in connection to their much lower working pressure compared to the small, fully porous particles yielding similar efficiencies. As we have discussed before, very small particles should afford smaller H values according to the van Deemter equation, what means superior efficiencies. Nevertheless, Darcy's law indicates that such small particles should also dramatically increase the resistance of the column. That would raise the working pressure causing a drop in the efficiency due to the frictional heating, as mentioned before.

The lower backpressures allow to use highly viscous organic/aqueous mixtures or analysing complex matrices or analytes (bio- and macromolecules) [84]. In HILIC separations, it has been demonstrated that the working backpressures with 2.7 µm core-shell particles can be up

to two times lower than those obtained with 1.7 µm fully porous particles, in columns of the same length and diameter, but sometimes at the expense of a certain loss in the efficiency [85]. Anyway, a progressive diminution in the particle diameter cannot ensure an increase in the efficiency. According to Carr *et al.* [1], the use of particles smaller than 1 µm will not be useful as it will require very narrow capillaries for the separations.

6. Performance and resolution of analytes chromatographied on superficially porous stationary phases

The van Deemter equation is a good model to define the column efficiency in absolute terms. Nevertheless, in the past years, the use of kinetic plots to explore the columns' efficiencies, and particularly to compare efficiencies among different columns, is becoming the most widespread choice. Kinetics plots represent how a column performs by relating its efficiency to the time needed to achieve it, for a certain limiting working pressure. This constitutes a better approach to study the practical performance of the column within an analytical scope.

One of the most popular kinetic plots is the Poppe plot. It consists of a representation of the separation speed vs. the number of theoretical plates (t_0/N vs. N) [86]. The modification introduced by Desmet (plotting t_0/N^2 vs. N and reversing the scale of the axes so the plot looks more like a conventional van Deemter equation) is also frequently employed [87] (Figure 9).

Theoretical considerations concerning the extrapolation of kinetic plots from isocratic to gradient elution have been critically discussed and experimentally validated on traditional C-18 and core-shell C-18 particles as stationary phases [88]. Comparison of kinetic plots for monolithic, superficially and totally porous particle columns shows that the best time of analysis allowing to achieve a high efficiency and at certain backpressures depends on the characteristics of the column. Thus, at 1000 bar, a 1.7 µm totally porous column provides similar performance than a 2.7 µm core-shell column working at 600 bar. The best performance for the monolithic column is reached at 200 bar [89]. Brice *et al.* came to analogue conclusions [90]. These authors compared the separation times, linear velocities and backpressures generated on monolithic, totally (1.7 µm) and superficially (2.7 µm) porous columns. Also, they studied the influence of pH on the stability of the stationary phase as well as on the separation. In the case of monolithic columns, pH had to be kept around 7. This fact constrained its applicability and leaded to longer time of analysis. The performances and kinetic plots for superficially porous and monolithic columns were higher in the case of monolithic column than for the columns packed with superficially porous particles, however the values obtained for the terms in the van Deemter equation were better in the case of core-shell particles [91].

The study of the kinetic performance of different columns packed with superficially and totally porous particles shows the significance of the thickness of the shell. In a paper which studied different 1.7 µm and 1.8 µm core shell and fully porous particles, the highest efficiencies were achieved with the particles possessing the thinnest porous shell. This work also underlined the contribution of the extra-column volume to the band broadening, being more affected the compounds with retention factors under 1 [72]. The narrow distribution of the particle diameter was found to be a critical variable to reach better efficiencies. The narrowest particle distribution was obtained for EiS-150-C-18 followed by Kinetex-1.7 µm-C-18.

Shaaban *et al.* have recently compared the efficiency, selectivity and resolution of the separation of pharmaceutically interesting compounds using totally (1.8 µm) and superficially porous particles (2.7 µm) [92]. The optimum

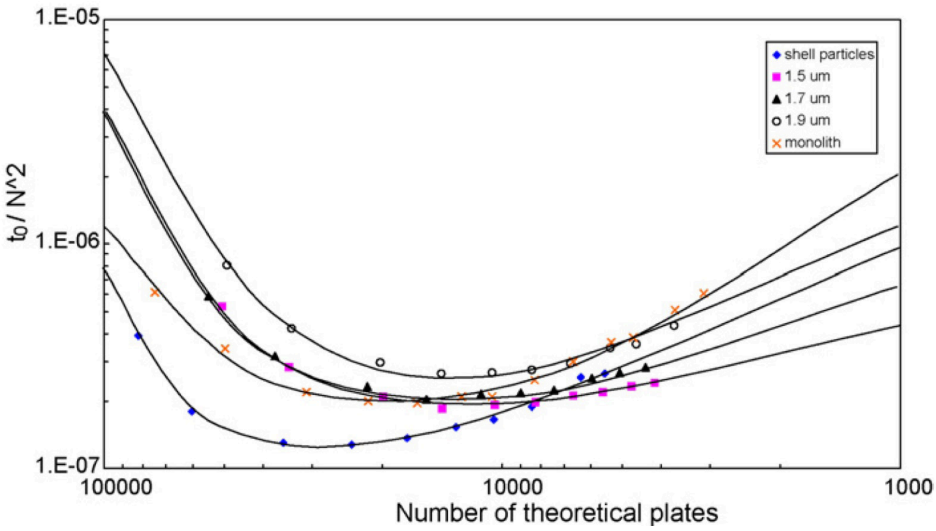

Figure 9
Example of a kinetic plot according to Desmet's modification. The similarity to a van Deemter plot makes easy to find the best kinetic efficiency point, achieved by the core-shell particles at around 30 000 plates. Taken from [89].

flow rates were similar in both columns, but the maximum flow rate was 2-3 folds higher in the case of the core-shell particles, thanks to the lower backpressures (32%) developed by the core-shell stationary phases. The efficiency of the separations afforded similar values (25 000 plates) in both cases. The resolution and retentions were also comparable but slightly higher in the case of the totally porous particles. An important conclusion is about the connection of two columns to increase the total column length. Such setup was expected to increase both the backpressure and the efficiency of the system. Although fully porous particles behaved as expected, the tandem connection of more than one core-shell column achieved a raise in the efficiency fairly larger than in the pressure. Cunliffe *et al.* described how good efficiencies at low back-pressures, with only a slight sacrifice in peak efficiency, could be reached in the separation of benzene, toluene and naphthalene under isocratic and gradient elution by using 2.7 µm superficially porous particles instead of 1.8 µm totally porous [93].

Another useful procedure to compare the performance of totally and superficially porous particles is analysing the *N*/pressure ratio using the experimental values corresponding to the plate height minimum. This quotient is 2-3 times higher for the columns packed with core-shell particles than for columns packed with totally porous particles of 1.7-1.9 µm. This feature makes them very suitable to be employed in conventional instruments operating at high mobile phase velocities achieving a notable performance enhancement [94].

7. Retention, selectivity, loading capacity and peak capacity on superficially porous stationary phases

The reduction of the particle size also affects to the chemical interactions between analyte and stationary phase, and thus the retention factors and overall separation will become affected. One of the methodologies useful to study such differences is the so-called carotenoid test. This test has been applied to study the effect of the particle size and the chemical behaviour of the stationary phases within a large number of commercial columns packed with totally and superficially porous silica [42,95]. The differences in the chemical surface properties of core-shell phases should be considered to provide better selectivity and retention. The core-shell particles also presented lower hydrophobic character than the corresponding totally porous columns, what has been explained considering the lower specific surface area of the superficially porous particles. The retention factors and the elution order became modified as a consequence of the variation of the chemical nature of the hydrophobic stationary phases. In comparison to C-18 or C-8, phenylhexyl stationary phase presented higher polar surface activity and showed higher selectivity.

The selectivity obtained for 2.7 µm core-shell particles and totally porous sub-2 µm particles can be considered similar, but columns packed with core-shell particles provided considerably enhanced selectivity profile [96]. It was also observed that superficially porous particles yielded lower retention factors, what was explained considering the lower accessible surface area

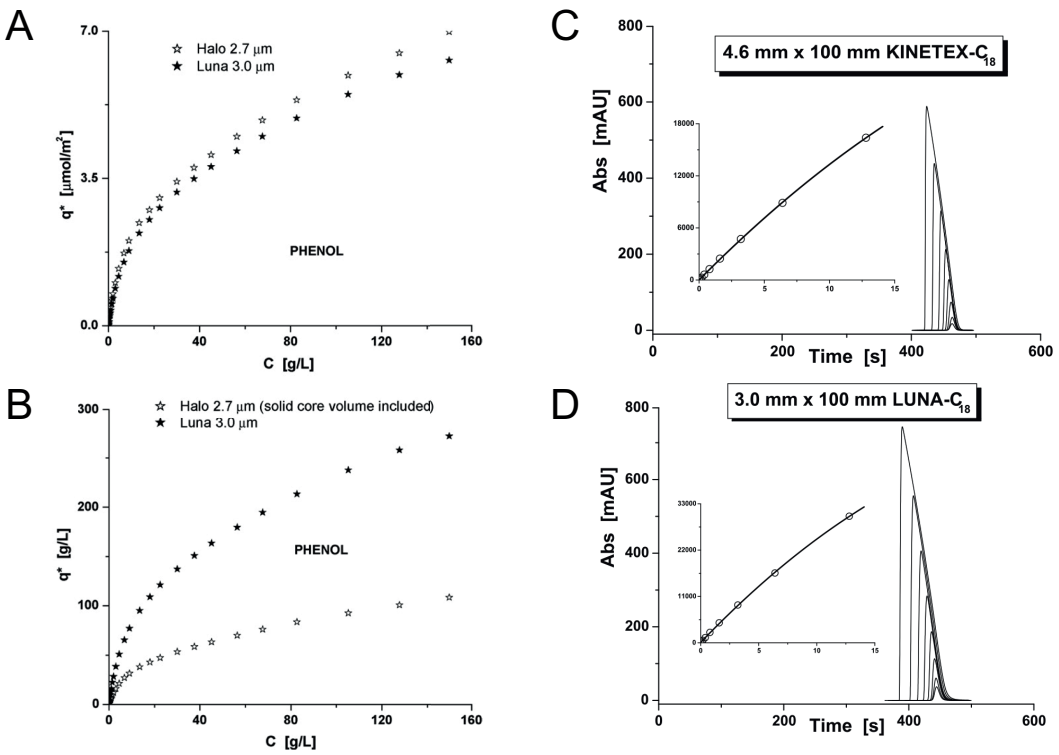

Figure 10.
(A/B) Adsorption isotherms of phenol measured on fully-porous and core-shell columns. Note that the adsorption capacity per surface unit is quite similar for both columns (A) but in the core-shell particles it drops to less than a half when expressed per mass unit (B). (A/B) Taken from Gritti & Guiochon (2007), Journal of Chromatography A, 1176 (1-2), 107–122.
(C/D) Overload effect on peak shape and area for a core-shell (C) and a fully-porous (D) column. (C/D) from [98].

due to the lower carbon loading in the case of the core-shell stationary phases. The carbon loading percentage also explains the lower (≈ 25%) loading capacity of the superficially porous particles with regard to those observed for totally porous sub-2 µm particles.

From a physicochemical point of view, the overloading phenomenon happens when the concentration of the analyte is locally higher than the adsorption capacity of the stationary phase, it's to say, the concentration is above the linear region on the adsorption isotherm. This means that the amount of a certain analyte exceeds the limits of what the stationary phase is able to effectively separate. It is often shown as strongly asymmetrical peaks in the chromatogram. Under extreme overload conditions, the apparent retention factors could seem altered [97]. Two variables constraint the loading capacity of a certain stationary phase: the specific surface area and the carbon load (Figure 10A).

The loading capacity of a column is a relevant issue on superficially porous particles because the reduction in the porous fraction of the particle with regard to the totally porous particles decreases the amount of sample that can be appropriately retained and separated onto the column. The most efficient columns happen to be the most strongly affected by peak overloading. Gritti and Guiochon [98] developed a method to allow accurate comparison of overloading behaviour among different columns, including core-shell and fully-porous particles (Figure 10B). The proposed methodology involved the integration of the first and the second central moments of the thermodynamic band profiles in order to calculate the thermodynamic contribution to the efficiency evaluated as HETP.

Depending on the manufacturer and the size of the particles, the porous volume constitutes from two thirds to three fourths of the total volume of the particles (75% for HALO, 61% Kinetex). Important differences in the overloading behaviour were found depending on the chemical characteristics of the analytes. Neutral analytes did not exhibit overload in comparison to charged analytes for the same type of column [99]. The loading of acid or basic ionisable compounds can be particularly problematic on the basis of the chemistry of the bonded phase and due to the smaller porous volume of the core-shell particles. The results by Fallas *et al.* [100] showed that columns with the same bonded chemistries but exhibiting differences in the porosities of the stationary phases presented similar loading capacity, even if they were supplied by different manufacturers. The capacity was increased for ionisable compounds at low pH values and at high buffer concentrations, however the use of formic acid or other low ionic strength buffers exerted a very poor performance enhancement, so their uses were advised only when mass spectrometry detection was employed.

Peak capacity is a magnitude of special relevance in the case of complex samples containing a large number of compounds. This concept should not be confused with the number of compounds separated and can be defined as the maximum number of peaks that can be inserted into a given chromatographic space with a resolution of 1.0 for all adjacent peaks [101]. Therefore, the peak capacity should be constant independently of the linear velocity. When the peak capacities of core-shell columns (Halo C-18 and Kinetex C-18) were compared with a totally porous BEH C-18 (1.7 µm) it was observed that, at low linear velocities, all three columns showed similar peak capacities for the separation of proteins. However, at higher flow rates Kinetex column maintained its performance and even enhanced its peak capacity with regard to the two other columns [102]. Peak capacities and efficiencies have been also compared under fast gradient elution for totally (1.7 µm) and superficially porous (2.7 µm) silica as well as for monolithic columns. The peak capacities were in the range of 27-30 for all of the columns studied. The monolithic columns with smaller I. D. presented the lowest peak capacity, efficiency and back pressures [103,104].

Vaast *et al.* [105] compared the peak capacity of monolithic, totally porous (3 µm) and superficially porous (2.7 µm) columns for the separation of proteins under gradient elution. The highest peak capacity was obtained for monolithic columns and this result can be attributed to the smaller peak widths compared to both fully and superficially porous particles. It seems to be the consequence of the large permeability of the monolithic columns, around 40% higher than the core-shell particles columns. For steroids, peak capacities from 130 to 150 were obtained with totally porous particles of 1.7 µm as well as for core-shell particles. A drop in the peak capacity near to 120 was observed in the case of the monolithic columns [89]. Columns packed with totally porous (1.7 µm) and superficially porous particles (2.7 µm) presented very similar peak capacities, as the peak capacity was enhanced for columns with totally porous particles of 1.5 µm [106]. This means that a small increase in the particle diameter dramatically affects to the peak capacity for totally porous stationary phases.

The effect of pH and temperature on the kinetic performance of the separations of peptides has been also studied. The increase of temperature favours the efficiency with all of the different mobile phase modifiers employed. Among the different acids (formic, acetic and trifluoroacetic acids as well as their corresponding ammonium salts) the best efficiencies and peak capacities were obtained in the presence of ammonium acetate [107].

8. Reduction in analysis time and solvent consumption using fused core silica packed columns

One of the most important goals achieved by means of columns packed with core-shell particles is the reduction in the time of analysis per run and consequently in the volume of wastes generated (Figure 11). The comparison of a conventional column (C-18, 5 µm, 2.1 mm × 50 mm at 0.4 mL/min) with a superficially porous column (C-18, 2.7 µm, 2.1 mm × 20 mm at 1.0 mL/min) proved a notable reduction in the total run time from 4.7 min to 1.80 min, with a nice resolution and performance. The time reduction achieved (up to 0.90 min) could be higher in the case of using flow rates of 3.0 mL/min with the column packed with core-shell particles. This important reduction is consequence of the lower operating pressures [108].

Time of analysis, peak capacity and kinetic plots have been employed to evidence the influence of the temperature (from 30 to 90 °C) on the separations of peptides and proteins (myoglobin, lactoglobulin, casein...) comparing 5.0 µm and 1.7 µm totally porous particles, 2.7 µm superficially porous particles and monolithic columns. A notably shorter time of analysis was obtained by increasing the temperature from 30 to 60 °C. Promising results were obtained for 1.7 µm-totally porous and 2.7 µm-core-shell particles compared to traditional or monolithic columns [109]. By using a core-shell column to carry out the separation of a mixture of NSAIDs, DeStefano *et al.* needed half the time employed with a totally porous column while achieving a 60% efficiency enhancement [74].

Time of analysis and performance were critically studied and compared on the basis of the chromatographic behaviour and Poppe plots of the results obtained on C-18 1.7 µm totally porous and 2.7 µm-superficially porous particles as stationary phases [110]. Ultrafast separations (2-3 min) of aryl-cetones mixtures were carried out. The efficiencies of both stationary phases were comparable, however considerably lower pressures and shorter analysis times were required in the case of core-shell particles. Core-shell columns outmatch the efficiency of sub-2 µm totally porous columns at longer analysis time because of the reduction in the longitudinal diffusion and the larger particle size.

McCalley [111] compared the efficiency of HALO silica columns in HILIC and obtained a 50% reduction in the time of analysis with regard to totally porous particles. Besides, the serial connection of three 5 cm HALO silica columns allowed to achieve similar run times than traditional columns, reaching 4 times higher efficiencies.

Due to the low pressures generated by the columns packed with core-shell particles, the peak capacity can be maximized by coupling two or more columns packed with superficially porous particles. This configuration provided quantitative examples of separation saving time (46%) and solvents by operating at 1200 bar [112]. The performance enhancement derived from the work with parallel and serially connected multi-column is described [113].

Shorter run times allowed to analyse more samples per time unit. Gradient elution is routinely employed in chromatography with the disadvantage of requiring re-equilibration time of the column. The re-equilibration time has been determined and studied in C-18 columns of superficially porous particles (Halo, Kinetex, Poroshell), and it was found to proceed quickly, with less than three column volumes of conditioning solvent. The use of a pressure raise is the simplest method to obtain a faster re-equilibration. The greater pore diameter of the superficially porous stationary phases makes possible

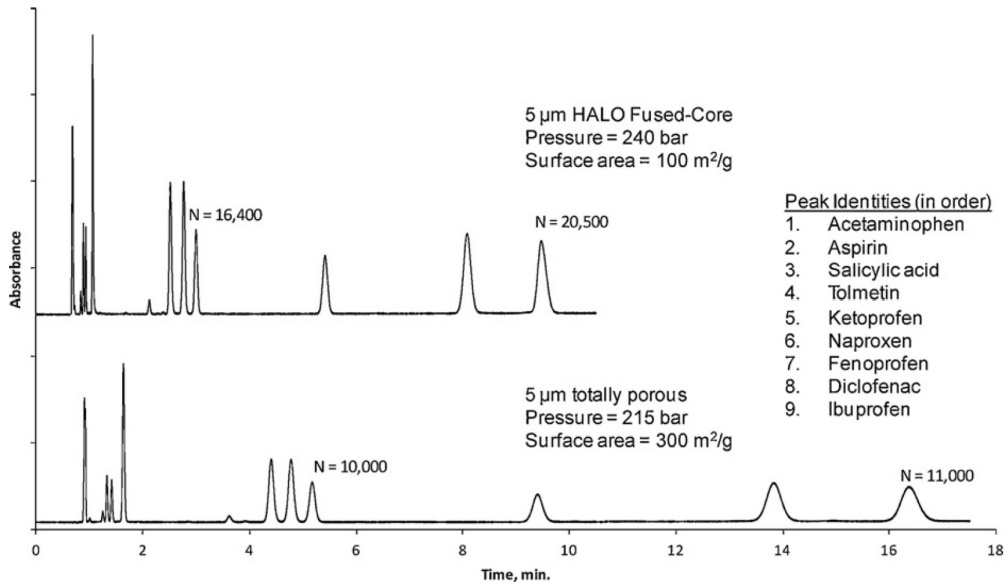

Figure 11.
Separation of several non-steroidal anti-inflammatory drugs using core-shell and fully-porous particles. A noticeable reduction in the time of analysis and an increase of the efficiencies expressed as number of theoretical plates are achieved. From [74].

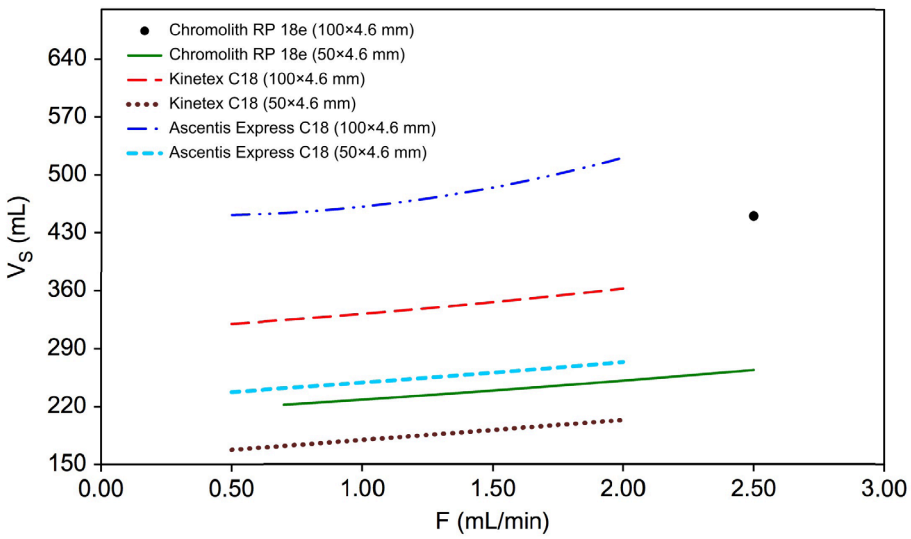

Figure 12. Volume of solvent employed to analyse 100 samples expressed as a function of the flow rate, compared to a reference method using a monolith column (black circle). From [253].

to increase the pressure to drive the aqueous phase into the particles [114].

A great number of papers devoted to the applications of the core-shell particles for the analysis of interesting compounds described the important reduction in the time of analysis (up to 4 times lower) as well as in the solvent consumption. Most of them are compiled in the Analytical Applications Section.

9. Brief remarks about the LC instruments employing columns packed with core-shell silica particles

As shown before, the use of core-shell particles as stationary phases notably increases the efficiency of the chromatographic separations. The number of theoretical plates can be multiplied by 3 - 10 times with regard to the traditional stationary phases. Efficiencies comparable to those obtained working with UHPLC instruments, but requiring lower working pressures, lower solvent consumption and shorter analysis times [115]. However, the optimum separation performance of these columns cannot be achieved if extra-column peak broadening is taking place in other elements of the system.

The efficiency loss experienced by core-shell particles when used on non-optimized HPLC system has been studied and quantified (about 30-55%) with commercially available chromatographs [116]. Several strategies have been proposed to overcome these problems [117]: shortening the connection tubes (pumps-column-detector), reducing the internal diameter of the tubing (0.12 mm I. D.), using small volume loops (1-5 µL), decreasing the needle seat, and replacing the detectors' cell from few µL to the range of nL are some of the modifications employed to boost the capabilities of conventional HPLC systems. All of these modifications are devoted to increase the efficiency and performance of the separations by reducing the extra-column volume [94,105,117].

Additional peak dispersion can be associated to the design or volume of the auto-injector [118]. The column end-fittings and the column frits also showed to affect to the shape of the peaks causing band broadening and peak tailing leading to loss in the efficiency. The optimization of connections and fits in the different components ant tubes of the LC equipment does not only reduce the band spreading but also affords the additional advantage of reducing solvent consumption [119].

Alternatives to conventional injection systems have been proposed for controlling the dispersion of the chromatographic bands. Sequential injection analysis (SIA) consisting of an eight-port selection valve to program and control the flow of the solvents involved in the chromatographic separations has been successfully applied to the quantitation of four estrogens with C-18 columns packed with core-shell particles. The efficiency and reduction in the analysis time was discussed in comparison to those obtained by using longer monolith columns [120]. POISe (Performance Optimizing Injection Sequence) is also an injection mode designed to reduce the band dispersion. This injection technique is not strictly speaking an instrument modification but an operational procedure, and it affords significant benefits to the performance of the separations. It consists of injecting a constant volume of weak solvent after the sample with the aim to "focus" (concentrate) the analytes at the head of the column by temporarily increasing their retention factors during the sample loading. The efficiencies obtained by using this methodology with different columns packed with superficially and fully porous particles have described and discussed [121].

A recent article [122] reviews most of the improvements that can be implemented to tune-up existing HPLC systems to achieve UHPLC-like separations by using columns packed

with core-shell particles at a fraction of the investment needed to purchase a new UHPLC chromatograph.

10. Analytical applications using core-shell particles columns

As shown in Figure 1, in the 2009-2012 period, the number of papers describing analytical applications of the core-shell columns has doubled yearly, and that pattern seems to continue also in the on-going 2013 year. Such increase arises from the interest of researchers working on diverse fields to take advantage of the attractive analytical features of this class of columns in terms of efficiency, sensitivity, time of analysis and solvent consumption as reviewed before. Furthermore, the fact that most of these columns can be successfully operated in conventional non-UHPLC systems with excellent performance has pushed in the direction of the core-shell particles to many researchers that were unable to adopt the sub-2 µm technology due to budget restrictions.

These columns are becoming widely employed in almost any analytical field. Many of the published applications compare the analytical performance of fully-porous vs. core-shell columns, and how the use of the new column technology allows improving the analytical outcome with little method development. Literature describes applications of core-shell particles for quantitation of compounds of diverse analytical interest, in different matrices, with various pretreatments, and making use of a variety of detectors.

From the side of manufacturers, they are making a huge effort to be the first to provide analysts with new core-shell stationary phases of assorted particle diameters and bonded chemistries affording different retention mechanisms. They are also continuously making available new analytical methodologies that researches can access as application notes to serve as a basis for their own method development. The number of application notes electronically available on the websites of representative manufacturers is shown in Table 1.

Other than the change in the column, most of these methods make use of well-known pretreatments strategies, mobile phases and detection methods. Thus, some characteristics can be outlined as the most frequently shared among the reviewed papers: 1) pretreatment usually is carried out by deproteinization, LLE, SLE or SPE; 2) gradient elution is the most common one, usually using formic or acetic acid-containing acetonitrile/water mixtures; 3) C18 is, by far, the most widely employed stationary phase, although PFP is becoming increasingly popular; 4) UV-Vis (mainly DAD) and MS are the preferred detection techniques.

In this section, we try to give an overview of the variety of uses that core-shell columns have been applied to in the recent years. Below can be found a selection of recently published analytical applications that make use of this column technology, grouped by the nature of their main analyte of interest. For additional summarized information of every paper (analytes, kind of sample, pretreatment, column details, mobile phase, detection and special remarks), readers are referred to Table 3. This should be useful as a starting point in the solving of analytical challenges taking advantage of core-shell particles columns.

10.1. Analysis of drug molecules

Drugs outstand among many other analytes because they are a subject of attention not only from the pharmacological point of view (along the many steps of the development of new medicines, in finished-product control or in patients), but also as illicit substances (sports or veterinary abuse) and pollutants in the environment.

The need for drug quantitation starts at the earliest steps of their development. Methods to analyse naproxcinod [123] and atazanavir [124] in degradation studies using core-shell columns were fully validated. Kawano analysed impurities in streptomycin [125], and a 2D method [126] was developed to detect several impurities in drug products. Cellular matrices are also of interest during *in vitro* biological assays and the quantitation of several drug candidates on Caco-2 and hepatocytes [127] using 40 µm controlled surface porosity particles was one of the earliest applications described. Paclitaxel has been independently analysed [128] in different intracellular compartments. Due to the frequent use of animals in preclinical studies, applications of core-shell particles to pharmacokinetics studies have been developed. Imipramine and desipramine [129] were quantified in rat plasma with improved figures of merit when compared to 5 µm fully porous particles. Several other methods analysed swertiamarin [130], an arginase inhibitor [131], protein kinase inhibitors [132] and sinafloxacin [133] in rat serum; and rimonabant [134] in mouse plasma, all of them with excellent results.

Human blood is one of the most relevant matrices to investigate the presence of drugs. Therefore, methods have been optimized for the monitorization of carbapenems [135], carboplatin [136], (*S*)-(+)- and (*R*)-(−)-ibuprofen [137], eletriptan [138], clopidogrel [139], GABA derivatives [140], 3-nitrotyrosine [141], and several drug diastereomers [142] in plasma with excellent validation results. Theophiline and several metabolites were analysed in whole blood [143] and the content of atenolol [144], protein kinase inhibitors [145] and a cyclosporine [146] in dried blood spots were also determined using

core-shell particles columns. Other body fluids and tissues were also studied. Mazzarino [147], developed a fast screening method to analyse the presence of a panel of doping substances in urine. β-adrenergic agonists and blockers have been chirally differentiated by using 2D chromatography with non-chiral core-shell HILIC columns on the first dimension [148]. Androgenic steroids were also determined in urine with improved time of analysis [149]. A recent application describes the use of fused-core columns in both dimensions for column-switching HPLC of propranolol in urine [150]. Packed sorbent microextraction and on-line SPE were successfully applied as pretreatment for the quantitation of several NSAIDs [151] and quinolones [152] respectively, in this matrix. Oral fluid was examined for cannabinoids [153,154] and human hair for benzodiazepines and "z-drugs" [155] using core-shell columns. Several protein kinase inhibitors [156] were quantified in serum with a remarkable enhancement over a previously described method that employed fully porous columns.

In the case of pharmaceutical preparations, penicillins have been quantified in injectable suspensions [157], cytarabine, methotrexate and ethylprednisolone in intrathecal solutions [158]; betamethasone-17-valerate and impurities in an ointment [159], and aspirin and atorvastatin in capsules [160].

Core-shell columns have been applied to the detection and quantification of drugs and metabolites in foodstuffs. Toltrazuril metabolytes were successfully analysed in meat [161]. Penicillins and amphenicols [162] exhibited improved figures of merit compared to fused core and monolithic when analysed in milk. This matrix was also investigated for sulphonamides [163] using a nano-LC format. Chloramphenicol was quantified in several matrices (egg, honey and milk) [164], and β-agonists and blockers [165] have been investigated in animal feeds. A fully validated method for sulfamides in honey shortened the analysis time and was employed in a national monitoring program [166]. Nitroimidazole antiparasitics [167] and lincomycin [168] have been analysed in plasma, milk, muscles, eggs, honey and feeds with very short analysis times. Sulfonamides [169] could be quantified in animal feeds with better figures of merit than methods using fully porous particles. Methods achieving improved performance and shorter analysis times have been developed for drugs in animal tissues from grass carp [170], cows [171] and pigs [172].

From the environmental point of view, turtle tissues were investigated for chloramphenicol [173], and water samples [174,175] were successfully screened for top-prescribed drugs with minimum solvent wastes.

Not only pharmacologically active compounds, but also excipients and preservatives were subject to analysis employing core-shell columns. Some examples include the quantification of polysorbates and polyethylene-glycol in protein-containing solutions with condensation nucleation light scattering detection [176,177], the analysis of mixtures of methylated cyclodextrins with better results than monolithic columns [178] and the analysis of parabens in hygiene wipes [179] using narrow-bore columns.

10.2. Analysis of vegetal metabolites

Plant metabolites are widely exploited in medicinal preparations and foodstuffs for their therapeutic and functional properties. They have also found its place when it comes to certifying the identity of raw or processed vegetal materials by means of vegetal metabolic fingerprinting.

Carotenoids have been separated in bidimensional liquid chromatography using core-shell particles columns in the second dimension [180]. Flavonoids were analysed (Figure 13) using different arrangements [181,182], but among them it is specially remarkable the hyphenation of CPC-Evaporative Light Scattering Detector (CPC-ELSD) with High Performance Liquid Chromatography-UV [183]. Another

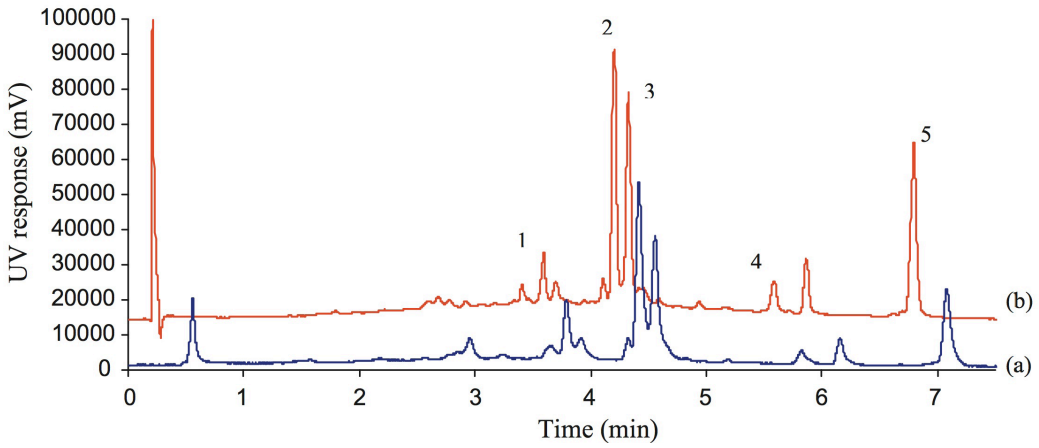

Figure 13. Chromatograms obtained from the separation of a complex mixture of flavonoids using both a 100 mm long monolith (blue line, 3 mL min^{-1}) and a 50 mm long core-shell C18 column (red line, 2 mL min^{-1}). Observe the reduction in the solvent consumption and analysis time, while improving the efficiency and resolution of the analysis. From [183].

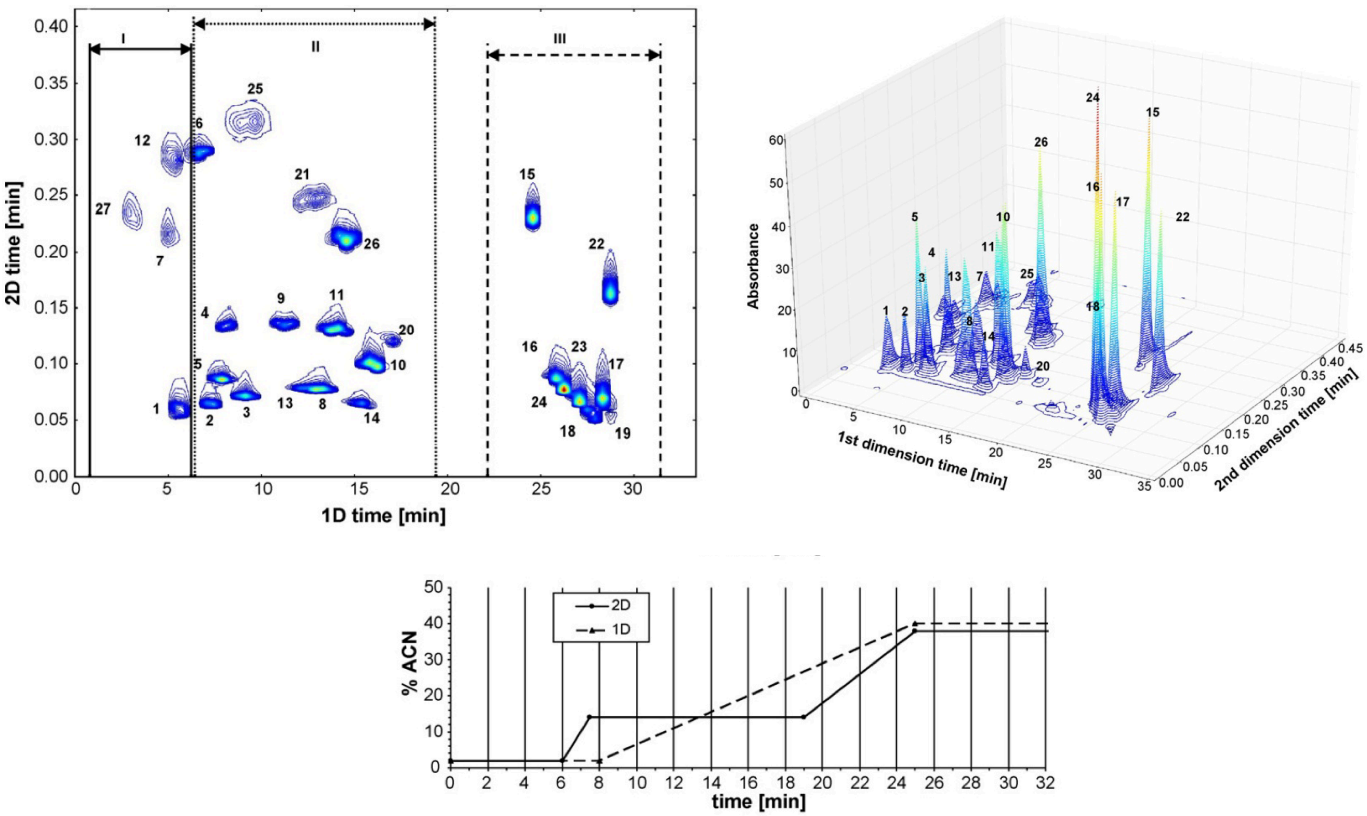

Figure 14.
Because of their high peak capacity and separation speed, core-shell particles perfectly fit the demands of the second-dimension separation on 2D-chromatography. This figure shows an example applied to the separation of a mixture of antioxidants. Second-dimension run times as fast as 0.45 min are achieved with a short and narrow 2.7 µm core-shell particles column. Taken from [210].

work also used ELSD with HILIC core-shell columns for betaine detection [184].

Vegetal metabolic fingerprinting has also found a useful companion in improved separations using core-shell particles. Isoflavones [185], saikosaponins [186], chromones and coumarines [187] have all of them been used with batch origin certification purposes. Raw vegetal materials [188] and tinctures [189] were analysed with this purpose employing core-shell particles achieving performance comparable to UHPLC columns, and using simple pretreatments such as dilution or ultrasound-assisted SLE. Complex traditional Chinese medicines have also been characterized by using these columns [190] and MS with dynamic multiple reaction monitoring.

Atropine and scopolamine [191], ginsenosides [192] or phloroglucinols [193], are other few examples of natural products for which HPLC analysis using core-shell columns has been described. A work by Wang took recently advantage of multivariate analysis to study the content of phorbolesters in plants [194]. The influence of the temperature on the quantification of saponins using fused-core columns has been depicted [195].

Faster separations with higher simple outputs and improved figures of merit were achieved by means of fused-core columns in the analyses of anthraquinones and naphtha-γ-pyrones [196], caffeoylquinic acid derivatives [197], and other various plant metabolites [198].

Heads, leaves, roots or fruits, either raw or dried, were investigated. Heat reflux, ultrasounds or microwave assisted extraction were the preferred techniques for sample pretreatment.

Foodstuffs are also a complex matrix were plant substances need to be quantified. Juices [199,200] have been investigated for flavonoids and anthocyanines. A determination of phenolic compounds in olive oil three folds shorter than traditional methods [201] and triacylglycerols in several vegetable oils [202] including application to predict the botanical origin [203] have also been reported. Seicoiridoids from different olive oils have been recently identified and quantified [204]. More complex samples such as canned artichoke [205], soy-containing foodstuffs [206] and several drinks [207] have also been examined.

Polyphenols have been analysed in tea bags by using nano-liquid chromatography and capillary columns packed with core-shell particles [208,209]. Several resources such as bidimensional chromatography (Figure 14) [210] or multiwalled carbon nanotubes as sorbent for online solid-phase extraction [211] have been employed in combination with core-shell columns for investigation of vegetal metabolytes in foods. By using this technology, versatile methods valid for different matrices have been also developed [212].

Various other samples have been reported. Dugo worked on the separation of all oxygen heterocyclic components present in differ-

ent *Citrus* sp. scents [213]. Sera from rat [214] and humans [215] were analysed in very short times, and sequential injection chromatography was applied to the quantitation of neat samples [216] by using core-shell column technology. Environmental samples such as soils and water were also processed for further analysis in search for artemisinin, dihydroartemisinin, and artemether [217].

10.3. Pollutants and contaminants

Xenobiotics pollutants can reach human organism through different ways. Wode analysed the presence of 72 pollutants of diverse origin in aqueous samples [218] coupling on-line SPE to liquid chromatography employing core-shell particles. Urban leachates [219] were analysed on PFP stationary phases achieving a four times faster separation than the previous isomer specific method for perfluorinated compounds, sulfonates and sulphonamides. Core shell particles chromatography and liquid-liquid microextraction combined in a method for analysis of polycyclic aromatic hydrocarbons in rainwater [220] led to a 59% shorter analysis time and 75% less solvent consumption. Naphthenic acids were analysed in surface waters by using in-column preconcentration and large-volume injection [221].

Automated on-line solid-phase extraction and core-shell particles were advantageously combined for the detection of contaminants in soft drinks [222]. Also canned products [223], grains [224] and several other foods [225] were analysed with improved analysis time and figures of merit compared to fully-porous particles.

Fatty acids and fatty alcohols derivatives were analysed with core-shell columns in order to monitor industrial processes [226] or wastes [227].

10.4. Proteins and peptides

As explained before, core-shell particles afford great advantages to the separation of proteins and other large molecular weight compounds. This is because the enhancement in the mass transfer equilibrium is more notorious for larger molecules than for smaller ones when superficially porous particles are employed. Most applications for whole proteins feature the use of 300 Å pore diameter particles, while the separations of peptides and digests can be carried out using particles with pore diameters around 100 Å.

Intact desalted proteins have been separated using commercial core-shell particles packed in capillary format [228] and MS detection. Disulfide isomers of a recombinant human immunoglobulin were analysed employing 300 Å pore diameter columns with high temperature, eluotropic strength and flow rate [229]. Peptides of α-zeins were identified from maize with ultrasound-assisted SLE followed by digestion [230].

The performances of the analyses of several synthetic peptides and tryptic digests have been compared when employing capillary columns packed with core-shell and fully-porous particles [231]. Seven proteins, including β-lactoglobulins, have been separated using columns modified for working at 1200 bar, and coupling up to six of them in tandem configuration [232].

Soymetide was analysed using fused-core particles packed into conventional and capillary columns, and compared with fully-porous particles [233]. Other dipeptides were also successfully quantified following a similar tandem-coupling strategy [234]. Core-shell columns were also employed as the second dimension separation in bidimensional chromatography of bovine albumin and myoglobin [235]. Peptidic biomarkers, peptides from apolipoproteins and insulin-like growth factor I have also been investigated using this column technology [236,237].

Yet another comparison of core-shell particles efficiency, fully-porous particles of different diameters and monolithic columns was carried out on the basis of an analytical procedure to investigate cleaning enzimes [238].

10.5. Non-vegetal metabolites

Although being the biggest one, plant metabolites are not the only group of metabolites for which core-shell columns have found application. Bacterial quorum sensing acylhomoserine lactones [239], industrially relevant botryococcenes [240] or non-canonical aminoacids norvaline and norleucine [241] have been quantified in bacterial and microalgae cultures.

Considering their relevance in gene expression, the quantification of the methylation status of DNA from cell cultures was compared using core-shell and fully-porous columns [242]. Tetrahydrobiopterin, dihydrobiopterin, and biopterin were investigated in human umbilical endothelial cells [243]. Catecholamines and indolamines were quantified in rat microdyalisates with derivatization [244] and removing the salts interference on MS/MS by using low particle size column and gradient programs. Cathecolamines were also studied in sheep encephalon comparing the results obtained from several different core-shell and fully-porous stationary phases and porous graphitic carbon [245]. Fetal mouse lung was the matrix for a lipidomics investigation of phosphorylcholine-containing lipids with shorter analysis time than methods employing fully-porous particles [246].

A large number of natural compounds were quantified in human samples. Metabolites of D2 and D3 vitamins were analysed in human plasma. One paper choose deproteinization as

sample pretreatment, and core-shell particles showed a performance comparable to sub-2 µm fully-porous particles [247]. Another publication employed deproteinization followed by online enrichment [248]. Endocannabinoids [249] and aldosterone [250] were also analysed in human plasma, using miniaturized SPE and core-shell particles. Modified nucleosides [251] in serum and urine were analysed with biomarking purposes for several diseases.

All eight natural tocopherols and tocotrienols were rapidly analysed in plasma and liver [252], and retinol and α-tocopherol in breast milk [253] by using core-shell particles. In a recent paper [254], porphyrins were chromatografied and quantified from urine and faeces using fluorescence detection; core-shell and several fully-porous particles were compared. A methodology allowing to obtain a human metabolic fingerprint was successfully developed by combining in-vial liquid-liquid dual extraction of human serum and MS detection [255].

10.6. Natural toxins

Routine inspection of products in search for toxins requires short time of analysis, low solvent consumption and excellent limit of detection. These features are improved when existing analytical methods are transferred to core-shell particles columns, making them remarkably attractive for this kind of analysis.

Mycotoxins were investigated in cereals and foodstuffs with an immunoaffinity step in the pretreatment procedure and using a photochemical reaction for sensitivity improvement [256,257]. Tölgyesi *et al.* carried out the full validation of a method for quantitation of mycotoxins in cereals, and found that core-shell particles columns remarkably improved the peak shapes compared to fully-porous ones [258]. Ochratoxin A was determined in wine with fluorescence detector using core-shell columns and the results compared to those of using fully-porous particles, showing better effectiveness and faster separations [259]. Paralytic shellfish toxins were analysed using core-shell columns and fluorescence detection, and when compared to the reference AOAC method, it was shown that just exchanging the fully-porous with the core-shell particles column led to a 66% reduction of analysis time and improved resolution [260,261] (Figure 15). Microcystins were quantified in water using core-shell PFP stationary phases and pre-column excimer-forming derivatization [262].

11. Conclusions and future trends

Although the concept of applying core-shell particles to chromatographic separations was born in the 60's, it took until the late 2000's to develop large-scale manufacturing methods adequate for these particles. This made them widely available to many scientists aiming to explore the insights of their physicochemical properties as well as to incorporate them into the analytical work. Only in the last years, our knowledge about their chromatographic behaviour and why they are able to exhibit such adequate features for HPLC applications has considerably changed.

The synthetic process employed to build these particles affords a very homogeneous product. This contributes directly (and indirectly, through a more homogenous packing) to reduce the eddy dispersion inside the column. Longitudinal diffusion processes are also reduced, as the larger permeability makes possible to work at higher flow than fully-porous particles. Mass transfer equilibrium between the particles and the stationary phase is slightly improved, although this effect is specially important when working with high molecular weight analytes and at fast flow rates. A better thermal conductivity also contributes to reduce the magnitude of radial temperature gradients inside the column that would spoil the efficien-

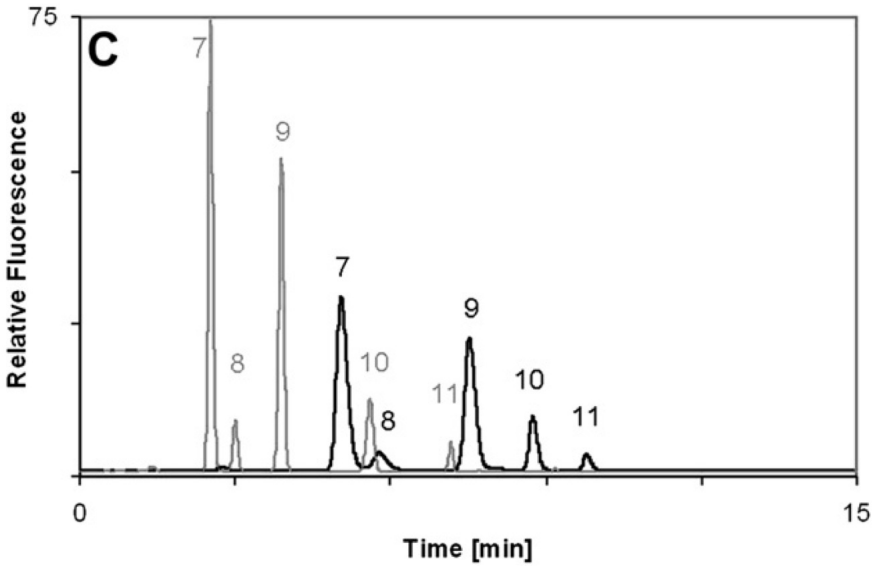

Figure 15.
Improvement in the selectivity and the speed of analysis achieved in the separation of paralytic shellfish toxins by using core-shell columns (grey line) instead of the original fully-porous columns (black line) ruled by the current AOAC official method. Taken from [260].

cy. As a drawback from using core-shell particles, the total loading capacity of the column becomes reduced, making them less appropriate for preparative HPLC or other uses where large analyte load is expected.

Chromatography applications taking advantage of core-shell particles immediately benefit from increased efficiency and resolution. The reduction time of analysis and solvent consumption become HPLC into a greener, higher throughput analytical technique with little need for changes on the analytical method or the instrument. Core-shell particles have proven to equal or overcome the resolution and the efficiency of fully-porous particles of smaller sizes and monolith columns, not only in terms of height equivalent to a theoretical plate, but also in overall kinetic performance. The number of papers depicting applications that take advantage of core-shell columns demonstrates that the adoption pace of this technology is exponentially growing among practitioners in virtually any field of analytical chemistry.

Most of the published methodologies include classical pretreatment procedures and conventional HPLC instruments, solvents and detectors. It shows how existing methods and hardware can be easily transferred to use core-shell columns. Also, new applications demanding outstanding levels of performance that could hardly been achieved before, are now more accessible. An extensive number of applications and their separation conditions have been included in Table 3 to help the interested chromatographists to find a good starting point to develop their own analytical methodologies using core-shell columns.

Core-shell particles of smallest diameters packed into narrow-bore columns are able to deliver a level of performance that exceeds the capabilities of the most powerful chromatographs currently available. Most practising chromatographists would be able to benefit from an immediate improvement on their analytical separations just by replacing their current fully-porous columns with core-shell ones. Nevertheless, those aiming to unveil the actual full performance that the most sophisticated core-shell columns are able to provide, will have to tune up their instruments, upgrade to state-of-the-art chromatographs or, ultimately, wait for the arrival of a new generation of instruments able to match the level of excellence that such columns and their users demand.

Table 3. Recently published applications of the core-shell column technology to different analytes and matrices (continues on next pages)

Ref.	Analytes	Matrix	Pretreatment	Core-shell column	Mobile phase	Detector	Notes
				Drugs (continued)			
[157]	Penicillins	Injectable suspensions	Dilution	Kinetex C18 2.6 µm (150 × 4.6)	50 mM CH_3COONH_4 in water / MeCN	UV-Vis	Compares with 5 µm and monolithic columns
[162]	Penicillins, amphenicols,	Milk	QuEChERS in ultrasonically assisted MSPD format	Kinetex C18 2.6 µm (150 × 4.6)	50 mM CH_3COONH_4in water / MeCN	UV-Vis	
[135]	Imipenem, ertapenem, doripenem and meropenem	Human plasma	Deproteinization with acetonitrile	Kinetex PFP 2.6 µm (100 × 4.6)	0.1 M Na_2HPO_4/H_3PO_4 (pH = 7) in water / MeOH	UV-Vis	
[152]	Quinolones	Water and human urine	On-line anion SPE	Kinetex C18 2.6 µm (150 × 4.6)	10 mM sodium citrate (pH = 4.0) / MeCN	FL	
[133]	Sinafloxacin	Rat plasma	Deproteinization with acetonitrile	HALO C18 2.7 µm (50 × 4.6)	0.5% TEA / H_3PO_4 (pH = 3) in water / MeCN	FL	
[173]	Chloramphenicol	Soft-shelled turtle tissues	On-line matrix solid-phase dispersion	HALO C18 2.7 µm (50 × 2.1)	0.1% HCOOH in water / MeCN	MS	
[164]	Chloramphenicol	Egg, honey and milk	SPE using multi-walled carbon nanotubes as sorbent	HALO C18 2.7 µm (50 × 2.1)	0.1% HCOOH in water / MeCN	MS	
[168]	Lincomycin	Foodstuffs	SPE	Kinetex C18 2.6 µm (100 × 3)	0.1% HCOOH in water / MeCN	MS	
[169]	Sulfonamides	Animal feeds	SLE. Derivatization with fluorescamine	Kinetex C18 2.6 µm (150 × 4.6)	10 mM HCOOH/HCOONa (pH = 3.4) in water / MeCN	FL	Comparison with fully porous 5 µm column
[163]	Sulfonamides	Milk	Deproteinization, SPE	Kinetex C18 2.6 µm particles, 100 Å pore size, packed into 250 mm × 100 µm capillary columns	0.1% HCOOH in water / MeCN	UV-Vis, MS	Capillary HPLC. Comparison of C18 core-shell with fully-porous C18 and phenyl 3 µm
[170]	Sulfonamides	Grass carp tissues	On-line matrix solid-phase dispersion	HALO C18 2.7 µm (50 × 2.1)	0.1% HCOOH in water / MeCN	MS	
[166]	Sulfonamides	Honey	SPE	Kinetex C18 2.6 µm (100 × 3)	0.1% HCOOH in water / MeCN	MS	
[125]	Impurities in streptomycin and dihydrostreptomycin	Neat samples	Direct injection	HALO HILIC 2.7 µm (100 × 2.1)	0.1–0.2 M $HCOONH_4$ (pH 3.0–4.5) / MeCN	MS	
[167]	Nitroimidazole antiparasitics	Plasma, milk, muscle, egg, honey and feeds	SPE	Kinetex C18 2.6 µm (100 × 3)	0.1% HCOOH in water (pH = 2.6) / MeOH	MS	
[263]	Telaprevir	Human plasma	LLE	Accucore C18 2.6 µm (150 × 2.1)	0.01% NH_3 water / MeCN / MeOH	MS	
[124]	Impurities in atazanavir sulphate	Neat samples	Direct injection	Ascentis Express C8 2.7 µm (150 × 4.6)	20 mM KH_2PO_4 (pH= 3.5) in water / MeCN	UV-Vis	
[146]	NIM811 (a cyclosporin)	Dried blood spots	SLE, LLE	HALO C18 2.7 µm (50 × 2.1)	10 mM CH_3COONH_4in water / MeCN	MS	
[161]	Toltrazuril and metabolytes	Foodstuffs	Ultrasound-assisted solid-liquid extraction, SPE	Ascentis Express C18 2.7 µm (150 × 2.1)	Water / MeOH	MS	
[136]	Carboplatin	Human plasma	Deproteinization	Accucore HILIC 2.6 µm (50 × 2.1)	0.1% CH_3COOH in water / MeCN	MS	

Table 3. (continued)

Ref.	Analytes	Matrix	Pretreatment	Core-shell column	Mobile phase	Detector	Notes
				Drugs (continued)			
[128]	Paclitaxel	Intracellular compartments in cell cultures	Cellular compartments fractionation, protein precipitation, LLE	Ascentis Express C18 2.7 µm (50 × 4.6)	0.1% HCOOH in water / MeCN	MS	
[158]	Cytarabine, methotrexate, ethylprednisolone	Intrathecal solution	Direct injection	HALO C18 2.7 µm (150 × 4.6)	0.1% CH_3COOH in water / MeOH	UV-Vis, MS	
[171]	Corticosteroids	Bovine tissues	SPE	Kinetex phenyl-hexyl 2.6 µm (100 × 4.6)	5 mM CH_3COONH_4/0.01% CH_3-COOH in water (pH 5.4) / MeOH	MS	
[172]	Corticosteroids	Pig fat	Liquid-liquid extraction, SPE	Ascentis Express C18 2.7 µm (150 × 4.6)	5 mM CH_3COONH_4 / 0.01% CH_3-COOH (pH = 5.4) in water / MeOH	MS	
[149]	Androgenic steroids	Urine	Enzimatic hydrolysis, SPE, LLE, SPE	Poroshell C18 2.7 µm (150 × 2.1)	Water / MeOH	MS	Comparison with fully porous 5 µm columns
[264]	Stanozolol metabolites	Bovine, pig and sheep urines	Deconjugation, SPE	Kinetex C18 2.6 µm (100 × 4.6)	0.1% HCOOH (pH=2.3) in water / MeOH	MS	Comparison of several pretreatment methodologies
[159]	Betamethasone-17-valerate and two impurities	Ointment	Dilution, cold precipitation	HALO C18 2.7 µm (100 × 4.6)	Water / MeCN	UV-Vis	Comparison with fully porous 3 µm and monolythic columns
[137]	(*S*)-(+)- and (*R*)-(−)-ibuprofen	Human plasma	Deproteinization with MeOH, LLE, derivatization	Kinetex PFP 2.6 µm (50 × 4.6)	1 mM CH_3COONH_4 in water / MeCN	MS	Derivatization with (*S*)-(-)-1-(1-napthyl) ethylamine using 1-hydroxybenzotriazole and 1-ethyl-3-(3-dimethylaminopropyl)carbodiimide
[123]	Naproxcinod and related substances	Neat samples	Direct injection	Ascentis Express C8 2.7 µm (150 × 4.6)	20 mM KH_2PO_4/0.2% H_3PO_4 / MeCN	UV-Vis	Comparison with several fully porous columns
[160]	Aspirin and atorvastatin	Capsules	Ultrasounds-assisted SLE, cristalization	HALO C18 2.7 µm (100 × 4.6)	50 mM H_3PO_4/KH_2PO_4 (pH= 2.3) in water / MeCN	UV-Vis	
[265]	Cimicoxib	Dog plasma	Protein precipitation, LLE	Kinetex C18 2.6 µm (100 × 4.6)	10 mM CH_3COONH_4 (pH=4.5) in water / MeCN	MS	
[151]	Several NSAIDs	Human urine	Packed sorbent microextraction (C18)	Poroshell C18 2.7 µm (100 × 3)	0.05% CF_3COOH in water / MeCN	UV-Vis	
[266]	Acetaminophen	Plasma, cerebrospinal fluid and dried blood spots	Protein precipitation or automatized DBS pretreatment	Kinetex PFP 2.6 µm (100 × 4.6)	0.1% CH_3COOH in water / MeCN	MS	
[132]	Protein kinase inhibitors	Rat serum	Deproteinization with MeCN	Poroshell C18 2.7 µm (50 × 4.6)	0.1% HCOOH in water / MeCN	MS	
[145]	Protein kinase inhibitors	Dried blood spots	Deproteinization and 96-well format SPE	Kinetex C18 2.6 µm (50 × 2.1)	0.1% HCOOH in water / MeCN	MS	
[131]	Arginase inhibitor	Rat plasma	SPE and on-line pre-column derivatization with o-phthaldialdehyde and 3-mercaptopropionic acid	Kinetex C18 2.6 µm (100 × 3)	HCOOH in water (pH = 3) / MeOH	FL	
[156]	Protein kinase inhibitors	Serum	LLE	Kinetex C8 2.6 µm (150 × 4.6)	H_3PO_4 (pH= 2) in water / MeCN	UV-Vis	Two columns serial setup (150+100 × 4.6) tested

Table 3. (continued)

Ref.	Analytes	Matrix	Pretreatment	Core-shell column	Mobile phase	Detector	Notes
				Drugs (continued)			
[138]	Eletriptan	Human plasma	Deproteinization, LLE	Ascentis Express C18 2.7 µm (50 × 4.6)	0.1% HCOOH in water / MeOH	MS	
[267]	Clopidogrel	Human plasma	Stabilization with 2-bromo-3-methoxyacetophenon, centrifugation	Ascentis Amide C8 2.7 µm (100 × 2.1)	0.1% HCOOH in water / MeOH / MeCN	MS	
[139]	Clopidogrel	Human plasma	Deproteinization with/without 96-well format SPE	Ascentis Express C8 2.7 µm (100 × 2.1) Ascentis RP-Amide 2.7 µm (100 × 2.1)	0.1% HCOOH in water / MeOH	MS	Three different deproteinization methods are compared. Comparison with fully-porous 5 µm column.
[268]	Opiates, methadone, buprenorphine	Urine	Deconjugation, LLE	Poroshell C18 2.7 µm (100 × 2.1)	0.1% HCOOH in water / MeOH	MS	
[269]	Cannabinoids	Urine	Enzimatic deconjugation, precipitation	Kinetex C18 2.6 µm (50 × 3)	0.1% HCOOH in water / MeCN	MS	
[270]	Cannabinoids	Oral fluid	SPE	Kinetex C18	0.01% CH_3COOH in water / MeOH	MS	
[154]	Cannabinoids	Oral fluid	Micro extraction by packed sorbent	Kinetex C18 2.6 µm (100 × 2.1)	1.25 mM CH_3COONH_4 in water / MeOH	MS	
[153]	Cannabinoids	Oral fluid	SPE	Kinetex C18 2.6 µm (150 × 2.1)	5 mM CH_3COONH_4 (pH = 6.8) in water / MeCN	MS	
[271]	Febuxostat	Human plasma	LLE	Ascentis Express C18 3.5 µm (50 × 4.6)	10 mM $HCOONH_4$ in water / MeCN	MS	
[134]	Rimonabant	Mouse plasma	Protein precipitation with MeCN/MeOH	HALO C18 2.7 µm (50 × 2.1)	0.1% HCOOH in water / MeCN	MS	Comparison with fully porous 1.7 µm column
[272]	Indapamide	Human whole blood	Automated SPE	Kinetex C18 1.7 µm (100 × 2.1)	2 mM CH_3COONH_4 /HCOOH in water / MeCN	MS	
[273]	Tamsulosin	Human serum	LLE	Ascentis Express C18 2.7 µm (100 × 3)	2 mM CH_3COONH_4 in water / MeOH	MS	
[165]	β-agonists and β-blockers	Animal foods	Hydrolysis, acidic extraction, SPE, MeOH cleanup	Ascentis Express Amide 2.7 µm (150 × 2.1)	0.1% HCOOH in water / MeOH	MS	
[148]	Salbutamol, salmeterol and atenolol	Urine	Hydrolysis, SPE	Kinetex HILIC 2.6 µm (150 × 2.1)	5 mM CH_3COONH_4 (pH = 6) in water / MeCN / MeOH	MS	2D separation: 1st dimension using core-shell particles, and 2nd dimension using a chiral column
[150]	Propranolol	Urine	Column switching	Ascentis Express Amide 2.7 µm(100 × 4.6)	0.5% triethylamine / CH_3COOH (pH = 4.5) in water / MeCN	FL	The pretreatment column is an Ascentis Express C18 2.7 µm (5 × 4.6) precolumn
[144]	Atenolol	Dried blood spots	Ultrasound-assisted SLE	Ascentis Express C18 2.7 µm (100 × 2.1)	0.1% HCOOH in water / MeCN	MS	
[143]	Theophilline and metabolites	Human whole blood	Precipitation with MeCN	Poroshell C18 2.7 µm (100 × 2.1)	0.1% HCOOH in water / MeCN	MS	
[274]	Boldine	Rat plasma, urine and bile	LLE / LL back-extraction	Kinetex PFP 2.6 µm (150 × 3)	5 mM $HCOONH_4$ (pH = 3.8) in water / MeCN	FL	

Table 3. (continued)

Ref.	Analytes	Matrix	Pretreatment	Core-shell column	Mobile phase	Detector	Notes
				Drugs (continued)			
[129]	Imipramine and desipramine	Rat plasma	Protein precipitation with MeCN / NH_4OH	HALO C18 2.7 µm (30 × 2.1)	10 mM CH_3COONH_4/0.1% NH_4OH (pH = 8.5) in water / 0.2% morpholine or TEA in MeCN	UV-Vis MS	Comparison with fully porous 5 µm column
[155]	Benzodiazepines and "z-drugs"	Human hair	Hair washing, pulverization, SLE	Kinetex C18 2.6 µm (50 × 2.1)	5 mM $HCOONH_4$ (pH = 3.5) in water / MeOH	MS	
[140]	Gabapentin, pregabalin, and vigabatrin	Human serum	Protein precipitation with MeCN	Kinetex C18 2.6 µm (50 × 2.1)	2 mM CH_3COONH_4/0.1% HCOOH in water / MeCN	MS	
[275]	Diosmetin metabolytes	Human plasma and urine	Deconjungation, centrifugation	Ascentis Express amide 5 µm (150 × 2.1) HALO C18 2.7 µm (50 × 0.3)	0.1% HCOOH in water / MeOH 2% CH_3COOH in water / MeCN	MS	Comparison among a fully porous and two different core-shell columns (one of them was a micro-bore column)
[130]	Swertiamarin	Rat plasma and tissues homogenates	SPE	Kinetex C18 2.6 µm (100 × 2.1)	0.1% CH_3COOH in water / MeOH	MS	
[141]	3-nitrotyrosine	Human plasma	SPE	Kinetex PFP 2.6 µm (100 × 2.1)	0.01% CH_3COOH in water / MeCN	UV-Vis	Comparison with fully porous 3 µm column
[142]	Drugs diastereomers	Human plasma	96-well protein precipitation and phospholipid removal plate	Poroshell C18 2.7 µm (50 × 2.1)	0.1% HCOOH in water / MeCN / MeOH	MS	Comparison with fully-porous 3.5 µm column. Comparison with classic deproteinization with MeCN.
[127]	Drug candidates	Caco-2 and hepatocyte samples	Protein precipitation, dilution	Optimize Technologies pellicular C18 40 µm (15 × 1)	2 mM CH_3COONH_4 in water / MeCN / MeOH	MS	2 columns switching for high-throughput screening
[174]	Top-used drugs	Influent wastewater	SPE	Kinetex C18 2.6 µm (100 × 2.1)	5 mM CH_3COONH_4/0.1% HCOOH in water / MeCN	MS	
[175]	Various drugs	Waste- and surface waters	SPE	Kinetex C18 2.6 µm (150 × 4.6)	0.5% CH_3COOH in water / MeCN	UV-Vis	Comparison with fully porous 1.8 µm column
[126]	Various drugs	Neat samples	Direct injection	Ascentis Express C18 2.7 µm (50 × 3.0)	50 mM or 10 mM CH_3COONH_4 in water / MeCN	UV-Vis	2D HPLC, with double parallel separation and detection on the 2nd dimension
[147]	Doping xenobiotics	Urine	LLE	HALO C18 2.7 µm (150 × 2.1 and 100 × 2.1)	0.1% HCOOH in water / MeCN	MS	Comparison with fully porous 5 µm column
[276]	Smoking biomarkers	Urine	LLE, SPE	Kinetex PFP 2.6 µm (100 × 4.6)	Water / MeOH	MS	
				Vegetal metabolites			
[277]	Caffeine and metabolites	Rat plasma	Protein precipitation	Poroshell C18 2.7 µm (50 × 4.6)	0.2% HCOOH in water / MeOH	MS	
[278]	β-artemether and lumefantrine	Anti-malarial tablets and powder for oral suspension	Dilution, filtration	HALO C18 2.7 µm (50 × 4.6) HALO Amide 2.7 µm (50 × 4.6) HALO Phenyl-Hexyl 2.7 µm (50 × 4.6)	1 mM H_3PO_4 / NaH_2PO_4 (pH = 3) in water / MeCN	UV-Vis	Comparison of different column chemistries

Table 3. (continued)

Ref.	Analytes	Matrix	Pretreatment	Core-shell column	Mobile phase	Detector	Notes
				Vegetal metabolites (continued)			
[217]	Artemisinin, dihydroartemisinin, and artemether	Soil, surface water, groundwater, plant extracts of *Artemisia annua*	SLE, LLE, SPE	Kinetex C18 2.6 µm (150 × 2.1)	10 mM CH_3COONH_4/0.01% CH_3-COOH in water / MeOH	UV-Vis MS	Pre-column derivatization. Comparison with fully porous 5 µm phenyl-hexyl column
[191]	Atropine and scopolamine	Plant parts of *Datura* sp.	Ultrasound-assisted SLE	Ascentis Express C18 2.7 µm (50 × 2.1)	1% HCOOH in water / MeOH	MS	
[197]	Caffeoylquinic acid derivatives	Heads and leaves of *Cynara scolymus* (artichoque)	SLE	HALO C18 2.7 µm (50 × 2.1)	0.1% HCOOH in water / MeCN	MS	
[205]	Caffeoylquinic acids	Canned artichoke	Reflux extraction	HALO C18 2.7 µm (50 × 2.1)	Water / MeOH	MS	Comparison with 1.8 µm column
[279]	Nicotine	Liquid for electronic cigarettes	Dilution	Ascentis Express HILIC 5.0 µm (150 × 2.1)	10 mM $HCOONH_4$/ 0.01% HCOOH in water / MeCN	MS	
[280]	Carotenoids	Food supplements	Saponification, SLE, on-line column-switching	Ascentis Express C18 2.7 µm (30 × 4.6)	Water / MeOH	UV-Vis	Pretreatment colum was a Chromolith Guard Cartridge RP-18e (Merck), 10 × 4.6 mm
[180]	Carotenoids	Red chili peppers	SLE	Ascentis Express C18 2.7 µm (30 × 4.6)	Water / MeCN / IPA	UV-Vis MS	2D separation, using core-shell on the 2nd dimension in single o tandem-coupled arrangement.
[187]	Chromones and coumarins	Dried root of *Saposhnikovia divaricata*	Ultrasounds assisted SLE	Ascentis Express C18 2.7 µm (100 × 4.6) Kinetex C18 2.6 µm (100 × 2.1)	Water / MeCN	UV-Vis, MS	
[181]	Flavonoid aglycones	Plant extracts	Reflux, hydrolysis, filtration, SPE	Ascentis Express C18 2.7 µm (150 × 4.6)	0.5% H_3PO_4 (pH = 2) in water / MeCN / THF	UV-Vis	
[281]	Flavonoids	*Citrus bergamia* juice	Centrifugation, liophylization, reconstitution in MeOH	Kinetex C18 1.7 µm (100 × 2.1)	0.1% HCOOH in water / MeCN	UV-Vis MS	
[183]	Flavonoids	Berries of *Hippophaë rhamnoides* (buckthorn)	Pressurized solvent-free microwave extraction	HALO C18 2.7 µm (50 × 4.6)	1.0% CH_3COOH in water / MeOH or MeCN	MS	Hyphenation of Centrifugal Partition Chromatography -Evaporative Light Scattering Detector (CPC-ELSD) with HPLC-UV
[199]	Flavonoids	Apple juice	SPE	HALO C18 2.7 µm (100 × 4.6)	Water / MeCN	UV-Vis	
[213]	Furocoumarins, coumarins, polymethoxylated flavones	*Citrus* sp. scents	Dilution or LLE	Ascentis Express C18 2.7 µm (150 × 4.6)	Water / MeCN / MeOH / THF	UV-Vis	
[282]	Genistein	Mouse tissues	Deproteinization / homogenization, SLE	Kinetex C18 2.6 µm (150 × 2.1)	10 mM NaH_2PO_4 in water (pH = 2.5) / MeOH	UV-Vis	
[185]	Isoflavones	*Radix puerariae*	Microwave-assisted SLE	Kinetex C18 2.6 µm (50 × 2.1)	0.2% HCOOH in water / MeOH	MS	
[214]	Isoflavones	Rat serum	Ultrasound-assisted LLE	Kinetex PFP 2.6 µm (50 × 2.1)	0.1% HCOOH in water / MeOH or MeCN	MS	Comparison with fully-porous 3.5 µm (C18) and 1.8 µm (CN) columns and Kinetex C18

Table 3. (continued)

Ref.	Analytes	Matrix	Pretreatment	Core-shell column	Mobile phase	Detector	Notes
				Vegetal metabolites (continued)			
[283]	Isoflavones	Soy-containing foodstuffs	Ultrasound-assisted SLE	Kinetex C18 2.6 µm (100 × 4.6)	1% CH_3COOH in water / MeCN	UV-Vis	
[284]	Multiple red-wine components	Red wine		Kinetex C18 2.6 µm (100 × 4.6)	0.1% CF_3COOH in water / MeCN	UV-Vis	Core-shell column employed on the second dimension of a 2D separation
[212]	Non-anthocyanin monomeric phenolics, condensed tannins and anthocyanins	Wine and grapes	Direct injection or SPE, LLE, optionally hydrolysis	Kinetex C18 2.6 µm (100 × 4.6) Kinetex PFP 2.6 µm (100 × 2.1)	H_3PO_4 in water / MeCN or MeOH	UV-Vis	
[216]	Phenolic acids	Neat samples	Direct injection	Ascentis Express amide Ascentis Express phenyl-hexyl Ascentis Express C18 2.7 µm (30 × 4.6 in all cases)	0.065% H_3PO_4 (pH= 2.4) in water / MeCN	UV-Vis	Sequential injection chromatography. Comparison of three column chemistries.
[207]	Phenolic compounds and caffeine	Mate, instant coffee, soft drink and energetic drink	Ultrasound-assisted SLE or direct injection after degassing	Kinetex C18 2.6 µm (100 × 4.6)	1% H_3PO_4 in water / MeCN	UV-Vis FL	
[182]	Phenolic acids and flavonoids	Raw propolis	Closed vessel microwave-assisted extraction	Ascentis Express C18 2.7 µm (150 × 3.0)	0.1% HCOOH in water / MeCN	UV-Vis MS	
[201]	Phenolic compounds	Olive oil	SPE	Kinetex C18 2.6 µm (100 × 4.6)	$HClO_4$ (pH=3.1) in water / MeCN / MeOH in presence of 60 mM $LiClO_4$	Coulometric Electrochemical Detector (ECD)	
[200]	Anthocyanins and other phenolic compounds	Pomegranate juice	Filtration	Poroshell C18 2.7 µm (100 × 3)	5% HCOOH in water / MeCN 1% CH_3COOH in water / MeCN	UV-Vis MS	
[210]	Phenols and flavones	White wine	Filtration	Ascentis Express C18 2.7 µm (100 × 3.0)	10 mM CH_3COONH_4/HCOOH in water / MeCN	UV-Vis	2D gradient
[192]	Ginsenosides	Harvested white ginsens	Ultrasounds-assisted SLE or reflux	Poroshell C18 2.7 µm (100 × 3)	Water / MeCN	UV-Vis	
[204]	Secoiridoids	Virgin olive oil	LLE	HALO C18 2.7 µm (100 × 2.1)	0.1% HCOOH in water / MeOH	MS	
[211]	Resveratrol	Red wine	Online SPE with multiwalled carbon nanotubes	HALO C18 2.7 µm (50 × 2.1)	0.1% HCOOH in water / MeCN	MS	
[193]	Phloroglucinols	Aerial parts *Dryopteris fragrans*	Ionic liquid-based surfactant and microwave-assisted extraction	Kinetex C18 2.6 µm (100 × 4.6)	0.15% HCOOH in water / MeCN	UV-Vis	
[285]	Polyphenols	*Salvia* sp.	Infusion, ultrasound-assisted SLE or microwave-assisted SLE	Kinetex C18 2.6 µm (100 × 4.6)	1% HCOOH in water / MeCN	UV-Vis MS	Comparison with fully-porous and monolithic columns

Table 3. (continued)

Ref.	Analytes	Matrix	Pretreatment	Core-shell column	Mobile phase	Detector	Notes
				Vegetal metabolites (continued)			
[194]	Phorbolesters	Seeds of *Jatropha curcas*	Ultrasound-assisted SLE	HALO C18 2.7 µm (150 × 4.6)	0.2% HCOOH in water / MeCN	UV-Vis	Use of PCA, HCA, PLS-DA to categorize the plant materials. Comparison of core-shell with fully-porous 5 and 3.5 µm particles
[209]	Polyphenols	Bee polen	SLE, LLE	Kinetex C18 2.6 µm particles, 100 Å pore size, packed into 100 mm × 100 µm capillary columns	0.5% HCOOH in water / MeCN	UV-Vis	
[208]	Polyphenols and methylxantines	Tea bags	SLE	Kinetex C18 2.6 µm particles, 100 Å pore size, packed into 100 mm × 100 µm capillary columns	0.5% HCOOH in water / MeOH / MeCN	UV-Vis MS	Nano-HPLC. Comparison of core-shell with fully-porous sub-2 µm particles
[215]	Sterols, oxysterols and secosteroids	Plasma	Ultrasound-assisted LLE, hydrolysis, SPE	Kinetex C18 2.6 µm (150 × 2.1)	50 mM HCOOH in water / isopropanol / MeCN	MS	
[203]	Triacylglycerols	Vegetable oils	Dilution	Kinetex C18 2.6 µm (150 × 4.6)	MeCN / *n*-pentanol	UV-Vis MS	
[202]	Triacylglycerols	Vegetable oils	Dilution, reconstitution	Poroshell C18 2.7 µm (50 × 3)	IPA / MeOH	MS	
[286]	Spinach pigments	Spinach	Lyophilization, pulverization, SLE	Kinetex C18 2.6 µm (100 × 4.6)	0.1 M CH_3COO^- $^+NH(CH_2CH_3)$ / MeCN / MeOH	UV-Vis	
[184]	Betaine	Dried fruit of *Lycium chinense*	Ultrasound-assisted SLE	Kinetex HILIC 2.6 µm (100 × 2.1) HALO HILIC 2.7 µm (100 × 2.1)	10 mM $HCOONH_4$ (pH = 3) in water / MeCN	ELSD	Comparison of core-shell with fully-porous 5 µm particles
[196]	Anthraquinones and two naphtha-γ-pyrones	*Cassia obtusifolia*	Maceration, reflux	Poroshell C18 2.7 µm (100 × 2.1)	30 mM CH_3COONH_4 in water / MeCN	MS	
[287]	Obtusin and derivatives	Rat plasma after oral administration of Semen Cassiae extract	Deproteinization	Poroshell C18 2.7 µm (100 × 2.1)	30 mM CH_3COONH_4 in water / MeCN	MS	
[186]	Saikosaponins	*Bupleurum falcatum*	Ultrasounds assisted SLE	Ascentis Express C18 2.7 µm (100 × 4.6)	0.1% HCOOH in water / MeCN	ELSD MS	Comparison with other extractions methods such as maceration and reflux. HCA to categorize the origin of batches. Comparison of core-shell with fully-porous 5 µm particles
[195]	Saponins	Yam	Heat-reflux extraction	Kinetex C18 2.6 µm (100 × 2.1)	Water / MeCN	Pulsed amperometric detection	Comparison of core-shell with fully-porous 3 µm particles

Table 3. (continued)

Ref.	Analytes	Matrix	Pretreatment	Core-shell column	Mobile phase	Detector	Notes
				Vegetal metabolites (continued)			
[288]	Indole and oxindole alkaloids of *Uncaria Hook*	Rat plasma and brain after administration of the traditional Japanese medicine Yokukansan	Deproteinization on 96-well plate format	Ascentis Express Amide 2.7 µm (100 × 2.1)	0.2% HCOOH in water / MeCN		
[189]	Vegetal metabolites	Tinctures of *Passiflora incarnata*	Dilution	Ascentis Express C18 2.7 µm (150 × 2.1)	0.05% CH_3COOH in water / THF / MeOH / MeCN	UV-Vis	AutoCovariance Function analysis for fingerprinting and comparison among core-shell, fully porous 1.8 µm and monolithic columns. Multiple column serial coupling.
[289]	Vegetal metabolites	Complex Traditional Chinese Medicine vegetal preparations	Ultrasounds assisted SLE	Poroshell C18 2.7 µm (100 × 2.1)	0.1% HCOOH in water / MeCN	MS	
[190]	Vegetal metabolites	Complex Traditional Chinese Medicine vegetal preparations	Heat-reflux extraction	Kinetex C18 2.6 µm (100 × 2.1)	0.1% HCOOH in water / MeCN	MS	Comparison between dynamic multiple reaction monitoring and multiple reaction monitoring detection
[188]	Vegetal metabolites	Extracts of *Rhodiola rosea*	Ultrasounds assisted SLE	HALO C18 2.7 µm (150 × 4.6)	0.1% HCOOH in water / MeCN	UV-Vis MS	Use of PCA, HCA and PLS-DA to categorize the origin of batches
[198]	Cytokinins, purines, indole-3-acetic acid, and abscisic acid	Leaves of *Arabidopsis thaliana*	Bieleski extraction, SPE	Kinetex C18 1.9 µm (100 × 2.1)	0.08% CH_3COOH in water / MeOH	MS	
				Proteins and peptides			
[228]	Intact proteins	Heterogeneous tissue homogenates, cell lysates	Desalting	Poroshell-300 C18 5 µm particles, 300 Å pore size, packed into 150 mm × 75 µm Picofrit columns with µESI spray tip	0.025% CF_3COOH and 0.3% HCOOH in water / MeCN / IPA	MS	Capillary format
[290]	Peptides	Intestinal multidrug transporter proteins	Cell lysis, protein extraction, denaturation, alkylation, digestion	Kinetex C18 2.6 µm (100 × 3)	0.1% HCOOH in water / MeCN	MS	
[235]	Peptides	Bovine serum albumin, bovine heart myoglobin	Digestion	HALO C18 2.7 µm (50 × 4.6)	0.1% CF_3COOH in water / MeCN	UV-Vis	2D chromatography. The core-shell column was on the 2nd dimension, optionally tandem-coupled to a fully porous5 µm column
[232]	Peptides	Seven proteins including β-lactoglobulins	Denaturation, reduction, alkylation, trypsination	Kinetex C18 2.6 µm (150 × 2.1)	0.05% HCOOH in water / MeCN	UV-Vis	Up to six tandem-coupled columns. Columns were modified for operation at 1200 bar

Table 3. (continued)

Ref.	Analytes	Matrix	Pretreatment	Core-shell column	Mobile phase	Detector	Notes
				Proteins and peptides (continued)			
[234]	Dipeptides	Alcoholic beverages	Deproteinization, derivatization with *N*-hydroxysuccinimidyl carbamate	Poroshell 120 C18 2.7 µm (150 × 3) Ascentis Express amide 2.7 µm (150 × 3)	0.1% HCOOH in water / MeCN	UV-Vis MS	Two core-shell columns tandem-coupled
[237]	Peptides from apolipoproteins A1, B48 and B100	Plasma	Reduction, digestion with/without deoxycholate	Kinetex C18 1.7 µm (50 × 2.1)	0.1% HCOOH in water / MeCN	MS	
[230]	Peptides from maize α-zeins	Maize kernels	Ultrasounds assisted SLE, digestion	Ascentis Express Peptide ES-C18 2.7 µm (100 × 2.1)	0.1% CF_3COOH in water / MeCN 0.3% CH_3COOH in water / MeCN	UV-Vis MS	
[236]	Peptidic biomarkers	Human plasma	SPE or MeCN protein depletion prior to tryptic digestion	Ascentis Express C18 2.7 µm (100 × 2.1)	0.1% HCOOH in water / MeCN	MS	
[229]	Recombinant human immunoglobulin gamma 2 (IgG2) disulfide isomers	Neat samples	Direct injection	Poroshell C8 300 Å 5 µm (75 × 2.1)	0.1% CF_3COOH in water, IPA, TFA, MeCN	UV-Vis	Comparison with totally-porous particles. Combination of high column temperature (85 °C), high eluotropic strength solvents (isopropanol) and high flow rate (1.5 mL/min)
[231]	Several synthetic peptides and tryptic digests	Isolated proteins or peptides	Alkylation, tryptic digestion	HALO Peptide ES-C18 2.7 µm, 160 Å pore size (50 × 2.1 or 50 × 0.2 or 150 × 0.2)	CF_3COOH or HCOOH or $HCOONH_4$/HCOOH in water / MeCN	UV-Vis	Comparison with fully porous 1.7 µm and monolythic columns
[233]	Soymetide	Soybean-derived foodstuffs	Protein extraction, fractionation and digestion are discussed	Ascentis Express C18 2.7 µm (50 × 2.1) Capillary Ascentis Express C18 2.7 µm (150 × 0.3)	0.1% CF_3COOH in water / Extrachrom®	MS	Comparison with fully porous 3.5 µm column
[238]	Tryptic digests of industrial cleaning enzimes	Cleaning products	Reduction, trypsinization	Kinetex C18 2.6 µm (100 × 3)	0.1% CF_3COOH in water / MeCN	UV-Vis	Comparison with fully porous 5 and 3 µm columns and with monolythic column
				Pollutants			
[218]	72 micropollutants from different origins	Aqueous samples	On-line SPE (12 µm particle size)	Accucore C18 2.6 µm (50 × 2.1)	0.1% HCOOH in water / MeOH	MS	
[222]	Bisphenols	Soft drinks	On-line SPE (12 µm particle size)	Ascentis Express C18 2.7 µm (50 × 2.1)	Water / MeOH	MS	
[223]	Diglycidyl ethers of bisphenols and derivatives	Canned foodstuffs and beverages	Ultrasound-assisted SLE or SPE	Ascentis Express C18 2.7 µm (50 × 2.1)	25 mM $HCOONH_4$/HCOOH (pH 3.75) in water / MeOH	MS	Comparison of core-shell with fully-porous 1.7 µm particles
[226]	Fatty acid alkyl esters	Biodiesel fuel reaction mixture	Dilution	Kinetex C18 2.6 µm (100 × 4.6)	Water / MeCN	MS	
[227]	Fatty alcohol ethoxylates	Industrial mixtures, cleaning products, river/sea water	SPE	Ascentis Express C8 2.7 µm (150 × 4.6)	0.1% CH_3COOH in water / MeCN	UV-Vis MS	Derivatisation with maleic anhydride in presence of urea

Table 3. (continued)

Ref.	Analytes	Matrix	Pretreatment	Core-shell column	Mobile phase	Detector	Notes
				Pollutants (continued)			
[225]	Perfluoroalkyl carboxylates, sulfonates and sulfonamides	Foodstuffs and drinking water	Alkaline digestion and high-flow SPE	Kinetex C18 2.6 µm (50 × 2.1)	10 mM *N*-methylmorpholine in water / MeOH	MS	
[219]	Perfluoroalkyl carboxylates, sulfonates and sulfonamides	Urban leachates	SPE	Ascentis Express PFP 2.7 µm (100 × 2.1)	20 mM $HCOONH_4$ in water / MeOH	MS	
[291]	Neonicotinoid insecticides	Beeswax	Fusion, dilution, clean-up on diatomaceous cartridges, LLE	Kinetex C18 2.6 µm (150 × 4.6)	0.1% HCOOH in water / MeCN	MS	
[224]	Pesticides	Grains	QuEChERS	Kinetex C18 2.6 µm (100 × 2.1)		MS	Comparison with fully porous 3 µm column
[220]	Polycyclic aromatic hydrocarbons	Rainwater	LL-microextraction	Kinetex C18 2.6 µm (100 × 4.6)	Water / MeCN	FL UV-Vis	
[221]	Naphthenic acids	Surface waters	In-column concentration	Poroshell C18 2.7 µm (50 × 3)	0.1% HCOOH in water / MeCN or MeOH	MS	Large volume injection and in-column "focusing", clean-up and concentration step at the beginning of the run
[239]	Acylhomoserine lactones	Bacterial culture	Centrifugation	Kinetex C18 5 µm (100 × 2)	0.1% CH_3COOH in water / MeCN	MS	Synthesis of the isotope-labeled internal standards
				Non-vegetal metabolites			
[241]	Norleucine and norvaline	*E. coli* culture samples	Cold shock, sonication, centrifugation	Sunshell C18 2.6 µm (150 × 2.1)	25 mM Na_2HPO_4/NaH_2PO_4 (pH 7.2) / THF / MeOH / MeCN	FL	OPA fully automated pre-column derivatization
[240]	Botryococcenes	Microalgae *Botryococcus braunii*	SLE	Kinetex C18 2.6 µm (100 × 4.6) Kinetex C18 2.6 µm (150 × 4.6)	Water / MeCN	UV-Vis	
[244]	Catecholamines	Rat microdyalisates	Derivatization	Poroshell C18 2.7 µm (100 × 4.6)	10 mM CH_3COONH_4/HCOOH (pH = 4) in water / MeCN	MS	Pre-column derivatization with dansyl chloride
[245]	Catecholamines and indolamines	Sheep encephalon	Perchloric acid digestion and centrifugation	HALO C18 2.7 µm (50 × 4.6)	1.25 mM nonafluoropentanoic acid in water / MeOH	UV-Vis MS	Comparison with fully-porous C18, PFP, porous graphitic carbon and monolithic columns. Ion pairing alternatives.
[254]	Porphyrins	Human urine and faeces	SPE	Poroshell C18 2.7 µm (50 × 4.6)	1 M CH_3COONH_4/CH_3COOH (pH = 5.16) in water / MeCN / MeOH	FL	Comparison with fully-porous 5, 2.4 and 1.9 µm particles
[249]	Endocannabinoids	Human plasma	µ-SPE	Kinetex C18 2.6 µm (100 × 2.1)	2.5 mM HCOOH in water / MeOH	MS	
[246]	Phosphorylcholine-containing lipids	Fetal mouse lung	LLE	Kinetex C18 2.6 µm (100 × 2.1)	20 mM CH_3COONH_4 in water / MeCN / MeOH	MS	Lipidomics / lipid profiling

Table 3. (continued)

Ref.	Analytes	Matrix	Pretreatment	Core-shell column	Mobile phase	Detector	Notes
				Non-vegetal metabolites (continued)			
[247]	Metabolites of D_2 and D_3 vitamins	Human plasma	Protein precipitation	Kinetex C18 2.6 µm (50 × 2.1)	$HCOONH_4$ (pH = 3) in water / MeOH	MS	Comparison of core-shell with fully-porous 1.9 µm particles
[248]	Metabolites of D_2 and D_3 vitamins	Human plasma	Protein precipitation, on-line enrichment	Kinetex PFP 2.6 µm (150 × 4.6)	0.5 mM $HCOONH_4$ in water / MeOH	MS	
[253]	Retinol and α-tocopherol	Breast milk	Protein precipitation, saponification, LLE	Kinetex C18 2.6 µm (100 × 4.6)	MeOH	UV-Vis	Comparison of core-shell columns with monolithic columns
[250]	Aldosterone	Human plasma	96-well plate SPE	Kinetex PFP 2.6 µm (100 × 2.1)	Water / MeOH	MS	
[292]	Sugars and sugar phosphates	Mouse heart tissue	Homogenization, reductive amination	Kinetex PFP 2.6 µm (150 × 2.1)	0.1% HCOOH / 1 mM $CH_3P(O)(OH)_2$ in water / MeCN	MS	
[242]	Methylated nucleotides	DNA from cell cultures	DNA extraction and hydrolysis	Kinetex C18 1.7 µm (100 × 2.1)	0.15% HCOOH in water / MeCN	MS	Comparison with fully porous 1.9 µm column
[251]	Modified nucleosides	Urine and serum	Direct injection	Kinetex C18 2.6 µm (150 × 4.6) Kinetex HILIC 2.6 µm (150 × 4.6)	Water / MeOH	UV-Vis	Comparison among several stationary phases diameters and chemistries
[243]	Tetrahydrobiopterin, dihydrobiopterin, and biopterin	Endothelial cells	Cell lysis in the presence of antioxidants	Poroshell 120 C18 2.7 µm (150 × 2.1)	150 mM CH_3COOH/12 mM heptafluorobutyric acid in water / MeOH	MS	
[252]	Tocopherols and tocotrienols	Plasma and liver	Saponification (for liver tissue), LLE	Kinetex PFP 2.6 µm (150 × 4.6)	Water / MeOH	FL	
[255]	Human metabolic fingerprinting	Human plasma	In-vial LL dual extraction	Poroshell 120 C8 2.7 µm (150 × 2.1)	10 mM $HCOONH_4$ / MeOH	MS	
				Pharmaceutical excipients and preservants			
[177]	Polysorbate 20 and polyethylene-glycol	Liquid pharmaceutical formulations containing proteins	Direct injection	Kinetex C18 2.6 µm (100 × 3)	0.1% CF_3COOH in water / MeCN	Condensation nucleation LSD-MS	
[176]	Polysorbate 80	Liquid pharmaceutical formulations containing proteins	Direct injection	Poroshell 300 C18 5 µm (75 × 2.1)	0.1% CF_3COOH in water / MeCN or MeOH	Charged aerosol detection MS	
[178]	Methylated cyclodextrins	Neat samples	Direct injection	HALO C18 2.7 µm (50 × 4.6)	Water / MeCN	ELSD	Comparison with 5 µm fully porous and monolythic columns.
[179]	Methyl-, ethyl- and propyl parabens	Hygiene wipes	Ultrasound-assisted SLE	Accucore C18 2.6 µm (50 × 2.1)	0.1% CH_3COOH in water (pH = 2.8) / MeCN /IPA	UV-Vis	

Table 3. (continued)

Ref.	Analytes	Matrix	Pretreatment	Core-shell column	Mobile phase	Detector	Notes
				Natural toxins			
[259]	Ochratoxin A	Red wine	Immunoaffinity SPE	Kinetex C18 2.6 µm (100 × 4.6)	1% HCOOH in water / MeCN	FL	Comparison with 5 µm and 3 µm fully porous columns
[258]	Mycotoxins	Cereals	SPE	Kinetex C18 2.6 µm (100 × 4.6)	5 mM CH_3COONH_4 in water (pH = 7) / MeOH	MS	Comparison with fully porous 5 µm column
[256]	Mycotoxins	Barley	SLE, immunoaffinity SPE, post-column photochemical derivatization	Ascentis Express C18 2.7 µm (150 × 2.1)	5 mM $HCOONH_4$ / 0.1% HCOOH in water / MeOH	FL	
[257]	Mycotoxins	Bread, crackers, minicakes and biscuits	SLE, immunoaffinity column	Kinetex C18 2.6 µm (150 × 2.1)	0.5% CH_3COOH in water / MeOH	MS	
[260]	Paralytic shellfish toxins	Shellfish extracts	SPE	Ascentis Express C18 2.7 µm (100 × 4.6)	0.1 M $HCOONH_4$/0.1 M CH_3COOH (pH = 6) in water / MeCN	FL	Comparison with fully porous 5 µm column (AOAC method)
[261]	Paralytic shellfish toxins	Mussels, oysters, cockles, hard clams, razors, and king scallops	Matrix precipitation, SPE, oxidation	Kinetex C18 2.6 µm (100 × 4.6) Poroshell C18 2.7 µm (100 × 4.6)	0.1 M $HCOONH_4$/ CH_3COOH (pH 6.0) in water / MeCN	FL	Comparison with fully porous 5 µm column (AOAC method)
[262]	Microcystins	Water samples	SPE, pre-column excimer fluorescence derivatization with 4-(1-pyrene) butanoic acid hydrazide	Accucore PFP 2.6 µm (50 × 3)	0.15% CF_3COOH/10 mM CH_3-$COONH_4$ in water / MeCN / MeOH	FL	

IPA: isopropyl alcohol, PCA: principal component analysis, HCA: hierarchical cluster analysis, PLS-DA: partial least square-discriminant analysis, LSD-MS: light scattering detection-mass spectrometry.

Referencias

1. P.W. Carr, D.R. Stoll, X. Wang, Perspectives on recent advances in the speed of high-performance liquid chromatography, Anal Chem. 83 (2011) 1890–1900.
2. T.K. Natishan, Developments In Fast Liquid Chromatographic Analysis Of Pharmaceuticals, J Liq Chromatogr Relat Technol. 34 (2011) 1133–1156.
3. S. Pieters, B. Dejaegher, Y. Vander Heyden, Emerging analytical separation techniques with high throughput potential for pharmaceutical analysis, part I: Stationary phase and instrumental developments in LC, Comb Chem High Throughput Screen. 13 (2010) 510–529.
4. M. de L. Guardia, Green analytical chemistry, Trends Anal Chem. 29 (2010) 577–577.
5. C.J. Welch, N. Wu, M. Biba, R. Hartman, T. Brkovic, X. Gong, et al., Greening analytical chromatography, Trends Anal Chem. 29 (2010) 667–680.
6. T.L. Chester, Recent Developments in High-Performance Liquid Chromatography Stationary Phases, Anal Chem. 85 (2013) 579–589.
7. J.J. Salisbury, Fused-core particles: a practical alternative to sub-2 micron particles, J Chromatogr Sci. 46 (2008) 883–886.
8. I. Ali, Z.A. AL-Othman, M. Al-Za'abi, Superficially porous particles columns for super fast HPLC separations, Biomed Chromatogr. 26 (2012) 1001–1008.
9. S. Fekete, E. Oláh, J. Fekete, Fast liquid chromatography: The domination of core–shell and very fine particles, J Chromatogr A. 1228 (2012) 57–71.
10. F. Gritti, G. Guiochon, The current revolution in column technology: How it began, where is it going? J Chromatogr A. 1228 (2012) 2–19.
11. F. Gritti, G. Guiochon, Mass transfer kinetics, band broadening and column efficiency, J Chromatogr A. 1221 (2012) 2–40.
12. S. Fekete, J.-L. Veuthey, D. Guillarme, New trends in reversed-phase liquid chromatographic separations of therapeutic peptides and proteins: theory and applications, J Pharm Biomed Anal. 69 (2012) 9–27.
13. O. Núñez, H. Gallart-Ayala, C.P.B. Martins, P. Lucci, New trends in fast liquid chromatography for food and environmental analysis, J Chromatogr A. 1228 (2012) 298–323.
14. Y. Wang, F. Ai, S.-C. Ng, T.T.Y. Tan, Sub-2 µm porous silica materials for enhanced separation performance in liquid chromatography, J Chromatogr A. 1228 (2012) 99–109.
15. D.V. McCalley, The challenges of the analysis of basic compounds by high performance liquid chromatography: some possible approaches for improved separations, J Chromatogr A. 1217 (2010) 858–880.
16. G. Guiochon, F. Gritti, Shell particles, trials, tribulations and triumphs, J Chromatogr A. 1218 (2011) 1915–1938.
17. X. Wang, W.E. Barber, W.J. Long, Applications of superficially porous particles: high speed, high efficiency or both? J Chromatogr A. 1228 (2012) 72–88.
18. I. Halász, C. Horváth, Micro Beads Coated with a Porous Thin Layer as Column Packing in Gas Chromatography, Anal Chem. 36 (1964) 1178–1186.
19. C.G. Horvath, B.A. Preiss, S.R. Lipsky, Fast liquid chromatography: an investigation of operating parameters and the separation of nucleotides on pellicular ion exchangers, Anal Chem. 39 (1967) 1422–1428.
20. C. Horvath, S.R. Lipsky, Column Design in High Pressure Liquid Chromatography, J Chromatogr Sci. 7 (1969) 109–116.
21. J.H. Knox, Evidence for Turbulence and Coupling in Chromatographic Columns, Anal Chem. 38 (1966) 253–261.
22. J.J. Kirkland, Controlled surface porosity supports for high-speed gas and liquid chromatography, Anal Chem. 41 (1969) 218–220.
23. K.K. Unger, O. Jilge, J.N. Kinkel, M.T.W. Hearn, Evaluation of advanced silica packings for the separation of biopolymers by high-performance liquid chromatography II. Performance of non-porous monodisperse 1.5-µm Silica beads in the separation of proteins by reversed-phase gradient elution high-performance liquid chromatography, J Chromatogr. 359 (1986) 61–72.
24. K. Kalghatgi, C. Horvath, Rapid analysis of proteins and peptides by reversed-phase chromatography, J Chromatogr. 398 (1987) 335–339.
25. J.J. Kirkland, Superficially porous silica microspheres for the fast high-performance liquid chromatography of macromolecules, Anal Chem. 64 (1992) 1239–1245.
26. J.J. Kirkland, F.A. Truszkowski, R.D. Ricker, Atypical silica-based column packings for high-performance liquid chromatography, J Chromatogr A. 965 (2002) 25–34.
27. J.J. Kirkland, F.A. Truszkowski, C.H. Dilks, G.S. Engel, Superficially porous silica microspheres for fast high-performance liquid chromatography of macromolecules, J Chromatogr A. 890 (2000) 3–13.
28. R.G. Chaudhuri, S. Paria, Core/shell nanoparticles: classes, properties, synthesis mechanisms, characterization, and applications, Chem Rev. 112 (2012) 2373–2433.
29. W. Stöber, A. Fink, E. Bohn, Controlled growth of monodisperse silica spheres in the micron size range, J Colloid Interf Sci. 26 (1968) 62–69.
30. R.T. Kennedy, I. German, J.E. Thompson, S.R. Witowski, Fast Analytical-Scale Separations by Capillary Electrophoresis and Liquid Chromatography, Chem Rev. 99 (1999) 3081–3132.
31. S.B. Yoon, J.-Y. Kim, J.H. Kim, Y.J. Park, K.R. Yoon, S.-K. Park, et al., Synthesis of monodisperse spherical silica particles with solid core and mesoporous shell: mesopore channels perpendicular to the surface, J. Mater. Chem. 17 (2007) 1758–1761.
32. A. Ahmed, W. Abdelmagid, H. Ritchie, P. Myers, H. Zhang, Investigation on synthesis of spheres-on-sphere silica particles and their assessment for high performance liquid chromatography applications, J Chromatogr A. 1270 (2012) 194–203.
33. J.-E. Jönsson, O.J. Karlsson, H. Hassander, B. Törnell, Shell-Layer Stability in Core–Shell Particles Prepared with Different Initiators, Macromolecules. 34 (2001) 1512–1514.
34. L.A. Wiest, D.S. Jensen, C.-H. Hung, R.E. Olsen, R.C. Davis, M.A. Vail, et al., Pellicular particles with spherical carbon cores and porous nanodiamond/polymer shells for reversed-phase HPLC, Anal Chem. 83 (2011) 5488–5501.
35. G. Saini, D.S. Jensen, L.A. Wiest, M.A. Vail, A. Dadson, M.L. Lee, et al., Core-shell diamond as a support for solid-phase extraction and high-performance liquid chromatography, Anal Chem. 82 (2010) 4448–4456.
36. F. Detobel, S. De Bruyne, J. Vangelooven, W. De Malsche, T. Aerts, H. Terryn, et al., Fabrication and chromatographic performance of porous-shell pillar-array columns, Anal Chem. 82 (2010) 7208–7217.
37. C. Paek, Y. Huang, M.R. Filgueira, A.V. McCormick, P.W. Carr, Development of a carbon clad core-shell silica for high speed two-dimensional liquid chromatography, J Chromatogr A. 1229 (2012) 129–139.
38. X. Wu, L. You, B. Di, W. Hao, M. Su, Y. Gu, et al., Novel chiral core-shell silica microspheres with trans-(1R,2R)-diaminocyclohexane bridged in the mesoporous shell: synthesis, characterization and application in high performance liquid chromatography, J Chromatogr A. 1299 (2013) 78–84.

39. A. El Fagui, F. Dalmas, C. Lorthioir, V. Wintgens, G. Volet, C. Amiel, Well-defined core-shell nanoparticles containing cyclodextrin in the shell: A comprehensive study, Polymer. 52 (2011) 3752–3761.
40. S. Bruns, U. Tallarek, Physical reconstruction of packed beds and their morphological analysis: core-shell packings as an example, J Chromatogr A. 1218 (2011) 1849–1860.
41. F. Gritti, I. Leonardis, D. Shock, P. Stevenson, A. Shalliker, G. Guiochon, Performance of columns packed with the new shell particles, Kinetex-C18, J Chromatogr A. 1217 (2010) 1589–1603.
42. E. Lesellier, Extension of the carotenoid test to superficially porous C18 bonded phases, aromatic ligand types and new classical C18 bonded phases, J Chromatogr A. 1266 (2012) 34–42.
43. A. Felinger, Diffusion time in core-shell packing materials, J Chromatogr A. 1218 (2011) 1939–1941.
44. J.O. Omamogho, J.P. Hanrahan, J. Tobin, J.D. Glennon, Structural variation of solid core and thickness of porous shell of 1.7 µm core-shell silica particles on chromatographic performance: narrow bore columns, J Chromatogr A. 1218 (2011) 1942–1953.
45. K. Horvath, F. Gritti, J.N. Fairchild, G. Guiochon, On the optimization of the shell thickness of superficially porous particles, J Chromatogr A. 1217 (2010) 6373–6381.
46. F. Gritti, J. Omamogho, G. Guiochon, Kinetic investigation of narrow-bore columns packed with prototype sub-2 µm superficially porous particles with various shell thickness, J Chromatogr A. 1218 (2011) 7078–7093.
47. F. Gritti, G. Guiochon, Theoretical investigation of diffusion along columns packed with fully and superficially porous particles, J Chromatogr A. 1218 (2011) 3476–3488.
48. F. Gritti, G. Guiochon, Comparative study of the performance of columns packed with several new fine silica particles. Would the external roughness of the particles affect column properties? J Chromatogr A. 1166 (2007) 30–46.
49. F. Gritti, A. Cavazzini, N. Marchetti, G. Guiochon, Comparison between the efficiencies of columns packed with fully and partially porous C18-bonded silica materials, J Chromatogr A. 1157 (2007) 289–303.
50. J. Urban, P. Jandera, Z. Kucerová, M.A. van Straten, H.A. Claessens, A study of the effects of column porosity on gradient separations of proteins, J Chromatogr A. 1167 (2007) 63–75.
51. F. Gritti, G. Guiochon, Experimental validation of physico-chemical models of effective diffusion in chromatographic columns packed with superficially porous particles, Chem Eng Sci. 66 (2011) 6168–6179.
52. F. Gritti, G. Guiochon, Diffusion models in chromatographic columns packed with fully and superficially porous particles, Chem Eng Sci. 66 (2011) 3773–3781.
53. A. Cavazzini, F. Gritti, K. Kaczmarski, N. Marchetti, G. Guiochon, Mass-transfer kinetics in a shell packing material for chromatography, Anal Chem. 79 (2007) 5972–5979.
54. F. Gritti, K. Horvath, G. Guiochon, How changing the particle structure can speed up protein mass transfer kinetics in liquid chromatography, J Chromatogr A. 1263 (2012) 84–98.
55. J. Kostka, F. Gritti, K. Kaczmarski, G. Guiochon, Modified Equilibrium-Dispersive Model for the interpretation of the efficiency of columns packed with core-shell particle, J Chromatogr A. 1218 (2011) 5449–5455.
56. F. Gritti, G. Guiochon, Speed-resolution properties of columns packed with new 4.6 µm Kinetex-C(18) core-shell particles, J Chromatogr A. 1280 (2013) 35–50.
57. A.C. Sanchez, G. Friedlander, S. Fekete, J. Anspach, D. Guillarme, M. Chitty, et al., Pushing the performance limits of reversed-phase ultra high performance liquid chromatography with 1.3µm core-shell particles, J Chromatogr A. 1311 (2013) 90–97.
58. K. Kaczmarski, G. Guiochon, Modeling of the mass-transfer kinetics in chromatographic columns packed with shell and pellicular particles, Anal Chem. 79 (2007) 4648–4656.
59. K. Miyabe, New moment equations for chromatography using various stationary phases of different structural characteristics, Anal Chem. 79 (2007) 7457–7472.
60. L. Nováková, H. Vlcková, A review of current trends and advances in modern bio-analytical methods: chromatography and sample preparation, Anal Chim Acta. 656 (2009) 8–35.
61. F. Gritti, G. Guiochon, Kinetic investigation of the relationship between the efficiency of columns and their diameter, J Chromatogr A. 1218 (2011) 1592–1602.
62. F. Gritti, G. Guiochon, Accurate measurements of peak variances: importance of this accuracy in the determination of the true corrected plate heights of chromatographic columns, J Chromatogr A. 1218 (2011) 4452–4461.
63. F. Gritti, G. Guiochon, Repeatability of the efficiency of columns packed with sub-3µm core-shell particles: Part I. 2.6µm Kinetex-C(18) particles in 4.6mm and 2.1mm×100mm column formats, J Chromatogr A. 1252 (2012) 31–44.
64. F. Gritti, G. Guiochon, Repeatability of the efficiency of columns packed with sub-3µm core-shell particles: Part II. 2.7 µm Halo-ES-Peptide-C18 particles in 4.6mm and 2.1mm×100mm column formats, J Chromatogr A. 1252 (2012) 45–55.
65. F. Gritti, G. Guiochon, Perspectives on the Evolution of the Column Efficiency in Liquid Chromatography, Anal Chem. 85 (2013) 3017–3035.
66. D. Cabooter, A. Fanigliulo, G. Bellazzi, B. Allieri, A. Rottigni, G. Desmet, Relationship between the particle size distribution of commercial fully porous and superficially porous high-performance liquid chromatography column packings and their chromatographic performance, J Chromatogr A. 1217 (2010) 7074–7081.
67. F. Gritti, G. Guiochon, Relationship between trans-column eddy diffusion and retention in liquid chromatography: theory and experimental evidence, J Chromatogr A. 1217 (2010) 6350–6365.
68. F. Gritti, I. Leonardis, J. Abia, G. Guiochon, Physical properties and structure of fine core-shell particles used as packing materials for chromatography Relationships between particle characteristics and column performance, J Chromatogr A. 1217 (2010) 3819–3843.
69. F. Gritti, G. Guiochon, Mass transfer mechanism in liquid chromatography columns packed with shell particles: would there be an optimum shell structure? J Chromatogr A. 1217 (2010) 8167–8180.
70. F. Gritti, G. Guiochon, A protocol for the measurement of all the parameters of the mass transfer kinetics in columns used in liquid chromatography, J Chromatogr A. 1217 (2010) 5137–5151.
71. F. Gritti, G. Guiochon, Non-invasive measurement of eddy diffusion in very efficient liquid chromatography columns packed with sub-3µm shell particles, Chem Eng Sci. 65 (2010) 6327–6340.
72. J.O. Omamogho, J.D. Glennon, Comparison between the Efficiencies of sub-2 µm C(18) Particles Packed in Narrow Bore Columns, Anal Chem. 83 (2011) 1547–1556.
73. F. Gritti, G. Guiochon, Unusual behavior of the height equivalent to a theoretical plate of a new poroshell stationary phase at high temperatures, J Chromatogr A. 1169 (2007) 125–138.
74. J.J. DeStefano, S.A. Schuster, J.M. Lawhorn, J.J. Kirkland, Performance characteristics of new superficially porous particles, J Chromatogr A. 1258 (2012) 76–83.

75. F. Gritti, G. Guiochon, The mass transfer kinetics in columns packed with Halo-ES shell particles, J Chromatogr A. 1218 (2011) 907–921.
76. S.A. Schuster, B.M. Wagner, B.E. Boyes, J.J. Kirkland, Wider pore superficially porous particles for peptide separations by HPLC, J Chromatogr Sci. 48 (2010) 566–571.
77. I. Ali, V.D. Gaitonde, A. Grahn, Halo Columns: New Generation Technology for High Speed Liquid Chromatography, J Chromatogr Sci. 48 (2010) 386–394.
78. S. Fekete, K. Ganzler, J. Fekete, Efficiency of the new sub-2 µm core-shell (Kinetex™) column in practice, applied for small and large molecule separation, J Pharm Biomed Anal. 54 (2011) 482–490.
79. E. Oláh, S. Fekete, J. Fekete, K. Ganzler, Comparative study of new shell-type, sub-2 micron fully porous and monolith stationary phases, focusing on mass-transfer resistance, J Chromatogr A. 1217 (2010) 3642–3653.
80. S. Fekete, R. Berky, J. Fekete, J.-L. Veuthey, D. Guillarme, Evaluation of recent very efficient wide-pore stationary phases for the reversed-phase separation of proteins, J Chromatogr A. 1252 (2012) 90–103.
81. F. Gritti, G. Guiochon, Optimization of the thermal environment of columns packed with very fine particles, J Chromatogr A. 1216 (2009) 1353–1362.
82. F. Gritti, G. Guiochon, Comparison of heat friction effects in narrow-bore columns packed with core–shell and totally porous particles, Chem Eng Sci. 65 (2010) 6310–6319.
83. F. Gritti, G. Guiochon, Mass transfer resistance in narrow-bore columns packed with 1.7 microm particles in very high pressure liquid chromatography, J Chromatogr A. 1217 (2010) 5069–5083.
84. D. Guillarme, J. Ruta, S. Rudaz, J.-L. Veuthey, New trends in fast and high-resolution liquid chromatography: a critical comparison of existing approaches, Anal Bioanal Chem. 397 (2010) 1069–1082.
85. B. Chauve, D. Guillarme, P. Cléon, J.-L. Veuthey, Evaluation of various HILIC materials for the fast separation of polar compounds, J. Sep. Sci. 33 (2010) 752–764.
86. H. Poppe, Some reflections on speed and efficiency of modern chromatographic methods, J Chromatogr A. 778 (1997) 3–21.
87. G. Desmet, D. Clicq, P. Gzil, Geometry-independent plate height representation methods for the direct comparison of the kinetic performance of LC supports with a different size or morphology, Anal Chem. 77 (2005) 4058–4070.
88. K. Broeckhoven, D. Cabooter, F. Lynen, P. Sandra, G. Desmet, The kinetic plot method applied to gradient chromatography: theoretical framework and experimental validation, J Chromatogr A. 1217 (2010) 2787–2795.
89. S. Fekete, J. Fekete, K. Ganzler, Characterization of new types of stationary phases for fast liquid chromatographic applications, J Pharm Biomed Anal. 50 (2009) 703–709.
90. R.W. Brice, X. Zhang, L.A. Colón, Fused-core, sub-2 microm packings, and monolithic HPLC columns: a comparative evaluation, J. Sep. Sci. 32 (2009) 2723–2731.
91. T.A. Diószegi, D.E. Raynie, Kinetic performance comparison of a capillary monolithic and a fused-core column in micro-scale liquid chromatography, J Chromatogr A. 1261 (2012) 107–112.
92. H. Shaaban, T. Górecki, Fused core particles as an alternative to fully porous sub-2 µm particles in pharmaceutical analysis using coupled columns at elevated temperature, Anal. Methods. 4 (2012) 2735–2743.
93. J.M. Cunliffe, T.D. Maloney, Fused-core particle technology as an alternative to sub-2-microm particles to achieve high separation efficiency with low backpressure, J. Sep. Sci. 30 (2007) 3104–3109.
94. J.J. Destefano, T.J. Langlois, J.J. Kirkland, Characteristics of Superficially-Porous Silica Particles for Fast HPLC: Some Performance Comparisons with Sub-2-m Particles, J Chromatogr Sci. 46 (2008) 254–260.
95. E. Lesellier, Extension of the C18 stationary phase knowledge by using the carotenoid test, J. Sep. Sci. 33 (2010) 3097–3105.
96. A. Abrahim, M. Al-Sayah, P. Skrdla, Y. Bereznitski, Y. Chen, N. Wu, Practical comparison of 2.7 microm fused-core silica particles and porous sub-2 microm particles for fast separations in pharmaceutical process development, J Pharm Biomed Anal. 51 (2010) 131–137.
97. Y. Kazakevich, R. LoBrutto, HPLC for Pharmaceutical Scientists, Wiley-Interscience, Hoboken, 2007.
98. F. Gritti, G. Guiochon, Overload behavior and apparent efficiencies in chromatography, J Chromatogr A. 1254 (2012) 30–42.
99. D.V. McCalley, Some practical comparisons of the efficiency and overloading behaviour of sub-2 µm porous and sub-3 µm shell particles in reversed-phase liquid chromatography, J Chromatogr A. 1218 (2011) 2887–2897.
100. M.M. Fallas, S.M.C. Buckenmaier, D.V. McCalley, A comparison of overload behaviour for some sub 2 µm totally porous and sub 3 µm shell particle columns with ionised solutes, J Chromatogr A. 1235 (2012) 49–59.
101. L.R. Snyder, J.J. Kirkland, J.W. Dolan, Introduction to Modern Liquid Chromatography, John Wiley & Sons, Inc, Hoboken, 2010.
102. F. Gritti, G. Guiochon, Performance of columns packed with the new shell Kinetex-C18 particles in gradient elution chromatography, J Chromatogr A. 1217 (2010) 1604–1615.
103. F. Gritti, N. Tanaka, G. Guiochon, Comparison of the fast gradient performance of new prototype silica monolithic columns and columns packed with fully porous and core-shell particles, J Chromatogr A. 1236 (2012) 28–41.
104. F. Gritti, G. Guiochon, Band broadening in fast gradient high-performance liquid chromatography: application to the second generation of 4.6 mm I.D. silica monolithic columns, J Chromatogr A. 1238 (2012) 77–90.
105. A. Vaast, K. Broeckhoven, S. Dolman, G. Desmet, S. Eeltink, Comparison of the gradient kinetic performance of silica monolithic capillary columns with columns packed with 3µm porous and 2.7µm fused-core silica particles, J Chromatogr A. 1228 (2012) 270–275.
106. S. Fekete, J. Fekete, K. Ganzler, Shell and small particles; evaluation of new column technology, J Pharm Biomed Anal. 49 (2009) 64–71.
107. S. Heinisch, A. D'Attoma, C. Grivel, Effect of pH additive and column temperature on kinetic performance of two different sub-2 µm stationary phases for ultrafast separation of charged analytes, J Chromatogr A. 1228 (2012) 135–147.
108. E.R. Badman, R.L. Beardsley, Z. Liang, S. Bansal, Accelerating high quality bioanalytical LC/MS/MS assays using fused-core columns, J Chromatogr B. 878 (2010) 2307–2313.
109. J. Ruta, D. Guillarme, S. Rudaz, J.-L. Veuthey, Comparison of columns packed with porous sub-2 microm particles and superficially porous sub-3 microm particles for peptide analysis at ambient and high temperature, J. Sep. Sci. 33 (2010) 2465–2477.
110. Y. Zhang, X. Wang, P. Mukherjee, P. Petersson, Critical comparison of performances of superficially porous particles and sub-2 microm particles under optimized ultra-high pressure conditions, J Chromatogr A. 1216 (2009) 4597–4605.

111. D.V. McCalley, Evaluation of the properties of a superficially porous silica stationary phase in hydrophilic interaction chromatography, J Chromatogr A. 1193 (2008) 85–91.
112. A. Vaast, J. De Vos, K. Broeckhoven, M. Verstraeten, S. Eeltink, G. Desmet, Maximizing the peak capacity using coupled columns packed with 2.6 µm core-shell particles operated at 1200 bar, J Chromatogr A. 1256 (2012) 72–79.
113. D. Cabooter, G. Desmet, Performance limits and kinetic optimization of parallel and serially connected multi-column systems spanning a wide range of efficiencies for liquid chromatography, J Chromatogr A. 1219 (2012) 114–127.
114. B.J. VanMiddlesworth, J.G. Dorsey, Reequilibration time of superficially porous silica based columns in gradient elution reversed phase liquid chromatography, J Chromatogr A. 1218 (2011) 7158–7165.
115. D.V. McCalley, Instrumental considerations for the effective operation of short, highly efficient fused-core columns. Investigation of performance at high flow rates and elevated temperatures, J Chromatogr A. 1217 (2010) 4561–4567.
116. S. Fekete, J. Fekete, The impact of extra-column band broadening on the chromatographic efficiency of 5 cm long narrow-bore very efficient columns, J Chromatogr A. 1218 (2011) 5286–5291.
117. F. Gritti, C.A. Sanchez, T. Farkas, G. Guiochon, Achieving the full performance of highly efficient columns by optimizing conventional benchmark high-performance liquid chromatography instruments, J Chromatogr A. 1217 (2010) 3000–3012.
118. A.J. Alexander, T.J. Waeghe, K.W. Himes, F.P. Tomasella, T.F. Hooker, Modifying conventional high-performance liquid chromatography systems to achieve fast separations with Fused-Core columns: a case study, J Chromatogr A. 1218 (2011) 5456–5469.
119. F. Gritti, G. Guiochon, Kinetic performance of narrow-bore columns on a micro-system for high performance liquid chromatography, J Chromatogr A. 1236 (2012) 105–114.
120. P. Chocholouš, L. Kosarová, D. Šatínský, H. Sklenárová, P. Solich, Enhanced capabilities of separation in Sequential Injection Chromatography--fused-core particle column and its comparison with narrow-bore monolithic column, Talanta. 85 (2011) 1129–1134.
121. A.C. Sanchez, J.A. Anspach, T. Farkas, Performance optimizing injection sequence for minimizing injection band broadening contributions in high efficiency liquid chromatographic separations, J Chromatogr A. 1228 (2012) 338–348.
122. S. Fekete, I. Kohler, S. Rudaz, D. Guillarme, Importance of instrumentation for fast liquid chromatography in pharmaceutical analysis, J Pharm Biomed Anal. (2013).
123. U.R. Inugala, N.R. Pothuraju, R.R. Vangala, Quality by design approach for the separation of naproxcinod and its related substances by fused core particle technology column, J Chromatogr Sci. 51 (2013) 453–459.
124. S.R. Chitturi, Y.S. Somannavar, B.G. Peruri, S. Nallapati, H.K. Sharma, S.R. Budidet, et al., Gradient RP-HPLC method for the determination of potential impurities in atazanavir sulfate, J Pharm Biomed Anal. 55 (2011) 31–47.
125. S.-I. Kawano, Analysis of impurities in streptomycin and dihydrostreptomycin by hydrophilic interaction chromatography/electrospray ionization quadrupole ion trap/time-of-flight mass spectrometry, Rapid Commun. Mass Spectrom. 23 (2009) 907–914.
126. A.J. Alexander, L. Ma, Comprehensive two-dimensional liquid chromatography separations of pharmaceutical samples using dual Fused-Core columns in the 2nd dimension, J Chromatogr A. 1216 (2009) 1338–1345.
127. J.S. Janiszewski, K.J. Rogers, K.M. Whalen, M.J. Cole, T.E. Liston, E. Duchoslav, et al., A High-Capacity LC/MS System for the Bioanalysis of Samples Generated from Plate-Based Metabolic Screening, Anal Chem. 73 (2001) 1495–1501.
128. T. Wang, W. Ma, Y. Sun, Y. Yang, W. Zhang, J.P. Fawcett, et al., Ultra-sensitive assay for paclitaxel in intracellular compartments of A549 cells using liquid chromatography–tandem mass spectrometry, J Chromatogr B. 912 (2013) 93–97.
129. W. Song, D. Pabbisetty, E.A. Groeber, R.C. Steenwyk, D.M. Fast, Comparison of fused-core and conventional particle size columns by LC-MS/MS and UV: application to pharmacokinetic study, J Pharm Biomed Anal. 50 (2009) 491–500.
130. H.-L. Li, J.-C. He, M. Bai, Q.-Y. Song, E.-F. Feng, G.-X. Rao, et al., Determination of the plasma pharmacokinetic and tissue distributions of swertiamarin in rats by liquid chromatography with tandem mass spectrometry, Arzneimittelforschung. 62 (2012) 138–144.
131. M. Hroch, Z. Havlínová, M. Nobilis, J. Chládek, HPLC determination of arginases inhibitor N-(ω)-hydroxy-nor-L-arginine using core-shell particle column and LC-MS/MS identification of principal metabolite in rat plasma, J Chromatogr B. 880 (2012) 90–99.
132. S.H. Bae, J.W. Hwang, S.J. Shin, G.H. Park, K.D. Yoon, S.K. Bae, Quantitation and pharmacokinetics of 1,4-diamino-2,3-dicyano-1,4-bis (2-aminophenylthio) butadiene (U0126) in rat plasma by liquid chromatography-tandem mass spectrometry, J. Sep. Sci. 36 (2013) 239–245.
133. S. Wang, J. Wen, L. Cui, X. Zhang, H. Wei, R. Xie, et al., Optimization and validation of a high performance liquid chromatography method for rapid determination of sinafloxacin, a novel fluoroquinolone in rat plasma using a fused-core C(18)-silica column, J Pharm Biomed Anal. 51 (2010) 889–893.
134. Y. Hsieh, C.J.G. Duncan, J.-M. Brisson, Fused-core silica column high-performance liquid chromatography/tandem mass spectrometric determination of rimonabant in mouse plasma, Anal Chem. 79 (2007) 5668–5673.
135. E. Dailly, R. Bouquié, G. Deslandes, P. Jolliet, R. Le Floch, A liquid chromatography assay for a quantification of doripenem, ertapenem, imipenem, meropenem concentrations in human plasma: application to a clinical pharmacokinetic study, J Chromatogr B. 879 (2011) 1137–1142.
136. H. Ito, H. Yamaguchi, A. Fujikawa, N. Shiida, N. Tanaka, J. Ogura, et al., Quantification of intact carboplatin in human plasma ultrafitrates using hydrophilic interaction liquid chromatography-tandem mass spectrometry and its application to a pharmacokinetic study, J Chromatogr B. 917-918 (2013) 18–23.
137. P. Sharma, S. Guttikar, G. Solanki, D.P. Patel, P.S. Shrivastav, Determination of (S)-(+)- and (R)-(-)-ibuprofen enantiomers in human plasma after chiral precolumn derivatization by reversed-phase LC-ESI-MS/MS, Bioanalysis. 4 (2012) 2909–2927.
138. V.S. Ponnuru, B.R. Challa, R. Nadendla, Quantitative analysis of eletriptan in human plasma by HPLC-MS/MS and its application to pharmacokinetic study, Anal Bioanal Chem. 401 (2011) 2539–2548.
139. L. Silvestro, M.C. Gheorghe, I. Tarcomnicu, S. Savu, S.R. Savu, A. Iordachescu, et al., Development and validation of an HPLC-MS/MS method to determine clopidogrel in human plasma. Use of incurred samples to test back-conversion, J Chromatogr B. 878 (2010) 3134–3142.

140. A. Chahbouni, A. Sinjewel, J.C.G. den Burger, R.M. Vos, A.J. Wilhelm, A.I. Veldkamp, et al., Rapid quantification of gabapentin, pregabalin, and vigabatrin in human serum by ultraperformance liquid chromatography with mass-spectrometric detection, Ther Drug Monit. 35 (2013) 48–53.
141. Y. Hui, M. Wong, S.S. Zhao, J.A. Love, D.M. Ansley, D.D.Y. Chen, A simple and robust LC-MS/MS method for quantification of free 3-nitrotyrosine in human plasma from patients receiving on-pump CABG surgery, Electrophoresis. 33 (2012) 697–704.
142. J.M. Cunliffe, J.X. Shen, X. Wei, D.P. Dreyer, R.N. Hayes, R.P. Clement, Implementation of high-temperature superficially porous technologies for rapid LC-MS/MS diastereomer bioanalysis, Bioanalysis. 3 (2011) 735–743.
143. T. Ogawa, H. Hattori, M. Iwai, K. Ito, K. Iwakura, A. Ishii, et al., A rapid and simultaneous analysis of theophylline and its metabolites in human whole blood by ultra-performance liquid chromatography-tandem mass spectrometry, Forensic Toxicol. 30 (2012) 142–148.
144. G. Lawson, E. Cocks, S. Tanna, Quantitative determination of atenolol in dried blood spot samples by LC-HRMS: a potential method for assessing medication adherence, J Chromatogr B. 897 (2012) 72–79.
145. E. Kralj, J. Trontelj, T. Pajic, A. Kristl, Simultaneous measurement of imatinib, nilotinib and dasatinib in dried blood spot by ultra high performance liquid chromatography tandem mass spectrometry, J Chromatogr B. 903 (2012) 150–156.
146. W. Li, S.M. Williams, H.T. Smith, F.L.S. Tse, Quantitative analysis of NIM811, a cyclophilin inhibitor, in human dried blood spots using liquid chromatography-tandem mass spectrometry, J Chromatogr B. 879 (2011) 2376–2382.
147. M. Mazzarino, X. de la Torre, F. Botrè, N. Gray, D. Cowan, A rapid screening LC-MS/MS method based on conventional HPLC pumps for the analysis of low molecular weight xenobiotics: application to doping control analysis, Drug Test Anal. 2 (2010) 311–322.
148. Y. Yang, N. Rosales-Conrado, V. Guillén-Casla, M.E. León-González, L.V. Pérez-Arribas, L.M. Polo-Díez, Chiral Determination of Salbutamol, Salmeterol and Atenolol by Two-Dimensional LC–LC: Application to Urine Samples, Chromatographia. 75 (2012) 1365–1375.
149. B. Wozniak, I. Matraszek-Zuchowska, J. Zmudzki, LC-MS/MS fast analysis of androgenic steroids in urine, Anal Bioanal Chem. 403 (2012) 2965–2972.
150. D. Šatínský, L. Havlíková, P. Solich, HPLC column-switching technique for sample preparation and fluorescence determination of propranolol in urine using fused-core columns in both dimensions, Anal Bioanal Chem. 405 (2013) 6583–6587.
151. S. Magiera, S. Gülmez, A. Michalik, I. Baranowska, Application of statistical experimental design to the optimisation of microextraction by packed sorbent for the analysis of nonsteroidal anti-inflammatory drugs in human urine by ultra-high pressure liquid chromatography, J Chromatogr A. 1304 (2013) 1–9.
152. F.J. Lara, M. del Olmo-Iruela, A.M. García-Campaña, On-line anion exchange solid-phase extraction coupled to liquid chromatography with fluorescence detection to determine quinolones in water and human urine, J Chromatogr A. 1310 (2013) 91–97.
153. M. Fabritius, C. Staub, P. Mangin, C. Giroud, Analysis of cannabinoids in oral fluid by liquid chromatography–tandem mass spectrometry, Forensic Toxicol. 31 (2012) 151–163.
154. M. Sergi, C. Montesano, S. Odoardi, L. Mainero Rocca, G. Fabrizi, D. Compagnone, et al., Micro extraction by packed sorbent coupled to liquid chromatography tandem mass spectrometry for the rapid and sensitive determination of cannabinoids in oral fluids, J Chromatogr A. 1301 (2013) 139–146.
155. K.Y. Rust, M.R. Baumgartner, N. Meggiolaro, T. Kraemer, Detection and validated quantification of 21 benzodiazepines and 3 “z-drugs” in human hair by LC-MS/MS, Forensic Sci Int. 215 (2012) 64–72.
156. M. Dziadosz, R. Lessig, H. Bartels, Protein kinase inhibitor analysis with the core-shell separation technique, Anal Bioanal Chem. 404 (2012) 2083–2086.
157. V.F. Samanidou, E.G. Karageorgou, On the use of Kinetex(™) -C(18) core-shell 2.6 µm stationary phase to the multiclass determination of antibiotics, Drug Test Anal. 3 (2011) 234–244.
158. M. D’Hondt, E. Vangheluwe, S. Van Dorpe, J. Boonen, T. Bauters, B. Pelfrene, et al., Stability of extemporaneously prepared cytarabine, methotrexate sodium, and methylprednisolone sodium succinate, Am J Health Syst Pharm. 69 (2012) 232–240.
159. J. Zheng, D. Patel, Q. Tang, R.J. Markovich, A.M. Rustum, Comparison study of porous, fused-core, and monolithic silica-based C18 HPLC columns for Celestoderm-V Ointment analysis, J Pharm Biomed Anal. 50 (2009) 815–822.
160. I. Ali, K. Saleem, A. Haque, W.A. Wani, V.D. Gaitode, New Generation Halo Column For Fast Analyses Of Aspirin And Atorvastatin In Pharmaceutical Preparation, J Liq Chromatogr Relat Technol. 36 (2013) 261–273.
161. A. Martínez-Villalba, E. Moyano, C.P.B. Martins, M.T. Galceran, Fast liquid chromatography/tandem mass spectrometry (highly selective selected reaction monitoring) for the determination of toltrazuril and its metabolites in food, Anal Bioanal Chem. 397 (2010) 2893–2901.
162. E.G. Karageorgou, V.F. Samanidou, Development and validation according to European Union Decision 2002/657/EC of an HPLC-DAD method for milk multi-residue analysis of penicillins and amphenicols based on dispersive extraction by QuEChERS in MSPD format, J. Sep. Sci. 34 (2011) 800–805.
163. G. D’Orazio, S. Rocchi, S. Fanali, Nano-liquid chromatography coupled with mass spectrometry: separation of sulfonamides employing non-porous core-shell particles, J Chromatogr A. 1255 (2012) 277–285.
164. Y. Lu, Q. Shen, Z. Dai, H. Zhang, Multi-walled carbon nanotubes as solid-phase extraction adsorbent for the ultra-fast determination of chloramphenicol in egg, honey, and milk by fused-core C18-based high-performance liquid chromatography–tandem mass spectrometry, Anal Bioanal Chem. 398 (2010) 1819–1826.
165. F. Sai, M. Hong, Z. Yunfeng, C. Huijing, W. Yongning, Simultaneous detection of residues of 25 β-agonists and 23 β-blockers in animal foods by high-performance liquid chromatography coupled with linear ion trap mass spectrometry, J Agric Food Chem. 60 (2012) 1898–1905.
166. A. Tölgyesi, R. Berky, K. Békési, S. Fekete, J. Fekete, V.K. Sharma, Analysis Of Sulfonamide Residues In Real Honey Samples Using Liquid Chromatography With Fluorescence And Tandem Mass Spectrometry Detection, J Liq Chromatogr Relat Technol. 36 (2013) 1105–1125.
167. A. Tölgyesi, V.K. Sharma, S. Fekete, J. Fekete, A. Simon, S. Farkas, Development of a rapid method for the determination and confirmation of nitroimidazoles in six matrices by fast liquid chromatography-tandem mass spectrometry, J Pharm Biomed Anal. 64-65 (2012) 40–48.
168. A. Tölgyesi, J. Fekete, S. Fekete, V.K. Sharma, K. Békési, E. Tóth, Analysis of sub µg/kg lincomycin in honey, muscle, milk, and eggs using fast liquid chromatography-tandem mass spectrometry, J Chromatogr Sci. 50 (2012) 190–198.

169. S. Borràs, R. Companyó, J. Guiteras, Analysis of sulfonamides in animal feeds by liquid chromatography with fluorescence detection, J Agric Food Chem. 59 (2011) 5240–5247.
170. Y. Lu, Q. Shen, Z. Dai, H. Zhang, Development of an on-line matrix solid-phase dispersion/fast liquid chromatography/tandem mass spectrometry system for the rapid and simultaneous determination of 13 sulfonamides in grass carp tissues, J Chromatogr A. 1218 (2011) 929–937.
171. A. Tölgyesi, V.K. Sharma, S. Fekete, D. Lukonics, J. Fekete, Simultaneous determination of eight corticosteroids in bovine tissues using liquid chromatography-tandem mass spectrometry, J Chromatogr B. 906 (2012) 75–84.
172. A. Tölgyesi, V.K. Sharma, J. Fekete, Development and validation of a method for determination of corticosteroids in pig fat using liquid chromatography-tandem mass spectrometry, J Chromatogr B. 879 (2011) 403–410.
173. Y. Lu, T. Zheng, X. He, X. Lin, L. Chen, Z. Dai, Rapid determination of chloramphenicol in soft-shelled turtle tissues using on-line MSPD-HPLC–MS/MS, Food Chem. 134 (2012) 533–539.
174. I. Tarcomnicu, A.L.N. van Nuijs, W. Simons, L. Bervoets, R. Blust, P.G. Jorens, et al., Simultaneous determination of 15 top-prescribed pharmaceuticals and their metabolites in influent wastewater by reversed-phase liquid chromatography coupled to tandem mass spectrometry, Talanta. 83 (2011) 795–803.
175. H. Shaaban, T. Górecki, Fast ultrahigh performance liquid chromatographic method for the simultaneous determination of 25 emerging contaminants in surface water and wastewater samples using superficially porous sub-3 µm particles as an alternative to fully porous sub-2µm particles, Talanta. 100 (2012) 80–89.
176. S. Fekete, K. Ganzler, J. Fekete, Fast and sensitive determination of Polysorbate 80 in solutions containing proteins, J Pharm Biomed Anal. 52 (2010) 672–679.
177. S. Fekete, K. Ganzler, J. Fekete, Simultaneous determination of polysorbate 20 and unbound polyethylene-glycol in protein solutions using new core-shell reversed phase column and condensation nucleation light scattering detection, J Chromatogr A. 1217 (2010) 6258–6266.
178. L. Fougère, C. Elfakir, M. Lafosse, Evaluation of a liquid chromatography method for quality control of methylated cyclodextrins, J Chromatogr A. 1277 (2013) 42–47.
179. P.D. Tzanavaras, T.D. Karakosta, P.G. Rigas, D.G. Themelis, A. Zotou, Isocratic liquid chromatographic determination of three paraben preservatives in hygiene wipes using a reversed phase core-shell narrow-bore column, Cent Eur J Chem. 10 (2012) 1459–1463.
180. F. Cacciola, P. Donato, D. Giuffrida, G. Torre, P. Dugo, L. Mondello, Ultra high pressure in the second dimension of a comprehensive two-dimensional liquid chromatographic system for carotenoid separation in red chili peppers, J Chromatogr A. 1255 (2012) 244–251.
181. M.A. Olszewska, New validated high-performance liquid chromatographic method for simultaneous analysis of ten flavonoid aglycones in plant extracts using a C18 fused-core column and acetonitrile-tetrahydrofuran gradient, J. Sep. Sci. 35 (2012) 2174–2183.
182. F. Pellati, F.P. Prencipe, D. Bertelli, S. Benvenuti, An efficient chemical analysis of phenolic acids and flavonoids in raw propolis by microwave-assisted extraction combined with high-performance liquid chromatography using the fused-core technology, J Pharm Biomed Anal. 81-82 (2013) 126–132.
183. T. Michel, E. Destandau, C. Elfakir, On-line hyphenation of centrifugal partition chromatography and high pressure liquid chromatography for the fractionation of flavonoids from Hippophaë rhamnoides L. berries, J Chromatogr A. 1218 (2011) 6173–6178.
184. H.-D. Shin, J.H. Suh, J.-H. Kim, H.-Y. Lee, H.Y. Eom, U.-Y. Kim, et al., Determination of Betaine in Fructus Lycii Using Hydrophilic Interaction Liquid Chromatography with Evaporative Light Scattering Detection, Bull. Korean Chem. Soc. 33 (2012) 553–558.
185. G. Du, H. Zhao, Y. Song, Q. Zhang, Y. Wang, Rapid simultaneous determination of isoflavones in Radix puerariae using high-performance liquid chromatography-triple quadrupole mass spectrometry with novel shell-type column, J. Sep. Sci. 34 (2011) 2576–2585.
186. J. Lee, D.-H. Yang, J.H. Suh, U. Kim, H.Y. Eom, J. Kim, et al., Species discrimination of Radix Bupleuri through the simultaneous determination of ten saikosaponins by high performance liquid chromatography with evaporative light scattering detection and electrospray ionization mass spectrometry, J Chromatogr B. 879 (2011) 3887–3895.
187. M.K. Kim, D.-H. Yang, M. Jung, E.H. Jung, H.Y. Eom, J.H. Suh, et al., Simultaneous determination of chromones and coumarins in Radix Saposhnikoviae by high performance liquid chromatography with diode array and tandem mass detectors, J Chromatogr A. 1218 (2011) 6319–6330.
188. Z. Wang, H. Hu, F. Chen, L. Zou, M. Yang, A. Wang, et al., Metabolic profiling assisted quality assessment of Rhodiola rosea extracts by high-performance liquid chromatography, Planta Med. 78 (2012) 740–746.
189. M.C. Pietrogrande, F. Dondi, A. Ciogli, F. Gasparrini, A. Piccin, M. Serafini, Characterization of new types of stationary phases for fast and ultra-fast liquid chromatography by signal processing based on AutoCovariance Function: a case study of application to Passiflora incarnata L. extract separations, J Chromatogr A. 1217 (2010) 4355–4364.
190. J. Liang, W.-Y. Wu, G.-X. Sun, D.-D. Wang, J.-J. Hou, W.-Z. Yang, et al., A dynamic multiple reaction monitoring method for the multiple components quantification of complex traditional Chinese medicine preparations: Niuhuang Shangqing pill as an example, J Chromatogr A. 1294 (2013) 58–69.
191. S. Jakabová, L. Vincze, Á. Farkas, F. Kilár, B. Boros, A. Felinger, Determination of tropane alkaloids atropine and scopolamine by liquid chromatography-mass spectrometry in plant organs of Datura species, J Chromatogr A. 1232 (2012) 295–301.
192. X. Jin, L.-Y. Zhu, H. Shen, J. Xu, S.-L. Li, X.-B. Jia, et al., Influence of sulphur-fumigation on the quality of white ginseng: a quantitative evaluation of major ginsenosides by high performance liquid chromatography, Food Chem. 135 (2012) 1141–1147.
193. X.-J. Li, H.-M. Yu, C. Gao, Y.-G. Zu, W. Wang, M. Luo, et al., Application of ionic liquid-based surfactants in the microwave-assisted extraction for the determination of four main phloroglucinols from Dryopteris fragrans, J. Sep. Sci. 35 (2012) 3600–3608.
194. Z. Wang, L. Tang, H. Hu, Y. Guo, T. Peng, F. Yan, et al., Metabolic Profiling Assisted Quality Control of Phorbolesters in Jatropha curcas Seed by High-Performance Liquid Chromatography Using a Fused-Core Column, J Agric Food Chem. 60 (2012) 9567–9572.
195. H.-J. Kwon, S.-H. Choi, C.-S. Yoo, H.-Y. Choi, S.-E. Lee, Y.-D. Park, Development of an analytical method for yam saponins using HPLC with pulsed amperometric detection at different column temperatures, J. Sep. Sci. 36 (2013) 690–698.

196. W.-D. Zhang, Y. Wang, Q. Wang, W.-J. Yang, Y. Gu, R. Wang, et al., Quality evaluation of Semen Cassiae (Cassia obtusifolia L.) by using ultra-high performance liquid chromatography coupled with mass spectrometry, J. Sep. Sci. 35 (2012) 2054–2062.
197. Q. Shen, Z. Dai, Y. Lu, Rapid determination of caffeoylquinic acid derivatives in Cynara scolymus L. by ultra-fast liquid chromatography/tandem mass spectrometry based on a fused core C18 column, J. Sep. Sci. 33 (2010) 3152–3158.
198. S.C. Farrow, R.N. Emery, Concurrent profiling of indole-3-acetic acid, abscisic acid, and cytokinins and structurally related purines by high-performance-liquid-chromatography tandem electrospray mass spectrometry, Plant Methods. 8 (2012) 42.
199. I. Ali, S.M.Z. Al-kindy, F.O. Suliman, S.D. Alam, Fast analysis of flavonoids in apple juice on new generation halo column by SPE-HPLC, Anal. Methods. 3 (2011) 2836.
200. A.M. Gómez-Caravaca, V. Verardo, M. Toselli, A. Segura-Carretero, A. Fernández-Gutiérrez, M.F. Caboni, Determination of the Major Phenolic Compounds in Pomegranate Juices by HPLC-DAD-ESI-MS, J Agric Food Chem. 61 (2013) 5328–5337.
201. B. Bayram, B. Ozcelik, G. Schultheiss, J. Frank, G. Rimbach, A validated method for the determination of selected phenolics in olive oil using high-performance liquid chromatography with coulometric electrochemical detection and a fused-core column, Food Chem. 138 (2013) 1663–1669.
202. J. La Nasa, E. Ghelardi, I. Degano, F. Modugno, M.P. Colombini, Core shell stationary phases for a novel separation of triglycerides in plant oils by high performance liquid chromatography with electrospray-quadrupole-time of flight mass spectrometer, J Chromatogr A. 1308 (2013) 114–124.
203. M.J. Lerma-García, R. Lusardi, E. Chiavaro, L. Cerretani, A. Bendini, G. Ramis-Ramos, et al., Use of triacylglycerol profiles established by high performance liquid chromatography with ultraviolet-visible detection to predict the botanical origin of vegetable oils, J Chromatogr A. 1218 (2011) 7521–7527.
204. S. Vichi, N. Cortés-Francisco, J. Caixach, Insight into virgin olive oil secoiridoids characterization by high-resolution mass spectrometry and accurate mass measurements, J Chromatogr A. 1301 (2013) 48–59.
205. J. Wu, Y. Qian, P. Mao, L. Chen, Y. Lu, H. Wang, Separation and identification of phenolic compounds in canned artichoke by LC/DAD/ESI-MS using core-shell C18 column: a comparative study, J Chromatogr B. 927 (2013) 173–180.
206. N. Manchón, M. D'Arrigo, A. García-Lafuente, E. Guillamón, A. Villares, J.A. Martínez, et al., Comparison of different types of stationary phases for the analysis of soy isoflavones by HPLC, Anal Bioanal Chem. 400 (2011) 1251–1261.
207. M.A. Rostagno, N. Manchón, M. D'Arrigo, E. Guillamón, A. Villares, A. García-Lafuente, et al., Fast and simultaneous determination of phenolic compounds and caffeine in teas, mate, instant coffee, soft drink and energetic drink by high-performance liquid chromatography using a fused-core column, Anal Chim Acta. 685 (2011) 204–211.
208. C. Fanali, A. Rocco, Z. Aturki, L. Mondello, S. Fanali, Analysis of polyphenols and methylxantines in tea samples by means of nano-liquid chromatography utilizing capillary columns packed with core-shell particles, J Chromatogr A. 1234 (2012) 38–44.
209. C. Fanali, L. Dugo, A. Rocco, Nano-liquid chromatography in nutraceutical analysis: Determination of polyphenols in bee pollen, J Chromatogr A. (2013).
210. P. Cesla, T. Hájek, P. Jandera, Optimization of two-dimensional gradient liquid chromatography separations, J Chromatogr A. 1216 (2009) 3443–3457.
211. Y. Lu, Q. Shen, Z. Dai, Multiwalled carbon nanotubes as sorbent for online solid-phase extraction of resveratrol in red wines prior to fused-core C18-based ultrahigh-performance liquid chromatography-tandem mass spectrometry quantification, J Agric Food Chem. 59 (2011) 70–77.
212. D.C. Manns, A.K. Mansfield, A core-shell column approach to a comprehensive high-performance liquid chromatography phenolic analysis of Vitis vinifera L. and interspecific hybrid grape juices, wines, and other matrices following either solid phase extraction or direct injection, J Chromatogr A. 1251 (2012) 111–121.
213. P. Dugo, A. Piperno, R. Romeo, M. Cambria, M. Russo, C. Carnovale, et al., Determination of oxygen heterocyclic components in citrus products by HPLC with UV detection, J Agric Food Chem. 57 (2009) 6543–6551.
214. J.M.A. Gavina, J. Priem, C.M. Wood, C.W. Xiao, Y.-L. Feng, Determination of isoflavones in rat serum using liquid chromatography-tandem mass spectrometry with a highly efficient core-shell column, Anal Bioanal Chem. 405 (2013) 2643-2651.
215. J.G. McDonald, D.D. Smith, A.R. Stiles, D.W. Russell, A comprehensive method for extraction and quantitative analysis of sterols and secosteroids from human plasma, J. Lipid Res. 53 (2012) 1399–1409.
216. P. Chocholouš, J. Vacková, I. Šrámková, D. Šatínský, P. Solich, Advantages of core–shell particle columns in Sequential Injection Chromatography for determination of phenolic acids, Talanta. 103 (2012) 221–227.
217. K.K. Jessing, R.K. Juhler, B.W. Strobel, Monitoring of artemisinin, dihydroartemisinin, and artemether in environmental matrices using high-performance liquid chromatography-tandem mass spectrometry (LC-MS/MS), J Agric Food Chem. 59 (2011) 11735–11743.
218. F. Wode, C. Reilich, P. van Baar, U. Dünnbier, M. Jekel, T. Reemtsma, Multiresidue analytical method for the simultaneous determination of 72 micropollutants in aqueous samples with ultra high performance liquid chromatography-high resolution mass spectrometry, J Chromatogr A. 1270 (2012) 118–126.
219. J.P. Benskin, M.G. Ikonomou, M.B. Woudneh, J.R. Cosgrove, Rapid characterization of perfluoralkyl carboxylate, sulfonate, and sulfonamide isomers by high-performance liquid chromatography-tandem mass spectrometry, J Chromatogr A. 1247 (2012) 165–170.
220. G. Vinci, M.L. Antonelli, R. Preti, Rapid determination of polycyclic aromatic hydrocarbons in rainwater by liquid-liquid microextraction and LC with core-shell particles column and fluorescence detection, J. Sep. Sci. 36 (2013) 461–468.
221. D. Shang, M. Kim, M. Haberl, A. Legzdins, Development of a rapid liquid chromatography tandem mass spectrometry method for screening of trace naphthenic acids in aqueous environments, J Chromatogr A. 1278 (2013) 98–107.
222. H. Gallart-Ayala, E. Moyano, M.T. Galceran, Analysis of bisphenols in soft drinks by on-line solid phase extraction fast liquid chromatography-tandem mass spectrometry, Anal Chim Acta. 683 (2011) 227–233.
223. H. Gallart-Ayala, E. Moyano, M.T. Galceran, Fast liquid chromatography-tandem mass spectrometry for the analysis of bisphenol A-diglycidyl ether, bisphenol F-diglycidyl ether and their derivatives in canned food and beverages, J Chromatogr A. 1218 (2011) 1603–1610.
224. J. Wang, W. Chow, W. Cheung, Application of a tandem mass spectrometer and core-shell particle column for the determination of 151 pesticides in grains, J Agric Food Chem. 59 (2011) 8589–8608.

225. Y.-C. Chang, W.-L. Chen, F.-Y. Bai, P.-C. Chen, G.-S. Wang, C.-Y. Chen, Determination of perfluorinated chemicals in food and drinking water using high-flow solid-phase extraction and ultra-high performance liquid chromatography/tandem mass spectrometry, Anal Bioanal Chem. 402 (2012) 1315–1325.
226. S.J. Allen, L.S. Ott, HPLC method for rapidly following biodiesel fuel transesterification reaction progress using a core-shell column, Anal Bioanal Chem. 404 (2012) 267–272.
227. A. Micó-Tormos, C. Collado-Soriano, J.R. Torres-Lapasió, E. Simó-Alfonso, G. Ramis-Ramos, Determination of fatty alcohol ethoxylates by derivatisation with maleic anhydride followed by liquid chromatography with UV-vis detection, J Chromatogr A. 1180 (2008) 32–41.
228. M.J. Roth, D.A. Plymire, A.N. Chang, J. Kim, E.M. Maresh, S.E. Larson, et al., Sensitive and reproducible intact mass analysis of complex protein mixtures with superficially porous capillary reversed-phase liquid chromatography mass spectrometry, Anal Chem. 83 (2011) 9586–9592.
229. Q. Wang, N.A. Lacher, B.K. Muralidhara, M.R. Schlittler, S. Aykent, C.W. Demarest, Rapid and refined separation of human IgG2 disulfide isomers using superficially porous particles, J. Sep. Sci. 33 (2010) 2671–2680.
230. P. Puchalska, M.L. Marina, M.C. García, Development of a reversed-phase high-performance liquid chromatography analytical methodology for the determination of antihypertensive peptides in maize crops, J Chromatogr A. 1234 (2012) 64–71.
231. S.A. Schuster, B.E. Boyes, B.M. Wagner, J.J. Kirkland, Fast high performance liquid chromatography separations for proteomic applications using Fused-Core® silica particles, J Chromatogr A. 1228 (2012) 232–241.
232. J. De Vos, C. Stassen, A. Vaast, G. Desmet, S. Eeltink, High-resolution separations of tryptic digest mixtures using core-shell particulate columns operated at 1200bar, J Chromatogr A. 1264 (2012) 57–62.
233. E. Domínguez-Vega, O. Kotkowska, M.C. García, A.L. Crego, M.L. Marina, Fast determination of the functional peptide soymetide in different soybean derived foods by capillary-high performance liquid chromatography, J Chromatogr A. 1218 (2011) 4928–4933.
234. K. Takahashi, M. Tokuoka, H. Kohno, N. Sawamura, Y. Myoken, A. Mizuno, Comprehensive analysis of dipeptides in alcoholic beverages by tag-based separation and determination using liquid chromatography/electrospray ionization tandem mass spectrometry and quadrupole-time-of-flight mass spectrometry, J Chromatogr A. 1242 (2012) 17–25.
235. N. Marchetti, J.N. Fairchild, G. Guiochon, Comprehensive off-line, two-dimensional liquid chromatography. Application to the separation of peptide digests, Anal Chem. 80 (2008) 2756–2767.
236. C. Barton, R.G. Kay, W. Gentzer, F. Vitzthum, S. Pleasance, Development of high-throughput chemical extraction techniques and quantitative HPLC-MS/MS (SRM) assays for clinically relevant plasma proteins, J. Proteome Res. 9 (2010) 333–340.
237. M.E. Lassman, T.M. McLaughlin, E.P. Somers, A.C. Stefanni, Z. Chen, B.A. Murphy, et al., A rapid method for cross-species quantitation of apolipoproteins A1, B48 and B100 in plasma by ultra-performance liquid chromatography/tandem mass spectrometry, Rapid Commun. Mass Spectrom. 26 (2012) 101–108.
238. M. Beneito-Cambra, J.M. Herrero-Martínez, G. Ramis-Ramos, W. Lindner, M. Lämmerhofer, Comparison of monolithic and microparticulate columns for reversed-phase liquid chromatography of tryptic digests of industrial enzymes in cleaning products, J Chromatogr A. 1218 (2011) 7275–7280.
239. A.L. May, M.E. Eisenhauer, K.S. Coulston, S.R. Campagna, Detection and quantitation of bacterial acyl-homoserine lactone quorum sensing molecules via liquid chromatography-isotope dilution tandem mass spectrometry, Anal Chem. 84 (2012) 1243–1252.
240. F. Gritti, M.-A. Perdu, G. Guiochon, Gradient HPLC of samples extracted from the green microalga Botryococcus braunii using highly efficient columns packed with 2.6 µm Kinetex core-shell particles, J Chromatogr A. 1229 (2012) 148–155.
241. M. Biermann, B. Bardl, S. Vollstädt, J. Linnemann, U. Knüpfer, G. Seidel, et al., Simultaneous analysis of the non-canonical amino acids norleucine and norvaline in biopharmaceutical-related fermentation processes by a new ultra-high performance liquid chromatography approach, Amino Acids. 44 (2013) 1225–1231.
242. I. Yang, M.C. Fortin, J.R. Richardson, B. Buckley, Fused-core silica column ultra-performance liquid chromatography-ion trap tandem mass spectrometry for determination of global DNA methylation status, Anal Biochem. 409 (2011) 138–143.
243. L. Fismen, T. Eide, R. Djurhuus, A.M. Svardal, Simultaneous quantification of tetrahydrobiopterin, dihydrobiopterin, and biopterin by liquid chromatography coupled electrospray tandem mass spectrometry, Anal Biochem. 430 (2012) 163–170.
244. R. Nirogi, P. Komarneni, V. Kandikere, R. Boggavarapu, G. Bhyrapuneni, V. Benade, et al., A sensitive and selective quantification of catecholamine neurotransmitters in rat microdialysates by pre-column dansyl chloride derivatization using liquid chromatography–tandem mass spectrometry, J Chromatogr B. 913-914 (2013) 41–47.
245. R.-I. Chirita, A.-L. Finaru, C. Elfakir, Evaluation of fused-core and monolithic versus porous silica-based C18 columns and porous graphitic carbon for ion-pairing liquid chromatography analysis of catecholamines and related compounds, J Chromatogr B. 879 (2011) 633–640.
246. C.-H. Tang, P.-N. Tsao, C.-Y. Lin, L.-S. Fang, S.-H. Lee, W.-H. Wang, Phosphorylcholine-containing lipid molecular species profiling in biological tissue using a fast HPLC/QqQ-MS method, Anal Bioanal Chem. 404 (2012) 2949–2961.
247. M.J. Bogusz, E. Al Enazi, M. Tahtamoni, J.A. Jawaad, M. Al Tufail, Determination of serum vitamins 25-OH-D2 and 25-OH-D3 with liquid chromatography-tandem mass spectrometry using atmospheric pressure chemical ionization or electrospray source and core-shell or sub-2 µm particle columns: a comparative study, Clin Biochem. 44 (2011) 1329–1337.
248. S. Baecher, A. Leinenbach, J.A. Wright, S. Pongratz, U. Kobold, R. Thiele, Simultaneous quantification of four vitamin D metabolites in human serum using high performance liquid chromatography tandem mass spectrometry for vitamin D profiling, Clin Biochem. 45 (2012) 1491–1496.
249. M. Sergi, N. Battista, C. Montesano, R. Curini, M. Maccarrone, D. Compagnone, Determination of the two major endocannabinoids in human plasma by µ-SPE followed by HPLC-MS/MS, Anal Bioanal Chem. 405 (2013) 785–793.
250. E. Hinchliffe, S. Carter, L.J. Owen, B.G. Keevil, Quantitation of aldosterone in human plasma by ultra high performance liquid chromatography tandem mass spectrometry, J Chromatogr B. 913-914 (2013) 19–23.
251. S. Studzinska, B. Buszewski, A new way to fast and high resolution determination of modified nucleosides, J Chromatogr B. 887-888 (2012) 93–101.

252. N. Grebenstein, J. Frank, Rapid baseline-separation of all eight tocopherols and tocotrienols by reversed-phase liquid-chromatography with a solid-core pentafluorophenyl column and their sensitive quantification in plasma and liver, J Chromatogr A. 1243 (2012) 39–46.
253. J. Plíšek, M. Kašparová, D. Solichová, L. Krcmová, B. Kucerová, L. Sobotka, et al., Application of core-shell technology for determination of retinol and alpha-tocopherol in breast milk, Talanta. 107 (2013) 382–388.
254. C.M. Benton, C.K. Lim, C. Moniz, D.J.L. Jones, Ultra high-performance liquid chromatography of porphyrins in clinical materials: column and mobile phase selection and optimisation, Biomed Chromatogr. 26 (2012) 714–719.
255. L. Whiley, J. Godzien, F.J. Ruperez, C. Legido-Quigley, C. Barbas, In-vial dual extraction for direct LC-MS analysis of plasma for comprehensive and highly reproducible metabolic fingerprinting, Anal Chem. 84 (2012) 5992–5999.
256. M. Ibáñez-Vea, L.A. Corcuera, R. Remiro, M.T. Murillo-Arbizu, E. González-Peñas, E. Lizarraga, Validation of a UHPLC-FLD method for the simultaneous quantification of aflatoxins, ochratoxin A and zearalenone in barley, Food Chem. 127 (2011) 351–358.
257. M. Suman, E. Bergamini, D. Catellani, A. Manzitti, Development and validation of a liquid chromatography/linear ion trap mass spectrometry method for the quantitative determination of deoxynivalenol-3-glucoside in processed cereal-derived products, Food Chem. 136 (2013) 1568–1576.
258. A. Tölgyesi, Z. Kunsági, Quantification of T-2 and HT-2 mycotoxins in cereals by liquid chromatography-multimode ionization-tandem mass spectrometry, Microchem J. 106 (2012) 300–306.
259. J. Mao, S. Lei, X. Yang, D. Xiao, Quantification of ochratoxin A in red wines by conventional HPLC–FLD using a column packed with core–shell particles, Food Control. 32 (2013) 505–511.
260. S.L. DeGrasse, J.A. DeGrasse, K. Reuter, Solid core column technology applied to HPLC-FD of paralytic shellfish toxins, Toxicon. 57 (2011) 179–182.
261. R.G. Hatfield, A.D. Turner, Rapid Liquid Chromatography for Paralytic Shellfish Toxin Analysis Using Superficially Porous Chromatography with AOAC Official MethodSM 2005.06, J AOAC Int. 95 (2012) 1089–1096.
262. T. Hayama, K. Katoh, T. Aoki, M. Itoyama, K. Todoroki, H. Yoshida, et al., Liquid chromatographic determination of microcystins in water samples following pre-column excimer fluorescence derivatization with 4-(1-pyrene)butanoic acid hydrazide, Anal Chim Acta. 755 (2012) 93–99.
263. S.D. Penchala, J. Tjia, O. El Sherif, D.J. Back, S.H. Khoo, L.J. Else, Validation of an electrospray ionisation LC-MS/MS method for quantitative analysis of telaprevir and its R-diastereomer, J Chromatogr B. 932 (2013) 100–110.
264. A. Tölgyesi, V.K. Sharma, J. Fekete, Confirmatory analysis of stanozolol metabolites in bovine, pig and sheep urines using an optimized clean-up and liquid chromatography-tandem mass spectrometry, J Pharm Biomed Anal. 88C (2013) 45–52.
265. M. Giorgi, T.-W. Kim, A. Saba, M.-R. Rouini, H. Yun, R. Ryschanova, et al., Detection and quantification of cimicoxib, a novel COX-2 inhibitor, in canine plasma by HPLC with spectrofluorimetric detection: development and validation of a new methodology, J Pharm Biomed Anal. 83 (2013) 28–33.
266. R.R. Taylor, K.L. Hoffman, B. Schniedewind, C. Clavijo, J.L. Galinkin, U. Christians, Comparison of the quantification of acetaminophen in plasma, cerebrospinal fluid and dried blood spots using high-performance liquid chromatography-tandem mass spectrometry, J Pharm Biomed Anal. 83 (2013) 1–9.
267. M.T. Furlong, I. Savant, M. Yuan, L. Scott, W. Mylott, T. Mariannino, et al., A validated HPLC-MS/MS assay for quantifying unstable pharmacologically active metabolites of clopidogrel in human plasma: application to a clinical pharmacokinetic study, J Chromatogr B. 926 (2013) 36–41.
268. H.-R. Lin, C.-L. Chen, C.-L. Huang, S.-T. Chen, A.-C. Lua, Simultaneous determination of opiates, methadone, buprenorphine and metabolites in human urine by superficially porous liquid chromatography tandem mass spectrometry, J Chromatogr B. 925 (2013) 10–15.
269. A. Wohlfarth, K.B. Scheidweiler, X. Chen, H.-F. Liu, M.A. Huestis, Qualitative confirmation of 9 synthetic cannabinoids and 20 metabolites in human urine using LC-MS/MS and library search, Anal Chem. 85 (2013) 3730–3738.
270. K.B. Scheidweiler, S.K. Himes, X. Chen, H.-F. Liu, M.A. Huestis, 11-Nor-9-carboxy-Δ9-tetrahydrocannabinol quantification in human oral fluid by liquid chromatography-tandem mass spectrometry, Anal Bioanal Chem. 405 (2013) 6019–6027.
271. B.R. Chandu, K. Kanala, N.T. Hwisa, P. Katakam, M. Khagga, Bioequivalance and pharmacokinetic study of febuxostat in human plasma by using LC-MS/MS with liquid liquid extraction method, Springerplus. 2 (2013) 194.
272. N. Nakov, K. Mladenovska, N. Labacevski, A. Dimovski, R. Petkovska, A. Dimitrovska, et al., Development and validation of automated SPE-LC-MS/MS method for determination of indapamide in human whole blood and its application to real study samples, Biomed Chromatogr. (2013).
273. R. Upreti, N.Z.M. Homer, G. Naredo, D.F. Cobice, K.A. Hughes, L.H. Stewart, et al., Measurement of tamsulosin in human serum by liquid chromatography-tandem mass spectrometry, J Chromatogr B. 930 (2013) 121–128.
274. M. Hroch, S. Micuda, J. Cermanová, J. Chládek, P. Tomšík, Development of an HPLC fluorescence method for determination of boldine in plasma, bile and urine of rats and identification of its major metabolites by LC-MS/MS, J Chromatogr B. 936 (2013) 48–56.
275. L. Silvestro, I. Tarcomnicu, C. Dulea, N.R.B.N. Attili, V. Ciuca, D. Peru, et al., Confirmation of diosmetin 3-O-glucuronide as major metabolite of diosmin in humans, using micro-liquid-chromatography–mass spectrometry and ion mobility mass spectrometry, Anal Bioanal Chem. (2013).
276. L. Yao, S. Zheng, Y. Guan, J. Yang, B. Liu, W. Wang, et al., Development of a rapid method for the simultaneous separation and determination of 4-(methylnitrosamino)-1-(3-pyridyl)-1-butanol and its N- and O-glucuronides in human urine by liquid chromatography-tandem mass spectrometry, Anal Chim Acta. 788 (2013) 61–67.
277. E.J. Choi, S.H. Bae, J.B. Park, M.J. Kwon, S.M. Jang, Y.F. Zheng, et al., Simultaneous quantification of caffeine and its three primary metabolites in rat plasma by liquid chromatography-tandem mass spectrometry, Food Chem. 141 (2013) 2735–2742.
278. S. Suleman, K. Vandercruyssen, E. Wynendaele, M. D'Hondt, N. Bracke, L. Duchateau, et al., A rapid stability-indicating, fused-core HPLC method for simultaneous determination of β-artemether and lumefantrine in anti-malarial fixed dose combination products, Malar. J. 12 (2013) 145.
279. P. Kubica, A. Kot-Wasik, A. Wasik, J. Namiesnik, "Dilute & shoot" approach for rapid determination of trace amounts of nicotine in zero-level e-liquids by reversed phase liquid chromatography and hydrophilic interactions liquid chromatography coupled

with tandem mass spectrometry-electrospray ionization, J Chromatogr A. 1289 (2013) 13–18.

280. I. Brabcová, M. Hlavácková, D. Šatínský, P. Solich, A rapid HPLC column switching method for sample preparation and determination of β-carotene in food supplements, Food Chem. 141 (2013) 1433–1437.

281. E. Sommella, G. Pepe, F. Pagano, G.C. Tenore, P. Dugo, M. Manfra, et al., Ultra high performance liquid chromatography with ion-trap TOF-MS for the fast characterization of flavonoids in *Citrus bergamia* juice, J. Sep. Sci. 36 (2013) 3351-3355.

282. C. Tamames-Tabar, E. Imbuluzqueta, M.A. Campanero, P. Horcajada, M.J. Blanco-Prieto, A simple and robust high-performance liquid chromatography coupled to a diode-array detector method for the analysis of genistein in mouse tissues, J Chromatogr B. 935 (2013) 47–53.

283. N. Manchón, M. D'Arrigo, A. García-Lafuente, E. Guillamón, A. Villares, A. Ramos, et al., Fast analysis of isoflavones by high-performance liquid chromatography using a column packed with fused-core particles, Talanta. 82 (2010) 1986–1994.

284. P.G. Stevenson, D.N. Bassanese, N.W. Barnett, X.A. Conlan, Improved 2-D HPLC of Red Wine by incorporating pre-process signal smoothing algorithms, J. Sep. Sci. 36 (2013) 21-22.

285. I. Cvetkovikj, G. Stefkov, J. Acevska, J.P. Stanoeva, M. Karapandzova, M. Stefova, et al., Polyphenolic characterization and chromatographic methods for fast assessment of culinary Salvia species from South East Europe, J Chromatogr A. 1282 (2013) 38–45.

286. B. Simonovska, I. Vovk, V. Glavnik, K. CerneliC, Effects of extraction and high-performance liquid chromatographic conditions on the determination of lutein in spinach, J Chromatogr A. 1276 (2013) 95–101.

287. W.-D. Zhang, P.-Y. Wang, Y. Wang, Q. Wang, Y. Gu, J. Cao, et al., Simultaneous determination of aurantio-obtusin, chrysoobtusin, obtusin and 1-desmethylobtusin in rat plasma by UHPLC-MS/MS, Biomed Chromatogr. 28 (2014) 369-374.

288. H. Kushida, M. Fukutake, M. Tabuchi, T. Katsuhara, H. Nishimura, Y. Ikarashi, et al., Simultaneous quantitative analyses of indole and oxindole alkaloids of Uncaria Hook in rat plasma and brain after oral administration of the traditional Japanese medicine Yokukansan using high-performance liquid chromatography with tandem mass spectrometry, Biomed Chromatogr. 27 (2013) 1647-1656.

289. Y. Ling, Z. Li, M. Chen, Z. Sun, M. Fan, C. Huang, Analysis of Multiple Constituents in Cong-Ming-Tang, a Chinese Herbal Formula for the Treatment of Amnesia, by High-performance Liquid Chromatography with Quadrupole Time-of-flight Mass Spectrometry, Phytochem. Anal. 24 (2013) 677-688.

290. C. Gröer, S. Brück, Y. Lai, A. Paulick, A. Busemann, C.D. Heidecke, et al., LC-MS/MS-based quantification of clinically relevant intestinal uptake and efflux transporter proteins, J Pharm Biomed Anal. 85 (2013) 253–261.

291. K.P. Yáñez, J.L. Bernal, M.J. Nozal, M.T. Martín, J. Bernal, Determination of seven neonicotinoid insecticides in beeswax by liquid chromatography coupled to electrospray-mass spectrometry using a fused-core column, J Chromatogr A. 1285 (2013) 110–117.

292. J. Han, V. Tschernutter, J. Yang, T. Eckle, C.H. Borchers, Analysis of selected sugars and sugar phosphates in mouse heart tissue by reductive amination and liquid chromatography-electrospray ionization mass spectrometry, Anal Chem. 85 (2013) 5965–5973.

7

Recursos para mejorar la sostenibilidad de la etapa de pretratamiento de las muestras

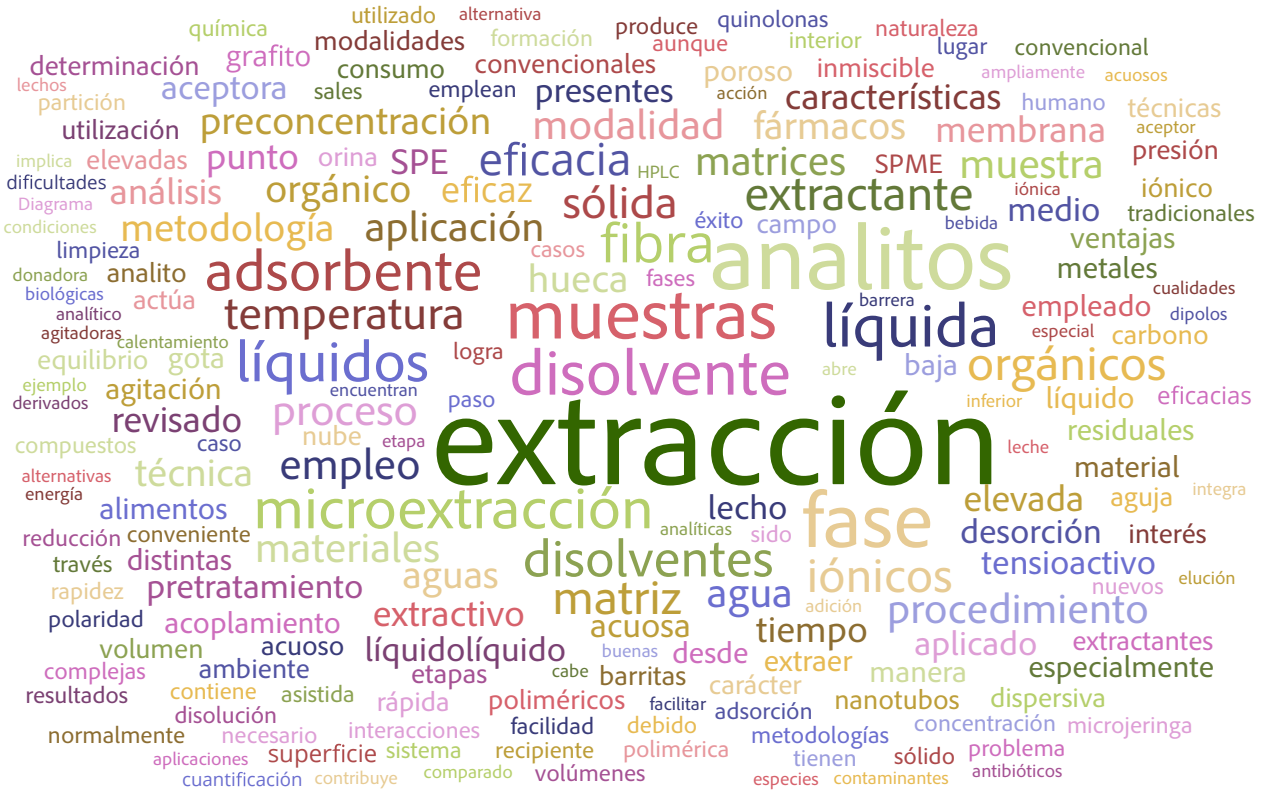

Nube de palabras que representa el número de veces que un término aparece en este capítulo

A pesar de los considerables avances que se han producido en la técnicas analíticas durante las últimas décadas, la mayoría de ellas requieren de un procedimiento previo de limpieza, extracción y, en muchos casos, pre-concentración de los analitos de interés. Estos procedimientos han de seleccionarse cuidadosamente atendiendo a las características de los analitos a determinar, a la matriz en la que se encuentran y a la técnica analítica elegida para la cuantificación.

Los métodos que podríamos denominar convencionales, como la extracción líquido-líquido (LLE) o la extracción en fase sólida (SPE), son ampliamente utilizados, si bien, poco a poco, otras metodologías [1] que proporcionan resultados reproducibles en tiempos cortos se van abriendo camino con gran pujanza. Tobiszewski *et al.* [2] han revisado los distintos métodos de preparación y pre-tratamiento de las muestras con un claro enfoque hacia las metodologías analíticas en las que se aplican los principios de la química verde. Centrándose en al análisis inorgánico, Rocha *et al.* [3] han revisado distintas estrategias sostenibles para la preparación de las muestras.

La utilización de los denominados "nuevos materiales" como el grafeno, los fulerenos y los líquidos orgánicos poliméricos como materiales adsorbentes en los procedimientos de extracción y pre-tratamiento de las muestras, abre nuevos caminos hacia la reducción de los disolventes nocivos en esta etapa del análisis [4] (Figura 1).

1. Extracción en fase sólida (SPE)

Esta modalidad de extracción está muy difundida por sus características de versatilidad,

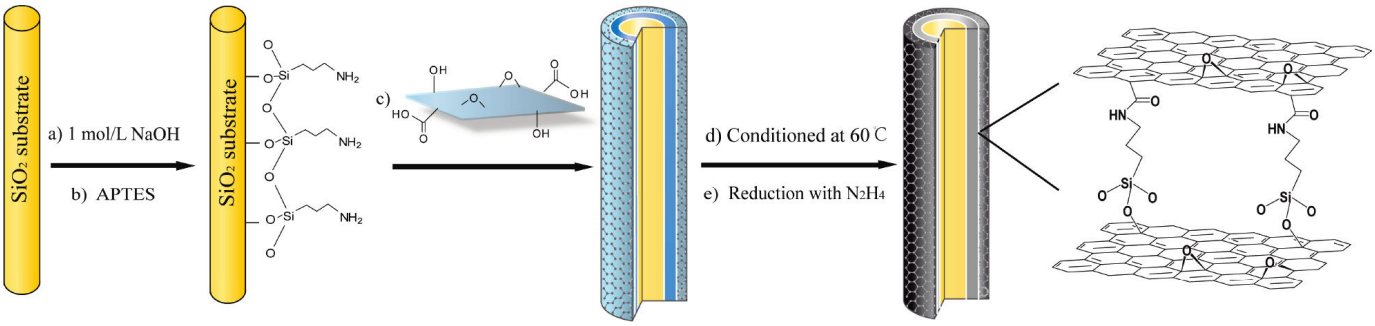

Figura 1. Fibra de microextracción en fase sólida recubierta con grafeno [4].

reproducibilidad y, muy especialmente, por su potencial analítico, ya que puede acoplarse a otras técnicas de pre-tratamiento logrando una sinergia en el proceso que permite elevadas recuperaciones de los analitos incluso en matrices muy complejas.

Este procedimiento de extracción se basa en la retención electiva de los analitos sobre un soporte sólido adsorbente y se lleva a cabo en varias etapas. Se comienza con un acondicionamiento del lecho extractante, seguido de las etapas de cargado de la muestra, lavado de interferencias y elución del analito de interés (Figura 2). A día de hoy, se comercializa una gran variedad de materiales adsorbentes susceptibles de retener los analitos mediante muy diversos mecanismos de interacción, tales como enlaces de hidrógeno, interacciones por fuerzas de Van der Waals, interacciones hidrofóbicas, interacciones π-π, así como procesos de intercambio iónico (aniónico o catiónico). Una de las ventajas del empleo de resinas intercambiadoras de iones es que evita las incompatibilidades propias del empleo de lechos extractantes de una polaridad concreta (elevada o baja). En tales casos, se emplean disolventes para la elución de los analitos que generalmente presentan serias dificultades de compatibilidad con las fases móviles en HPLC, lo que dificulta su acoplamiento "on-line". Un ejemplo reciente del acoplamiento de SPE a HPLC con detección fluorimétrica ha sido aplicado para la determinación de quinolonas en aguas de bebida y en orina humana [5].

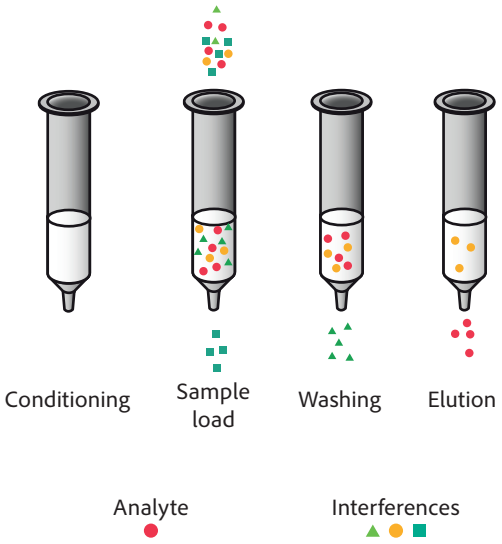

Figura 2. Esquema de las etapas en el proceso de extracción en fase sólida (SPE) [57].

Adoptando las características propias de la SPE se pueden utilizar otros materiales adsorbentes altamente selectivos, como es el caso de los polímeros impresos (MIP, *molecularly imprinted polymers*) que amplían el potencial analítico de la técnica [6]. De ese modo, se ha podido extraer con una gran eficacia diclofenaco de muestra de aguas residuales [7]. La utilización de MIP como metodología selectiva de pre-tratamiento de las muestras y concentración de los analitos abre nuevos campos de aplicación combinados con la cromatografía de líquidos empleando columnas monolíticas [8].

Además de los soportes tradicionales (sílica, sílicas modificadas, materiales adsorbentes de grafito poroso, materiales adsorbentes poliméricos) en los últimos años se han introducido líquidos iónicos inmovilizados en sílica o bien enlazados a soportes poliméricos como nuevos lechos extractantes para SPE. Estos materiales se han aplicado con una buena eficacia a la extracción de contaminantes orgánicos de muestras de interés mediambiental, metales en muestras de agua y a la obtención de muy diversos extractos vegetales [9].

Manteniendo la eficacia de extracción propia de la SPE se pueden alcanzar resultados satisfactorios en matrices complejas (por ejemplo, análisis de medicamentos en muestras de aguas residuales) gracias al acoplamiento de la SPE con otras técnicas de extracción.

1.1. Extracción asistida con ultrasonidos (UAE)-SPE

La energía de las ondas ultrasónicas provoca en el interior de la disolución el fenómeno denominado cavitación, generando temperaturas y presiones localmente elevadas, acompañadas de sus correspondientes gradientes y dando lugar a la formación de las denominadas "manchas calientes" que facilitan la rápida extracción de los analitos de las matrices sólidas. Asimismo, los ultrasonidos facilitan la dispersión del extractante orgánico en un medio mayoritariamente acuoso gracias a la formación de pequeñas vesículas que conllevan una elevada eficacia de extracción. Esta modalidad resulta particularmente conveniente cuando se trata de extraer

analitos lábiles, ya que la extracción se realiza a temperatura ambiente y en un periodo de tiempo muy corto. Esta técnica se ha utilizado con gran éxito para la extracción de medicamentos en sedimentos de plantas de tratamiento de aguas residuales [10].

1.2. Ultrafiltración-SPE

Este acoplamiento es especialmente útil cuando se requiere la preconcentración de los analitos debido a su extremadamente baja concentración en las muestras. Es un procedimiento especialmente eficaz para la aplicación a muestras biológicas o en matrices de alimentos donde la ultrafiltración posibilita la rápida separación de las macromoléculas de pesos moleculares elevados (proteínas, polisacáridos), por lo que se ha aplicado a la determinación de fármacos en saliva [11].

1.3. Extracción asistida con microondas-SPE (MAE-SPE)

Este acoplamiento es el más difundido para la extracción de analitos en matrices sólidas por su eficacia y rapidez [12]. El calentamiento por acción de las microondas se produce gracias a la interacción del campo electromagnético con los dipolos, las moléculas polares y las partículas cargadas presentes en las muestras objeto de análisis. Estas especies absorben la energía a través de dos mecanismos: conductancia iónica y rotación de los dipolos, incrementando el rendimiento del proceso de extracción debido al calentamiento rápido de las muestras. Esta metodología supone una reducción en el consumo de disolventes orgánicos (25-50 mL) y en el tiempo de análisis por muestra. Los resultados obtenidos con esta metodología se han comparado críticamente con los conseguidos por la extracción Soxhlet [13].

2. Micro-extracción en fase sólida (SPME)

Esta modalidad de extracción reúne todas las características de sostenibilidad, ya que además de requerir un mínimo empleo de disolventes orgánicos, integra los procesos de extracción, pre-concentración y limpieza en un solo paso. El volumen de muestra requerido para el proceso de extracción es de unos pocos microlitros. Los analitos se distribuyen entre la muestra y la superficie adsorbente de una fibra sólida de naturaleza polimérica que se dispone sobre la aguja de una jeringa [14].

Con la finalidad de extraer los analitos, la aguja que soporta la fibra polimérica se introduce en la disolución problema y, una vez transcurrido el tiempo necesario para la extracción, se retrae la aguja y se procede a la desorción térmica o química de los analitos. Se ha de tener especial precaución en la manipulación de las fibras, ya que pueden romperse con facilidad, así como en la elección del disolvente orgánico para la desorción, puesto que no todos los recubrimientos poliméricos son compatibles con aquéllos. En general, se recomienda trabajar a temperatura ambiente, lo que implica que el proceso de adsorción puede resultar lento. La aplicación de esta metodología en el campo de la farmacología, la toxicología y, en general, del ámbito clínico [15] se ha revisado en profundidad. Asimismo, ha demostrado ser de gran utilidad para la extracción de componentes explosivos [16] y de anti-inflamatorios en diversas matrices (suero humano, agua...) [17].

La SPME puede ser utilizada en los denominados formatos de alto rendimiento, bien sea en los sistemas adorbentes multipocillo, o bien en las configuraciones de “thin-film” o “in-tip”. Además del elevado número de muestras que pueden procesarse en tiempos reducidos, cabe señalar sus características idóneas para la extracción de analitos de matrices complejas (sangre completa) o de elevada viscosidad que suponen serias dificultades de aplicación en el caso de la SPME convencional. Su aplicación en clínica puede decirse que está ampliamente extendida [18].

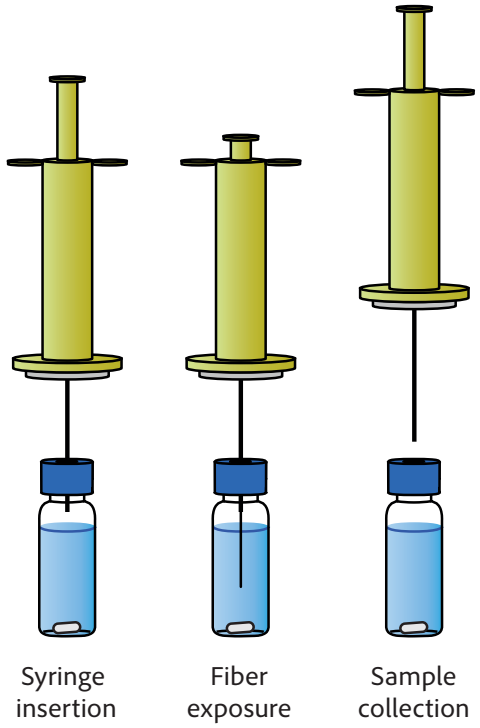

Figura 3.
Esquema del procedimiento de microextracción en fase sólida [57].

3. Extracción dispersiva en fase sólida (dispersive SPE)

La más popular aplicación de la extracción dispersiva en fase sólida es la metodología conocida con el nombre de QuEChERS, denominada así por sus cualidades de rapidez, facilidad, economía, efectividad, resistencia y seguridad (Quick, Easy, Cheap, Effective, Rugged and Safe). Esta modalidad de extracción implica dos etapas. En

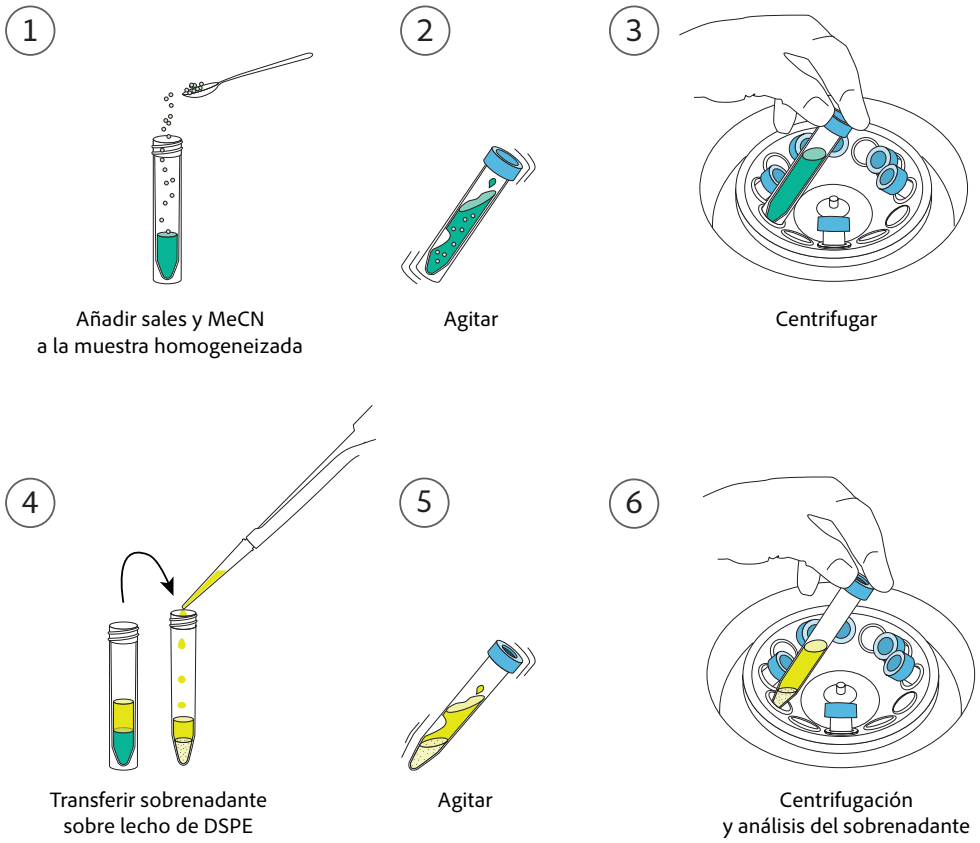

Figura 4. Resumen de los pasos fundamentales en la extracción usando QuEChERS. En este caso el adsorbente retira interferentes del sobrenadante que contiene el analito.

la primera tiene lugar la extracción de los analitos gracias al equilibrio de distribución de éstos entre una fase acuosa y una fase orgánica en la que el efecto salino por incremento de la fuerza iónica es determinante. En la segunda etapa tiene lugar la eliminación de interferentes en un lecho extractante sólido, pudiendo utilizarse combinaciones de sulfato de magnesio con distintos adsorbentes (C-18, amino, grafito) (Figura 4). Este sistema de extracción está muy extendido en el análisis medioambiental de pesticidas, pero también se ha empleado para la extracción y purificación de varios tipos de residuos de fármacos en alimentos, entre ellos diversos antibióticos [19,20], como cefalosporinas [21], quinolonas en leche [22], quinolonas en miel, jalea real y própolis [23]. Otros compuestos como micotoxinas presentes en la leche del cardo mariano también se han determinado de manera eficaz mediante esta metodología [24].

4. Extracción con barras agitadoras adsorbentes (SBSE)

Ésta es una técnica de extracción en fase sólida en la que el lecho adsorbente no está situado en vertical (en una pequeña columna, SPE, o en una aguja, SPME). Normalmente se emplean barritas de hierro, de unos 4 cm de longitud que están recubiertas con el material polimérico adsorbente (polar o apolar), a elegir según la polaridad de los analitos a extraer. Estas barritas agitadoras se introducen en el recipiente que contiene la muestra y se ponen en agitación para facilitar el que se alcance de forma rápida el equilibrio de partición de los analitos entre la matriz líquida y el lecho extractante sólido. Una vez adsorbidos los analitos y, por tanto, finalizada la extracción, se sacan las barritas de la matriz líquida y se procede a la desorción bien mediante un volumen reducido de un disolvente apropiado, o bien, mediante desorción térmica en el caso analitos volátiles.

Esta aproximación se ha utilizado para la extracción de fármacos de muestras de agua dulce (ríos, lagos) [25]. Recientemente, se han preparado barritas de sílice recubiertas con β-ciclodextrina como nuevo material adsorbente para la extracción de compuestos fenólicos de muestras de agua [26].

5. Extracción por adición de adsorbentes sobre matrices líquidas

Basándose en principios similares a los descritos en los apartados precedentes, pueden utilizarse otros materiales como discos adsorbentes, en los que el lecho extractante es un material poroso que se atrapa entre dos filtros de fibra de vidrio y se hace pasar la matriz líquida a través de ellos a un caudal relativamente rápido. Los analitos quedan retenidos selectivamente en el material poroso. También se puede embeber el lecho adsorbente en una película de teflón poroso.

El empleo de nanotubos de carbono para la retención y extracción de analitos de baja polaridad de medios acuosos suscita un gran interés debido a su gran superficie adsorbente y a sus características estructurales. Se pueden agrupar en dos categorías según estén formados por una lámina de grafito enrollada sobre si misma (monocapa) o por varias láminas de grafito enrolladas también sobre si mismas (multicapa). Tienen un amplio campo de aplicación desde la extracción de fármacos en muestras de agua mediante nanotubos de carbono multicapa [27] hasta la adsorción de metales pesados para su determinación mediante espectrometría atómica [28]. En todos los casos se produce una preconcentración eficaz de los analitos y la desorción de los mismos de la matriz extractante se logra de manera sencilla con la adición de un pequeño volumen de un disolvente orgánico adecuado.

A pesar de las excelentes propiedades mecánicas, térmicas y eléctricas, uno de los inconvenientes de los nanotubos de carbono reside en su gran facilidad para formar agregados en los medios líquidos, sin embargo se ha comprobado que estos se dispersan considerablemente mejor en el seno de líquidos iónicos de sales de imidazolinio que en disolventes orgánicos tradicionales. Las aplicaciones de los nanotubos de carbono dispersados en líquidos iónicos y sus aplicaciones han sido revisadas recientemente [29].

6. Extracción en fase líquida

La extracción líquido-líquido convencional se ha visto sustituida paulatinamente por atractivas y eficaces alternativas en las que, aunque tanto la matriz como el extractante siguen siendo líquidos, el formato de la técnica se ha miniaturizado o bien se ha apostado por líquidos extractantes respetuosos con el medio ambiente. A las metodologías convencionales se han unido recursos como el empleo de la formación de pares iónicos con sustancias de carácter tensioactivo, así como la utilización de bromuro de hexadeciltrimetilamonio, que permite la extracción de antibióticos (cefalosporinas) de muestras de alimentos [30].

7. Extracción por punto de nube (CPE)

En esta modalidad se pueden extraer y pre-concentrar tanto analitos orgánicos como inorgánicos presentes en un medio acuoso. Para lograr una extracción eficaz, se emplea como medio extractante disoluciones acuosas diluidas de un tensioactivo no iónico. A partir de una determinada temperatura (temperatura del punto de nube), que depende de la naturaleza anfifílica del tensioactivo y de la concentración del mismo, las micelas formadas por el tensioactivo se deshidratan y agregan. De esa manera se separan dos fases líquidas: el disolvente acuoso y la fase rica en surfactante que contiene el analito (Figura 5). Así se alcanza una eficacia de extracción muy elevada. Puesto que la temperatura es característica para alcanzar el punto de nube de un determinado tensioactivo, se hace necesario el control estricto de esta variable crítica.

Una de las ventajas de esta metodología es que los tensioactivos utilizados no son volátiles, ni tóxicos, además se pueden considerar como materiales adsorbentes seguros. Por ello, se han empleado con éxito para la extracción de flurbiprofeno de plasma [31] después de su administración por vía oral. Este procedimiento de extracción también se ha utilizado para la extracción de las vitaminas A y E [32], si bien requiriendo un tiempo de extracción de 30 minutos.

8. Extracción mediante el empleo de líquidos iónicos (ILsE)

Los líquidos iónicos actúan como mediadores y extractantes en muy diversas modalidades de extracción tanto en fase líquida como en fase sólida y, por ello, se ha revisado su papel en las distintas modalidades de micro-extracción [33]. Poco a poco los líquidos iónicos han ido

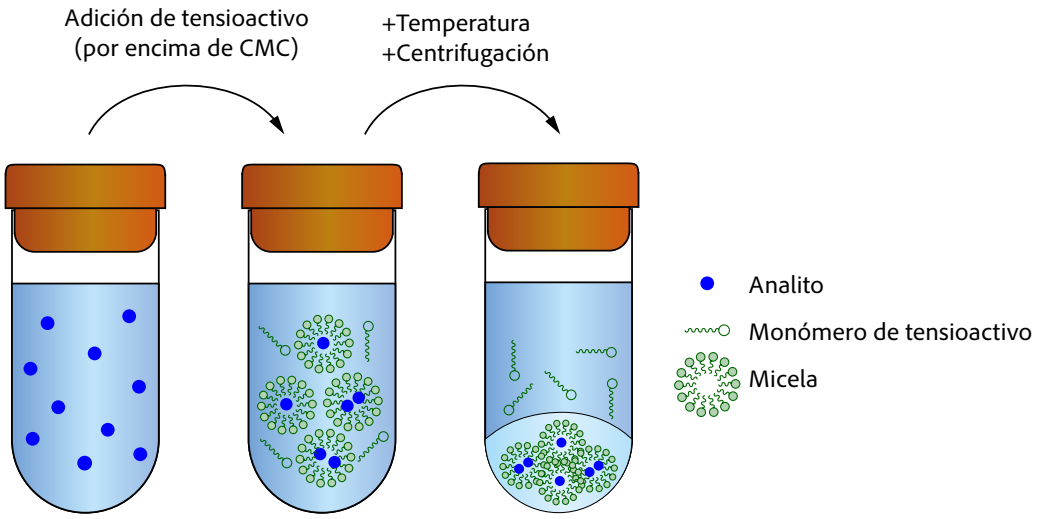

Figura 5.
Proceso de concentración/extracción de un analito en la fase rica en tensioactivo por aumento de la temperatura por encima del punto de nube. Adaptado de: L. H. Keith, L. U. Gron, J. L. Young, Chem. Rev. 2007, 107, 2695-2708.

ganando terreno como disolventes alternativos, especialmente como disolventes "verdes" [34]. Lamentablemente, este carácter sostenible no está exento de controversia, ya que desde un punto de vista estricto debe tenerse en cuenta su toxicidad [35] y su carácter no biodegradable, por lo que pueden producirse bio- y ecoacumulación de los mismos en el entorno. Aunque las sales de derivados nitrogenados orgánicos son conocidas desde comienzos del siglo XX, sin embargo en la década de los 90 se describe el uso del tetrafluoroborato de etilmetilimidazolinio como nuevo líquido iónico para catálisis homogénea.

Los líquidos iónicos son sales con un punto de fusión por debajo de la temperatura ambiente, lo que los hace líquidos en condiciones operativas normales. Son estables térmicamente, no inflamables, tienen una presión de vapor muy baja y, por tanto, poseen muy baja volatilidad, siendo miscibles tanto con el agua como con los disolventes orgánicos. Estas singulares características de los líquidos iónicos [36] se reflejan en sus buenas cualidades extractivas y se pueden considerar como una alternativa a los disolventes orgánicos tradicionales, por lo que se han clasificado como disolventes "limpios".

Se ha comparado la eficacia de la extracción para 8 líquidos iónicos en la extracción de floroglucinoles (derivados de 1,3,5-trihidroxibenceno) presentes en especies vegetales [37]. El hexafluorofosfato de 1-butil-3-metil-imidazolio es un líquido iónico que se ha empleado en la micro-extracción en fase líquida de diversos derivados de fenotiazina presentes en muestras de orina humana [38]. La preconcentración de los analitos gracias al procedimiento de extracción contribuye significativamente a mejorar la sensibilidad del método cromatográfico empleado en su cuantificación.

9. Extracción mediante el empleo de líquidos a presión (PLE)

Esta modalidad de extracción, también denominada extracción con fluidos presurizados, utiliza disolventes orgánicos o acuosos convencionales a elevadas presiones (10-14 MPa) y temperaturas (50-200 °C) (Figura 6). La extracción se realiza de forma rápida y eficaz con un gran ahorro en el consumo de disolvente extractivo y una significativa reducción en el tiempo de extracción. Puede afirmarse que en unos 5-10 minutos se logra la extracción de los analitos de una muestra de 10 g con tan solo 15 mL de disolvente. La temperatura empleada, por encima del punto de ebullición del disolvente, mejora ostensiblemente la cinética de desorción de los analitos de la matriz en la que se encuentran. Se produce un incremento de la solubilidad de los analitos en el disolvente extractivo a las condiciones de presión y temperatura empleadas, lo que incide en la eficacia del proceso y contribuye a la disminución del consumo energético si

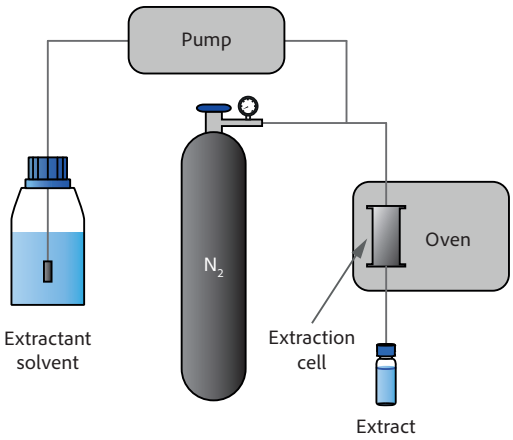

Figura 6.
Diagrama del funcionamiento de un sistema de extracción de analitos a alta presión y temperatura [57].

se compara con un proceso de extracción estático clásico (16 h en Soxhlet).

Esta técnica, considerada respetuosa con el medioambiente [39], se ha empleado en la extracción de 32 fármacos de uso humano y veterinario en muestras de suelos y de sedimentos [40]. Su aplicación a la extracción de analitos de muestras de alimentos y plantas se ha revisado exhaustivamente [41].

10. Micro-extracción en fase líquida (LPME)

La micro-extracción en fase líquida es una modalidad miniaturizada de extracción líquido-líquido en la que se emplean volúmenes del orden de unos microlitros de un disolvente orgánico inmiscible con el agua (fase aceptora), que captura los analitos contenidos en un medio acuoso (fase donadora) [42]. Las diferentes modalidades de micro-extracción en fase líquida suponen un consumo de disolventes orgánicos entre 100 y 1000 veces inferior a los volúmenes empleados en las extracciones líquido-líquido convencionales.

Las distintas alternativas de micro-extracción en fase líquida se han revisado en el contexto de la química verde [43] o en su aplicación al análisis de contaminantes [44] en distintas matrices.

10.1. Micro-extracción en fase líquida mediante fibra hueca (HF-LPME)

La fibra hueca está constituida por un material poroso y una membrana que actúa de barrera entre la muestra líquida (fase donadora) y el disolvente que actúa como extractante (fase aceptora) (Figura 7). La fibra hueca puede tener forma cilíndrica y cerrada en la parte inferior (modalidad trifásica) o bien en forma de "U" de tal manera que los dos extremos se hallan conectados a través de unos tubos guía (modalidad bifásica).

Cuando se introduce en la muestra líquida la fibra hueca con la fase aceptora, los analitos son transferidos al disolvente extractante. La eficacia de extracción y limpieza de las muestras es elevada, ya que la membrana que actúa como barrera impide el paso a los compuestos de alto peso molecular, por lo que resulta muy conveniente en el pre-tratamiento de muestras biológicas, si bien ha de evitarse el bloqueo de la fibra porosa por la adsorción excesiva de analitos hidrofóbicos. Además, la membrana tiene el inconveniente de que prolonga el tiempo necesario para la extracción.

Si los analitos tienen grupos ionizables con carácter ácido o básico, entonces es conveniente utilizar la modalidad trifásica. En ésta, los analitos son transferidos desde una matriz al disolvente orgánico que se encuentra alojado en los poros de la fibra hueca y posteriormente a una disolución acuosa aceptora que está situada en la luz de la fibra. De esta forma, regulando el pH de la fase acuosa aceptora, se logra la extracción y pre-concentración de los analitos en la misma. También se pueden utilizar líquidos iónicos como fase aceptora acuosa, en base a sus buenas propiedades peliculares que favorecen su inmovilización en el interior de la fibra hueca. Este procedimiento proporciona unas elevadas eficacias de extracción con factores de enriquecimiento que varían entre 200 y 800. Esta alternativa se ha aplicado con éxito a la extracción y pre-concentración de metales en aguas naturales [45], a la extracción de fármacos de aguas fluviales [46] y residuales [47,48] así como en plasma humano [49].

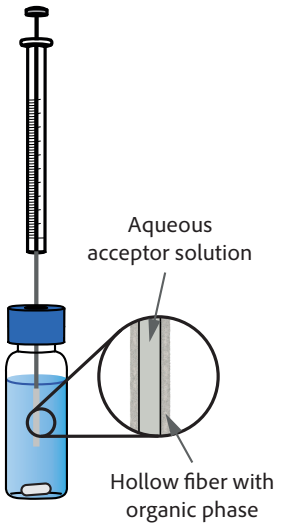

Figura 7.
Dispositivo para la microextracción en fase líquida mediante fibra hueca, mostrando en la ampliación el detalle de la membrana que conecta ambas fases [57]

10.2. Micro-extracción en fase líquida mediante gota única (SD-LLME)

La micro-extracción en fase líquida mediante el procedimiento denominado "single-drop" consiste en introducir en la matriz líquida, usando una microjeringa, una gota (de aproximadamente 1-10 µL) de un disolvente extractante inmiscible con el medio líquido problema. Se deja un tiempo para que se establezca el equilibrio de partición entre los dos disolventes inmiscibles y el analito pase de la disolución problema a la gota de extractante. Después se retrae la gota con la microjeringa y puede procederse a la inyección directa en el cromatógrafo. La eficacia de la extracción no es muy elevada y la pre-concentración de los analitos tampoco. Uno de los inconvenientes de esta metodología es la inestabilidad de la gota especialmente cuando se aplica agitación o se sube la temperatura [50].

10.3. Micro-extracción en fase líquida mediante membrana agitadora (SM-LLME)

El empleo de la membrana con agitación en una micro-extracción líquido-líquido, facilita la extracción de los analitos de una manera sencilla y eficaz. Se emplea un recipiente de PTFE dentro del cual se introduce un alambre férrico que sirve para agitar bajo la acción del campo magnético externo. La cámara interior del recipiente está recubierta con una membrana de naturaleza polimérica que evita la pérdidas del disolvente aceptor durante el proceso de extracción y está llena con el disolvente aceptor (Figura 8). Este sistema integra las ventajas de la micro-extracción en fase líquida, en lo que a reducido volumen de disolventes se refiere junto con la rapidez en alcanzar el equilibrio de partición que es consecuencia del proceso de agitación magnética. Este procedimiento se ha aplicado a la extracción de fármacos y sus metabolitos en muestras de orina [51].

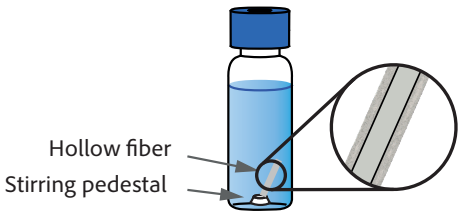

Figura 8.
Diagrama de un dispositivo que combina la extracción por fibra hueca y la agitación magnética de la misma [57]

10.4. Micro-extracción dispersiva líquido-líquido (DLLME)

Esta técnica de pre-tratamiento de muestras proporciona altas eficacias de extracción a la vez que requiere volúmenes de disolvente extractivo muy pequeños. Estas eficacias son consecuencia de la elevada superficie de contacto que se establece entre el líquido extractivo que se dispersa en forma de pequeñas gotículas en el seno de una matriz líquida inmiscible con aquél. Para lograr la extracción de los analitos, una mezcla del disolvente extractivo y un dis-

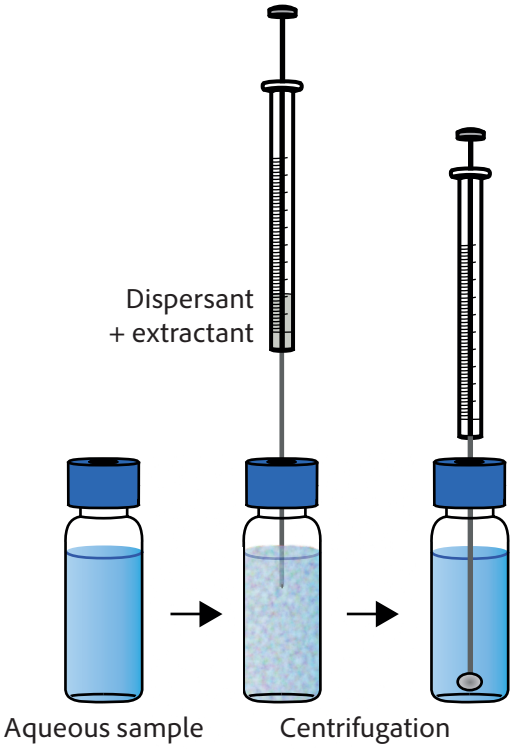

Figura 9. Etapas del procedimiento de microextracción dispersiva líquido-líquido [57].

persante se inyecta en la matriz acuosa. Los analitos hidrofóbicos se transfieren desde la matriz acuosa a las gotículas del disolvente orgánico dispersado. La suspensión así obtenida se centrifuga y finalmente con ayuda de una microjeringa se toma la fase orgánica que contiene los analitos a cuantificar (Figura 9). Para facilitar este último paso, normalmente se emplea como disolvente extractivo un líquido orgánico de elevada densidad e inmiscible con el agua. Por el contrario el disolvente que actúa como dispersante debe ser tanto miscible con agua como con el disolvente orgánico extractivo, usándose normalmente metanol, etanol, acetona o acetonitrilo [52,53].

Esta técnica se ha aplicado mayoritariamente a la extracción de pesticidas presentes en muestras de aguas [54], aunque también se ha descrito su utilización para la determinación de fármacos en orina [38].

Las ventajas del empleo de esta modalidad para la extracción de metales de muy diversas muestras (agua de bebida, aguas residuales, cereales, cabello...) se ha revisado con especial atención en su acoplamiento a técnicas espectroanalíticas y cromatográficas [55]. La utilidad del empleo de líquidos iónicos en combinación con distintas modalidades de micro-extracción dispersiva líquido-líquido entre las que cabe citar la modalidad convencional, la de temperatura controlada, o la asistida por microondas, han sido revisadas y aplicadas tanto a la extracción de analitos orgánicos como de metales [56].

11. Referencias

1. L. Nováková, H. Vlcková, A review of current trends and advances in modern bio-analytical methods: chromatography and sample preparation, Anal Chim Acta. 656 (2009) 8–35.
2. M. Tobiszewski, A. Mechlinska, B. Zygmunt, J. Namiesnik, Green analytical chemistry in sample preparation for determination of trace organic pollutants, Trends Anal Chem. 28 (2009) 943–951.
3. D.L. Rocha, A.D. Batista, F.R.P. Rocha, G.L. Donati, J.A. Nóbrega, Greening sample preparation in inorganic analysis, Trends Anal Chem. 45 (2013) 79–92.
4. Z. Huang, H.K. Lee, Materials-based approaches to minimizing solvent usage in analytical sample preparation, Trends Anal Chem. 39 (2012) 228–244.
5. F.J. Lara, M. del Olmo-Iruela, A.M. García-Campaña, On-line anion exchange solid-phase extraction coupled to liquid chromatography with fluorescence detection to determine quinolones in water and human urine, J Chromatogr A. 1310 (2013) 91–97.
6. S. Rubio, D. Pérez-Bendito, Recent advances in environmental analysis, Anal Chem. 81 (2009) 4601–4622.
7. C.-M. Dai, X.-F. Zhou, Y.-L. Zhang, S.-G. Liu, J. Zhang, Synthesis by precipitation polymerization of molecularly imprinted polymer for the selective extraction of diclofenac from water samples, J Hazard Mater. 198 (2011) 175–181.
8. J. Tan, Z.-T. Jiang, R. Li, X.-P. Yan, Molecularly-imprinted monoliths for sample treatment and separation, Trends Anal Chem. 39 (2012) 207–217.
9. N. Fontanals, F. Borrull, R.M. Marcé, Ionic liquids in solid-phase extraction, Trends Anal Chem. 41 (2012) 15–26.
10. J. Martín, J.L. Santos, I. Aparicio, E. Alonso, Multi-residue method for the analysis of pharmaceutical compounds in sewage sludge, compost and sediments by sonication-assisted extraction and LC determination, J. Sep. Sci. 33 (2010) 1760–1766.
11. S. Almeda, L. Arce, M. Valcárcel, Combination of solid-phase extraction and large-volume stacking with polarity switching in micellar electrokinetic capillary chromatography for the determination of traces of nonsteroidal anti-inflammatory drugs in saliva, Electrophoresis. 29 (2008) 3074–3080.
12. A. Azzouz, E. Ballesteros, Combined microwave-assisted extraction and continuous solid-phase extraction prior to gas chromatography-mass spectrometry determination of pharmaceuticals, personal care products and hormones in soils, sediments and sludge, The Sci Total Environ. 419 (2012) 208–215.

13. J. Antonic, E. Heath, Determination of NSAIDs in river sediment samples, Anal Bioanal Chem. 387 (2007) 1337–1342.
14. L. Vera-Candioti, M.D. Gil García, M. Martínez Galera, H.C. Goicoechea, Chemometric assisted solid-phase microextraction for the determination of anti-inflammatory and antiepileptic drugs in river water by liquid chromatography-diode array detection, J Chromatogr A. 1211 (2008) 22–32.
15. B. Bojko, E. Cudjoe, J. Pawliszyn, M. Wasowicz, Solid-phase microextraction. How far are we from clinical practice? Trends Anal Chem. 30 (2011) 1505–1512.
16. Gaurav, V. Kaur, A. Kumar, A.K. Malik, P.K. Rai, SPME-HPLC: A new approach to the analysis of explosives, J Hazard Mater. 147 (2007) 691–697.
17. Q.-W. Yu, X. Wang, Q. Ma, B.-F. Yuan, H.-B. He, Y.-Q. Feng, Automated analysis of non-steroidal anti-inflammatory drugs in human plasma and water samples by in-tube solid-phase microextraction coupled to liquid chromatography-mass spectrometry based on a poly(4-vinyl -pyridine-co-ethylene dimethacrylate) monolith, Anal. Methods. 4 (2012) 1538.
18. D. Vuckovic, High-throughput solid-phase microextraction in multi-well-plate format, Trends Anal Chem. 45 (2013) 136–153.
19. A. Garrido Frenich, M.D.M. Aguilera-Luiz, J.L. Martínez Vidal, R. Romero-González, Comparison of several extraction techniques for multiclass analysis of veterinary drugs in eggs using ultra-high pressure liquid chromatography-tandem mass spectrometry, Anal Chim Acta. 661 (2010) 150–160.
20. C. Blasco, A. Masia, F.G. Morillas, Y. Picó, Comparison of the effectiveness of recent extraction procedures for antibiotic residues in bovine muscle tissues, J AOAC Int. 94 (2011) 991–1003.
21. R. Pérez-Burgos, E.M. Grzelak, G. Gokce, J. Saurina, J. Barbosa, D. Barrón, Quechers methodologies as an alternative to solid phase extraction (SPE) for the determination and characterization of residues of cephalosporins in beef muscle using LC-MS/MS, J Chromatogr B. 899 (2012) 57–65.
22. M. Lombardo-Agüí, L. Gámiz-Gracia, C. Cruces-Blanco, A.M. García-Campaña, Comparison of different sample treatments for the analysis of quinolones in milk by capillary-liquid chromatography with laser induced fluorescence detection, J Chromatogr A. 1218 (2011) 4966–4971.
23. M. Lombardo-Agüí, A.M. García-Campaña, L. Gámiz-Gracia, C. Cruces-Blanco, Determination of quinolones of veterinary use in bee products by ultra-high performance liquid chromatography–tandem mass spectrometry using a QuEChERS extraction procedure, Talanta. 93 (2012) 193–199.
24. N. Arroyo-Manzanares, A.M. García-Campaña, L. Gámiz-Gracia, Multiclass mycotoxin analysis in *Silybum marianum* by ultra high performance liquid chromatography–tandem mass spectrometry using a procedure based on QuEChERS and dispersive liquid–liquid microextraction. J Chromatogr A. 1282 (2013) 11–19.
25. Y.-B. Luo, H.-B. Zheng, J.-X. Wang, Q. Gao, Q.-W. Yu, Y.-Q. Feng, An anionic exchange stir rod sorptive extraction based on monolithic material for the extraction of non-steroidal anti-inflammatory drugs in environmental aqueous samples, Talanta. 86 (2011) 103–108.
26. H. Faraji, S.W. Husain, M. Helalizadeh, β-cyclodextrin-bonded silica particles as novel sorbent for stir bar sorptive extraction of phenolic compounds, J Chromatogr Sci. 49 (2011) 482–487.
27. A. Sarafraz-Yazdi, A. Amiri, G. Rounaghi, H. Eshtiagh-Hosseini, Determination of non-steroidal anti-inflammatory drugs in water samples by solid-phase microextraction based sol-gel technique using poly(ethylene glycol) grafted multi-walled carbon nanotubes coated fiber, Anal Chim Acta. 720 (2012) 134–141.
28. M. Tuzen, K.O. Saygi, M. Soylak, Solid phase extraction of heavy metal ions in environmental samples on multiwalled carbon nanotubes, J Hazard Mater. 152 (2008) 632–639.
29. M.L. Polo-Luque, B.M. Simonet, M. Valcárcel, Functionalization and dispersion of carbon nanotubes in ionic liquids, Trends Anal Chem. 47 (2013) 99–110.
30. C. Quesada-Molina, A.M. García-Campaña, M. del Olmo-Iruela, Ion-paired extraction of cephalosporins in acetone prior to their analysis by capillary liquid chromatography in environmental water and meat samples, Talanta. 115 (2013) 943–949.
31. F. Han, R. Yin, X.-L. Shi, Q. Jia, H.-Z. Liu, H.-M. Yao, et al., Cloud point extraction-HPLC method for determination and pharmacokinetic study of flurbiprofen in rat plasma after oral and transdermal administration, J Chromatogr B. 868 (2008) 64–69.
32. A.C. Ortega, D.C. da Silva, J.V. Visentainer, N.E. de Souza, V. de Cinque Almeida, C.C. Oliveira, Determination of Vitamins A and E Exploiting Cloud Point Extraction and Micellar Liquid Chromatography, Analytical Letters. 44 (2011) 778–786.
33. E. Aguilera-Herrador, R. Lucena, S. Cárdenas, M. Valcárcel, The roles of ionic liquids in sorptive microextraction techniques, Trends Anal Chem. 29 (2010) 602–616.
34. Z. Li, Y. Pei, H. Wang, J. Fan, J. Wang, Ionic liquid-based aqueous two-phase systems and their applications in green separation processes, Trends Anal Chem. 29 (2010) 1336–1346.
35. T.P.T. Pham, C.-W. Cho, Y.-S. Yun, Environmental fate and toxicity of ionic liquids: A review, Water Research. 44 (2010) 352–372.
36. Z.-Q. Tan, J.-F. Liu, L. Pang, Advances in analytical chemistry using the unique properties of

ionic liquids, Trends Anal Chem. 39 (2012) 218–227.

37. X.-J. Li, H.-M. Yu, C. Gao, Y.-G. Zu, W. Wang, M. Luo, et al., Application of ionic liquid-based surfactants in the microwave-assisted extraction for the determination of four main phloroglucinols from Dryopteris fragrans, J. Sep. Sci. 35 (2012) 3600–3608.
38. M. Cruz-Vera, R. Lucena, S. Cárdenas, M. Valcárcel, One-step in-syringe ionic liquid-based dispersive liquid-liquid microextraction, J Chromatogr A. 1216 (2009) 6459–6465.
39. S. Morales-Muñoz, J.L. Luque-García, M.D. Luque de Castro, Pure and modified water assisted by auxiliary energies: An environmental friendly extractant for sample preparation, Anal Chim Acta. 557 (2006) 278–286.
40. E. Pérez-Carrera, M. Hansen, V.M. León, E. Björklund, K.A. Krogh, B. Halling-Sørensen, et al., Multiresidue method for the determination of 32 human and veterinary pharmaceuticals in soil and sediment by pressurized-liquid extraction and LC-MS/MS, Anal Bioanal Chem. 398 (2010) 1173–1184.
41. A. Mustafa, C. Turner, Pressurized liquid extraction as a green approach in food and herbal plants extraction: A review, Anal Chim Acta. 703 (2011) 8–18.
42. A. Sarafraz-Yazdi, A. Amiri, Liquid-phase microextraction, Trends Anal Chem. 29 (2010) 1–14.
43. F. Pena-Pereira, I. Lavilla, C. Bendicho, Liquid-phase microextraction techniques within the framework of green chemistry, Trends Anal Chem. 29 (2010) 617–628.
44. C. Mahugo-Santana, Z. Sosa-Ferrera, M.E. Torres-Padrón, J.J. Santana-Rodríguez, Application of new approaches to liquid-phase microextraction for the determination of emerging pollutants, Trends Anal Chem. 30 (2011) 731–748.
45. C. Vergel, R. Montoya, C. Mendiguchía, M. García-Vargas, C. Moreno, HF-LPME as a green alternative for the preconcentration of nickel in natural waters, Anal Bioanal Chem. 404 (2012) 665–670.
46. Z. Es'haghi, Determination of widely used non-steroidal anti-inflammatory drugs in water samples by in situ derivatization, continuous hollow fiber liquid-phase microextraction and gas chromatography-flame ionization detector, Anal Chim Acta. 641 (2009) 83–88.
47. N. Larsson, E. Petersson, M. Rylander, J.Å. Jönsson, Continuous flow hollow fiber liquid-phase microextraction and monitoring of NSAID pharmaceuticals in a sewage treatment plant effluent, Anal. Methods. 1 (2009) 59.
48. A. Saleh, E. Larsson, Y. Yamini, J.Å. Jönsson, Hollow fiber liquid phase microextraction as a preconcentration and clean-up step after pressurized hot water extraction for the determination of non-steroidal anti-inflammatory drugs in sewage sludge, J Chromatogr A. 1218 (2011) 1331–1339.
49. W.W. Yang, H.F. Zhang, Y.R. Jia, T. Zhao, Y.L. Zhao, L.J. Tong, et al., Hollow fiber liquid-phase microextraction for the determination of nimesulide in human plasma and its application to a pharmacokinetic study, Pharmazie. 66 (2011) 564–569.
50. M.A. Jeannot, A. Przyjazny, J.M. Kokosa, Single drop microextraction--development, applications and future trends, J Chromatogr A. 1217 (2010) 2326–2336.
51. S. Riaño, M.C. Alcudia-León, R. Lucena, S. Cárdenas, M. Valcárcel, Determination of non-steroidal anti-inflammatory drugs in urine by the combination of stir membrane liquid-liquid-liquid microextraction and liquid chromatography, Anal Bioanal Chem. 403 (2012) 2583–2589.
52. A.V. Herrera-Herrera, M. Asensio-Ramos, J. Hernández-Borges, M.Á. Rodríguez-Delgado, Dispersive liquid-liquid microextraction for determination of organic analytes, Trends Anal Chem. 29 (2010) 728–751.
53. M. Rezaee, Y. Yamini, M. Faraji, Evolution of dispersive liquid-liquid microextraction method, J Chromatogr A. 1217 (2010) 2342–2357.
54. A.Z.A.-G. Kowiak, T. Grzeskowiak, Dispersive liquid-liquid microextraction, Trends Anal Chem. 30 (2011) 1382–1399.
55. M.S. El-Shahawi, H.M. Al-Saidi, Dispersive liquid-liquid microextraction for chemical speciation and determination of ultra-trace concentrations of metal ions, Trends Anal Chem. 44 (2013) 12–24.
56. M.J. Trujillo-Rodríguez, P. Rocío-Bautista, V. Pino, A.M. Afonso, Ionic liquids in dispersive liquid-liquid microextraction, Trends Anal Chem. 51 (2013) 87–106.
57. A.I. Olives, V. González-Ruiz, M.A. Martín. Isolation and Quantitative Methods for Analysis of Non-Steroidal Anti-Inflammatory Drugs. Anti-Inflammatory&Anti-Allergy Agents in Medicinal Chemistry (Formerly Current Medicinal Chemistry - Anti-Inflammatory and Anti-Allergy Agents), 11 (2012), 65–95.

PARTE 2

Justificación y objetivos

Esta página se ha dejado en blanco intencionadamente.

Justificación y Objetivos

A día de hoy, la cromatografía de líquidos (HPLC) es la técnica analítica de mayor proyección y aplicación en la industria farmacéutica y otros muchos ámbitos: plantas de producción, laboratorios control de calidad de materias primas y productos terminados, laboratorios clínicos, etc. La producción de residuos de disolventes orgánicos como consecuencia de los análisis a realizar es algo inevitable y, por ello, la reducción en la generación de los mismos constituye un reto atractivo en el contexto de la Química Analítica Sostenible. Welch [1] afirma que cada cromatógrafo de líquidos (trabajando a pleno rendimiento en una planta industrial) genera aproximadamente 1 L de residuos orgánicos cada 24 h. Así, ha sugerido distintas alternativas como el empleo de disolventes orgánicos biodegradables en clara sintonía con lo propuesto por Kerton [2] y De La Guardia [3]. Poco a poco, y especialmente en los últimos diez años, se ha ido arraigando en la comunidad científica la necesidad de desarrollar estrategias analíticas limpias y respetuosas con el medio ambiente. Así, se van introduciendo distintas metodologías y técnicas analíticas con menor impacto medioambiental que las ya existentes [4].

El desarrollo de nuevos fármacos antitumorales que presenten menores efectos adversos que los actualmente disponibles es uno de los campos de mayor interés en la investigación relacionada con la terapia anticancerosa. La naturaleza nos brinda extraordinarios modelos de compuestos naturales con actividad antitumoral. Así, desde los alcaloides presentes en plantas superiores o en tejidos de mamíferos, hasta los heterociclos producidos por algas y organismos marinos microscópicos, sirven de plataforma para el diseño racional de nuevos candidatos que presenten mayor eficacia terapéutica y menor toxicidad. Los inhibidores de la enzima topoisomerasa I constituyen un grupo terapéutico de gran interés, ya que presentan una buena selectividad al actuar sobre una de las enzimas involucradas en procesos clave para las células que se encuentran en rápido crecimiento y división, como la transcripción, la replicación y la reparación del material genético. Estos compuestos interaccionan tanto con ADN como con la enzima en lo que Pommier [5] ha venido a denominar "el paradigma de la inhibición interfacial". La determinación de los mismos en matrices biológicas y el estudio de su actividad antitumoral requieren técnicas analíticas sensibles, versátiles y rápidas para su determinación en los organismos que los producen, en líneas celulares tumorales, en tejidos y fluidos biológicos durante los ensayos preclínicos, o en las formas farmacéuticas acabadas.

Basándonos en lo anteriormente expuesto, nos propusimos **desarrollar metodologías analíticas limpias y sostenibles para la determinación de heterociclos que desempeñan actividades biológicas diversas**. Así, nos planteamos mejorar la sostenibilidad de metodologías de separación por cromatografía de líquidos (HPLC) incorporando **ciclodextrinas como modificadores de las fases móviles**. Las ciclodextrinas son oligosacáridos cíclicos naturales obtenidos del almidón, completamente biodegradables, renovables y exentos de toxicidad. La adición de estos peculiares macrociclos a las fases móviles introduce un equilibrio químico secundario al de separación cromatográfica, lo cual permite utilizar disolventes de mínima toxicidad y renovables, como el etanol, como componente orgánico en la fase móvil. Desde el punto de vista medioambiental este disolvente ofrece considerables ventajas, sin embargo, su utilización en HPLC [6] es poco frecuente. Para demostrar la viabilidad de este planteamiento, se ha utilizado como modelo la separación de varios alcaloides derivados de β-carbolina.

Focalizando nuestra atención en el desarrollo de otras alternativas cromatográficas sostenibles, nos planteamos el diseño de **separaciones por HPLC para un grupo de alcaloides antitumorales derivados de camptotecina y luotonina A**. Partiendo del empleo de fases estacionarias convencionales en lo que a dimensiones y porosidad se refiere, abordamos el reto de la separación de este grupo de compuestos en columnas **C-18**, **pentafluoro-fenil-propil** y **fenil-hexil**. En paralelo, nos propusimos optimizar las condiciones de separación que condujeran a la reducción del volumen de fase móvil mediante el empleo

de **columnas de menor diámetro interno** y, seguidamente abordamos la utilización de fases estacionarias novedosas y de reciente introducción: las empaquetadas con partículas **"core-shell"**. El empleo de estas fases estacionarias no convencionales de tamaño de partícula sub-3-µm presenta atractivas cualidades, tanto desde el punto de vista de la técnica cromatográfica en sí misma, como desde el de las mejoras que aportan a la sostenibilidad del método. En la presente memoria exploramos las potenciales ventajas (reducción en el tiempo de análisis y del consumo de disolventes, mayores eficacia y resolución) derivadas del empleo de este nuevo tipo de fases estacionarias, que parecen estar abriendo un nuevo camino en lo que a la evolución de la cromatografía de líquidos se refiere.

En los últimos años, la aplicación de las técnicas espectroscópicas miniaturizadas (lectores multi-placa o multipocillo) ha experimientado un creciente y renovado interés. Las determinaciones analíticas con lector multipocillo se aplican no sólo a la resolución de problemas "típicos" (para la determinación de actividades enzimáticas u otros parámetros en biología molecular), sino que se están aplicando con éxito en reacciones y metodologías analíticas "clásicas" a escala miniaturizada. Entre sus ventajas destacan el elevado número de muestras que se analizan por unidad de tiempo y la drástica reducción en los volúmenes de disolvente y reactivos requeridos. Por ello, estas técnicas de alto rendimiento pueden considerarse metodologías analíticas sostenibles.

En consecuencia, otro de los objetivos de nuestro trabajo ha consistido en la **adaptación de determinaciones analíticas espectrofluorimétricas al formato de lectura de placas multi-pocillo**. Estas técnicas de alto rendimiento además pueden utilizarse de forma automatizada. Sin embargo, para poder emplear estas metodologías como técnicas de análisis en rutina, es necesaria la caracterización fiable previa de los compuestos a determinar. Por ello, dado que la estructura química de los antitumorales derivados de luotonina A sugiere una luminiscencia con propiedades singulares que hasta el momento no se ha descrito, otro de los objetivos a alcanzar fue el **estudio de su fluorescencia**. Además, este paso es indispensable antes de poder emplear la espectrofluorimetría como técnica analítica para cuantificarlos en muestras reales o para obtener una detección fluorimétrica sensible tras su separación por HPLC.

En el contexto interdisciplinar en el que estamos implicados, otro de los objetivos propuestos se centró en los ensayos de actividad biológica de los compuestos estudiados. Uno de los problemas que podrían aparecer es la baja solubilidad en agua de los derivados de luotonina A. Para minimizar este inconveniente, y contando con nuestra experiencia previa, nos propusimos estudiar cómo la **solubilidad de los antitumorales podía mejorarse** mediante la formación de complejos de inclusión con ciclodextrinas.

Finalmente, otro de nuestros retos fue explorar nuevos detalles del **mecanismo de acción de estos análogos**, de su potencia antitumoral y de la relación existente entre ambos. Nos planteamos llevar a cabo ensayos de **inhibición de topoisomerasa 1** y estudios de **citotoxicidad sobre líneas celulares tumorales**. Con el objetivo de conocer mejor los detalles de la influencia de la estructura de los compuestos estudiados en su actividad, también consideramos la utilidad de los estudios de **modelado y docking molecular para establecer los modos de interacción** entre cada uno de ellos y el complejo DNA-topoisomerasa 1. Éste constituyó uno de los retos más ambiciosos de los propuestos, pero de proyección más motivadora, no sólo desde el punto de vista analítico sino por su relevancia farmacológica.

Referencias

1. C. J. Welch, N. Wu, M. Biba, R. Hartman, T. Brkovic, X. Gong, R. Helmy, W. Schafer, J. Cuff, Z. Pirzada, L Zhou, Trend. Anal. Chem., 2010, 29, 667-680.
2. F. M. Kerton, Alternative Solvents for Green Chemistry, RSC, Cambridge, 2009.
3. M. de la Guardia, S. Armenta, Green Analytical Chemistry. Theory and Practice, vol 57, en D. Barceló (Ed.), Comprehensive Analytical Chemistry, Elsevier 2010.
4. L.H Keith., L.U. Gron, J.L. Young, Chem. Rev., 2007, 107, 2695-2708.
5. Y. Pommier (Ed.), DNA Topoisomerases and Cancer, in Teicher BA (Series Ed.), Cancer Drug Discovery and Development, Springer, New York, 2012.
6. C.J. Welch, T. Brkovic, W. Schafer, X. Gong, Green Chem., 2009, 11, 1232–1238.

PARTE 3

Parte experimental, resultados y discusión

- Resumen de equipos empleados
- Derivados de la luotonina A
- Eco-friendly liquid chromatographic separations based on the use of cyclodextrins as mobile phase additives
- SPE/RP-HPLC using C1 columns: an environmentally friendly alternative to conventional reverse phase separations for quantitation of β-carboline alkaloids in human serum samples
- Fluorescence properties of the natural anti-tumour alkaloid luotonin A and new analogues: pH modulation as an approach to their fluorimetric quantitation in biological samples
- Liquid chromatographic analysis of the anti-cancer alkaloid luotonin A and some new derivatives in human serum samples
- A down-scaled fluorimetric determination of the solubility properties of drugs to minimize waste generation
- Challenging core-shell stationary phases with the separation of closely related anti-cancer compounds: performance studies and application to drug quantitation in cell cultures with multi-well plate clean-up
- B-Ring-aryl substituted luotonin A analogues with a new binding mode to the topoisomerase 1-DNA complex show enhanced cytotoxic activity

Esta página se ha dejado en blanco intencionadamente.

Resumen de equipos empleados

1. Cromatógrafos

Merck-Hitachi (Tokyo, Japón)		
Equipo 1	Bomba de gradiente LaChrom L-7100	Caudal de 0,001 a 9,999 mL/min Exactitud del caudal: ± 2% hasta 5 mL/min Precisión del caudal: ≤ 0,2 RSD a 1 mL/min Presión de trabajo máxima: 412 barGradiente de hasta 4 canales, con proporción por tiempo de apertura de válvulas en incrementos del 1%; mezclador estático en línea.
	Detector de fluores-cencia LaChrom L-7485	Lámpara de arco de Xe de 150 W Exactitud de los monocromadores: ± 3 nm Ancho de rendijas: 15 nm Volumen de la celda de detección: 12 µL Detector de trabajo: fotomultiplicador Detector de referencia: fotodiodo
Equipo 2	Bomba isocrática L-6000	Caudal de 0,001 a 9,990 mL/min Exactitud del caudal: ± 2% hasta 5 mL/min Precisión del caudal: ≤ 0,3 RSD a 1 mL/min Presión de trabajo máxima: 420 bar
	Detector de fluores-cencia F-1050	Lámpara de arco de Xe de 150 W Exactitud de los monocromadores: ± 7 nm Ancho de rendijas: 15 nm, fijo. Volumen de la celda de detección: 12 µL Detectores de trabajo y referencia: fotomultiplicadores
Elementos comunes	Horno para columnas LaChrom ELITE L-2300	Horno termostático por efecto Peltier con sección de precalentamiento. Aire circulante. Rango de temperaturas: ambiente -15 °C a 65 °C Precisión: ±0,1 °C entre 20 y 65 °C
	Interfaz D-7000	
	PC ejecutando el software HPLC System Manager 4.1 en Windows 2000 para control de los sistemas y adquisición de datos.	
Rheodyne (Rohnert Park, CA, EE.UU.)		
Inyector	2 × 7725i	
Bucles de carga	Volumen dependiente de la aplicación.	
VICI (Houston, TX, EE.UU.)		
Restrictor	Regulador de presión JR-BPR1 en la salida de la celda de detección, ajustado a +1.5 bar.	

2. Fluorímetro

FluoroMax-4P de Horiba-Jovin Yvon (Edison, NJ, EE.UU.)	
Fuentes de radiación	Lámpara de arco de Xe de 150 W (fluorescencia) Lámpara pulsante de descarga de Xe (fosforescencia)
Monocromadores	Redes de difracción por reflexión de 1200 líneas/mm Rango óptico: 220-600 nm (excitación) y 290-800 nm (emisión) Dispersión: 4,25 nm/mm Resolución: 0,3 nm Rendijas: ajustables entre 0 y 30 nm de ancho de banda
Detector de emisión	Fotomultiplicador R928P Rango de trabajo: 180-850 nm, lineal hasta 2×10^6 cps Corriente oscura: < 1000 cps, relación S:R = 3000:1
Detector de referencia	Fotodiodo analógico, con respuesta lineal entre 190 y 980 nm
Polarizadores	Material: calcita Disposición: en L Cálculo del factor G: automático por software
Lector de placas multi-pocillo	MicroMax 384 Conexión óptica por haces de fibra de vidrio al espectrofluorímetro Soporte para lectura automatizada de placas de 96 y 384 pocillos
Control y adquisición de datos	PC ejecutando FluorEssence 3.5 con módulo MultiGroup en Windows XP.

3. Equipos externos

Equipo	Fabricante	Centro
Espectrómetro de masas	ABSciex TRIPLETOFT 5600 Fuente de ionización ESI/APCI y analizador híbrido de triple cuadrupolo-tiempo de vuelo	Servicio Central de Apoyo a la Investigación Experimental, Universidad de Valencia
Espectrómetro de RMN	Bruker Avance 250 MHz	Centro de Apoyo a la Investigación de Resonancia Magnética Nuclear y de Spin Electrónico, Universidad Complutense de Madrid
Espectrómetro de RMN	Bruker Avance III 700 MHz	Centro de Apoyo a la Investigación de Resonancia Magnética Nuclear y de Spin Electrónico, Universidad Complutense de Madrid

4. Otros equipos

Equipo	Fabricante	
Espectrofotómetro de absorción UV-Vis	Kontron Uvikon 810	Doble haz
Bomba vacío	Eyela A-3S	Caudal de 40 L min-1
Microevaporador	Selecta Vacuo-Temp	Con trampa de frío
Agitador tipo noria	Stuart Rotator SB3	
Baño de ultrasonidos	Elmasonic S15	
Cascada de frío	Labconco Lyph-Lock 12	
Medidor de pH	Crison Micro-pH 2001	
Balanza	Sartorius Handy H51	

Derivados de la luotonina A

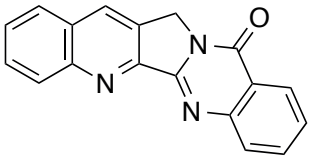

Luotonina A, (1)
$C_{18}H_{11}N_3O$
285,31 g/mol
CAS 205989-12-4

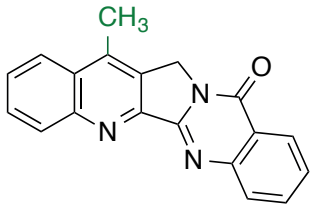

2
$C_{19}H_{13}N_3O$
299,33 g/mol
CAS 441732-36-1

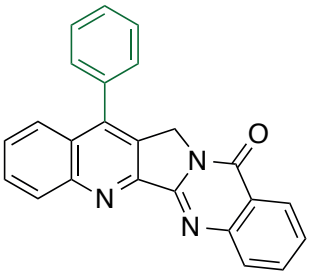

3
$C_{24}H_{15}N_3O$
361,40 g/mol
CAS 1242965-49-6

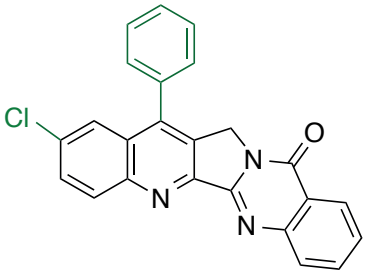

4
$C_{24}H_{14}ClN_3O$
395,85 g/mol
CAS 1242965-52-1

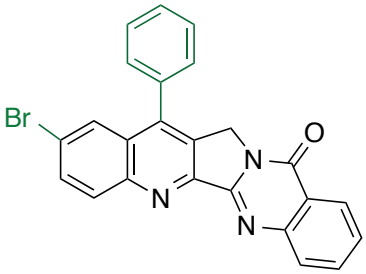

5
$C_{24}H_{14}BrN_3O$
440,30 g/mol
CAS 1274936-21-8

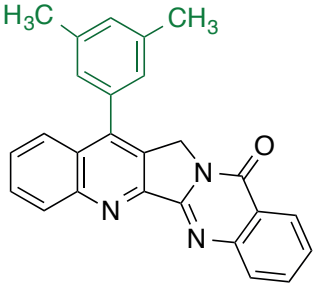

6
$C_{26}H_{19}N_3O$
389,46 g/mol
CAS 1242965-55-4

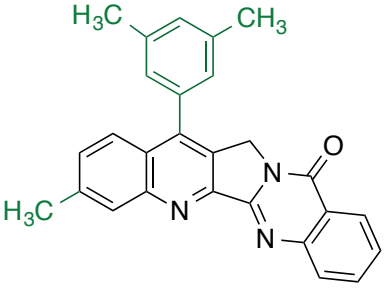

7
$C_{27}H_{21}N_3O$
403,49 g/mol
CAS 1242965-56-5

Esta página se ha dejado en blanco intencionadamente.

8

Eco-friendly liquid chromatographic separations based on the use of cyclodextrins as mobile phase additives

Published in: González-Ruiz, V., León, A. G., Olives, A. I., Martín, M. A., & Menéndez, J. C. (2011). Green Chem., 13(1), 115–126.

ABSTRACT ▶ Acetonitrile and methanol are the most popular solvents employed in analytical HPLC, but they suffer from a number of drawbacks from the environmental point of view. Alternative, greener mobile phases employing methanol or the less toxic solvent ethanol as the sole organic solvent are proposed in this paper, and applied to the problem of the separation of β-carbolines on C18-stationary phases. The use of β-cyclodextrin (β-CD) and (2-hydroxypropyl)-β-cyclodextrin (HPβ-CD) as mobile phase additives allowed us to increase the proportion of water in the mobile phases without loss in the resolution or efficiency of the separations, leading initially to a considerable reduction of the proportion of methanol in the mobile phase (from 70% to 50%) and at a later stage, to the development of a mobile phase containing only 30% of ethanol. The β-carboline–cyclodextrin association constants were determined by HPLC, and the inclusion complexes were also characterized by ^{1}H-NMR, ^{13}C-NMR and 2D-ROESY experiments, and these studies were used to explain the chromatographic behaviour. The new chromatographic methodology developed was validated and applied to the quantitation of β-carboline derivatives in spiked human serum samples. For the extraction of β-carboline alkaloids from serum samples, liquid–liquid extraction (LLE) and solid-phase extraction (SPE) procedures were compared. It was concluded that the combination of a pre-treatment procedure (ionic exchange SPE) with a water-enriched chromatographic separation leads to a promising, environmentally friendly new methodology.

DOI ▼
10.1039/c0gc00456a

ABBREVIATIONS ▼
- **β-CD:** β-cyclodextrin
- **HPβ-CD:** (2-hydroxypropyl)-β-cyclodextrin
- **LLE:** liquid-liquid extraction
- **SPE:** solid-phase extraction
- **CDs:** cyclodextrins
- **MPA:** mobile phase additives

1. Introduction

Cyclodextrins (CDs) are cyclic oligosaccharides with fascinating molecular recognition properties that have been exploited for the design of other host molecules. As stated by Sezjtli [1], CDs are very attractive for the development of environmentally friendly technologies because they are semi-natural compounds produced from starch, a renewable material, by enzymatic conversion. They present a variety of applications in chemistry [2] and also in pharmaceutical, food and cosmetic industries because they are non-toxic and inexpensive. Furthermore, chemically modified CDs with tailor-made cavity dimensions are easily synthesized and they can be designed to be soluble in water or organic solvents. In analytical chemistry, they are employed in separation techniques [3], including GC, SFC, HPLC and CZE. Their use as mobile phase additives (MPA) in HPLC is less developed, in spite of the fact that CDs have the advantage over other additives of being transparent in the UV-Vis range and that they also enhance the HPLC resolution of non-chiral compounds like indole derivatives [4] or steroids [5]. CDs are also very popular in HPLC and CZE as chiral selectors, and thus CDs enhance the enantiomeric HPLC resolution of chiral compounds like norgestrel [6] and sertraline [7]. The effects of the addition of neutral and charged CDs in CZE and to the mobile phase in HPLC have been compared to establish the stereoselective interactions that contribute to chiral discrimination [8].

A favourable consequence of the presence of CDs in the mobile phases is the possibility to reduce the organic solvent/water ratio without a decrease

in the selectivity or resolution. For instance, the separation of several pharmaceutically interesting compounds (citalopram, pantoprazol, nitrofurazone, trans-resveratrol) was performed in acetonitrile:buffered aqueous solution [6,9] or in methanol:buffered aqueous solution [4,10] in the presence of different types of CDs as MPA.

β-Carbolines are natural alkaloids occurring in plants and mammalian tissues. They have a great variety of biological activities, including mutagenic behaviour due to their capability of binding to DNA [11] and varied neurological effects due to their interactions with benzodiazepine and imidazoline receptors [12]. Clinical studies correlated increased plasma concentrations of β-carbolines [13] with neurological diseases [14] and also with high consumption of alcohol [15], heroin [16] and tobacco [17]. The structures of the β-carboline alkaloids studied in this paper are shown in figure 1.

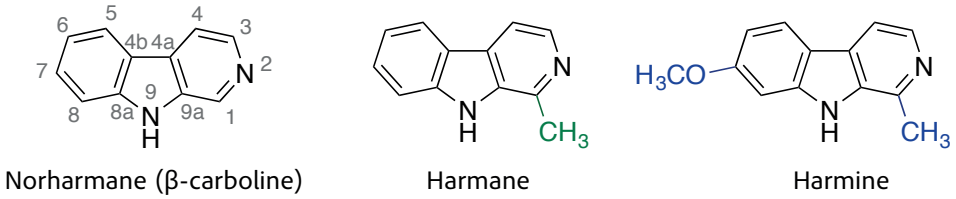

Figure 1. β-Carboline alkaloids studied in this paper.

Different chromatographic methods [18] have been employed for the determination of β-carbolines in several samples and matrices. Thus, RP-HPLC coupled to mass spectrometry, fluorimetric and UV-Vis detection has been employed to quantify β-carboline in food and foodstuffs [19], human blood [20] and hair [21] and HPLC with electrochemical detection is useful for determining β-carboline in foods and beverages [22] as an alternative to gas chromatographic [23] or capillary electrophoretic techniques [24]. Among the liquid chromatographic procedures described for quantitation of β-carbolines, isocratic or gradient elution has been found to require aqueous mixtures with a high proportion of acetonitrile [25] or methanol [14,20] or alternatively, acetonitrile and methanol mixtures [22,26]. Lowering the pH of the aqueous component to pH 3.0 allows the reduction of the organic solvent proportion in the mobile phase [19a, 21] but these conditions increase the degradation of the stationary phases.

HPLC is a powerful analytical technique that allows the fast separation and quantification of compounds in complex matrices with high efficiency, resolution and sensitivity and is the most widely employed separation technique for routine analysis in industrial settings. The volume of organic solvent waste originated from HPLC analysis is very high, due to the huge number of instruments in operation worldwide. Reversed Phase HPLC, the most popular separation method, traditionally involves the use of mixtures of water and acetonitrile. Due to the toxicity of acetonitrile, these mixtures have to be treated as chemical waste and for this reason there is a growing interest in the use of non-toxic solvents, specially alcohols, as an alternative [27]. Replacing acetonitrile is not an easy task because acetonitrile:water mobile phases have a number of advantages including their lower viscosity and higher transparency in the UV region, coupled with better chromatographic efficiencies. There is a growing interest in the replacement of acetonitrile by ethanol to solve some specific chromatographic problems [28] but these methodologies are still in their early stages. In the case of ionic analytes such as uric acid, an efficient RP-HPLC separation can be achieved employing ammonium phosphate as the mobile phase but this requires a guard column to avoid the easy degradation of the analytical column [29]. Other

alternatives to reduce the organic solvent consumption involve the use of micellar liquid chromatography (MLC), an approach that combines conventional stationary phases with mobile phases modified by the presence of surfactants and a reduced proportion of organic solvents [30]. One drawback of this technique is the tendency of the surfactants to become adsorbed on the chromatographic stationary phases.

The present paper describes the potential of β-CD and HPβ-CD as MPA for greener RP-HPLC separations. β-CD and HPβ-CD were selected over other CDs taking into account their benefit/cost ratio. We present here our results on the use for this purpose of modified methanolic mobile phases, which are compared with the greener ethanolic mobile phases. This has been illustrated for the case of the separation of the biologically relevant β-carboline alkaloids norharmane, harmane and harmine in human serum samples. Taking into account that the complexation equilibrium competes with the chromatographic distribution equilibrium, and in order to achieve the maximum reduction in the organic solvent proportion we also considered relevant a detailed knowledge of the stability and structure of the inclusion complexes to obtain a more detailed picture of its influence on the chromatographic process. To this end, we undertook the chromatographic determination of the CD-carboline association constants and the structural characterization of the complexes by NMR techniques. In order to reduce the use of organic solvents also at the pre-treatment stage, our study involves the comparison of the traditional Liquid-Liquid Extraction (LLE) protocol with another one based on Solid Phase Extraction (SPE), which requires a much lower amount of organic solvent and which had not been previously applied to the analysis of carboline derivatives in blood or serum samples.

2. Experimental Section

2.1. Apparatus and reagents

All reagents and solvents were analytical, spectroscopic or chromatographic grade and were used without further purification. Water was doubly distilled and deionized (Milli-Q system) prior to its use. Norharmane, harmane and harmine were purchased from Sigma (Steinheim, Germany) as well as the cyclodextrins employed, namely β-CD and HPβ-CD (average degree of substitution: 0.8 hydroxypropyl groups per glucose unit).

NMR spectra were recorded with a Bruker Advance 250 spectrometer (Servicio de Resonancia Magnética Nuclear, UCM) using D_2O or d_6-DMSO as solvents.

A liquid chromatographic system (Hitachi-Merck, Tokyo, Japan) consisted of a quaternary gradient pump L-7100 coupled with a fluorescence detector L-7485 and a second was equipped with an isocratic pump L-6000 coupled to a fluorescence detector F-1050. For both instruments the temperature of the columns was controlled with a L-2300 oven and the samples were injected through a Rheodyne 7725i injector (20 µL loop). The two chromatographic systems were under computer control through the HPLC System Manager software, version 4.1. The analytical C18 columns (Spherisorb, ODS2, 5 µm, 150 × 4.6 mm) were purchased to Waters (Milford, Massachusetts) and they were utilized in combination with ethanolic and methanolic mobile phases. The mobile phases were filtered through a 0.45 µm × 47 mm membrane filter (GPH, Waters, Bedford, MA, USA and Sartorius Stedim Biotech GmbH, Goettigen, Germany) under vacuum followed by the application of ultrasound during 5 minutes. The flow rate was 0.9 mL × min^{-1} (pressures of 80-120 bar). The fluorescence detection conditions employed were: excitation wavelength of 290 nm and emission wavelength of 430 nm.

2.2. Procedures

Stock solutions of norharmane, harmane or harmine 3.0×10^{-3} M in ethanol were freshly prepared. Aliquots of these stocks were taken to prepare solutions around 3.0×10^{-5} M of the alkaloids in 0.1 M HCl. These acidic solutions were spectrophotometrically measured and their molar absorptivities were considered in order to calculate accurately the real concentration of the stock solutions [31]. Then, suitable volumes of the standarized stock solutions were employed to prepare the standards for validation of chromatographic procedure and also to spike the serum samples studied.

The β-carbolines-CDs solid inclusion complexes were prepared at stochiometric ratios of 1:1 and 1:2. An appropriate amount of norharmane, harmane and harmine was weighed. Then the corresponding amount of CD was added to the solid β-carboline derivative and an adequate volume of water to assure the solubilization of the cyclodextrins. The mixture was magnetically stirred in a water bath at 50 ºC for 1 week. The mixture was then cooled to 8 ºC and the solid complexes obtained were filtered and washed with ethanol followed by water to eliminate free β-carboline and free CDs. Finally, the complexes were freeze-dried for 48 h. Then, adequate amounts of the complexes obtained were dissolved in d_6-DMSO or deuterium oxide containing a trace of 4,4-dimethyl-4-silapentane-1-sulfonic acid (DSS) as an internal standard, at a concentration 1×10^{-2} M for β-CD and 1×10^{-1} M for HPβ-CD, in order to obtain the ^{1}H-NMR and ^{13}C-NMR spectra.

For the chromatographic determination of the association constants, isocratic mobile phases methanol:buffered phosphate (pH 7.8), 50:50, (v:v) and isocratic mobile phases ethanol:buffered phosphate (pH 7.8), 30:70, (v:v) were employed. The mobile phases were modified by the addition of appropriate amounts of CDs. The range of concentrations assayed was from 0-3.0 mM (7 levels of concentration, methanolic mobile phases) and 0-11.0 mM (7 levels of concentration, ethanolic mobile phases) for β-CD and from 0-17 mM for HPβ-CD (10 levels of concentration, methanolic and ethanolic mobile phases). The association constants were determined at 25, 35 and 45 ºC. The columns were washed daily according to a previously described procedure [32] which allowed each column to be employed at least in 370-400 assays for the analysis of β-carbolines in serum samples.

With the aim to demonstrate the applicability of the method to the separation and quantitation of β-carbolines in real samples, human serum specimens (≈ 2-3 mL) belonging to 20 healthy volunteers were mixed to obtain a representative serum pool exempt from β-carboline derivatives. Two aliquots (S_1 and S_2) were taken from this pool and then adequate volumes of standard solutions containing norharmane, harmane and harmine were added to the serum samples, the concentration of each alkaloid (norharmane, harmane and harmine) being 0.250 µM (S_1) and 0.500 µM (S_2). The serum samples were spiked with the standard solutions of the alkaloids in a volume no higher than 5% of the initial serum volume. Two different procedures for sample clean-up were employed, namely the liquid-liquid extraction (LLE) procedure [20a] for the determination of harmane and harmine in blood samples and the solid phase extraction (SPE) procedure described for analysis of β-carboline derivatives in food samples [19]. SPE was carried out employing cartridges of 3 mL capacity packed with 200 mg propylsulphonic acid-derivatized silica gel (Isolute SCX 2, International Sorbent Technology, Mid Glamorgan, UK) placed in a vacuum manifold. The purified samples were then injected onto the chromatographic system using methanolic and ethanolic mobile phases modified by the addition of appropriate amounts of CDs (3 mM β-CD or 15 mM HPβ-CD) [33].

3. Results and discussion

3.1. ^{1}H- and ^{13}C-NMR Characterization of the β-carboline-cyclodextrin Inclusion Complexes

Although different methodologies and instrumental techniques can be employed for the structural characterization of CD inclusion complexes, NMR is well established as a powerful tool for investigating the through-space interactions of CDs and their ligands, both inside and outside the CD cavities. In the present work, we have employed for this purpose a combination of 1D ^{1}H-NMR and ^{13}C-NMR and 2D ROESY data. We have previuosly described a preliminary 1D NMR study of the harmane and harmine CD inclusion complexes, but under the conditions employed the carboline signals could not be observed, and the study was based on the changes observed in the glucose signals [34a]. We report now the use of more sensitive conditions that allow to observe the alkaloid signals and perform a much more refined structural study.

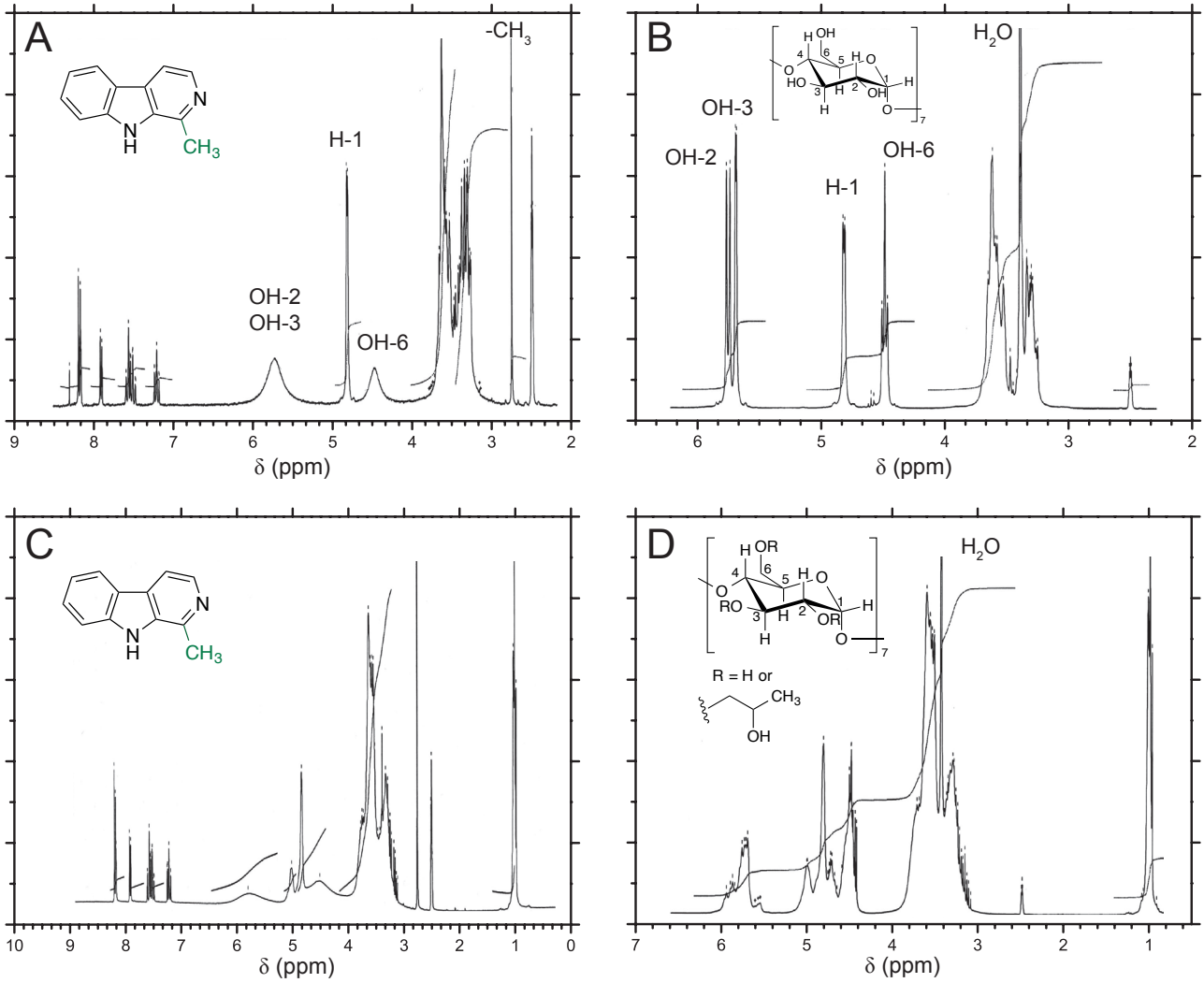

Figure 2.
^{1}H-NMR spectra of (A) harmane–β-CD complex (1:1), (B) β-CD, (C) harmane–HPβ-CD complex (1:1) and (D) HPβ-CD. Spectra obtained at 250 MHz in d_6- DMSO.

Several significant changes were observed in the ^{1}H-NMR spectra of the complexes in comparison to those of the corresponding free cyclodextrin and guest. As an example, figures 2 A and B show the ^{1}H-NMR spectrum of β-CD and its 1:1 complex with harmane. CD complexation led to decoupling of the OH groups at C2, C3 and C6. This reflects a fast proton exchange, which is a consequence of alterations of the hydrogen-bonding network at the rims of the cyclodextrin. Related changes were observed for HPβ-CD (figure 2, C and D). Comparison of the ^{1}H-NMR spectra of free CDs with

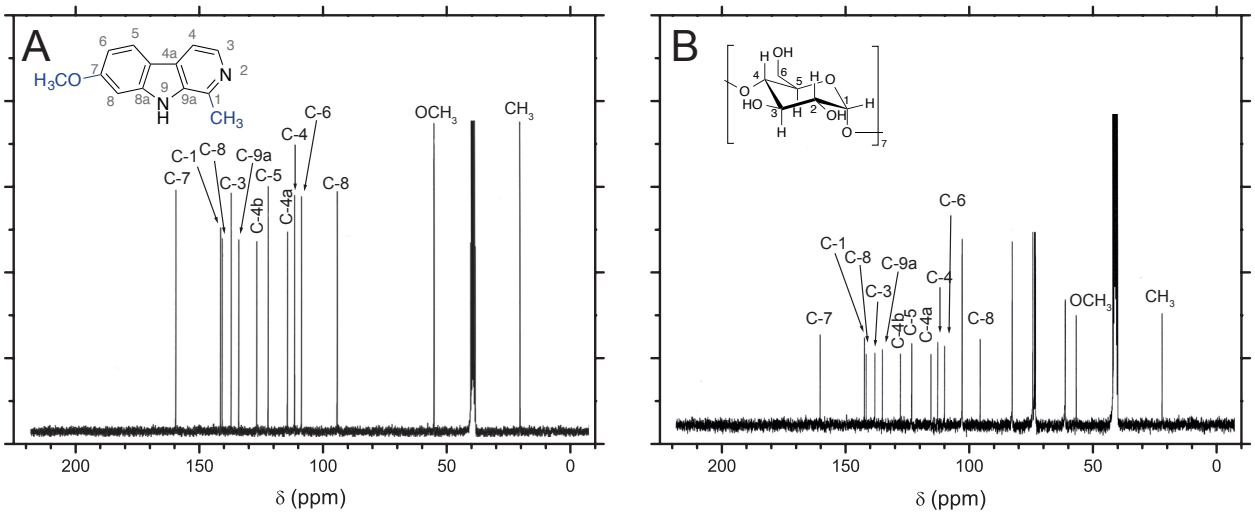

Figure 3. ^{13}C-NMR spectra of (A) harmine and (B) harmine–β-CD complex (1:2). Spectra obtained at 250 MHz in d_6- DMSO.

the ones obtained for the inclusion complexes, significant spectral changes can also be observed in the 3.40 ppm zone. In the case of free CDs, an intense peak is observed in this region due to the water molecules included inside the CD cavity [34b] but for the inclusion complexes this signal disappears because water is displaced from the CD cavity by the β-carboline molecules.

^{13}C-NMR measurements showed increased displacements for harmine (Figure 3), norharmane and harmane, chosen as a representative example for this discussion, and higher displacements for the 1:2 stoichiometry, showing a deeper penetration of the ligands inside the CD cavities. In the case of the 1:1 complexes, the signals that showed the highest displacements were those of C-5, C-6, C-7 and C-8 (Table 1), which proved that the more lipophilic benzene rings of the alkaloids enter the cavity first. The significant increase in Δδ for C-4 for the 1:2 stoichiometry is consistent with a complex containing two CD molecules per ligand. The absence of changes in the CH_3 group suggests that, due to geometrical reasons, this group is outside the CD. Figure 4 summarizes the displacements found for the carbon signals of harmane. Harmine showed a very similar behaviour to harmane in all respects. However, in the case of norharmane the signals due to the benzene ring and those of the pyridine ring showed similar displacements, and indeed the most significant one corresponded to C-1. This

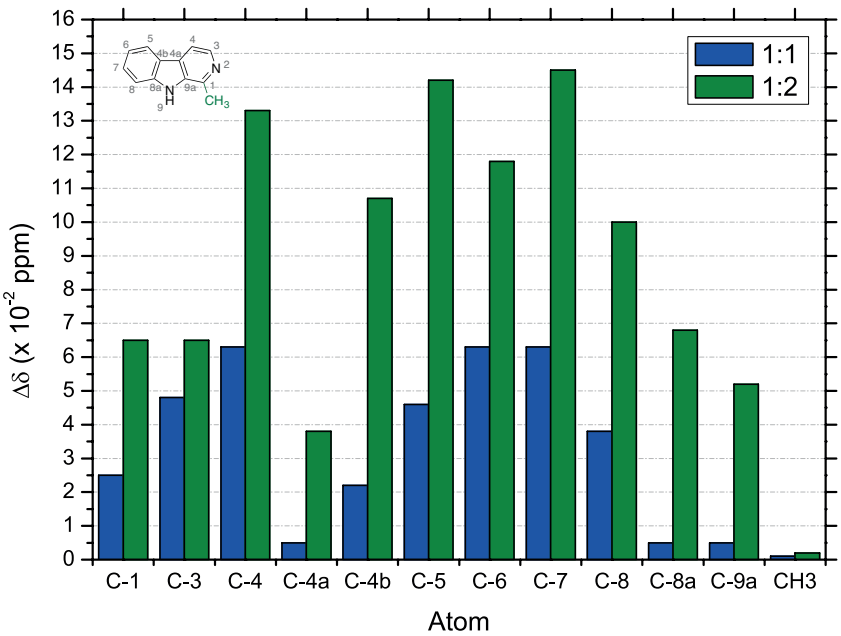

Figure 4. Comparison of the changes in the chemical shifts (Δδ) of the C-signals of harmane in inclusion complexes with HPβ-CD, relative to free harmane.

Table 1. Increase in the ^{13}C-NMR chemical shifts (× 10^{-2} ppm) for the 1:1 and 1:2 alkaloids:CDs inclusion complexes. Data are given as $\Delta\delta = \delta_{complex} - \delta_{guest\ molecule}$. NHE: norharmane; HAE: harmane; HIE: harmine.

	NHE/β-CD		NHE/HPβ-CD		HAE/β-CD		HAE/HPβ-CD		HIE/β-CD		HIE/HPβ-CD	
Atom	**1:1**	**1:2**	**1:1**	**1:2**	**1:1**	**1:2**	**1:1**	**1:2**	**1:1**	**1:2**	**1:1**	**1:2**
C-1	17.8	14.9	6.1	-1.3	2.9	8.8	2.5	6.5	-0.5	4.5	1.7	5.0
C-3	-3.7	-2.2	7.6	3.5	5.0	7.8	4.8	6.5	1.0	2.8	2.2	3.0
C-4	3.6	7.8	4.0	8.5	6.9	16.7	6.3	13.3	2.3	7.6	4.5	7.8
C-4a	-1.4	-0.5	-2.4	0.9	0.4	4.8	0.5	3.8	-0.8	1.8	0.6	2.0
C-4b	1.7	6.7	4.2	8.7	2.3	13.4	2.2	10.7	0.4	6.4	2.6	7.0
C-5	4.2	8.9	4.3	9.6	7.0	17.7	4.6	14.2	3.0	7.8	4.8	7.7
C-6	3.4	6.6	3.5	2.1	6.9	14.9	6.3	11.8	3.2	3.4	4.6	8.5
C-7	4.4	9.4	5.2	10.2	7.0	18.4	6.3	14.5	0.5	5.3	2.4	5.6
C-8	0.8	4.3	0.8	30.0	4.2	12.1	3.8	10.0	0.3	4.0	2.0	4.5
C-8a	0.4	3.0	0.8	4.2	0.8	9.0	0.5	6.8	0.0	2.9	1.4	3.0
C-9a	-2.6	-0.2	3.6	0.2	0.6	7.0	0.5	5.2	-0.7	2.7	0.9	3.1
CH_3	-	-	-	-	0.3	0.8	0.1	0.2	-0.7	-0.7	-0.3	-0.6
OCH_3	-	-	-	-	-	-	-	-	2.5	6.5	4.1	6.6

suggests a different mode of inclusion, where both the benzene and the pyridine rings at the ends of the molecule can enter the CD cavities.

A more detailed picture of the solution geometry of the complexes can be obtained by measuring NOE enhancements, which show the spatial proximity of protons. However, cyclodextrin complexes fall in the region where $\omega t_c \approx 1$, and consequently small NOE effects are expected. Therefore, rotating frame nuclear Overhauser effect (ROE) experiments, which give a positive response over the whole molecular weight range [35], were employed. 2D ROESY experiments for the 1:1 and 1:2 harmane/HPβ-CD complexes are shown in Figure 5 as representative examples. Clear correlations were observed between the signals corresponding to the protons of the benzene rings

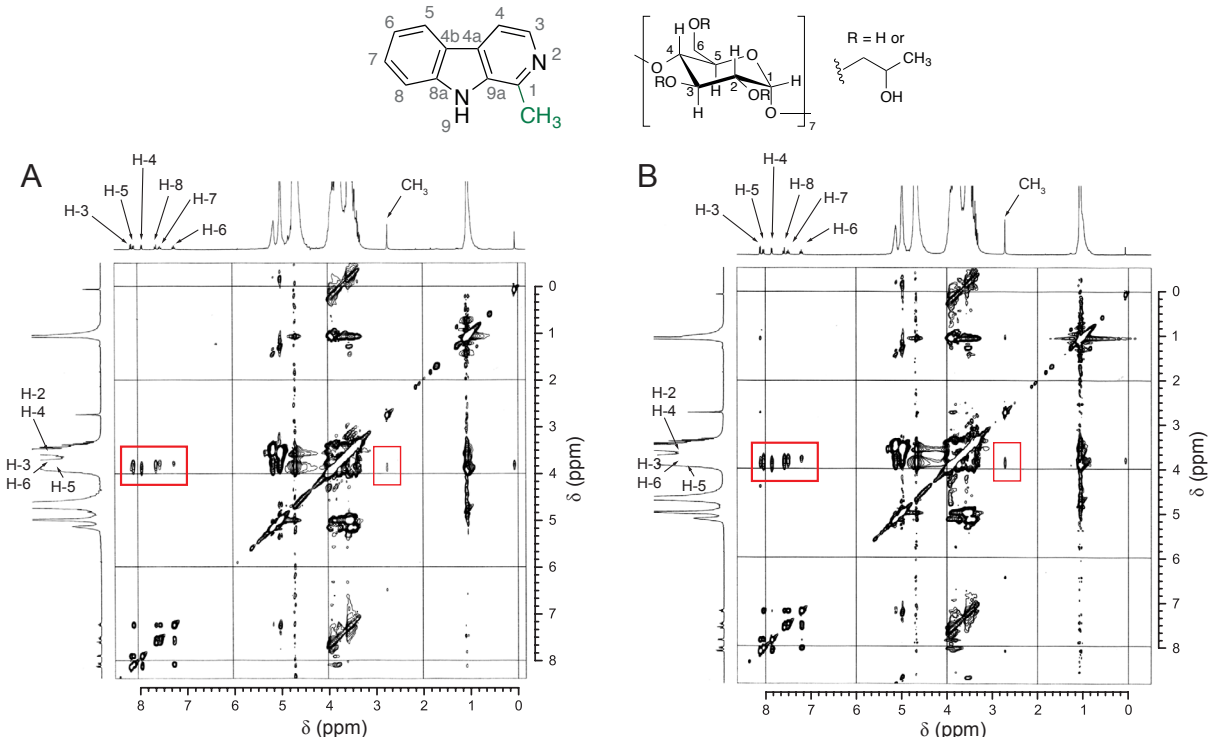

Figure 5.
Contour plots of 2D-ROESY experiments (D_2O, 250 MHz) corresponding to the inclusion complexes (A) harmane–HPβ-CD (1:1) and (B) harmane–HPβ-CD (1:2)

H-5, H-6, H-7 and H-8 on the β-carboline ring and the group of signals corresponding to protons H-3, H-5 and H-6 of the glucose rings, but not to H-2 and H-4. Since H-3 and H-5 are oriented towards the inner side of the CD cavities and H-2 and H-4 are outside, these results prove the penetration of the alkaloids into the host molecules. Another intense correlation is observed for H-4 of the carboline system, which is sufficiently close to the rim of the CD molecule, while H-3 shows a clear correlation only for the case of the 1:2 complex. The methyl group of harmane also shows a correlation, although rather weak. Harmine shows a similar behaviour to harmane. In the case of norharmane, strong ROESY correlations were observed for H-1, H-3, H-4, H-5, H-6, H-7 and H-8, confirming that the benzene and pyridine rings can be included with similar probability (Figure 6).

The ^{13}C-NMR studies, coupled with the ROESY correlations, lead us to propose the schematic model for the inclusion of harmane and harmine shown in Figure 7A. On the other hand, the 1:1 norharmane complexes can be considered as mixtures of two species, where the inclusion takes place by either end of the molecule (Figure 7B). According to these models, the more lipophilic part of the molecule, which is the one responsible for the interaction with the stationary phases, is inside the CD cavity. Therefore, diminished retention times can be expected in the presence of CDs, even in mobile phases containing high proportions of water, in comparison with the situation in the absence of cyclodextrins. For the case of norharmane, the effective interactions of both aromatic rings (benzene and pyridine) with the CDs increase the solubility of the ligand in the aqueous mobile phases and thus decrease its retention on the stationary phase, contributing to a further reduction of the retention times. This is in agreement with the higher values found for the association constants found for norharmane in comparison with harmane and harmine (see below).

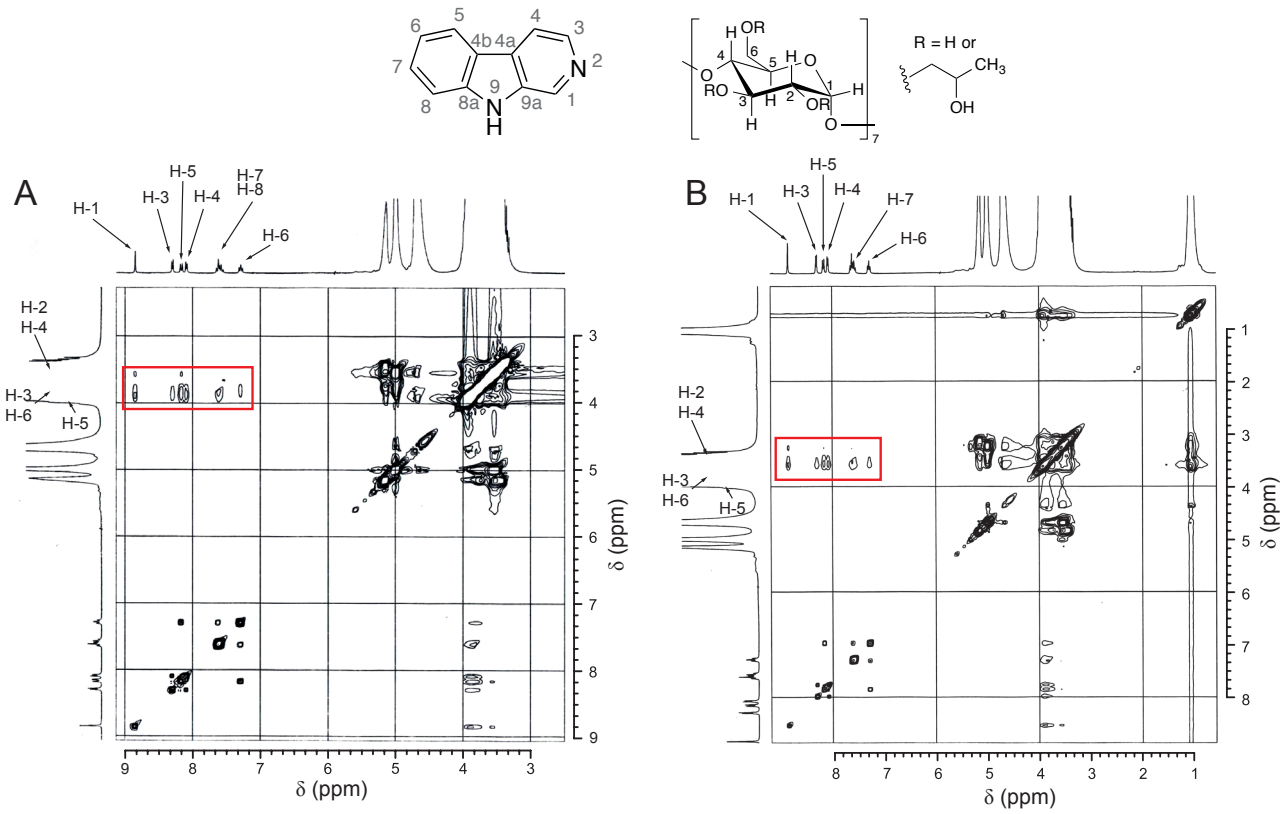

Figure 6.
Contour plots of 2D-ROESY experiments (D_2O, 250 MHz) corresponding to the inclusion complexes (A) norharmane–HPβ-CD (1:1) and (B) norharmane–HPβ-CD (1:2)

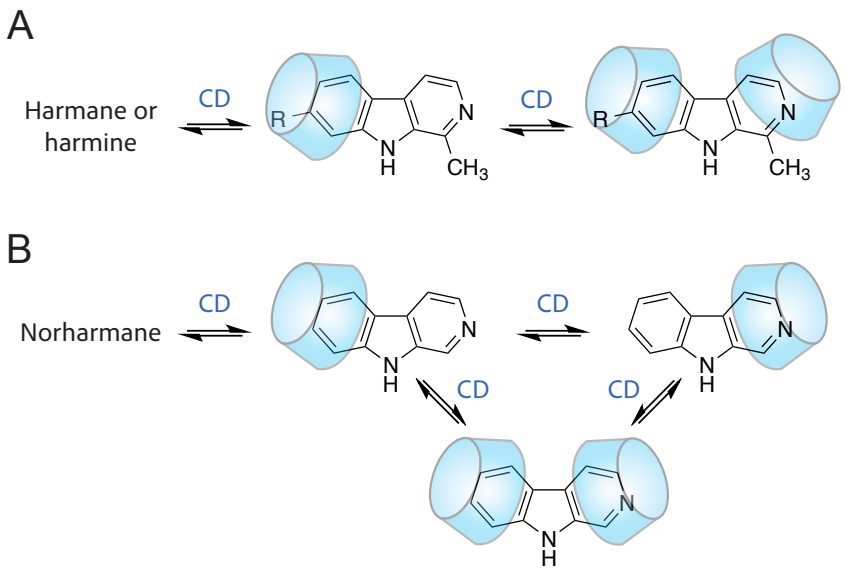

Figure 7.
Proposed models of the inclusion of β-carboline alkaloids into the CD cavities. (A) Inclusion complexes of harmane or harmine. (B) Inclusion complexes of norharmane.

3.2. Chromatographic determination of the β-carboline-cyclodextrins association constants

The presence of CDs in the mobile phases has been used to enhance the chromatographic separation of closely related compounds [3,36]. When CDs are added to the mobile phases, the retention factors decrease as a consequence of the formation of inclusion complexes during the chromatographic separation. The determination of the complex stability constants and the evaluation of the strength of guest-host interactions by HPLC are of interest because the existence of competitive chromatographic and inclusion equilibria can lead to alterations not only of the retention factors but also of the elution order and the selectivity. Studying the association constants can therefore contribute to optimize the mobile phase and the chromatographic conditions for routine analysis. Mobile phases with a very high water proportion favour the formation of CD inclusion complexes but they cannot be employed in practice because the retention times became prohibitively long, even in the presence of CDs in the mobile phase.

The apparent association constants (K_{ass}) can be determined using Equation 1 [37], where k and k_0 are the retention factor values in the presence and absence of cyclodextrin, respectively. The plot of $1/k$ *vs.* [CD] gives a straight line, where the value of K_{ass} can be calculated as slope/ordinate.

$$\frac{1}{k} = \frac{1}{k_0} + \frac{K_{ass}[\mathrm{CD}]}{k_0} \qquad \textbf{Equation 1}$$

Table 2 shows the values obtained for the β-carboline-CD association constants (K_{ass}), which can be seen to bear an inverse relationship with temperature. Inclusion complexes were more stable in ethanol-water mixtures than in methanol, and complexes with HPβ-CD were more stable than those with β-CD for the ethanolic mobile phases, which is an important result in terms of the use of ethanol as real alternative in the design of greener mobile phases. It is well known that increased temperatures are accompanied by better chromatographic features, and for this reason we undertook a brief study of the influence of temperature on complex stability. As shown in Table 2, it can be observed that increasing temperatures favour the dissociation of the β-carboline-CD complexes, an effect that is well documented in the literature for

Table 2. Apparent association constants values (K_{ass}) and standard deviations obtained by RP-HPLC for the β-carboline derivatives-CD complexes in two different hydroalcoholic mobile phases. Stationary phase octadecylsilane (C18). Values obtained considering the total concentration of CD. The values of K_{ass} calculated considering the competition of the solvent appear in parenthesis. All the values expressed as $K_{ass} \pm \sigma_{n-1}$, (M^{-1}).

		MeOH:buffer			EtOH:buffer			
	β-CD	HPβ-CD			β-CD		HPβ-CD	
		25 °C	35 °C	45 °C	35 °C	45 °C	35 °C	45 °C
Norharmane	[a]	19.82 ± 0.16	10.05 ± 0.44	10.63 ± 1.63	11.21 ± 2.07 (64.78 ± 11.95)	6.70 ± 0.28 (38.71 ± 1.64)	21.59 ± 2.47	15.99 ± 0.96
Harmane	[a]	16.48 ± 0.35	5.81 ± 0.43	9.19 ± 1.78	8.30 ± 1.68 (47.98 ± 9.74)	4.89 ± 0.94 (28.30 ± 5.42)	16.46 ± 2.11	13.06 ± 0.34
Harmine	[a]	18.01 ± 0.28	[a]	9.47 ± 2.09	6.62±3.03 ([a])	[a] ([a])	12.58 ± 3.23	11.49 ± 0.51

[a] *The values obtained were not processable because of the poor correlation coefficient.*

some types of ligands. This observation led us to exclude the use of temperatures above 35 °C to increase the chromatographic efficiency. For both mobile phases and both CDs, the magnitude of the association constants for the three β-carbolines studied varied as follows: norharmane > harmane > harmine. These values are in agreement with NMR results and with the models of inclusion proposed in Figure 7.

The literature association constants for the methanol/β-CD and ethanol/β-CD complexes are 0.32 and 0.93 M^{-1}, respectively [38]. Considering these values, the alkaloids should be more easily displaced from the CD cavities by ethanol than by methanol, but the presence of a higher water proportion in the ethanolic mobile phases more than makes up for this effect, as previously observed by other workers, who noticed that an increase of 5% in the water proportion of the mobile phases produced a significant enhancement of the association constant values for terpene derivatives [39]. This effect can be attributed to the predominance of hydrophobic interactions inside the CD cavity, which favours the formation of analyte inclusion complexes [40]. Table 2 also includes the values of K_{ass} calculated considering the competition of the solvent and β-carboline alkaloids, where $K_{solvent}$ is 0.32 for methanol and 0.93 for ethanol, and free CD concentration present in the mobile phase ($[CD]_M$) can be determined as shown in Equation 2 [38,41].

$$[CD]_M = \frac{[CD]_{total}}{1 + K_{solvent}[solvent]} \qquad \text{Equation 2}$$

As expected, a notable increase in the stability constants was observed when the competition of the solvent for the β-CD was considered (Table 2). From these results can be deduced that the water:organic solvent ratio employed in our experiments is adequate to obtain a reasonable time of analysis and the combination C-18 and ethanol:buffered aqueous solution with HPβ-CD as MPA is a valuable approach to the development of green chromatographic separations.

3.3. Influence of CDs on the chromatographic separation and quantitation of β-carbolines

The concentration of CDs in the mobile phases needs to be adjusted to the experimental conditions. Higher CD concentrations reduced the retention factor although, due to the limited solubility of CDs in the alcoholic-water mixtures, the pressure in the column is increased and therefore the column efficiency is reduced. Based on our previous experience on the influence of the composition of the mobile and stationary phases, temperature and CDs concentration in the mobile phase on the separation

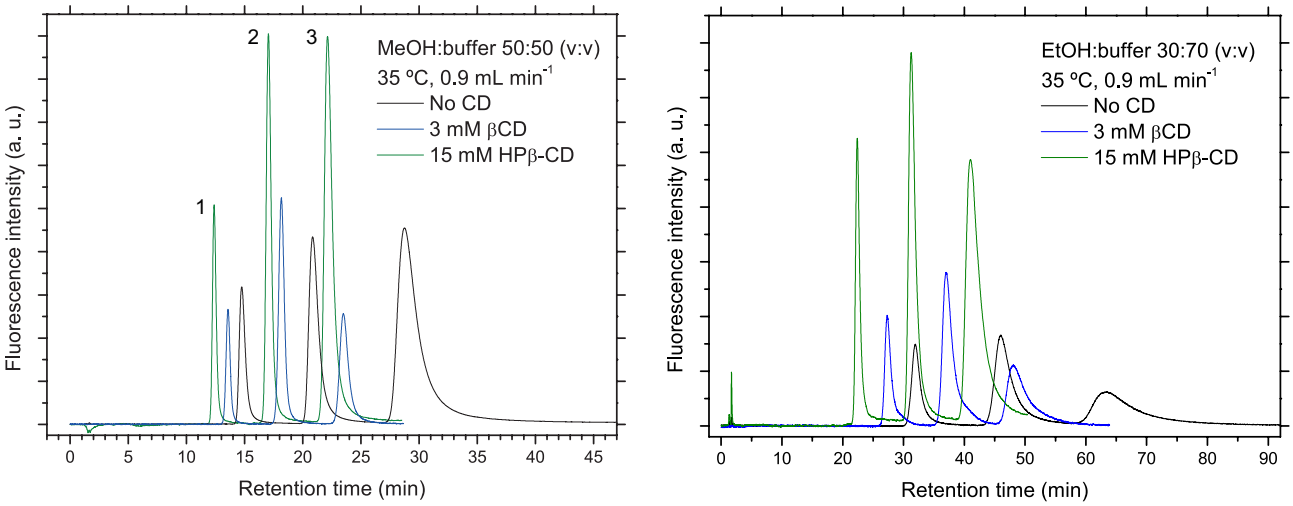

Figure 8.
Effects of CDs as mobile phase additives on the separation of β-carboline alkaloids in the standard solutions. Elution order: 1, norharmane; 2, harmane; 3, harmine

of β-carboline alkaloids [33] 15 mM HPβ-CD and 3 mM β-CD concentrations were chosen for the quantitation of norharmane, harmane and harmine in biological samples. We have also described the chromatographic determination of the association constants of 2,6-di-*O*-methyl-β-cyclodextrin and 2,3,6-tri-*O*-methyl-β-cyclodextrin and β-carboline alkaloids [32], but these CDs are too expensive for routine chromatographic analysis, compared to native β-CD and HPβ-CD.

The addition of β-CD and HPβ-CD as MPA caused a notable decrease in the retention times and in the retention factors of the β-carboline alkaloids under study, as shown in Figure 8 for the separation of the solutions of standards (see also Figure 10 below for the results obtained for spiked serum samples). The chromatographic behaviour obtained was the same for the standards and for real samples. The decrease in the retention time was higher for the ethanolic than for methanolic mobile phases and the decrease observed in the retention factors was higher for HPβ-CD than for β-CD. These effects can be explained considering that the concentration of β-CD is lower than that of HPβ-CD, the water proportion was higher in the ethanolic mixtures than in the methanolic ones and hence the formation of inclusion complexes is favoured in the ethanolic mobile phases, and also taking into account that the association constant values are higher for HPβ-CD than for β-CD. The decrease in the retention factors is a consequence of the higher solubility of the inclusion complexes in the mobile phase [36] in comparison to free alkaloids present in the non-modified mobile phases.

The realiability of the chromatographic method was shown by the agreement in the retention time obtained for β-carbolines in the standard solutions and those obtained for the spiked serum samples. A good reproducibility in the retention times was obtained in non-modified mobile phases and in the presence of CDs. Thus, after 12 consecutive injections of the standard solutions, the change in the retention times was in the 0.5 - 2% range for all the analytes using mobile phases without CDs. Similarly, no significant changes in the retention times were observed in the presence of CDs (1-3%). A percentage of reduction in the retention time of 3-7% was observed after 35-40 injections in three consecutive days with CDs. The highest reduction was observed in ethanolic mobile phases for both β-CD and HPβ-CD. The peak area reproducibility was also evaluated by injecting the standard solutions.

3.4. Validation of the chromatographic method

Linearity ranges and limits of detection were deduced using standard solutions of norharmane, harmane and harmine dissolved in the mobile phases in the 0.1 µM - 1.0 µM

concentration range. Duplicate injections were made for each standard solution. The limit of detection (Table 3) was determined by injecting 6 times a solution of concentration 0.1 µM and then calculated as described by Zheng [20a] The calibration curves for the β-carbolines studied were linear over the 0.1 - 1.0 µM concentration range. The correlation coefficients (R^2) were obtained from linear regression treatment, using the peak area *versus* concentration for each standard compound. An increase in the correlation and in the slopes of the calibration curves was observed in the presence of CDs in ethanolic or methanolic mobile phases. When HPβ-CD was employed as mobile phase additive, the slopes for the three alkaloids were twice as high in comparison with the non-modified mobile phases. The Limits of Detection (LODs) obtained in the presence of CDs were better than the ones obtained in non-modified mobile phases for both types of CDs and mobile phases studied (Table 3). The enhancement of LODs was most noticeable for ethanolic mobile phase and HPβ-CD. Fluorimetric detection is adequate for the quantitation of these alkaloids, whose high native fluorescence is enhanced by the formation of CD inclusion complexes, increasing the sensitivity for their detection [42]. The LOD values obtained (2 - 6 × 10^{-8} M, which corresponds to 3.6 - 10.8 ng mL^{-1}) were in the same range to other chromatographic procedures described for the determination of β-carbolines in blood samples [20a-c]. These values were better than those required for the analysis of the alkaloids [17,18b] in foodstuffs, cigarrette smoke condensates or plant extracts.

Precision was evaluated by the intra-day and inter-day repeatability Relative Standard Deviation (RSD, %). For intra-day assays the standard solution containing the mixture of alkaloids was injected 6 times in the same day. For the inter-day RSD calculation the standard solutions containing the mixture of alkaloids were injected in

Table 3. Linear regression study (0.1-1.0 µM) and limit of detection obtained for β-carbolines under different experimental conditions

Mobile phase	Compound	R^2	LOD
	Without CDs in the mobile phase		
MeOH:Buffer 50:50	Norharmane	0.9970	5.92 × 10^{-8} M
	Harmane	0.9960	6.10 × 10^{-8} M
	Harmine	0.9959	3.77 × 10^{-8} M
EtOH:Buffer 30:70	Norharmane	0.9887	1.04 × 10^{-7} M
	Harmane	0.9903	1.20 × 10^{-7} M
	Harmine	0.9521	1.41 × 10^{-7} M
	3 mM β-CD in the mobile phase		
MeOH:Buffer 50:50	Norharmane	0.9993	2.03 ×10^{-8} M
	Harmane	0.9996	2.07 ×10^{-8} M
	Harmine	0.9997	3.66 ×10^{-8} M
EtOH:Buffer 30:70	Norharmane	0.9975	6.33 ×10^{-8} M
	Harmane	0.9987	5.30 ×10^{-8} M
	Harmine	0.9940	7.46 ×10^{-8} M
	15 mM HPβ-CD in the mobile phase		
MeOH:Buffer 50:50	Norharmane	0.9987	5.15 ×10^{-8} M
	Harmane	0.9991	5.36 ×10^{-8} M
	Harmine	0.9992	4.70 ×10^{-8} M
EtOH:Buffer 30:70	Norharmane	0.9978	6.14 ×10^{-8} M
	Harmane	0.9974	5.83 ×10^{-8} M
	Harmine	0.9975	5.47 ×10^{-8} M

R^2 Coefficient of determination; LOD limit of detection (n = 6).

duplicate sets during 6 consecutive days. Intra-day and inter-day precision studies were carried out at two levels of concentration: 0.1 μM and 1.0 μM (Table 4). The precision of the method was good, as shown by the fact that RSD values were lower than 8% in 64 cases out of 72. The RSD values were higher for the ethanolic mobile phases than for the methanolic ones for both concentration levels. These results are a consequence of the efficiency of the chromatographic conditions, since the peaks are wider in ethanol than in methanol and this affects the quantitation based on peak areas. The intra-day precision was enhanced in the presence of β-CD as MPA for both mobile phases with regard to the results obtained without CDs (for a graphical comparison, see figure 9). The intra-day precision for β-CD was better than in the case of HPβ-CD for both mobile phases. The differences between the RSD values for intra-day assay and inter-day assay are negligible, which shows a good response of the chromatographic system in the presence of CD additives in the mobile phase, owing to the adequate selection of CD concentrations and the efficiency of the daily washing procedure [32,33]. Thus, comparing the same mobile phase and the same CD as MPA, the RSD values for inter-day assay are lower than the corresponding intra-day assay RSD values. These results can be ascribed to the fact that the inter-assay experiments were developed each day after the night washing procedure and hence the detrimental effect of the presence of CDs in the mobile phases during several hours is avoided.

Accuracy was estimated as the percentage of the measured concentration (on the calibration curves) over the nominal concentrations. The accuracy of the chromatographic separation and of the total methodology including the pre-treatment

Table 4. Evaluation of the precision of the chromatographic method at two levels of concentration: 0.1 μM and 1.0 μM

Compound	Intra-day precision[a] (%RSD)		Inter-day precision[a] (%RSD)	
	MeOH:Buffer 50:50	EtOH:Buffer 30:70	MeOH:Buffer 50:50	EtOH:Buffer 30:70
Without CDs in the mobile phase				
Norharmane[b]	3.31	3.09	1.55	9.20
Harmane[b]	2.87	11.53	1.91	4.29
Harmine[b]	4.97	11.42	1.50	3.60
Norharmane[c]	3.55	4.31	1.85	6.27
Harmane[c]	2.30	1.19	1.94	6.06
Harmine[c]	4.32	7.74	1.35	5.53
3 mM β-CD in the mobile phase				
Norharmane[b]	3.10	4.14	1.82	7.39
Harmane[b]	1.79	2.75	2.95	8.15
Harmine[b]	6.09	9.73	4.76	5.97
Norharmane[c]	1.85	2.40	3.85	3.79
Harmane[c]	1.62	2.20	4.53	3.91
Harmine[c]	2.61	4.02	5.16	4.04
15 mM HPβ-CD in the mobile phase				
Norharmane[b]	5.25	7.64	5.42	8.27
Harmane[b]	7.23	5.86	6.33	8.51
Harmine[b]	4.52	6.40	8.53	6.73
Norharmane[c]	4.72	5.49	3.83	3.10
Harmane[c]	4.02	5.34	2.69	2.88
Harmine[c]	4.08	6.37	3.77	6.19

[a] *n = 6.* [b] *0.1 μM.* [c] *1.0 μM*

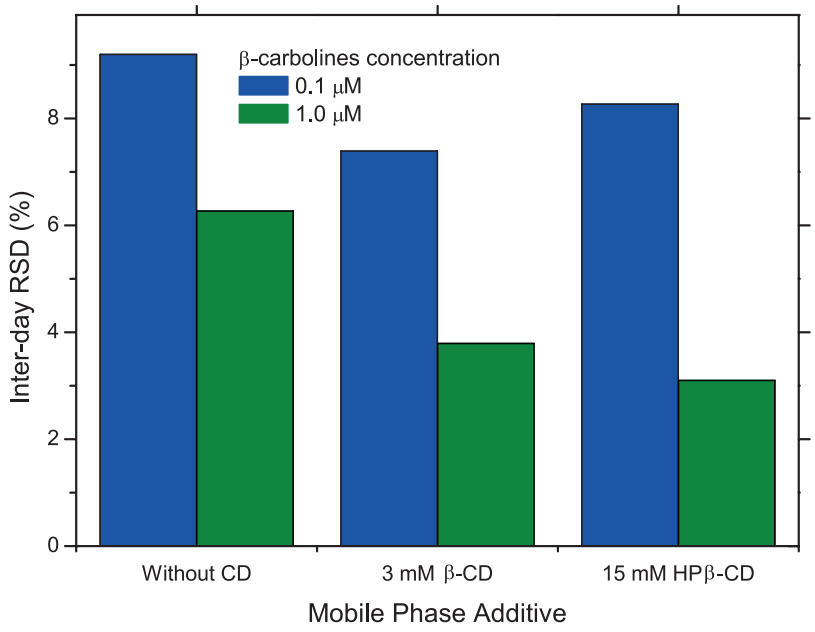

Figure 9. Effect of CDs as MPA on the inter-day precision obtained in the separation of norharmane. Mobile phase: EtOH:buffered aqueous solution, 30:70 (v:v).

procedures has been determined to show the utility of CDs as MPA. The accuracy of the chromatographic procedure was evaluated in terms of recovered concentrations. An exactly measured volume of the standarized solutions of the β-carbolines under study was added to the extracted serum samples containing a concentration of 0.5 μM of each β-carboline alkaloids. Then the samples were injected (n=3) under the different chromatographic conditions. The results are presented in Table 5. The recoveries obtained (91-113%) are very satisfactory for the experimental conditions including CDs as MPA.

In order to verify the accuracy of the methodology (extraction and chromatographic procedures) for the determination of β-carboline derivatives in biological samples, absolute recoveries were calculated. Thus, a known amount of each β-carboline studied was added to the spiked serum samples containing 0.500 μM concentration and then the complete analytical protocol was applied. The recoveries obtained are

Table 5. Accuracy of the chromatographic procedure for β-carbolines in different experimental conditions. The accuracy was evaluated in terms of recovery (%).

Compound	Recoveries (%)[a]	
	MeOH:Buffer 50:50	EtOH:Buffer 30:70
	Without CDs in the mobile phase	
Norharmane	101.3	113.0
Harmane	108.8	107.9
Harmine	106.2	103.6
	3 mM β-CD in the mobile phase	
Norharmane	98.5	100.0
Harmane	99.1	102.1
Harmine	89.8	92.7
	15 mM HPβ-CD in the mobile phase	
Norharmane	96.4	106.6
Harmane	101.6	107.7
Harmine	91.7	92.6

[a] *β-Carboline alkaloids were added (c = 0.250 μM) to the previously extracted spiked serum samples containing the alkaloids in concentrations 0.500 μM.*

Table 6. Absolute recoveries (as %) obtained for β-carbolines in human serum samples.

Compound	LLE		SPE	
	MeOH:Buffer 50:50	EtOH:Buffer 30:70	MeOH:Buffer 50:50	EtOH:Buffer 30:70
Without CDs in the mobile phase				
Norharmane[a]	133.0	109.2	94.8	91.7
Harmane[a]	114.2	109.1	107.5	90.1
Harmine[a]	112.1	111.9	102.6	115.5
Norharmane[b]	89.0	107.8	82.1	101.4
Harmane[b]	110.4	112.9	95.0	95.6
Harmine[b]	100.7	134.7	87.2	111.8
3 mM β-CD in the mobile phase				
Norharmane[a]	115.8	146.8	102.7	70.7
Harmane[a]	92.4	122.7	109.2	87.7
Harmine[a]	84.3	119.2	84.8	92.3
Norharmane[b]	74.5	144.4	107.3	91.8
Harmane[b]	99.8	149.5	105.2	83.0
Harmine[b]	87.9	134.7	97.4	95.0
15 mM HPβ-CD in the mobile phase				
Norharmane[a]	123.5	146.9	77.3	85.3
Harmane[a]	115.5	153.1	83.0	96.6
Harmine[a]	112.0	159.5	92.1	97.6
Norharmane[b]	76.9	136.8	78.7	81.8
Harmane[b]	100.1	151.4	81.0	78.6
Harmine[b]	92.3	147.4	82.3	93.0

[a]The alkaloid was added up to a final 0.125 μM concentration. [b]The alkaloid was added up to a final 0.250 μM concentration.

presented in Table 6. The chromatographic recoveries were close to 100%, while for the overall method the recoveries present a greater dispersion. The values obtained for the absolute recoveries are in a range similar or better than those described in the literature for different analytes in real samples, *i.e.* β-carbolines in serum samples (70-130%) [20a], phenotiazine derivatives in human urine (67-105%) [43] and anti-depressant drugs in plasma (52-110%) [44].

Regarding the extraction procedures employed, it can be appreciated that the recoveries obtained for the aliquots extracted by SPE are better than those obtained from the LLE using the method described by Zheng [20a]. The absolute recoveries obtained for the SPE method were in the range of 81-115% in 33 out of 36 cases, but the recoveries for LLE-extracted samples were less adequate. These results can be explained considering that the extracts obtained by both extraction procedures are in different solvents, since the eluates obtained from SPE are in a methanol:acidic aqueous solution and the acid pH assures the protonation of the alkaloids, thus increasing their solubilities and allowing the use of a reduced volume of organic solvent. On the other hand, liquid-liquid extraction according to the Zheng protocol [20a] requires tedious evaporation of each individual fraction and subsequent re-dissolution of the dry residues in a small volume of methanol to avoid dilution of the analytes, and in these conditions the residue is not completely dissolved. Since these methanol solutions are then directly injected into the chromatograph, these problems lead to an increase in the width of the chromatographic peaks for the case of the LLE-extracted samples (Figure 10), for both methanolic and ethanolic mobile phases. This behaviour

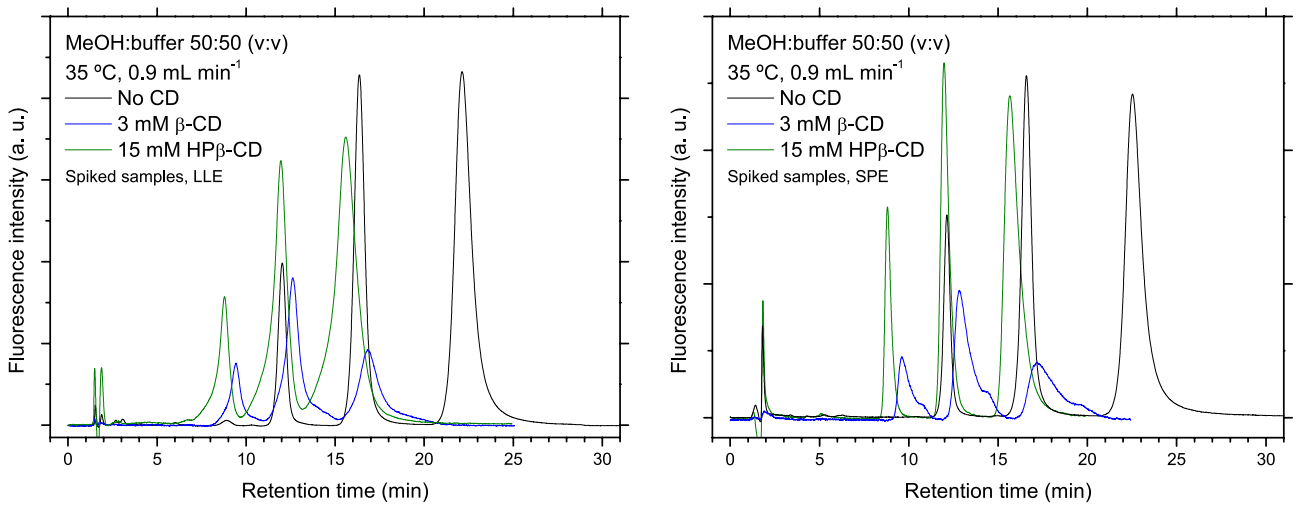

Figure 10. Effects of CDs on the separation of β-carboline alkaloids in the spiked and extracted serum samples. Peaks corresponding to compounds as in Figure 8.

was not observed for the SPE extracts, explaining why accuracy values obtained in the validation for SPE are better than for LLE. As an additional advantage, SPE results in a lower volume of extractive mixtures, which have a higher proportion of water; this is possible due to the ionic exchange retention mechanism. Besides, SPE requires less operator time and simpler experimental conditions.

Table 7. Determination of β-carbolines in spiked human serum samples. Experimental values obtained employing the chromatographic procedures and clean-up protocols developed in this paper (liquid–liquid extraction, LLE and solid-phase extraction, SPE)

Compound	LLE		SPE	
	MeOH:Buffer 50:50	EtOH:Buffer 30:70	MeOH:Buffer 50:50	EtOH:Buffer 30:70
Without CDs in the mobile phase				
Norharmane[a]	0.248	0.285	0.205	0.243
Harmane[a]	0.285	0.261	0.231	0.217
Harmine[a]	0.290	0.294	0.230	0.258
Norharmane[b]	0.435	0.457	0.379	0.458
Harmane[b]	0.494	0.448	0.419	0.436
Harmine[b]	0.482	0.469	0.405	0.460
3 mM β-CD in the mobile phase				
Norharmane[a]	0.240	0.255	0.261	0.214
Harmane[a]	0.272	0.271	0.278	0.234
Harmine[a]	0.237	0.272	0.253	0.210
Norharmane[b]	0.408	0.422	0.523	0.418
Harmane[b]	0.460	0.473	0.562	0.449
Harmine[b]	0.418	0.488	0.504	0.413
15 mM HPβ-CD in the mobile phase				
Norharmane[a]	0.231	0.233	0.202	0.198
Harmane[a]	0.255	0.256	0.229	0.213
Harmine[a]	0.243	0.246	0.206	0.179
Norharmane[b]	0.387	0.424	0.386	0.423
Harmane[b]	0.438	0.461	0.439	0.438
Harmine[b]	0.401	0.416	0.385	0.381

[a]*The theoretical value was 0.250 μM.* [b]*The theoretical value was 0.500 μM.*

3.5. Application of the developed methodology to the analysis of β-carbolines in human serum samples

The pooled serum samples spiked with β-carbolines at 0.250 μM and 0.500 μM concentrations were analyzed by the proposed RP-HPLC procedures after sample clean-up (LLE or SPE). The experimental concentrations of β-carbolines were calculated considering the areas under the peaks and comparing to those obtained from the standard calibration curves. The values of alkaloid concentrations found in the samples are shown in Table 7. According to the figures of merit obtained, the differences among the theoretical values of β-carbolines and the experimental values obtained are related to the extraction methodology employed. In conclusion, these chromatographic procedures can be successfully applied to the quantitation of β-carbolines in biological samples.

3.6. Comparison to other chromatographic separations (RP-HPLC) of β-carbolines

The proposed method was compared to some of the most representative HPLC quantitation methods for β-carboline alkaloids [14,18b,20a,26a] in terms of solvent consumption. The methodology described here avoided the use of acetonitrile and also allowed a considerable reduction of the proportion of methanol in the mobile phase (from 70% to 50%). It also allowed the use of ethanol as mobile phase, which was unprecedented. Furthermore, the presence of CDs as MPA increased the sensitivity for detection of the analytes and did not reduce the accuracy or precision of the methodology.

4. Conclusions

The inclusion complexes from norhamane, harmane and harmine with β-CD and HPβ-CD have been characterized by 1D- and 2D-NMR experiments. For the cases of harmane and harmine, and for inclusion complexes with both 1:1 and 1:2 alkaloid:CD stoichiometries, these studies show that inclusion takes place through the benzene ring of the host molecules, and the pyridine moiety remains partially outside the CD cavities. In the case of norharmane, either the benzene or the pyridine rings at the ends of the molecule can enter the CD cavities. Interestingly, these structural studies are in good agreement with the association constant values obtained by RP-HPLC, where the highest K_{ass} were those obtained for the case of norhamane because the more effective interactions with the CDs reduce the interaction with the stationary phases and hence the retention times. This correlation between structural data obtained by NMR and chromatographic behaviour constitutes another innovative aspect of our work. The addition of CDs allows a reduction of the organic solvent content in the HPLC mobile phases. Furthermore, it also allows the use of renewable solvents (methanol and ethanol) as the organic component, avoiding the use of the more toxic acetonitrile, the most frequent organic component in the analysis of β-carbolines by RP-HPLC. It has been demonstrated that the presence of β-CD and HPβ-CD as MPA does not exert a negative influence on the analytical performance of the chromatographic procedure. On the contrary, the sensitivity is increased in the presence of CDs and the accuracy and precision of the method are very satisfactory for the analysis of these interesting compounds in complex biological matrices. The use of SPE pre-treatment was compared with LLE and had the advantage of a lower use of organic solvents while it led to better analytical results and a good compatibility of the extraction solvents with the mobile phase composition. Therefore the presence of CDs in the mobile phases potentially allows the traditional HPLC technique to become

an attractive eco-separation technique using conventional and inexpensive columns and stationary phases, under simple and user-friendly experimental conditions.

5. Acknowledgements

Financial support from Ministerio de Ciencia e Innovación (Spain) through grants CTQ 2009-11312-BQU and CTQ 2009-12320-BQU as well as from Grupos de Investigación UCM (920234) is gratefully acknowledged. The authors are also grateful to MEC for the award of a FPU research fellowship to V. González-Ruiz.

6. References

1. J. Sezjtli, Chem. Rev., 1998, 98, 1743-1753.
2. (a) H. Bricout, F. Hapiot, A. Ponchel, S. Tilloy and E. Monflier, Sustainability, 2009, 1, 924-945 (b) B. Chankvetadze, in: H. Dodziuk (Ed.), Cyclodextrins and their complexes, Wiley-VCH, Weinheim, 2006, pp. 119-146. (c) S. Tilloy, H. Bricout and E. Monflier, Green Chem., 2002, 4, 188-193.
3. T. Cserháti and E. Forgacs, Cyclodextrins in Chromatography, Royal Society of Chemistry, Cambridge, 2003.
4. C. Gazpio, M. Sánchez, I. X. García-Zubiri, I. Velaz, C. Martínez-Ohárriz, C. Martín and A. Zornoza, J. Pharm. Biomed. Anal., 2005, 37, 487-492.
5. P. K. Zarzycki, H. Ohta, Y. Saito and K. Jinno, Anal. Bioanal. Chem., 2008, 391, 2793-2801.
6. J. Ye, G. Chen and S. Zeng, J. Chromatogr. B, 2006, 843, 289-294.
7. D. Chen, S. Jiang, Y. Chen and Y. Hu, J. Pharm. Biomed. Anal., 2004, 34, 239-245.
8. A. Kwaterczak, K. Duszczyk and A. Bielejewska, Anal. Chim. Acta, 2009, 645, 98-104.
9. (a) A. El-Gindy, S. Emara, M. K. Mesbah and G. M. Hadad, J. Assoc. Off. Anal. Chem., 2006, 89, 65-70. (b) N. F. S. de Melo, R. Grillo, A. H. Rosa and L. F. Fraceto, J. Pharm. Biomed. Anal., 2008, 47, 865-869. (c) R. Grillo, N. F. S. de Melo, C. M. Moraes, R. Lima, C. M. S. Menezes, E. I. Ferreira, A. H. Rosa and L. F. Fraceto, J. Pharm. Biomed. Anal., 2008, 47, 295-302. (d) J. M. López-Nicolás and F. García-Carmona, Food Chem., 2008, 109, 868-875. (e) P. Rodríguez-Bonilla, J. M. López-Nicolás and F. García-Carmona, J. Chromatogr. B, 2010, 878, 1569-1575. (f) J. Guan, J. Yang, Y. Bi, S. Shi, F. Yan, and F. Li, J. Sep. Sci., 2008, 31, 288-293.
10. (a) J. M. López-Nicolás, E. Núñez-Delicado, A. J. Pérez-López, A. Carbonell-Barrachina and P. Cuadra-Crespo, J. Chromatogr. A, 2006, 1135, 158-165. J. Pan, G. Kai, C. Yuan and R. Jin, Chromatographia, 2007, 66, 121-123. J. Pan, G. Kai, C. Yuan, B. Zhou, R. Jin and Y. Yuan, Chin. J. Chromatogr., 2007, 25, 316-318.
11. (a) A. M. Soban, S. A. Ebrahimi and M. Mahmoudian, J. Pharm. Sci., 2002, 5, 19-23. (b) Y. Totsuka, H. Ushiyama, J. Ishihara, R. Sinha, S. Goto, T. Sugimura and K. Wakabayashi, Cancer Lett., 1999, 143, 139-143.
12. R. A. Glennon, B. Grella, R. J. Tyacke, A. Lau, J. Westaway and A. L. Hudson, Bioorg. Med. Chem. Lett., 2004, 14, 999-1002.
13. (a) D. Fekkes, A. Tuite, I. Bom and L. Pepplinkhuizen, Life Sci., 2001, 69, 2113-2121. (b) A. Greube and H. Rommelspacher, J. Chromatogr. B, 2003, 784, 155-168.
14. E. D. Louis, W. Jiang, K. M. Pellegrino, E. Ríos, P. Factor-Litvak, C. Henchcliffe and W. Zheng, NeuroToxicology, 2008, 29, 294-300.
15. N. Wodarz, G. A. Wiesbeck, H. Rommelspacher, P. Riederer and J. Böning, Alcohol Clin. Exp. Res., 1996, 20, 706-710.
16. R. Stohler, H. Rommelspacher and D. Ladewig, Eur. Psychiat., 1995, 10, 56-58.
17. U. Breyer-Pfaff, G. Wiatr, I. Stevens, H. J. Gaertner, G. Mundle and K. Mann, Life Sci., 1996, 58, 1425-1432.
18. (a) T. Herraiz, J. Chromatogr. A, 2000, 881, 483- 499. (b) M. Kartal, M. Altun and S. Kurucu, J. Pharm. Biomed. Anal., 2003, 31, 263-269.
19. (a) J. Adachi, Y. Mizoi, T Naito, K. Yamamoto, S. Fujiwara and I. Ninomiya, J. Chromatogr., 1991, 538, 331-339. (b) T. Herraiz and C. Chaparro, J. Chromatogr. A, 2006, 1120, 237-243.
20. (a) W. Zheng, S. Wang, L. F. Barnes, Y. Guan and E. D. Louis, Anal Biochem., 2000, 279, 125-129. (b) E. D. Louis, W. Zheng, E. C. Jurewicz, D. Watner, J. Chen, P. Factor-litvak and M. Parides, Neurology, 2002, 59, 1940-1944.(c) Y. Guan, E. D. Louis and W. Zheng, J. Toxicol. Env. Health A 2001, 64, 645-660. (d) T. R. Bosin and K. F. Faull, J. Chromatogr. 1988, 428, 229-236.
21. H. Tsuchiya, J. Chromatogr. A, 2004, 1031, 325-330.
22. L. Agüí, C. Peña-Farfal, P. Yánez-Sedeño and J. M. Pingarrón, Anal. Chim. Acta, 2007, 585, 323-330.
23. (a) C. J. Smith, S. Qian, Q. Zha and S. C. Moldoveanu, J. Chromatogr. A, 2004, 1046, 211-216. (b) S. Casal, E. Mendes, J. O. Fernandes, M. B. P. P. Oliveira and M. A. Ferreira, J. Chromatogr. A, 2004, 1040, 105-114. (c) T. Herráiz and C. Chaparro, Biochem. Biophys. Res. Commun., 2005, 326, 378-386.
24. J. Stöckigt, Y. Sheludko, M. Unger, I. Gerasimenko, H. Warzecha and D. Stöckigt, J. Chromatogr. A, 2002, 967, 85-113.

25. (a) T. Herraiz, Food Chem., 1999, 66, 313-321. (b) T. Herraiz, Food Addit. Contam., 2002, 19, 748-754. (c) N. Rosales-Conrado, M. E. León-Gonzáles, L. V. Pérez-Arribas and L. M. Polo-Díez, Anal. Bioanal. Chem., 2008, 391, 1433-1442. (d) T. Herraiz, H. Guillén and V. J. Arán, Chem. Res. Toxicol., 2008, 21, 2172-2180. (e) Y. M. Back, J. H. Lee, H. S. Shin and K.G. Lee, Food Addit. Contam., 2009, 26, 298-305. (f) T. Herraiz, D. González, C. Ancín-Azpilicueta, V. J. Arán and H. Guillén, Food Chem. Toxicol., 2010, 48, 839-845.
26. (a) M. Yritia, J. Riba, J. Ortuño, A. Ramírez, A. Castillo, Y. Alfaro, R. de la Torre and M. J. Barbanoj, J. Chromatogr. B, 2002, 779, 271-281. (b) Moncrieff, J. Chromatogr., 1989, 496, 269-278.
27. F. M. Kerton, Alternative Solvents for Green Chemistry, Royal Society of Chemistry, Cambridge, 2009, pp. 97-117.
28. (a) C. Capelo, U. Fischer and K. Hungerbühler, Green Chem., 2007, 9, 927-934. (b) C. J. Welch, T. Brkovic, W. Shafer and X. Gong, Green Chem., 2009, 11, 1232-1238.
29. J.-F. Jen, S.-L. Hsiao and K. H. Liu, Talanta, 2002, 58, 711-717.
30. L. Zhu, L. Ding, Q. Zhang, L. Wang, F. Tang, Q. Liu and S. Yao, Green Chem., 2009, 11, 132-137. (a) T. Cserháti and E. Forgács, J. Chromatogr. A, 1996, 722, 33-40. (b) O. Jiménez, M. A. García and M. L. Marina, J. Chromatogr. A, 1996, 719, 15-26.
31. A. C. Moffat, J. V. Jackson, S. M. Moss and B. Widdop, Clarke's Isolation and Identification of Drugs (2nd Edition), Pharmaceutical Press, London, 1986.
32. A. G. León, A. I. Olives, B. del Castillo and M. A. Martín, J. Chromatogr. A, 2008, 1192, 254-258.
33. A. G. León, A. I. Olives, M. A. Martín and B. del Castillo, J. Incl. Phenom. Macrocycl. Chem., 2007, 57, 577-583.
34. (a) L. Martín, A. León, M. A. Martín, B. del Castillo, J. C. Menéndez, J. Pharm. Biomed. Anal. 2003, 32, 991-1001 (b) L. Liu and Q.-X. Guo, J. Incl. Phenom. Macrocycl. Chem., 2002, 42, 1-14.
35. (a) H.-J. Schneider, F. Hacket, V. Rüdiger and H. Ikeda, Chem. Rev., 1998, 98, 1755-1785. (b) G. Fronza, A. Mele, E. Redenti and P. Ventura, J. Org. Chem., 1996, 61, 909- 914. (c) P. K. Owens, A. F. Fell, M. W. Coleman, M. Kinns and J. C. Berridge, J. Pharm. Biomed. Anal. 1997, 15, 1603- 1619. (d) C. Danel, N. Azaroual, C. Foulon, J.-F. Goosens, G. Vermeersch, J.-P. Bonte, C. Vaccher, Tetrahedron: Asym., 2006, 17, 975-983. (e) M. C. Bergonzi, A. R. Bilia, L. Di Bari, G. Mazzi and F. F. Vincieri, Bioorg. Med. Chem. Lett., 2007, 17, 5744-5748.
36. K. G. Flood, E. R. Reynolds and N. H. Snow, J. Chromatogr. A, 2000, 903, 49-65.
37. J. Szejtli and T. Osa (Eds.) Comprehensive Supramolecular Chemistry: Cyclodextrins, Elsevier, Oxford, 1996, p. 228.
38. (a) A. Bielejewska, K. Duszczyk and D. Sybilska, J. Chromatogr. A, 2001, 931, 81-93. (b) K. A. Connors, J. Pharm. Sci., 1995, 84, 843- 848. (c) Y. Matsui and K. Mochida, Bull. Chem. Soc. Jpn., 1979, 52, 2808- 2814.
39. I. Clarot, D. Clédat, S. Battu and P. J. P. Cardot, J. Chromatogr. A, 2000, 903, 67-76.
40. B. Claude, Ph. Morin, M. Lafosse and P. Andre, J. Chromatogr. A, 2004, 1049, 37-42.
41. J. Zukowski, D. Sybilska and J. Jurczak, Anal. Chem., 1985, 57, 2215-2219.
42. P. Prognon, A. Kasselouri, M. C. Desroches and G. Mahuzier, Analusis, 2000, 28, 664-669.
43. M. Cruz-Vera, R. Lucena, S. Cárdenas and M. Valcárcel, J. Chromatogr. B, 2009, 877, 37-42.
44. A. R. Chaves, S. M. Silva, R. H. C. Queiroz, F. M. Lanças and M. E. C. Queiroz, J. Chromatogr. B, 2007, 850, 295-302

This page intentionally left blank

9

SPE/RP-HPLC using C1 columns: an environmentally friendly alternative to conventional reverse phase separations for quantitation of β-carboline alkaloids in human serum samples

Published in: González-Ruiz, V., Olives, A. I., & Martín, M. A. (2011). Anal. Bioanal. Chem., 400(2), 395–401.

ABSTRACT ▶ The analysis of beta-carboline alkaloids presents a renewed interest due to their biological relevance and their increasing popularity as recreational drugs. In the present work a novel chromatographic RP-HPLC method with fluorimetric detection has been applied to the determination of β-carbolines spiked in human serum samples. The chromatographic procedure involves the use of less retentive, unusual C1 columns combined with hydro-alcoholic mobile phases and the use of β-cyclodextrin or (2-hydroxypropyl)-β-cyclodextrin as mobile phase additives. The effective combination of C1 columns and the modified mobile phases with cyclodextrins leads to a considerable reduction in the organic proportion in the mobile phase (up to 50%) with good resolution and efficiency. Besides, the presence of cyclodextrins allows the use of ethanol, a green solvent, as the organic component in the mobile phase. Traditional RP-HPLC thus becomes an attractive eco-separation technique using conventional stationary phases under simple and user-friendly experimental conditions. Solid phase extraction was employed as sample clean-up protocol with attractive features, i.e a low consumption of organic solvents, time and step economy and diminished need for sample handling. The analytical procedure was completely validated showing satisfactory figures of merit. Limits of detection of 10^{-9}-10^{-10} M can be achieved. The recoveries obtained for the total methodology (sample pre-treatment and chromatographic determination in the case of the mobile phases containing cyclodextrins) were very satisfactory (95-107%) as well as the intra-day (2-3%) and inter-day precision values (3-7%). The use of 3-hydroxymethyl-β-carboline as an internal standard allows the comparison of the goodness of response of the analytical methodology in the presence or absence of cyclodextrins.

DOI ▼
10.1007/s00216-010-4562-2

ABBREVIATIONS ▼
- **β-CD:** β-cyclodextrin
- **3HMBC:** 3-Hydroxymethyl-β-carboline
- **CDs:** Cyclodextrins
- **HPβ-CD:** 2-Hydroxypropyl-β-cyclodextrin
- **HPLC:** High-performance liquid chromatography
- **IS:** Internal standard
- **MPA:** Mobile phase additives
- **QC:** Quality control samples
- **RP-HPLC:** Reverse phase-HPLC
- **SPE:** Solid-phase extraction

1. Introduction

β-Carboline alkaloids are natural products generated in the metabolism of indole-3-ethylamines [1] that occur in a great variety of samples including plant extracts [2,3], animal tissues, biological fluids [4], foods and foodstuffs [5] specially meat and fish, alcoholic beverages [6] and tobacco [7,8]. The extracts of seeds or roots from *Peganum harmala* [9-11] and *Banisteriopsis caapi* [12] are rich in these alkaloids. They also appear in marine sponges [13,14], termites [15] and mammalian tissues [16], and thus they are known as indole mammalian alkaloids. Inhalation of the smoke from dried plants or the consumption of plant extracts containing β-carboline alkaloids are popular in some traditional ceremonies of Amazonian tribes [12,17]. Similar rituals have been described in Iran during the pre-Islamic times [18], and their effects are associated to the psychoactive and hallucinogenic properties of these alkaloids, which are able to interact with different neural receptors such as benzodiazepine or imidazoline receptors. Their psychotropic and neurotoxic effects, together with other symptoms (gastrointestinal and cardiac problems) could produce severe clinical disorders. Therefore, the analysis of β-carboline alkaloids presents a renewed interest, not only due to their occurrence in foodstuffs and biological fluids, but also due to

the recent report of intoxications produced among young people in North America and Europe following the intake of infusions prepared from seeds and roots of *Peganum harmala*. Those dried vegetable parts are easily available through the Internet [10,19] and thus beyond the control of health authorities.

One of the challenges of modern analytical chemistry is the search for new techniques and methodologies able to reduce the use of environmentally hazardous solvents and reagents. This issue is especially relevant in the case of HPLC, because of the widespread use of this analytical technique in most chemical, pharmaceutical and government laboratories. Different alternatives have been proposed to reduce the generation of organic solvents waste in HPLC including microflow-HPLC [20, 21] or the use of stationary phases allowing a high water proportion in the mobile phases [22]. Another alternative aimed at reducing the organic solvent consumption involves the use of mobile phase additives (MPA) such as surfactants [23] (micellar liquid chromatography, MLC) or cyclodextrins (CDs) in the mobile phases. Thus, the use of β-CD as MPA makes possible to use a higher proportion of water in mobile phases for the separation of citalopram [24] and *trans*-resveratrol in methanol:buffered aqueous solution (50:50) [25], and also employing mixtures of CDs [26] in the mobile phase has been described. Furthemore, CDs are natural products, easy to produce and completely biodegradable and it has been shown that they may help to solve complicated separation problems [27,28].

Acetonitrile is one of the most popular solvents employed in HPLC due to its low viscosity and UV transparency, but its toxicity has led to an increasing interest in replacing it by alcohols [29,30]. Furthermore, acetonitrile is obtained as a by-product in the manufacture of acrylonitrile polymers and cannot be considered as a renewable resource. In the case of the analysis of β-carboline alkaloids the use of acetonitrile is much more common than methanol as the organic component in the mobile phase.

In the present work we describe the separation of the β-carboline alkaloids norharmane, harmane and harmine (Figure 1) by HPLC, employing the uncommon reverse phase C1 columns. The use of this stationary phase, combined with the presence of CDs as MPA, allows a notable increase in the proportion of water in the mobile phase. The proposed methodology involves the use of less or non-toxic, renewable solvents (alcohols), which is an attractive feature that makes it an eco-separation. In an effort to reduce the organic solvent consumption also in the sample pre-treatment, SPE has been employed. The validation of the developed methodology (SPE/HPLC) was ca-

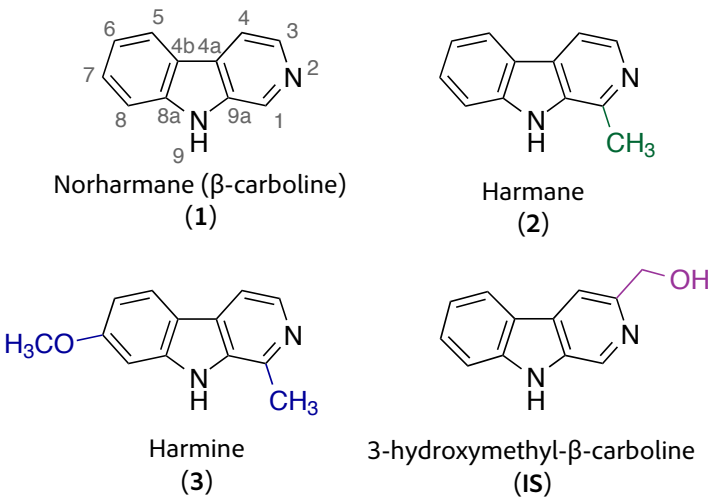

Figure 1.
Chemical structures of the β-carboline alkaloids analyzed in spiked human serum samples.

rried out to show the utility of the combination of both methods, and excellent results were obtained. We used β-carboline spiked serum samples as model biological matrices, taking into account the toxicological relevance of the presence of these alkaloids in human serum.

2. Materials and methods

A Hitachi (Tokyo, Japan) liquid chromatographic system equipped with a quaternary gradient pump model L-7100 and a fluorescence detector model L-7485 was employed and a Hitachi (Tokyo, Japan) liquid chromatographic system equipped with an isocratic pump model L-6000 and a F-1050 fluorescence detector was also used. For all experiments the detection conditions were λ_{ex}= 290 nm, λ_{em}= 430 nm. Both chromatographic systems were equipped with a Rheodyne 7725i injector (20 µL loop) and they were under computer control through the HPLC System Manager software, version 4.1. The column temperature was kept constant at 35 ^{o}C with a Merck Hitachi oven model L-2300. Separations were developed in isocratic reverse phase using C1 columns (Kromasil 100 C1, 5 µm, 125 × 4 mm, Teknokroma, Barcelona, Spain). The flow rate was 0.9 mL min^{-1}.

UV-Vis absorption spectra were obtained with a Kontron (Zurich, Switzerland) Uvikon 810 double beam spectrophotometer. Excitation and emission spectra and measurements at fixed wavelengths were obtained with a Horiba-Jobin Yvon (Edison, NJ, USA) FluoroMax-4P spectrofluorometer equipped with the control and data acquisition software FluorEssence 2.1.

All reagents (analytical grade) and solvents (spectroscopic or chromatographic grade) were from Panreac (Barcelona, Spain) and were used without further purification. Water was doubly distilled and deionized (Milli-Q purification system, Millipore, Molsheim, France). Norharmane, harmane, harmine and (2-hydroxypropyl)-β-CD (HPβ-CD) were purchased from Sigma (Steinheim, Germany). 3-Hydroxymethyl-β-carboline (3HMBC) was supplied by Research Biochemicals Incorporated (Natick, MA, USA). Native β-cyclodextrin (β-CD) was acquired from Fluka (Steinheim, Germany). Propylsulfonic acid-derivatized silica SPE cartridges (Isolute SCX 2, 3 mL capacity) were obtained from International Sorbent Technology, Mid Glamorgan, UK.

Six mobile phases were compared. Solvent mixtures consisting of methanol:aqueous buffer 40:60 v:v and ethanol:aqueous buffer 25:75 v:v were employed without CDs and with 3 mM β-CD and 15 mM HPβ-CD. Phosphate 0.02 M at pH 7.8 was used as aqueous buffer. To prepare the mobile phases containing CDs as additives, an appropriate amount of the cyclodextrin was weighed and dissolved in the corresponding hydro-alcoholic mixture, up to a final volume of 500 mL. Finally, sonication was applied until full dissolution. All mobile phases were filtered through 0.45 µm pore membrane filter (Sartorius Stedim Biotech GmbH, Göttigen, Germany) under vacuum and degassed by sonication for 5 minutes.

Accurately weighed amounts of norharmane, harmane, harmine and 3-hydroxymethyl-β-carboline were diluted in ethanol to get 3.0 × 10^{-3} M stock solutions of every compound. Aliquots of these stocks were diluted up ten times in 0.1 M HCl. These acidic solutions were spectrophotometrically measured to calculate the actual concentration of the stock solutions by using the molar absorptivities of the alkaloids [31]. Suitable volumes of the standarized stocks of the three analytes were mixed and diluted up to get a solution "A" containing each compound in a concentration 3.0 × 10^{-5} M in ethanol.

Equal aliquots of pooled human sera, obtained from 30 healthy individuals, were spiked with solution "A" or adequate dilutions in ethanol, to get sets of sera with β-carboline at six concentration levels ranging from 5.0×10^{-7} M to 5.1×10^{-8} M (calibrators). Blank sera spiked with the same volume of ethanol were also prepared. The spiked volume was always less than 5% of serum volume in order to avoid distorting the nature of the matrix.

The same procedure was followed to prepare quality control samples (QC) at final concentrations of 3.0×10^{-7} M, 1.0×10^{-7} M and 5.1×10^{-8} M. Both calibrators and QC samples were spiked with 3-hydroxymethyl-β-carboline as internal standard at a concentration of 3.8×10^{-7} M.

Solid phase extraction of the sera was carried out by following a procedure previously described for the analysis of β-carbolines in foodstuffs [32]. Briefly, the SPE cartridges placed on a vacuum manifold were conditioned with methanol (2 × 3 mL) and 0.1 M HCl (2 × 3 mL). Then, 2 mL aliquots of the samples acidified to pH 1.5 with concentrated HCl were loaded and passed through the cartridges. The cartridges were washed with 6 mL of H_2O and 3 mL of 0.4 M phosphate buffer (pH 9.1). Finally, the compounds were eluted with 1 mL of a 50:50 v:v mixture of methanol and 0.2 M phosphate buffer pH 8.8. Collected eluates were directly injected into the chromatographic system.

In order to validate the chromatographic methods under study, linearity, limit of detection (LOD), limit of quantitation (LOQ), accuracy and precision were determined following the recommendations of IUPAC, FDA and ICH [33-35].

Calibration curves were constructed by measuring extracted spiked sera (calibrators) at six levels of concentrations plus a blank, and then plotting the peak area ratio (analyte/IS) versus the theoretical concentration. Calibration curves were measured by quadruplicate in different days in order to minimize effects due to intra- and inter-day variation. LOD and LOQ were determined from five replicated measurements of quality control solution at 5.1×10^{-8} M concentration and then calculated as previously described in the literature [4]:

$$\text{LOD} = 3 \times \frac{\text{SD of the experimental concentration} \times \text{theoretical concentration}}{\text{mean of the experimental concentration}} \qquad \textbf{Eq. 1}$$

$$\text{LOQ} = 10 \times \frac{\text{SD of the experimental concentration} \times \text{theoretical concentration}}{\text{mean of the experimental concentration}} \qquad \textbf{Eq. 2}$$

Accuracy was determined by six replicate analyses of spiked QC at three levels of concentration (3.0×10^{-7} M, 1.0×10^{-7} M and 5.1×10^{-8} M) which were then compared with the calibration curves previously prepared. Intra-day precision was calculated from six runs conducted on the same day, and the experiments were also performed using the previous three levels of concentration. Inter-day precision was determined from duplicate injections of the same concentration over five different days, also at three levels of concentration.

3. Results and discussion

The environmental conscience is growing up day after day in the different chemical areas. Water is the most environmentally friendly solvent, however HPLC separations require the use of organic solvents in high proportions generating a large volume of waste. Alcohols are considered green and renewable solvents, as they can be obtained from renewable feedstocks [36]. Considering that the existing HPLC methods for

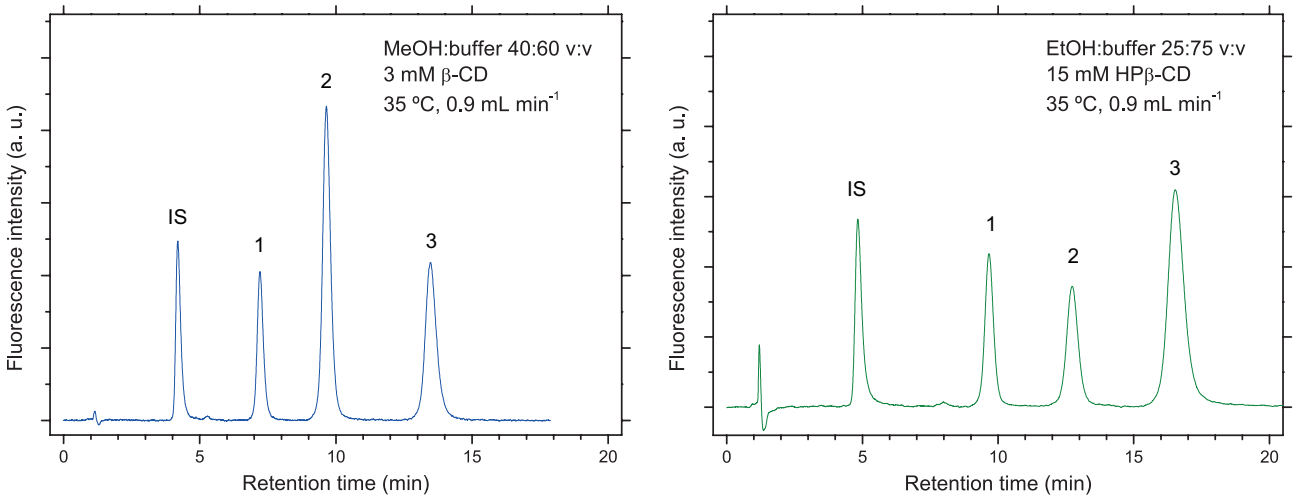

Figure 2.
Chromatographic separation of standard solutions of β-carboline alkaloids. 1, norhamane; 2, harmane; 3, harmine. IS internal standard (3-hydroxymethyl-β-carboline).

quantitation of β-carbolines involved the use of acetonitrile or methanol as organic component of the mobile phase, we selected a methanolic mobile phase as the starting point of our study on the development of greener chromatographic procedures. The effects of replacing methanol by ethanol in the mobile phase and adding CDs as mobile phase additives were studied. As can be appreciated in Figure 2, the standard solutions containing a mixture of β-carboline alkaloids can be separated using hydro-alcoholic (methanolic or ethanolic) mobile phases. Various solvent mixtures containing different proportions of methanol or ethanol and also different concentrations of CDs in the mobile phase were tested [37]. The highest CDs concentrations reduced the retention factor, shortening the run time. Nevertheless, due to the limited solubility of CDs in the alcoholic-water mixtures and the higher viscosity, the pressure in the column was increased and therefore the chromatographic efficiency was reduced. Under the optimized experimental conditions (ethanol:aqueous buffer 25:75 or methanol:aqueous buffer 40:60 v:v), a reasonable compromise between the chromatographic parameters (retention time, selectivity factor, resolution and efficiency) and a maximum water proportion in the mobile phases was reached. Reverse-phase silica C1 columns do not present the same efficiency and resolution as C18 columns, due to their lower retentive effect on the analytes. Nevertheless, good peak shapes and symmetries were obtained, keeping the efficiency and resolution high while achieving a considerable reduction in the organic solvent proportion in the mobile phase, thanks to the use of a less retentive stationary phase.

Environmentally friendly separations using hydro-ethanolic mobile phases modified with β-CD and HPβ-CD were also assayed. A notable reduction in the retention times for harmine in methanolic mobile phases (5% in the presence of β-CD and 12% in the presence of HPβ-CD) as well as in ethanolic mobile phases (23% in the presence of β-CD and 28% the presence of HPβ-CD) was achieved by using CDs as mobile phase additives.

To carry out the validation of the conditions developed with analytical purposes, 3-hydroxymethyl-β-carboline was chosen as internal standard. This compound was employed due to its structural similarity to β-carboline alkaloids and also considering the suitable retention time obtained under the experimental conditions employing CDs as mobile phase additives. This IS conveniently eluted between the void time and the β-carboline derivatives under study, was commercially available and had been previously employed for this purpose [16,38].

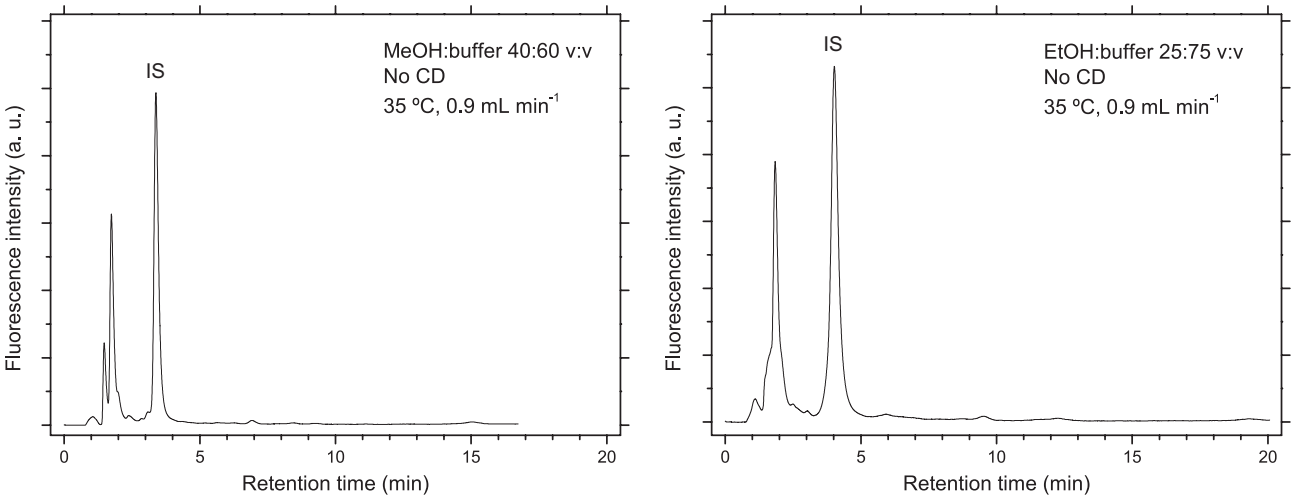

Figure 3. Chromatograms of the blank sera spiked with the internal standard 3-hydroxymethyl-β-carboline.

The selectivity of the methods was proved by the absence of chromatographic peaks at the retention times of the analytes after analysis of serum samples spiked only with the IS (Figure 3). For all of the experimental conditions, no differences were observed in the retention times of the compounds analysed in human serum extracts with regard to the retention times obtained with standard samples prepared in the mobile phase.

The method of unweighed least squares was employed to calculate the linear regression parameters. As showed by the determination coefficients of the calibration curves (Table 1), the response obtained was linear with respect to concentration for all of the analytes and over the whole working concentration range, from 5.0×10^{-7} M to 5.12×10^{-8} M. The regression parameters intercept and slope (Table 1) showed an excellent reproducibility along time.

LOD and LOQ were calculated according to the equations listed in the Materials and Methods Section. The LODs obtained (Table 2) were in agreement with other chromatographic procedures described for the determination of β-carboline alkaloids in blood samples [4,39]. LODs are in the range of $1 - 4 \times 10^{-9}$ M for chromatographic separations without CDs and became slightly higher ($3 \times 10^{-9} - 1.5 \times 10^{-8}$ M) when CDs

Table 1. Figures of merit obtained from the validation of the different assayed methodologies. Compounds: 1, norharmane; 2, harmane; 3, harmine

Comp.	MeOH:aqueous buffer pH 7.8 40:60 v:v			EtOH:aqueous buffer pH 7.8 25:75 v:v		
	Slope ± SD	Intercept ± SD	R^2	Slope ± SD	Intercept ± SD	R^2
Without CDs in the mobile phase						
1	$3.77 \times 10^6 \pm 1.79 \times 10^4$	$4.30 \times 10^{-3} \pm 4.30 \times 10^{-3}$	0.9999	$3.38 \times 10^6 \pm 1.80 \times 10^4$	$-1.90 \times 10^{-3} \pm 4.30 \times 10^{-3}$	0.9998
2	$1.03 \times 10^7 \pm 4.95 \times 10^4$	$1.97 \times 10^{-2} \pm 1.18 \times 10^{-2}$	0.9999	$8.87 \times 10^6 \pm 6.88 \times 10^4$	$2.59 \times 10^{-2} \pm 1.64 \times 10^{-2}$	0.9996
3	$7.51 \times 10^6 \pm 3.71 \times 10^4$	$2.20 \times 10^{-3} \pm 8.90 \times 10^{-3}$	0.9998	$6.83 \times 10^6 \pm 2.87 \times 10^4$	$9.70 \times 10^{-3} \pm 6.85 \times 10^{-3}$	0.9999
With 3 mM β-CD in the mobile phase						
1	$3.71 \times 10^6 \pm 1.80 \times 10^4$	$6.60 \times 10^{-3} \pm 4.30 \times 10^{-3}$	0.9999	$3.73 \times 10^6 \pm 3.01 \times 10^4$	$1.88 \times 10^{-2} \pm 7.20 \times 10^{-3}$	0.9996
2	$1.03 \times 10^7 \pm 4.50 \times 10^4$	$2.53 \times 10^{-2} \pm 1.08 \times 10^{-2}$	0.9999	$9.75 \times 10^6 \pm 6.99 \times 10^4$	$5.20 \times 10^{-2} \pm 1.67 \times 10^{-2}$	0.9997
3	$7.39 \times 10^6 \pm 3.86 \times 10^4$	$1.35 \times 10^{-2} \pm 9.20 \times 10^{-3}$	0.9998	$6.19 \times 10^6 \pm 4.69 \times 10^4$	$2.99 \times 10^{-2} \pm 1.12 \times 10^{-2}$	0.9997
With 15 mM HPβ-CD in the mobile phase						
1	$3.28 \times 10^6 \pm 1.11 \times 10^4$	$5.80 \times 10^{-3} \pm 2.64 \times 10^{-3}$	0.9999	$3.54 \times 10^6 \pm 1.90 \times 10^4$	$5.70 \times 10^{-3} \pm 4.50 \times 10^{-3}$	0.9998
2	$7.65 \times 10^6 \pm 4.78 \times 10^4$	$3.57 \times 10^{-2} \pm 1.14 \times 10^{-2}$	0.9998	$7.93 \times 10^6 \pm 5.29 \times 10^4$	$-1.08 \times 10^{-2} \pm 1.27 \times 10^{-2}$	0.9997
3	$1.17 \times 10^7 \pm 4.99 \times 10^4$	$2.80 \times 10^{-3} \pm 1.19 \times 10^{-2}$	0.9999	$1.08 \times 10^7 \pm 9.96 \times 10^4$	$2.89 \times 10^{-2} \pm 2.38 \times 10^{-2}$	0.9995

were employed as MPA. Comparing the LOQ and LOD for both mobile phases and CDs, it can be observed that LOD values obtained when β-CD was used as MPA were somehow better in the case of ethanolic than in methanolic mobile phase. However, when using HPβ-CD as additive, lower LOD and LOQ can be obtained in methanolic mobile phases. When CDs were added as MPA, no significant differences were observed depending on the alcohol (methanol or ethanol) employed, nor on the CD added to the mobile phase (Table 2).

Figure 4 shows the chromatographic separation of norharmane, harmane and harmine in human serum samples following two of the proposed methodologies. Slight differences in the chromatograms corresponding to the serum samples can be appreciated with regard to those obtained for the standard solutions of β-carboline alkaloids (Figure 2), mostly at the void time.

The accuracy of the proposed methodology was evaluated in terms of concentration of β-carbolines found at three different levels of QC concentration. Recoveries (as percentage) were also calculated. The figures of merit are summarized in Table 2 for all of the experimental conditions. The E_R% obtained in all the different experimental conditions (mobile phases and in the presence o absence of CDs) was lower than 5%, showing excellent accuracy values even for the concentration levels closest to the LOQ. The accuracy was better in the presence of CDs (found concentration = 95-107%) than for the mobile phases without CDs (found concentration = 88-99%). The enhancement in the accuracy values in the presence of CDs was observed for both methanolic and ethanolic mobile phases. The more accurate results were obtained for the couples ethanolic mobile phase + β-CD and methanolic mobile phase + HPβ-CD as can be deduced from the values on Table 2. The excellent recovery values obtained showed that the sample pre-treatment (SPE) coupled to the proposed HPLC quantitation methods are suitable for the analysis of β-carboline alkaloids in biological samples.

Precision was evaluated by means of the determination of the intra-day (n=6) and inter-day (n=5) relative standard deviation at three levels of concentration (QC). Satisfactory RSD values (< 7%) were obtained in all cases. Precision values were better for methanolic than for ethanolic mobile phases. In both cases, the addition of CDs as MPA increased the RSD. In ethanolic mobile phases, the reduction in the precision was smaller with β-CD

Table 2. Figures of merit obtained from the validation of the different assayed methodologies.

	Compound	MeOH:aqueous buffer pH 7.8 40:60 v:v									EtOH:aqueous buffer pH 7.8 25:75 v:v								
		LOD (M)	LOQ (M)	Accuracy (found concentration)			Intra-day precision (%RSD)			Inter-day precision (%RSD)			LOD (M)	LOQ (M)	Accuracy (found concentration)			Intra-day precision (%RSD)			Inter-day precision (%RSD)		
				C_1	C_2	C_3	C_1	C_2	C_3	C_1	C_2	C_3			C_1	C_2	C_3	C_1	C_2	C_3	C_1	C_2	C_3
No CD	1	1.42×10^{-9}	4.74×10^{-9}	4.95×10^{-8}	9.65×10^{-8}	2.93×10^{-7}	0.90	0.34	0.50	4.97	5.33	5.06	2.40×10^{-9}	8.02×10^{-9}	5.10×10^{-8}	9.51×10^{-8}	2.88×10^{-7}	1.58	3.01	1.40	4.63	3.37	3.46
	2	1.75×10^{-9}	5.82×10^{-9}	5.06×10^{-8}	9.72×10^{-8}	2.95×10^{-7}	1.09	0.27	0.37	3.96	3.30	3.13	2.58×10^{-9}	8.62×10^{-9}	5.07×10^{-8}	9.73×10^{-8}	2.98×10^{-7}	1.59	4.30	1.86	3.07	1.60	3.07
	3	1.17×10^{-9}	3.91×10^{-9}	5.02×10^{-8}	9.69×10^{-8}	2.96×10^{-7}	0.77	0.38	0.68	3.09	2.49	2.92	3.28×10^{-9}	1.09×10^{-8}	4.69×10^{-8}	8.79×10^{-8}	2.64×10^{-7}	2.07	1.84	2.05	4.43	2.87	2.64
β-CD	1	3.25×10^{-9}	1.08×10^{-8}	5.13×10^{-8}	9.67×10^{-8}	2.94×10^{-7}	2.04	1.72	1.59	1.41	5.03	4.48	4.13×10^{-9}	1.38×10^{-8}	5.11×10^{-8}	1.00×10^{-7}	3.06×10^{-7}	2.44	0.68	3.33	2.23	2.08	1.62
	2	7.32×10^{-9}	2.44×10^{-8}	5.18×10^{-8}	1.02×10^{-7}	2.99×10^{-7}	2.79	1.39	3.42	3.01	2.86	2.81	6.16×10^{-9}	2.05×10^{-8}	5.13×10^{-8}	1.01×10^{-7}	3.03×10^{-7}	3.63	1.01	3.52	2.51	2.84	1.56
	3	1.23×10^{-8}	4.10×10^{-8}	5.23×10^{-8}	1.01×10^{-7}	3.02×10^{-7}	1.64	1.37	3.09	1.47	3.65	1.76	6.52×10^{-9}	2.17×10^{-8}	5.29×10^{-8}	9.96×10^{-8}	3.05×10^{-7}	3.90	1.43	4.51	3.52	2.44	1.82
HPβ-CD	1	3.51×10^{-9}	1.17×10^{-8}	5.20×10^{-8}	1.01×10^{-7}	3.01×10^{-7}	2.21	0.39	0.52	1.24	1.06	1.51	9.24×10^{-9}	3.08×10^{-8}	5.28×10^{-8}	9.99×10^{-8}	2.90×10^{-7}	5.83	2.48	1.69	4.33	2.70	2.73
	2	3.81×10^{-9}	1.27×10^{-8}	5.18×10^{-8}	9.97×10^{-8}	2.95×10^{-7}	2.28	1.06	0.54	3.15	2.85	1.79	1.00×10^{-8}	3.33×10^{-8}	5.50×10^{-8}	9.86×10^{-8}	2.88×10^{-7}	6.68	3.32	1.96	4.86	1.78	1.59
	3	3.44×10^{-9}	1.15×10^{-8}	5.33×10^{-8}	1.01×10^{-7}	2.98×10^{-7}	2.23	1.01	0.55	3.01	1.84	1.04	6.95×10^{-9}	2.32×10^{-8}	5.36×10^{-8}	9.75×10^{-8}	2.84×10^{-7}	4.29	2.67	2.11	6.56	3.84	2.70

Compounds: 1, norharmane; 2, harmane; 3, harmine. Quality control samples: C_1= 5.12 × 10^{-8} M; C_2=1.00 × 10^{-7} M; C_3=3.00 × 10^{-7} M. HPβ-CD concentration: 15 mM; β-CD concentration: 3 mM.

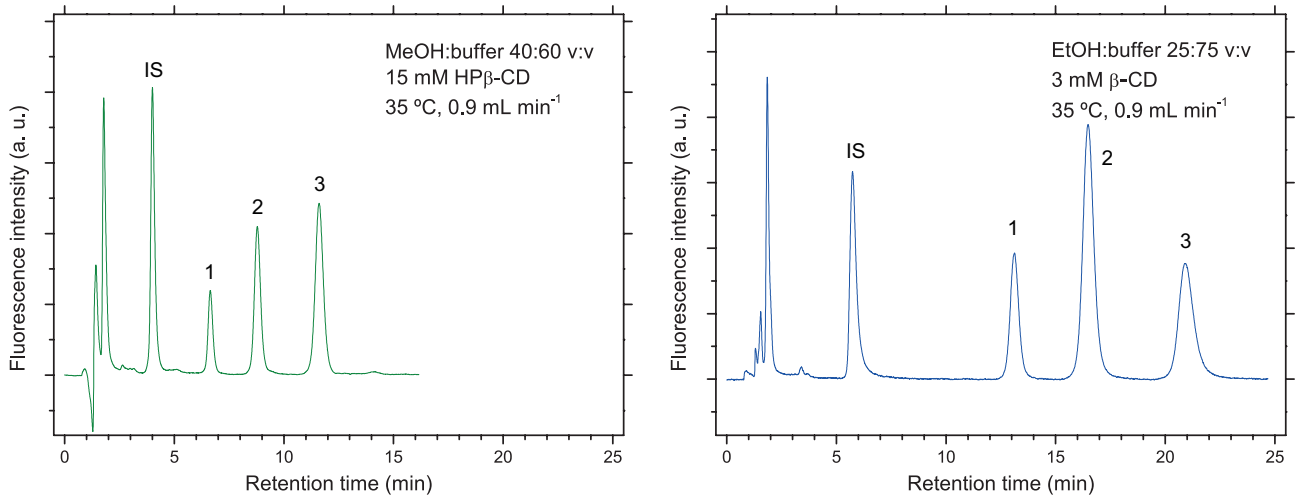

Figure 4. Chromatograms showing the quantification β- carboline alkaloids quantified in spiked and SPE-extracted human sera. Elution order as in Figure 2.

than with HPβ-CD. In the case of methanolic mobile phases, the effect of both CDs was similar and smaller than in ethanolic mobile phases.

Table 3 shows a comparative study of the organic solvent consumption in different HPLC methods employed for β-carboline analysis [4, 40-43] and in our proposed methodologies. A significant reduction in the organic solvent proportion (50-70%) is reached and this, together with the excellent figures of merit obtained in the validation studies, prove that the present SPE-HPLC combination can be successfully applied to the determination of β-carbolines with a lower organic solvent waste production.

4. Conclusion

The use of C1 stationary phase allows a considerable increase of the proportion of water in the mobile phase with adequate retention times and good resolution and efficiency. The developed methodologies employ only renewable solvents (methanol and ethanol) as organic component in the mobile phases and biodegradable and renewable additives (CDs). The combination of the C1 stationary phase with CDs as mobile phase additives provides a noticeable reduction (50-70%) in the organic solvent proportion necessary for RP-HPLC analysis. The proposed methodologies have been completely validated showing excellent figures of merit in all the cases. The use of CDs in the mobile phases turns the traditional HPLC into an attractive eco-separation technique using conventional and inexpensive columns under ordinary and

Table 3. Comparative study of the of the organic solvent consumption in different methodologies proposed for β-carbolines analysis.

	Previous methodologies					Proposed methodologies	
	Yritia *et al.* (2002) [40]	Back *et al.* [a] (2009) [41]	Kartal *et al.* (2003) [42]	Zheng *et al.* (2000) [4]	Herráiz *et al.* (2008) [43]	MeOH:Buffer 40:60 + HPβ-CD 15 mM	EtOH:Buffer 25:75 + HPβ-CD 15 mM
Elution	Gradient	Gradient	Isocratic	Isocratic	Gradient	Isocratic	Isocratic
Run time (min)	16	33	16	11	18	12	18
MeOH (mL)	8.31			7.7		4.32	
EtOH (mL)							4.05
^{i}PrOH (mL)			4.80				
Acetonitrile (mL)	5.54	9.24	4.80		5.90		
Total (mL)	13.85	9.24	9.60	7.70	5.90	4.32	4.05

[a] *Narrow bore column (2.1 mm)*

user-friendly experimental conditions, making possible to carry out an accurate and simple analysis of β-carbolines in blood samples.

5. Acknowledgements

Financial support from Ministerio de Ciencia e Innovación (SPAIN) through grant CTQ2009-11312 as well as from Grupos de Investigación UCM grant 920234 is gratefully acknowledged. The authors are grateful to MEC for a FPU research fellowship for V. González-Ruiz.

6. References

1. Casal S, Mendes E, Fernandes JO, Oliveira MBPP, Ferreira MA (2004) J Chromatogr A 1040:105-114
2. Stöckigt J, Sheludko Y, Unger M, Gerasimenko I, Warzecha H, Stöckigt D (2002) J Chromatogr B 802:115-126
3. Hemmateenejad B, Abbaspour A, Maghami H, Miri R, Panjehshahin MR (2006) Anal Chim Acta 575:290-299
4. Zheng W, Wang S, Barnes LF, Guan Y, Louis ED (2000) Anal Biochem 279:125-129
5. Herraiz T, Chaparro C (2006) J Chromatogr A 1120:237-243
6. Aguí L, Peña-Farfal C. Yáñez-Sedeño P, Pingarrón JM (2007) Anal Chim Acta 585:323-330
7. Smith CJ, Qian X, Zha Q, Moldoveanu SC (2004) J Chromatogr A 1046:211-216.
8. Herraiz T, Chaparro C (2005) Biochem Biophys Res Commun 326:378-386
9. Pfau W, Skog K (2004) J Chromatogr A 1046:211-216
10. Frison G, Favretto D, Zancanaro F, Fazzin G, Ferrara SD (2008) Foresic Sci Int 179:e37-e43
11. Herraiz T, González D, Ancín-Azpilicueta C, Arán VJ, Guillén H (2010) Food Chem Toxicol 48:839-845
12. Callaway JC (2005) J Psichoact Drugs 37:151-155
13. Inman W D, Bray WM, Gassner NC, Lokey RS,-Tenney K, Shen YY, Tendyke K, Suh T, Crews P (2010) J Nat Prod 73:255-257
14. Charan RD, McKee TC, Gustafson KR, Pannell LK, Boyd MR (2002) Tetrahedron Lett 43:5201-5204
15. Chouvenc T, Su N, Elliot M (2008) J Invertebr Pathol 99:345-347
16. Tsuchiya H (2004) J Chromatogr A 1031:325-330
17. Mckenna DJ (2004) Pharmacol Ther 102:11-129
18. Pieroni A, Muenzc H, Akbulut M, Baser KH, Durmuskahya C (2005) J Ethnopharmacol 102:69-88
19. Boyer EW, Shannon, M Hibberd PL (2001) N Eng J Med 345:469-471
20. Welch CJ, Sajonz P, Biba M, Gouker J, Fairchild J (2006) J Liq Chromatogr 29:2185-2200
21. Sajonz P, Schafer W, Gong X, Schultz S, Rosner T, Welch CJ (2007) J Chromatogr A 1147: 149-154
22. Jandera P, Bocian S, Molíková M, Buszewski B (2009) J Chromatogr A 1216:237-248
23. Zhu L, Ding L, Zhang Q, Wang L, Tang F, Liu Q, Yao S (2009) Green Chem 11:132-137
24. El-Gindy A, Emara S, Mesbah MK, Hadad GM (2006) J Assoc Off Anal Chem 89:65-70
25. López-Nicolás JM, Núñez-Delicado E, Pérez-López AJ, Carbonell-Barrachina A, Cuadra-Crespo P (2006) J Chromatogr A 1135:158-165
26. López-Nicolás JM, García-Carmona F (2008) Food Chem 109:868-875.
27. Sezjtli J (1998) Chem Rev 98:1743-1753
28. Cserháti T, Forgacs E (2003) Cyclodextrins in Chromatography, Royal Society of Chemistry, Cambridge
29. Capelo C, Fisher U, Hungerbühler K (2007) Gren Chem 9: 927-934
30. Welch CJ, Brkovic T, Schafer W, Gong X (2007) Green Chem 11:1232-1238
31. Moffat AC, Jackson JV, Moss SM, Widdop B (1986) Clarke's Isolation and Identification of Drugs, Pharmaceutical Press, London
32. Adachi J, Mizoi Y, Naito T, Yamamoto K, Fujiwara S, Ninomiya I (1991) J Chromatogr 531:331-339
33. Food and Drug Administration (2001) Guidance for Industry - Bioanalytical Method Validation
34. International Conference on Harmonisation (1996) ICH Topic Q 2 B. Validation of analytical procedures methodology
35. Thompson M, Ellison SLR, Wood R (2002) Pure Appl Chem 74:835-855
36. Kerton FM (2009) Alternative Solvents for Green Chemistry, Royal Society of Chemistry, Cambridge
37. León AG, Olives AI, Martín MA, del Castillo B (2007) J Incl Phenom Macrocycl Chem 57:577-583
38. Tsuchiya H, Shimizu H, Iimuna M (1999) Chem Pharm Bull 47:440-443

39. Louis ED, Zheng W, Jurewicz EC, Watner D, Chen J, Factor-litvak P, Parides M (2002) Neurology 59:1940-1944
40. Yritia M, Riba J, Ortuño J, Ramírez A, Castillo A, Alfaro Y, de la Torre R, Barbanoj M. J. (2002) J Chromatogr B 779:271-281
41. Back YM, Lee JH, Shin HS, Lee KG (2009) Food Addit Contam 26:298-305
42. Kartal M, Altun M, Kurucu S (2003) J Pharm Biomed Anal 31:263-269
43. Herraiz T, Guillén H, Arán VJ (2008) Chem Res Toxicol 21:2172-2180

10

Fluorescence properties of the anti-tumour alkaloid luotonin A and new synthetic analogues: pH modulation as an approach to their fluorimetric quantitation in biological samples

Published in: González-Ruiz, V., González-Cuevas, Y., Arunachalam, S., Martín, M. A., Olives, A. I., Ribelles, P., Ramos, M. T. & Menéndez, J. C. (2012). J. Lumines., 132(9), 2468-2475.

ABSTRACT ▶ Luotonin A is an alkaloid structurally related to the natural anti-tumour agent camptothecin. The fluorescence behaviour of luotonin A and a series of six analogues is described in the present work. The influence of solvent polarity and pH on the native fluorescence properties of these alkaloids was studied, finding that in organic solvents or in aqueous solutions (pH 5.5–7.2) the neutral form of the luotonin derivatives emit in the region of 410–450 nm but, in both media, acidification to pH values below 3.0 causes a new emission band to appear at about 500 nm. An ESPT reaction occurs due to the protonation of the basic nitrogen atoms of the pentacyclic ring. Acid-base titrations of luotonin A and its derivatives in aqueous and acetonitrile media were carried out in order to determine their pK_a^* values which were around 2, showing these compounds to be very weak bases. In aqueous media, the absence of an iso-emissive point in the emission spectra suggests the existence of more than two species in the proton transfer equilibria. The basicity of the luotonin A derivatives is increased in organic media, and a good correlation between the pK_a^* values and the chemical structure was found. The protonation of luotonin A was also studied by ^{1}H-NMR and ^{13}C-NMR experiments, which proved the protonation of the nitrogen atoms at the positions 5 and 6 of the pentacyclic ring. The fluorescence quantum yields were determined in organic solvents and in aqueous solutions under neutral and acidic conditions. The fluorescence quantum yields were higher in water for the case of the more polar compounds, and the opposite result was obtained for the more hydrophobic ones. The remarkable and interesting fluorescence properties of luotonin A prompted the development of its fluorimetric analytical quantitation, obtaining very good analytical features.

DOI ▼
10.1016/j.jlumin.2012.03.056

ABBREVIATIONS ▼

- **ESPT:** Excited state proton transfer reactions
- **HPLC:** High Performance Liquid Chromatography
- **HTS:** High Throughput Screening
- **LOD:** limit of detection
- **LOQ:** limit of quantitation
- **NMR:** Nuclear Magnetic Resonance
- **QY:** Quantum Yield
- **UV-Vis:** Ultraviolet-visible electromagnetic radiation

1. Introduction

Fluorescence techniques have shown a wide range of application in life sciences including molecular biology and pharmacology, and also in medical and clinical fields[1-4]. The different fluorescence methodologies display relevant analytical features (selectivity, sensitivity, wide linear response, accuracy and precision) and they can be applied to solve diverse analytical challenges. Thus, molecular events can be directly studied on the cells, in real time, by means of the use of appropriate fluorescent sensors and fluorescence microscopy techniques [5-7]. Interactions between drugs and biological macromolecules (proteins or DNA) can be monitored by steady state or time-resolved fluorescence spectroscopy, allowing evidencing the nature of such interactions and helping to establish the mechanisms responsible for the biological activity [8-12]. Fluorescence measurements involving micro-plate well format (HTS systems) facilitate this kind of studies as well as the biological activity assays of potential drugs in cell cultures. This approach allows the assay of different drug candidates in one single

test with very low consumption of reagents and samples (micro- or nano-format). Besides it provides sensitive, robust and low-cost analyses [13,14].

Separation techniques (HPLC and CE) coupled to fluorescence detection allow the rapid and simultaneous identification and quantitation of drugs and their metabolites in biological fluids that are essential aspects of pharmacokinetic studies [15-17]. Therefore, the characterization of the fluorescence properties of newly synthesized compounds is a part of their pharmaceutical development that makes further studies possible.

The design and development of new anti-cancer drugs possessing good therapeutical response and acceptable toxicity is a research field of growing interest. *Peganum nigellastrum* is a plant used traditional Chinese medical practice whose extracts present anti-tumour and anti-inflamatory effects [18,19]. The main component of this extract is luotonin A, a molecule structurally related to the alkaloid camptothecin, a cytotoxic natural product whose analogues have found widespread application in the treatment of several types of cancers [20-24]. The mechanism of action of luotonin A seems to be identical to that of camptothecin, and involves the stabilization of the complex formed between DNA and human topoisomerase 1, inducing cellular apoptosis [25,26]. In this context, a considerable effort has been devoted to the development of synthetic routes to the natural product and its analogues [27-30]. Camptothecin and its derivatives, such as topotecan and irinotecan, show a notable fluorescence emission, and their quantitation has been described by means of direct fluorescence or fluorescence coupled to HPLC [31–34]. Luotonin A combines in its structure quinoline and quinazoline rings, which behave as potent fluorophores.

In the present paper we explore the steady state fluorescence properties of luotonin A and six newly synthesized derivatives of this alkaloid (Figure 1). With the aim to develop a chromatographic analysis of these compounds, we considered of relevance the study of the influence of solvent polarity on their native fluorescence together with the determination of fluorescence QYs in aqueous and organic solvents. The presence of heterocyclic basic nitrogens allows prototropic reactions and for this reason ESPT processes in aqueous and organic solvents were also studied. The attractive fluorescence properties of luotonin A led us to develop a preliminary methodology for its direct fluorimetric analysis.

2. Experimental

2.1. Apparatus and reagents

Corrected excitation and emission spectra and fluorescence measurements at fixed wavelengths were obtained with a Horiba-Jobin Yvon (Edison, NJ, USA) FluoroMax-4P spectrofluorometer equipped with the control and data acquisition software

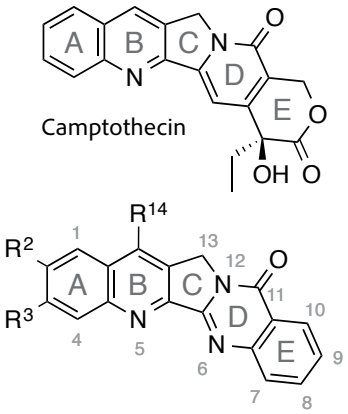

Compound	R^2	R^3	R^{14}
1 (Luotonin A)	H	H	H
2	H	H	CH_3
3	H	H	C_6H_5
4	Cl	H	C_6H_5
5	Br	H	C_6H_5
6	H	H	3,5-$Me_2C_6H_3$
7	H	CH_3	3,5-$Me_2C_6H_3$

Figure 1. Chemical structures of luotonin A and its derivatives under study, and the closely related anti-tumour agent camptothecin.

FluorEssence 2.1. UV-Vis absorption spectra were recorded with an automatic double beam Kontron (Zurich, Switzerland) Uvikon 810 spectrophotometer. A Crison micro-pH 2001 pH-meter was used to monitor the final pH values of the buffer solutions. ^{1}H-NMR and ^{13}C-NMR spectra were recorded in d_6-DMSO with a Bruker Avance III 700 MHz spectrometer (Servicio de Resonancia Magnética Nuclear, UCM).

All reagents and solvents were analytical or spectroscopic grade and were used without further purification. Water was doubly distilled and deionized (Milli-Q 50, Millipore, Molsheim, France) prior to its use. Luotonin A and its derivatives were synthesized using modified Friedländer conditions under Ce(IV) ammonium nitrate catalysis [29].

2.2. Procedures

2.2.1. Absorption UV-Vis and fluorescence characterization

For the spectrophotometric and spectrofluorimetric characterization of luotonins, stock solutions were prepared in DMSO or ethanol at 5.0×10^{-4} M. Appropriate aliquots of these stock solutions were taken to prepare ethanolic solutions around 1.0×10^{-4} M which were spectrophotometrically measured. Considering the molar absorptivities [35] the actual concentrations of the stocks solutions were accurately determined. Suitable volumes of the solutions were employed for the different experiments.

Fluorescence excitation and emission spectra were obtained by diluting aliquots from the stock solutions of luotonins in water, ethanol, and hydrochloric acid 0.316 M, the final concentrations being 5.0×10^{-7} M.

The fluorescence QYs of luotonin A and its derivatives, in water (pH 5.5), ethanol, methanol, acetonitrile and hydrochloric acid 0.316 M (pH 0.5) were determined from the corrected fluorescence spectra, integrating the whole fluorescence emission area and using quinine sulfate in H_2SO_4 0.1 M as a fluorescence standard (Φ_F = 0.577) [4, 36]. The fluorescence measurements were carried out for diluted solutions showing absorbance values below 0.05 at the excitation wavelengths. For the calculation of the fluorescence QYs the refractive indexes of the solvents were considered (Eq. 1).

$$\Phi_F = \Phi_F^r \frac{I}{I_r} \frac{A_r}{A} \frac{n^2}{n_r^2} \qquad \text{Eq. 1}$$

Where Φ_F, I, A and *n* correspond to the fluorescence quantum yield, the emission intensity, the absorbance and the refractive index, respectively, of the studied unknown and the reference solutions.

2.2.2. Solvent polarity effect on UV-Vis absorption and fluorescence behaviour

To study the influence of solvent polarity on luotonin A and derivatives, three model compounds were selected (**1**, **2** and **4**, Figure 1). To avoid the presence of trace amounts of solvent arising from the stock solutions, these solutions were prepared in ethanol. Aliquots (10-100 µL) of the ethanolic stock solutions were taken and then the solvent was evaporated under vacuum at room temperature. The films obtained after evaporation were diluted up to an appropriate volume of each solvent and the solutions were maintained under magnetic stirring for 1 h. The final concentrations were 1.0×10^{-5} M for the spectrophotometric determination and 1.0×10^{-6} M for fluorescence measurements.

2.2.3. Excited State Proton Transfer (ESPT) study of luotonin A and derivatives

Preliminary studies concerning the influence of pH on the native fluorescence of luotonins involved buffered solutions consisting of a 0.2 M citric acid solution titrated with 0.2 M sodium hydroxide (pH 2.0-5.0 range) and 0.2 M potassium dihydrogenphosphate solution titrated with 0.2 M sodium hydroxide (pH 6.0-9.0 range) [37]. For further studies involving pH values from –1.0 to 4.0, titrated solutions of HCl (sodium carbonate) were employed. Duplicate or triplicate sets of 17 solutions of luotonin A and derivatives were prepared for studying the ESPT reaction in the pH range from -1.0 to 4.0. The final concentration of compounds was 5.0×10^{-7} M in all cases.

As consequence of the results obtained in aqueous media, and considering that luotonins are very weak bases, the prototropic reactions were studied also in organic media. Appropriate aliquots of the standardized luotonin stock solutions in DMSO were taken and diluted up to a final concentration of 5.0×10^{-7} M in acetonitrile. Then successive aliquots of 10 or 20 µL of $HClO_4$ solutions were added to the luotonin A derivative solutions and fluorescence spectra were recorded after every addition. $HClO_4$ solutions for the titration were prepared in acetonitrile containing a 10% of acetic anhydride, with the aim to eliminate of water present in the commercially available solution [38]. The small volumes of $HClO_4$ added during the titration caused a negligible dilution effect.

2.2.4. ^{1}H and ^{13}C-NMR studies of the proton transfer reactions of luotonin A

With the aim to confirm the presence of protonated forms of luotonin A in the acid-base equilibria, ^{1}H- and ^{13}C-NMR spectra of luotonin A were obtained. 14.6 mM solutions of luotonin A were prepared in d_6-DMSO. Then ^{1}H- and ^{13}C-NMR spectra were recorded during the titration with $HClO_4$ covering a molar ratio from 1:0.5 to 1:5 (luotonin A:$HClO_4$) and then a final addition an excess of $HClO_4$ was carried out.

3. Results and discussion

3.1. UV-Vis absorption and fluorescence studies of luotonin A and derivatives in different solvents

The UV-Vis absorption spectra of luotonin A and its derivatives (Figure 2) showed two bands in the region of 200-300 nm with a well-defined peak close to 250 nm with high molar absorptivity values. A broad band with lower molar absorptivity was pre-

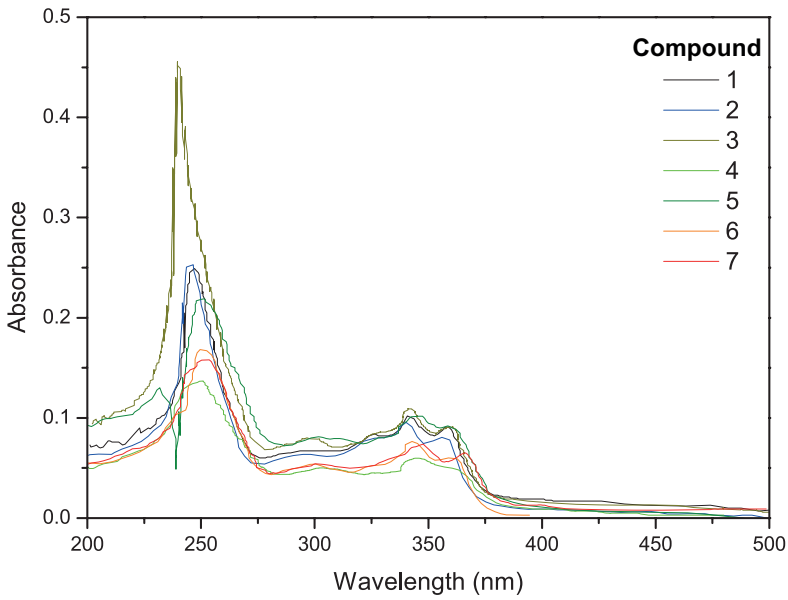

Figure 2.
UV-Vis absorption spectra of compounds **1**-**7** in ethanol.

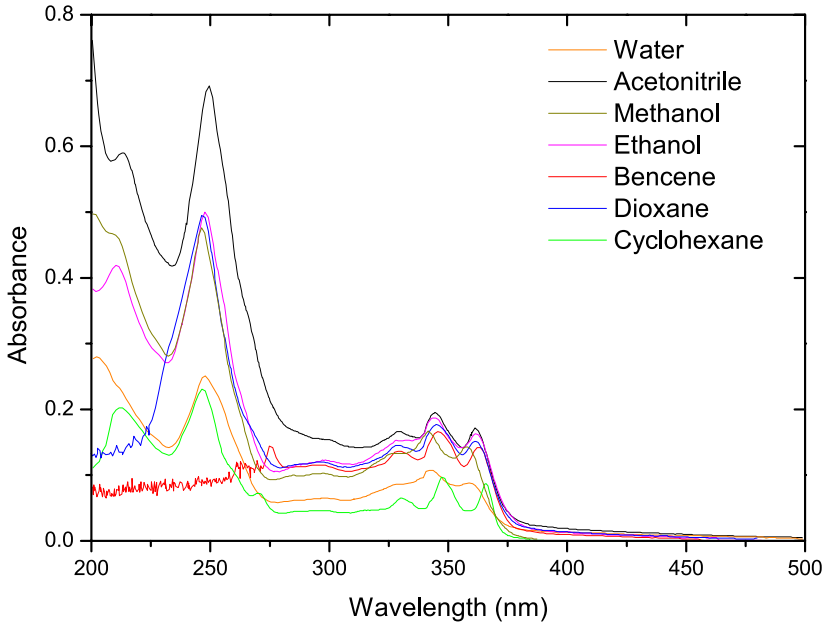

Figure 3.
UV-Vis absorption spectra of compound **2** in different solvents

sent in the 300-400 nm region, resolved in two peaks. It can be appreciated that the presence of substituents on R^2, R^3 and R^{14} of the pentacyclic system does not affect the position or intensity of the absorption maxima (Figure 2), showing that the quinoline and pyrroloquinazolinone moieties are the main chromophores responsible for the transitions in the UV-Vis region.

The influence of solvent polarity on the absorption properties of these compounds was investigated. The solvents studied covered a wide range of polarity from the apolar solvents to polar protic and aprotic ones. The spectral shape of the band at 340-370 nm is the same in all solvents studied and the absorbance of the maximum near 340 nm was always higher than the corresponding absorbance at the maximum of 360 nm in all the cases. Only small shifts (2-8 nm) in the position of the absorption maxima were observed with the change of the solvents (Figure 3). However, it is important to remark that for the compounds studied a slight red shift in the absorption maxima took place in cyclohexane with regard to the other solvents and especially to more polar protic solvents (methanol and water). This behaviour is similar to that described for camptothecin in different solvents [39] and it can been attributed to the fact that polar solvents stabilize the ground states to a greater extent than the excited states and hence the absorption maximum is blue-shifted with increasing solvent polarity [40].

The fluorescence excitation spectra presented the same two resolved peaks in the 340-370 nm region corresponding to those observed in the absorption spectra. In the case of polar protic and aprotic solvents, the shapes of the emission spectra consisted of a broad emission band (Figure 4). It is well established that the hydrogen bonding interactions between fluorophore and solvent contribute to the low resolution of the fluorescence spectra and cause inhomogeneous broadening spectral shapes [41,42]. Better-defined emission peaks were appreciated in the case of low polarity solvents (cyclohexane, benzene and dioxane). In polar protic or aprotic solvents a good correlation between the emission maxima and solvent polarity was obtained. For the polar protic or aprotic solvents a red shift of the emission maximum wavelength from cyclohexane to water was observed (Figure 4). The fluorescence maxima were red-shifted with polar solvents with regard to those observed in benzene or dioxane and the fluorescence intensity was higher for the polar protic and aprotic solvents, which

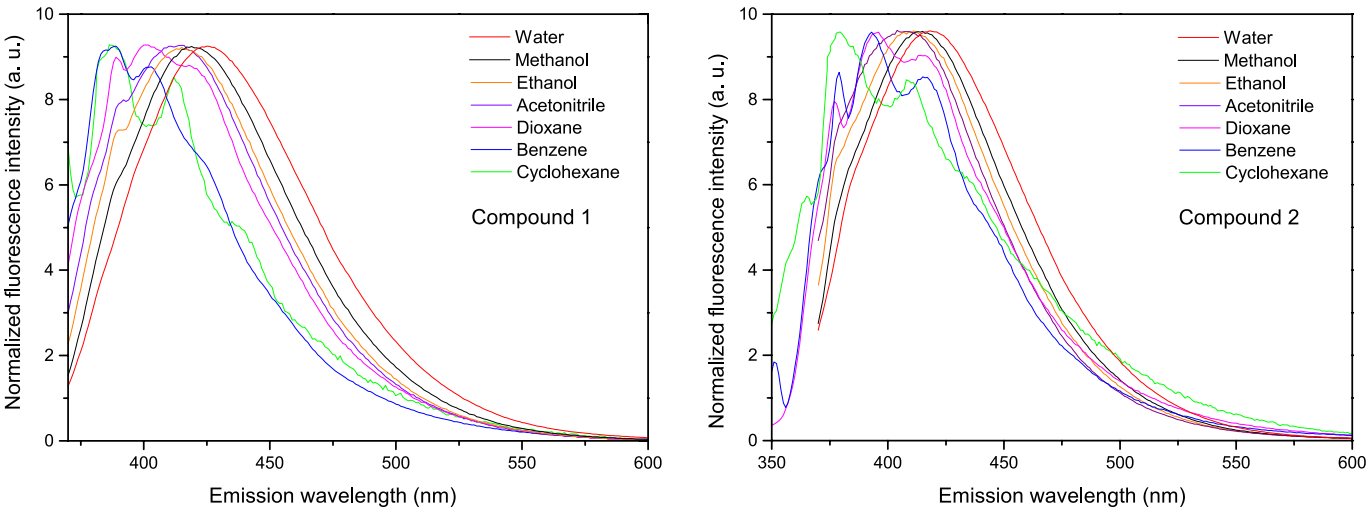

Figure 4. Effect of the solvent polarity on the fluorescence emission spectra of compounds **1** and **2**.

can be attributed to the stabilization of the quinoline and quinazoline moieties by hydrogen bonding with the solvents. The fluorescence emission maxima obtained in different solvents are summarized in Table 1.

The fluorescence QYs were remarkably lower in the case of protonated forms (pH=0.5) with regard to the values obtained in aqueous solution at pH=5.5. A clear structure-fluorescence QYs correlation was established for the derivatives of luotonin A in different solvents. Thus, the fluorescence QYs for these compounds vary according to the electron-donating or electron-withdrawing nature of the substituents on the luotonin A skeleton, with a high electron density on the fluorophore ring favouring the fluorescence emission. A comparison of the values of QYs for compounds **1**–**2** and **6**–**7** leads to the conclusion that the fluorescence efficiency was higher for the methyl derivatives (**2** and **7**), which can be ascribed to the electron-donating effect of this substituent. In the case of compound **5**, the fluorescence QYs in the different solvents were lower due to the inner quenching effect associated with the presence of the heavy halogen atom.

Solvent also plays an important role, and a decrease in the fluorescence QY was observed in aqueous solution from compound **1** (0.31) to compound **7** (0.08). The opposite trend was found for the QYs in organic solvents. The fluorescence efficiency in ethanol or acetonitrile increased from compound **1** (0.08) to compound **7** (0.23). Variations in the fluorescence QYs with the nature of the solvent have also been described for camptothecin (more hydrophilic than luotonin A) where the fluorescence

Table 2. Fluorescence quantum yields (QYs) obtained for the compounds studied in different environments

	Fuorescence Quantum Yields, $\Phi_F \pm 0.001$, (λ_{ex} = 350 nm)				
Comp.	**Water (pH=5.5)**	**Water (pH=0.5)**	**Methanol**	**Ethanol**	**Acetonitrile**
1	0.314	0.043	0.139	0.093	0.084
2	0.346	0.064	0.082	0.057	0.050
3	0.103	0.053	0.227	0.141	0.137
4	0.077	0.015	0.237	0.218	0.194
5	0.020	0.026	0.072	0.087	0.102
6	0.051	0.007	0.224	0.177	0.166
7	0.086	0.049	0.170	0.280	0.236

QY is higher in aqueous solution than in apolar solvents [40], but its derivative 9-aminocamptothecin exhibits a very low fluorescent QYs in alcohols or water compared to those obtained in chloroform or dioxane [43]

3.2. ESPT reactions of luotonin A and derivatives in aqueous media

Luotonin A has three nitrogen atoms, two of which belong to an acylamidine moiety inherent to a quinazolinone unit and the third one belongs to a quinoline system. Hence luotonin A possesses two basic centers (N-5, N-6) and a non-basic nitrogen (N-12). The protonation of the basic nitrogens on luotonine A should be possible and, therefore, changes in the UV-Vis and fluorescence spectra should be expected. Consequently, the influence of pH on the native fluorescence of luotonin A and its analogues was studied.

Considering the pK_a values of related simpler heterocycles (quinoline, pK_a = 4.90; isoquinoline pK_a = 5.40; quinazoline pK_a =1.94 —for metastable equilibrium— and 3.43 —for stable equilibrium—) [44], preliminary studies involved the use of buffered aqueous solutions in the 2.0-9.0 pH range. The UV-Vis absorption spectra of luotonin A at different pH values are shown in Figure 5. No spectral changes were observed in the 3.0-9.0 pH range. The band in the 300-370 nm region is resolved into two peaks at 340 nm and 360 nm. The absorbance of this band increases with decreasing pH values (7.5-2.5). A shoulder at around 400 nm appeared below pH 3 and it was increased as pH decreased, suggesting the appearance of a protonated species. Only in strongly acidic media (pH ≤ 0.75) the increase in the absorbance at 400 nm was accompanied by a decrease of the absorbance values of the peaks at 340 nm and 360 nm.

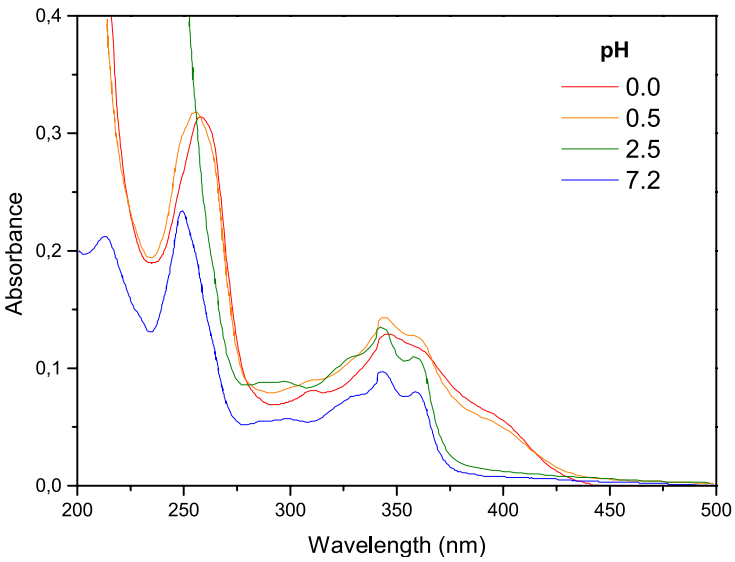

Figure 5.
Representative absorption UV-Vis spectra of compound **1** in buffered aqueous solutions at selected pH values.

Table 1. Excitation and fluorescence emission wavelengths, in nm, of the compounds studied in organic solvents and aqueous solutions at two pH values.

Comp.	MeCN	EtOH	MeOH	Ciclohexane	1,4-Dioxane	Benzene	Water (pH = 5.5)	Water (pH = 0.5)
1	λ_{ex}=248,340,357 λ_{em}=412	λ_{ex}=248,341,358 λ_{em}=416	λ_{ex}=248,341,357 λ_{em}=422	λ_{ex}=249,343,359 λ_{em}=414	λ_{ex}=255,328(sh),345,360 λ_{em}=384(sh),402,421(sh)	λ_{ex}=330,346,363 λ_{em}=380(sh),399,420	λ_{ex}=249,341,358 λ_{em}=426	λ_{ex}=251,341,358,390 (sh) λ_{em}= 517
2	λ_{ex}=248,338,355 λ_{em}=407	λ_{ex}=248,340,357 λ_{em}=411	λ_{ex}=248,339,356 λ_{em}=416	λ_{ex}=249,341,358 λ_{em}=408	λ_{ex}=255,326,342,358 λ_{em}=378(sh),396,419	λ_{ex}=328,344,361 λ_{em}=372,393,417,443(sh)	λ_{ex}=248,340,357 λ_{em}=420	λ_{ex}=252,340,369,402 (sh) λ_{em}=497
3	λ_{ex}= 252,343,361 λ_{em}=417	λ_{ex}= 253,344,360 λ_{em}=418	λ_{ex}= 252,343,360 λ_{em}=425				λ_{ex}= 255,345,361 λ_{em}=429	λ_{ex}= 348,363,397 λ_{em}=513
4	λ_{ex}=253,347,361 λ_{em}=423	λ_{ex}=254,347,362 λ_{em}=427	λ_{ex}=254,346,361 λ_{em}=431	λ_{ex}=255,351,364 λ_{em}=420	λ_{ex}=260,335,352,366 λ_{em}=392(sh),413,433(sh)	λ_{ex}=337,353,361 λ_{em}=387,410,430,459(sh)	λ_{ex}=259,347,361 λ_{em}=436	λ_{ex}=259,348,362,396 (sh) λ_{em}=514
5	λ_{ex}= 255,348,362 λ_{em}=426	λ_{ex}= 257,349,363 λ_{em}=427	λ_{ex}= 258,347,362 λ_{em}=432				λ_{ex}= 260,349,362 λ_{em}=437	λ_{ex}= 260,352,364,400 λ_{em}=523
6	λ_{ex}= 251,342,360 λ_{em}=415	λ_{ex}=254,342,361 λ_{em}=417	λ_{ex}=254,343,360 λ_{em}=422				λ_{ex}=256,345,362 λ_{em}=426	λ_{ex}=268,347,369,395 λ_{em}=513
7	λ_{ex}=254,346,364 λ_{em}=400	λ_{ex}=256,348,365 λ_{em}=406	λ_{ex}=255,347,365 λ_{em}=410				λ_{ex}=259,356,374 λ_{em}=455	λ_{ex}=262,355,375,398 λ_{em}=492/525

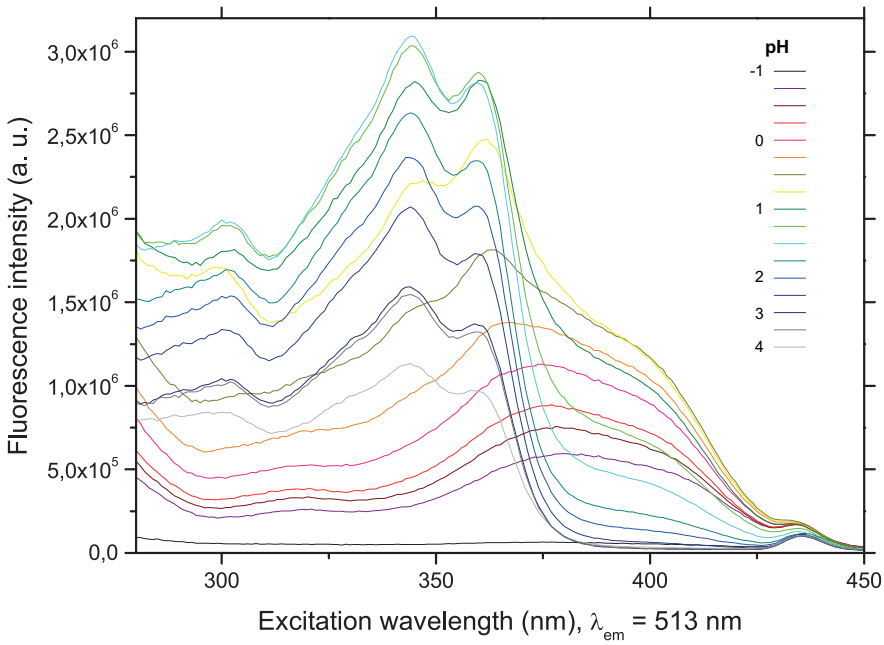

Figure 6. Effect of the pH on the fluorescence excitation spectra of compound 3 in buffered aqueous solutions.

The changes observed in the UV-Vis absorption spectra were parallel to those obtained in the fluorescence excitation spectra. However, due to the experience gained in the previous studies, the fluorescence was examined only from pH -1.0 to 4.0. In aqueous solutions at pH 4.0-2.0, the fluorescence excitation spectra exhibited two resolved peaks at 340 and 360 nm. The fluorescence intensity was higher at 340 nm than at 360 nm. When the pH was decreased the fluorescence intensity of both peaks decreased and the intensity at 340 nm became similar to the intensity at 360 nm, and then a new excitation band appeared around 400 nm. At pH 1.0 the excitation spectra consisted of a broad band with two badly defined maxima at 360 nm and 400 nm. (Figure 6).

The shape of the fluorescence emission spectra also changed with the pH modifications. The intensity of the broad emission band in the region of 390-440 nm (the position of the maximum depends on the luotonin A derivative studied) decreased together with the pH value (Figure 7A). When pH 2.0 was reached a new broad emission band appeared at around 500 nm (the precise position of the maxima depended on the compound, Table 1). This emission band must be attributed to the protonated species in the acid-base equilibria. The fluorescence emission at 500 nm (Figure 7B)

Figure 7. Effect of pH on the fluorescence emission spectra of compound **3** in buffered aqueous solutions. (A) λ_{ex} = 344 nm. (B) λ_{ex} = 397 nm.

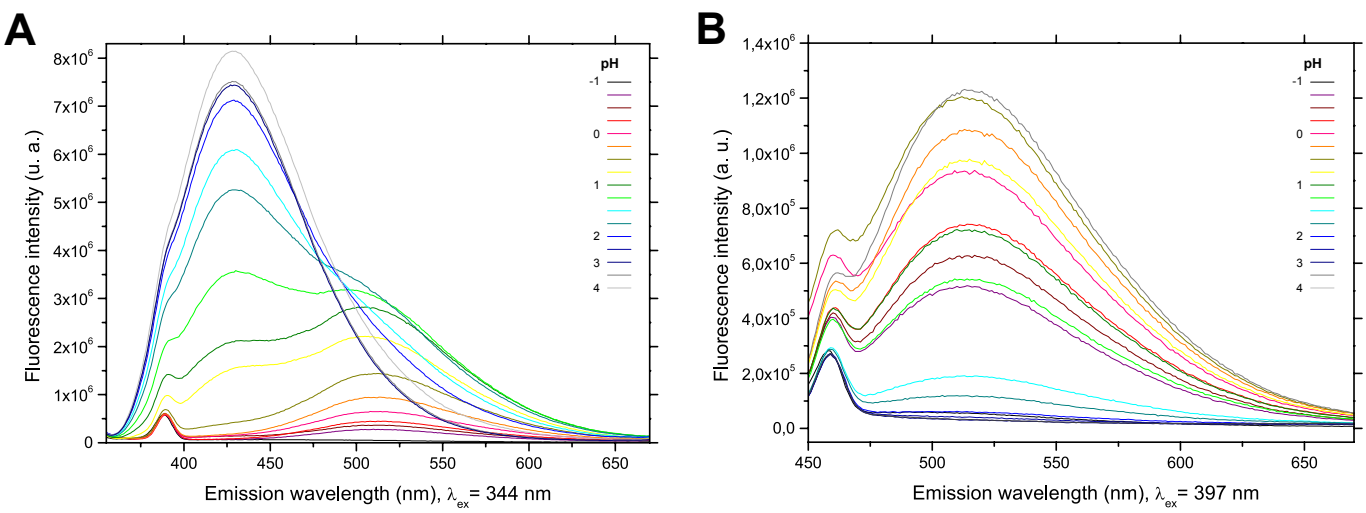

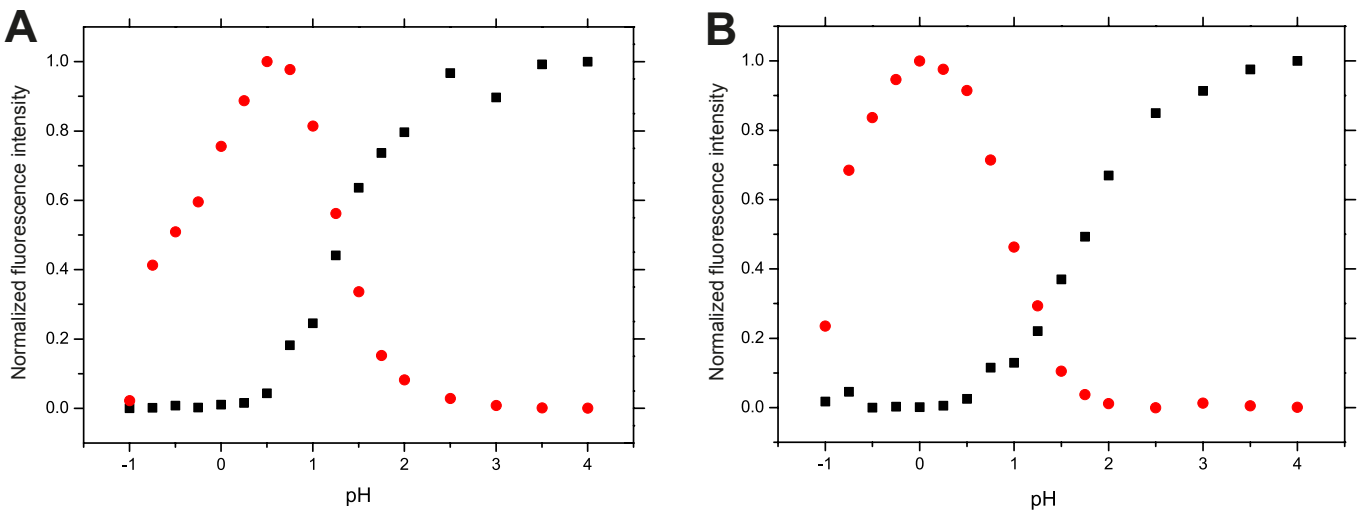

Figure 8.
Fluorescence titration curves obtained in aqueous media.
(A) compound **3**
(B) compound **6**.
■ Fluorescence intensity at the emission wavelength of the neutral form.
● Fluorescence intensity at the emission wavelength of the protonated form.

was increased in the pH range from 2 to 0.5 and, from this point, higher proton concentrations in the media induced a decrease in its fluorescence intensity, as can be appreciated in the titration curves (Figures 8A and 8B). The above-mentioned behaviour is present in all of the compounds, although each one has its own peculiarities. Both the neutral and the cationic species can be excited using the maxima around 340 nm. Under these conditions and at very low pH values, the emission corresponding to the cationic species can be observed even in the case of compounds with a protonated form presenting a very low QY compared to the neutral one (compound **6**, Figure 9).

The fluorescence emission spectra obtained in the titration of all of the compounds do not present an iso-emissive point, indicating the existence of more than two species in the proton transfer reaction in the excited state. Thus, it can be inferred that diprotonated and monoprotonated species (in any of the two nitrogens) can coexist in the prototropic equilibria in aqueous media. This conclusion will be discussed below in connection with the results obtained for non-aqueous titrations and NMR experiments. The plots of the normalized fluorescence intensity versus pH values (Figure 8) of the aqueous solutions allowed the determination of the pK_a^* values of the luotonin A derivatives studied (Table 3). These pK_a^* values are in the same range as the one described in the literature for the conjugate acid of camptothecin in the excited state,

Table 3. pK_a^* values obtained in aqueous media by steady- state fluorimetric titration.

Comp.	pK_a^*
1	1.87
2	2.10
3	1.32
4	1.36
5	0.89
6	1.73
7	1.01

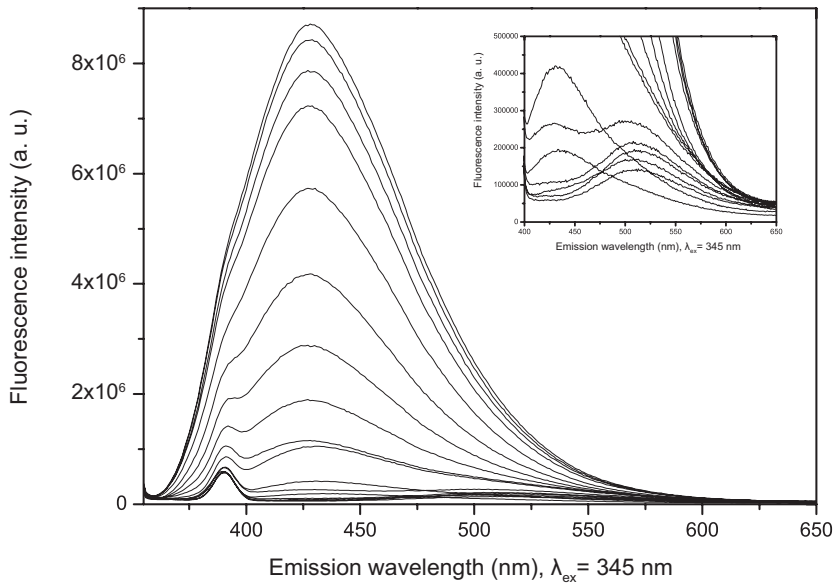

Figure 9.
Effect of the pH on the fluorescence emission spectra of compound **6** in buffered aqueous solutions.
Inset: expanded zone corresponding to highest acid concentrations.

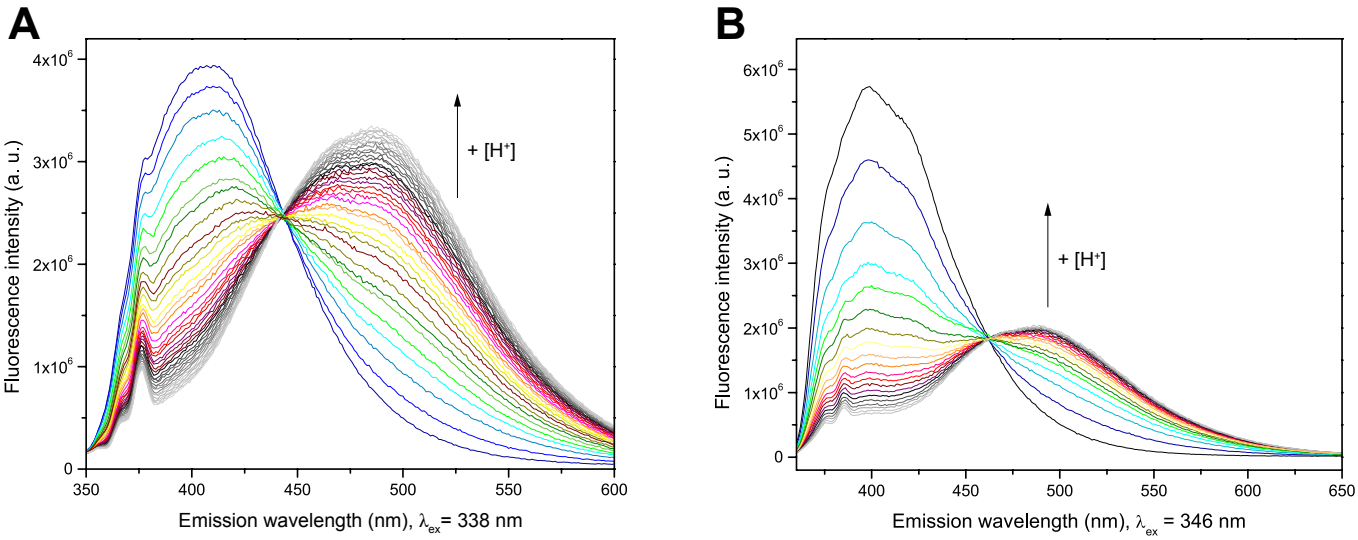

Figure 10. Fluorescence emission spectra of luotonin derivatives obtained in the titration with $HClO_4$ in acetonitrile. (A) Compound 2. (B) Compound 7.

pK_a^* = 1.65 [45, 46], showing that excited state protonation of luotonin A and its derivatives takes place only in strong acidic media. More recently, a pK_a^* value of 1.85 has been reported for camptothecin, differentiating the catonic (pH < 1.5) and neutral (at pH > 3.0) forms by means of their different fluorescence lifetimes [47]. These values show that luotonin A, similarly to camptothecin, behaves as a very weak base even in excited state. The notable decrease in the basicity of luotonin or camptothecin with regard to quinoline can be explained by the higher degree of delocalization of the non-bonding electron pair of the basic nitrogens.

3.3. ESPT reactions of luotonin A and derivatives in organic media (acetonitrile)

The relative strength of a weak base and then the possibility to be titrated satisfactorily depends on the nature of the solvent in which the proton-transfer reaction proceeds. Acetonitrile is a polar aprotic solvent widely employed in analytical chemistry (electrochemistry, spectroscopic studies and chromatographic separations). It has good properties (UV transparent, strong eluent power, high dielectric constant, low solvating power and small autoprotolysis constant, pK_s=33.6) and it behaves as differentiating solvent for the very weak bases that are not convenient titrated and differentiated in aqueous media [48]. As titrant acid solution we chose $HClO_4$, as it is a very strong acid that is completely dissociated in organic media even at 10 M concentration [44].

Two different behaviours were found in the titration of luotonin A and derivatives in acetonitrile. In the case of compounds **2** and **7**, the additions of successive aliquots of $HClO_4$ caused a decrease in the fluorescence emission of the band at 400-430 nm while a new maximum appeared in the region of 500 nm, with a characteristic iso-emissive point between both maxima (Figure 10). The presence of this point reveals the existence of only two species in the proton transfer equilibrium, namely the neutral and fully protonated forms.

Nevertheless, in the case of compounds **1** and **3**-**6**, the absence of an iso-emissive point (see Figure 11) suggests that the neutral, monocation and dication species of luotonin A coexist in the equilibria and that the ESPT proceeds in two steps. At the beginning of the titration the 420 nm emission of the neutral form was red shifted to 450 nm as its intensity decreased; in a second stage, an iso-emissive point appeared between the decreasing 450 maximum and the new emission growing at 500 nm corresponding to the dicationic form.

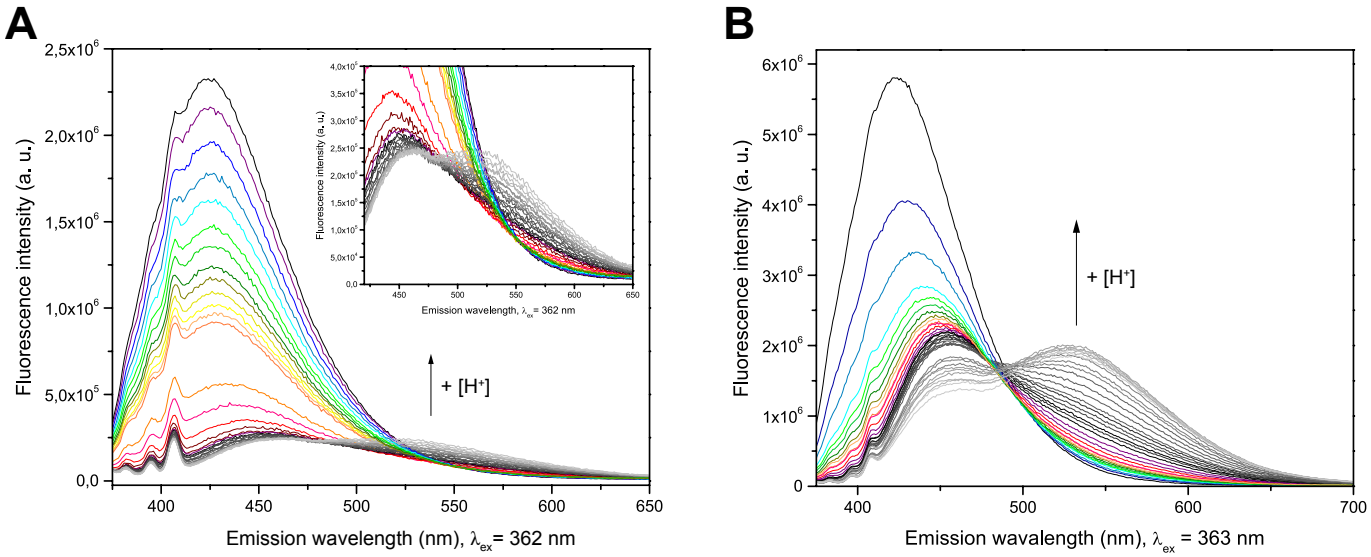

Figure 11.
Fluorescence emission spectra of luotonin derivatives obtained in the titration with $HClO_4$ in acetonitrile.
(A) Compound **5**.
(B) Compound **4**.

These two proposed pathways for the ESPT are schemed in Figure 12. The different observed behaviours can be explained considering the different electronic and structural features present in methyl derivatives **2** and **7**, which can be protonated more easily than the other compounds owing to the electron-releasing effect of the substituents. Therefore, **2** and **7** are able to yield the dicationic form in a single step, as indicated by the existence of the iso-emissive point.

The plots of normalized fluorescence intensity versus -log[$HClO_4$] (Figure 13) allowed the tentative deduction of the pK_a^* values in organic media considering the acid concentration required for the protonation of the half of the molecules population [49]. The $HClO_4$ concentrations values necessary to reach the half-protonation of the bases present a good correlation to the chemical structure (see Figure 14). Although all compounds behaved as weak bases, their basicity was clearly increased in acetonitrile media with regard to the aqueous solutions. Compounds **2** and **7**, with electron-donating methyl groups, were the most basic ones, as expected, while compounds presenting electron-withdrawing halogen substituents (**4** and **5**) were the weakest bases of the series (Table 4).

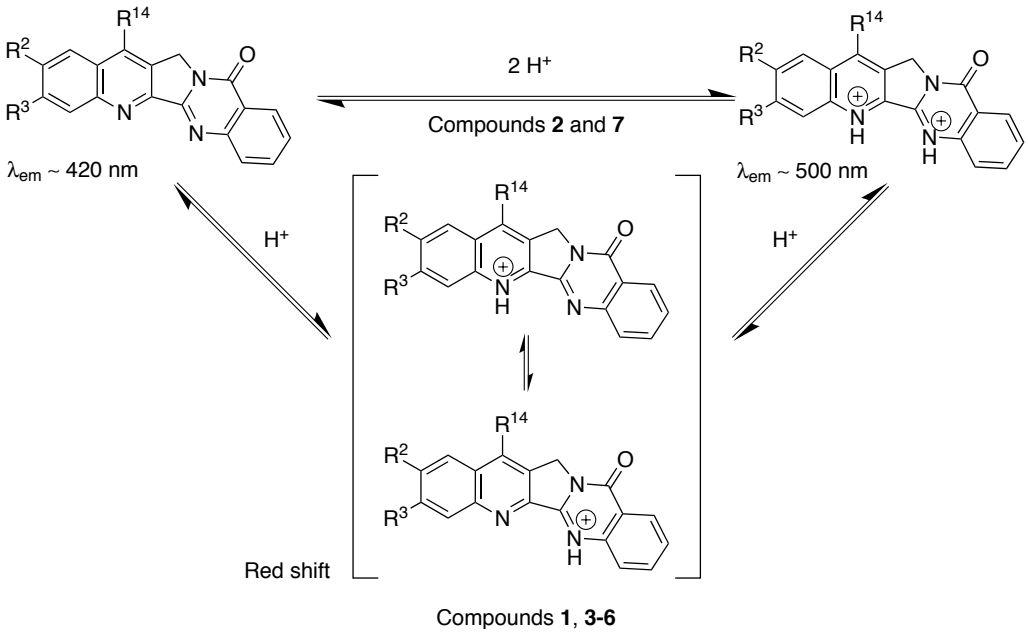

Figure 12.
Scheme proposed for the ESPT reactions of luotonin A and the derivatives studied in the present work.

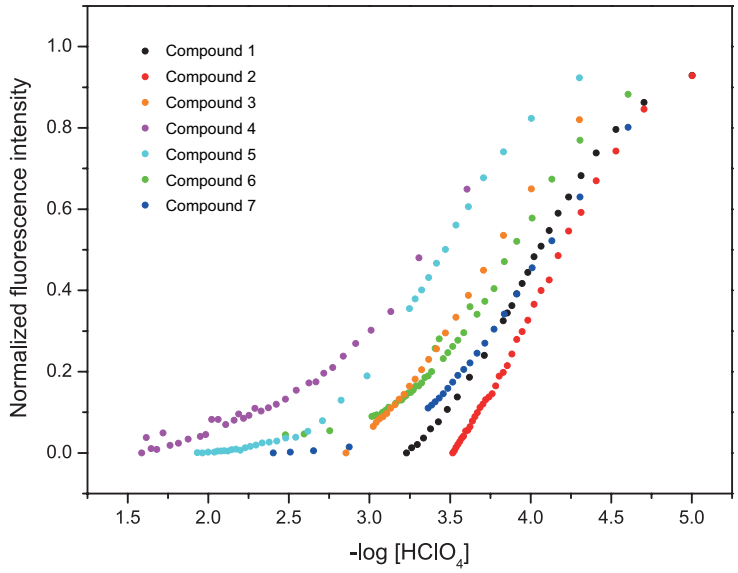

Figure 13. Titration curves obtained in acetonitrile media obtained for the luotonin A and derivatives. Excitation and emission wavelengths correspond to the neutral form.

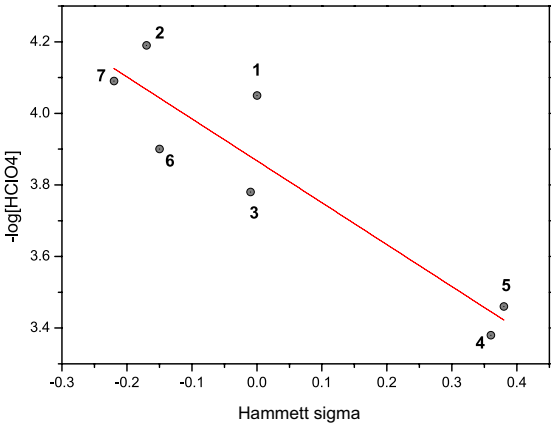

Figure 14. Plot of the pK_a^* value obtained in the titration luotonin A derivatives with $HClO_4$ in acetonitrile versus the σ Hammett parameter calculated for each compound.

Table 4. pK_a^* values obtained in acetonitrile by steady-state fluorescence measurements.

Comp.	Hammett σ value	-log[$HClO_4$]#
1	0	4.05
2	-0.17	4.19
3	-0.01	3.78
4	0.36	3.38
5	0.38	3.46
6	-0.15	3.90
7	-0.22	4.09

#Concentration of $HClO_4$ required to drop the normalized fluorescence of the neutral form by 50%.

3.4. ^{1}H and ^{13}C-NMR studies of the proton transfer reactions of luotonin A

With the aim to demonstrate the protonation of the basic nitrogens, ^{1}H and ^{13}C-NMR experiments were carried out using d_6-DMSO as solvent and non-deuterated $HClO_4$ as titrating agent. The additions of increasing amounts of acid caused the protonation of both quinoline nitrogen (N-5) and quinazoline nitrogen (N-6) as can be observed in Figure 15A. In the ^{1}H-NMR experiments, the protonation of nitrogens was evidenced by the down-field shifts of the signals corresponding to the protons in *para* with regard to the protonation positions. This is the case of the signals of the protons H-2 and H-14 (*para* to N-5) and the signals of the proton H-9 (*para* to N-6). These changes showed that the simultaneous protonation of both nitrogens is possible. In the ^{13}C-NMR spectra, important changes in the chemical shifts (see Figure 15B) were observed for the signals of the carbons closest to the basic quinoline (C-4a and C-5a) and quinazoline nitrogens (C-5b and C-6a), which demonstrated the protonation of both of them.

3.5. Quantitative analysis of luotonin A and derivatives

In view of these studies, fluorescence measurements constitute a technique of choice for the quantitation of luotonin A and its derivatives. With the aim to carry out this

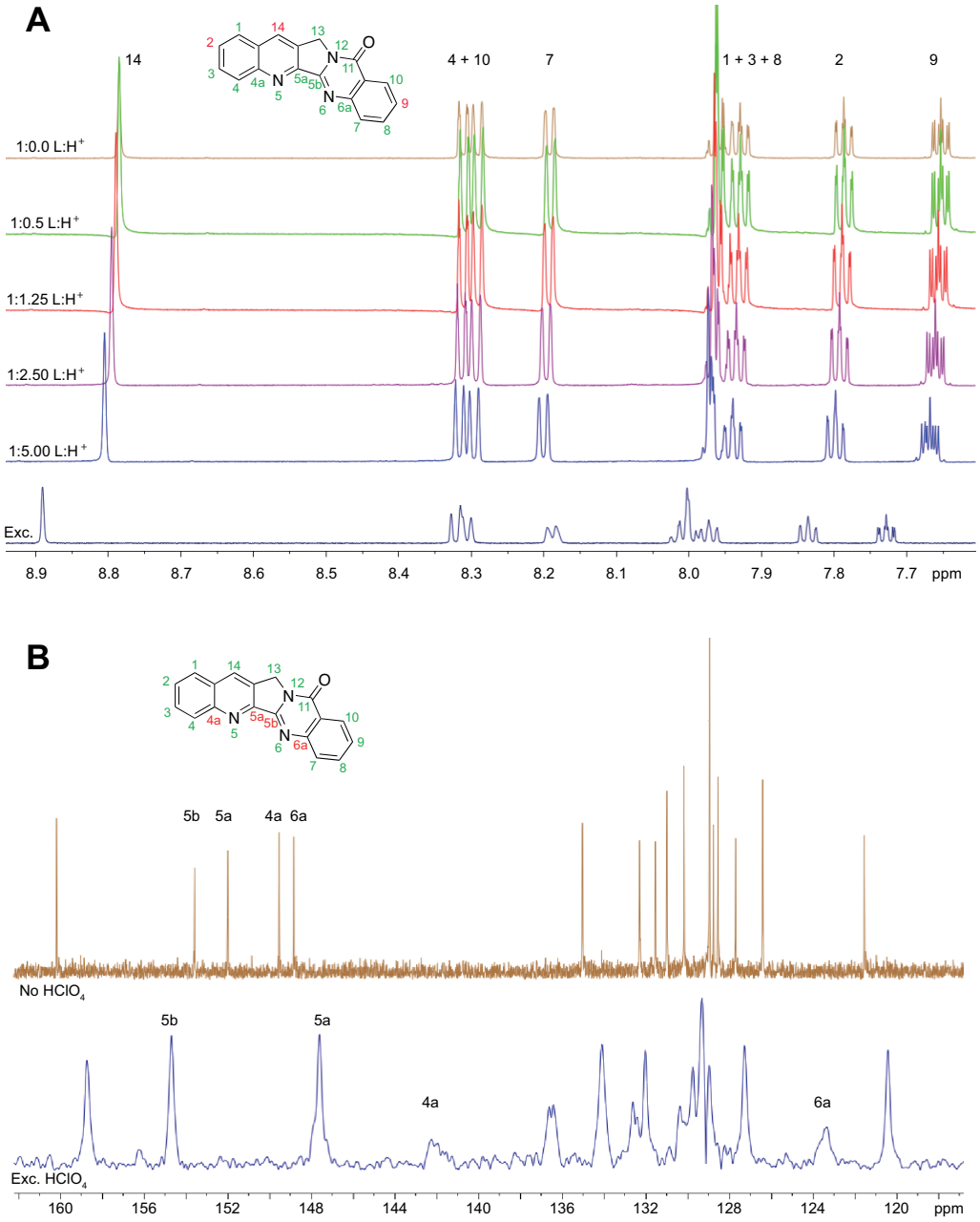

Figure 15.
Overlay of ^{1}H- (A) and ^{13}C-NMR(B) spectra of free luotonin A and luotonin A and $HClO_4$ in increasing stoichiometric ratio, and $HClO_4$ concentration in excess.
Both figures have been expanded into the region of the atoms involved in the proton transfer reaction.

kind of assays applied to forthcoming *in vitro* biological activity evaluation and pharmacokinetic studies, we were prompted to develop a simple methodology for their quantitation. From this approach, we have determined the linear range and sensitivity of this method evaluated as limit of detection (LOD). The results obtained are summarized in Table 5, with remarkably good analytical features. Concentrations in the range of 10^{-9} M can be determined for all compounds studied in standard samples. Besides, comparing the LOD and LOQ obtained in aqueous (pH 5.5) and ethanolic solutions with those obtained in acid aqueous solution (pH 0.5) where the cationic species are responsible for the fluorescence emission, no apreciable differences in the sensitivity were obtained.

Despite the fact that the QYs of the neutral forms are higher, the cationic forms allow the quantitative analysis to be performed in acidic media with a sensitive LOQ and measuring at 500 nm emission wavelength. These conditions avoid the potential interference coming from the auto-fluorescence emission of biomolecules present in biological matrices.

Table 5. Sensitivity of the quantitative analysis of luotonin A and derivatives. Limit of detection and limit of quantitation obtained at the excitation and emission maxima wavelengths selected.

Compound	Solvent	LOD (M)	LOQ (M)
1	Ethanol	3.42×10^{-9}	1.14×10^{-8}
	Water (pH=5.5)	2.46×10^{-9}	8.19×10^{-9}
	Water (pH=0.5)	1.93×10^{-9}	6.45×10^{-9}
2	Ethanol	4.39×10^{-9}	1.46×10^{-8}
	Water (pH=5.5)	1.48×10^{-9}	4.92×10^{-9}
	Water (pH=0.5)	4.04×10^{-10}	1.35×10^{-9}
3	Ethanol	1.45×10^{-9}	4.84×10^{-9}
	Water (pH=5.5)	4.84×10^{-10}	1.61×10^{-9}
	Water (pH=0.5)	3.46×10^{-9}	1.15×10^{-8}
4	Ethanol	3.30×10^{-9}	1.10×10^{-8}
	Water (pH=5.5)	2.66×10^{-9}	8.88×10^{-9}
	Water (pH=0.5)	4.64×10^{-9}	1.55×10^{-8}
5	Ethanol	3.24×10^{-9}	1.08×10^{-8}
	Water (pH=5.5)	3.26×10^{-9}	1.09×10^{-8}
	Water (pH=0.5)	3.04×10^{-9}	1.01×10^{-8}
6	Ethanol	7.86×10^{-9}	2.62×10^{-8}
	Water (pH=5.5)	2.79×10^{-9}	9.30×10^{-9}
	Water (pH=0.5)	3.04×10^{-9}	1.01×10^{-8}
7	Ethanol	1.36×10^{-9}	4.35×10^{-9}
	Water (pH=5.5)	1.10×10^{-9}	3.66×10^{-9}
	Water (pH=0.5)	4.36×10^{-9}	1.45×10^{-8}

In all of cases the correlation (R^2) obtained from the linear regression analysis was higher than 0.99. The linear range of concentrations studied covers from 1.0×10^{-10} M to 1.0×10^{-7} M.

4. Conclusions

The present work shows that luotonin A and the six new derivatives studied present rich ESPT equilibria, with neutral and cationic species coexisting in the excited state. Fluorescence measurements as well as ^{1}H- and ^{13}C-NMR spectra demonstrate that the two basic nitrogens present on luotonin A structure are protonated under strong acidic conditions. The pK_a^* values obtained in aqueous media are in concordance with those described for camptothecin. The fluorescence properties of luotonin A and the six new compounds are described here for the first time and their relative acid-base strength is well correlated with their chemical structures. In organic solvents, the basicity of these compounds is increased with regard to aqueous media, with compounds possessing electron-withdrawing substituents showing lower basicities. Fluorescence quantum yields are dependent not only on the chemical structure but also on the solvent and pH value. The complex proton transfer equilibria of these compounds will require further studies that can contribute to clarify not only their particular behaviour but also the peculiar acid-base equilibria of camptothecin which, 50 years after its isolation, are still not fully understood. The remarkable fluorescence observed for the new luotonin A derivatives, coupled with their good analytical properties, make spectrofluorimetry an attractive and adequate technique for the analysis of these compounds in biological matrices.

5. Acknowledgements

We gratefully acknowledge financial support of this work by MICINN, Spain (grants CTQ 2009-11312-BQU and CTQ2009-12320-BQU) and Universidad Complutense (Grupos de Investigación Consolidados, grant GR35/10-A-920234). V. González-Ruiz is grateful to MEC, Spain, for a FPU Research Fellowship. S. Arunachalam expresses his thanks to MEC for supporting his Sabbatical leave on Spain (SAB-2006-0059).

6. References

1. A.P. Demchenko, Introduction to Fluorescence Sensing, Springer, Berlin, 2009.
2. M. Hof, R. Hutterrer, V. Fidler (Eds.), Fluorescence Spectroscopy in Biology. Advances Methods and their Applications to Membranes, Proteins, DNA and Cells, Springer, Berlin, 2005.
3. B. Valeur, Molecular Fluorescence. Principles and Applications, Wiley-VCH, Weinheim, 2001.
4. J.R. Lakowicz, Principles of Fluorescence Spectroscopy, 3rd Ed, Springer, 2006.
5. R.H. Newman, M.D. Fosbrink, J. Zhang, Chem. Rev. 111 (2011) 3614-3666.
6. X. Fang, W. Tang, Acc. Chem. Res. 43 (2010) 48-57.
7. J. Guo, L. Yu, N.J. Turro, J. Ju, Acc. Chem. Res. 43 (2010) 551-563.
8. Y. Sun, S. Bi, D. Song, C. Quiao, D. Mu, H. Zhang, Sensor Actuat. B Chem. 129 (2008) 799-810.
9. L. He, X. Wang, B. Liu, J. Wang, Y. Sun, E. Gao, S. Xu, J. Lumin. 131 (2011) 285-290.
10. Y. Yue, Y. Zhang, Y. Li, J. Zhu, J. Qin, X. Chen, J. Lumin. 128 (2008) 513-520.
11. G.-W. Song, Z.-X. Cai, Y. He, Z.-W. Lou, Sensor Actuat B Chem. 102 (2004) 320-324.
12. P. Mussardo, E. Corda, V. González-Ruiz, J. Rajesh, S. Girotti, M. A. Martín, A. I. Olives, Anal. Bioanal. Chem. 400 (2011) 321-327.
13. P. Zuck, G.T. O'Donnell, J. Cassaday, P. Chase, P. Hodder, B. Strulovici, M. Ferrer, Anal. Biochem. 342 (2005) 254-259.
14. R.A. Pufahl, T.P. Kasten, R. Hills, J.K. Gierse, B.A. Reitz, R.A. Weinberg, J.L. Masferrer, Anal. Biochem. 364 (2007) 204-212.
15. E. Gravel, P. Bourget, L. Mercier, A. Paci, J. Pharm. Biomed. Anal. 39 (2005) 581-586.
16. P.M. Loadman, C.R. Calabrese, J. Chromatogr. B 764 (2001) 193-206.
17. M. Espinosa-Bosch, A.J. Ruiz-Sánchez, F. Sánchez-Rojas, C. Bosch-Ojeda, J. Pharm. Biomed. Anal. 48 (2008) 519-532.
18. Z.-Z. Ma, Y. Hano, T. Nomura, Y.-J. Chen, Heterocycles 46 (1997) 541-546.
19. K. Nacro, C. Zha, P.R. Guzzo, R.J. Herr, D. Peace, T.D. Friedrich, Bioorg. Med. Chem. 15 (2007) 4237-4246.
20. C. Avendaño, J. C. Menéndez, Medicinal Chemistry of Anticancer Drugs, Elsevier, Amsterdam, 2008, chapter 7.
21. B.A. Teicher, Biochem. Pharm. 75 (2008) 1262-1271.
22. V.J. Venditto, E. E. Simanek, Mol. Pharmaceut. 7 (2010) 307-349.
23. Y. Pommier, E. Leo, H.L. Zhang, C. Marchand, Chem. Biol. 17 (2010) 421-433.
24. J. F Pizzolato, L.B Saltz, Lancet 361 (2003) 2235-2242
25. A. Cagir, S.H. Jones, R. Gao, B.M. Eisenhauer, S. M. Hecht, J. Am. Chem. Soc. 125 (2003) 13628-13629.
26. C.J. Thomas, N.J. Rahier, S.M. Hecht, Bioorg. Med. Chem. 12 (2004) 1585-1604.
27. Z. Ma, Y. Hano, T. Nomura, Heterocycles 65 (2005) 2203-2219.
28. N. Malecki, P. Carato, B. Rigo, J.-F. Goossens, R. Houssin, C. Bailly, J.-P. Hénicharta, Bioorg. Med. Chem. 12 (2004) 641-647.
29. V. Sridharan, P. Ribelles, M. T. Ramos, J. C. Menéndez, J. Org. Chem. 74 (2009) 5715-5718.
30. J.L. Liang, H.C. Cha, Y. Jahng, Molecules 16 (2011) 4861-4883.
31. J.-J. Aaron, S. Trajkovska, Curr. Drug Targets 7 (2006) 1067-1081.
32. Z.P. Hu, X.X. Yang, X. Chen, E. Chan, W. Duan, J. Chromatogr. B, 850 (2007) 575-580.
33. X. Liu, Y. Wang, D. Vardeman, Z. Cao, B. Giovanella, J. Chromatogr. B 867 (2008) 84-89.
34. T. Oguma, J. Chromatogr. B 764 (2001) 49-58.
35. V. González-Ruiz, P. Mussardo, E. Corda, S. Girotti, A.I. Olives, M.A. Martín, J. Sep. Sci. 33 (2010) 2086-2093.
36. J.W. Eastman, Photochem. Photobiol. 6 (1967) 55 - 72.
37. W.S. Haynes (Ed.), CRC Handbook of Chemistry and Physics, 92 nd Edition, CRC Press, Boca Raton, 2011.
38. British Pharmacopoeia Commission Office, British Pharmacopoeia, Apendix VIII A, vol.4, Stationery Office (MHRA), London, 2009.
39. J. Dey, I.M. Warner, J. Lumin. 71 (1997) 105-114.
40. Y. Posokhov, H. Biner, S. Icli, J. Photochem. Photobiol. A: Chem. 158 (2003) 13-20.
41. E.L. Wehry, Effects of Molecular Environment on Fluorescence and Phosphorecence, in G.G. Guilbault, Practical Fluorescence, Marcel Dekker Inc., New York, 1990.
42. S.K. Droga, J. Lumin. 114 (2005) 101-117.

43. J. Dey, I.M. Warner, J. Photochem. Photobiol. A: Chem. 116 (1998) 27-37.
44. A. Albert, E.P. Serjeant, The Determination of Ionization Constants. A Laboratory Manual, Chapman and Hall, London, 1984.
45. J. Dey, I.M. Warner, J. Photochem. Photobiol. A: Chem. 101 (1996), 21-27.
46. B. Selvi, S. Patel, M. Savva, J. Pharm. Sci. 97 (2008) 4379-4390.
47. M.R. di Nunzio, B. Cohen, A. Douhal, J. Phys. Chem. A 115 (2011) 5094-5104.
48. G. Jahanbakhsh, A. Shahin, K. Mikael, F. Amin, J. Chem. Eng. Data 48 (2003) 1178-1182.
49. R. F. Cookson, Chem. Rev. 74 (1974) 5-28

11

Liquid chromatographic analysis of the anti-cancer alkaloid luotonin A and some new derivatives in human serum samples

Published in: González-Ruiz, V., Mussardo, P., Corda, E., Girotti, S., Olives, A. I. & Martín, M. A. (2010). J. Sep. Sci., 33(14), 2086-2093.

ABSTRACT ▶ The quantitation of the natural cytotoxic and anti-inflammatory alkaloid luotonin A and five recently synthesized derivatives is described, constituting the first report of a HPLC method for the analysis of these compounds in human serum samples. The conditions for the chromatographic separation were optimized and the method was validated for the analysis of these compounds in biological samples according to international guidelines. An RP-HPLC method with fluorimetric detection and a C-18 stationary phase was applied. Different MeCN/water mobile phases were assayed, including 0–4% of a mobile phase modifier such as tetrahydrofuran, dioxane or *tert*-butyl methyl ether. Isocratic and gradient elution conditions are compared. The influence of pH on the efficiency and resolution of the separation was also considered. The developed method was applied to the determination of luotonins in pooled human serum samples by gradient elution RP-HPLC using a simple clean-up procedure. The proposed chromatographic method exhibits satisfactory analytical figures of merit, with LOD from 1.0×10^{-10} to 2.0×10^{-10} M, intra-day and inter-day precision below 6% except for the concentration level closest to LOD, and good agreement between experimental and theoretical concentrations. Therefore, the developed method is suitable, reliable, rapid, and simple.

DOI ▼
10.1002/jssc.201000175

ABBREVIATIONS ▼
- **FL:** fluorescence
- **QC:** quality control
- **^{t}BME:** *tert*-butyl methyl ether
- **RP-HPLC:** reverse phase-HPLC

1. Introduction

The design and development of new anti-cancer drugs possessing better pharmacological properties and lower toxicities is a research field of renewed interest. The analysis of the concentrations of drug candidates in biological samples makes it possible to establish correlations between those concentrations and many of their pharmacological and pharmacokinetic properties. The use of sensitive, versatile and rapid analytical techniques being able to process a large number of samples is essential to perform this kind of studies.

Luotonin A (Figure 1) is a derivative of the quino[2',3'-3,4]pyrrolo[2,1-*b*] quinazoline ring system which was first isolated in 1997 from the plant *Peganum nigellastrum*. This plant has been used for a long time in Chinese traditional medicine as a remedy for inflammatory disorders [1]. Luotonin A also exhibits cytotoxic activity against several mouse tumor cells due to its topoisomerase I poisoning properties [2,3]. Luotonin A is structurally close to the strong topoisomerase I inhibitor camptothecin and other related anticancer drugs (Figure 1) [4]. There is a considerable interest in the synthesis of new analogues of luotonin A and the study of their biological properties [5-7] because of its lower toxicity and higher chemical stability compared to camptothecin. The anti-proliferative activity of new A-ring- and E-ring-modified derivatives has been assayed in different cancer cell lines showing an equivalent activity to the parent luotonin A [5]. These studies have shown that some structural modifications, specially in ring E, may lead to pronounced changes in the ability to stabilize the topoisomerase I-DNA binary complex [7].

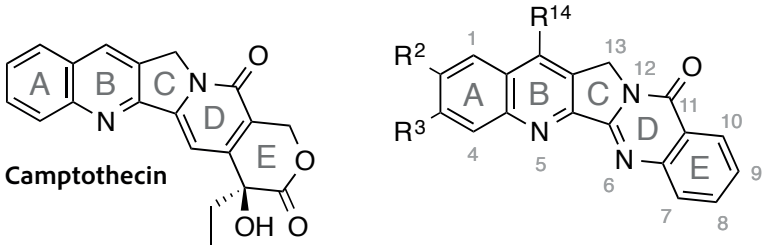

Compound	R^2	R^3	R^{14}
1 (Luotonin A)	H	H	H
2	H	H	CH_3
3	H	H	C_6H_5
4	Cl	H	C_6H_5
5	Br	H	C_6H_5
6	H	H	3,5-$Me_2C_6H_3$
7	H	CH_3	3,5-$Me_2C_6H_3$

Figure 1.
Chemical structures of the anticancer drug camptothecin, and of the luotonin A and its derivatives studied in the present work.

The presence of aromatic and heteroaromatic rings on the structures of camptothecin and luotonin A affords the notable native fluorescence of these compounds. This property makes it possible to use fluorescence measurements with analytical and biomedical purposes [8]. The studies of cytotoxicity and selectivity of new antitumor agents in tumor cells require sensitive and selective analytical methods. Several HPLC procedures have been described for the determination of camptothecin [8-20], including the isocratic elution of camptothecin and its analogues using MeCN:phosphate buffer as mobile phase [13]. Isocratic and gradient separations coupled to UV-Vis [14,15] and diode array detection [16] have been employed successfully. Other detection methods for camptothecin and analogues include fluorimetry [17-19] and mass spectrometry [20,21]. Nevertheless there is not any previously described analytical method for the separation and quantitative determination of luotonin A.

Considering the emerging potential of the luotonin A family of compounds, human serum has been selected as a representative model of biological matrices in which these compounds should be quantified along their pharmaceutical development. In the present work we describe for the first time a RP-HPLC method with fluorimetric detection allowing the separation and quantitation of luotonin A and several recently synthesized derivatives (Figure 1) in human serum. The optimized method has shown to be simple, fast and will allow for the correlation of physico-chemical properties of every compound and their biological activities through cell-culture assays, thus paving the way for the search of new candidates as a less toxic alternative to camptothecin derivatives.

2. Experimental

2.1. Apparatus and reagents

UV-Vis absorption spectra were obtained using a Kontron (Zurich, Switterland) Uvikon 810 double beam spectrophotometer and quartz cells of 1 cm of path length. Corrected excitation and emission fluorescence spectra as well as fluorescence emission at fixed wavelengths were carried out with a Horiba-Jobin Yvon (Edison, NJ, USA) FluoroMax-4P spectrofluorometer equipped with the control and data acquisition software FluorEssence 2.1.

For the HPLC quantitation of luotonin derivatives, a Merck-Hitachi (Tokyo, Japan) chromatographic system (quaternary gradient pump L-7100, fluorescence detector L-7450, oven L-2300 and a Rheodyne model 7725i injector with 20 µL loop) was employed. The chromatographic system was under computer control through the HPLC System Manager software, version 4.1. Separations were developed under isocratic or gradient reverse phase using Spherisorb C-18 columns (ODS2, 5 µm, 150 × 4.6 mm) from Teknokroma (Barcelona, Spain).

Luotonin A and its analogues (Figure 1) were kindly provided by the Organic and Pharmaceutical Chemistry Department at the Faculty of Pharmacy (Universidad Complutense de Madrid), and they were synthesized by modified Friedländer conditions as described elsewhere [22]. All reagents and solvents were analytical, spectroscopic or chromatographic grade (from Panreac, Barcelona, Spain) and they were used without further purification. Water was doubly distilled and deionized (Milli-Q purification system, Millipore, Molsheim, France).

2.2. Procedures

2.2.1. Standard solutions and characterisation of new luotonin A derivatives

Stock solutions (5.0×10^{-4} M) of lutonin A and its derivatives in DMSO were prepared from an accurately weighed amount of each compound. A series of solutions for each luotonin A derivative was prepared in ethanol in the range of concentration 1.0×10^{-6} M to 1.0×10^{-4} M in order to obtain the UV-Vis absorption spectra and the values of molar absorptivities (Table 1).

Fluorescence excitation and emission spectra were obtained as a previous step to reach the sensitive luminescent quantitation of these compounds. For this purpose, 5.0×10^{-7} M and 1.0×10^{-6} M ethanolic solutions were prepared and measured. Both excitation and emission slits were set at 3 nm bandpass.

2.2.2. Conditions of the chromatographic analysis

For isocratic elution the optimized mobile phase was H_2O:MeCN:^{t}BME, 60:38:2 (v:v:v) at 35 °C. In gradient elution, a combination of H_2O and MeCN was employed at a flow rate of 1 mL min^{-1}. The column was firstly equilibrated with 60% H_2O and 40% MeCN for 5 minutes. Then, the sample was injected and the proportion of MeCN was increased from 40 to 60% over 20 minutes; after 5 minutes kept at 60%, the proportion of MeCN was returned to 40% over 2 minutes. The separation took 24 minutes. Temperature was fixed at 25 °C. For all experiments the fluorescence detection conditions were λ_{ex}= 340 nm, λ_{em}= 420 nm. All solvents were filtered through a 0.45 µm pore membrane and sonicated prior to their use. For every experimental condition, each compound was injected individually to be identified by its retention factor.

2.2.3. Preparation of the standard solutions and spiked serum samples for chromatographic analysis

Separate stock solutions around 5.0×10^{-4} M in DMSO were prepared by weighing an appropriate amount of each compound. The concentrations of the stock solutions were checked using the previously determined UV-Vis molar absorptivity values. Suitable volumes of every luotonin derivative stock solution were mixed and diluted to get a solution A containing each compound in a concentration of 5.0×10^{-6} M in H_2O:MeCN, 50:50 (v:v). From this solution (A), a serial dilution was carried out to prepare a set of solutions (B-G) of concentrations 2.5×10^{-6} M, 1.25×10^{-6} M, 5.0×10^{-7} M, 5.0×10^{-8} M, 5.0×10^{-9} M and 2.5×10^{-9} M in the same solvent mixture.

Equal aliquots of pooled human sera, obtained from 20 healthy individuals, were spiked with solutions A-G to get a set of sera with luotonin concentrations ranging from 5.0×10^{-7} M to 2.5×10^{-10} M (calibrators). Blank sera spiked with the same volume of solvent mixture were also prepared. The spiked volume was always less than 10% of serum volume to avoid distorting the nature of the matrix.

The same procedure was followed to prepare quality control samples (QC) at final concentrations of 5.0×10^{-7} M, 5.0×10^{-8} M and 5.0×10^{-10} M.

Furthermore, aliquots of solutions A-G were also diluted using mobile phase to get a series of standard solutions matching the concentrations of the calibrators but being free of matrix effects.

2.2.4. Human serum samples pre-treatment for chromatographic analysis

A previously described sample clean-up procedure was followed because of its simplicity, low time-consumption and good extraction efficiency [23]. This treatment consisted of a protein precipitation using 0.5% glacial acetic acid in MeCN followed by centrifugation. The supernatant was transferred to a clean tube and evaporated under vacuum at 50 °C, then the solid residue obtained was dissolved in the mobile phase. This clean-up methodology was followed for preparing both calibrators and QC samples.

2.2.5. Validation of the chromatographic method for the analysis of luotonins in human serum samples

To validate the developed chromatographic method, linearity, limit of detection (LOD), limit of quantitation (LOQ), accuracy, precision and evaluation of matrix effects were determined following the recommendations of IUPAC, FDA and ICH [24-26].

Calibration curves were constructed by measuring extracted spiked sera (calibrators) at seven levels of concentrations plus a blank, and then plotting the areas of the chromatographic peaks *versus* the theoretical concentration. Calibration curves were measured by quadruplicate in different days to minimize effects due to intra- and inter-day variation. LOD and LOQ were determined from five replicated measurements of QC solutions at 5.0×10^{-10} M concentration and then calculated as shown in Equations 1 and 2 [27].

$$\text{LOD} = 3 \times \frac{\text{SD of the experimental concentration} \times \text{theoretical concentration}}{\text{mean of the experimental concentration}} \qquad \textbf{Eq. 1}$$

$$\text{LOQ} = 10 \times \frac{\text{SD of the experimental concentration} \times \text{theoretical concentration}}{\text{mean of the experimental concentration}} \qquad \textbf{Eq. 2}$$

Accuracy was determined by six replicate analyses of spiked QC samples (QC) at three levels of concentration (5.0×10^{-7} M, 5.0×10^{-8} M and 5.0×10^{-10} M) which were then compared with the calibration curves previously prepared. Intra-day precision was calculated from six runs conducted on the same day, and the experiments were also performed using the previous three levels of concentration. Inter-day precision was determined from duplicate injections of the same concentration over five different days, also at three levels of concentration. Matrix effects were evaluated using a Student's *t*-test to compare the slope of the calibration curve obtained from standard solutions prepared in mobile phase and the slope of the calibration curve constructed from calibrators prepared in sera and following the extraction procedure.

3. Results and discussion

3.1. Spectroscopic properties of luotonin A and derivatives

UV-Vis absorption spectra of the different compounds under study showed a band in the region of 300-375 nm with two resolved peaks appearing near to 340 and 360 nm. The relative position of these two maxima changes depending on substituents attached to the pattern ring as can be observed in Table 1. The UV-Vis spectral shape of luotonin A derivatives as well as the molar absorptivity values were in agreement with those described for camptothecin [28]. The molar absorptivities were calculated from the slope of the calibration curves in ethanol, using the maxima wavelengths of every compound. These values are significant to characterize the derivatives studied and they were also used to ensure the accuracy of the concentration of stock solutions for chromatographic analysis.

It is well known that fluorescence emission provides a better sensitivity than UV-Vis absorption methods with an enhancement in the LOD varying from 10 to 1000 times. Therefore, fluorescence is one of the most widespread detection techniques in liquid chromatographic analysis, and particularly for the determination of pharmaceutical interesting compounds present in different matrices at very low concentrations. The fused aromatic rings in luotonin A and derivatives afford a noticeable native fluorescence. The emission spectra exhibited a broad emission band (Figure 2) with a maximum placed at 410-430 nm depending on the compound being studied (Table 1). The spectral shape and the position of the emission maxima are close to those described for camptothecin [28]. Thus fluorescence measurements are an elegant and sensitive technique for their detection in HPLC.

Table 1. Spectrophotometric and spectrofluorimetric properties of the compounds studied. Maximum absorption wavelength and fluorescence emission maximum obtained for luotonin A and derivatives. The molar absorptivity values were calculated for the different luotonin A derivatives at two wavelengths and using 90:10 (v:v) EtOH:DMSO as solvent. The values of log ε are showed in parenthesis.

Compound	UV-Vis absorption λ_{max} (log ε)#	Fluorescence emission $\lambda_{ex}/\lambda_{em}$ #
1	342 (4.21), 359 (4.15)	341/416
2	341 (4.23), 358 (4.16)	340/403
3	344 (4.26), 361 (4.19)	343/420
4	348 (4.02), 364 (3.97)	347/424
5	349 (4.26), 363 (4.21)	349/425
6	345 (4.18), 361 (4.11)	343/415
7	348 (4.04), 366 (3.99)	348/405

Wavelengths are given in nm.

3.2. Development and optimization of the chromatographic methodology

To study the influence of several experimental variables on the chromatographic separation of the compounds, isocratic elution experiments were carried out. Thus, organic solvent proportion, pH, temperature and mobile phase modifiers were considered. Mobile phases containing different H_2O:MeCN proportions (from 80% to 40% of MeCN) were tested. The best resolution/retention times ratio was obtained with a H_2O:MeCN 60:40 (v:v) mobile phase. Several modifiers were assayed, such as dioxane, tetrahydrofurane and *tert*-butyl methyl ether (^{t}BME). Dioxane and tetrahydrofurane (THF) had no significant effect on the separation process. However, ^{t}BME showed the ability to shorten the retention times without a loss in peak resolution and, thus,

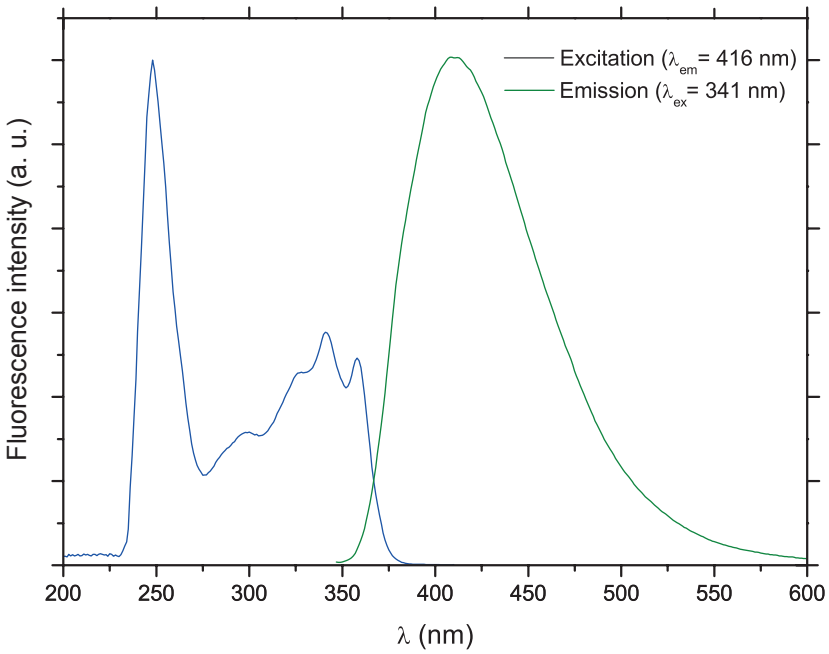

Figure 2. Corrected excitation and fluorescence emission spectra of luotonin A, 2.5×10^{-6} M in ethanol. The intensity of fluorescence excitation and emission spectra is normalized to the same intensity value

^{t}BME from 0-4% was tested in the above selected H_2O:MeCN mobile phase. The best results were obtained with a mobile phase composition of H_2O:MeCN:^{t}BME 60:38:2 (v:v:v) (Figure 3). The influence of the pH of the aqueous proportion in the mobile phase was also considered by using 50 mM phosphate buffer in the pH range from 3.0 to 9.0. This parameter was not found to exert a remarkable effect on the separations, neither changing the retention factors nor the efficiency of the separation, thus avoiding the use of buffer solutions in the mobile phases (Table 2). Nevertheless, none of the assayed conditions allowed getting a reasonable time of analysis (chromatographic runs required 50 min). Additionally, the effect of temperature (25 °C, 35 °C and 45 °C) on the chromatographic process was tested. As it was expected, higher temperatures shortened the retention times and the resolution of the compounds was kept constant.

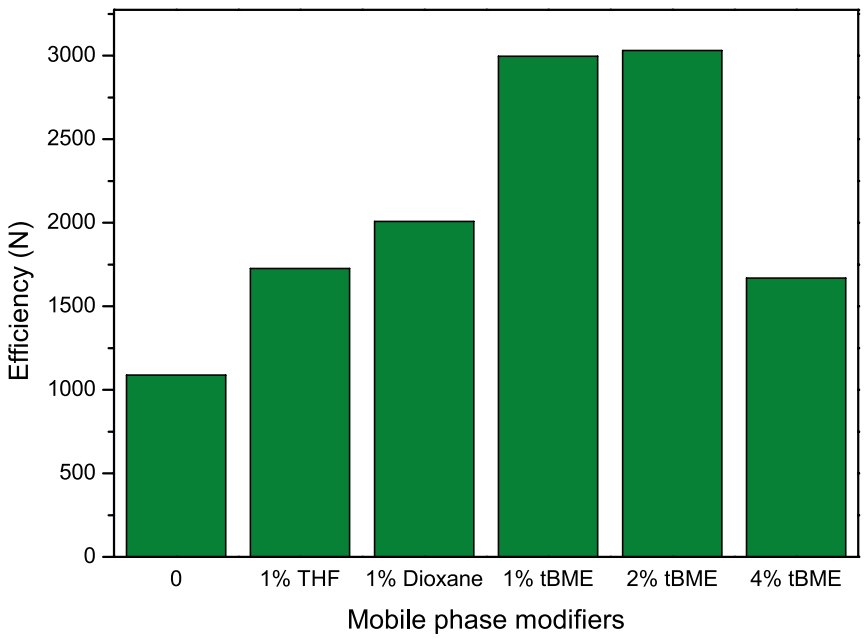

Figure 3. Influence of the organic modifier in the mobile phase on the efficiency of the separation under isocratic conditions. Mobile phase: (modifier + MeCN):H_2O 40:60 (v:v). Modifiers proportions are expressed as percentage of the total volume. Temperature: 25°C. Compound **4**.

Table 2. Retention factors (*k'*) obtained for three representative compounds depending on the pH of the aqueous component of the mobile phase. Mobile phase: 50 mM phosphate buffer:MeCN 50:50 (v:v). Temperature: 25 ºC.

pH	Retention factors (*k'*)		
	Compound 1	Compound 2	Compound 4
pH 3.0	1.21	1.57	6.97
pH 5.8	1.30	1.68	7.40
pH 7.0	1.34	1.70	7.28
pH 9.0	1.26	1.60	6.79

Finally, for isocratic elution, the chosen optimized conditions implied using a mobile phase composition of H_2O:MeCN:^{t}BME 60:38:2 (v:v:v) and carrying out the separation at 35 ºC (Figure 4A).

With the aim to improve the separation efficiency and to get shorter retention times, a gradient elution was developed. Different gradient profiles were assayed (Figure 4B-4D), all of them starting with H_2O:MeCN 60:40 (v:v). Isocratic elution experiments revealed that this proportion was the best MeCN one allowing the resolution of compounds **1** and **2**. It was observed then that a controlled increase in the proportion of acetonitrile would shorten the retention time for compound 6 in order to achieve a reasonable analysis time, without spoiling the resolution of compounds **1** and **2**. After exploring several options, this goal was reached by using the gradient detailed in the Experimental section 2.2.2 (Figure 4D).

Gradient elution provided good resolution, efficiency and shortened in a half the run time at 25 ºC. Therefore, it was chosen for routine analysis and validation of the method. These results also suggest that the developed method could be applied to

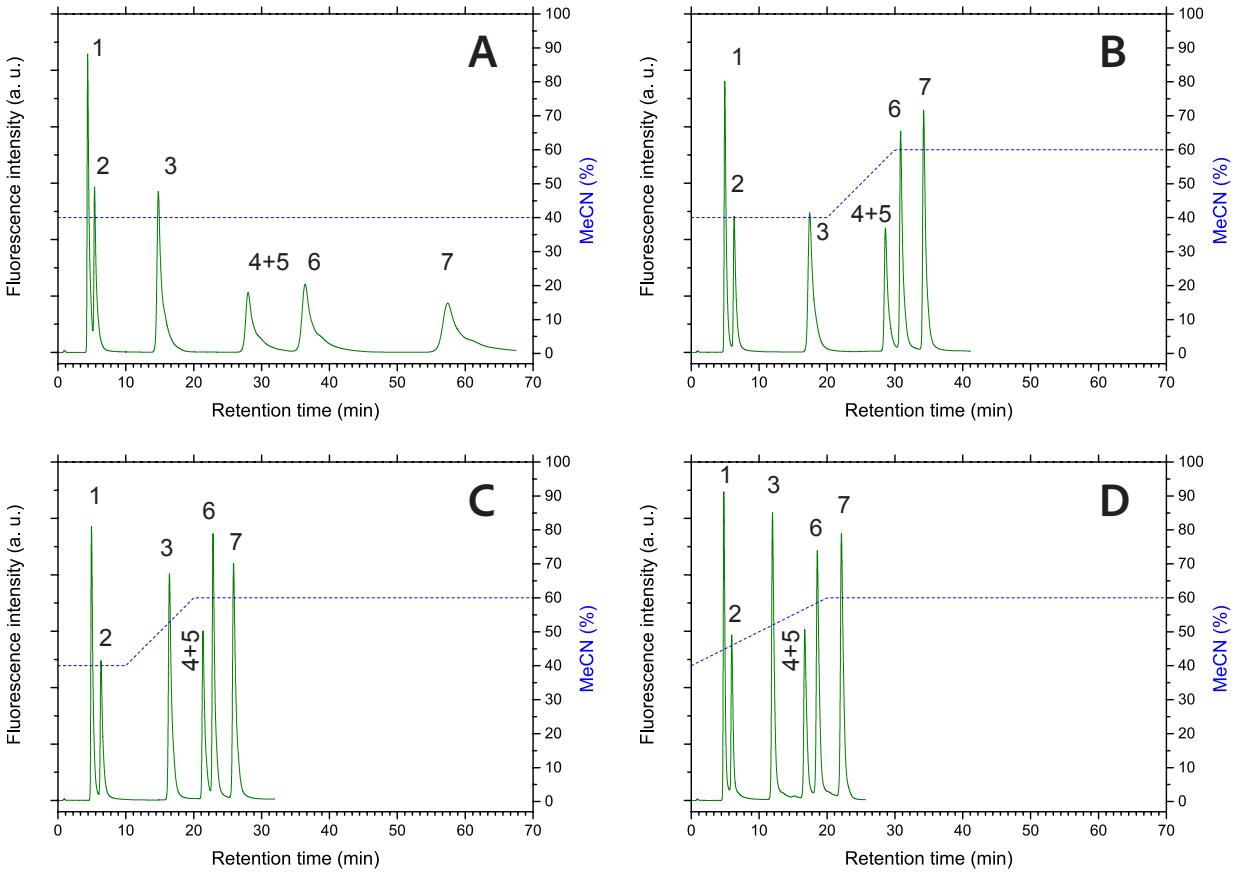

Figure 4.
Chromatographic separation obtained for the compounds studied under several conditions.
(A) Isocratic elution, mobile phase H_2O:MeCN:^{t}BME 60:38:2, 35 ºC.
(B to D): Gradient elution with H_2O:MeCN mixtures as shown by dashed plots, 25 ºC.
General conditions: flow = 1 mL min^{-1}, λ_{ex} = 340 nm, λ_{em} = 420 nm, column Waters Spherisorb 5 µm ODS2 4.6 × 150 mm, compounds concentration = 0.5 µM.

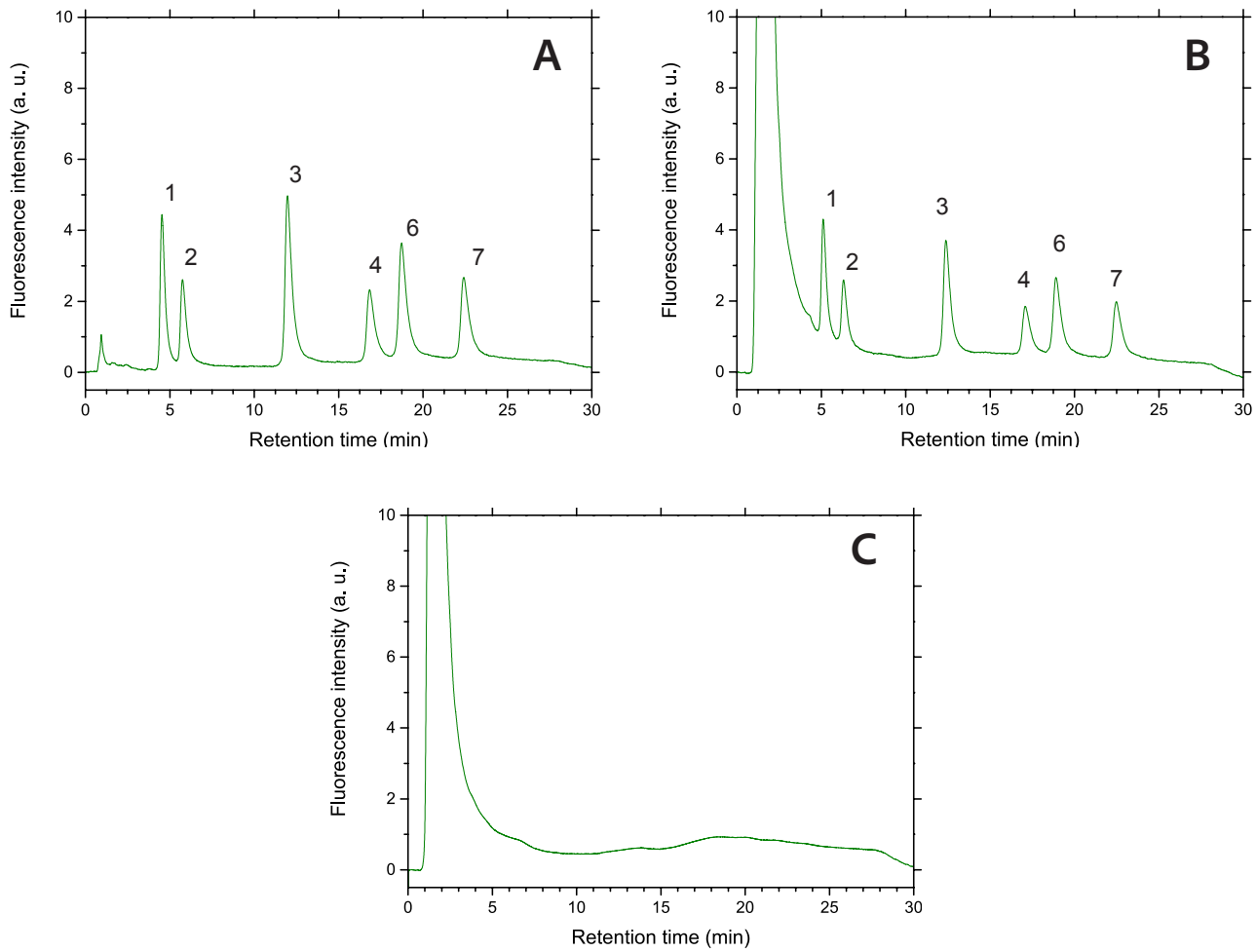

Figure 5. Chromatograms obtained after analysis of the studied compounds in a 5 × 10^{-9} M standard solution (A) or extracts from serum spiked at 5 × 10^{-9} M (B). Chromatogram corresponding to the extract of a blank serum under the same conditions (C). All the separations were carried out at 25 ºC and using the gradient detailed in Section 2.2.2 and depicted in Figure 4D.

the separation of structurally close compounds (drugs and their metabolites), being a good candidate for further pharmacokinetic studies.

Noteworthy, compounds **4** and **5** were not separatedad equately under none of the isocratic or gradient conditions assayed. Because of this, compound **5** was not included in the validation experiments carried out with spiked sera.

3.3. Validation of the chromatographic analytical method (HPLC-FL)

Figure 5 shows the chromatograms corresponding to the standard solutions of luotonins dissolved in mobile phase (Figure 5A) and the luotonin A and derivatives extracted from the spiked serum samples (Figure 5B). As can be observed in the latter Figure, neither the retention times nor the resolution of the studied compounds were affected by the extraction procedure, and the only remarkable change on the chromatogram is the peak appearing at the dead time. To check the specificity of the technique, blank samples from pooled sera were processed and injected onto the chromatographic system. The absence of chromatographic peaks in blank samples (Figure 5C) together with the good separation of the luotonins obtained in spiked serum samples analyzed confirmed the specificity of the method under the developed conditions.

The method of unweighted least squares was employed to calculate the linear regression parameters. As showed by the determination coefficients of the calibration curves (Table 3), the response obtained was linear with the concentration for all of the analytes and over the whole working concentration range, from 5.0 × 10^{-7} M to 2.5 × 10^{-10} M. The regression parameters intercept and slope (Table 3) showed excellent reproducibility along time.

Table 3. Linear regression parameters obtained for the quantitative analysis of luotonin A derivatives by HPLC-FL.

Comp	Calibrators in serum			Calibrators in mobile phase		
	Slope ± SD	Intercept ± SD	R^2	Slope ± SD	Intercept ± SD	R^2
1	$1.54\times10^{13} \pm 0.77\times10^{11}$	$-1.97\times10^{4} \pm 1.57\times10^{4}$	0.9998	$2.13\times10^{13} \pm 1.17\times10^{11}$	$-7.35\times10^{3} \pm 2.38\times10^{4}$	0.9998
2	$1.12\times10^{13} \pm 1.08\times10^{11}$	$-3.52\times10^{4} \pm 2.20\times10^{4}$	0.9993	$1.52\times10^{13} \pm 0.74\times10^{11}$	$-1.27\times10^{3} \pm 1.51\times10^{4}$	0.9998
3	$2.15\times10^{13} \pm 1.29\times10^{11}$	$-2.31\times10^{4} \pm 2.63\times10^{4}$	0.9997	$3.30\times10^{13} \pm 1.45\times10^{11}$	$-5.40\times10^{3} \pm 2.94\times10^{4}$	0.9999
4	$9.44\times10^{12} \pm 0.62\times10^{11}$	$-8.45\times10 \pm 1.26\times10^{4}$	0.9997	$1.56\times10^{13} \pm 0.70\times10^{11}$	$-3.39\times10^{3} \pm 1.42\times10^{4}$	0.9999
6	$1.66\times10^{13} \pm 1.23\times10^{11}$	$-7.92\times10^{3} \pm 2.50\times10^{4}$	0.9996	$2.64\times10^{13} \pm 0.96\times10^{11}$	$-1.20\times10^{4} \pm 1.96\times10^{4}$	0.9999
7	$1.15\times10^{13} \pm 1.22\times10^{11}$	$-3.11\times10^{3} \pm 2.48\times10^{4}$	0.9992	$1.88\times10^{13} \pm 0.77\times10^{11}$	$-9.63\times10^{3} \pm 1.56\times10^{4}$	0.9999

The LOQ and LOD were calculated according to the equations listed in Section 2.2.5. LODs were below 1.8×10^{-10} M and LOQs under 5.9×10^{-10} M, except for the case of compound **4**, in which they were slightly higher. However, biologically effective concentrations of luotonin A and other different derivatives were in the range from 10^{-6} to 10^{-7} M [7], so the obtained LOD and LOQ were at least 1000 folds lower than the concentrations needed for biological and clinical assays.

The accuracy and precision of the HPLC methodology were checked through the analysis of QC samples at three levels of concentration as detailed in Section 2.2.5. Table 4 shows the figures of merit. Accuracy of the method was expressed as experimentally found concentrations. Precision was calculated as % relative standard deviation (% RSD) for intra- and inter-day assays. The obtained values were below acceptance limits (< 10%), and proved that the developed method is suitable for the analysis of these compounds in biological matrices. Nevertheless, accuracy and precision were lowered when working at the lowest QC concentration value (5.0×10^{-10} M), due to the closeness of this concentration to the LOD and LOQ.

A Student's *t*-test was employed to compare the slopes obtained from calibration curves constructed using calibrators (extracted spiked sera) or using standard solutions directly diluted with the mobile phase. For every compound, the slopes were statistically different ($p > 0.01$), which evidenced the presence of matrix effects coming from serum and/or extraction procedure. These facts did not affect to the quantitation of the luotonins in the samples as deduced from the accuracy and precision of the concentration values obtained. Therefore, the good values obtained for the figures of merit prove that this method provides a reliable quantitation of these anticancer drugs in human serum.

Table 4. Figures of merit (sensitivity, accuracy and precision) obtained in the validation of the proposed HPLC-FL method.

Comp	Sensitivity		Accuracy as found concentration (%RE)			Intra-day precision as %RSD			Inter-day precision as %RSD		
	LOD (M)	LOQ (M)	QC_1	QC_2	QC_3	QC_1	QC_2	QC_3	QC_1	QC_2	QC_3
1	1.518×10^{-10}	5.060×10^{-10}	5.003×10^{-7} (0.06)	4.700×10^{-8} (6.00)	4.330×10^{-10} (13.40)	4.02	3.22	10.12	2.76	4.09	8.54
2	1.154×10^{-10}	3.846×10^{-10}	5.005×10^{-7} (0.10)	4.537×10^{-8} (9.26)	4.658×10^{-10} (6.30)	2.16	3.22	7.69	1.87	3.44	7.77
3	1.140×10^{-10}	3.802×10^{-10}	5.005×10^{-7} (0.10)	4.585×10^{-8} (8.30)	5.585×10^{-10} (11.70)	3.66	4.03	7.60	1.63	4.21	9.62
4	2.322×10^{-10}	7.740×10^{-10}	5.004×10^{-7} (0.08)	4.543×10^{-8} (9.14)	7.953×10^{-10} (#)	4.07	3.05	15.48	3.85	5.38	12.22
6	1.429×10^{-10}	4.764×10^{-10}	5.004×10^{-7} (0.08)	4.555×10^{-8} (8.90)	5.926×10^{-10} (#)	3.32	3.38	9.53	1.46	5.08	6.73
7	1.751×10^{-10}	5.837×10^{-10}	5.005×10^{-7} (0.10)	4.502×10^{-8} (9.96)	9.339×10^{-10} (#)	3.03	2.42	11.67	1.44	3.70	6.46

Theoretical concentrations: $QC_1 = 5.000 \times 10^{-7}$ M, $QC_2 = 5.000 \times 10^{-8}$ M, $QC_3 = 5.000 \times 10^{-10}$ M.
% RE: Relative error (percentage), % RSD: Relative standard deviation (percentage)
LOD: Limit of detection, LOQ: Limit of quantitation, # Non-admisible error

4. Conclusion

This is the first time that a HPLC-FL method has been successfully developed and validated for the quantitation of natural alkaloid luotonin A and some derivatives. This work also describes absorption and luminescent characteristics of these molecules. These properties can be exploited to reach their reliable and sensitive detection. The influence of several variables in the separation of this series of very similar compounds has been studied. Furthermore the developed chromatographic method provides a high sample throughput being quick and simple and requiring small sample volumes.

The use of human serum as a biological sample model allows the tuning up of new analytical methods for the quantitation of new drugs since the early stages of their pharmaceutical development, without the need for experimentation in animals, which will be unavoidable in following steps.

The good analytical characteristics of the proposed chromatographic method proved it to be a useful tool for the quantitation of these compounds in biological samples, a main issue in the structure-activity relationship research. This will lead to a better knowledge of their pharmacology and pharmacodynamics, in the way of finding less toxic alternatives to camptothecin analogues being currently used in clinical treatments.

5. Acknowledgements

Financial support from Ministerio de Ciencia e Innovación (SPAIN) through grant CTQ2009-11312 as well as from Grupos de Investigación UCM-CAM (920234/2009) is gratefully acknowledged. The authors are grateful to MEC for a FPU research fellowship for V. González-Ruiz.

6. References

1. Ma, Z., Hano, Y., Nomura, T., Chen, Y., Heterocycles. 1997, 46, 541-546.
2. Ma, Z., Hano, Y., Nomura, T., Heterocycles. 2005, 65, 2203-2219.
3. Lee, E. S., Park, J. G., Kim, S. I., Jahng, Y., Heterocycles. 2006, 68, 151-158.
4. Avendaño, C., Menéndez, J. C., Medicinal Chemistry of Anticancer Drugs, Elsevier, Amsterdam 2008.
5. Nacro, K., Zha, C., Guzzo, P. R., Herr, R. J., Peace, D., Frieddrich, T. D., Bioorg. Med. Chem. 2007, 15, 4237-4246.
6. Cagir, A., Eisenhauer, B. M., Gao, R., Thomas, S. J., Hecht, S. M., Bioorg. Med. Chem. 2004, 12, 6287-6299.
7. Cagir, A., Jones, S. H., Eisenhauer, B. M., Gao, R., Hecht, S. M., Bioorg. Med. Chem. Lett. 2004, 14, 2051-2054.
8. Aaron, J. J., Trajkovska, S., Curr. Drug Targets. 2006, 7, 1067-1081.
9. Oguma, T., J. Chromatogr. B. 2001, 764, 49-58.
10. Palumbo, M., Sissi, C., Gatto, B., Moro, S., Zagotto, G., J. Chromatogr. B. 2001, 764, 121-140.
11. Zufía, L., Aldaz, A., Giraldez, J., J. Chromatogr. B. 2001, 764, 141-159.
12. Loos, W. J., de Bruijn, P., Verweij, J., Sparreboom, A., Anti-Cancer Drugs. 2000, 11, 315-324.
13. Yang, X., Hu, Z., Chan, S. Y., Goh, B. C., Duan, W., Chan, E., Zhou, S., J. Chromatogr. B. 2005, 821, 221-228.
14. Bansal, T., Awasthi, A., Jaggi, M., Khar, R. K., Talegaonkar, S., Talanta. 2008, 76, 1015-1021.
15. Wen, Y., Fan, Y., Zhang, M., Feng, Y. Q., Anal. Bioanal. Chem. 2005, 382, 204-210.
16. Goossens, J., Foulon, C., Bailly, C., Bigg, D. C. H., Bonte, J. P., Vaccher, C., Chromatographia. 2004, 59, 305-313.
17. Hu, Z. P., Yang, X. X., Chen, X., Chan, E., Duan, W., Zhou, S. F., J. Chromatogr. B. 2007, 850, 575-580.
18. Liu, X., Wang, Y., Vardeman, D., Cao, Z., Giovanella, B., J. Chromatogr. B. 2008, 867, 84-89.
19. Gravel, E., Bourget, P., Mercier, L., Paci, A., J. Pharm. Biomed. Anal. 2005, 39, 581-585.
20. Badaloni, E., Cabri, W., Ciogli, A., Deias, R., Gasparrini, F., Giorgi, F., Vigevani, A., Villani, C., Anal. Chem. 2007, 79, 6013-6019.
21. Ragot, S., Marquet, P., Lachâtre, F., Rousseau, A., Lacassie, E., Gaulier, J. M., Dupuy, J. L., Lachâtre, G., J. Chromatogr. B. 1999, 736, 175-184.

22. Sridharan, V., Ribelles, P., Ramos, M. T., Menéndez, J. C., J. Org. Chem. 2009, 74, 5715–5718.
23. Bardin, S., Guo, W., Johnson, J. L., Khan, S., Ahmad, A., Duggan, J. X., Ayoub, J., Ahmad, I., J. Chromatogr. A. 2005, 1073, 249-255.
24. Food and Drug Administration. Guidance for Industry - Bioanalytical Method Validation. FDA, Rockville 2001.
25. International Conference on Harmonisation. ICH Topic Q 2 B. Validation of analytical procedures methodology. ICH, Rockville1996.
26. Thompson, M., Ellison, S. L. R., Wood, R., Pure Appl. Chem. 2002, 74, 835-855.
27. Zheng, W., Wang, S., Barnes, L. F., Guan, Y., Louis, E. D., Anal. Biochem. 2000, 279, 125-129.
28. Dey, J., Warner, I. M., J. Lumin. 1997, 71, 105-114.

This page intentionally left blank

12

A down-scaled fluorimetric determination of the solubility properties of drugs to minimize waste generation

Published in: González-Ruiz, V., Olives, A. I. & Martín, M. A. (2013). Green Chem., 15(9), 2558-2565.

ABSTRACT ► A miniaturized fluorescence assay on multi-well plates has been developed to study the solubility enhancement effect of (2-hydroxypropyl)-β-cyclodextrin on three anti-tumor alkaloids. The measurement of the fluorescence emission on a multi-well plate format has been proved to be a rapid and efficient technique to evaluate the solubility of pharmaceutical formulations of new drugs that help save time, reagents and wastes in the search for greener analytical strategies. The proposed methodology was compared with a reference HPLC solubility study and was employed to examine the enhancement of the solubility of camptothecin, luotonin A, and a synthetic derivative of the latter in the presence of (2-hydroxypropyl)-β-cyclodextrin. Considerable reductions in the time of analysis (almost 50 times faster) and the volume of organic solvents employed (close to 25 times less acetonitrile needed) were achieved. The nature of the inclusion complexes was investigated by analysis of the phase-solubility diagrams obtained by the newly developed method and was complemented with spectrofluorimetry and ESI-MS experiments. The concentrations of solubilised compounds found by both methodologies were in good agreement ($R^2 > 0.98$). The analytical figures of merit of both methodologies were compared and the adequacy of the proposed method for the development of drug solubilisation studies is discussed.

DOI ▼
10.1039/c3gc40974k

ABBREVIATIONS ▼
- **CD:** cyclodextrin
- **β-CD:** β-cyclodextrin
- **HPβ-CD:** (2-hydroxypropyl)-β-cyclodextrin
- **CPT:** camptothecin
- **HPLC-FL:** high performance liquid chromatography with fluorescence detection
- **HTS:** high-throughput screening
- **MS:** mass spectrometry
- **MALDI:** matrix-assisted laser desorption/Ionization
- **LOD:** limit of deteceion
- **LOQ:** limit of quantitation

1. Introduction

Greener analytical methodologies are in high demand due to the need for environmentally friendly techniques able to reduce the volume of reagents and wastes, thus minimizing their environmental impact [1]. In this context, considerable efforts have been focused on sample pre-treatment procedures [2], quantitative analysis by liquid chromatographic techniques [3], and capillary electrophoresis [4].

Miniaturization through down-scaled approaches employing high-throughput screening (HTS) assays affords important advantages *i.e.* low cost, small volumes of reaction, reduction in the reagents and analytes consumption and minimization of wastes. UV-Vis absorption and fluorescence spectrophotometry assays on multi-well plates are widely employed, among other uses, in the evaluation of the biological activity of drugs at pharmaceutical industries, or in hundreds of routine determinations in the areas of biochemistry and molecular biology [5].

Screening methodologies based on multi-well plates are employed in qualitative assays with satisfactory results, but they are not so often used for quantitative determinations in the field of Analytical Chemistry. More recently, quantitative applications with multi-well plate readers are becoming popular and successful for well established analytical methods such as chloride determination according to the classical Volhard determination [6], vitamin C in fruit and tomatoes by derivatization reaction of dehydroascorbate with orthophenylenediamine [7] or lipid analysis by the Van Handel method [8]. The multi-well plate reader format presents a good analytical efficiency together with a notable reduction in time of analysis as well as

in the volumes of the reagents and samples. Furthermore, its feasibility, high throughput and reduced cost make it attractive from a practical point of view, and thus HTS assays are being adapted for a variety of determinations including those of inorganic phosphate [9], arsenic in soil [10], chlorhexidine in oral preparations, [11] quinones in spiked human serum [12] or biogenic amines in foods [13]. Furthermore, from the analytical point of view, the parallelized measurement of samples and calibrators contributes to a robust recording of the analytical response.

Solubility tests of drugs are required during the development of new compounds of therapeutic interest, and they are routinely conducted at pharmaceutical companies. Cyclodextrins are natural products able to include poorly soluble drugs into their cavities, thus enhancing their solubility, absorption, release and bioavailability [14].

Topoisomerase 1 is the molecular target for camptothecin, the lead structure of a class of anticancer drugs widely employed in the treatment of several types of cancer [15]. Therapeutic uses of natural camptothecin are limited principally by its low hydrosolubility and its chemical instability due to the opening of the lactone ring at physiological pH. The formation of the inclusion complexes camptothecin-CDs has led to an important increase of its hydrosolubility [16] and chemical stability [17]. Luotonin A shares with camptothecin the mechanism of action, behaving as a selective inhibitor of topoisomerase 1 [18]. It also has advantages over its parent drug in terms of chemical stability and having fewer side-effects. Nevertheless, the poor hydrosolubility of luotonin A precludes its promising pharmacological activity. For this reason, the study of the effect of solubility enhancers on its pharmaceutical properties becomes a keystone not only for carrying out biological activity assays, but also aiming at its future clinical development.

Considering that solubility studies are routine assays not only for drugs, but also for pesticides, cosmetics, dietary complements and other compounds with industrial uses, in the present work we propose a downscaled fluorimentric assay as a model environmentally friendly methodology for the evaluation of the solubility enhancement of the topoisomerase inhibitors camptothecin, luotonin A and 14-(3,5-dimethyl-phenyl)-3-methylquinolino[2',3':3,4]pyrrolo[2,1-*b*]quinazolin-11-(13*H*)-one (compounds CPT, **1** and **7**, Figure 1). The multi-well plates format makes it possible to prepare the drug-CD complexes on a reduced scale (10 times lower than traditional solubilisation studies) and to conduct the solubility tests in a small volume of solvent. The high-throughput nature of the technique allows one to simultaneously process a large number of samples. The determinations were carried out in a short time span and the samples were measured automatically through a fiber optical device connecting the automated multi-well plate reader to a conventional spectrofluorometer. This methodology required very small amounts of the tested compounds and notably reduced the use of organic solvents employed as mobile phases in HPLC quantitation of the solubilised drug.

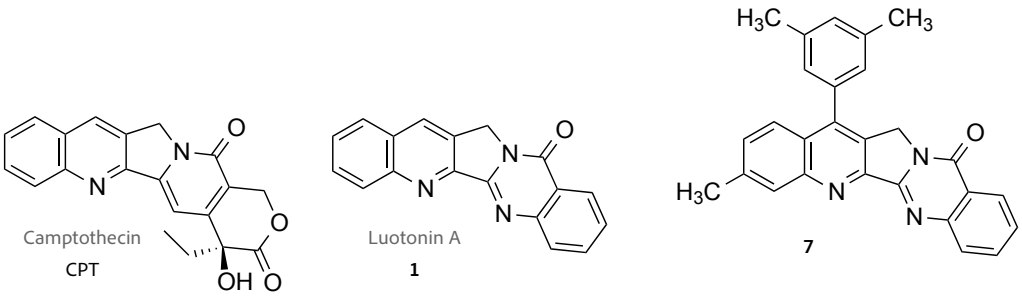

Figure 1.
Chemical structures of the compounds studied.

2. Experimental

2.1. Apparatus and reagents

Fluorescence measurements at fixed wavelength were obtained using a MicroMax 384 multi-well plate reader coupled to a FluoroMax-4P spectrofluorometer (both from Horiba-Jobin Yvon, Edison, NJ, USA) equipped with the control and data acquisition software FluorEssence 3.5. 96-well black plates (BD Falcon, Franklin Lakes, NJ, USA) were employed in the downscaled analysis. Corrected excitation and emission spectra and measurements at fixed wavelengths were obtained on the FluoroMax-4P using 1 cm path length quartz cells.

The liquid chromatographic system (Merck-Hitachi, Tokyo, Japan) consisted of a quaternary gradient pump L-7100 and a fluorescence detector L-7485. The temperature of the column was controlled with a L-2300 oven and the samples were injected through a Rheodyne 7725i injector (20 µL loop). The chromatographic system was under computer control through the HPLC System Manager software, version 4.1. The analytical C-18 columns (Luna, C18(2), 5 µm, 150 × 3.00 mm) was purchased from Phenomenex (Torrance, CA, USA).

Mass spectrometry experiments were performed using a TripleTOF 5600 system by AB Sciex (Framingham, MA, USA) with ESI/APCI ionization source and a hybrid triple quadrupole-time of flying analyser. System control and data acquisition were done from a PC running Analyst software. Spectra processing and analysis was performed using the free mMass software [19].

A Stuart Rotator SB3 rotatory shaker and an Elmasonic S15 ultrasonic bath were employed for the preparation of the inclusion complexes. Commercially available camptothecin, luotonin A and 1.0 molar substitution (2-hydroxypropyl)-β-cyclodextrin (HPβ-CD) were purchased from Sigma-Aldrich (Steinheim, Germany). Compound **7** was synthesized using modified Friedländer conditions as described elsewhere [20]. All reagents and solvents were chromatographic grade and were used without further purification. Ultrapure water was obtained from a Milli-Q Direct 8 system (Millipore, Molsheim, France).

2.2. Procedures

2.2.1. Study of the effect of complex formation on the fluorescence spectra of the alkaloids

To study the fluorescence properties of the solubilised drugs in the presence of HPβ-CD, conventional fluorescence spectrometry experiments were carried out in quartz cuvettes. The concentrations of the anti-tumor agents were fixed at 5.0×10^{-7} M, and the HPβ-CD concentration was 1.0×10^{-2} M. The solutions were kept under magnetic stirring at room temperature for 48 h. Then, the fluorescence emission spectra of the complexes was recorded and compared to those of free-drug aqueous solutions.

2.2.2. Solubility enhancement determination

To obtain the phase solubility diagrams, an excess of a single solid alkaloid (approx. 0.3 mg mL^{-1}) was added to a small volume (1.0 mL) of each of the six different solutions of HPβ-CD (0, 5, 10, 15, 20 and 25% w/v). The suspensions were kept under ultrasound stirring for 30 minutes and then placed on a rotatory shaker at room temperature for 7 days. After this period, the suspensions were filtered (0.45 µm pore size, regenerated cellulose membrane, Phenomenex, Torrance, CA, USA) to separate the soluble complexes containing the alkaloid from the solid drug. Aliquots of the filtrates were diluted using 50% aqueous acetonitrile, and the amount of solubilised

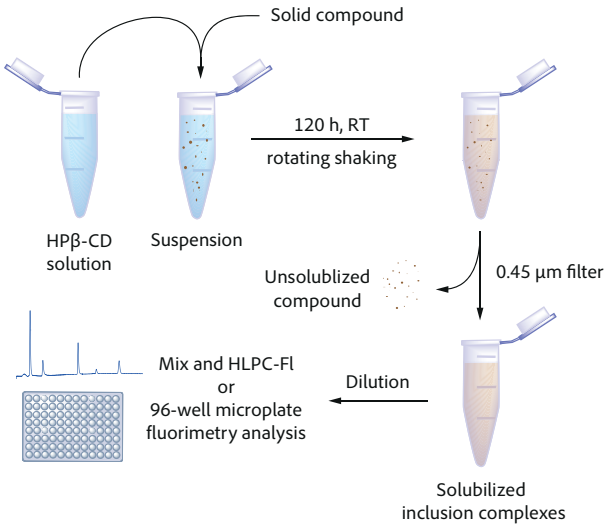

Scheme 1. Protocol followed for the development of the solubility assays

compound was quantified by both of the compared methodologies (Scheme 1). All of the measurements were carried out at least in triplicate sets. The solubility phase diagrams were plotted according to Brewster [14b,21] and taking into account the Equations 1a-c and 2.

$$S_t = S_0 + K_{1:1}S_0[CD] \quad \textbf{Eq. 1a}$$

$$S_t = S_0 + K_{1:1}S_0[CD] + K_{1:1}K_{1:2}S_0[CD]^2 \quad \textbf{Eq. 1b}$$

$$S_t = S_0 + K_{1:1}S_0[CD] + K_{1:1}K_{1:2}S_0[CD]^2 + K_{1:1}K_{1:2}K_{1:3}S_0[CD]^3 \quad \textbf{Eq. 1c}$$

$$K_{ass} = K_{1:1} \cdot K_{1:2} \cdot K_{1:3} \quad \textbf{Eq. 2}$$

2.2.3. Downscaled fluorescence quantitation of the solubilised anti-tumor agents

200 µL aliquots of the diluted filtrates were placed on the multi-well plate for fluorescence measurement. Every plate contained triplicate sets of the diluted samples as well as triplicate calibration curves. The concentration of the solubilised drugs was deduced by interpolation in the calibration curves. LOD was calculated as the concentration interpolated from the signal value corresponding to the ordinate in the origin of the calibration curve plus three times its standard deviation.

2.2.4. HPLC-fluorescence quantitation

As HPLC allowed the separation of the three compounds under study, samples coming from different compounds with the same level of cyclodextrins were combined prior to their dilution and chromatography analysis. The mixtures were separated on a C-18 analytical column under modified gradient elution conditions [22] (40 to 65% acetonitrile in water in 10.5 mins, 25 °C, flow rate 0.5 mL min^{-1}). Detector was set at $\lambda_{ex}/\lambda_{em}$=340/420 nm. The concentrations were deduced from the areas under the peaks and using calibration curves constructed from standard solutions. LOD was calculated as described in the previous section.

2.2.5. ESI-MS characterization of the complexes

Electrospray-mass spectrometry spectra were obtained from the filtrated liquors of the complexes prepared with the 25% w/v of HPβ-CD and diluted with water. The system was operated in positive ionization mode under mild conditions: vaporization temperature of 450 °C, capillary voltage of 5500 V and declustering potential of

50 V. A constant flow of 10 mM aqueous ammonium formiate:MeCN 90:10 v:v was employed as carrier at 0.2 mL min^{-1} to introduce the samples into the spectrometer.

3. Results and discussion

Conventional solubility studies require an appreciable volume of solvents (10.0-25.0 mL) for quantitative determinations [23]. Although spectrophotometric methods (UV-Vis absorption or fluorescence) require higher volumes of a solvent reaction mixture than chromatographic methods (HPLC), additional organic solvents are employed in the mobile phases needed for the chromatographic determinations. The multi-well plate determination avoids the need for either larger volumes of reaction or running mobile phases.

3.1. Effect of the HPβ-CD on the fluorescence spectra of the studied alkaloids

The spectral shape and fluorescence emission maxima obtained in the presence and absence of HPβ-CD are shown in Figure 2. As can be appreciated, there are no significant shifts in the emission maxima with regard to those described for these compounds in aqueous solutions [24]. Therefore, the following excitation and emission maxima were employed for the quantitation and determination of the solubilities in the multi-well plates: CPT $\lambda_{ex}/\lambda_{em}$ = 369/428 nm, **1** $\lambda_{ex}/\lambda_{em}$ = 341/416 nm and **7** $\lambda_{ex}/\lambda_{em}$ = 348/404 nm. The change in the fluorescence emission intensity confirmed the formation of the complexes in all of the three compounds.

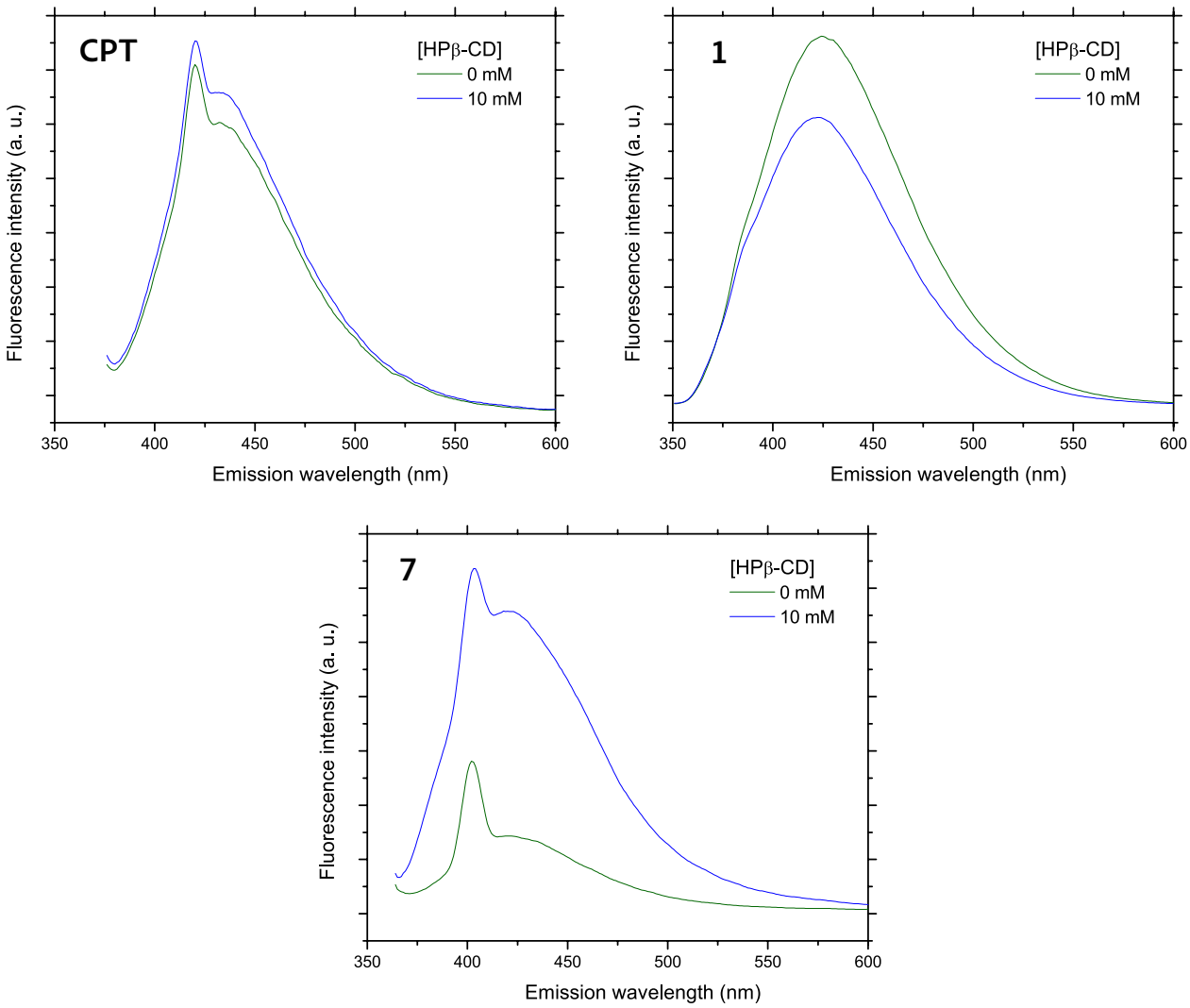

Figure 2.
Fluorescence emission spectra of the alkaloids studied (5×10^{-7} M in water) in the absence and in the presence of HPβ-CD 10 mM.

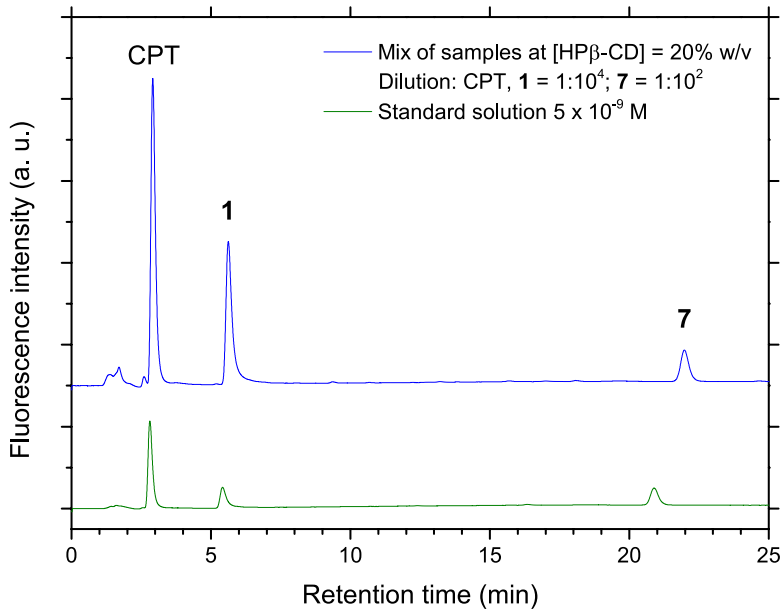

Figure 3. Overlayed chromatograms corresponding to a mix of compounds solubilized in the presence of HPβ-CD (top) and a calibration solution of the alkaloids (bottom). The cyclodextrin inclusion complexes were prepared individually (as described in the Experimental Section) and simultaneously chromatographed.

3.2. HPLC quantitation of the solubilised fraction of the studied compounds

Figure 3 shows the chromatograms obtained from the HPLC analysis of one of the calibration solutions and from the analysis of the mixture of filtrates. The method allowed the separation and simultaneous quantitation of the three compounds under study, with a high concordance in the retention time between the standard solutions and the samples. This methodology yielded very good sensitivity (LODs ranged from 0.32 to 0.64 nM) and reproducibility (between 1.6 and 2.7% RSD, Table 1). The linearity of the response was checked for concentrations ranging from 1×10^{-10} to 1×10^{-7} M, obtaining a correlation $R^2 > 0.99$. On closer inspection, this method revealed three main drawbacks: a) the analysis was quite slow (22 minutes for three combined samples); b) it required a considerable amount of organic solvent (7.0 mL of acetonitrile as the organic component of the mobile phase) and c) the samples required a high degree of dilution prior to its analysis, thus consuming additional time and organic solvents and increasing the risk of inaccuracy due to the dilution process.

3.3. Miniaturized fluorescence assay using multi-well plates

The miniaturized fluorescence measurement on multi-well plates was found to afford a more modest analytical outcome (Table 1), with LODs comprised in the 1×10^{-7} M order, a precision ranging from 6.3 to 16.7% RSD and a linear response checked in the span between 3×10^{-7} to 6×10^{-6} M, with $R^2 > 0.98$. From the practical and environmental points of view, this technique was found to provide an excellent performance in terms of time (90 seconds per three samples analysed in triplicate) and organic solvent consumption (100 µL of acetonitrile per well). Furthermore, the samples required less dilution prior to the analysis, what also contributes to decreasing the organic solvent volume employed and decreases the amount of generated wastes.

Table 1. Limits of detection deduced from the calibration curves for the downscaled spectrofluorimetry (multi-well plate) determination of the anti-tumour agents studied.

Compound	LOD (multi-well plate)	LOD (HPLC)
CPT	2.1×10^{-7} M	3.2×10^{-10} M
1	2.7×10^{-7} M	6.4×10^{-10} M
7	2.0×10^{-7}M	6.3×10^{-10} M

Several reasons account for the lower sensitivity and accuracy achieved with the multi-well plate reading arrangement compared to the reference HPLC method. One reason is the much more complex optic path (including mirrors and optical fibers) that the light must follow in the automated plate reader compared to the neat path through the HPLC detector flow cell. Also, the bigger dispersion happening on the bottom and the walls of the wells in the miniaturized assay contributes to this loss in sensitivity and accuracy with increasing the background signal. Nevertheless, LODs obtained with the multi-well plate method adequately fit the demands of the solubility assays, taking into account that, as mentioned, the samples need less dilution for the newly proposed methodology than for the reference chromatography method.

3.4. Comparison of the reference HPLC method and the proposed downscaled multi-well method

The capability of the proposed downscaled fluorescence assay was evaluated by a comparison to the reference HPLC method by following the well-established procedure [25] of plotting the concentrations of solubilised alkaloids determined by the down-scaled fluorescence method *vs.* those determined by HPLC. These plots demonstrated notably good agreement between both analytical methodologies, showing satisfactory linear correlation (CPT, $R^2 > 0.98$; **1**, $R^2 > 0.97$, and **7**, $R^2 > 0.99$) as can be appreciated in Figure 4.

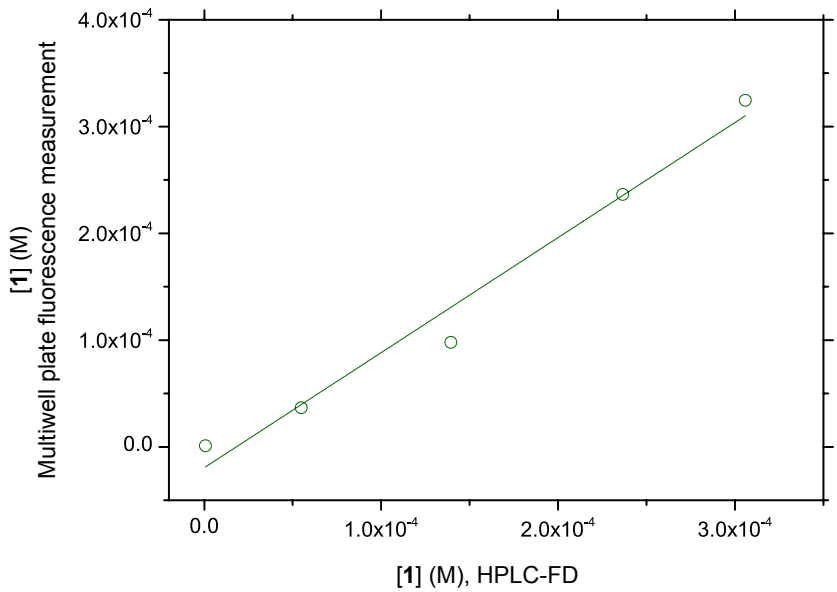

Figure 4.
Correlation between the concentrations of solubilized luotonin A obtained by using the two different assayed methodologies.

3.5. Application of the developed methodology to study the effect of HPβ-CD on the solubility of the compounds

The concentrations of the solubilised alkaloids were determined by HPLC-FL and the down-scaled fluorescence assay at different HPβ-CD concentrations, and these data were used to obtain the phase-solubility diagrams. Similar phase-solubility plots were deduced from the chromatographic and multi-well plate fluorimetric determination (Figure 5). In these figures, two different behaviours can be observed: camptothecin and luotonin A exhibited a linear relationship when the solubilised alkaloid concentration was plotted *versus* the HPβ-CD concentrations, while in the case of **7** a curved line diagram was obtained.

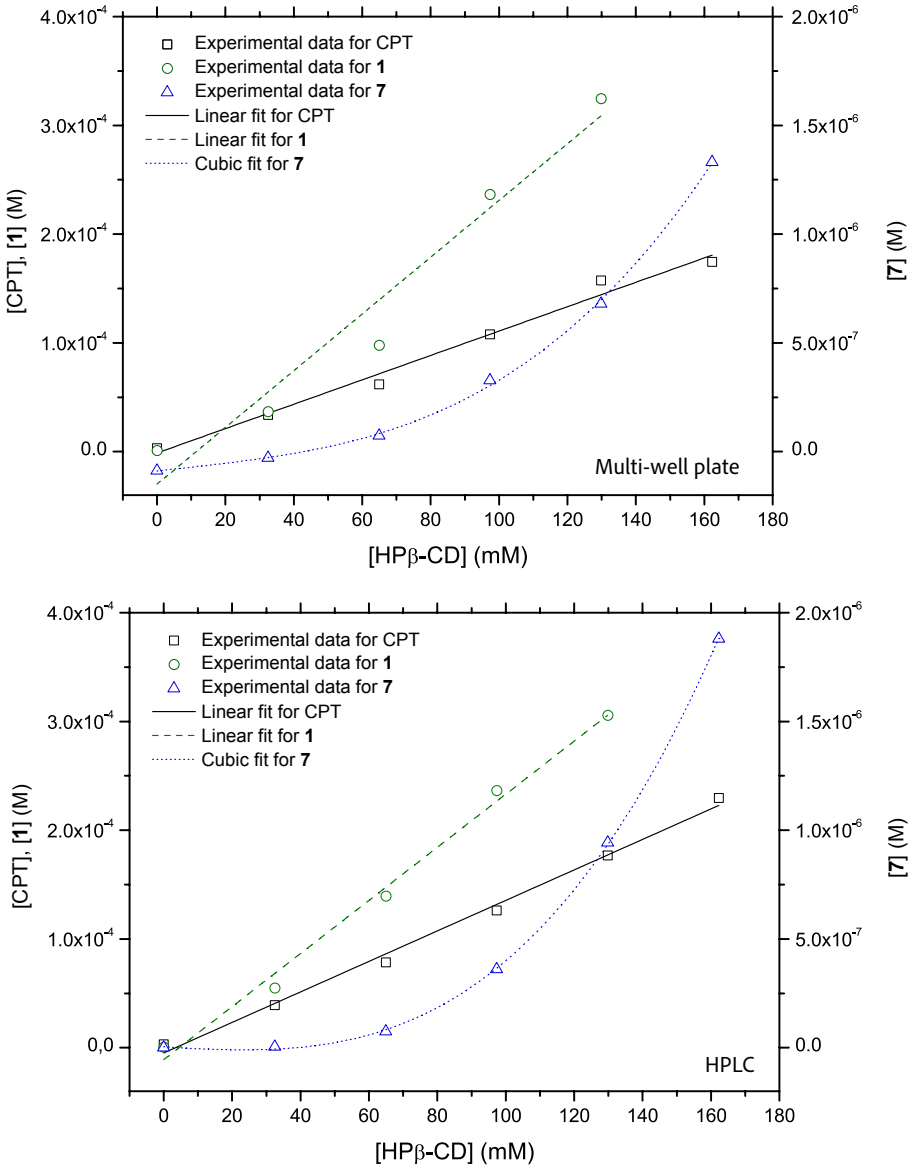

Figure 5. Phase solubility diagrams obtained for the alkaloids under study in the presence of increasing amounts of HPβ-CD by multi-well plate fluorescence measurements (top) and HPLC (bottom).

Typical phase-solubility diagrams corresponding to an A-type profile (A_L or A_P) [14b,21], could be either linearly increased with the CD concentration (A_L type) or positively deviated from the linearity (A_P profile). Camptothecin and luotonin A showed an A_L behaviour, but in the case of the more hydrophobic and more substituted compound **7**, an A_P behaviour was obtained.

The best-fit to a linear plot indicated the presence of complexes with a 1:1 drug:CD stoichiometry in the case of camptothecin and luotonin A. The found slopes, lower than one, confirmed that only one drug molecule is associated with a host CD molecule. These results are in agreement with the solubilisation behaviour described for camptothecin in the presence of HPβ-CD [17]. However, **7** showed a positive deviation from linearity in the solubility diagrams, suggesting the existence of complexes with two or more molecules of CD associated with one molecule of **7**. The best fit of the experimental values to a cubic equation indicates the existence of complexes involving a 1:3 **7**:CD stoichiometry.

The alkaloid/HPβ-CD apparent association constants K_{ass} can be deduced from the phase solubility diagrams [14b,21,26] which were plotted after the experimental de-

Table 2. Values of the association constants (K_{ass}) obtained for the alkaloid/HPβ-CD complexes using the two methodologies compared.

Compound	log K_{ass} (HPLC)	log K_{ass} (multi-well plate)
CPT	2.64	2.54
1	3.55	3.58

termination of the amount of solubilised compound at every HPβ-CD concentration by HPLC and by the fluorescence measurement onto the multi-well plates (Table 2).

In the case of **7**, the fit of the cubic equation yielded a negative second order coefficient and, thus, the calculation of its K_{ass} value was hindered. Good agreement between solubility phase diagrams obtained by HPLC-FL and the fluorescence assay on multi-well plate was obtained, as well as in the association constant values (K_{ass}) or stoichiometry deduced from these equations that define the chemical behaviour of the compounds showing that the enhancement in the aqueous solubility of these alkaloids is higher for the more lipophilic alkaloids (**7**). Furthermore, the presence of a phenyl group on the quinoline moiety of **7** favours the association of more than one molecule of HPβ-CD, coexisting complexes with different stoichiometric ratios. Therefore, the ability to form inclusion complexes has been shown to be closely related to the lipophillicity and spatial disposition of the substituents on the luotonin A backbone. The solubility increase in the presence of HPβ-CD proceeds according to the series: **7** > luotonin A > camptothecin.

3.6. Study of the solubilised anti-tumor agents by using electrospay ionization-mass spectrometry (ESI-MS)

One of the outstanding characteristics of MS is its usefulness as a confirmatory analytical technique. In the case of the solubilisation assays involving HPβ-CD, the mass spectra make it possible to evidence not only the solubilised fraction of free alkaloid but also the different complexes of solubilised drug present in the filtrated liquors. Taking into account that the solubility phase diagrams showed different behaviours for the compounds and suggested various drug:HPβ-CD stoichiometric ratios, we decided to confirm these results. In the context of our goal to save reagents and avoid wastes generation, mass spectrometry analysis (MS) becomes a convenient method for the confirmatory analysis of stoichiometry as an alternative to the traditional continuous variation method (Jobs plots).

Among the different modes of ionization employed in the analysis of inclusion complexes using mass spectrometry, ESI is preferred as a soft ionization technique adequate to evaluate species in which non-covalent interactions are present [27]. Moreover, in ESI the analytes are instantaneously transferred from the solution to the vacuum, allowing an excellent correspondence between the species present in the sample and those that are able to reach intact the detector, provided they are kinetically stable under the conditions of the experiment. Nevertheless, non-specific adducts can be formed as a consequence of the electrostatic interactions among the charged surface droplets [28]. Besides, MS allows the simultaneous detection of complexes with different association grades of host and guest molecules and, due to the intrinsic sensitivity of the technique, the detection of the inclusion complexes is possible even if the host:guest molar ratio is higher than 1000 [29].

Firstly, we explored several different ionisation conditions. We found that MALDI ionisation did not allow us to detect the peaks corresponding to the drug:CD complexes under our experimental conditions (data not shown). When using ESI, higher

cone voltages (90 V) lead us to the same dead end. We found that cone voltages as low as 50 V were needed in order to prevent the dissociation of the non-covalent complexes, allowing for their detection. As cone potential is a critical parameter for the detection of the complexes, potentials down to 10 V have been previously reported in the literature to avoid dissociation when ESI ionization is employed [30]. The existence of the stable complexes of the compound 14-aza-camptothecin with α-, β-, and γ-CD in gas-phase has been recently described employing ESI-MS, but the experiment was performed under MALDI ionization, which led not only to the dissociation of the complexes, but also to the fragmentation of the parent molecules [31].

MS experiments were carried out with the complexes formed using the highest HPβ-CD concentration (25% w/v). That cyclodextrin concentration was 1000 to 50000 times higher than the final solubilized amount of compound, causing the signals of the complexes to be very weak compared to those of the free cyclodextrins [29,32]. Therefore, the most abundant peaks can be observed at *m/z* distributions in the range from 1540 to 1590 Da, which corresponds to the free HPβ-CD molecules (Figure 6). Such peaks appear at 1541.67 (HPβ-CD + H^+), 1558.69 (HPβ-CD + NH_4^+), 1563.65 (HPβ-CD + Na^+) and 1579.62 (HPβ-CD + K^+). The group of signals appearing in the region ranging from 770 to 830 Da corresponds to the free molecules of HPβ-CD associated with two cations, normally 2 H^+ (771.33), 2 Na^+ (793.31) and 2 NH_4^+ (788.36). In the case of camptothecin, the signals appearing 1889.78 and 1924.82 Da confirm that the complexes of camptothecin with HPβ-CD + H^+ and camptothecin with HPβ-CD + NH_4^+ are present as well the complexes with camptothecin:HPβ-CD 1:1 stoichiometry but possessing two charges (H^+ and NH_4^+) at *m/z* 953.91. The relative abundance and the peak distribution in the mass spectra are in agreement with the results reported using ESI-MS to study the complexes of β-CD with camptothecin and homocamp-

Figure 6.
(Continues on opposite page)
Mass spectra of the inclusion complexes with HPβ-CD. The HPβ-CD concentration was 25% w/v.

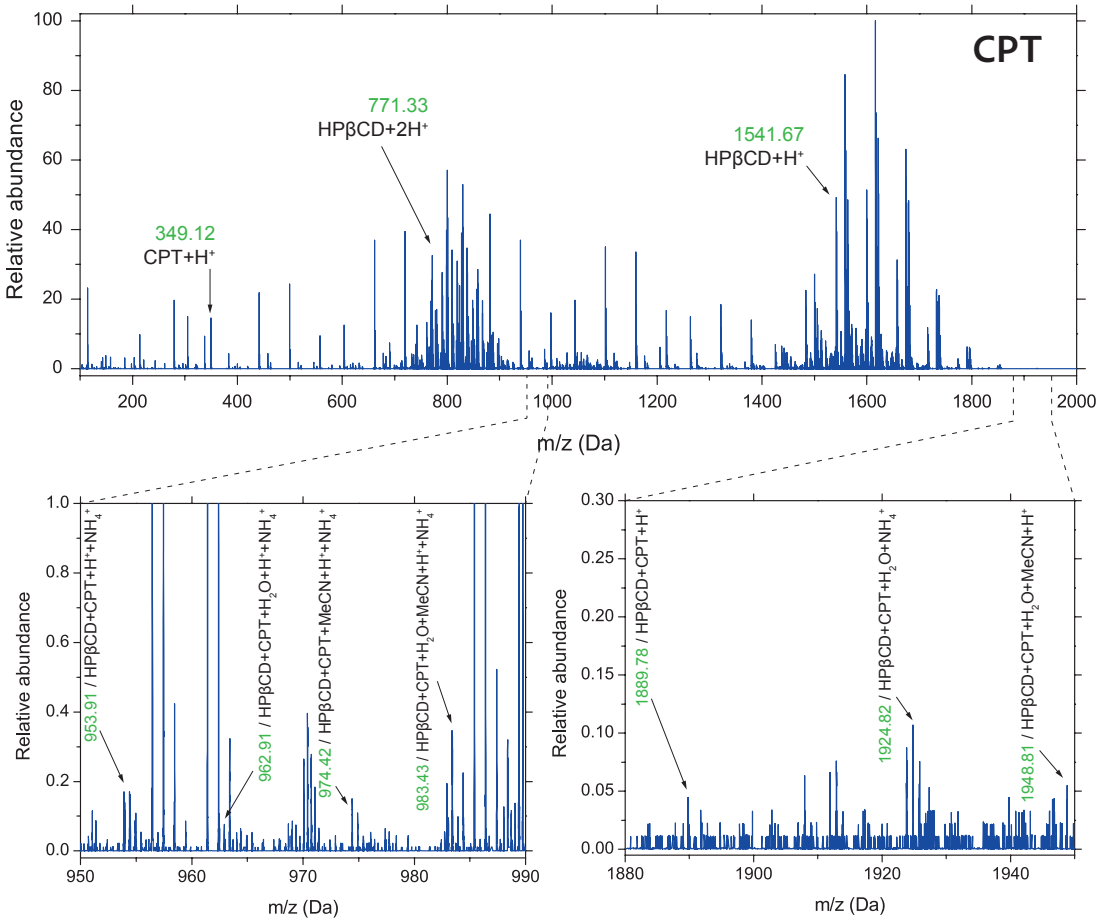

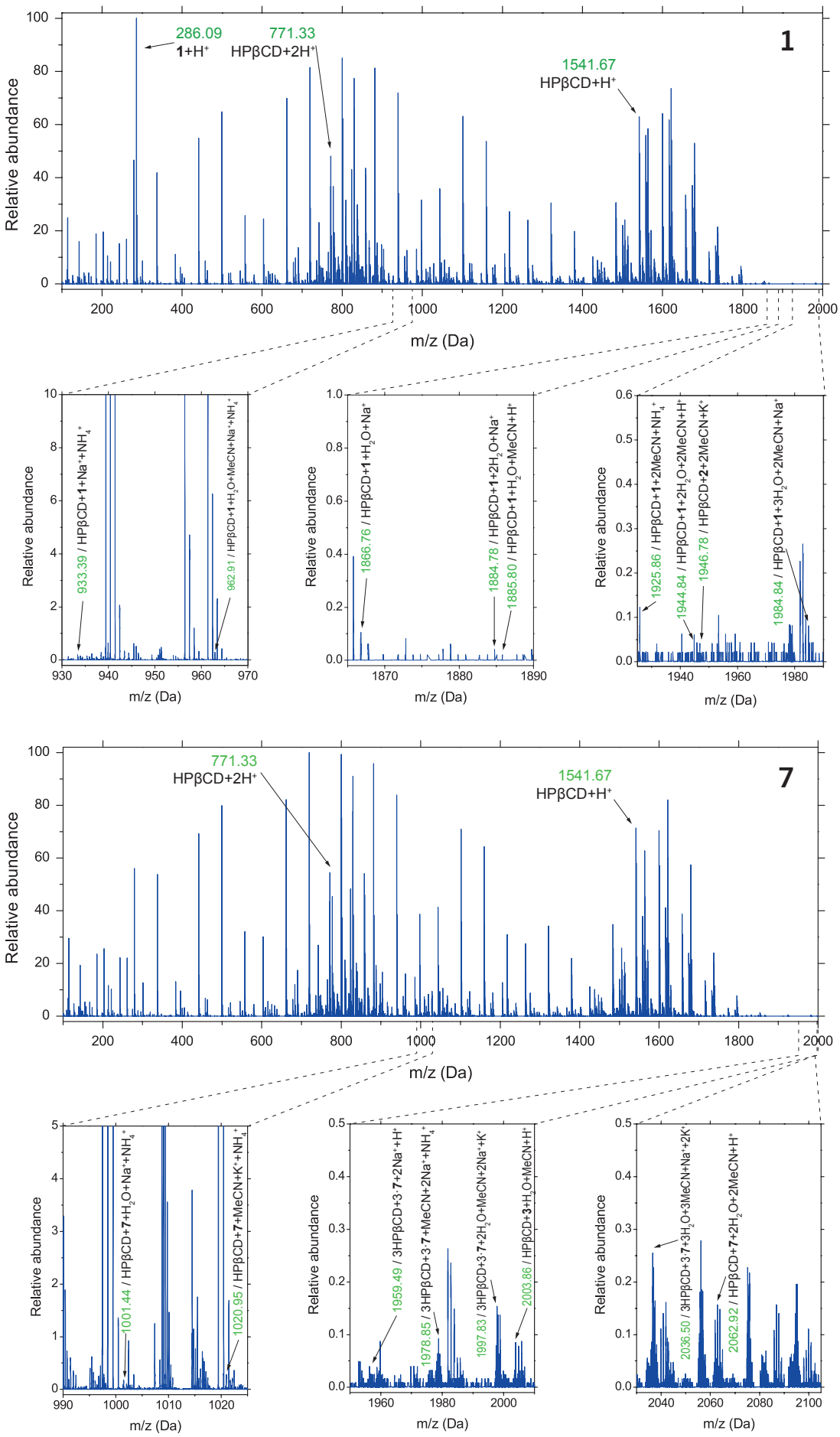

Figure 6.
(Comes from previous page)

Table 3. Comparison of the features of the proposed down-scaled fluorimetric assay and the reference HPLC methodology.

	Multi-well plate	HPLC
Solvent for solubility assays	Water: 1.0 mL	Water: 1.0 mL
Volume of solvents required for quantitative determinations*	Water: 300 µL MeCN: 300 µL	Water: 4.5 mL MeCN: 6.5 mL
Wastes produced*	MeCN: 300 µL	7.0 mL of MeCN per run including column stabilization
Time of analysis	30 seconds	22 min

** For the determination of the three studied compounds, simultaneously chromatographied or fluorimetrically determined*

tothecin derivatives [32]. Similarly, in the case of the solubilised luotonin A into the cyclodextrin cavities, the signals with *m/z* values from 1867.69 to 1946.78 Da correspond to the luotonin A/HPβ-CD complexes with different charged species (H^+, Na^+, K^+ and NH_4^+) incorporating one or more neutral molecules of the solvent (H_2O and acetonitrile). Besides, the presence of complexes with a 1:1 luotonin A:HPβ-CD stoichiometry, was confirmed by the peaks appearing at 933.39 and 962.91 Da that corresponds to the complexes associated to two charged species (Na^+ and NH_4^+). However, in the case of **7**, a unique complex with a 1:1 stoichiometry was found with H^+ as charged species and two neutral molecules (H_2O and acetonitrile) at *m/z* 2003.88. The signals in the region of 1959.49 to 1998.85 can be ascribed to the entities of 3 molecules of HPβ-CD with 3 molecules of compound **7** with 3 charged species (H^+, Na^+, K^+ and NH_4^+) and also including neutral molecules. These aggregates cannot be assigned to a **7**:HPβ-CD 1:3 stoichiometry, but these associations are only present in the case of **7**. The formation of these entities during the ionization onto the electrospray source cannot be discarded. Nevertheless, the practically absence of 1:1 stoichiometry complexes together with the 3:3 associations allows to establish a satisfactory concordance between the results obtained in the solubility-phase diagrams and those deduced from the analysis of the mass spectra

4. Conclusions

The downscaled fluorimetric assay has proven to be a rapid, efficient, inexpensive, and environmentally friendly methodology for the determination of the solubility of drugs and can be applied for the solubilisation studies of many other compounds. The evaluation of the solubility enhancement has been compared to a HPLC reference method, obtaining very satisfactory agreement in the different parameters determined for both methodologies.

Table 3 reveals the green analytical features of the down-scaled fluorimetric assay. This assay requires only 300 µL of an organic solvent for the quantitation of the three compounds studied, instead of the 7.0 mL of acetonitrile required by the HPLC-FL analysis.

Besides the savings in organic solvents and waste, an important saving of energy was observed as three samples can be analysed in 30 seconds in comparison with the 22 minutes required for the analysis of the three compounds by HPLC. Furthermore, although the sensitivity of the down-scaled fluorimetric assay is lower than that of the HPLC or conventional fluorescence determinations, it perfectly fits the demands of the solubilisation studies, where the concentration of the analyte does not seem to

be a critical limitation of the assays. Its ability to process a high number of samples in an automated fashion makes this technique meet the requirements for the routine, high-throughput analysis in the pharmaceutical development of new drugs that help save reagents and time of analysis. Therefore, down-scaled fluorescence analysis is proposed as an environmentally friendly analytical alternative methodology to conventional solubilisation studies.

5. Acknowledgements

The authors are grateful to MICINN, Spain and Universidad Complutense for financial support through grants CTQ2009-11312/BQU and GR35/10-A-920234. The authors are also grateful to MEC for the award of a FPU research fellowship to V. González-Ruiz.

6. References

1. S. Armenta, S. Garrigues, M. de la Guardia, Trends Anal. Chem., 2008, 27, 497-511.
2. (a) M. Tobiszewski, A. Mechlinska, B. Zygmunt, J. Namiesnik, Trends Anal. Chem., 2009, 28, 943-951. (b) C. Mahugo-Santana, Z. Sosa-Ferrera, M. E. Torres-Padrón, J. J. Santana-Rodríguez, Trends Anal. Chem., 2011, 30, 731-748.
3. (a) C. J. Welch, N. Wu, M. Biba, R. Hartman, T. Brkovic, X. Gong, R. Helmy, W. Schafer, J. Cuff, Z. Pirzada, L. Zhou, Trends Anal. Chem., 2010, 29, 667-680. (b) R. Hartman, R. Helmy, M. Al-Sayah, C. J. Welch, Green Chem., 2011, 13, 934-939. (c) V. González-Ruiz, A. G. León, A. I. Olives, M. A. Martín, J. C. Menéndez, Green Chem., 2011, 13, 115-126. (d) D. G. Drueckhammer, S. Q. Gao, X. Liang, J. Liao, ACS Sustainable Chem. Eng., 2013, 1, 87-90.
4. H.-Y. Xie, Y.-Z. He, Trends Anal. Chem., 2010, 29, 629-635.
5. (a) A. G. Gehring, D. M. Albin, S. A. Reed, S.-I. Tu, J. D, Brewster, Anal. Bioanal. Chem., 2008, 391, 497-506. (b) V. Hoerr, W. Ziebuhr, S. Kozitskaya, E. Katzowitsch, U. Holzgrabe, Anal. Chem., 2007, 79, 7510-7518. (c) R. A. Pufahl, T. P. Kasten, R. Hills, J. K. Gierse, B. A. Reitz, R. A. Weinberg, J. L. Masferrer, Anal. Biochem., 2007, 364, 204-212.
6. T. Rojanarata, K. Sumran, P. Nateetaweewat, W. Winotapun, S. Sukpisit, P. Opanasopit, T. Ngawhirunpat, Talanta, 2011, 85, 1324-1329.
7. R. Stevens, M. Buret, C. Garchery, Y. Carretero, M. Causse, J. Agric. Food Chem., 2006, 54, 6159-6165.
8. L. S. Inouye, G. R. Lotufo, Talanta, 2006, 70, 584-587.
9. P. Zuck, G. T. O'Donnell, J. Cassaday, P. Chase, P. Hodder, B. Strulovici, M. Ferrer, Anal. Biochem., 2005, 342, 254-259.
10. K. C. Makris, P. Punamiya, D. Sarkar, R. Datta, Analyst, 2008, 133, 191-196.
11. T. Attin, T. Abouassi, K. Becker, A. Wiegand, M. Roos, R. Attin, Clin. Oral Investig., 2008, 12, 189-196.
12. M. S. Elgawish, C. Shimomai, N. Kishikawa, K. Ohyama, K. Nakashima, N. Kuroda, Analyst, 2012, 137, 4802-4808.
13. H. A. Azab, S. A. El-Korashy, Z. M. Anwar, G. M. Khairy, M.-S. Steinerb, A. Duerkop, Analyst, 2011, 136, 4492-4499.
14. (a) K. Uekama, F. Hirayama, H. Arima, Pharmaceutical Applications of Cyclodextrins and their Derivatives in Cyclodextrins and their Complexes. Chemistry, Analytical Methods and Applications, ed. H. Dodziuk, Wiley-VCH, Weinheimm, 2006. (b) M. E. Brewster, T. Loftsson, Adv. Drug Delivery Rev., 2007, 59, 645-666. (c) A. Vyas, S. Saraf, S. Saraf, J. Inclusion Phenom. Macrocyclic Chem., 2008, 62, 23-42.
15. (a) C. Avendaño, J. C. Menéndez, Medicinal Chemistry of Anticancer Drugs, Elsevier, Amsterdam, 2008. (b) Y. Pommier, DNA Topoisomerases and Cancer in B. A. Teicher (Series Ed.) Cancer Drug Discovery and Development, Springer, New York, 2012.
16. J. Kang, V. Kumar, D. Yang, P. R. Chowdhury, R. J. Hold, Eur. J. Pharm. Sci., 2002, 15, 163-170.
17. A. M. Sætern, N. B. Nguyen, A. Bauer-Brandl, M. Brandl, Int J Pharm., 2004, 284, 61-68.
18. (a) A. Cagir, S. H. Jones, R. Gao, B. M. Eisenhauer, S. M. Hecht, J. Am. Chem. Soc., 2003, 125, 13628-13629. (b) A. Cagir, S. H. Jones, B. M. Eisenhauer, R. Gao, S. M. Hecht, Bioorg Med Chem Lett., 2004, 14, 2051-2054. (c) A. Cagir, B. M. Eisenhauer, R. Gao, S. J. Thomas, S. M. Hecht, Bioorg Med. Chem., 2004, 12, 6287-6299.
19. M. Strohalm, D. Kavan, P. Novák, M. Volný, V. Havlíček, mMass 3: A Cross-Platform Software Environment for Precise Analysis of Mass Spectrometric Data. Anal. Chem., 2010, 11, 4648-4651.
20. V. Sridharan, P. Ribelles, M. T. Ramos, J. C. Menéndez, J. Org. Chem., 2009, 74, 5715-5718.
21. T. Loftsson, D. Hreinsdottir, M. Masson Int J Pharm., 2005, 302, 18-28.
22. V. González-Ruiz, P. Mussardo, E. Corda, S. Girotti, A. I. Olives, M. A. Martín, J. Sep. Sci., 2010, 33, 2086-2093.

23. (a) H. Maeda, Y. Ogawa, H. Nakayama J. Inclusion Phenom. Macrocyclic Chem., 2013, DOI 10.1007/s10847-013-0290-5. (b) C. Shen, X. Yang, Y. Wang, J. Zhou, C. Chen, J. Inclusion Phenom. Macrocyclic Chem., 2012, 72, 263-274. (c) X. Zhu, W. Tan, F. Zhou, Z. Li, L. Duan, J. Inclusion Phenom. Macrocyclic Chem., 2012, 73, 193-198.
24. V. González-Ruiz, Y. González-Cuevas, S. Arunachalam, M. A. Martín, A. I. Olives, P. Ribelles, M. T. Ramos, J. C. Menéndez, J. Lumin., 2012, 132, 2468-2475.
25. G. S. Cembrowsky, A. M. Sullivan, Quality Control and Statistics, in Clinical Chemistry, eds. M. L. Bishop, J. L. Duben-Engelkirk, E. P. Fody, J. B. Lippincott Company, Philadelphia, 1992.
26. K. A. Connors, Binding constants: the measurement of molecular complex stability, Wiley-Interscience, New York, 1987.
27. (a) W. Danikiewicz, Mass Spectrometry of Cyclodextrins and their Complexes, in Cyclodextrins and their Complexes. Chemistry, Analytical Methods and Applications, ed. H. Dodziuk, Wiley-VCH, Weinheimm, 2006; (b) D. P. Weimann, M. Kogej, C. A. Schalley Mass Spectrometry and Gas Phase Chemistry of Supramolecules, in C. A. Schalley (Ed.) Analytical Methods in Supramolecular Chemistry, vol. 1, Wiley-VCH, Weinheim, 2012.
28. V. Gabelica, N. Galic E. De Pauw, J. Am. Soc. Mass Spectrom., 2002, 13, 946 – 953.
29. R. Kobetic, B. S. Jursic, S. Bonnette, J. S.-C. Tsai, S. J. Salvatore Tetrahedron Lett., 2001, 42, 6077-6082.
30. (a) L. Caron, S. Tilloy, E. Monflier, J.-M. Wieruszeski, G. Lippens, D. Landy, S. Fourmentin, G. Surpateanu, J. Inclusion Phenom. Macrocyclic Chem., 2000, 38, 361 - 379. (b) Y. Dotsikas, Y. L. Loukas, J. Am. Soc. Mass Spectrom., 2003, 14, 1123–1129. (c) B. D. Wagner, N. Stojanovic, G. Leclair, C. K. Jankowski, J. Inclusion Phenom. Macrocyclic Chem., 2003, 45, 275–283.
31. B. Ivanova, M. Spiteller, J. Inclusion Phenom. Macrocyclic Chem., 2013, 76, 87-98.
32. C. Foulon, J. Tedou, T. Queruau Lamerie, C. Vaccher, J. P. Bonte, J. F. Goossens, Tetrahedron: Asymmetry 2009, 20, 2482–2489.

13

Challenging core-shell stationary phases with the separation of closely related anti-cancer compounds: performance studies and application to drug quantitation in cell cultures with multi-well plate clean-up

In preparation for submission: González-Ruiz, V., Olives, A. I. & Martín, M. A.

ABSTRACT ▶ Nowadays, the wide variety of commercially available HPLC stationary phases makes it possible to solve most of the analytical problems that a chromatographist may need to face. For this reason, an increasing number of analysts are focusing not only on achieving good separations, but also on raising the efficiency of the separations in terms of speed and sustainability. In the present paper, we describe the chromatographic behaviour of six different stationary phases (5 µm fully porous and 2.6 µm core-shell particles, each featuring octadecyl-, pentafluorophenyl-propyl- and phenyl-hexyl- functionalizations) for the separation of camptothecin and a family of closely related analogues of the natural anti-cancer drug luotonin A. We compared the efficiency of these three chemistries in separating and resolving all of the eight compounds under different experimental conditions achieved by varying the organic solvent nature and proportion, the temperature and by adding modifiers. These studies allowed us to infer the nature of the interactions established between each compound and the different stationary phases. We also studied the efficiency and performance of both types of supports (fully porous *vs.* core-shell particles) by means of van Deemter and kinetic plots, using an optimized conventional HPLC system. As expected, columns packing core-shell particles afforded better efficiencies, higher permeabilities and a significant decrease in the analysis time and the consumption of solvents. The replacement of acetonitrile with methanol had a dramatic effect in the selectivity and efficiency of the PFP stationary phase. Taken in the aggregate, these results allowed us the selection and optimization of the best combination of stationary and mobile phases (core-shell C-18, H_2O:MeCN gradient) for the rapid, cost-effective and sustainable quantitation of the anti-tumour agents under study in cell cultures. A simple and rapid clean-up step was optimized using 96-well deproteinization and delipidization plates. The validation of the proposed analytical method showed excellent figures of merit. The combination of this sample pre-treatment procedure with the separation on core-shell particles yielded a fast methodology able to process a large number of samples with minimal waste generation and environmental impact.

ABBREVIATIONS ▼

- **C-18:** octadecyl-silane
- **PFP:** pentafluorophenyl-propyl-silane
- **PH:** phenyl-hexil-silane
- **CPT:** camptothecin
- **LOD:** limit of deteceion
- **LOQ:** limit of quantitation

1. Introduction

Human DNA topoisomesases are enzymes able to reduce the supercoiling of the DNA structure, thus allowing molecular processes with key roles in cell survival such as DNA replication or damage repair [1]. Topoisomerase I is the molecular target for camptothecin, the lead compound of a class of anticancer drugs widely employed in the treatment of several types of cancer [2-5]. The therapeutic uses of natural camptothecin (Figure 1) are limited mainly by its cytotoxicity and chemical instability due to the hydrolysis of its E ring. This ring bears a lactone moiety that quickly opens at physiological pH yielding the inactive carboxylate form of the drug. Luotonin A (Figure 1) is a natural pentacyclic alkaloid whose structure resembles that of camptothecin, and therefore it also behaves as a topoisomerase I inhibitor [6-9]. Since Hecht and co-workers [10] demonstrated that topoisomerase I was the target of luotonin A, a notable number of papers devoted to the synthesis of luotonin A derivatives and their structure-activity relationships have been published [11,12] because their better chemical stability is a promise

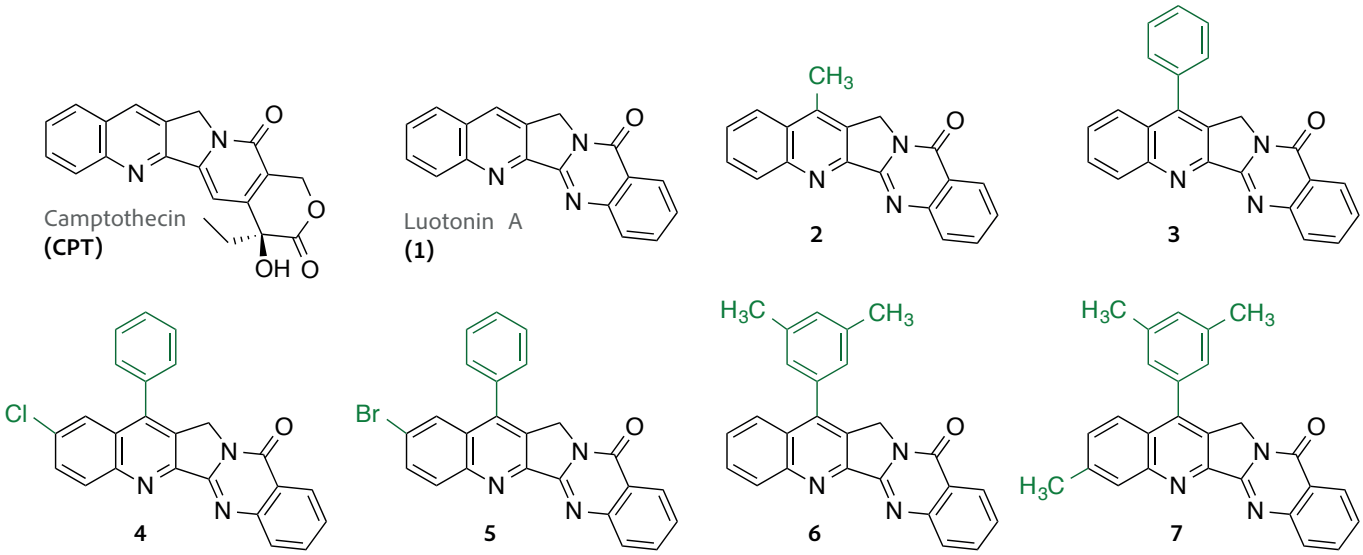

Figure 1. Chemical structures of camptothecin, luotonin A and its six derivatives.

for an improved bioavailability. As natural luotonin A exhibits a lower *in vitro* cytotoxic activity than camptothecin [13], the search for new analogues with improved activity is increasingly important. *In vitro* and pharmacokinetic studies require analytical methodologies able to quantify the drugs in cell cultures, tissues and biological fluids from experimentation animals, as well as human samples in the last research stages.

The alternatives for the analysis of anti-cancer drugs, including camptothecin, have been reviewed [14]. Different chromatographic approaches to the analysis of camptothecin and its clinically available derivatives (irinotecan and topotecan) have been summarized [15]. Due to the notable fluorescence of these pentacyclic compounds, fluorescence detection has been widely employed [16], since the sensitivity obtained is adequate for the determination of camptothecins levels in biological fluids and tissues [17-19]. Some HPLC methods were developed with the aim to distinguish and quantify separately its lactone and carboxylate forms [20], a useful piece of information in clinical practice. Furthermore, the use of commercially available chiral stationary phases or the inverted chirality columns approach, has made possible the chiral resolution of enantiomers of the drugs [21].

Luotonin A derivatives also exhibit a strong fluorescence [22,23]. Nevertheless, the literature about the separation of luotonin A analogues is very scarce [24,25]. We have previously reported a methodology for the quantification of luotonin A derivatives in human serum samples [24]. Following this initial approach to the separation and quantification of luotonin A analogues in biological samples, our research interest has been focused on overcoming its main drawbacks: compounds **4** and **5** were not properly separated, the analysis time and solvent consumption were susceptible of improvement, and the manual one-by-one deproteinization step was a bottleneck leading to a low throughput of the method.

Columns packed with core-shell particles are one of the most promising innovations currently changing the analytical chromatography panorama. They are built by synthesizing a porous silica shell onto a fused, non-porous silica nucleus [26,27]. This methodology affords particles with a narrow size dispersion that can be packed with an exceptional homogeneity into the HPLC columns. Measurements of the three terms of the van Deemter equation showed that smaller B-, C- and, remarkably, A-term, account for the surprisingly good chromatographic behaviour of such columns [28,29].

They can deliver efficiencies comparable to those of smaller fully porous HPLC particles while keeping the working pressures under 600 bars [30,31]. Furthermore, they do not require the investment in special ultra-high pressures pumps needed for operating UHPLC columns. They are also capable to separate a large number of peaks per time unit in columns of reduced length and diameter, decreasing the analysis time and solvent consumption [29,32-36]. For these reasons, their use has become widespread in the past five years.

Some recent examples of analysis using superficially porous particles include polycyclic aromatic hydrocarbons in rainwater [37], phenolic compounds in food samples [38-40], isoflavones in serum [41], toxins [42], pharmaceutically interesting compounds [43], protein kinase inhibitors [44], corticosteroids in bovine tissues [45], and complex protein mixtures [46], among many others.

The use of fast chromatographic methodologies allowing rapid separations in the 1-5 minutes timescale requires comparably quick methods for sample preparation. Conventional methodologies for the clean-up of biological samples involve the precipitation of proteins with an ice-cold organic solvent (usually acetonitrile, methanol or ethyl acetate) acidified with formic, acetic or phosphoric acid followed by centrifugation of the individual tubes and separation of the supernatant [19,24,47-49]. This procedure is tedious and involves individual or small-batch processing of the samples. On the contrary, multi-well format sample clean-up allows the simultaneous processing of 96 samples, and is also susceptible of full automatization. Multi-well sample format employing different configurations increases the throughput capabilities of HPLC [50].

The aim of this work is to compare the performance of columns packed with superficially and totally porous particles bearing different bonded chemistries. Chromatographic behaviour was studied in terms of their ability to separate the family of structurally close compounds under different proportions of organic solvents, mobile phase modifiers and temperatures. Efficiencies and analysis time were compared by means of van Deemter and kinetic plots. These studies allowed us not only to investigate the analyte-stationary phase interactions, but also to find the best starting point to optimize a gradient elution that we successfully applied to the quantitation of the compounds in cell cultures. A simple an efficient sample clean-up procedure is also employed.

2. Experimental

2.1. Apparatus

The liquid chromatographic system (Merck-Hitachi, Tokyo, Japan) consisted of a quaternary gradient pump L-7100, able to handle a maximum backpressure of 412 bar, and a fluorescence detector L-7485. The column was thermostated inside a L-2300 oven with circulating air and a heat exchanger region for the inlet capillary. A backpressure regulator adjusted at +1.5 bar (VICI-Jour, Schenkon, Switzerland) was placed after the detector. The chromatographic system was controlled and the data was acquired through a PC running HPLC System Manager software, version 4.1 (Merk-Hitachi). The samples were injected through a Rheodyne 7725i injector.

Short columns packed with core-shell particles are able to deliver exceptionally good efficiencies, but such good results can be easily spoiled by peak broadening arising from extra-column volume in conventional instruments [51]. Consequently, such HPLC instruments are advised to undergo some easy and inexpensive modifications prior to the use of core-shell columns [52,53]. Thus, we used two different connection

setups (designed as "unmodified" and "optimized") during the present work. The unmodified setup was used for the experiments where conventional fully porous columns were employed, and consisted of a 1000 × 0.2 mm (L × I. D.) stainless steel capillary between the injector and the column, and a 450 × 0.2 mm (L × I. D.) PTFE capillary placed at the exit of the column. The injector was equipped with a 20 µL sample loop. In the optimized setup, Viper (Dionex, Germering, Germany) capillary tubes were chosen because of their advantageous features: they are available in different pre-cut sizes and have built-in fittings that guarantee zero-dead-volume connections. Two capillaries of 750 × 0.13 mm (L × I. D.) and 350 × 0.13 mm (L × I. D.) were placed at the inlet and the outlet of the column, respectively. In this second setup, a smaller 5 µL sample loop was chosen in order to minimize the influence of the sample solvent on the shape of the peaks eluting at short retention times and considering the smaller loading capacity and better sensitivity expected from core-shell columns [54-56]. The replacement of the flow cell to reduce its extra-column volume contribution is also a good practice to improve the performance of optimized systems using core-shell particles. Nevertheless, no smaller-volume flow cell was manufactured for our fluorescence detector, so the original 12 µL flow cell was employed in both configurations.

2.2. Columns

Columns were all manufactured by Phenomenex (Torrance, California, USA), and are detailed in Table 1. The pore size was 100 Å in all cases. Kinetex columns were equipped with adequate SecurityGuard (Phenomenex) guard cartridges.

Table 1. Details of the columns employed in the present work.

Brand	Type	Functio-nalization	L × I. D. (mm)	Particle size (µm)	Ref. #	Batch / Serial
Luna	Fully-porous	C-18(2)	150 × 3.0	5.0	00F-4252-Y0	5291-83 / 544253-13
Luna	Fully-porous	PFP(2)	150 × 3.0	5.0	00F-4448-Y0	5537-38 / 546984-1
Luna	Fully-porous	PH	150 × 3.0	5.0	00F-4257-Y0	5296-31 / 547127-1
Kinetex	Core-shell	C18	50 × 3.0	2.6	00B-4462-Y0	5569-159 / 644641-53
Kinetex	Core-shell	PFP	50 × 3.0	2.6	00B-4477-Y0	5576-52 / 617410-27
Kinetex	Core-shell	PH	50 × 3.0	2.6	Made on-demand	43339

2.3. Chemicals and mobile phases

Commercially available camptothecin was purchased from Sigma-Aldrich (Steinheim, Germany). Compounds **1**-**7** were synthesized using modified Friedländer conditions as described elsewhere [7]. Acetonitrile and methanol (UHPLC grade), as well as formic and acetic acids (HPLC gradient grade) were from VWR BDH-Prolabo (Fontenay-sous-Bois, France). Tetrahydrofuran and *tert*-butyl methyl ether (HPLC grade) were from Sigma-Aldrich. Ultrapure water was produced in-lab with a Milli-Q Direct 8 system (Millipore, Molsheim, France).

Mobile phases were filtered under low-pressure and ultrasonically degassed prior to their use. Polyamid 47 mm filters (Sartolon 0.45 µM pore size, Sartorius Stedim Biotech, Goettingen, Germany) were employed for mobile phases intended to be used in conventional columns. For core-shell columns, mobile phases were filtered through Phenex nylon membranes (47 mm, 0.2 µm pore size, Phenomenex).

2.4. Procedures

2.4.1. Preparation of problem mixtures

Individual stock solutions of the compounds under study (CPT and **1**-**7**) were prepared from accurately weighed amounts of the solid products, dissolved in DMSO at 5 × 10^{-4} M concentration. Fresh working mixtures were prepared by combining adequate aliquots of the stock solutions and diluting up to 5 × 10^{-7} M concentration with 50% aqueous MeCN. All the solutions were filtered through 4 mm syringe filters (Phenex, regenerated cellulose, 0.2 µm pore size, Phenomenex) prior to their injection. These working solutions were employed for all experiments except for the final validation of the analytical method.

At the beginning of the experiments with every different column, the compounds were injected individually in order to check the elution order. This parameter was found to remain constant in all the assayed columns and conditions, being as follows: CPT, **1**, **2**, **3**, **4**, **5**, **6** and **7** (from shorter to longer retention times). Most retained compounds (**6** and **7**, or **4**-**7**) were removed from the working solutions when the lowest flow rates or organic solvent proportions yielded exceptionally long run times (over 180 mins).

2.4.2. Influence of the organic solvent proportion and of the temperature in the chromatographic behaviour

Different intervals of organic solvent proportions were assayed in each column at 0.5 mL min^{-1} flow rate and 25 ºC, as detailed in table Table 2. The influence of the temperature on the chromatographic behaviour of the columns was explored by running the separations at temperatures ranging from 25 to 65 °C using 60:40 H_2O:MeCN mobile phases at a flow rate of 0.5 mL min^{-1}. The van't Hoff plots were obtained by plotting the experimental values of retention factors *versus* the reciprocal of the absolute temperature values, according to Eq. 1, where β is V_{FM}/V_{FE}. The total free energy could then be calculated using Eq. 2.

Eq. 1

$$\ln k' = -\frac{\Delta H^0}{R}\cdot\frac{1}{T} + \frac{\Delta S^0}{R} - \ln \beta$$

Eq. 2

$$\Delta G^0 = \Delta H^0 - T\Delta S^0$$

Table 2. Organic solvent ratios assayed in every stationary phase.

Column	φ MeCN (v:v)	φ MeOH (v:v)
Luna C-18	0.40 – 0.50	-
Luna PFP	0.40 – 0.60	0.60 – 0.80
Luna PH	0.40 – 0.60	-
Kinetex C-18	0.35 – 0.60	-
Kinetex PFP	0.35 – 0.60	-
Kinetex PH	0.35 – 0.60	-

2.4.3. Van Deemter and kinetic plots

In order to get the experimental data allowing the construction of the van Deemter and kinetic plots for every column, flow rate was varied between 0.1 and 0.7 mL min^{-1} with fixed temperature and organic solvent proportion (25 °C and H_2O:MeCN 55:45 v:v).

Efficiencies for each peak were calculated from the retention time of the peak apex and its half-height width. Although this classical method provides inaccurate results in the measured efficiency [57], it was chosen for three main reasons. The first one is that, although other methods can afford a better accuracy for most circumstances, they can also actually fail to provide correct values under certain conditions. Second,

the selected method is the best known by most chromatographists, specially by those researchers more interested in analytical applications than in chemical engineering of the separation process. The third one is that the peak efficiency calculation based on the retention time and the half-height width is implemented in most control and data acquisition software suites and, consequently, it can be calculated in a straightforward manner without the need for development of specific software.

Another keystone of our work is that we have not considered the extra-column peak broadening influence on the efficiency values reported. Again, this decision was made after a careful evaluation of the available literature and the aim our work. Firstly, no robust method had been reported to date allowing an accurate measurement of the extra-column peak broadening [58,59] until the time when this manuscript was already under preparation [60]. Furthermore, and being the driving motivation for us, it is our aim to report actual efficiency values that can be achieved with conventional instruments, specially the ones using the detectors best known for their large volume flow-cells, *i.e.* fluorescence detectors.

The linear velocity of the mobile phase was calculated, at every flow rate and in every column, from the elution time of the unretained peak (sample solvent). Experimental (u_0, H) data were plotted and fitted to the Knox equation with $n = {}^1/_3$ (Eq. 3).

$$H = A \cdot u_0^n + B / u_0 + C \cdot u_0 \qquad \text{Eq. 3}$$

The experimentally obtained efficiency data pairs (u_0, H) were transformed into kinetic data following the method developed by Desmet [61], using Equations 4 and 5.

$$N = \frac{\Delta P}{\eta}\left(\frac{K_V}{u_0 H}\right) \qquad \text{Eq. 4}$$

$$t_0 = \frac{\Delta P}{\eta}\left(\frac{K_V}{u_0^2}\right) \qquad \text{Eq. 5}$$

Where u_0 and H are the experimentally determined velocity and efficiency values, ΔP is the maximum allowable working pressure (for our instrument, it was set at 400 bar, 4×10^7 Pa), η is the viscosity of the H_2O:MeCN 55:45 v:v mobile phase at 25 °C (8.52×10^{-4} kg (m·s)$^{-1}$) [62] and K_V is the permeability of the chromatographic bed, experimentally calculated for every column by means of Eq. 6.

$$K_v = \frac{u_0 \eta L}{\Delta P} \qquad \text{Eq. 6}$$

2.4.4. Optimization of the separation method

On the basis of the results obtained in the previous experiments, the combination of C-18 Kinetex column and H_2O:MeCN mobile phase was chosen for further optimization. With this purpose, we assayed the influence of different mobile phase modifiers on the separation, so several formic or acetic acid concentrations, as well as tetrahydrofuran and *tert*-butyl methyl ether, were added to the mobile phases and their effects were studied. A remarkable number of gradient profiles were also designed and assayed, all of them aimed at shortening the total chromatographic run time while maintaining the good resolution of all compounds.

The optimized chromatographic separation selected for quantitative purposes in cell lysates consisted of the C-18 Kinetex column working at 45 °C with a flow rate of 0.7 mL min^{-1} and H_2O:MeCN mobile phase under gradient elution as follows: MeCN

from 35 to 60% over 5.5 minutes, kept at 60% for 3 minutes and then back to 35% in 0.5 min. The column was re-equilibrated after each run for 3 minutes.

2.4.5. Analysis of luotonin A and derivatives in cell culture lysates

Murine embryonic fibroblasts were incubated (37 °C, 5% CO_2) in 100 mm polystyrene plates (Becton Dickinson, Franklin Lakes, USA). Culture medium was DMEM (Dulbecco's Modified Eagle Medium from Gibco-Life Technologies, Carlsbad, USA) supplemented with fetal bovine serum, antibiotics (penicillin G, streptomycin, amphotericin B) and mycoplasma elimination reagent (MycoZap, Lonza, Basel, Switzerland). At confluence, plates were washed four times with cold DPBS (Dulbecco's Phosphate-Buffered Saline, Gibco-Life Technologies) and scrapped. Cells were then transferred to polypropylene tubes and washed four times by resuspension in DPBS and centrifugation at 110 × *g* (3 min, 4 °C). Pellets were frozen at -20 °C until the time of the analysis. Prior to their use, cells were lysated by adding 0.1X DPBS into the sample tubes and keeping them in an ice-cold ultrasonic bath for 20 minutes. As a reference, protein concentration in the resulting lysates was determined to be 0.1 µg/µL by routine Bradford assay (absorbance measurement at 595 nm after reaction with Coomassie brilliant blue G-250, Bio-Rad, Hercules, USA).

The concentrations of individual stock solutions of the compounds **1**-**7** (around 5×10^{-4} M in DMSO) were accurately determined by spectrophotometry [24] using a double-beam Kontron (Zurich, Switzerland) Uvikon 810 spectrophotometer, and then adequate aliquots were mixed and diluted with H_2O:MeCN 50:50 v:v to obtain a solution containing compounds **1**-**7** at 2.0×10^{-5} M. Subsequent dilution from that mixture and using the same solvent allowed to obtain a set of solutions of the compounds covering the 2.0×10^{-5} – 1.0×10^{-8} M range. Aliquots of these solutions (25 µL) were added to 475 µL of the cell lysates to obtain fortified samples of concentrations between 1.0×10^{-6} and 5.0×10^{-10} M without distorting the nature of the matrix (spiking volume was 5% of the total volume). Camptothecin solutions for use as internal standard were prepared following the same procedure.

2.4.6. Sample clean-up

For the clean-up step we chose a multi-well plate format that allowed to process up to 96 samples simultaneously with very little time consumption. The Phree proteins and phospholipids removal plates (Phenomenex, Torrance, CA) combine on the bottom of each well a membrane for precipitated protein retention and a selective sorption material able to retain phospholipids from cell membranes. Briefly, a protein precipitation solution (1% HCOOH in MeCN containing camptothecin 1×10^{-8} M as internal standard) was placed into each well, and then the samples were added. After vortex mixing for 3 mins, clean supernatants were eluted from the bottom of each well into a clean collection plate by applying a soft vacuum (-0.15 bar, 3 mins). Samples eluted in acetonitrile were diluted (50:50 v:v) with water (a weak solvent) to minimize peak distortion (Figure 2) and injected into the chromatograph [59]. Preliminary studies were conducted in order to determine the most adequate sample-to-precipitant volume ratio (see the Results and Discussion section). Finally, volumes of 900 µL of precipitant solution and 100 µL of cell lysates were used for the validation of the method.

2.4.7. Validation of the analytical method

Validation of the method was carried out by determining linearity, limit of detection (LOD), limit of quantitation (LOQ), accuracy and precision according to international bioanalytical method validation guidelines [63-65]. Two kinds of samples were analysed: calibrator solutions and quality controls (QC). Calibrators were cell lysates

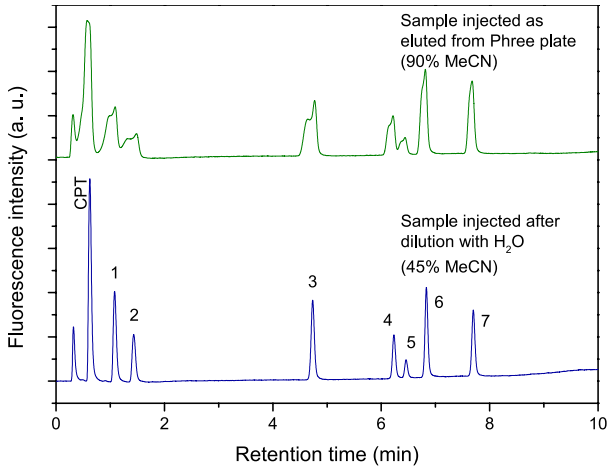

Figure 2. Improvement of the peak shape obtained by diluting the samples with a weak solvent such as water prior to the injection. Chromatographic conditions were the optimized ones (see Section 2.4.4).

samples fortified at six levels of concentrations (1.0×10^{-6} to 5.0×10^{-10} M) plus a blank cell lysate. Quality controls were cell lysates containing the compounds at three levels of concentration: 1.0×10^{-6}, 1.0×10^{-7} and 5.0×10^{-9} M (QC1, QC2 and QC3 respectively). Calibrators and QC samples were conducted through the clean-up process and the optimized chromatographic analysis previously described. Calibration curves were constructed by measuring the calibrator solutions and plotting the analyte/IS peaks area ratio *versus* the theoretical concentration. In order to minimize the influence of intra- and inter-day variation, calibration curves were measured by quadruplicate and in different days. LOD and LOQ were determined from five replicated measurements of QC3 solutions (5.0×10^{-9} M) and calculated as previously described in the literature [66] according to Eqs. 7 and 8. Accuracy was determined from six replicate analyses of QC samples at the three levels of concentration. Intra-day precision was calculated from six runs conducted on the same day, and inter-day precision from duplicate injections of the same concentration over five different days, both at the QC1, QC2 and QC3 levels of concentration.

$$\mathrm{LOD} = 3\frac{\text{SD of the experim. conc.} \times \text{theoret. conc.}}{\text{mean of the experim. conc.}} \qquad \textbf{Eq. 7}$$

$$\mathrm{LOQ} = 10\frac{\text{SD of the experim. conc.} \times \text{theoret. conc.}}{\text{mean of the experim. conc.}} \qquad \textbf{Eq. 8}$$

3. Results and discussion

3.1. Influence of the chromatographic conditions on the behaviour of the different stationary phases.

3.1.1. Selectivity

Columns packed with fully porous particles

The growing number of commercially available chemically modified silica stationary phases broadens the spectrum of retention mechanisms that can be exploited to increase the selectivity among closely related compounds [67]. Considering the structures of the compounds under study, we were prompted to investigate the separation capabilities of PH and PFP-bonded silica stationary phases. PH bonded silica is able to interact through π-π interactions with the aromatic rings present in the structure of the drugs under study, and PFP-functionalized stationary phases can establish hydrogen bonding and dipole-dipole interactions with polar functional groups or by inducing the polarization of the aromatic moieties on the analytes. Both interactions add

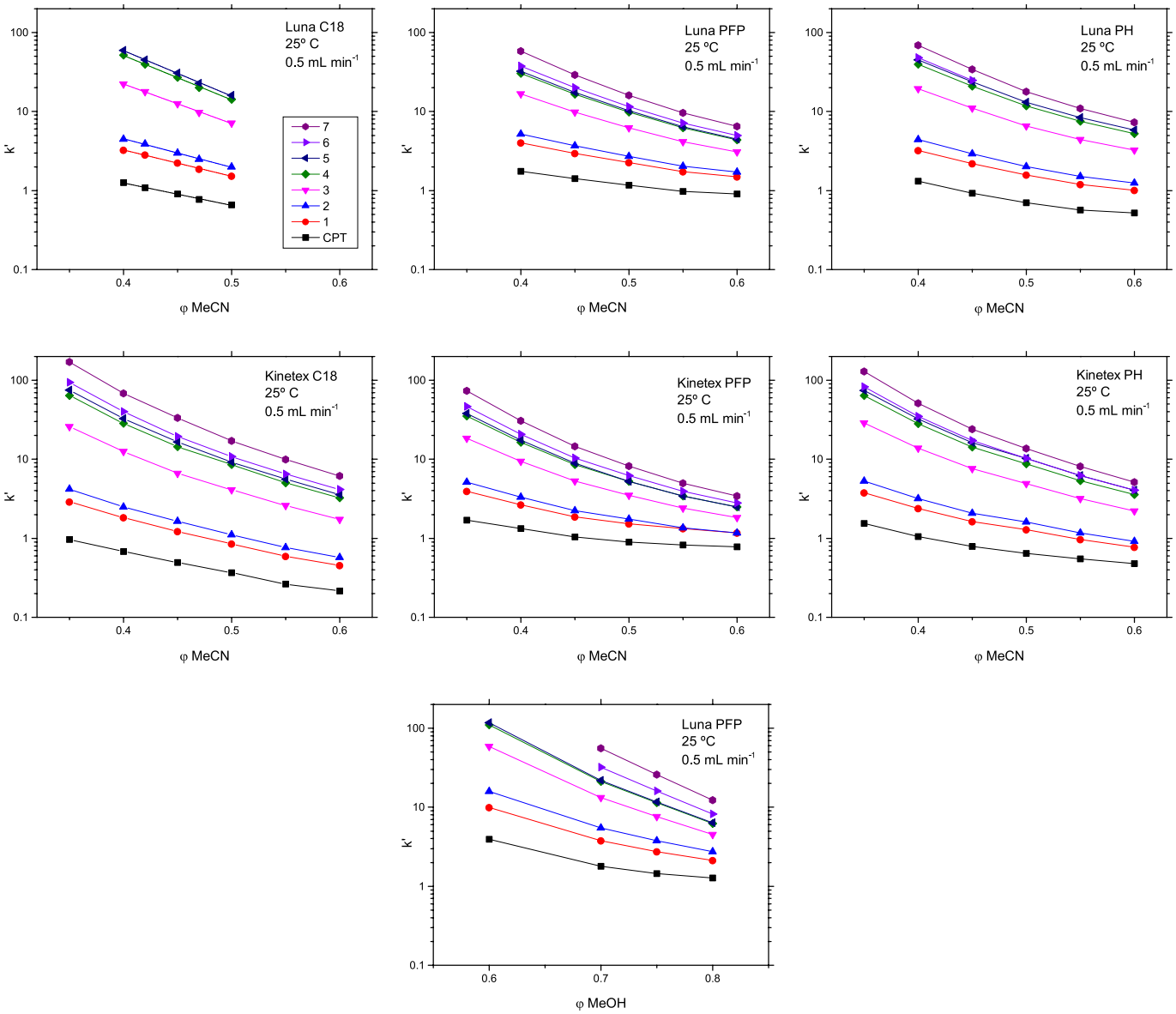

Figure 3.
Evolution of the retention factors with increasing organic solvent proportion for all the compounds and stationary phases assayed. Note the poor resolutions attained for some pairs of compounds, as shown by the overlapping lines.

to the hydrophobic ones that are also present in these stationary phases and, thus, an improved selectivity can be expected with regard to C-18. Bearing in mind that C-18 columns are widely employed in routine and official analysis methods, we decided to use them as a reference for comparison with the results achieved by PH and PFP in the separation of the complex mixture of anti-tumor agents under study.

The study of the variation of *k'* caused by the different proportions of organic solvent in the mobile phase revealed, as expected, a reduction in the *k'* values with increasing MeCN or MeOH content (Figure 3). The library of molecules under study shared a common trend over the whole range of solvent ratios, fitting to a quadratic model with an excellent R^2 (higher than 0.999 except for case of the core-shell PH stationary phase, which remained over 0.996). These results support a classical reverse-phase mechanism for the separation of the analytes in all the stationary phases [68]. These plots also allow for an easy visualization of the pairs of compounds that are poorly resolved with any stationary phase/mobile phase combination, as detailed below.

The Luna C-18 stationary phase was able to successfully separate all the compounds using a 50:50 H_2O:MeCN mobile phase composition, but at the expense of

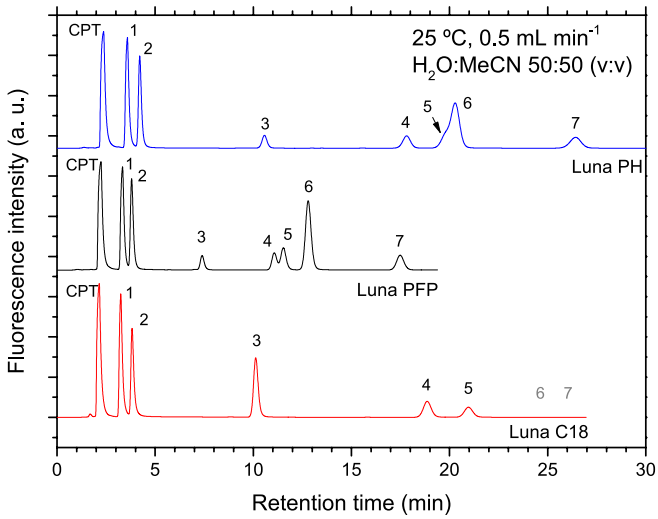

Figure 4. Chromatographic behaviour of the three different columns packed with fully-porous particles. Compounds **6** and **7** were not present in the test mixture separated on the Luna C-18 column under the detailed experimental conditions.

yielding undesirable analysis times over 30 minutes (Figure 4). This drawback arose from the well-known isocratic elution problem: when the organic solvent proportion is increased in order to shorten the retention time of the most-retained solutes, the resolution of the compounds with smallest *k*' values is lost. Inversely, when the proportion of organic solvent was reduced, the resolution of compounds **1** and **2** (differing only in a methyl group) was improved, but the time of analysis increased even further.

We found that all the compounds could be separated with good resolution by using a 60:40 H_2O:MeCN mobile phase on the PFP column. Again, the analysis time needed to obtain such results extended over 30 minutes. Nevertheless, the retention afforded by this stationary phase was remarkably lower than those of C-18 and PH at comparable organic solvent proportions (Figure 4). Organic solvent ratios higher than 60:40 H_2O:MeCN harmed not only the resolution of the **1**/**2** pair, but also that of compounds **4**/**5**, which bear a different halogen (Cl or Br) at the same position of the pentacyclic structure (Figure 5A). With the aim to circumvent this problem, and reasoning that hydrogen bonds play a key role on the PFP retention mechanism, we decide to test how a hydrogen-bonding donor solvent affected the selectivity of the separation. Our choice was methanol because it shares with acetonitrile many desirable chromatographic features and is also widely employed in reverse-phase separations. The results were quite different from those obtained with acetonitrile. We needed meth-

Figure 5. Chromatograms obtained with PFP columns using different proportions of (A) MeCN and (B) MeOH in the mobile phases. Note how the resolution of compounds **4**/**5** is always lost (black arrows, A and B). Pair **1**/**2** is poorly resolved with MeCN (A, black arrows) while its resolution is kept under MeOH elution (B, green arrows). The retention time of compound **7** using H_2O:MeOH 30:70 v:v mobile phase was of 65 minutes (not shown for clarity).

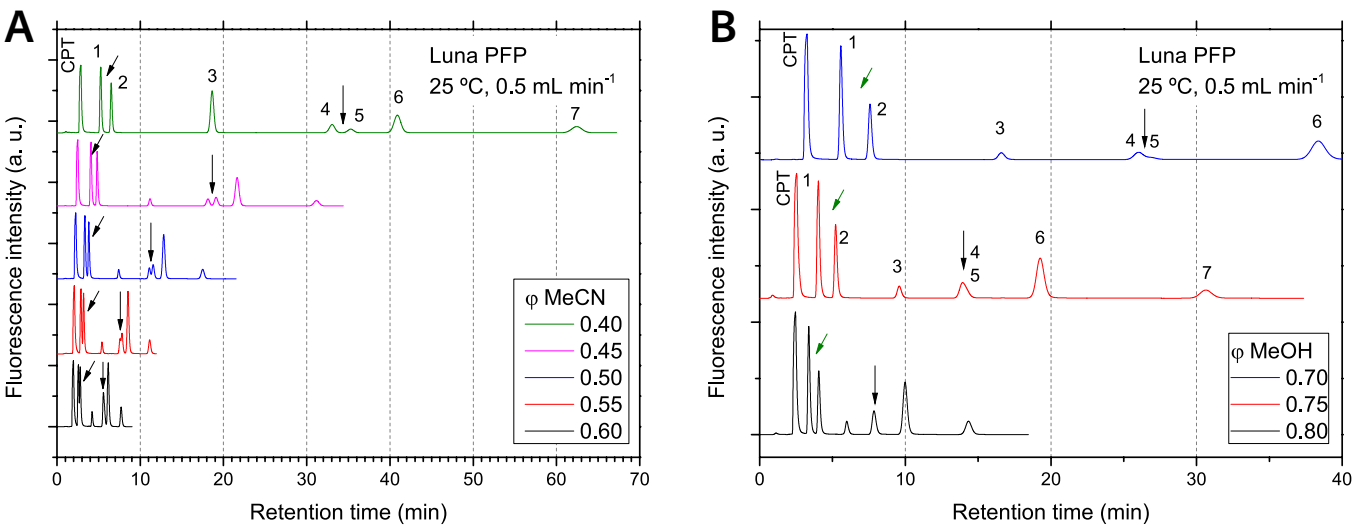

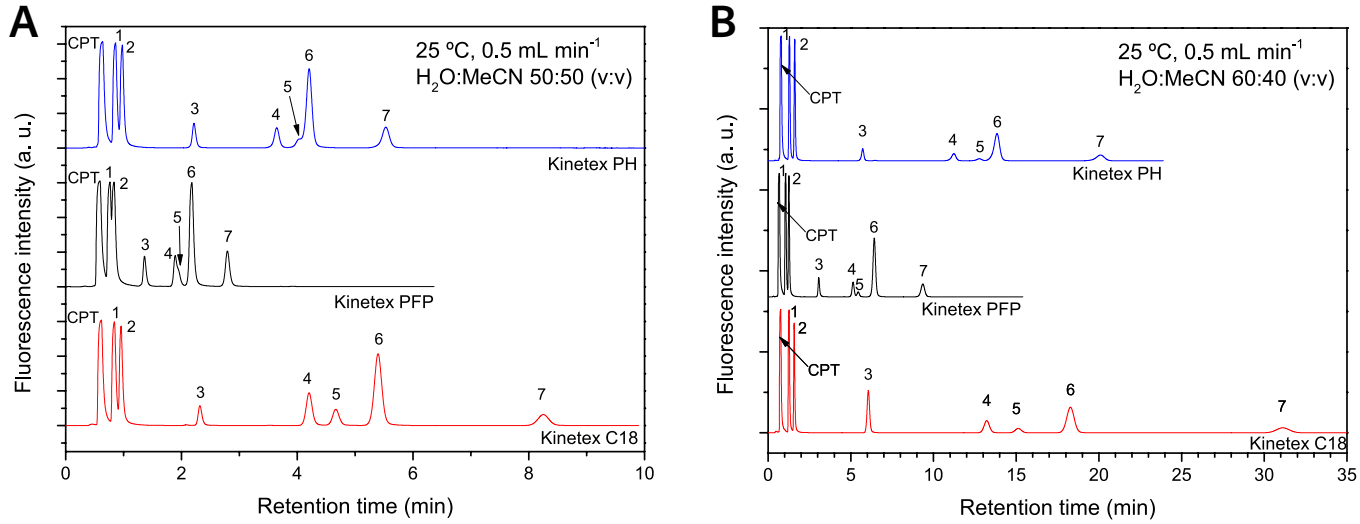

Figure 6.
Separations obtained using core-shell columns. (A) H_2O:MeCN 50:50 (same as in Fig. 4) and (B) H_2O:MeCN 60:40 (times closer to those of fully-porous in Fig. 4).

anol proportions as high as H_2O:MeOH 25:75 (v:v) to obtain analysis times similar to those of acetonitrile (around 30 minutes). The **4**/**5** pair of compounds was especially sensitive to the organic phase composition and, under the mentioned conditions, could not be properly separated (Figure 5B). Separation of these compounds was only achieved by using a H_2O:MeOH 40:60 (v:v) proportion, yielding a run time close to 150 minutes. On the contrary, we obtained an excellent resolution for compounds **1**/**2** (Rs = 2.37) even at the highest assayed methanol proportion (H_2O:MeOH 20:80 (v:v)). This allowed us to carry out a fast, isocratic separation where acetonitrile was replaced by the more environmentally friendly methanol, although at the cost of not being able to resolve compounds **4**/**5**. As one of the aims of the present work was the development of a method able to separate all the compounds under study, this combination, although interesting, had to be abandoned.

In the PH stationary phase, the worst selectivity values were obtained for a third pair of compounds: **5**/**6**. This outcome was totally unexpected, as pairs of compounds **1**/**2**, **4**/**5** and **6**/**7** present a higher degree of similarity between them, as shown in (Figure 1). The analyses times were comparable to those of the C-18 column (in the 20-30 minutes time range, Figure 4), but the aromatic stationary phase presented the drawback of being unable to separate compounds **5**/**6**, unless high temperatures were employed, as discussed below.

Core-shell columns

A general picture of the core-shell columns compared to the fully-porous ones shows that their retentivities were remarkably lower and their efficiencies notably better (Figure 6). Thus, similar separations could be obtained in shorter analysis times and employing lower organic solvent ratios. Table 3 shows how the evolution of the resolution of the critical pairs in the three chemistries assayed clearly follows this trend. The core-shell columns are able to achieve resolution values comparable to those of the fully-porous columns with mobile phases containing less MeCN and in shorter analysis times. Consequently, it allows using water-rich mobile phases which are more environmentally friendly, while the chromatographic features (efficiency, resolution and analysis time) are kept constant or, more frequently, improved.

Table 3. Resolution of the critical pairs on the different columns and with varying organic solvent contents.

φ	Luna C-18		Luna PFP (MeCN)		Luna PFP (MeOH)		Luna PH		Kinetex C-18		Kinetex PFP (MeCN)		Kinetex PH	
	1/2	4/5	1/2	4/5	1/2	4/5	1/2	5/6	1/2	4/5	1/2	4/5	1/2	5/6
0.35									3.2	3.0	2.2	1.7	3.2	2.1
0.40	4.3	3.5	3.2	1.7		N/R	4.2	1.4	2.2	2.9	1.4	1.2	2.1	1.8
0.42	3.8	3.3												
0.45	3.1	3.1	2.2	1.3			2.9	0.9	1.5	2.6	0.9	0.9	1.4	1.4
0.47	2.7	2.9									N/R	N/R		
0.50	2.3	2.8	1.6	0.9			2.1	N/R	1.0	2.3			1.0	N/R
0.55			1.1	0.6			1.5		0.7	1.9			0.7	
0.60			0.8	N/R	6.8		1.1		N/R	1.5			N/R	
0.70					5.0									
0.75					3.6									
0.80					2.4									

N/R: not resolved at the specified or higher organic solvent proportions.

3.1.2. Thermodynamics

Considering the results from the previous experiments, all the different stationary phases seemed to share very similar retention mechanisms. With the aim to further elucidate the nature of such mechanisms driving the separation process on every stationary phase, we studied the influence of the temperature on the separation of the series of compounds on the different columns. Such experiments allowed us to construct the so-called van't Hoff plots for every compound and stationary phase. These plots, although showing several limitations [69], make it possible to calculate the standard entropy and enthalpy of the transfer process of the solute from the mobile to the stationary phase.

In C-18- and PFP-functionalized columns (both fully-porous and core-shell), a good lineal correlation was found between the natural logarithm of the *k'* and the inverse of the absolute temperature (Figure 7A), meaning that the mode of interaction between the analyte and the stationary phase remained unchanged along the whole range of temperatures studied. Remarkably, when a single compound was inspected, very similar standard enthalpy values were found across all of these stationary phases (see Table 4).

Figure 7. Van't Hoff plots of the studied compounds on two of the core-shell columns assayed. (A) Straight lines observed on C-18-functionalised stationary phase. (B) On the PH column, two different regions can be observed, depending on the working temperature.

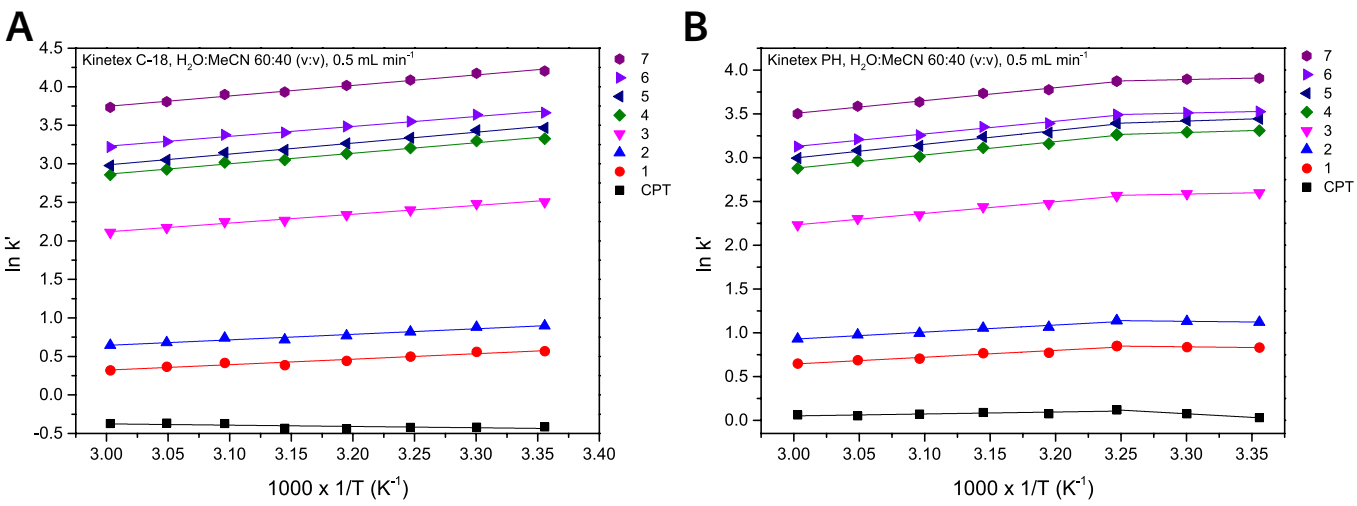

Table 4. Entropy and enthalpy values calculated for the transfer process of the analytes from the mobile to the stationary phase.

Compound	Energy (J/mol)	Luna C18	Luna PFP	Luna PH (40-60 °C)	Luna PH (25-40 °C)	Kinetex C18	Kinetex PFP	Kinetex PH (35-60 °C)	Kinetex PH (25-35 °C)
CPT	ΔS	-4.58	-2.66	1.48	14.49	4.40	-9.21	-2.97	25.49
	ΔH	-3164.31	-2455.64	-1905.74	2211.90	1406.47	-2839.30	-1852.00	6877.27
1	ΔS	-14.05	-9.30	-6.65	3.48	-16.52	-15.52	-11.93	13.49
	ΔH	-8527.19	-6496.73	-6472.52	-3285.29	-7342.94	-6390.97	-6481.54	1316.40
2	ΔS	-10.79	-7.15	-4.75	6.40	-13.97	-14.42	-10.23	15.81
	ΔH	-8389.15	-6489.43	-6701.62	-3195.19	-7385.62	-6606.49	-6702.60	1284.71
3	ΔS	-7.32	-6.66	-6.47	8.06	-7.72	-16.21	-12.58	15.95
	ΔH	-11406.05	-9235.40	-10932.69	-6362.83	-9514.27	-9708.18	-11097.92	-2335.35
4	ΔS	-6.58	-5.11	-6.31	10.03	-6.97	-15.18	-12.06	17.55
	ΔH	-13254.10	-10257.56	-12662.65	-7523.93	-11334.70	-10778.76	-12718.26	-3622.72
5	ΔS	-7.38	-5.35	-6.57	10.03	-7.33	-15.69	-12.30	17.47
	ΔH	-13835.63	-10494.50	-13083.84	-7864.07	-11791.17	-11080.92	-13122.11	-3975.09
6	ΔS	N/A	-1.60	-2.49	14.41	-2.04	-12.06	-7.99	22.30
	ΔH	N/A	-9755.35	-12021.21	-6703.63	-10698.87	-10405.47	-12051.77	-2741.26
7	ΔS	N/A	0.75	-0.26	17.94	0.38	-10.24	-5.48	25.84
	ΔH	N/A	-10128.42	-12272.66	-6547.56	-11326.58	-10809.94	-12260.94	-2635.71

N/A: Compounds not analysed under these conditions

Interestingly, a quite different behavior was observed on the PH-stationary phase (Figure 7B). In these columns, two lineal ranges could be observed. The first straight line corresponded to the temperature interval from 35 to 60 °C and ran parallel to the C-18 and PFP plots. This observation means that between these two temperatures, an enthalpy value comparable to that of the other stationary phases drove the transfer process. The second straight line, appearing between 25 and 35 °C, had a much lower slope indicating a process defined by higher entropy and lower enthalpy values. It is noteworthy that the decrease in the enthalpy is balanced by the raise of the entropy in this range of temperatures, leading to a total free energy that remains almost unaltered over the whole 25-60 °C temperature interval.

These observations allowed a better comprehension of the critical pairs not being adequately resolved on every stationary phase. A close examination of the estimated enthalpy and entropy values, shows how on the C-18 columns the transfer enthalpy progressively increases from the less to the most retained solutes. For compounds **4**-**7**, the calculated enthalpies remain almost constant or even drop but, interestingly, the entropy values grow and eventually become positive, making the total free energy of the transfer process much more favourable for the last-eluting compounds. In other words, in the case of the C-18 columns, the less retained solutes are separated because of their different enthalpy values, while entropy is the driving force allowing the separation of the most retained compounds. When the energy values obtained with the PFP column are compared, similar results are obtained for the poorly resolved pair **4**/**5**, that share almost identical enthalpy and entropy values. This explains why their separation is so hard to achieve.

The data from the PH columns reveal a more complicated behaviour, in very good agreement with the two different branches observed in their van't Hoff plots and the fact that compounds **5**/**6** were separated only at the highest assayed temperatures. The enthalpy and entropy values deduced from the "right" branch of the plots (the region corresponding to temperatures between 25 and 35 °C) are quite different between compounds **5** and **6**. Surprisingly, these apparently different values cancel

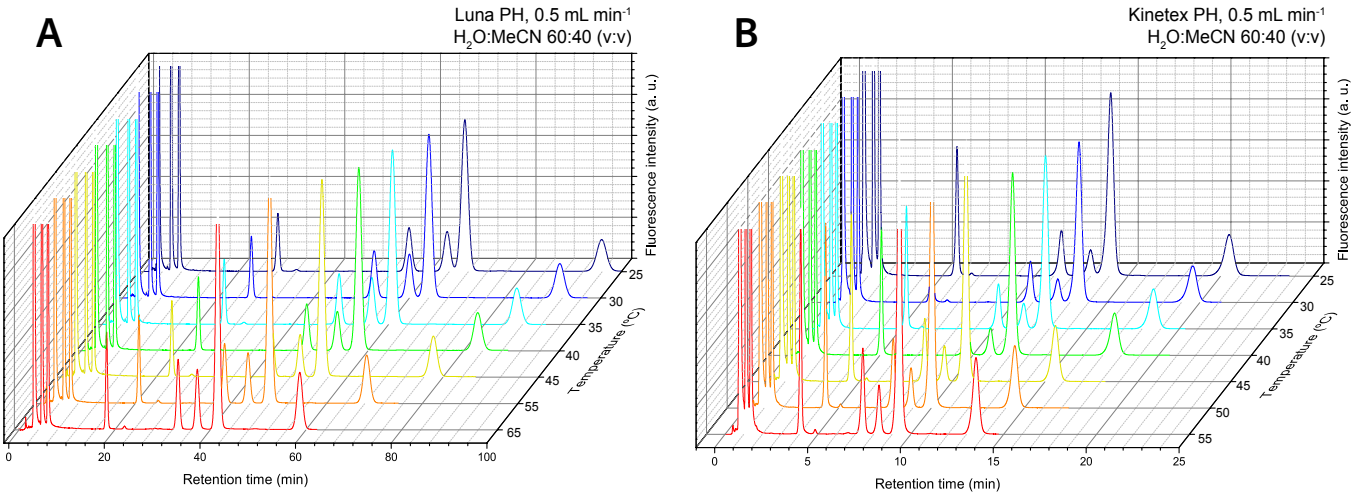

Figure 8. Influence of the temperature on the chromatograms obtained on the (A) Luna fully-porous and (B) Kinetex core-shell PH stationary phases. Note how the resolution of the peaks corresponding to the compounds **5** and **6** improves at highest temperatures.

each other yielding an almost identical total free energy for the transfer processes of both compounds [70], explaining why they are so poorly separated. On the "left" branch, enthalpies are very similar, but the different and negative entropy values afford a total free energy values that differ by almost 300 J/mol, doubling the difference deduced at room temperature. From the analytical point of view, this interesting behavior explains why the ability of the PH columns to distinguish compounds **5** and **6** improves above 35 °C (Figure 8).

Several reasons have been proposed to explain the lack of linearity in van't Hoff plots, such as the inhomogeneity of the stationary phase [71], or changes in the ionization degree of the analytes as a consequence of temperature modification [72]. Another explanation is the modification of the characteristics of the stationary phase upon temperature changes [73]. These precedents led us to the conclusion that any kind of temperature-related modification must occur in the PH stationary phase at 35 - 40 °C. Above that temperature, the stationary phase behaves in the same fashion as C-18 and PFP. Below 35 °C, the change in the properties of the PH stationary phase causes a drop in the enthalpy values as shown by the slope of the van't Hoff plots.

3.2. Comparison of the column efficiencies and the optimum achievable plate heights

The interest of evaluating the efficiency of the columns on the basis on their van Deemter plots (*H vs. u*), arises from the fact that it allows for an immediate comparison of the practical efficiency delivered by each column in an uncorrected, raw manner. We chose compound **3** as a probe because of its adequate *k'* (7-8 under the selected experimental conditions). The composition of the mobile phase was not adjusted across the different columns to keep a constant value *k'* because it would have caused additional variability in terms of viscosity, and diffusion coefficients of the analytes, and in order to be able to compare columns possessing different chemical functionalizations [32].

Figure 9 shows the typical van Deemter plots obtained for this compound on the six different stationary phases studied. The columns packed with 5 µm totally porous particles present well-defined H_{min} values at linear velocities below 1 mm s^{-1} (Table 5). Increasing the linear velocity above this point produces a drastic reduction in the column efficiency (higher *H* values) due to the increase in the C-term of the van Deemter equation, accounting for the mass transfer resistance. All the fully-porous stationary phases share this same behavior.

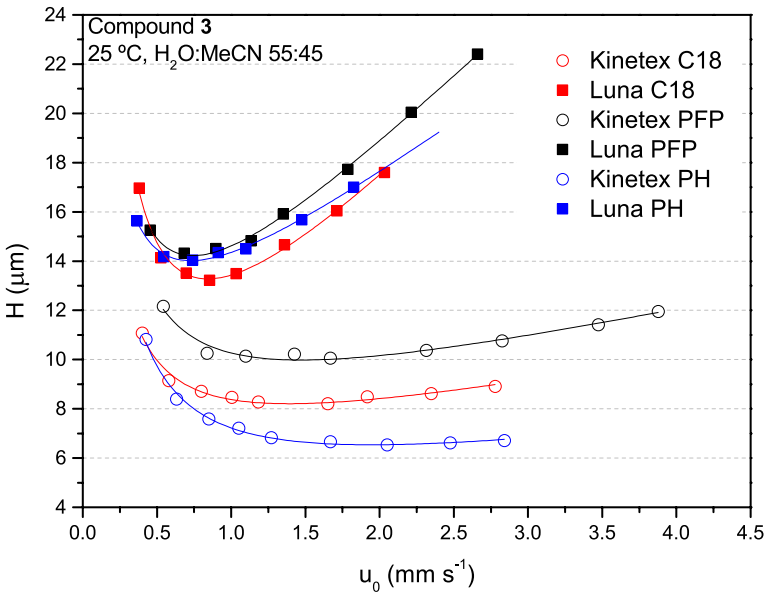

Figure 9. Van Deemter plots corresponding to the separation of compound **3** on the six stationary phases under study.

In the case of the columns packed with core-shell particles of 2.6 µm, H_{min} are clearly lower, meaning that the total efficiencies delivered are better than those obtained with the fully porous particles. Remarkably, these H_{min} values are achieved at faster linear velocities and the right branches of the curves have a smaller slope, evidencing that faster separations at higher flow rates can be achieved without causing a significant enlargement of the obtained *H* values. An obvious limitation to this observation is caused by the backpressure limit of the instrument. Increased backpressures should be expected when working with columns packed with particles of smaller diameter. Nevertheless, the improved permeability of the core-shell structure and the shorter length of the columns makes possible to work at keeping the backpressures under the 200 bar limit (Table 5 and Figure 10 on next page).

To summarize these results, we can state that using core-shell particles instead of conventional fully-porous particles, makes possible an immediate improvement of the efficiencies afforded. Moreover, a flatter C-term branch and a larger permeability allows working at higher flow rates without spoiling such efficiencies nor needing special UHPLC pumps.

These results reflect an overview of the analytical advantages of using core-shell particles rather than the fully-porous ones, although they must be taken with the proper caution in order to avoid biased conclusions. First, it must be taken into account that the sizes of both kinds of particles are not equal (fully-porous were 5 µm while the only core-shell columns commercially available by the time our experiments started were 2.6 µm). This difference affords favours the core-shell columns,

Table 5. Permeability, efficiency and kinetic parameters calculated for the different columns under study.

Column	K_v (m²)	H_{min} (µm)	h_{min} (µm)	u_0 for H_{min} (mm s⁻¹)	N_{opt} (/)	Knox and Saleem limit (s)
Luna C-18	2.46×10^{-14}	13.24	2.65	0.84	104044.6	1645.82
Luna PFP	4.67×10^{-14}	14.16	2.83	0.74	208785.3	3990.66
Luna PH	3.36×10^{-14}	13.98	2.80	0.71	159852.1	3165.84
Kinetex C18	6.73×10^{-15}	8.25	3.17	1.32	29010.91	181.12
Kinetex PFP	1.03×10^{-14}	9.97	3.84	1.38	35090.31	252.97
Kinetex PH	6.86×10^{-14}	6.58	2.53	1.90	24639.06	81.56

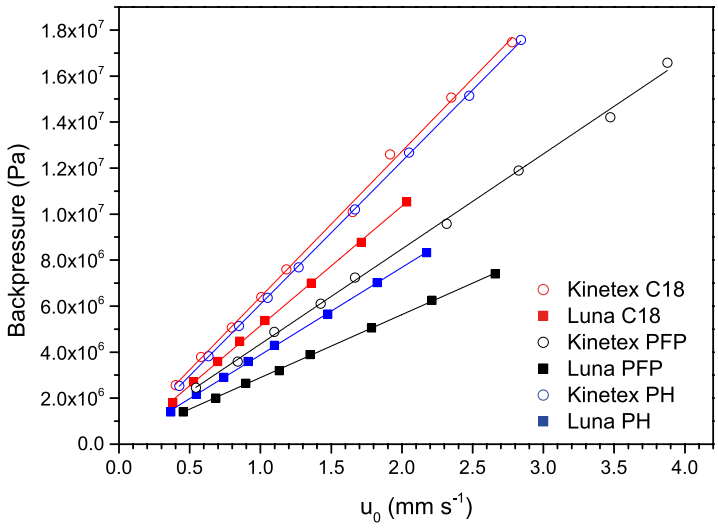

Figure 10. Evolution of the backpressures with increasing flow rates in the different chromatographic supports. Mobile phase H_2O:MeCN 55:45 v:v, 25 ºC.

since better performances are expected from columns packed with smaller particles. Furthermore, core-shell columns are a 66% shorter (150 *vs.* 50 mm long) than the fully porous ones, which reduces both their efficiencies and their working pressures. We assumed these differences because it is our purpose to compare the analytical possibilities of conventional, widely employed 5 µm fully-porous particles to those of the core-shell columns with biggest diameter available by the time our experiments started.

For these reasons, a method allowing for a realistic comparison of packed beds having different geometries and particle sizes and structures is needed. A first approach to allow such a comparison among different particle sizes involves using the reduced form of the H value, h (Eq. 9):

$$h = \frac{H}{d_p} \qquad \text{Eq. 9}$$

This way, the H_{min} values previously obtained can be normalized and made particle-size-independent (see Table 5). From these values, it could seem that the improvements in the H_{min} values obtained by the core-shell particles were only related to particle size, because their h_{min} values seem to be actually larger than the ones of the fully-porous ones (except for the case of the PH stationary phase). This apparent contradiction can be explained attending to two key considerations [74]. On one side, the h_{min} values yielded by core-shell particles decrease when longer columns are employed, because extra-column band broadening effect is reduced when the volume of the column increases [75]. Thus, extra-column contribution to the peak broadening becomes more important as the size of the columns decreases [76] and this issue is of particular relevance when the instrument is optimized but not conceived and built to minimize such effect [51]. Furthermore, it is not uncommon to observe that apparently big differences in H values become much closer after conversion into h_{min} [77]. Taking into account that the calculated H values have not been corrected for extra-column variations, it seems totally plausible to obtain the reported h_{min} values under our experimental conditions.

Reduced plate heights are still unable to allow direct comparisons among packed beds with different geometries or particle shapes. To solve this problem, the separation impedance number (E_0) has been employed for years as the ultimate figure of merit for chromatography supports [78,79]. This value, being a dimensionless number, cannot give any real idea about the speed of a separation. With the aim to provide

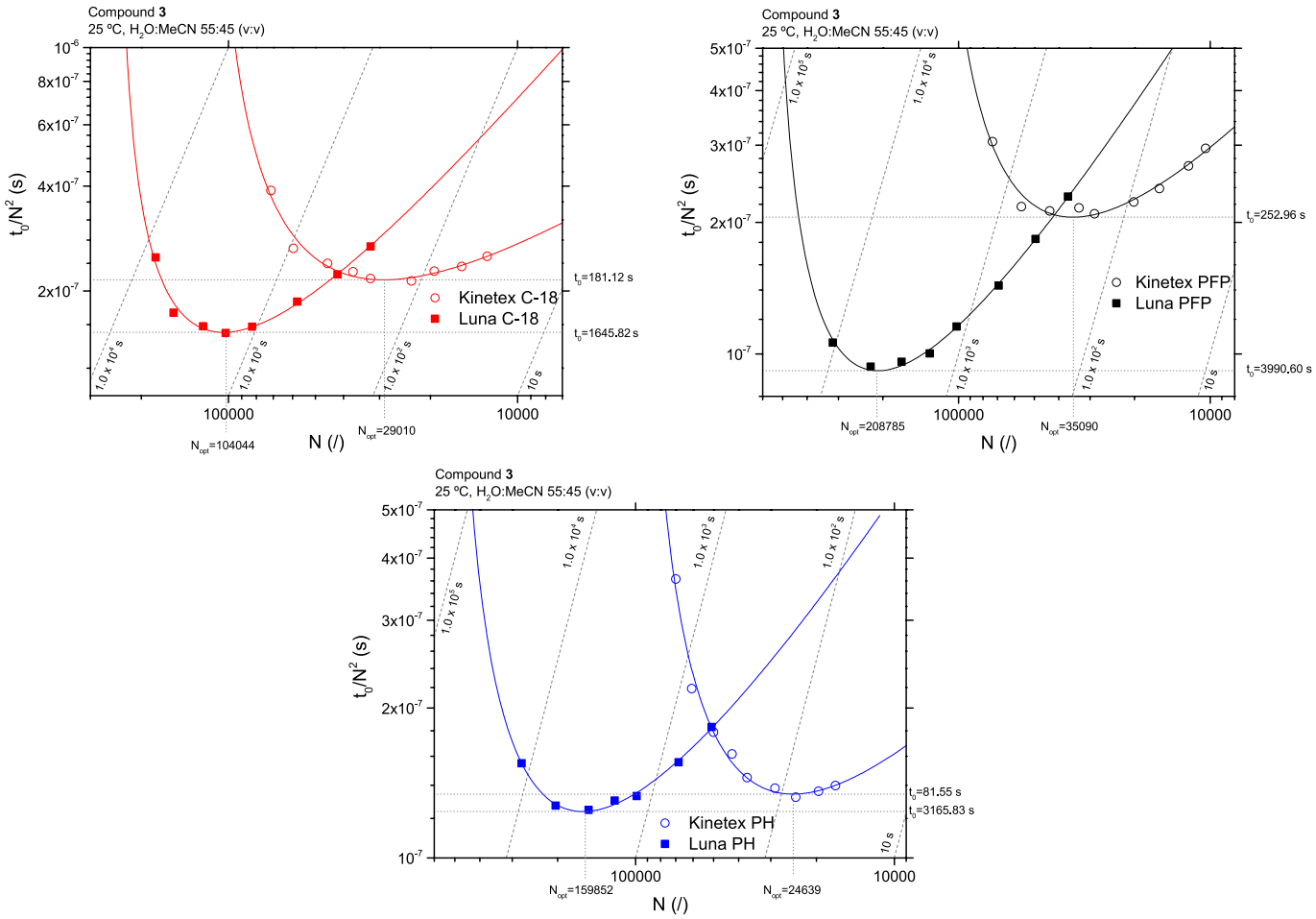

Figure 11.
Kinetic plots calculated as described in the text, showing the kinetic behaviour of the six chromatographic supports under study. Best kinetic performances are obtained when the minima of the curves are closer to the right-bottom corner of the plots, indicating better efficiencies in shorter analysis times.

an easy method allowing such kind of comparisons, kinetic plots afford a valuable tool to obtain a solution for two common chromatography optimization problems: achieving a maximal number of plates in a certain time of analysis and minimizing the time required to achieve a desired number of plates. Kinetic plots were firstly used to compare GC columns in the mid sixties, but it was decades later when Poppe laid their foundations [78]. From a practical point of view, the generation of kinetic plots required complex numerical methods until Desmet [61] proposed a clever methodology to make the calculation of N and t_0 values easily accessible. That procedure has found a widespread application since then, and it is the one that we have chosen to compare our six different supports. Plotted as t_0/N^2 *vs.* N values, with reversed x axis, these graphs resemble the typical shape of van Deemter plots, allowing for an intuitive interpretation of the data they represent.

From the kinetic plots obtained for every couple of columns with the same functionalization (Figure 11, and Table 5), it can be deduced that the optimum number of theoretical plates (N_{opt}) is 3 to 5 times smaller for the core-shell columns than the corresponding to the fully-porous ones. Interestingly, such smaller N_{opt} are achievable in a remarkably shorter analysis time (10 to 40 times). This evidence is in accordance with the well established knowledge [78,79] that shorter columns packed with smaller size particles are more appropriated for faster separations, while longer columns with larger size particles are able to reach higher N at the expense of much longer analysis times.

In our search for a fast chromatographic method, core-shell particles were a clear choice under the light of the data derived from the kinetic plots, as they had the better N_{opt} to time of analysis ratio. Among the three core-shell chemistries, C-18 gave the best relationship between N_{opt} and time of analysis. Consequently, the Kinetex C-18 column was chosen for further gradient optimization and analytical method development.

3.3. Development and validation of an analytical application

3.3.1. Optimization of the elution conditions

In a first approach, we had assayed the effect of several modifiers on the selectivity, resolution and time of analysis obtained with the Luna C-18 stationary phase under isocratic conditions. Considering that the analytes had been adequately separated on this column eluting with H_2O:MeCN 60:40 (v:v), we replaced 0, 2 and 4% of the organic fraction with tetrahydrofuran or *tert*-butyl methyl ether. As expected, the elution strength was increased, but no useful advantages were found in these experiments, as no noticeable enhancements in the separation features could be obtained. We also assayed the effect of 0.1% (v:v) formic or acetic acid on the separation, resulting in identically inappreciable enhancement of the separation.

Considering the precedent results in the aggregate, we took a different approach in our search for optimal conditions and decided to explore the possibilities of gradient elution in all of the core-shell stationary phases. We designed and tried many different gradients with the aim to adequately separate the critical pairs on PH and PFP. Unfortunately, under none of the profiles, temperatures (25-45 ºC) and flow rates (0.5-0.7 mL min^{-1}) that were tried, the resolution was improved without unacceptably affecting the efficiencies, the analysis times or the resolution of the compounds with smallest retention factors. As gradient elution on PFP and PH stationary phases did not achieve the standards we were aiming at, we focused on the C-18 colum.

Many different combinations were checked (a few of them are shown in Figure 12), and we finally opted for the linear gradient described in the Experimental Section. This gradient achieved the full resolution of all compounds in a run time as short as

Figure 12. A few representative chromatograms of several gradients assayed on the Kinetex C-18 columns, showing the effect of different profiles and flow rates on the separation.

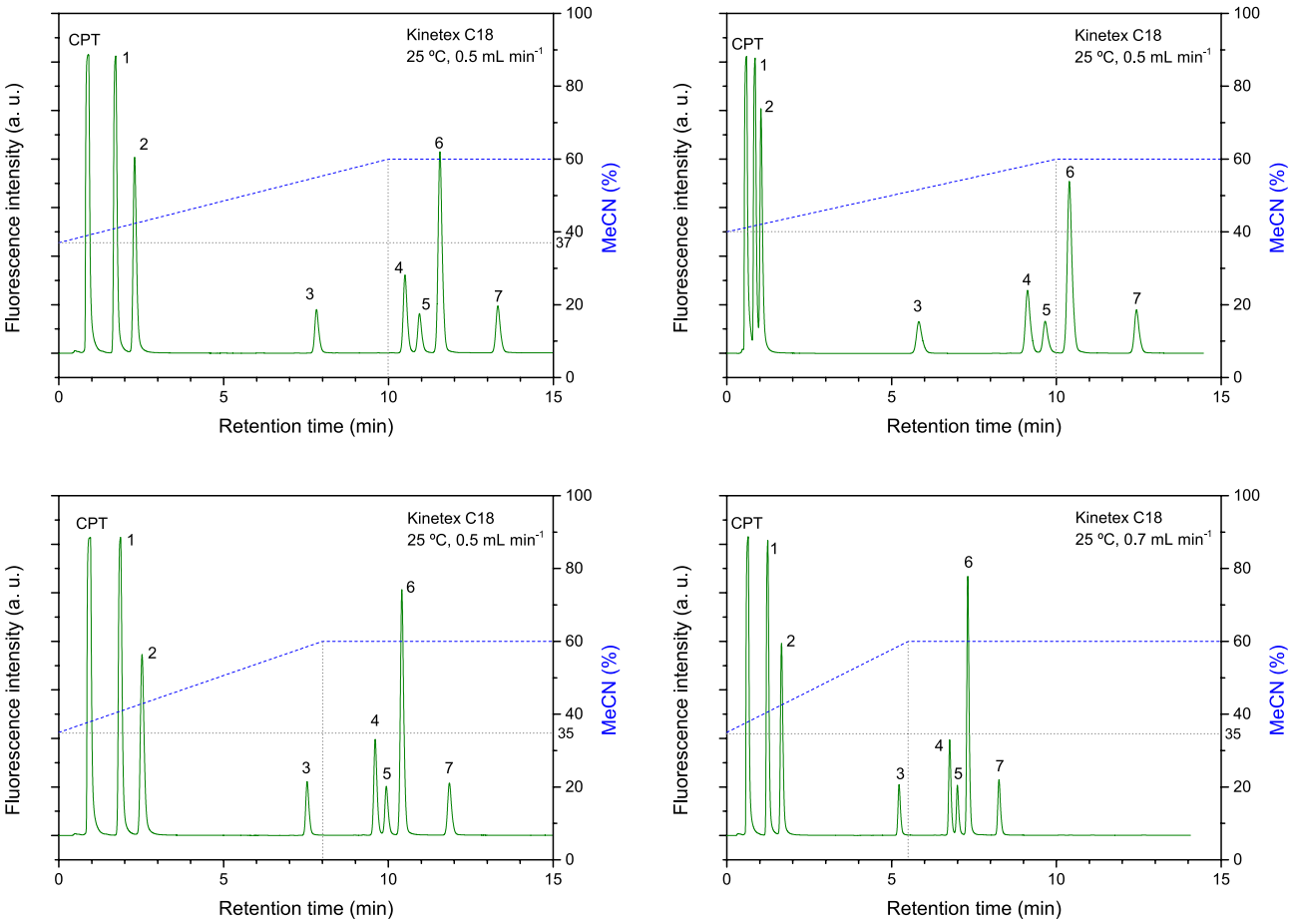

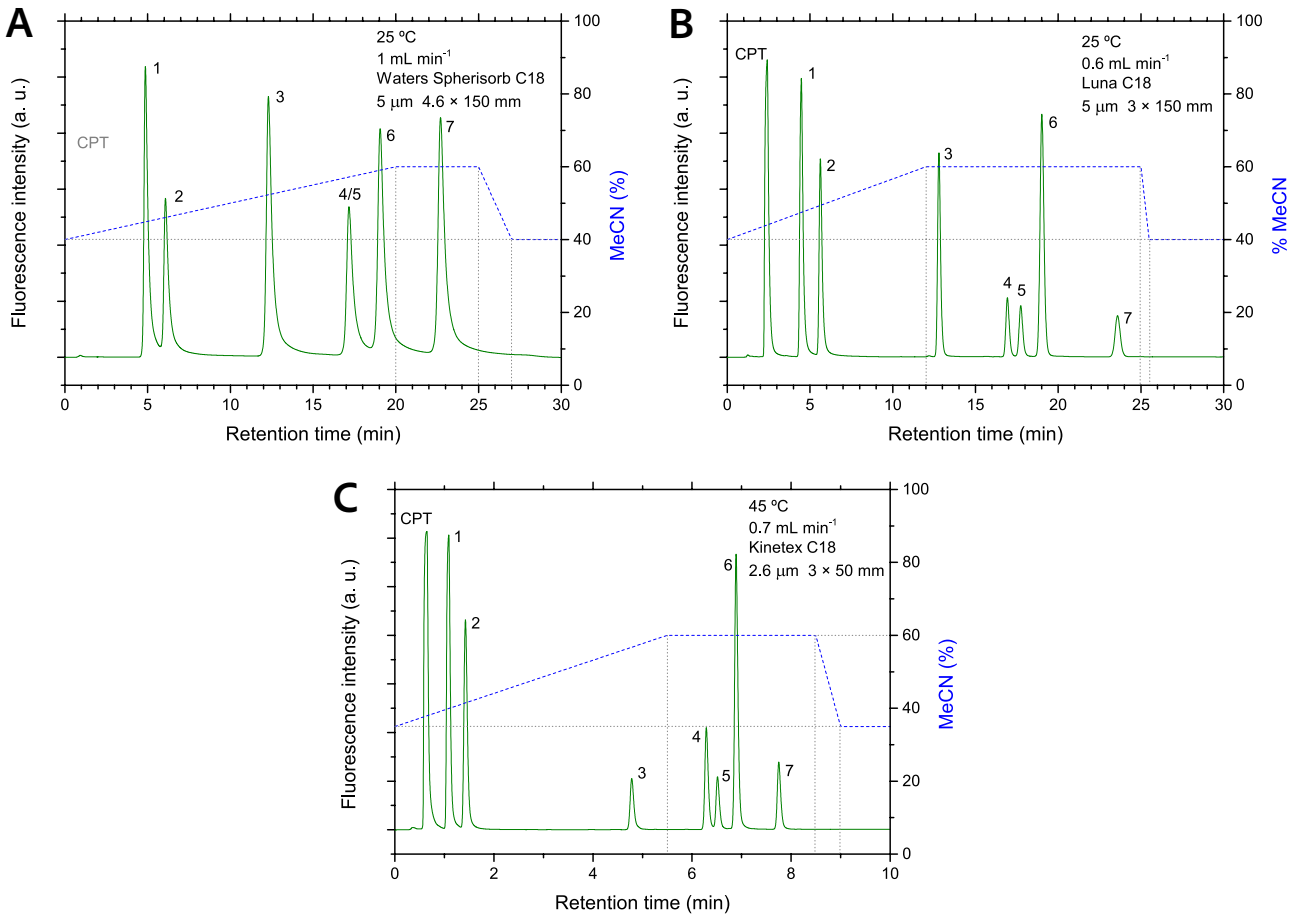

Figure 13.
Comparison of gradient elutions on different columns. (A) Waters Spherisorb C-18 (Chapter 11, p. 217, CPT was not analyzed). (B) Fully-porous Luna C-18 column. (C) Kinetex C-18 (chosen for the analyses in cell cultures).

8.5 minutes using a moderate flow rate (0.7 mL min^{-1}), thus minimizing the amount of acetonitrile required for the analysis. Compared to the previously described separation [24], this column and elution conditions was able not only to separate compounds **4** and **5**, but also shortened the analysis time and increased the efficiency and the number of peaks per time unit. Figure 13 shows the selected profile (Figure 13C) compared to the one optimized in [24] (Figure 13A) and an unoptimized gradient on the fully-porous C-18 column (Figure 13B).

3.3.2. Optimization of the sample clean-up

Acetonitrile containing 1% (v:v) HCOOH was employed as a protein-precipitant solution and to solubilize and detach the analytes from the cellular components. According to the manufacturer of the Phree plates, a sample-to-precipitant ratio of 1:4 should yield satisfactory results for most analytes and biological matrices. Nevertheless, for molecules showing a remarkable lipophilicity, such as the ones under study, ratios up to 1:9 are advised in order to improve the recoveries. From this starting point, we planned a panel of experiments aimed at discerning which ratio could better fit our analytical needs.

We checked both 1:4 (100 + 400 µL) and 1:9 (100 + 900 µL) sample-to-precipitant ratios. This was done at three concentrations of the analytes (1×10^{-6}, 1×10^{-7} and 1×10^{-8} M), and for three consecutive extractions of the same cell lysates. Our goals were: (a) recovering as much analyte as possible in one single extraction; (b) minimizing the inter-sample variability; (c) reducing the amount of organic solvent employed.

About 100 µL of the sample + precipitating mixture had been reported by the manufacturer (and confirmed by us) to remain in the well after the elution process. In

very good agreement with this data, we found that approximately a 10% of the total analyte in the case of the 1:9 ratio and a 20% in the 1:4 was not extracted in the first elution and was recovered only after a second one. In the case of the third extraction step, a negligible amount of the analytes (< 0.04% of the original amount) was found in the 1:9 eluates, even in the case of the highest concentration level assayed (1×10^{-6} M). This remnant was 10 times larger for the 1:4 ratio. All of these data pointed towards the direction that the losses due to the non-eluting volume of the wells were remarkably higher in the 1:4 than in the 1:9 ratio.

On the other hand, the reproducibility of the recoveries increased under the 1:9 ratio elution conditions. At the 1×10^{-6} M concentration level, the RSD of the recoveries of the analytes ranged from 0.04 to 0.10% with a 1:9 ratio. Instead, RSD values rose up to the 0.07 - 0.21% interval for the samples extracted using the 1:4 ratio. A similar behaviour was found at the 1×10^{-7} and 1×10^{-8} M levels.

These results, taken as a whole, led us to choose the 1:9 ratio for the final clean-up procedure. Nevertheless, this decision presented the drawback of requiring more acetonitrile. This fact not only had a worse profile from the environmental point of view, but also increased the dilution factor of the samples during the process (1:10 from cell lysate to final eluate). This undesirable problem could be circumvented by evaporating the eluate (totally or partially) prior to its HPLC analysis. Nevertheless, we discarded this option for two reasons. First, it involved one more step on the analytical process, thus going against our goal to develop a fast method amenable to automation. Second, the amount of drugs expected to be found in cell culture lysates, taking into account the cytotoxicity reported for luotonin A derivatives, is in the micromolar range [10,13, and our results in Chapter 14 of this thesis], so we preferred a clean-up method able to extend the upper limit of the dynamic range rather than the lower one. Indeed, the validated methodology keeps the door open to the possibility to evaporate the eluates with the purpose to concentrate them prior to their analysis.

With the aim to compare the results of the multi well plate clean-up procedure with those obtained with the classical MeCN precipitation + centrifugation clean-up protocol, we also processed some samples through this previously described methodology [24]. As can be appreciated in Figure 14A, comparable results are obtained. Although the non-retained peak is somewhat larger in the case of the Phree-processed samples, such fluorescence does not interfere with the quantitation of any other peaks. Taking into account the much shorter time required per processed sam-

Figure 14.
(A) Chromatograms of blank and spiked (5×10^{-8} M) samples. Comparison of deproteinization achieved by means of the conventional centrifugation method (green) or using the Phree multi-well plates (blue). (B) Chromatograms of a blank sample and samples spiked at two concentration levels and submitted to the multi-well plate deproteinization process. Chromatographic conditions are as in Figure 13C.

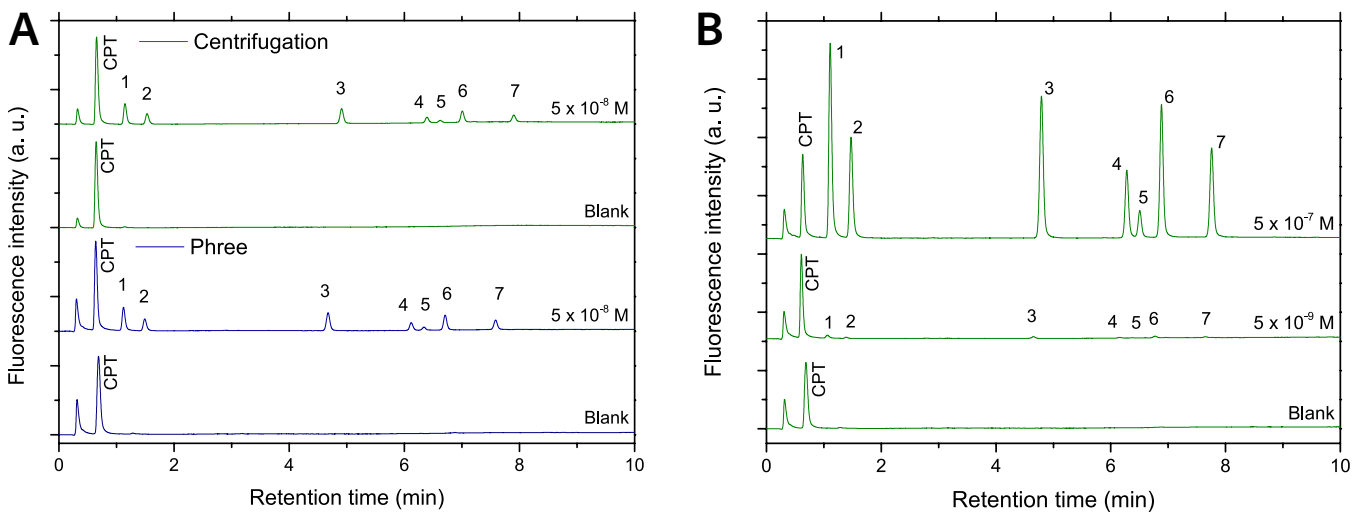

Table 6. Figures of merit of the developed analytical method.

Param.	Conc. level (M)	Compounds						
		1	2	3	4	5	6	7
R^2		0.9997	0.9998	0.9997	0.9997	0.9995	0.9997	0.9997
Slope ± SD		$4.8562 \times 10^6 \pm 3.3904 \times 10^4$	$2.7815 \times 10^6 \pm 1.6040 \times 10^4$	$4.1780 \times 10^6 \pm 2.5958 \times 10^4$	$1.8835 \times 10^6 \pm 1.1655 \times 10^4$	$7.6836 \times 10^5 \pm 6.2494 \times 10^3$	$3.8463 \times 10^6 \pm 2.5397 \times 10^4$	$2.6608 \times 10^6 \pm 2.2055 \times 10^4$
Intercept ± SD		$1.0485 \times 10^{-2} \pm 1.4399 \times 10^{-2}$	$6.6258 \times 10^{-3} \pm 6.3720 \times 10^{-3}$	$1.1779 \times 10^{-2} \pm 1.0312 \times 10^{-2}$	$-1.8121 \times 10^{-3} \pm 4.7349 \times 10^{-3}$	$-1.8620 \times 10^{-3} \pm 2.5295 \times 10^{-3}$	$-1.4310 \times 10^{-3} \pm 1.0089 \times 10^{-2}$	$-1.3139 \times 10^{-2} \pm 1.0308 \times 10^{-2}$
Accuracy (M)	5.00×10^{-9}	5.750×10^{-9}	5.233×10^{-9}	5.526×10^{-9}	5.252×10^{-9}	5.109×10^{-9}	5.173×10^{-9}	5.107×10^{-9}
	1.00×10^{-7}	1.082×10^{-7}	1.042×10^{-7}	1.097×10^{-7}	9.782×10^{-8}	9.525×10^{-8}	9.548×10^{-8}	9.492×10^{-8}
	1.00×10^{-6}	1.035×10^{-6}	1.037×10^{-6}	1.033×10^{-6}	1.054×10^{-6}	1.048×10^{-6}	1.012×10^{-6}	1.057×10^{-6}
Intra-day %RSD	5.00×10^{-9}	4.47	4.21	2.54	2.58	3.90	2.16	9.73
	1.00×10^{-7}	0.49	1.16	1.63	1.73	1.56	2.20	1.59
	1.00×10^{-6}	1.54	1.58	0.65	1.63	0.97	1.78	1.74
Inter-day %RSD	5.00×10^{-9}	5.25	3.63	2.34	4.44	6.59	5.48	9.55
	1.00×10^{-7}	4.74	5.08	1.05	4.53	5.30	3.27	4.74
	1.00×10^{-6}	3.72	3.91	1.46	2.11	1.75	3.16	2.74
LOD (M)		3.41×10^{-10}	4.08×10^{-10}	6.75×10^{-10}	4.48×10^{-10}	7.74×10^{-10}	1.26×10^{-9}	4.43×10^{-10}
LOQ (M)		1.14×10^{-9}	1.36×10^{-9}	2.25×10^{-9}	1.49×10^{-9}	2.58×10^{-9}	4.18×10^{-9}	1.48×10^{-9}

ple, the Phree plates clearly outstood as the best alternative for the rapid analysis of numerous samples.

3.3.3. Validation of the chromatographic method

When the chromatograms of the pre-treated cell lysates (Figure 14B) are compared to the ones corresponding to the compounds diluted in mobile phase (Figure 13C), it becomes clear that neither the retention times nor the resolution of the studied compounds were affected by the clean-up procedure. Eluates from blank samples chromatographed under our experimental conditions did not show any extra peaks coming from the lysates, confirming the specifity of the newly developed methodology.

The figures of merit obtained in the validation process are summarized in Table 6. The response of the method proved to be linear ($R^2 > 0.9997$ except for compound **5**, $R^2 = 0.9995$) over the whole range of concentrations assayed (1.0×10^{-6} to 5.0×10^{-10} M). The parameters of the calibration curves were calculated using the method of unweighted least squares, and showed an excellent consistency over time. The sensitivity obtained in each case was directly related to the fluorescence quantum yield of the drugs [22].

LOD were under 7.75×10^{-10} M for all of the compounds except for **6** (1.26×10^{-9} M). LOQ were lower than 2.60×10^{-9}, again, except in the case of compound **6** (4.18×10^{-9} M). These LOD and LOQ are in the same range that the ones we previously reported for serum samples [24] and far below the micromolar concentrations of the compounds in cell cultures. Although in our earlier work the reported values were slightly better, this can be explained considering a few experimental differences between both methodologies. The first one is related to the clean-up process: while in the previous method the analytes from the serum sample were preconcentrated (2×) in the pretreatment step, in the newly developed method, as it has been explained previously, they were diluted twenty times due to the elution in a larger acetonitrile volume and to the further dilution with water needed to avoid the peak shape distortion (Figure 2, p. 250). Thus, the differences in the clean-up step are responsible

for a 40× difference in the concentration of the extracts injected into the chromatograph. Therefore, the size of the sample loop accounts for an additional 4× difference between both methodologies because, as described in the Experimental section, the volume of the sample loop had been reduced from 20 to 5 µL to better fit the load capacity of the core-shell columns. This means that, considered all together, differences in sample clean-up methodology and loop size constitute a 160× drop in the amount of analytes injected into the column, and this places in an appropriate context the present LOD and LOQ limits afforded by core-shell columns.

Intra-day precisions expressed as %RSD were lower than 5.0% except in the case of compound **7** at the 5×10^{-9} M level of concentration (9.73%). Inter-day variation was below 5.5% in most cases and always under 10%. The accuracy of the method calculated as found concentration was excellent at the 1×10^{-6} and 1×10^{-7} M concentration levels, and good for the 5×10^{-9} M level except for compound **1** (15% deviation from expected concentration), which can be explained considering the closeness to the LOD and LOQ of the method.

To investigate the presence of matrix effects, the slopes of the calibration curves built using fortified cell lysates submitted to the clean-up process, and the ones obtained from clean mixtures of the compounds diluted in mobile phase, were compared by means of a Student's *t*-test. For every compound, the slopes were statistically different ($p > 0.01$), which reveals the existence of matrix effects arising from the cells and/or the extraction procedure. Such effects did not seem to appreciably affect to the quantitation of the drugs in the samples, as deduced from the good figures of merit obtained.

3.4. Comparison of the overall sustainability of the method

All features of the method were chosen bearing in mind the minimization of organic solvent and time consumption, and waste generation. Since our earlier reported method, three characteristics of the columns were improved. The first one is the choice of shorter columns with a reduced inner diameter. Compared to the previous Waters Spherisorb (4.6 × 150 mm), this allowed us to develop our separations using a lower flow rate (0.7 mL min^{-1} *vs.* 1.0 mL min^{-1}) and in a shorter time. The two other improved characteristics also accounted for this working conditions: the smaller particle size (2.6 µm *vs.* 5.0 µm) yielded better efficiencies and resolution, and the nature of the silica particles (core-shell *vs.* fully porous) made possible faster separations keeping the backpressures far below the maximum pressure allowable for conventional pumps.

Under conditions validated in the present work, the volume of MeCN employed in one chromatographic run was reduced by a 75.0% compared to the previous methodology (Table 7). Furthermore, the analysis time was shortened by more than 50.0% and compounds **4** and **5** were successfully resolved for the first time. Together with the multi-well plate clean-up methodology, a total saving of acetonitrile of 71.2% was reached together with a considerable reduction of time and energy required to an-

Table 7. MeCN required for the sample clean-up and the chromatographic analysis of one sample according to the previously described and the current methodology.

Method	Sample clean-up	Chromatographic analysis	Total
[24]	1.0 mL 0.5% CH_3COOH in MeCN / 500 uL sample	16.0 mL of MeCN	17.0 mL
Current	0.9 mL 1.0% HCOOH in MeCN / 100 uL sample	4.0 mL of MeCN	4.90 mL
Saving	10.0%	75.0%	71.2%

alyse one sample. Thus, a bird's eye view of the present multi-well plate coupled to HPLC method reveals it as a remarkable step in the direction of developing greener, more sustainable methodologies saving time and reagents and producing smaller volumes of wastes.

4. Conclusions

We have employed a family of eight structurally related compounds to explore the selectivities of two stationary phases (PFP and PH) allowing additional interactions besides the hydrophobic ones that operate in the widely employed C-18. Although several proportions of organic solvents (MeCN and MeOH), additives, temperatures and gradient profiles were assayed, only the C-18 stationary phases were able to properly resolve all of the compounds within an acceptable time of analysis. The pair of compounds **4**/**5** was poorly separated on the PFP stationary phases, and an analogue result was obtained for the **5**/**6** pair on the PH columns. These observations could be explained using the enthalpy and entropy values calculated for every compound / stationary phase combination by means of the van't Hoff plots. While the overall free energy was different for every compound in the case of the C-18 stationary phases, the values obtained for **4** and **5** on the PFP columns were almost identical. A temperature-dependent change affecting the enthalpy and the entropy values explained the improvement of the separation of **5** and **6** found above 35-40 °C on the PH columns.

By using 50 mm-long columns packed with 2.6 µm core-shell particles, we were able to develop fast separations with better efficiencies than the delivered by the 150 mm-long columns packed with 5.0 µm fully-porous particles and without remarkably raising the working backpressure. Although our chromatography system was optimized to reduce the extra-column volume, the efficiencies obtained were much lower than the ones obtained with state-of-the-art instruments designed to minimize extra-column band broadening. Although an improvement on the efficiency and the time of analysis was reached effortless, the large extra-column volume of conventional systems makes it impossible to obtain the full efficiencies delivered by small-volume columns packed with core-shell particles. Kinetic plots showed that columns packed with C-18-functionalized core-shell particles exhibited the best efficiency-to-time of analysis relationship.

Using these columns, we optimized a gradient elution profile able to successfully separate all the compounds within 8.5 minutes. We have developed an analytical application taking advantage of these good chromatographic features in combination with a clean-up step carried out using 96-well deproteinization and delipidization plates. Such pre-treatment method minimized the time consumption and is amenable for automation. The validation of the whole methodology was conducted on cell culture samples, obtaining excellent analytical figures of merit.

The newly developed methodology has reduced the analysis time by 2.6 folds compared to the previous one that our group had published, and achieves the full separation of all the compounds while reducing a 71% the amount of acetonitrile required per sample. Thus, not only the chromatographic performance has become notably improved, but also the sustainability features and throughput capacity of the whole methodology. Hopefully, this article will be useful to other chromatographists as a real-life example on how the performance of conventional HPLC systems can be improved by using core-shell technology and carrying out some inexpensive tuning of the chromatograph, without the need for high-budget investments on UHPLC systems.

5. References

1. S.H. Chen, N.-L. Chan, T.-S. Hsieh, New mechanistic and functional insights into DNA topoisomerases, Annu Rev Biochem. 82 (2013) 139–170.
2. C. Avendaño, J.C. Menéndez, Medicinal Chemistry of Anticancer Drugs, 1st ed., Elsevier, Amsterdam, 2008.
3. Y. Pommier, DNA Topoisomerases and Cancer, Springer, New York, 2012.
4. V.R. Adams, T.G. Burke, Camptothecins in Cancer Therapy, Springer, Totowa, NJ, 2005.
5. J.B. Leppard, J.J. Champoux, Human DNA topoisomerase I: relaxation, roles, and damage control, Chromosoma. 114 (2005) 75–85.
6. J.L. Liang, H.C. Cha, Y. Jahng, Recent advances in the studies on luotonins, Molecules. 16 (2011) 4861–4883.
7. V. Sridharan, P. Ribelles, M.T. Ramos, J.C. Menéndez, Cerium(IV) ammonium nitrate is an excellent, general catalyst for the Friedländer and Friedländer-Borsche quinoline syntheses: very efficient access to the antitumor alkaloid luotonin A, J Org Chem. 74 (2009) 5715–5718.
8. A. Cagir, S. Jones, B. Eisenhauer, R. Gao, S. Hecht, Synthesis and biochemical properties of E-ring modified luotonin A derivatives, Bioorg Med Chem Lett. 14 (2004) 2051–2054.
9. A. Cagir, B.M. Eisenhauer, R. Gao, S.J. Thomas, S.M. Hecht, Synthesis and topoisomerase I inhibitory properties of luotonin A analogues, Bioorg Med Chem Lett. 12 (2004) 6287–6299.
10. Ali Cagir, Shannon H Jones, Rong Gao, A. Brian M Eisenhauer, S.M. Hecht, Luotonin A. A Naturally Occurring Human DNA Topoisomerase I Poison, J Am Chem Soc. 125 (2003) 13628–13629.
11. K. Nacro, C. Zha, P.R. Guzzo, R.J. Herr, D. Peace, T.D. Friedrich, Synthesis and topoisomerase poisoning activity of A-ring and E-ring substituted luotonin A derivatives, Bioorg Med Chem Lett. 15 (2007) 4237–4246.
12. M.-C. Tseng, Y.-W. Chu, H.-P. Tsai, C.-M. Lin, J. Hwang, Y.-H. Chu, One-pot synthesis of luotonin A and its analogues, Org Lett. 13 (2011) 920–923.
13. S. Dallavalle, L. Merlini, G. Beretta, S. Tinelli, F. Zunino, Synthesis and cytotoxic activity of substituted Luotonin A derivatives, Bioorg Med Chem Lett. 14 (2004) 5757–5761.
14. S. Nussbaumer, P. Bonnabry, J.-L. Veuthey, S. Fleury-Souverain, Analysis of anticancer drugs: A review, Talanta. 85 (2011) 2265–2289.
15. M. Ramesh, P. Ahlawat, N.R. Srinivas, Irinotecan and its active metabolite, SN-38: review of bioanalytical methods and recent update from clinical pharmacology perspectives, Biomed Chromatogr. 24 (2010) 104–123.
16. J. Aaron, S. Trajkovska, Fluorescence Studies of Anti-Cancer Drugs-Analytical and Biomedical Applications, Curr Drug Targets. 7 (2006) 1067–1081.
17. E. Tsakalozou, J. Horn, M. Leggas, An HPLC assay for the lipophilic camptothecin analog AR-67 carboxylate and lactone in human whole blood, Biomed Chromatogr. 24 (2010) 1045–1051.
18. M.-T. Baylatry, A.-C. Joly, J.-P. Pelage, L. Bengrine-Lefevre, J.-L. Prugnaud, A. Laurent, et al., Simple liquid chromatography method for the quantification of irinotecan and SN38 in sheep plasma: application to in vivo pharmacokinetics after pulmonary artery chemoembolization using drug eluting beads, J Chromatogr B. 878 (2010) 738–742.
19. T. Bansal, A. Awasthi, M. Jaggi, R. Khar, S. Talegaonkar, Development and validation of reversed phase liquid chromatographic method utilizing ultraviolet detection for quantification of irinotecan (CPT-11) and its active metabolite, SN-38, in rat plasma and bile samples: Application to pharmacokinetic studies, Talanta. 76 (2008) 1015–1021.
20. M. Pistolozzi, G. Varchi, A. Degli Esposti, A. Guerrini, G. Sotgiu, M. Ballestri, et al., Camptothecin and thiocamptothecin: the role of sulfur in shifting the hydrolysis equilibrium towards the closed lactone form, ChemMedChem. 6 (2011) 1706–1714.
21. E. Badaloni, W. Cabri, A. Ciogli, I. D'Acquarica, R. Deias, F. Gasparrini, et al., Extending the use of "Inverted Chirality Columns Approach" for enantiomeric excess determination in absence of reference samples: Application to a water-soluble camptothecin derivative, J Chromatogr A. 1217 (2010) 1024–1032.
22. V. González-Ruiz, Y. González-Cuevas, S. Arunachalam, M.A. Martín, A.I. Olives, P. Ribelles, et al., Fluorescence properties of the anti-tumour alkaloid luotonin A and new synthetic analogues: pH modulation as an approach to their fluorimetric quantitation in biological samples, J Lumines. 132 (2012) 2468–2475.
23. Z. Miskolczy, L. Biczók, Effect of hydrogen bonding and complexation with metal ions on the fluorescence of luotonin A, Photochem. Photobiol. Sci. 12 (2013) 936–943.
24. V. González-Ruiz, P. Mussardo, E. Corda, S. Girotti, A.I. Olives, M.A. Martín, Liquid chromatographic analysis of the anticancer alkaloid luotonin A and some new derivatives in human serum samples, J. Sep. Sci. 33 (2010) 2086–2093.
25. S. Lee, J. Lee, Y. Jahng, T.C. Jeong, D.H. Kim, Characterization of in vitro metabolites of luotonin A in human liver microsomes using electrospray/tandem mass spectrometry, Xenobiotica. 43 (2013) 527–533.

26. A. Ahmed, W. Abdelmagid, H. Ritchie, P. Myers, H. Zhang, Investigation on synthesis of spheres-on-sphere silica particles and their assessment for high performance liquid chromatography applications, J Chromatogr A. 1270 (2012) 194–203.
27. R.G. Chaudhuri, S. Paria, Core/shell nanoparticles: classes, properties, synthesis mechanisms, characterization, and applications, Chem Rev. 112 (2012) 2373–2433.
28. F. Gritti, G. Guiochon, Mass transfer kinetics, band broadening and column efficiency, J Chromatogr A. 1221 (2012) 2–40.
29. G. Guiochon, F. Gritti, Shell particles, trials, tribulations and triumphs, J Chromatogr A. 1218 (2011) 1915–1938.
30. F. Gritti, G. Guiochon, Speed-resolution properties of columns packed with new 4.6μm Kinetex-C(18) core-shell particles, J Chromatogr A. 1280 (2013) 35–50.
31. J.M. Cunliffe, T.D. Maloney, Fused-core particle technology as an alternative to sub-2-microm particles to achieve high separation efficiency with low backpressure, J. Sep. Sci. 30 (2007) 3104–3109.
32. S. Fekete, E. Oláh, J. Fekete, Fast liquid chromatography: The domination of core–shell and very fine particles, J Chromatogr A. 1228 (2012) 57–71.
33. S. Fekete, J.-L. Veuthey, D. Guillarme, New trends in reversed-phase liquid chromatographic separations of therapeutic peptides and proteins: theory and applications, J Pharm Biomed Anal. 69 (2012) 9–27.
34. D. Guillarme, J. Ruta, S. Rudaz, J.-L. Veuthey, New trends in fast and high-resolution liquid chromatography: a critical comparison of existing approaches, Anal Bioanal Chem. 397 (2010) 1069–1082.
35. I. Ali, Z.A. AL-Othman, M. Al-Za'abi, Superficially porous particles columns for super fast HPLC separations, Biomed Chromatogr. 26 (2012) 1001–1008.
36. J.J. Salisbury, Fused-core particles: a practical alternative to sub-2 micron particles, J Chromatogr Sci. 46 (2008) 883–886.
37. G. Vinci, M.L. Antonelli, R. Preti, Rapid determination of polycyclic aromatic hydrocarbons in rainwater by liquid-liquid microextraction and LC with core-shell particles column and fluorescence detection, J. Sep. Sci. 36 (2013) 461–468.
38. J. Wu, Y. Qian, P. Mao, L. Chen, Y. Lu, H. Wang, Separation and identification of phenolic compounds in canned artichoke by LC/DAD/ESI-MS using core-shell C18 column: a comparative study, J Chromatogr B. 927 (2013) 173–180.
39. P. Chocholouš, J. Vacková, I. Šrámková, D. Šatínský, P. Solich, Advantages of core–shell particle columns in Sequential Injection Chromatography for determination of phenolic acids, Talanta. 103 (2012) 221–227.
40. M.A. Rostagno, N. Manchón, M. D'Arrigo, E. Guillamón, A. Villares, A. García-Lafuente, et al., Fast and simultaneous determination of phenolic compounds and caffeine in teas, mate, instant coffee, soft drink and energetic drink by high-performance liquid chromatography using a fused-core column, Anal Chim Acta. 685 (2011) 204–211.
41. J.M.A. Gavina, J. Priem, C.M. Wood, C.W. Xiao, Y.-L. Feng, Determination of isoflavones in rat serum using liquid chromatography-tandem mass spectrometry with a highly efficient core-shell column, Anal Bioanal Chem. 405 (2013) 2643–2651.
42. S.L. DeGrasse, J.A. DeGrasse, K. Reuter, Solid core column technology applied to HPLC-FD of paralytic shellfish toxins, Toxicon. 57 (2011) 179–182.
43. J. Ruta, D. Zurlino, C. Grivel, S. Heinisch, J.-L. Veuthey, D. Guillarme, Evaluation of columns packed with shell particles with compounds of pharmaceutical interest, J Chromatogr A. 1228 (2012) 221–231.
44. M. Dziadosz, R. Lessig, H. Bartels, Protein kinase inhibitor analysis with the core-shell separation technique, Anal Bioanal Chem. 404 (2012) 2083–2086.
45. A. Tölgyesi, V.K. Sharma, S. Fekete, D. Lukonics, J. Fekete, Simultaneous determination of eight corticosteroids in bovine tissues using liquid chromatography-tandem mass spectrometry, J Chromatogr B. 906 (2012) 75–84.
46. M.J. Roth, D.A. Plymire, A.N. Chang, J. Kim, E.M. Maresh, S.E. Larson, et al., Sensitive and reproducible intact mass analysis of complex protein mixtures with superficially porous capillary reversed-phase liquid chromatography mass spectrometry, Anal Chem. 83 (2011) 9586–9592.
47. L. Whiley, J. Godzien, F.J. Ruperez, C. Legido-Quigley, C. Barbas, In-vial dual extraction for direct LC-MS analysis of plasma for comprehensive and highly reproducible metabolic fingerprinting, Anal Chem. 84 (2012) 5992–5999.
48. S.M. Martins, T. Wendling, V.M.F. Gonçalves, B. Sarmento, D.C. Ferreira, Development and validation of a simple reversed-phase HPLC method for the determination of camptothecin in animal organs following administration in solid lipid nanoparticles, J Chromatogr B. 880 (2012) 100–107.
49. Y.-X. Zhao, J.-Q. Gao, H.-L. Qiao, H.-L. Chen, W.-Q. Liang, Development and validation of a sensitive reversed-phase HPLC method to determine intracellular accumulation of hydroxycamptothecin, J Pharm Biomed Anal. 41 (2006) 1007–1010.

50. D. Vuckovic, High-throughput solid-phase microextraction in multi-well-plate format, Trends Anal Chem. 45 (2013) 136–153.
51. S. Fekete, I. Kohler, S. Rudaz, D. Guillarme, Importance of instrumentation for fast liquid chromatography in pharmaceutical analysis, J Pharm Biomed Anal. 87 (2014) 105–119.
52. D.V. McCalley, Instrumental considerations for the effective operation of short, highly efficient fused-core columns. Investigation of performance at high flow rates and elevated temperatures, J Chromatogr A. 1217 (2010) 4561–4567.
53. A.J. Alexander, T.J. Waeghe, K.W. Himes, F.P. Tomasella, T.F. Hooker, Modifying conventional high-performance liquid chromatography systems to achieve fast separations with Fused-Core columns: a case study, J Chromatogr A. 1218 (2011) 5456–5469.
54. F. Gritti, G. Guiochon, Overload behavior and apparent efficiencies in chromatography, J Chromatogr A. 1254 (2012) 30–42.
55. D.V. McCalley, Some practical comparisons of the efficiency and overloading behaviour of sub-2 µm porous and sub-3 µm shell particles in reversed-phase liquid chromatography, J Chromatogr A. 1218 (2011) 2887–2897.
56. M.M. Fallas, S.M.C. Buckenmaier, D.V. McCalley, A comparison of overload behaviour for some sub 2 µm totally porous and sub 3 µm shell particle columns with ionised solutes, J Chromatogr A. 1235 (2012) 49–59.
57. F. Gritti, G. Guiochon, Accurate measurements of peak variances: importance of this accuracy in the determination of the true corrected plate heights of chromatographic columns, J Chromatogr A. 1218 (2011) 4452–4461.
58. A.C. Sanchez, G. Friedlander, S. Fekete, J. Anspach, D. Guillarme, M. Chitty, et al., Pushing the performance limits of reversed-phase ultra high performance liquid chromatography with 1.3µm core-shell particles, J Chromatogr A. 1311 (2013) 90–97.
59. A.C. Sanchez, J.A. Anspach, T. Farkas, Performance optimizing injection sequence for minimizing injection band broadening contributions in high efficiency liquid chromatographic separations, J Chromatogr A. 1228 (2012) 338–348.
60. F. Gritti, G. Guiochon, Accurate measurements of the true column efficiency and of the instrument band broadening contributions in the presence of a chromatographic column, J Chromatogr A. 1327 (2014) 49–56.
61. G. Desmet, D. Clicq, P. Gzil, Geometry-independent plate height representation methods for the direct comparison of the kinetic performance of LC supports with a different size or morphology, Anal Chem. 77 (2005) 4058–4070.
62. J.W. Thompson, T.J. Kaiser, J.W. Jorgenson, Viscosity measurements of methanol–water and acetonitrile–water mixtures at pressures up to 3500bar using a novel capillary time-of-flight viscometer, J Chromatogr A. 1134 (2006) 201–209.
63. European Medicines Agency, Guideline on bioanalytical method validation, 21st ed., Committee for Medicinal Products for Human Use (CHMP), European Medicines Agency, London, 2011.
64. International Conference on Harmonisation, Validation Of Analytical Procedures: Text And Methodology Q2(R1), (2007) 1–17.
65. S. Ellison, M. Thompson, Harmonized guidelines for single-laboratory validation of methods of analysis (IUPAC Technical Report), Pure Appl. Chem. 74 (2002) 835.
66. W. Zheng, S. Wang, L. Barnes, Y. Guan, E. Louis, Determination of harmane and harmine in human blood using reversed-phased high-performance liquid chromatography and fluorescence detection, Anal Biochem. 279 (2000) 125–129.
67. L.R. Snyder, J.W. Dolan, P.W. Carr, The hydrophobic-subtraction model of reversed-phase column selectivity, J Chromatogr A. 1060 (2004) 77–116.
68. C.F. Poole, The essence of chromatography, Elsevier, Amsterdam, 2003.
69. F. Gritti, G. Guiochon, Adsorption mechanisms and effect of temperature in reversed-phase liquid chromatography. meaning of the classical Van't Hoff plot in chromatography, Anal Chem. 78 (2006) 4642–4653.
70. N. Wu, Y. Liu, M.L. Lee, Sub-2 microm porous and nonporous particles for fast separation in reversed-phase high performance liquid chromatography, J Chromatogr A. 1131 (2006) 142–150.
71. F. Gritti, G. Guiochon, A chromatographic estimate of the degree of heterogeneity of RPLC packing materials. 1. Non-endcapped polymeric C30-bonded stationary phase, J Chromatogr A. 1103 (2006) 43–56.
72. D.S. Bell, H.M. Cramer, A.D. Jones, Rational method development strategies on a fluorinated liquid chromatography stationary phase: Mobile phase ion concentration and temperature effects on the separation of ephedrine alkaloids, J Chromatogr A. 1095 (2005) 113–118.
73. C.A. Doyle, T.J. Vickers, C.K. Mann, J.G. Dorsey, Characterization of C18-bonded liquid chromatographic stationary phases by Raman spectroscopy: the effect of temperature, J Chromatogr A. 877 (2000) 41–59.
74. S. Fekete, J. Fekete, The impact of extra-column band broadening on the chromatographic efficiency of 5 cm long narrow-bore very

efficient columns, J Chromatogr A. 1218 (2011) 5286–5291.

75. J.J. Destefano, T.J. Langlois, J.J. Kirkland, Characteristics of Superficially-Porous Silica Particles for Fast HPLC: Some Performance Comparisons with Sub-2-m Particles, J Chromatogr Sci. 46 (2008) 254–260.
76. S. Fekete, J. Fekete, K. Ganzler, Shell and small particles; evaluation of new column technology, J Pharm Biomed Anal. 49 (2009) 64–71.
77. F. Gritti, G. Guiochon, Comparative study of the performance of columns packed with several new fine silica particles. Would the external roughness of the particles affect column properties? J Chromatogr A. 1166 (2007) 30–46.
78. H. Poppe, Some reflections on speed and efficiency of modern chromatographic methods, J Chromatogr A. 778 (1997) 3–21.
79. J.H. Knox, Theoretical Aspects of LC with Packed and Open Small-Bore Columns, J Chromatogr Sci. 18 (1980) 453–461.

This page intentionally left blank

14

B-Ring-aryl substituted luotonin A analogues with a new binding mode to the topoisomerase 1-DNA complex show enhanced cytotoxic activity

Accepted in PLOS ONE, González-Ruiz, V., Pascua, I., Fernández-Marcelo, T., Ribelles, P., Bianchini, G., Sridharan, V., Iniesta, P., Ramos, M. T., Olives, A. I., Martín, M. A., Menéndez, J. C.

ABSTRACT ▶ Topoisomerase 1 inhibition is an important strategy in targeted cancer chemotherapy. The drugs currently in use acting on this enzyme belong to the family of the camptothecins, and suffer severe limitations because of their low stability, which is associated with the hydrolysis of the δ-lactone moiety in their E ring. Luotonin A is a natural camptothecin analogue that lacks this functional group and therefore shows a much-improved stability, but at the cost of a lower activity. Therefore, the development of luotonin A analogues with an increased potency is important for progress in this area. In the present paper, a small library of luotonin A analogues modified at their A and B rings was generated by cerium(IV) ammonium nitrate-catalyzed Friedländer reactions. All analogues showed an activity similar or higher than the natural luotonin A in terms of topoisomerase 1 inhibition and some compounds had an activity comparable to that of camptothecin. Furthermore, most compounds showed a better activity than luotonin A in cell cytotoxicity assays. In order to rationalize these results, the first docking studies of luotonin-topoisomerase 1-DNA ternary complexes were undertaken. Most compounds bound in a manner similar to luotonin A and to standard topoisomerase poisons such as topotecan but, interestingly, the two most promising analogues, bearing a 3,5-dimethylphenyl substituent at ring B, docked in a different orientation. This binding mode allows the hydrophobic moiety to be shielded from the aqueous environment by being buried between the deoxyribose belonging to the G(+1) guanine in the scissile strand and the Arg364 on the surface of the protein, and makes also possible a hydrogen bond between the D-ring carbonyl and the basic amino acid. The discovery of this new binding mode and its associated higher inhibitory potency is a significant advance in the design of new topoisomerase 1 inhibitors.

NOTE ON AUTHORSHIP: Víctor González Ruiz did not contribute to the synthesis part of the present chapter. Nevertheless, some experimental details corresponding to the synthesis of the studied compounds are reported in order to maintain the integrity of the multidisciplinary approach that drove the present work as a whole.

Ms. ID ▼
PONE-S-14-04819

ABBREVIATIONS ▼
- **CAN:** Ce(IV) ammonium nitrate
- **THF:** tetrahydrofurane
- **CPT:** camptothecin
- **DMEM:** Dulbecco's modified Eagle's medium
- **FBS:** fetal bovine serum
- **PEG:** polyethylene glycol
- **RMSD:** root-mean-square deviation

1. Introduction

Cancer continues to be one of the leading causes of death worldwide. According to the latest data from the International Agency for Research on Cancer, in 2012 there were 14.1 million new cancer cases, 8.2 million cancer deaths and 32.6 million people living with cancer (within 5 years of diagnosis). Cancer is no longer a disease of the developed world, with 57% of newly diagnosed cases of cancer and 65% of deaths being associated with less developed regions [1].

Cancer therapy is still founded on the pillars of surgery, radiotherapy and chemotherapy, with immunotherapy having recently entered the stage as a fourth approach [2]. Nevertheless, the development of new anticancer drugs continues to be essential in the fight against the disease [3].

Topoisomerases are present in all living organisms and are crucial for relieving torsional tension in supercoiled DNA in the course of DNA replication, transcription and reparation [4]. Topoisomerases, and topoisomerase 1 in particular, are among the most relevant anticancer targets [5,6].

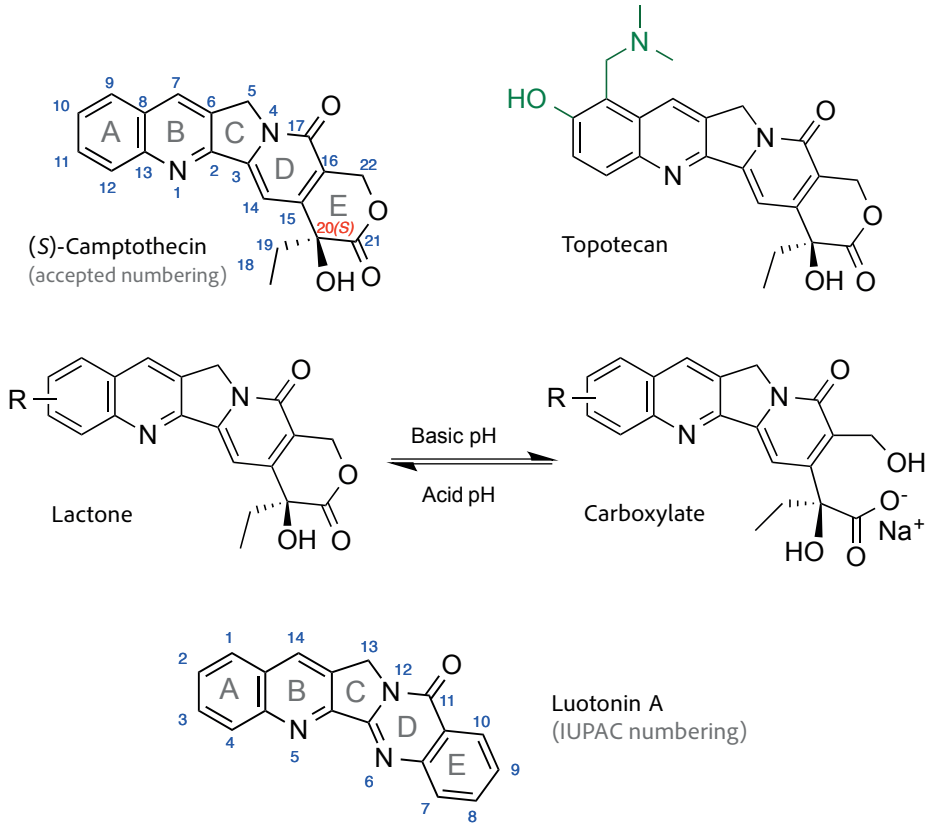

Figure 1.
Structure of representative camptothecins and luotonin A. Camptothecin is a natural topoisomerase 1 inhibitor that has been used as a lead for the development of a family of anti-cancer agents in clinical use, exemplified by topotecan. Nevertheless, the camptothecins suffer severe limitations because of their low stability, which is associated with the hydrolysis of the δ-lactone moiety in their E ring that leads to an inactive carboxylate form. Luotonin A is a plant alkaloid whose structure strongly resembles that of camptothecin but lacks the lactone moiety. The discovery that luotonin A is also a topoisomerase 1 inhibitor, although less potent than the camptothecins, provided a unique opportunity for drug discovery in the anti-cancer area.

The camptothecins, specially irinotecan, topotecan and belotecan (Figure 1), are the main family of clinically relevant topoisomerase 1 inhibitors [7]. These compounds have a planar, pentacyclic core comprising a lactone functional group in ring E and containing a stereocenter at C-20, which must be in the *S* configuration for camptothecins to be active. Their pharmacologic target is the covalent topoisomerase 1-DNA binary complex, where they can bind non-covalently at the interphase formed between both macromolecules during the enzimatic catalytic cycle. This binding stabilizes the complex and retards its dissociation, finally leading to irreversible DNA damage and cell death [6,8].

In spite of their widespread use, they show severe undesired effects, their main dose-limiting toxicities being myelosupression, diarrhea and bone marrow toxicity [9]. Another serious problem with the camptothecins is their low stability [10], which is due to the easy opening of its lactone E ring to give an inactive hydroxy acid form (camptothecin carboxylate) that is sequestered by seric albumin [11]. The lactone-hydroxy acid equilibrium is relevant to bladder toxicity, another problem associated to the clinical use of the camptothecins that is due to accumulation of the active lactone form owing to lactonization at the acidic pH of urine [12].

Against this background, camptothecin analogues lacking the lactone ring seem attractive, but during decades this structural feature was believed to be essential for activity. The discovery of the stabilization of the human topoisomerase 1-DNA covalent binary complex by the alkaloid luotonin A, closely related to the camptothecins but having an aromatic E ring, brought about a landmark change in this paradigm [13]. Furthermore, luotonin A is achiral, a feature that can be viewed as an advantage in terms of its potential role as a lead compound in drug discovery and development because it simplifies synthetic access to new analogues and their analytical control. In summary, although the potency of luotonin is much lower than that of the camp-

tothecins [14], it does provide an excellent opportunity for the discovery of improved topoisomerase 1 inhibitors.

The low potency of the natural luotonin A has prompted the synthesis and biological evaluation of a considerable number of analogues [15-18]. Nevertheless, these studies have been limited by the constraints found in known synthetic methodologies, specially in terms of A and B ring modification. Among the methods allowing access to the luotonin A framework, the Friedländer reaction between precursors corresponding to the C-D-E fragment and aromatic *o*-aminoketones or aldehydes provides the best opportunity for this type of structural manipulation. We have recently reported a protocol that improves the yields of this classical reaction by employing Ce(IV) ammonium nitrate (CAN) as a catalyst [19], and describe now its application to the synthesis of A and B ring-modified luotonin A analogues, together with studies of their activity as topoisomerase 1 poisons and cytotoxic agents.

2. Materials and methods

2.1. Synthesis

2.1.1. General experimental information

All reagents were of commercial origin (Aldrich, Fluka, Acros) and were used as received. Melting points reported in this work were measured in open capillaries. Flash chromatography was performed on silica gel (230-400 mesh) or neutral alumina having the activity grade reported in each case. ^{1}H and ^{13}C-NMR spectra were measured at 250/300 and 63/75 MHz, respectively, with a Bruker 250 and 300 MHz (Avance) instruments maintained by the CAI de Resonancia Magnética Nuclear, Universidad Complutense. $CDCl_3$ was the solvent in all cases, using the signal due to the residual non-deuterated solvent as internal standard. Chemical shifts are reported as δ values (ppm). All one- and two-dimensional NMR spectra were obtained using standard Bruker software throughout. IR spectra were recorded on a Perkin-Elmer FT-IR Paragon 1000 spectrometer in film form, prepared by evaporation of a few drops of sample solution over a sodium chloride window. Combustion elemental analyses were obtained by the CAI de Microanálisis, Universidad Complutense, using a Leco CHN 932 Elemental Analyzer.

2.1.2. Synthesis of starting 2-aminophenylketones 8

2-Aminobenzaldehyde **8a**, 2-aminoacetophenone **8b**, 2-aminobenzophenone **8c** and (4-chloro-2-amino)benzophenone **8d** were purchased from Aldrich. (5-Bromo-2-amino)benzophenone **8e** was prepared according to a literature method [20]. For preparation of compounds **8f** and **8g**, a solution of the corresponding 2-aminonitrile (5 mmol, 1 eq) in anhydrous THF (10 mL) was added dropwise over a solution of 3,5-dimethylphenylmagnesium bromide (15 mmol, 3 eq) and the reaction mixture was refluxed for 2.5 h. After cooling, the reaction mixture was slowly poured onto ice water (30 mL). A 3M aqueous solution of hydrochloric acid (21.5 mL) was then added, the mixture was stirred at room temperature for 1 h, and the organic phase was separated. The aqueous layer was extracted with ethyl ether (2 × 20 mL). The combined organic layers were washed with water (1 × 20 mL), brine (1 × 20 mL), dried over $MgSO_4$ and filtered. The filtrate was concentrated *in vacuo* and the residue was either crystallized from ethanol or purified by column chromatography on silica gel eluting with petroleum ether:ethyl acetate to give compounds **8f** or **8g**.

2.1.3. Synthesis of luotonin A and its analogues (1-7)

A solution of 1,2-dihydropyrrolo[2,1-*b*]quinazoline-3,9-dione (**9**) (1 or 1.5 eq), the corresponding aminophenone **8** (1 eq) and cerium(IV) ammonium nitrate, CAN (15 mol %) in ethanol (5 mL) was refluxed for the time period specified in each case. After completion of the reaction, as indicated by TLC, the mixture was cooled, diluted with dichloromethane (20 mL), washed with water (2 × 10 mL) and brine (1 × 10 mL), and dried over anhydrous Na_2SO_4. The solvent was evaporated under reduced pressure and the crude reaction mixture was purified by silica gel column chromatography eluting with a petroleum ether:ethyl acetate (4:1, v:v) mixture to afford compounds **1-7**. Analytical samples were recrystalized in ethanol. In two of the reactions, small amounts of intermediates **10** were also isolated.

2.2. Pharmacological studies

2.2.1. DNA relaxation assay

DNA relaxation assay was carried out to investigate the inhibitory effect of luotonin A derivatives on the activity of the human topoisomerase 1 enzyme. A final reaction volume of 20 µL containing 200 ng of pGEM-5Zf(+) plasmid (Promega, Madison, Wisconsin) in its native supercoiled form, the corresponding drug diluted in 1 µL DMSO for a final concentration of 10 µM, 1 unit of human topoisomerase 1 (Sigma-Aldrich, St. Louis, Missouri) and the enzyme reaction buffer (TopoGEN, Port Orange, Florida) was incubated over 15 minutes at 37 °C.

Control reactions containing native supercoiled and fully relaxed forms were run from a mixture containing the reaction buffer and plasmid, for the first one; and the reaction buffer, plasmid and human topoisomerase 1, for the latter.

After incubation, all the reactions were stopped by addition of a mixture of electrophoresis loading buffer and 20% SDS to yield a final 10% SDS concentration. The reaction products were loaded into a 1% agarose gel (Bio-Rad, Hercules, California) and separated for 3 h at 60 V in Tris-borate-EDTA buffer.

The gels were stained using GelRed dye (Biotium, Hayward, California) according to the manufacturer's protocol (soaking in 3× GelRed solution for 30 minutes under gentle shaking and then rinsed with water), and photographed in 254 nm UV light using a ChemiDoc XRS+ (Bio-Rad) system.

The bands were analysed using OriginPro 8.6 software (OriginLab, Northampton, Massachusetts) and the inhibitory activity of the drugs was calculated for each one as the supercoiled to unwinded bands ratio, and normalised to the activity of camptothecin (CPT) (Sigma-Aldrich, St. Louis, Missouri).

2.2.2. Cell culture and *in vitro* anti-proliferation assay

Three human cell lines were used; HeLa (cervical carcinoma), A549 (lung adenocarcinoma) and SW480 (colon adenocarcinoma) were obtained from the American Type Culture Collection (ATCC, Manassas, USA). All cell lines were seeded in 96-well plates at a density of 19000 (HeLa) and 5000 (A549 and SW480) cells/well in 200 µl of Dulbecco's modified Eagle's medium (DMEM, Life Technologies, Carlsbad, USA) supplemented with 10% fetal bovine serum (FBS) (Life Technologies). Cell cultures were maintained at 37 °C under 5% CO_2.

After 5 h, cells were treated with compounds **1**-**7**: 1 µL DMSO containing a compound to yield final concentrations of 25.0, 12.5, 6.3 and 3.1 µM per well, the final concentration of DMSO being 0.5%. Every concentration of the drugs was assayed in triplicate. In addition, every 96-well plate contained wild type cells, negative control wells (0.5% DMSO) and positive control wells containing CPT to final concentrations of 25.0 and 2.5 µM which caused 100% cell mortality. The plate was incubated for 72 h before the fixation step.

Moreover, a no-growth control 96-well plate was seeded in every experiment. The cells on this plate were allowed to adhere for 5 h as in the experiment plate and then directly fixed, dried and stored until dying as described below, with no exposure to any compound. This no-growth plate was used to calculate the cell growth in every well of the experiment plate by subtraction of the no-growth values to the 72 h time values of the experiment plate. Experiments for every cell line were performed in triplicate.

Cells were fixed by addition of 100 µL of cold 30% (w/v) trichloroacetic acid into every well and incubated at 4 °C for 1 h. Plates were then washed with water four times and dried. Protein dying was carried out with 100 µL per well of 0.057% (w/v) sulforhodamine B (Sigma-Aldrich, St. Louis, Missouri) in 1% (v:v) acetic acid, kept at room temperature for 30 minutes. After that, excess of sulforhodamine B was removed by quickly rinsing the plates four times with 1% (v:v) acetic acid. After drying, sulforhodamine B was redissolved by adding 100 µL unbuffered Tris base solution to each well and shaking for 45 minutes on a gyratory shaker. Sulforhodamine B was quantified by its absorbance measured at 510 nm [22].

2.3. Docking studies

2.3.1. Crystal structure preparation

The crystal structure of topotecan bound to the topoisomerase 1-DNA covalent complex was downloaded from Protein Data Bank (PDB code 1K4T) [23]. Its choice as the starting point was dictated by the fact that topotecan is the only camptothecin in clinical use that has been crystallized in its site of action. To prepare the crystal structure for docking, firstly an atom of Hg, a molecule of PEG and the two forms of topotecan (the closed lactone and the opened carboxylate) were deleted; later the Dockprep tool of the UCSF Chimera package [24] was used. This tool allows to automatically delete water molecules, add hydrogens to both the enzyme and the DNA, repair truncated side chains (Dunbrack rotamer library [25]) and assign Gasteiger charges with the AMBER ff12SB force field [26]. The input file for docking was generated with AutoDock Tools 1.5.6 [27]. The docking site was defined as a box with dimensions 15 ×15 × 20 Å, whose centroid was calculated using the coordinates of the closed lactone form of topotecan (x= 21.377, y= -4.068, z= 28.192 Å).

2.3.2. Ligand preparation

Individual PDB files of ligands were prepared by *ab initio* energy minimization with Spartan '10 (Wavefunction, Irvin, USA) at the 3-21G level. Hydrogens were added to all ligands and the root of torsion tree was detected. The input file for docking was generated with AutoDock Tools 1.5.6.

2.3.3. Docking studies

Docking was performed with AutoDock Vina [28] using the same parameters described above. The best pose for each ligand was selected and analyzed. To validate the docking protocol, we docked the closed lactone form of topotecan into the target binding site, after preparing both files as described above. The best resulting pose was compared with the pose of the crystal structure, and a RMSD value of 0.492 Å was calculated for the differences between the positions of the atoms in both pentacyclic scaffolds.

3. Results and discussion

3.1. Synthesis

As commented before, the planned Friedländer disconnection of the target compounds **1**-**7** required the preparation of two kinds of starting materials, compounds **8** and **9**. Compound **9**, which can be regarded as an oxidised derivative of the alkaloid vasicinone, was prepared using a literature method [29]. Some of the compounds **8**, namely **8a**-**d**, were commercially available, while access to **8e** was secured by a literature method involving the bromination of **8c** with potassium bromide under oxidative conditions [20]. Finally, compounds **8f** and **8g** were prepared by treatment of the corresponding derivatives of 2-aminobenzonitrile with 3,5-dimethylphenylmagnesium bromide followed by acidic hydrolysis (Figure 2A).

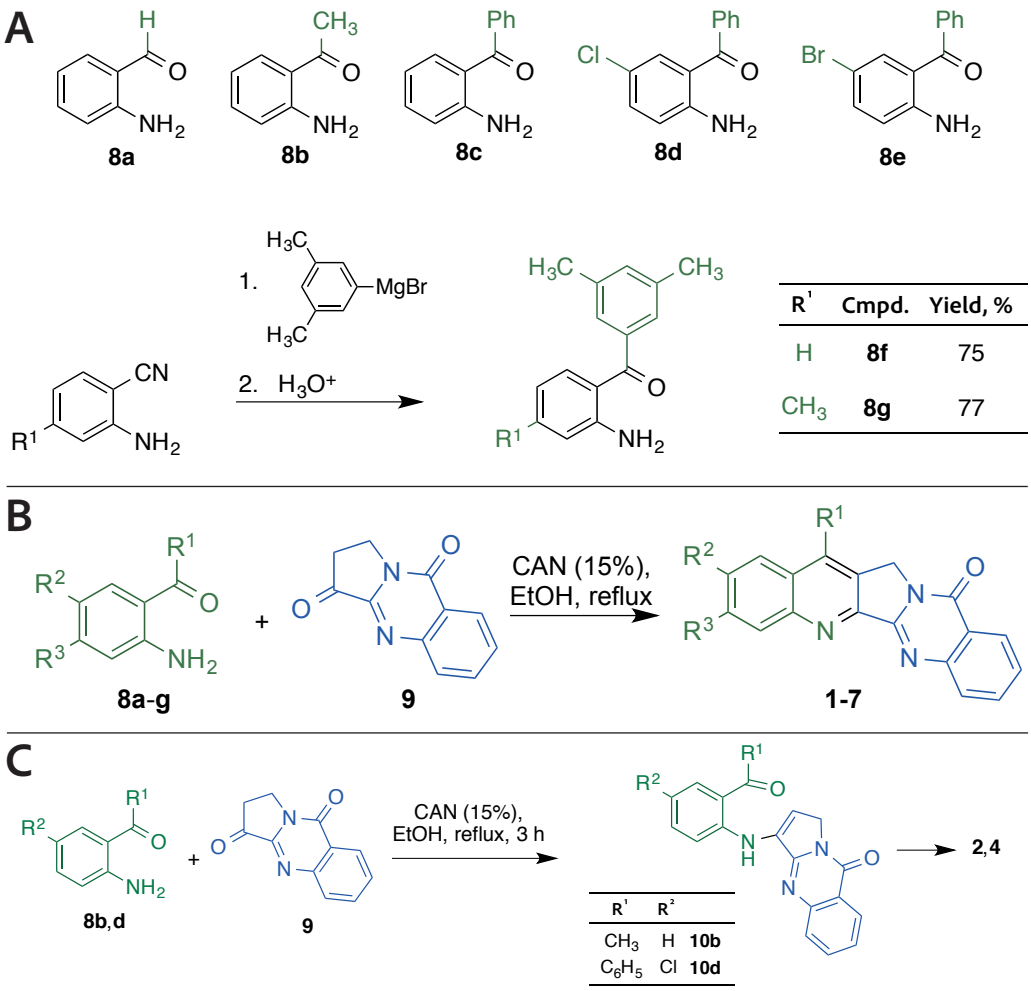

Figure 2. *Schemes on the synthesis of the luotonin A derivatives.* (A) Preparation of the synthetic precursors. **8e**, **8f** and **8g** were not commercially available. (B) The reaction between the *o*-aminocarbonyl compounds **8** and the oxidised vasicinone derivative **9** was performed in refluxing ethanol, in the presence of CAN as a Lewis acid. (C) Isolation of open luotonin analogues that behave as intermediates of the Friedländer reaction.

With compounds **8** and **9** in hand, we studied their Friedländer coupling under conditions previously established by our group [19] that involved heating of the starting materials in refluxing ethanol in the presence of CAN as a Lewis acid catalyst [30] (Figure 2B). The reaction proceeded in good to excellent yields (64-90%) and furnished a small library of luotonin analogues with a variety of substituents at the A and B rings.

During the initial optimization studies, we carried out two of the reactions for shorter reaction times (3 h) and obtained the open luotonin analogues **10**, finding subsequently that they were transformed into the corresponding final products **1**-**7** by use of longer reaction times. This result proves that compounds **10** are intermediates of the CAN-catalyzed Friedländer reaction, a conclusion that is of some mechanistic interest because there is not a general agreement on whether the Friedländer reaction is initiated by an aldol reaction or by the formation of a β-enaminone like compounds **10** (Figure 2C) [32].

3.2. DNA relaxation assay

A representative electrophoresis gel showing the separation of DNA topomers after incubation of the plasmid in the presence of human topoisomerase 1 and the inhibitors under assay is shown in Figure 3.

When normalised to the activity of CPT, luotonin A (**1**) showed a lower inhibitory activity (++), as expected. Interestingly, all the newly synthesized analogues exhibited an inhibitory activity similar or better than that of the reference compound, luotonin A (**1**). Compounds **2**, **3** and **5** exhibited an activity similar to that of **1** (++). The chlorine-containing compound **4** and the dimethylphenyl derivative **6** showed an inhibitory potential (+++) higher than the lead compound **1**. Finally, the dimethylphenyl methyl derivative **7** demonstrated an excellent activity and achieved the best poisoning capacity (++++), which was close to that of CPT. This level of potency is

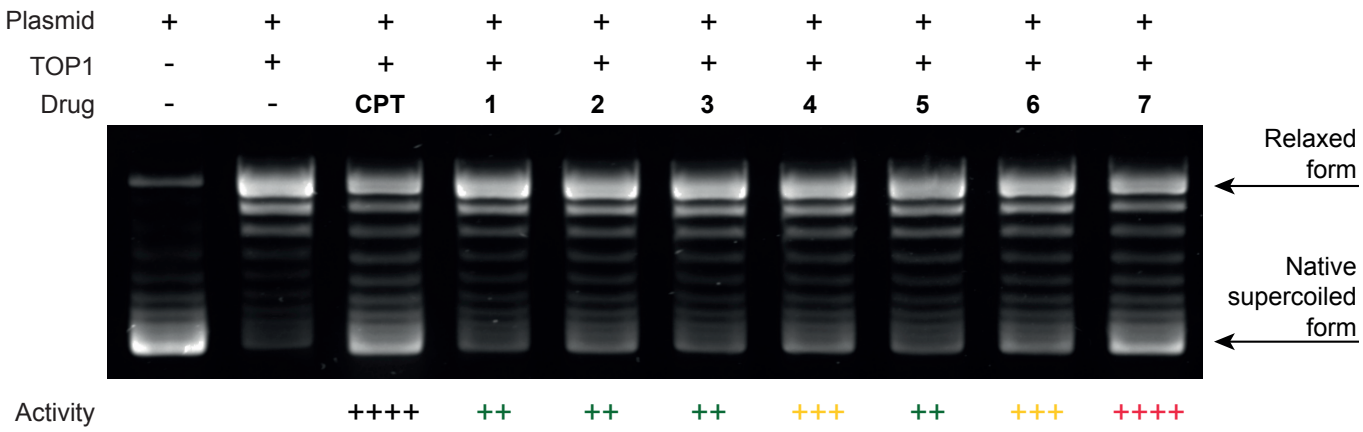

Figure 3.
DNA relaxation inhibition assay. Drug concentration was 10 μM. Activities are expressed relative to that of CPT: (+) 1-25%, (++) 26-50%, (+++) 51-75%, (++++) 76-100% of the CPT inhibition. All compounds were at least as potent as luotonin A and compound **7** showed a remarkable activity, comparable to that of CPT.

remarkable in that it has very rarely been found in the inhibition of human topoisomerase by luotonin analogues [16].

3.3. *In silico* studies

In order to rationalize the high activity as topoisomerase poisons of some of our luotonin analogues, and also with a view of using the information thus obtained for planning improved analogues in the future, we undertook *in silico* studies. There is no crystal structure available for the luotonin-DNA-topoisomerase 1 ternary complex and, furthermore, to the best of our knowledge, this is the first time that docking of luotonin A derivatives onto the DNA-topoisomerase 1 complex has been carried out. For this reason, we started this part of our work by studying the behaviour of luotonin A itself (**1**), the lead compound in this series. As shown in Figures 4A and 4B, it stacked between the base pairs (-1) and (+1) and also gave hydrogen bonding interactions between N5 and Arg364. A comparison between the docking pose of luotonin A with the crystal structure of the complex formed

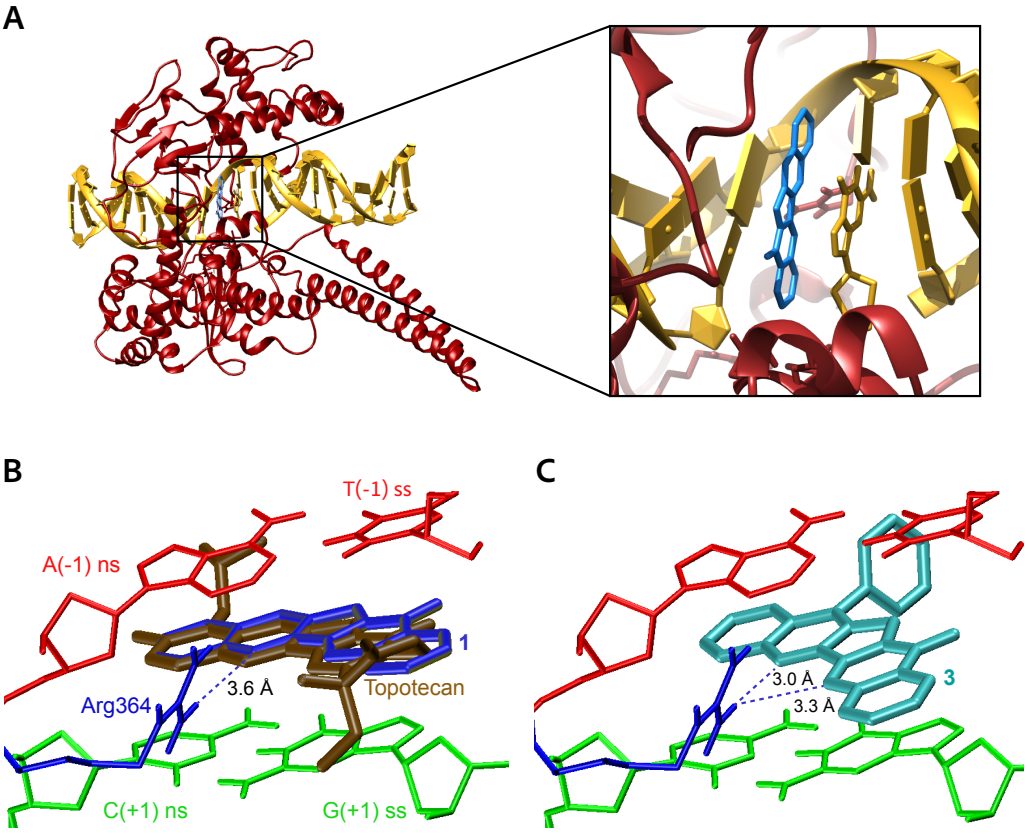

Figure 4.
*Docking of luotonin A, topotecan and compound **1**.*
(A) A full view of the topoisomerase 1-DNA complex with luotonin A docked onto the active site.
(B) Expansion of the binding site. Luotonin A (navy blue) is shown compared with the position found for topotecan (brown) by crystallography, showing an excellent concordance between both poses. The base pairs are coloured in red (-1) and green (+1). The topoisomerase Arg364 residue responsible for hydrogen bonding with the compounds is displayed in blue.
(C) Docking of compound **3**, showing the hydrogen bonding interaction of Arg364 with both nitrogens N5 and N6

Table 1. Quantification of the affinities of compounds **1**-**7** for their binding sites and its correlation with their inhibitory activity

Comp.	Score (kcal/mol)	Inhibitory activity
1	-11.4	++
2	-11.7	++
3	-11.8	++
4	-12.0	+++
5	-11.7	++
6	-13.3	+++
7	-13.7	++++
CPT	-12.4	++++
Topotecan	-12.1	N/A

by topotecan showed that the orientation of both molecules was the same. The docking of compound **3** is also shown (Figure 4C), showing a similar docking pose but a stronger interaction due to hydrogen bonding of its two nitrogen atoms, N5 and N6. This is a feature common to all our analogues, as will be discussed below.

The affinity of the examined molecules was quantified as the free-energy difference between the binary DNA-top1 complex and the ternary complexes formed upon binding of the drugs ("scores" in Table 1). Importantly, a good correlation was found between the ability of the molecules to stabilize the binary complex and their *in vitro* topoisomerase 1 inhibitory effects, as shown in Table 1. It is interesting to note that the two compounds bearing 3,5-dimethylphenyl substituents (**6** and **7**), which were the most potent of the series, were also the ones showing the highest scores.

Our docking studies revealed that the binding modes of the molecules under study could be grouped into two different types. Derivatives **1**-**5** (Figure 5A) bound the target site in the same fashion as the original crystallographic topotecan. All these compounds stacked between the (-1) and (+1) base pairs, perpendicular to the DNA main axis and with the two nitrogens at positions 5 and 6 facing the minor groove of the DNA. The aromatic rings in the pentacyclic structure established π-π stacking interactions, within a 3.6 Å range, with the four DNA bases flanking the molecule. A single direct protein-drug interaction was detected through hydrogen bonding between the Arg364 residue and the two basic nitrogen atoms in the molecule. Only in the case of halogenated compounds **4** and **5** a third class of interaction was found, as halogen bonding was possible between the chlorine or bromine atoms and the Glu356 side chain. This type of bonding is a subset of the so-called σ-hole bonds [33] and can play a significant role in molecular recognition in biological environments, as often evidenced by crystallographic studies of ligand-binding site interactions [34]. All compounds in this group pointed their E rings towards the scissile strand, although in the case of compound **2**, another pose was found with a similar score (-11.7 *vs.* -11.6 kcal/mol) that stacks the opposite way, with the A ring on the scissile strand side.

Interestingly, compounds **2**-**5** showed in all cases a better affinity ("score") than luotonin A itself in our computational studies. Upon examination of the 3D docking models, this was attributed to the fact that luotonin binds to the Arg364 residue by a single hydrogen bond by the nitrogen belonging to its quinoline fragment, while in the other cases the quinoline and quinazoline fragments are both within hydrogen bonding distance of Arg364. An overlay of all five compounds at their binding sites (Figure 5A) clearly shows that the docking pose of luotonin A is different from the others. This difference may be attributed to the steric effect of the R^1 substituent in

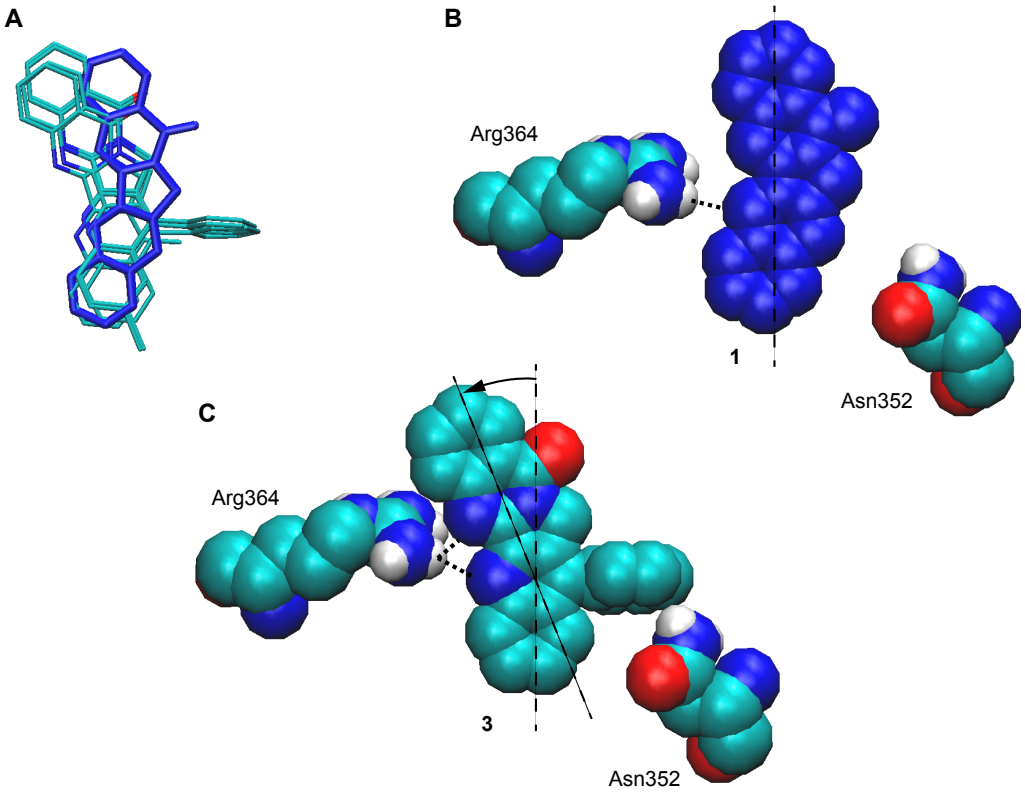

Figure 5.
B-ring substitution improves hydrogen bonding to Arg364.
(A) Overlay of luotonin A (**1**) and compounds **2**-**5** at their binding sites, showing that the presence of the substituent at the C-14 position of the B ring induces a rotation of the docking pose that leads to improved hydrogen bonding to Arg364 and hence to a better fit to the binding site.
(B) Docking of luotonin A showing the position of Asn352, which would interfere with any B ring substituent.
(C) Docking of the B-phenyl substituted compound **3**, also showing the position of Asn352.

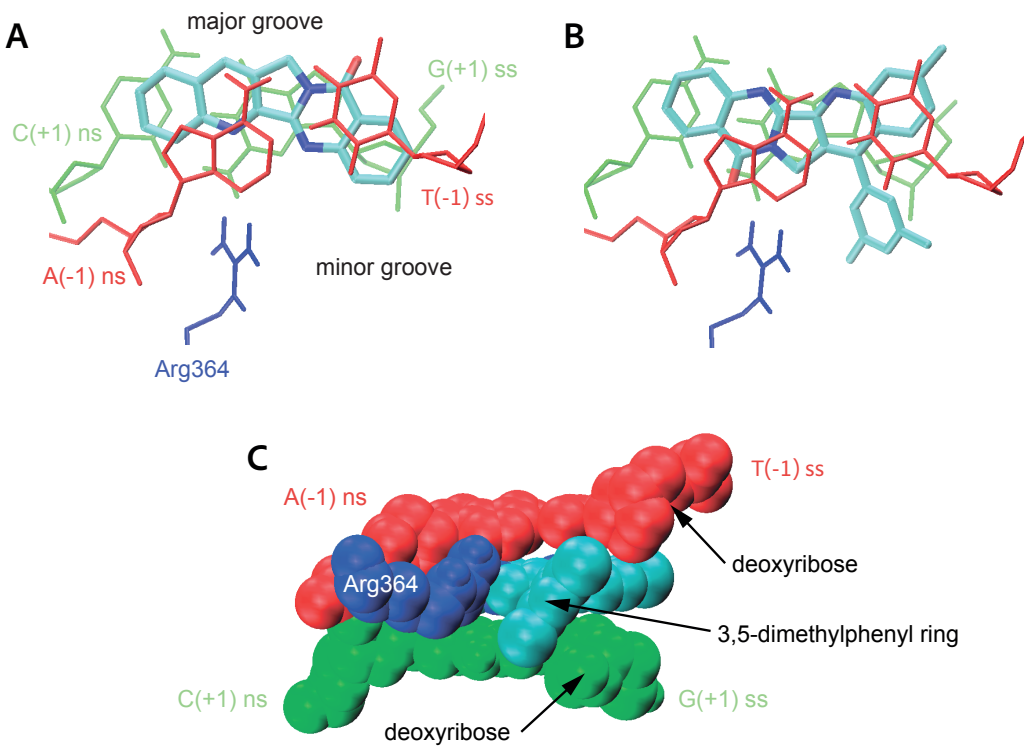

Figure 6.
*The two binding orientations of compounds **1**-**7**.*
Docking studies revealed two different modes of binding:
(A) In the case of compounds **1**-**5**, the docking pose was similar to the one found for topotecan by X-Ray crystallography.
(B) Compounds **6** and **7**, on the other hand, changed their mode of binding in order to shield the highly hydrophobic dimethylphenyl moiety from the aqueous environment by burying it between the base pairs of the scissile strand and the surface of the protein.
(C) Detail of the newly described binding feature of the human topoisomerase 1-DNA complex uncovered by our study.

compounds **2**-**5**, which would give repulsive interactions with Asn352 if their binding poses were superimposable with that of luotonin A (Figures 5B and 5C).

Compounds **6** and **7** showed a different binding mode (Figure 6B). Both molecules stacked between the (-1) and (+1) base pairs, but the orientation of the rings was modified. Both molecules bear a 3,5-dimethylphenyl substituent at the C-14 position of

Table 2. Quantification of the affinities of compounds **1**-**7** for their binding sites and its correlation with their inhibitory activity.

Comp.	H-bonding interactions	Stacking interactions
1	N5/Arg364 (3.6 Å)	Ring D,E/G(+1) (3.6 Å)
2	N5/Arg364 (2.5 Å) N6/Arg364 (2.7 Å)	Ring D,E/A(-1) (3.4 Å) Ring D,E/G(+1) (3.5 Å)
3	N5/Arg364 (3.0 Å) N6/Arg364 (3.3 Å)	Ring A,B/G(+1) (3.6 Å)
4[a]	N5/Arg364 (3.0 Å) N6/Arg364 (3.4 Å)	Ring A,B/A(-1) (3.6 Å) Ring A,B/G(+1) (3.5 Å)
5[b]	N5/Arg364 (3.1 Å) N6/Arg364 (3.5 Å)	Ring A,B/A(-1) (3.6 Å) Ring A,B/G(+1) (3.5 Å)
6	Carbonyl/Arg364 (1.9 Å)	Ring A,B/T(-1) (3.6 Å) Ring A,B/G(+1) (3.4 Å) Ring D,E/A(-1) (3.5 Å) Ring D,E/C(+1) (3.6 Å)
7	Carbonyl/Arg 364 (1.9 Å)	Ring A,B/T(-1) (3.6 Å) Ring A,B/G(+1) (3.4 Å) Ring D,E/A(-1) (3.5 Å) Ring D,E/C(+1) (3.6 Å)

Halogen bonds were found in these cases: [a] Cl – Glu356 (3.1 Å); [b] Br – Glu356 (3.1 Å).

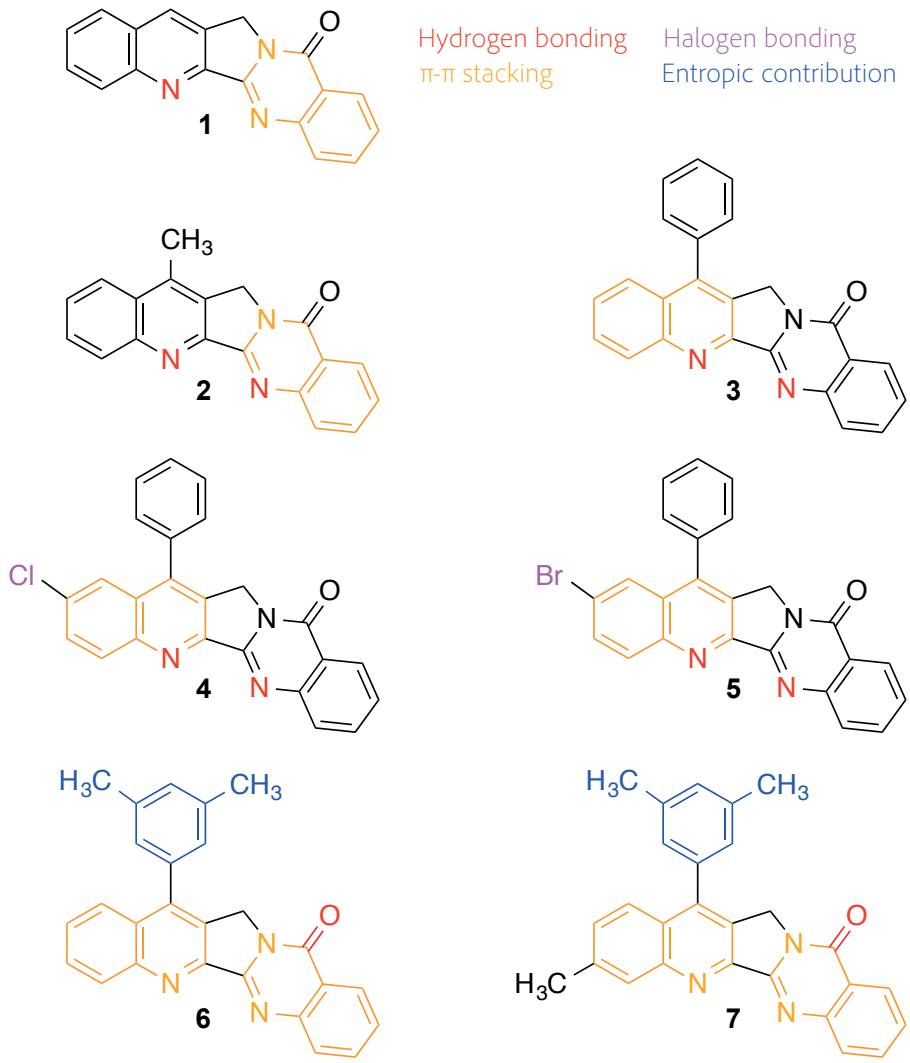

Figure 7. *Interaction sites ef every compound with the binary complex.* Compounds **1** and **3** stablish stacking interactions with DNA bases through one side of their aromatic rings only. The other compounds interact through both sides.

ring B that confers them a high lipophilicity [35]. Although the topotecan-like binding mode previously described allows the accommodation of large groups on position 14 of the luotonin B ring [36], nevertheless such substituents remain exposed to the highly polar environment. In this regards, it is worth noting that solvent accessible surface area for compounds **6** (530.45 Å^2) and **7** (562.76 Å^2) is at least 10% higher than the values calculated for the other luotonin derivatives [37]. The binding mode of **6** and **7** almost totally shields the hydrophobic dimethylphenyl moiety from the aqueous environment by burying it between the base pairs of the scissile strand and the surface of the protein, more specifically between Arg364 and the deoxyriboses belonging to G(+1) and T(-1). This minimizes the entropic effect of an ordered layer of water molecules covering the dimethylphenyl moiety [38] and enhances the stability of the ternary complex (Figure 6C). As a consequence of this binding mode, the hydrogen bonds between the basic nitrogens and Arg364 are lost. Nevertheless, this is compensated by the formation of a new, shorter hydrogen bond between the D-ring carbonyl and the basic amino acid. The dimethylphenyl group ceases to be orthogonal to the pentacyclic system in order to achieve a better fit with this binding pocket.

The main ligand-binding site interactions found in our docking studies are summarized in Table 2 and Figure 7.

3.4. Cell culture and *in vitro* anti-proliferation assays

The *in vitro* cytotoxic activity of the studied compounds was deduced from the percentage of cell growth observed when several cell cultures were exposed to 25 μM drug concentration, normalized with regard to the negative control (DMSO-treated), with the results shown in Figure 8. In the case of HeLa cells, cell growth reached an 80.3 ± 5.1% (mean ± standard error) in the presence of the reference compound luotonin A (**1**). The mean growth of the cells in the presence of the **2**-**7** derivatives was compared to that of compound **1**, in search for statistically significant differences. All the derivatives except **3** (91.2 ± 4.9%, $p = 0.038$) showed a higher cytotoxicity than luotonin A, being particularly remarkable the results of compounds **6** (37.1 ± 3.4%, $p < 0.001$) and **7** (49.3 ± 3.1%, $p < 0.001$).

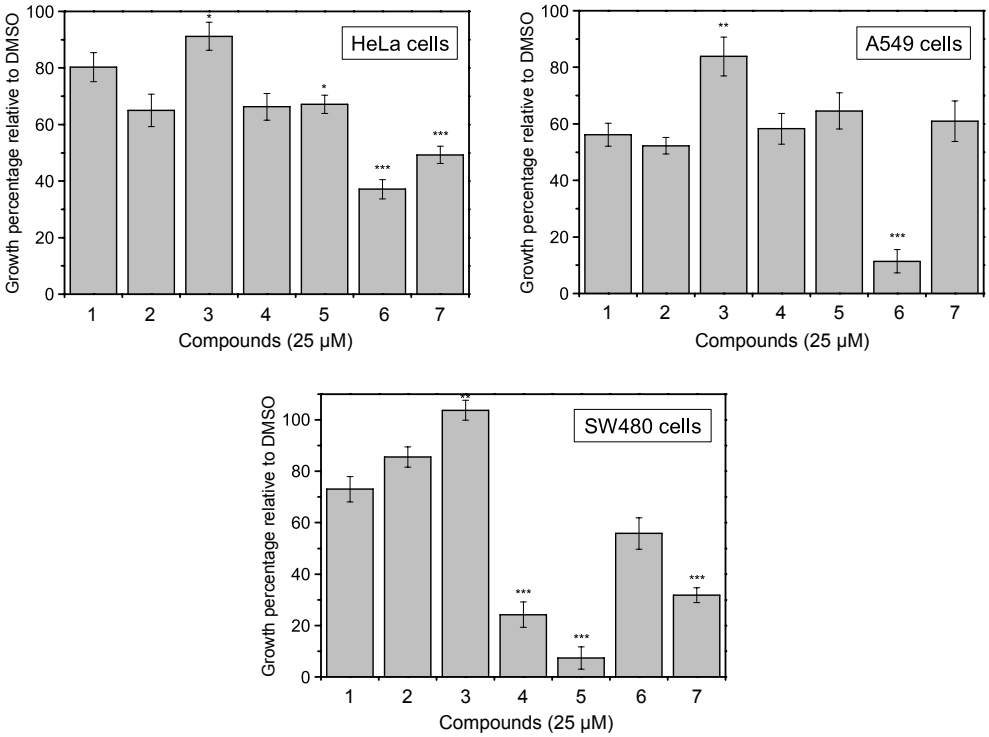

Figure 8.
Results of the citotoxicity assays. The cytotoxicities of compounds **1**-**7** are expressed as percentage of cell growth relative to the negative control. Error bars account for the standard error. Asterisks indicate statistically significant differences between a drug and the model compound **1**. CPT was employed as a positive control (0% growth) at 25 and 2.5 μM concentrations.

A similar profile was obtained in the case of lung adenocarcinoma A549 cells. All compounds showed a higher inhibitory effect in this culture than in HeLa cells, including luotonin A (56.2 ± 4.0%). Compound **3** was again the one with the lowest inhibitory activity (83.8 ± 6.8%, $p = 0.004$). On the other hand, compound **6** continued to be the most cytotoxic molecule, leading to a cell growth as low as 11.4 ± 4.1% ($p < 0.001$).

Interestingly, the tested compounds showed a different inhibition pattern in the case of SW480 (colon adenocarcinoma) cells. In this cell line, the largest inhibitory effect was exerted by compounds **4** (24.2 ± 4.9%), **5** (7.3 ± 4.3%) and **7** (31.8 ± 2.9%) all of them with a p value < 0.001 with respect to luotonin A (73.02 ± 4.9%). Taken in the aggregate, these results unveil a selectivity inhibitory activity pattern of the halogenated derivatives **4** and **5** against the colon adenocarcinoma cell line and of compound **6** against the lung adenocarcinoma cell line. This is an interesting feature, since a high potency against all cell lines is usually regarded as a proof of indiscriminate toxicity and therefore as an undesirable property.

The fact that the topoisomerase inhibition data showed a less than perfect correlation with the cytotoxicity results can be attributed to the participation in the latter of physicochemical characteristics and pharmacokinetic phenomena such as solubility and transport across membranes.

When examined together with the results from the topoisomerase 1 inhibition assay, the outcome from the cell cytotoxicity experiments supports the conclusion that compounds **6** and **7** are the most promising therapeutic candidates, showing a much higher potency than the reference luotonin A in the three cell lines assayed. Also compounds **4** and **5**, which showed a moderate activity in the topoisomerase 1 inhibition experiments, have been revealed as interesting alternatives, with good results in the colon adenocarcinoma cell line. The high selectivity of these chloro- and bromo- derivatives towards SW480 cells is remarkable and shall be the subject of further research.

4. Conclusions

The CAN-catalyzed Friedländer reaction provides a reliable and efficient method for the synthesis of luotonin A analogues modified at their A and B rings. All analogues showed an activity similar or higher in topoisomerase 1 inhibition in comparison to the reference compound luotonin A, and some compounds even had an activity comparable to camptothecin, which is an unusually good result for series of analogues of this alkaloid. Furthermore, almost all compounds showed a better activity than luotonin A in cell cytotoxicity assays. In order to rationalize these results, docking studies of luotonin A-topoisomerase 1-DNA ternary complexes were undertaken for the first time, and led to the conclusion that most compounds bound in a manner similar to standard topoisomerase poisons such as topotecan and also to luotonin A, although the presence of the substituent at the C-14 position of ring B induced in most cases a better fit to the binding site due to improved hydrogen bonding to Arg364. Interestingly, the two most promising compounds, bearing a 3,5-dimethylphenyl substituent at ring B, docked in a different orientation, with this hydrophobic moiety shielded from the aqueous environment by being buried between the deoxyribose belonging to the G(+1) in the scissile strand and the Arg364 on the surface of the protein, additionally forming a hydrogen bond between the D-ring carbonyl and the basic amino acid (Figure 9). The discovery of this new binding mode and its associated higher inhibitory potency is a significant advance that will find application in the design of new topoisomerase 1 inhibitors.

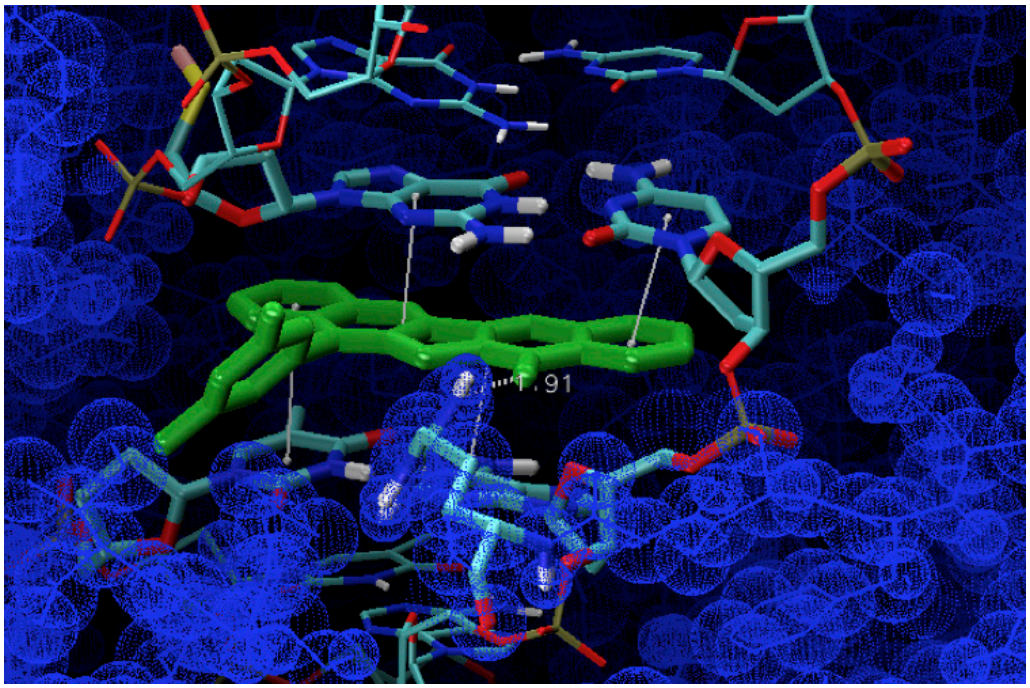

Figure 9.
*Molecular model of the binding mode of **6** to the topoisomerase 1-DNA complex..*

5. References

1. Ferlay J, Soerjomataram, Ervik M, Dikshit R, Eser S, Mathers C, Rebelo M, Parkin DM, Forman D, Bray, F. GLOBOCAN 2012 v1.0, Cancer incidence and mortality worldwide: IARC CancerBase No. 11 [Internet]. Lyon, France: International Agency for Research on Cancer; 2013. Available from: http://globocan.iarc.fr, accessed on 22/01/2014.
2. Levin B, Boyle P (Eds.) (2008) World cancer report. Lyon: International Agency for Research on Cancer, WHO Press.
3. Avendaño C, Menéndez JC (2008) Medicinal chemistry of anticancer drugs. Amsterdam: Elsevier.
4. Chen SH, Chan NL, Hsieh TS (2013) New mechanistic and functional insights into DNA topoisomerases. Ann Rev Biochem 82: 139–170.
5. Pommier Y (2011) DNA topoisomerases and cancer. New York: Springer.
6. Pommier Y (2013) Drugging topoisomerases: Lessons and challenges. ACS Chem Biol 8: 82-95.
7. Kacprzak KM (2013) Chemistry and biology of camptothecin and its derivatives, in Ramawat KG, Mérillon JM (Eds.) Natural Products (pp. 643–682). Heidelberg, Berlin: Springer.
8. Castelli S, Coletta A, D'Anness, I, Fiorani P, Tesauro C, Desideri A (2012) Interaction between natural compounds and human topoisomerase 1. Biol Chem 393:1327–1340
9. Venditto VJ, Simanek EE (2010) Cancer therapies utilizing the camptothecins: a review of the in vivo literature. Mol Pharmaceutics 7:307–349.
10. Pommier Y (2009) DNA topoisomerase 1 inhibitors: Chemistry, biology, and interfacial inhibition. Chem Rev 109: 2894–2902.
11. Marszałł, M. P., Buciński, A., Kruszewski, S., & Ziomkowska, B. (2011). A new approach to determine camptothecin and its analogues affinity to human serum albumin. J Pharm Sci 100:1142–1146.
12. Pizzolato JF, Saltz LB (2003) The camptothecins. Lancet 361: 2235–2242.
13. Cagir A, Jones SH, Gao R, Eisenhauer BMA, Hecht SM (2003). Luotonin A. A naturally occurring human DNA topoisomerase 1 poison. J Am Chem Soc 125: 13628–13629.
14. Dallavalle S, Merlini L, Beretta G, Tinelli S, Zunino F (2004). Synthesis and cytotoxic activity of substituted luotonin A derivatives. Bioorg Med Chem Lett 14: 5757–5761.
15. Liang JL, Cha HC, Jahng Y (2011) Recent advances in the studies on luotonins. Molecules 16: 4861–4883.
16. Tseng MC, Chu YW, Tsai HP, Lin CM, Hwang J, Chu YH (2011). One-pot synthesis of luotonin A and its analogues. Org Lett 13: 920–923.
17. Boisse T, Gavara ., Gautret P, Baldeyrou B, Lansiaux A et al (2011) Toward new camptothecins. Part 7: Synthesis of thioluotonine and its 5-methoxycarbonyl derivative. Tetrahedron Lett 52: 1592–1596
18. Golubev AS, Bogomolov VO, Shidlovskii AF, Dezhenkova LG, Peregudov AS et al (2011) Synthesis of fluoromethyl-containing analogs of antitumor alkaloid luotonin A. Russ Chem Bull, Int Edition 59: 209—218,
19. Sridharan V, Ribelles P, Ramos MT, Menéndez JC (2009) Cerium(IV) ammonium nitrate is an

excellent, general catalyst for the Friedländer and Friedländer-Borsche quinoline syntheses: Very efficient access to the antitumor alkaloid luotonin A. J Org Chem 74: 5715–5718.

20. Atechian S, Nock N, Norcross RD, Ratni H, Thomas, AW et al (2007) New vistas in quinoline synthesis. Tetrahedron 63:2811-2823.
21. Ma ZZ, Hano Y, Nomura T, Chen YJ (1997) Two new pyrroloquinazolino-quinoline alkaloids from Peganum nigellastrum. Heterocycles 46: 541-546.
22. Vichai V, Kirtikara K (2006) Sulforhodamine B colorimetric assay for cytotoxicity screening. Nature Protocols 1:1112–1116.
23. Staker BL, Hjerrild K, Feese MD, Behnke CA, Burgin AB, Stewart L (2002) The mechanism of topoisomerase 1 poisoning by a camptothecin analog. Proc Natl Acad Sci USA 99:15387–15392.
24. Pettersen EF, Goddard TD, Huang CC, Couch GS, Greenblatt DM, Meng EC, Ferrin TE (2004) UCSF Chimera - A visualization system for exploratory research and analysis. J Comput Chem 25:1605-1612.
25. Dunbrack Jr RL (2002) Rotamer libraries in the 21st century. Curr Opin Struct Biol 12:431-440
26. Wang J, Wang W, Kollman PA, Case DA (2006) Automatic atom type and bond type perception in molecular mechanical calculations. J Mol Graph Modelling 25:247-260.
27. Morris GM, Huey R, Lindstrom W, Sanner MF, Belew RK et al (2009) AutoDock4 and AutoDockTools4: automated docking with selective receptor flexiblity. J Comput Chem 16:2785-2791.
28. Trott O, Olson AJ (2010) AutoDock Vina: improving the speed and accuracy of docking with a new scoring function, efficient optimization and multithreading. J. Comput Chem 31:455-461
29. Molina P, Tárraga A, González-Tejero A (2000) A convenient divergent approach to the alkaloids isaindigotone and luotonin A. Synthesis 1523-1525.
30. Sridharan V, Menéndez JC (2010) Cerium(IV) ammonium nitrate as a catalyst in organic synthesis. Chem Rev 110:3805–3849.
31. Rahman AFMM, Kim DH, Liang JL, Lee ES, Na Y et al (2008) Synthesis and biological properties of luotonin A derivatives. Bull Kor Chem Soc 29:1988-1992.
32. Marco JL, Pérez-Mayoral E, Samadi A, Carreiras MC, Soriano E (2009) Recent advances in the Friedländer reaction. Chem Rev 109: 2652-2671.
33. Politzer P, Murray JS, Clark T (2013) Halogen bonding and other σ-hole interactions: A perspective. Phys Chem Chem Phys 15:11178-11189.
34. Howard EI, Sanishvili R, Cachau RE, Mitschler A, Chevrier B et al (2004) Ultrahigh resolution drug design I: Details of interactions in human aldose reductase-inhibitor complex at 0.66 Å. Prot Struct* Funct Bioin, 55:792-804.
35. González-Ruiz V, Mussardo P, Corda E, Girotti S, Olives AI, Martín MA (2010) Liquid chromatographic analysis of the anticancer alkaloid luotonin A and some new derivatives in human serum samples. J Sep Sci 33:2086–2093.
36. Verma RP, Hansch C (2009) Camptothecins: A SAR/QSAR study. Chem Rev 109:213–235.
37. www.chemicalize.org, accessed 22/01/2014.
38. Wadkins RM, Bearss D, Manikumar G, Wani MC, Wall ME, von Hoff DD (2004) Topoisomerase 1-DNA complex stability induced by camptothecins and its role in drug activity. Curr Med Chem-Anti-Cancer Agents 4:327–334.

PARTE 4

Perspectivas de futuro y Conclusiones

Esta página se ha dejado en blanco intencionadamente.

Perspectivas de futuro

Los resultados obtenidos con el uso de ciclodextrinas como modificadores de las fases móviles han demostrado que este recurso permite reducir la proporción de disolvente orgánico en la fase móvil de forma muy significativa gracias al acortamiento de los índices de retención. Por otro lado, las buenas características cromatográficas de las fases estacionarias basadas en partículas "core-shell" hacen evidente que son la base sobre la que la evolución de los lechos cromatográficos se desenvolverá en los próximos años.

Dado que las presiones de trabajo generadas en este tipo de columnas son significativamente menores que lo que cabría esperar para el diámetro de las partículas, las separaciones en las que se combinen fases estacionarias "core-shell" y ciclodextrinas como aditivos de las fases móviles constituyen uno de los retos más atractivos a abordar en nuestra línea de trabajo hacia una química analítica cada vez más sostenible.

Con el fin de poder lograr un diseño óptimo de las condiciones cromatográficas, es necesario llevar a cabo un estudio más detallado de la naturaleza de los complejos de inclusión formados por las ciclodextrinas con los derivados de la luotonina A y con la camptotecina. En este sentido, hemos comenzado por el estudio de la preparación de los complejos de inclusión en diferentes condiciones experimentales y su estudio mediante espectrofluorimetría y resonancia magnética nuclear (^{13}C y ^{1}H).

Puesto que tanto la camptotecina como la luotonina A y sus derivados presentan un equilibrio de transferencia de protón en estado excitado sensible al entorno, un recurso útil para poner de manifiesto la formación de los complejos de inclusión es estudiar cómo este equilibrio se altera como consecuencia de la inclusión de las moléculas en las cavidades de las ciclodextrinas (Figuras 1 y 2).

Con la finalidad de conocer la geometría de los complejos de inclusión, resulta de especial utilidad la información aportada por las técnicas de RMN. La magnitud de las variaciones de los desplazamientos químicos de los átomos de H o de C de la molécula incluida será consecuencia de la proximidad entre esos átomos y los de las

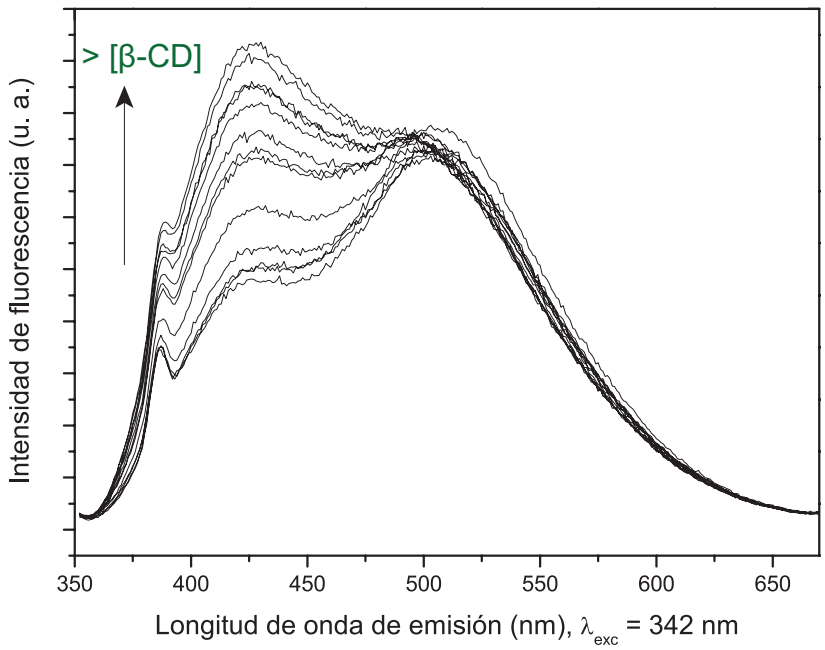

Figura 1.
Efecto de la presencia de concentraciones crecientes de ciclodextrinas sobre la fluorescencia de la luotonina A en medio acuoso ácido (pH=1). Nótese cómo en ausencia de ciclodextrina, la emisión de la forma catiónica (517 nm) es mayoritaria. Por el contrario, la formación del complejo de inclusión conlleva la aparición de la emisión de la forma neutra (426 nm), al quedar protegida en el interior de la cavidad de la ciclodextrina.

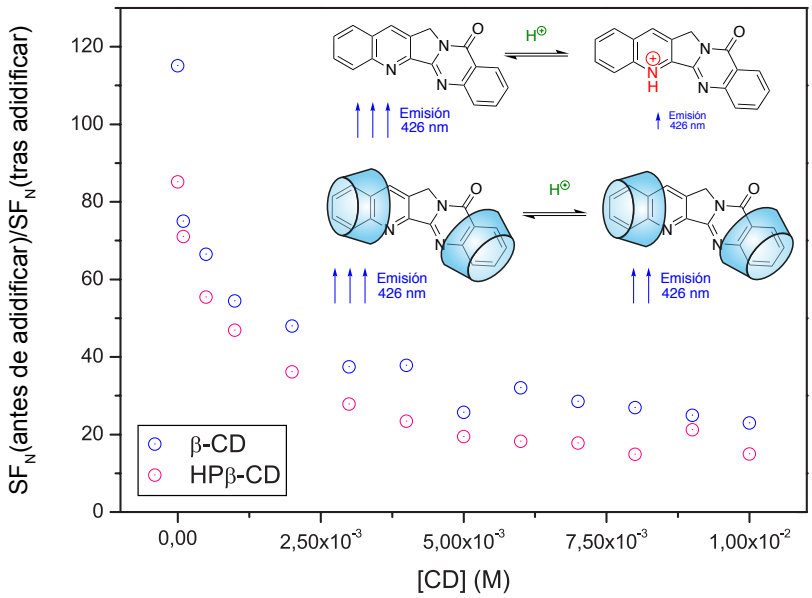

Figura 2. Demostración de la protección ejercida por las ciclodextrinas sobre la luotonina A. En ausencia de ciclodextrinas, la emisión de la forma neutra disminuye drásticamente después de acidificar el medio, como corresponde a una elevada relación de señales de fluorescencia antes/después. Cuando la acidificación se efectúa tras la formación de complejos de inclusión en presencia de cantidades crecientes de ciclodextrinas, la protección aportada por éstas dificulta la protonación y, por tanto, las emisiones de la forma neutra antes y después de acidificar son más parecidas (menor relación antes/después).

ciclodextrinas. Así, en los espectros de ^{1}H y ^{13}C de la camptotecina se pueden apreciar variaciones significativas en las señales correspondientes a los átomos del anillo aromático A. Sin embargo, las señales del anillo E, que es mucho más polar, resultan menos afectadas, lo que indica que un menor número de moléculas se han incluido por ese anillo. Por el contrario, en el caso de la luotonina A se pueden observar tales cambios tanto en la zona del anillo A como en la del anillo E. Este resultado confirma que la menor polaridad de este anillo en el caso de la luotonina A aumenta el grado de inclusión por ese extremo de la molécula (Figura 3).

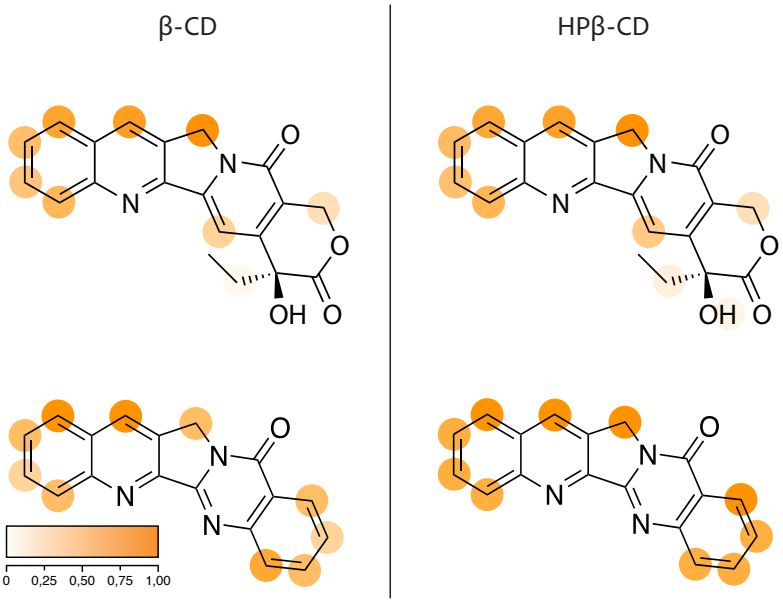

Figura 3. Diagramas que muestran la magnitud relativa del cambio en el desplazamiento químico de los átomos señalados como consecuencia de la inclusión en ciclodextrinas. La intensidad de color es proporcional al grado de variación del desplazamiento químico.

Así pues, la caracterización de los complejos de inclusión formados entre CDs y los fármacos antitumorales estudiados, así como el estudio de la presencia de CDs como aditivos en las fases móviles empleando columnas “core-shell”, son dos de las líneas de trabajo que nos encontramos actualmente comenzando.

Conclusiones

1. Se ha desarrollado un método cromatográfico para la determinación de la luotonina A y 5 de los 6 nuevos derivados. Se ha estudiado la influencia de distintas variables (elución gradiente/isocrático, pH, aditivos orgánicos en la fase móvil) en la separación. Las condiciones optimizadas se han aplicado a la determinación de estos derivados en muestras de suero humano. El método se ha validado de acuerdo a las normas internacionales demostrando ser sensible, preciso y exacto.

2. Se ha comparado la selectividad de tres fases estacionarias de características químicas distintas: fenil-hexil-, pentafluorofenil-propil- y octadecil-silano (PH, PFP y C-18, respectivamente). Sólo la fase estacionaria C-18 consigue resolver adecuadamente todos los compuestos. El estudio de la termodinámica de la adsorción revela que, en todas las fases estacionarias, las separaciones obedecen a un mecanismo de separación en fase inversa típico. En el caso de las fases PH, se observan dos comportamientos distintos que son dependientes de la temperatura.

3. Las eficacias de las columnas tipo "core-shell" evaluada como HEPT es significativamente mayor que la obtenida con las columnas de partículas totalmente porosas. Los "kinetic plots" revelan que estas columnas son ideales para separaciones rápidas. La sustitución de las columnas totalmente porosas por las tipo "core-shell" aporta una mejora inmediata en la eficacia y el tiempo de análisis sin comprometer las presiones de trabajo. Sin embargo, de nuestros resultados se desprende que sólo en equipos concebidos para minimizar el volumen extra-columna es posible aprovechar todo el potencial de este tipo de soportes cromatográficos.

4. Se han optimizado las condiciones de separación en la columna "core-shell" C-18 y se ha aplicado un gradiente que logra la separación de la camptotecina, la luotonina A y los 6 derivados de ésta reduciendo el tiempo de análisis en más de un 50% con respecto a las fases estacionarias convencionales. La metodología se ha aplicado a la determinación de los antitumorales derivados de luotonina A en líneas celulares, y en su validación se han obtenido excelentes parámetros de calidad.

5. En la etapa de pretratamiento se ha optimizado y aplicado un método de desproteinización empleando placas multipocillo que permite procesar un elevado número de muestras de manera rápida y automatizable. Esta estrategia, acoplada a la separación en columnas de tipo "core-shell", conlleva una reducción del consumo de disolventes orgánicos de un 72%. Puede afirmarse que se trata de una metodología sostenible y de alto rendimiento.

6. La incorporación de ciclodextrinas a las fases móviles causa un notable descenso en los índices de retención de los solutos sin sacrificar la eficacia de la separación. Por lo tanto, permite separaciones cromatográficas con fases móviles mayoritariamente acuosas y en las que el componente orgánico es

etanol, un disolvente no tóxico y biodegradable. Se ha logrado la separación de alcaloides de tipo β-carbolina en fases estacionarias convencionales C-18 o metilsilano (C-1). El uso de ciclodextrinas permite reducir el consumo de disolvente orgánico en un 37% (C-18). Las columnas C-1 permiten alcanzar un ahorro efectivo del 70% del componente orgánico de la fase móvil con respecto a métodos previamente descritos. Se consigue así disminuir la generación de residuos y que éstos tengan muy bajo o nulo impacto ambiental.

7. Se ha validado el método analítico empleando 2-hidroxipropil-β-ciclodextrina o β-ciclodextrina nativa tanto en fases estacionarias C-18 como C-1 para la determinación de β-carbolinas en muestras de suero humano. La elección de la SPE como método de pretratamiento permitió reducir aún más el impacto ambiental del método, al requerir menor cantidad de disolvente orgánico que la extracción líquido-líquido. En todos los casos, en la validación se obtuvieron buenos parámetros de calidad, sin bien la incorporación de un patrón interno mejoró notablemente los resultados de la misma.

8. Se han estudiado por primera vez las propiedades luminiscentes de la luotonina A y una serie de derivados. Los rendimientos cuánticos de fluorescencia de los siete compuestos son dependientes de la estructura química, el disolvente y el pH. Los equilibrios de transferencia de protón en estado excitado han revelado que los nitrógenos básicos se protonan en medios fuertemente ácidos. Las técnicas de ^{1}H y ^{13}C-RMN apoyan los resultados obtenidos por fluorescencia. La correlación estructura química-basicidad es notable para el conjunto de los derivados estudiados.

9. Se ha diseñado un método sostenible y miniaturizado en formato multi-pocillo para estudiar cómo aumenta la solubilidad de los derivados de luotonina A tras formar complejos de inclusión con (2-hidroxipropil)-β-ciclodextrina, y éstos se han caracterizado también mediante espectrometría de masas (ESI-MS). Usando este formato de alto rendimiento es posible procesar un elevado número de muestras de manera simultánea, mejorando notablemente los resultados de la técnica cromatográfica de referencia en cuanto a tiempo de análisis (30 s/muestra, 40 veces inferior), y del volumen de residuos generados (25 veces inferior).

10. Dado que la luotonina A presenta actividad antitumoral, se ha evaluado la potencia de los derivados estudiados mediante ensayos enzimáticos de inhibición de topoisomerasa 1 y el efecto citotóxico ejercido sobre líneas celulares tumorales de colon, cérvix y pulmón. La mayoría de los compuestos presentan mejores actividades que la luotonina A, obteniendo resultados más prometedores los derivados más lipófilos. Los resultados obtenidos mediante modelado molecular y “docking” han permitido proponer un nuevo modo de interacción de estas moléculas con el complejo enzima-ADN que explicaría su mejor actividad, y que destaca el papel de los sustituyentes aromáticos en el anillo B en la estabilidad del complejo.

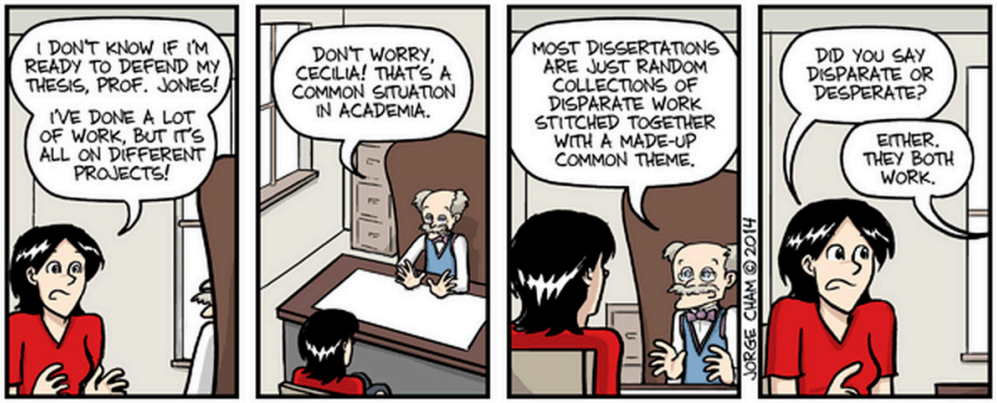

WWW.PHDCOMICS.COM

Proudly made on a Mac